AD-A170 212 THE NORDA (NAVAL OCEAN RESEARCH AND DEVELOPMENT ACTIVITY) REVIEW(U) NAVAL OCEAN RESEARCH AND DEVELOPMENT ACTIVITY NSTL STATION MS MAR 86

UNCLASSIFIED F/G 8/10 NL

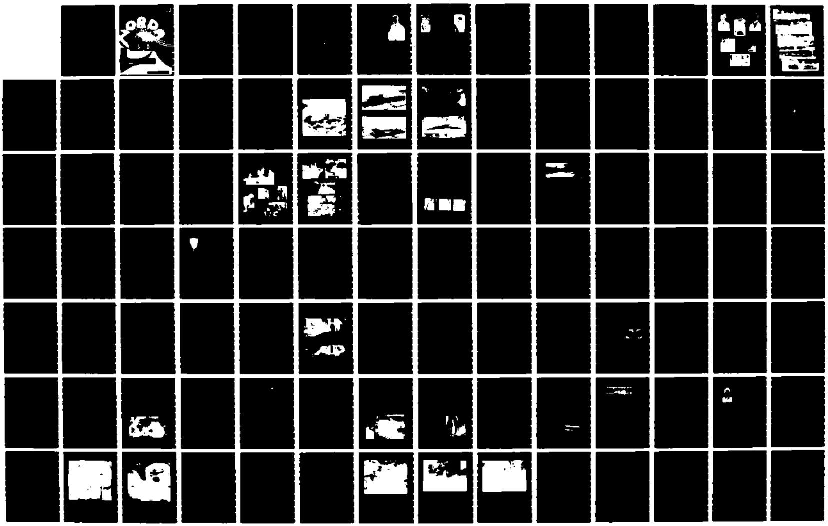

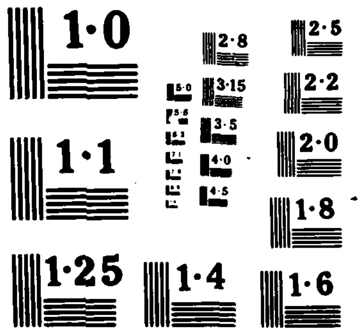
1·0
2·8
2·5
3·15
2·2
3·5
2·0
1·1
4·0
1·8
4·5
1·25
1·4
1·6

Naval Ocean Research and Development Activity

1

AD-A170 212

DTIC
S ELECTE D
JUL 2 5 1986
D

DISTRIBUTION STATEMENT A
Approved for public release;
Distribution Unlimited

NORDA Mission

The mission of the Naval Ocean Research and Development Activity is to carry out a broadly based RDT&E program in ocean science and technology, with emphasis on understanding ocean processes through measurement and analysis, and the effects of the ocean environment on Navy systems and operations.

UNCLASSIFIED
SECURITY CLASSIFICATION OF THIS PAGE

REPORT DOCUMENTATION PAGE

1a REPORT SECURITY CLASSIFICATION Unclassified	1b RESTRICTIVE MARKINGS None
2a SECURITY CLASSIFICATION AUTHORITY	3 DISTRIBUTION/AVAILABILITY OF REPORT Approved for public release; distribution is unlimited.
2b DECLASSIFICATION/DOWNGRADING SCHEDULE	
4 PERFORMING ORGANIZATION REPORT NUMBER(S)	5 MONITORING ORGANIZATION REPORT NUMBER(S)
6 NAME OF PERFORMING ORGANIZATION Naval Ocean Research and Development Activity	7a NAME OF MONITORING ORGANIZATION Naval Ocean Research and Development Activity
6c ADDRESS (City, State, and ZIP Code) NSTL, Mississippi 39529–5004	7b ADDRESS (City, State, and ZIP Code) NSTL, Mississippi 39529–5004
8a NAME OF FUNDING/SPONSORING ORGANIZATION Naval Ocean Research and Development Activity 8b OFFICE SYMBOL (If applicable)	9 PROCUREMENT INSTRUMENT IDENTIFICATION NUMBER
8c ADDRESS (City, State, and ZIP Code) NSTL, Mississippi 39529–5004	10 SOURCE OF FUNDING NOS. PROGRAM ELEMENT NO / PROJECT NO / TASK NO / WORK UNIT NO

11 TITLE (Include Security Classification)
The NORDA Review

12 PERSONAL AUTHOR(S)

13a TYPE OF REPORT	13b TIME COVERED	14 DATE OF REPORT (Yr., Mo., Day)	15 PAGE COUNT
Final	From 1976 To 1986	March 1986	238

16 SUPPLEMENTARY NOTATION

17 COSATI CODES			18 SUBJECT TERMS (Continue on reverse if necessary and identify by block number)
FIELD	GROUP	SUB. GR.	science, technology, environment, research

19 ABSTRACT (Continue on reverse if necessary and identify by block number)

This publication reviews the growth of NORDA and presents a cross section of NORDA's products as a multidisciplinary, full-spectrum, ocean science and engineering facility. NORDA's research program has been designed as a broad, balanced blend of basic and exploratory ocean research, model development and applications, systems concepts and designs, and advanced engineering developments. NORDA's corporate goals are to advance our knowledge of the marine environment, to apply and exploit this knowledge in support of Navy weapon systems development, and to resolve Fleet problems impacted by the ocean environment.

20 DISTRIBUTION/AVAILABILITY OF ABSTRACT UNCLASSIFIED/UNLIMITED [ ] SAME AS RPT ■ DTIC USERS [ ]	21 ABSTRACT SECURITY CLASSIFICATION Unclassified
22a NAME OF RESPONSIBLE INDIVIDUAL Jim Sullivan	22b TELEPHONE NUMBER (Include Area Code) (601) 688-4765 22c OFFICE SYMBOL Code 104

DD FORM 1473, 83 APR EDITION OF 1 JAN 73 IS OBSOLETE

UNCLASSIFIED
SECURITY CLASSIFICATION OF THIS PAGE

A

The NORDA Review

(March 31, 1976—March 31, 1986)

Naval Ocean Research and Development Activity
NSTL, Mississippi 39529-5004

Preface

Rear Admiral J. B. Mooney, Jr., USN
Chief of Naval Research

Oceanography has played a major role in the U.S. Navy since the time of Matthew Fontaine Maury. The importance of this knowledge in the deployment of our armed forces and the use of our weapon systems is more critical today than ever before.

As a former Oceanographer of the Navy, I was responsible for furnishing oceanographic products to our operational forces, and I needed support from strong oceanographic research and development programs. Now, as Chief of Naval Research (CNR), I am responsible for developing the oceanographic technical base necessary to satisfy these requirements.

With this unique privilege—working with NORDA as both CNR and Oceanographer of the Navy—I can personally attest to the dedication and capabilities of NORDA's people. Many of NORDA's accomplishments in ocean and acoustic modeling, instrumentation, and measurement techniques have been transitioned to the Fleet. I applaud this success and look forward to an exciting future, as we work together to implement oceanographic knowledge and multiply the capabilities of our operational forces.

J. B. Mooney, Jr., Rear Admiral, USN
Chief of Naval Research

Introduction

Captain Roger P. Onorati, USN, Commanding Officer
Dr. James E. Andrews, Technical Director

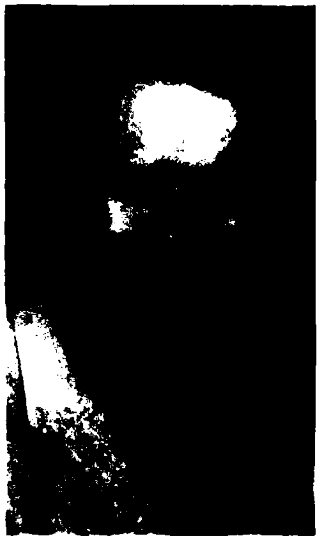

This publication reviews the growth of NORDA and presents a cross section of NORDA's products as a multidisciplinary, full-spectrum, ocean science and engineering facility. NORDA's research program has been designed as a broad, balanced blend of basic and exploratory ocean research, model development and applications, systems concepts and designs, and advanced engineering developments. NORDA's corporate goals are to advance our knowledge of the marine environment, to apply and exploit this knowledge in support of Navy weapon systems development, and to resolve Fleet problems impacted by the ocean environment.

The underlying theme of this document is that of progress throughout NORDA's relatively short history; progress displayed by the continuing growth of the high-quality scientific research staff and by the state-of-the-art facilities that support that staff. It is also apparent in the high quality of the administrative and technical support staff. The product of our research staff is exemplified in the content of the papers in the Review. The product of the other is reflected in the quality and polish of the physical aspects of this publication.

These pages reveal that NORDA has developed strong programs in oceanography; ocean remote sensing; ocean modeling; ocean acoustics; mapping, charting and geodesy; and geosciences. Innovative measurement systems, many of which are unique in the marine community, have been developed by NORDA scientists and engineers to support these programs. These programs and capabilities are the result of a series of well-planned investment initiatives and of the support provided by the Chief of Naval Research through the Office of Naval Research to implement these plans. Most importantly, the products of NORDA research presented here reflect the cumulative efforts and dedication of all the individuals who have been part of NORDA's first ten years, and set a standard to be maintained and advanced in future years.

Contents

The Origin of NORDA

The early 1960s constituted a brief period of prosperity for both oceanography and Department of Defense Research and Development. During these few years, the Vietnam War had not yet taken over either the Defense budget or the focus of national attention. President Kennedy had committed the nation to winning a race with Russia in space, and the mood of the Congress fostered a growing respect and support for scientific efforts. The ocean was beginning to be recognized as the final frontier for exploration on earth.

During those few years, Congress authorized the building of the first Navy-owned and operated ships specifically designed for oceanographic work, the Navy's ocean science budget more than doubled, and the size of the Naval Oceanographic Office (NAVOCEANO) grew by more than 50%.

At this time the Navy also began an effort to improve coordination of its ocean science programs, both internally and with those managed by other agencies. This effort included the establishment of the Oceanographer of the Navy (OCEANAV) as a separate command in 1966 to serve as the Navy's "czar" of oceanography, and to direct and manage the resources of the Naval Oceanographic Program. At the same time, the Naval Research Laboratory (NRL) and its higher headquarters, the Office of Naval Research (ONR), were reorganizing a number of their programs. These two organizations and NAVOCEANO were the only major Navy elements with significant ongoing research efforts in basic ocean science, programs not directly related to supporting fleet systems development.

The Assistant Secretary for the Navy for R&D, ONR, and NRL initiated plans to establish on one campus an ocean science center that would serve to improve coordination among the various Navy programs. The plan grew, eventually involving OCEANAV and NAVOCEANO, and began to take shape in the mid-1960s as the Matthew F. Maury Center for Ocean Science.

NAVOCEANO's growth during the preceding few years was beginning to cause severe space shortages at both its Suitland, Maryland, and Washington (D.C.) Navy Yard locations. Conversely, the completion of several new buildings at NRL had made several older buildings there surplus and subject to demolition. These buildings were chosen as the site of the incipient Maury Center and, within weeks, NAVOCEANO began relocating some of its research and development people to this site.

But now in the mid-1960s, the mood of the nation was beginning to change with its deepening involvement in Vietnam. The war's drain on the DoD budget and, later, negative public reaction to our national involvement in the war, began to impact drastically on the Navy ocean science budget and personnel ceilings. The available R&D funding began to diminish; at-sea ship time was cut back and several of the new AGS and AGOR ships were either mothballed for long periods or were disposed of. Navy influence in the overall national ocean science program thus diminished.

However, the rapid growth of NAVOCEANO was now forcing it to occupy office and laboratory space in parts of some 10 different buildings at four different locations (Suitland, NRL, the Washington Navy Yard, and the NRL facility at Chesapeake Beach, Maryland). NRL, itself experiencing renewed growth as a result of direct support of the war effort in some of its programs, forced NAVOCEANO to move many of its Maury Center people out of their spaces.

This need for space, together with the fact that the Navy was the largest federal employer in the D. C. area (with over 40,000 civilian employees) and was under pressure from Congress to decentralize and relocate its personnel to other parts of the country, pointed toward relocation of NAVOCEANO away from Washington.

NASA's National Space Technology Laboratories, located in southwestern Mississippi, near Bay St. Louis, was just one of the sites OCEANAV considered. The others included Newport, Rhode Island; the Philadelphia Navy Yard; Hyattsville, Maryland; and NASA's Michoud site near New Orleans. But because of the cutback in the space program, the Mississippi facility had approximately 45,000 square feet of modern (mid-1960s) office and laboratory space and about 100,000 square feet of warehouse space and other facilities that were either vacant or could be made available on short notice.

Because of the high cost, relocating just NAVOCEANO did not appear acceptable. So, in February of 1975, OCEANAV proposed to the Assistant Secretary of the Navy (R&D) a plan for consolidation of the Naval

Oceanographic Program at NSTL, with a number of existing components in addition to NAVOCEANO. These components were ONR Code 480, the Long Range Acoustic Propagation Project (LRAPP), the ONR Acoustic Environmental Support Detachment (AESD), ONR Code 102-OS, and six unspecified ocean science program managers from the Navy Systems Commands and the Chief of Naval Material.

For the most part, these (together with the R&D components of NAVOCEANO) were the same elements earmarked to compose the Maury Center back in the mid-1960s. But the Maury Center, although it had its own letterhead stationery and a sign on its main building, never did achieve official status as a command or even a component of a command. During its entire existence (1966–1976), it remained a loose confederation of co-located elements that had similar interests, but entirely different chains of command.

By relocating these elements along with the the rest of the NAVOCEANO organization, it was felt that the goals of the Maury Center could still be pursued and would stand a better chance of being achieved.

The preliminary plan was approved by the Assistant Secretary of the Navy (R&D), and the following month (March 1975) the Chief of Naval Research announced that a new R&D organization would be formed as a result of moving these elements to Mississippi. Although NAVOCEANO would continue to report to OCEANAV, NAVOCEANO's R&D components and the other ONR and SysCom elements involved would form the new R&D organization and would report to the Chief of Naval Research. This new organization would, however, be co-located with NAVOCEANO at NSTL; together, they would form the basis of a new Naval Oceanographic Center of Excellence.

The Chief of Naval Research appointed Dr. Roy Gaul, the manager of the Long Range Propagation Project, to head the planning group to form the new organization. Initially, Dr. Gaul informally named the new activity the Naval Ocean Research Laboratory (NORL); this was changed within a month to the Naval Ocean Science Activity (NOSA). Finally, on June 10, 1975, Dr. Gaul and his assistants agreed that the Naval Ocean Research and Development Activity (NORDA) should be the name of the new R&D organization.

On July 25, 1975, the Deputy Secretary of Defense announced that certain elements of the Navy's Oceanographic Program would be consolidated at NASA's NSTL base in Mississippi. Five days later, an OPNAV-NOTICE 5450 was issued, establishing NORDA in a development status, effective August 3, 1975. And, on March 31, 1976, NORDA became fully operational as a field activity under the Chief of Naval Research.

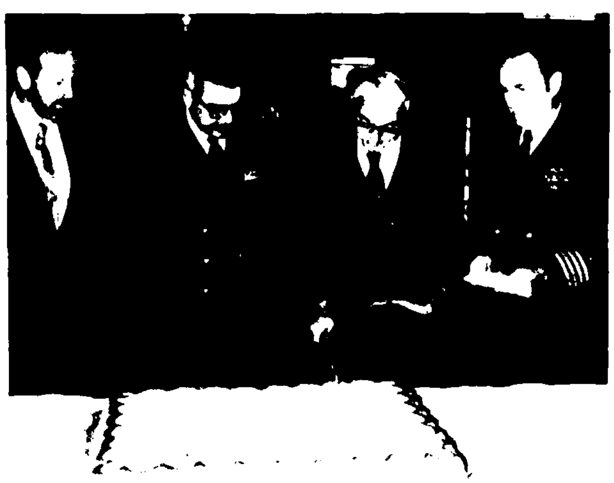

Significant Dates in the History of NORDA

The essential history of NORDA is contained in the documents of its research, development, and engineering activities. However, in the chronology of NORDA as an organization, a number of specific dates and milestones are worth noting in these pages.

February 1975—Commander B. Matthews is assigned to serve as Executive Officer of the organization-in-formation that will become NORDA.

December—Captain Charles G. Darrell is assigned as Commanding Officer of the new organization.

March 31, 1976—NORDA is officially established at NSTL as a field activity of the Chief of Naval Research. Dr. Ralph Goodman, Associate Director of Research for Oceanology at the Naval Research Laboratory, is named NORDA's first Technical Director. Commander George E. Lawniczak is assigned as first Director of the Navy Oceanographic Laboratory (NOL) at NORDA.

September—Commander R. J. Mace relieves Commander Matthews as Executive Officer.

April 25, 1977—NORDA's first ADP facility, featuring a CDC-1700 computer, is dedicated.

June—NORDA's first two reports are published: *The Geological Environment West of St. Croix*, by T. Holcomb, A. Einwich, F. Bowles, and J. Egloff, all of Code 360, and *The Oceanographic/Meteorological Environment West of St. Croix* by D. Burns of Code 330.

July 1—Captain Glenn D. Hamilton assumes directorship of NOL.

September—Commander John D. Hague relieves Commander Mace as NORDA Executive Officer.

January 3, 1979—Dr. David Mann, Assistant Secretary of the Navy for Research, Engineering and Systems, breaks ground for NORDA Remote Sensing Laboratory addition to Building 1105. (First dedicated NORDA construction project.)

July—Commander Kenneth G. Hinman relieves Captain Hague as NORDA Executive Officer.

June 15, 1980—Dr. Louis P. Solomon reports aboard as Head of NORDA's Ocean Programs Management Office (Code 500).

December 8—Captain G. Thomas Phelps assumes command of NORDA.

March 1, 1981—Dr. James E. Andrews assumes Directorship of NORDA's Ocean Science and Technology Laboratory (Code 300).

April 3—Navy Secretary John Lehman and U.S. Senator John Stennis are briefed on NORDA during a tour of NSTL.

May 11—Ground is broken for a second wing to Building 1105, dedicated to NORDA's Physical Oceanography Branch.

August—Dr. Goodman accepts reassignment to head the SACLANT ASW Research Centre at La Spezia, Italy.

November—Dr. Andrews is named NORDA Technical Director.

June 1, 1982—Dr. Herbert Eppert is named Director of NORDA's Ocean Science and Technology Laboratory.

July—Captain Hinman is reassigned to Naval Oceanography Command Center—Guam; Commander R. J. Coleman takes over as NORDA Executive Officer.

August 20—Ground is broken for the NORDA Ocean Science Center, the first new building dedicated exclusively to NORDA's use.

August 1983—NORDA's remote sensing capabilities are enhanced; one 10-m and two 5-m dish antennas are installed.

January 1984—NORDA reorganizes; Ocean Acoustics and Technology Directorate is established, and is headed by Dr. William Moseley.

March—Ocean Programs Management Office is disestablished.

July 20—NORDA's Magnetic Observatory opens.

September 7—NORDA's Ocean Science Center (Building 1005) opens.

September 25—Captain Roger P. Onorati relieves Captain Phelps as NORDA Commanding Officer.

November—Seven members of the Naval Research Advisory Committee (NRAC) pay first visit to NORDA.

July 1985—The Secretary of the Navy announces that an Institute for Naval Oceanography will be established at NSTL; Captain Onorati will be the first Officer-in-Charge.

August—Commander Roland Garcia relieves Commander Coleman as Chief Staff Officer (former Executive Officer position).

NORDA Major Scientific and Technical Accomplishments (1976–1986)

Since 1976, NORDA's efforts in ocean research and engineering, either directly or through programs it has sponsored, have resulted in specific and general accomplishments that increased our understanding of the ocean environment or had a beneficial impact on state-of-the-art systems, techniques, and equipment design, or on the Fleet, itself. This listing summarizes some of NORDA's more significant accomplishments.

- A technique to extract ocean bottom impulse response from reflectivity data was established.
- An improved model of resonant scattering from an individual swimbladder fish was developed.
- An acoustic model to estimate the distribution of fish school target strength for any schooling species was developed and refined.
- An advanced towable, high-frequency acoustic backscatter measurement system was completed and field tested to measure volume reverberation and to enable study of internal wave interaction and mixing processes and how they affect acoustic transmission.
- A new active sonar forecasting system, SHARPS III (Ship, Helicopter Acoustic Range Prediction System), was developed by NORDA.
- The Versatile Experimental Kevlar Array Program (VEKA) produced a family of instrumented arrays for various environmental acoustic experiments required by the Navy for a wide variety of underwater acoustic experiments.
- A series of detailed geological/geophysical maps that describe the sea floor in the eastern Caribbean and the northeast Pacific were produced.
- Geoacoustic models were derived for seven Northeast Atlantic sites.
- An electronic filter (EEF) was developed for use with the ASQ-81 MAD system for reducing geological noise during ASW operations.
- A cooperative NORDA/Canadian Defence Ministry experiment was conducted off the coast of Newfoundland. Results of the experiment indicated the possibility that radar beamed from a satellite can be used to locate ocean surface currents and eddies.
- The world's first ocean forecast model designed for operational use was developed and delivered to the Fleet Numerical Oceanography Center, Monterey, California. The Thermodynamical Ocean Prediction System (TOPS) provides real-time, large-scale forecasts of the thermodynamical structure of the upper mixed layer of the ocean.
- An electromechanical cable was developed for diverse sea applications. The cable allows for complete torque balance and provides a wide choice of strength for a given core size.
- A unique ocean measurement system that can measure and analyze the highly saline brine pumped from salt domes was developed and installed at the Bryan Mound salt dome near Freeport, Texas.
- A portable 33-GHz microwave radiometer and source has been developed and is now "Arctic-ready."
- The preliminary concept, design, and testing phases for a new deep ocean measurement technology—the Deep Towed Array Geophysical System (DTAGS)—has been completed.
- Development and field testing of a buried mine minehunting system has begun.
- Three large, uncharted seamounts were detected near Wake Island; linear, seafloor-spreading type anomalies were identified in the magnetic "quiet zone"; and new regional anomaly patterns and their boundaries were mapped.
- Numerical experiments on the Gulf of Mexico circulations verified theoretical predictions about the Loop Current and its eddy shedding, including eddy diameter, penetration into the Gulf and the latitude of westward bending.
- Conductivity-temperature-depth (CTD) processing software developed by the Naval Oceanographic Office has been streamlined and extensively documented.
- A major field experiment, Donde Va?, involved scientists from Spain, France, Germany, and the United States. The experiment was conducted near the Strait of Gibraltar.

Analysis of results revealed previously unknown features of the regional circulation, which have significant tactical implications about temporal and spatial environmental variability.

- A group of experiments was performed to study the evolution of steep, initially two-dimensional water waves. Experiments in a large towing tank and an outdoor basin revealed rapid, intense, nonlinear transitions leading to three-dimensional wave breakdown.
- Models have been developed to improve the basic understanding of the interaction of acoustic energy with the ocean boundaries.
- Vertical line array (VLA) performance measurements were conducted to support an experiment in a bottom-limited region of the Northeast Pacific. Data from these measurements served as a testbed for a maximum entropy beamformer, which provides beamwidths one-seventh as wide as those provided conventionally.
- A new analytical approach based on pyrolysis-mass spectrometry has been developed. The instrument analyzes the organics in water, sediments, and particles, and on surfaces in under 15 minutes.
- An Expendable Probes Data Acquisition System (EPDAS) has been developed and tested. The system can collect data from a variety of expendable sensors.
- The Air/Sea Interaction Measurement System was developed to provide a significant capability for precisely measuring ocean surface waves and their interactions with surface winds and subsurface currents.
- A marine geotechnical laboratory was established to improve understanding of the relationships among sediment geotechnical properties, seabed acoustic properties, and seafloor environmental processes.
- Two deep-ocean piezometer probes have been developed and tested.
- The Oceanographic Instrumentation Systems Project sponsored the development, evaluation, and implementation of new measurement systems: the expendable shear probe, the expendable dissipation probe; and air-expendable sound velocity probe; deep, accurate airborne expendable bathythermographs; digital data collection systems for use on surface and air platforms; microstructure profilers; and bathyphotometers.
- A shipboard oceanographic profiling system, including sensors and winch, was developed and used extensively to measure finescale ocean variability.
- For the first time, a global distribution of oceanic shear was obtained over the Northern Hemisphere in the upper layers of the ocean using the TOPS model developed by NORDA and surface momentum/heat fluxes derived from a global weather prediction model.
- In a cooperative effort with the Naval Underwater Systems Center, a wide-angle parabolic equation model was developed to predict acoustic propagation in range-dependent ocean environments.
- NORDA participated in a U.S. Navy Black Sea operation to determine how the Acoustic Performance Prediction (APP) system is used in the field and to provide NORDA with experience in its operational uses and problems.
- The AUTO OCEAN data base was updated in the Southern Hemisphere, and the Retrievable Sound Velocity Provile (RSVP) data base was updated.
- A continuing project, Basic Acoustic Model Users Support—BAMUS, provides support to the ASW community by making acoustic modeling services available.
- SHARPS III updates were completed, and the upgrade for the Fast Asymptotic Coherent Transmission (FACT) 9H model, FACT 10A, was evaluated and will replace the older version.
- A data system to provide altimeter-based products to the Fleet Numerical Oceanography Center and research to refine and improve the algorithms to derive oceanographic parameters from GEOSAT data is continuing.
- A towed underwater pumping system (TUPS) was successfully developed to make simultaneous chemical, biological, and light measurements in the oceans.
- Analysis of clay minerals from Quaternary sediments of the eastern Caribbean has led to positive identification of the Orinoco River as a source area and development of sediment transport models explaining the spatial/temporal distribution of Quaternary terrigenous sediments in the eastern Caribbean.
- A continuing objective is to improve hydrographic survey operations by collecting bathymetric data more accurately and efficiently. An in-depth analysis was performed for survey operations and the need for a centralized Fault Location System (FLS) was identified. The FLS will provide sound boat operators with immediate, continuous monitoring of the quality and operational availability of all data collection, navigation, recording, power, and environmental equipment in use.
- NORDA has conducted research and development to support amphibious preassault planning. A technique has been developed for using wave-refraction analysis to determine nearshore bathymetry in an amphibious objective area.
- A large-scale, complex, user-friendly interactive data processing system has been designed for use in hydrographic information handling. The software has already

proved useful in processing survey data onboard NAVOCEANO's hydrographic ships.

• A Remote Work Processing Facility was designed and established at NORDA for automatic feature extraction research. NORDA has been formally recognized as the Navy's Remote Work Processing Facility for the Defense Mapping Agency's tri-service capability.

• An automated system for extracting bathymetry from remotely sensed data was needed. NORDA tested and evaluated various image enhancement/digital filtering algorithms for use in improving stereocompilation of bathymetric images.

• The Navy needed a cavitation source to advance its understanding of ocean parameter influences on the generation of cavitation by propellers and moving hulls. The Cavitating Ocean Profiling System was developed and has been successfully demonstrated at sea.

• The South Atlantic Geocorridor project has obtained geomagnetic profiles that extend from the eastern coast of South America to the Mid-Atlantic Ridge.

• A Versatile Experimental Data Acquisition Buoy System (VEDABS) was developed to provide critical acoustic measurements.

• Maximum Entropy Method (MEM) beamforming, a high-resolution spatial processing technique, has been developed to provide increased resolution and decreased beamwidth without increasing the array aperture.

• Airborne Electromagnetic (AEM) bathymetry technology from geological prospecting applications is being applied to charting the depth of shallow coastal waters. Initial field testing shows good agreement with ground truth data, but further improvements in model inputs and equipment calibration techniques are required for improved resolution.

• An Airborne Bathymetric Survey (ABS) System is being developed for use in a Navy P-3 aircraft. This system will address the significant backlog of needed surveys in coastal areas, while performing those surveys more quickly, with higher coverage, and at less expense than conventional techniques. The ABS System will combine an active scanning laser sounder, a nine-channel passive multispectral scanner, and an active electromagnetic profiler.

• During a four-year period, NORDA led or participated in eight shallow-water, high-frequency, acoustic bottom scattering experiments.

• An operational Arctic Sea Ice Forecast Model was developed and delivered to the Fleet Numerical Oceanography Center. The model forecasts ice velocity, thickness, and compactness, as well as areas of convergence and divergence.

• Fleet Interaction: NORDA has been intensely involved in providing direct technical environmental support to Fleet operational commands.

• A vertical line array DIFAR acoustic prediction model was installed in the computer at Fleet Numerical Oceanography Center for daily use in Fleet broadcasts to predict the performance of the Fleet operational system.

• NORDA carried out data collection, analysis, and modeling as the lead U.S. participant in a two-part NATO Military Oceanography operation in a closed basin.

• A seasonal Secchi depth atlas documenting water clarity has been developed for the world's coastlines.

• NORDA has constructed a remotely located Magnetic Observatory to conduct measurements of the ambient magnetic field in a magnetically quiet environment, as well as other such magnetic phenomena as telluric potentials and low-frequency seismic vibrations in support of Navy mapping, charting, and geodesy requirements.

• An upgraded Thematic Mapper Scanner is being developed for use in the Airborne Bathymetric Survey (ABS) System. This multispectral scanner splits the blue and green bands to provide more accurate bathymetric information in the penetrating bands.

• Monte Carlo models have been developed to enable direct simulation of the laser volume backscatter radiance at off-axis detectors.

• A study was conducted to determine map and chart symbolization improvements that could be made available by computerized production methods. A 1:1,000,000 experimental map featuring illuminated contours and other special symbolizations was designed. Proof copies are being produced for evaluation.

• An opportunity to conduct two SWATHMAP surveys in the Red Sea and Gulf of Aden aboard the USS JOHN HANCOCK was exploited. The data acquired on these cruises demonstrate the validity of regional geoacoustic (backscatter) mapping using SQS or similar sonar systems.

• The WESTPAC Jurassic "Quiet Zone" study has been completed. Low-altitude aeromagnetic survey data were used to map sequences of linear magnetic anomalies in a region of subdued magnetic morphology east of the Mariana-Izu trench system. The anomalies are interpreted to be of the seafloor spreading variety and have been used to derive a new geomagnetic reversal time scale for the Jurassic.

• The Marine Seismic System (MSS) project successfully completed a SW Pacific operational deployment in a water depth of 18,600 ft.

Facilities

NORDA is located on the grounds of NASA's National Space Technology Laboratories, which is situated about 25 miles from the Mississippi Gulf Coast and 45 miles from New Orleans, Louisiana. Our facilities consist of administrative and support offices, laboratories, specialized work areas, and storage facilities. Selected articles on several of our facilities and systems are included here.

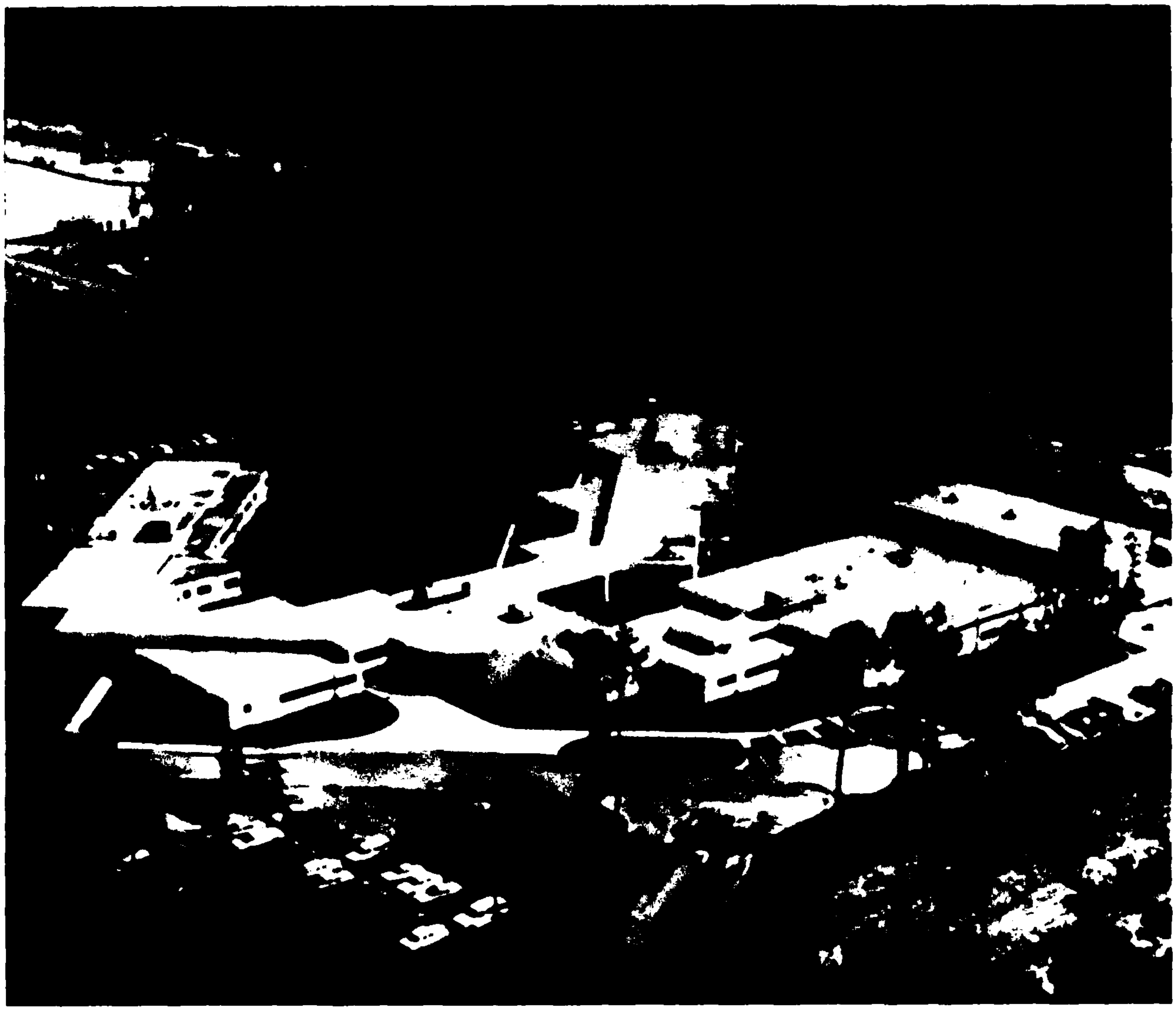

NORDA's first dedicated building, the Ocean Science Center, was officially open for business 17 August 1984. The Command's senior management staff and the Ocean Acoustics, Ocean Technology, and Seafloor Geosciences Divisions are located here.

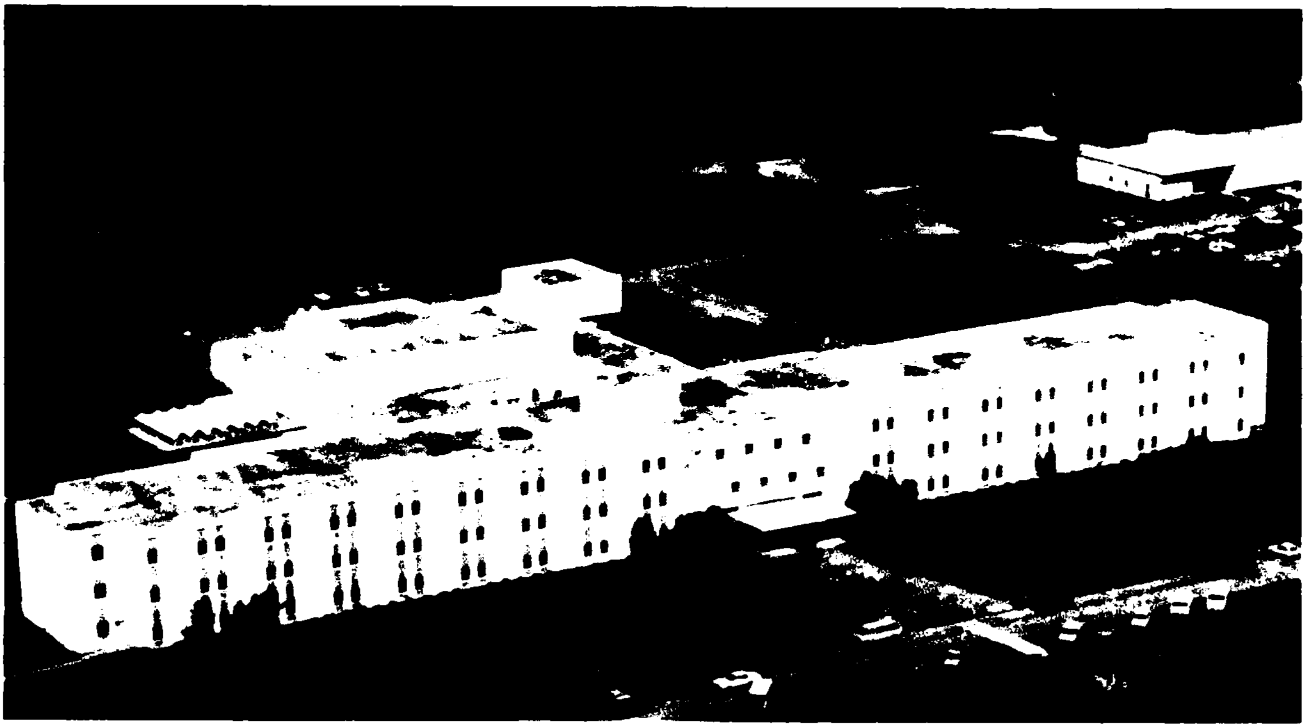

Some of NORDA's personnel share space with other government agencies and contractors in NSTL's main administration building.

This building houses NORDA's Oceanography Division and Ocean Sensing and Prediction Division personnel. Although space is shared with contractor personnel, this laboratory has two NORDA-dedicated wings.

A modular building houses NORDA's Financial Management and Personnel Division. NORDA is also using a 2400 square foot metal prefab office warehouse building for storage. NORDA has two double-wide trailers, one for the Public Affairs Office and one for training.

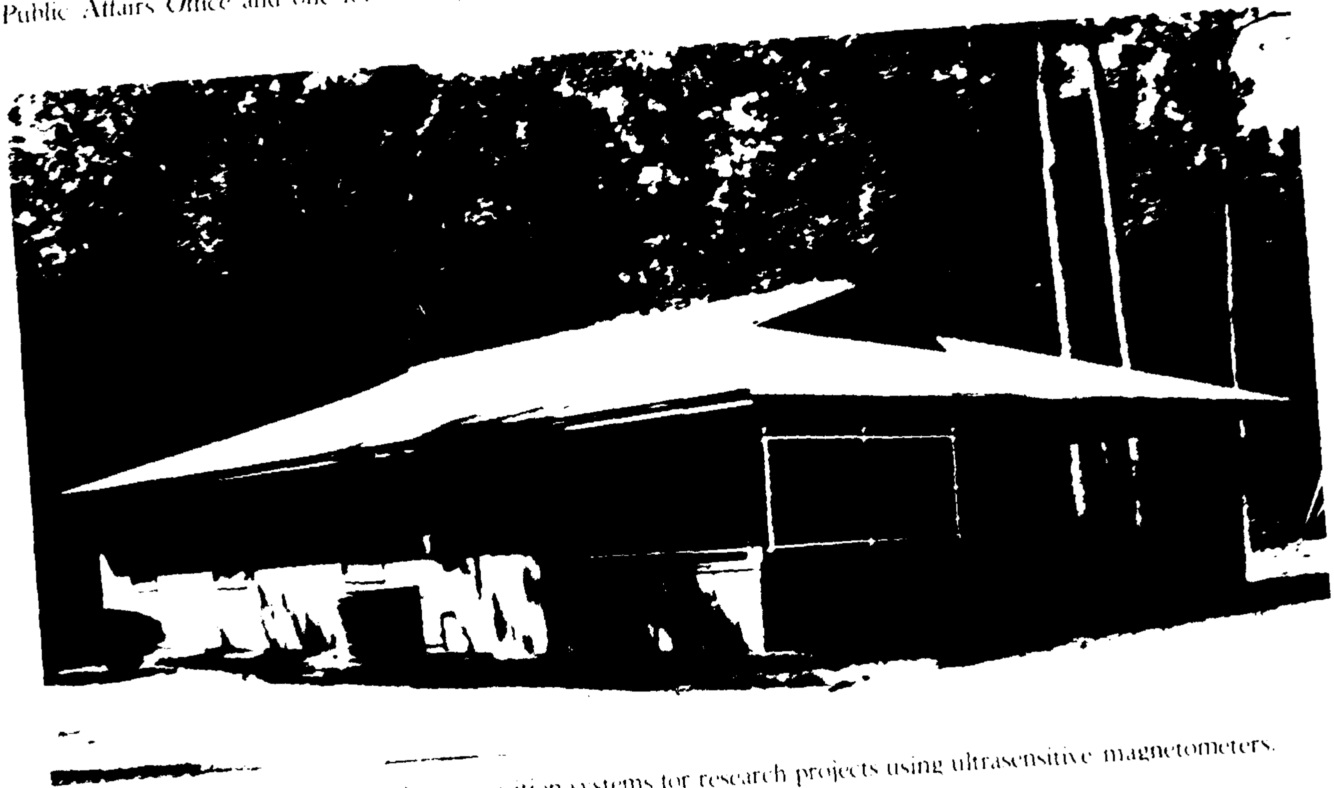

This observatory houses data acquisition systems for research projects using ultrasensitive magnetometers.

NORDA's data collection platforms range from a fleet of dedicated Navy ships and aircraft to a variety of satellites. Occasionally, research vessels belonging to contractors or cooperating academic institutions are used.

The equipment available to NORDA researchers is either developed for a particular purpose or is drawn from the most current technology. Examples of state-of-the-art equipment include a scanning electron microscope, an X-ray diffractometer, several computer facilities, an updated Interactive Digital Satellite Processing System, a Satellite Data Receiving and Processing System, a GEOSAT Oceanographic Applications Program facility, and a wave-making facility. Some of the equipment that has been developed by NORDA scientists and technicians includes a Deep Towed Array Geophysical System and a variety of other fabricated underwater sensors and acoustic arrays, ocean-going towers, various types of software, a portable field microwave radiometer and source (passive radiometer or active radar) for ground use, an Arctic survival kit to protect two people for approximately one week, and a navigation and communications package for use on floating sea-ice camps.

The printed circuit board prototyping facility consists of printed circuit artwork layout, photographic, and etchant equipment for the design and manufacture of single- or double-sided copper foil printed circuit boards. This facility provides NORDA with an in-house capability for rapid implementation and testing of electronic circuits used in specialized research instrumentation systems. In addition, this facility can be used to color-etch aluminum front panels for electronic equipment. This color etching capability permits color coding of operator control panels for clearer understanding of functional meaning.

The secondary standards control room provides a highly controlled temperature and humidity environment for the stabilization of secondary standards for calibration checking of general purpose electronic test equipment. Temperature of the room is maintained within one degree Celsius and five percent relative humidity. The secondary standards within this facility are traceable to the National Bureau of Standards.

The acoustic tower test bed facility consists of two 35-foot tall towers attached to catamaran hulls so that each tower can be towed to an offshore test site and sunk to the sea floor. These towers provide submerged mounting platforms for a wide variety of acoustic projector and receiving arrays. The pointing direction of mounted devices can be independently controlled in roll, pitch, and azimuth so that direct path or indirect path propagation can be investigated. On-board electronic systems provide for control and acquisition of data. The towers can be individually positioned and subsequently controlled by a single surface ship, which makes using the testbed facility more cost attractive.

Remote Work Processing Facility

R. Kent Clark
Mapping, Charting, and Geodesy Division

Introduction

Extracting cartographic and feature information from a variety of source imagery is a continuing requirement for the Defense Mapping Agency (DMA) and the military services. An active area of research is the development of automatic and computer-aided interactive feature extraction techniques. The Remote Work Processing Facility (RWPF) is an integrated hardware-software computer system that serves as a testbed for research into automatic feature extraction.

The RWPF was originally named the Automatic Feature Extraction System. When the system became operational in 1976, it used the most advanced minicomputers and off-the-shelf hardware, including a PDP 11/70 minicomputer and DeAnza IP5500 image processor. Since that time, sensor technology advances dictated a need for large-format imagery that far exceeded the memory limitations of the PDP 11/70. The advent of virtual memory architectures, along with advances in image processing systems, has made extremely large images feasible. The RWPF has been upgraded to incorporate the latest hardware and to allow the use of many more image types and sources.

As part of the upgrading process, DMA has developed a tri-service capability with an RWPF at each of the three service laboratories. NORDA houses the Navy's RWI ¨ Each RWPF contains a compatible set of haruware (Down.. et al., 1984) and software (PAR Upgrade Team, 1985) to make use of common software and communications among researchers much easier.

Discussion

RWPF Hardware

The current NORDA configuration of the RWPF (Fig. 1) consists of a VAX 11/780, an IP8500 image processor, an FPS 5205 array processor, and a Grinnell display system. The VAX 11/785 processor will allow large image input, tessellation, viewing, roaming, interactive image processing, and automatic processing. It also handles the software and project maintenance duties. The Gould IP8500 image processing system handles the image display and manipulation chores, and the Grinnell display system is provided to ensure compatibility with the Defense Advanced Research Projects Agency's image-understanding testbed. An upgrade of the IP8500, additional disk drives, and the symbolics processor are being procured.

The VAX 11/780 superminicomputer has become a standard for scientific computing. Its lower price has made it available to a wide variety of university, government, and private laboratories throughout the country, and its virtual memory architecture and speed make it a useful tool for medium- to heavy-duty computing. The NORDA RWPF VAX has 10 megabytes of physical memory (with up to four gigabytes of virtual memory) and a floating point accelerator. A massbus adapter interfaces the high-density tape drive and two unibus adapters connect the other peripherals.

The Floating Point Systems 5205 array processor provides very high speed computations (up to 12 million floating point operations per second) for compute bound programs. This 38-bit processor interfaces to the VAX via the Unibus. It has 256 kilowords of memory available for use. Because the large image arrays must undergo heavy manipulation, these devices have found a wide acceptance in image processing laboratories.

The Gould DeAnza IP8500 is a state-of-the-art, programmable, image display system that performs such functions as image data capture, image enhancement, and image analysis. The system contains RAM memory to store images, look-up tables for false coloring, and specialized hardware processors. Typical applications include medical imagery, animation software and special effects, and remote sensing. The IP8500 is interfaced with the VAX via Unibus and drives an RGB (red-green-blue) color monitor for image display. Currently, the NORDA IP8500 has 10 megabytes of memory for image storage and is capable of driving a 512 x 512 pixel monitor or 1024 x 1024 pixel high-resolution monitor.

A LISP processor is being procured for the NORDA RWPF. (A Symbolics 3670 has been installed at the DMA

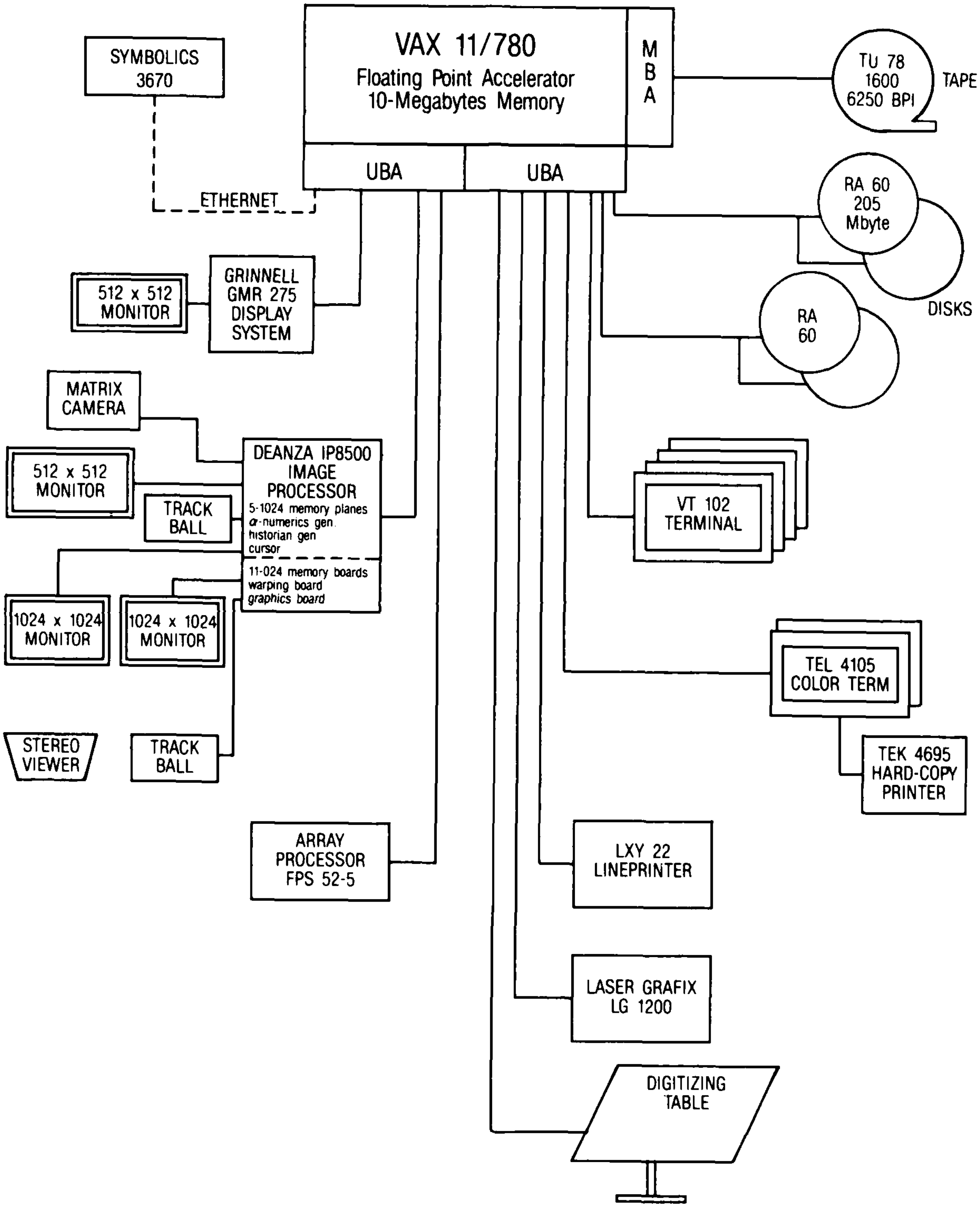

Figure 1. Remote work processing facility configuration.

RWPF.) This machine has been specifically designed to efficiently run programs written in the LISP programming language. It will be interfaced with the VAX via Ethernet. This machine will be used for symbolic manipulation and artificial intelligence image understanding research. This processor will be a valuable tool in the NORDA RWPF.

RWPF software

A large set of integrated software has been developed for the RWPF for feature extraction and general image processing. Many image processing primitives, such as edge detectors, statistical classifiers, filters, and multiband processors, are available and can be linked to perform specific operator-controlled functions. Software is available for image restoration and manipulation, symbolic matching for stereo compilation, symbolic change detection, and stereo cross correlation. An interactive aid for knowledge engineering is available to help construct knowledge bases for expert systems.

The software on the RWPF was designed to support a multiuser environment and, because the RWPF was meant to exist i a research and development arena, be easily modified and modular. Also, the software was signed to be independent of image source so that the RWPF could exploit the various present and future image sources.

The VAX 11/780 runs under the 4.2 Berkeley Software Distribution of UNIX (UNIX 4.2bsd), which is widely used by other image-processing and image understanding laboratories. This is a virtual memory operating system that offers several facilities not available under other UNIX systems.

Job control facilities let the user run jobs in foreground or background and even move running jobs from one state to the other. A history mechanism records previously executed commands, which the user can easily modify and/or reexecute.

Programming languages supported by UNIX 4.2bsd include LISP, C, FORTRAN77, Pascal, and APL. There is a full screen text editor, vi, as well as text formatters, troff and nroff. Finally, the relational data base management system, INGRES, is available to the user community.

One major piece of software in the RW the Symbolic Matching for Automatic Stereo Co ion (SMASC) (Barrett nd Kinn, 1983). The major problem in extracting thre dimensional information from stereo imagery is locating match points in the stereo pairs. SMASC uses probabilistic inferencing to match objects represented symbolically from two stereo images.

A second major piece of software is a program called Automatic Symbolic Change Detection (ASCD) (Kinn et al., 1983). ASCD is a knowledge-based system that compares features of interest in a reference data set with those in a mission data set. Output is the identification of the regions of change. ASCD first finds all features in the reference symbolic data file. This information is used to compile a list of features to look for in the mission image. The mission image is segmented and a mission symbolics data file is formed. Then, for each region in the reference symbolic data file, search areas in the mission image are scanned and a determination of whether or not significant change has occurred is made from a rule base. A change probability is assigned to each grid cell of the mission image.

Summary

The NORDA RWPF, operating in a research and development environment, provides a useful facility for research in automatic feature extraction. The system will be able to support research in various ocean science areas. Furthermore, because NORDA has scientists with expertise in a wide range of ocean science fields, development of feature extraction and image processing techniques will be rapid.

References

Barrett, Scott A. and Gerald J. Kinn (1983). *Symbolic Matching For Automatic Stereo Compilation*. PAR Technology Corporation, New Hartford, New York, Report 83-62.

Downs, A. L., J. H. Huss, E. H. Bohling, and P. M. Lentz (1984). *Hardware Specifications Documents for the RWPF Upgrade*. PAR Technology Corporation Report, New Hartford, New York.

Kinn, Gerald J., Scott A. Barrett, and Eric P. Firman (1983). *Automatic Symbolic Change Detection (ASCD) Final Report*. PAR Technology Corporation, New Hartford, New York, Report 83-143.

PAR Upgrade Team (1985). *Software Specification Reports for the RWPF Upgrade*. PAR Technology Report, New Hartford, New York.

Magnetic Observatory

Kuno Smits and F. Slade Barker
Mapping, Charting, and Geodesy Division

Conducting magnetic measurements of the ambient earth magnetic field with state-of-the-art superconducting quantum interference device (SQUID) gradiometers/magnetometers must be done in a magnetically quiet environment. To provide this ideal environment, NORDA constructed a magnetic observatory at an isolated location at NSTL.

Both the isolated location of the building and its wooden superstructure contribute to the magnetically quiet environment necessary to conduct these magnetic measurements. Additional phenomena, such as telluric potentials and low-frequency seismic vibration measurements, will also be investigated at the observatory site. These measurements are conducted to support Navy mapping, charting, and geodesy requirements, basic research needs, and Fleet requirements.

This research facility can also support airborne electromagnetic bathymetry measurement research. In addition, specialized environmental data are being developed at this facility to support fleet antisubmarine warfare, magnetic anomaly detection, and related sensor and weapons systems.

At present, the largest research effort at the observatory is the study of geomagnetic variability and its associated induced geoelectrical fields. These activities are the single largest noise source that affects naval extremely low-frequency (ELF) sensor systems and weapons support systems, such as the Magnetic Anomaly Detector (MAD).

NORDA is the only Navy laboratory with a dedicated program at the basic research level addressing ELF magnetic signals in and through the ocean environment. In FY83, a research program in geoelectric/geomagnetic variability was initiated to address all ELF magnetic signals in and near the ocean environment. The program includes theoretical studies and a comprehensive and detailed measurement program.

Various parts of the observed magnetic variation must be separated and identified to study ELF magnetic and electric signals in and near the ocean environment. A measurement program has been carefully planned to optimize separating and identifying various source signals. The program requires precision base measurements to be made and compared with various precision remote station measurements, which will consist of both land and sea measurements. The land remote station measurements will include both shore and inland domains; the sea measurements will include both surface and in situ measurements.

Figure 1 is the operational configuration of the total instrument suite at the observatory. Each instrument in the suite is used to help isolate and classify the sources of geomagnetic and geoelectric variability.

The heart of the observatory instrument suite is the Superconducting Quantum Interference Devices (SQUID). It consists of two S.H.E. vectors, SQUID magnetometers, and a Sperry SQUID Gradiometer/Magnetometer System (SGMS). The SQUID vector magnetometer has better vector resolution than the SGMS, but is difficult to set up in a gradiometer configuration with the same resolution as the SGMS. All SQUIDs are susceptible to the phase-lock loss in an intense radio-frequency environment or during heavy thunderstorms. To counter this loss of baseline reference, each SQUID is coupled with a flux-gate instrument. Absolute scalar standards are maintained by cesium and rubidium vapor quantum magnetometers. These two magnetometers are separated by a long baseline; one end is remote to all local traffic, the other is close to the observatory access road. This configuration allows them to act as a long baseline gradiometer for measuring local traffic. The inductions loop antennas, which were obtained from the U.S. Geological Survey (USGS), are as sensitive as the SQUID magnetometer at frequencies above 1 Hz. These instruments are used to measure the noise associated with the air conditioner, water pump, and other such equipment. The telluric current systems allow magneto-telluric sounding of the observatory area, which results in a conductivity profile of the area. Conductivity fluctuations are a measure of the influence of ground water intrusion, which will affect the correlation of the observatory measurements with the remote station measurements.

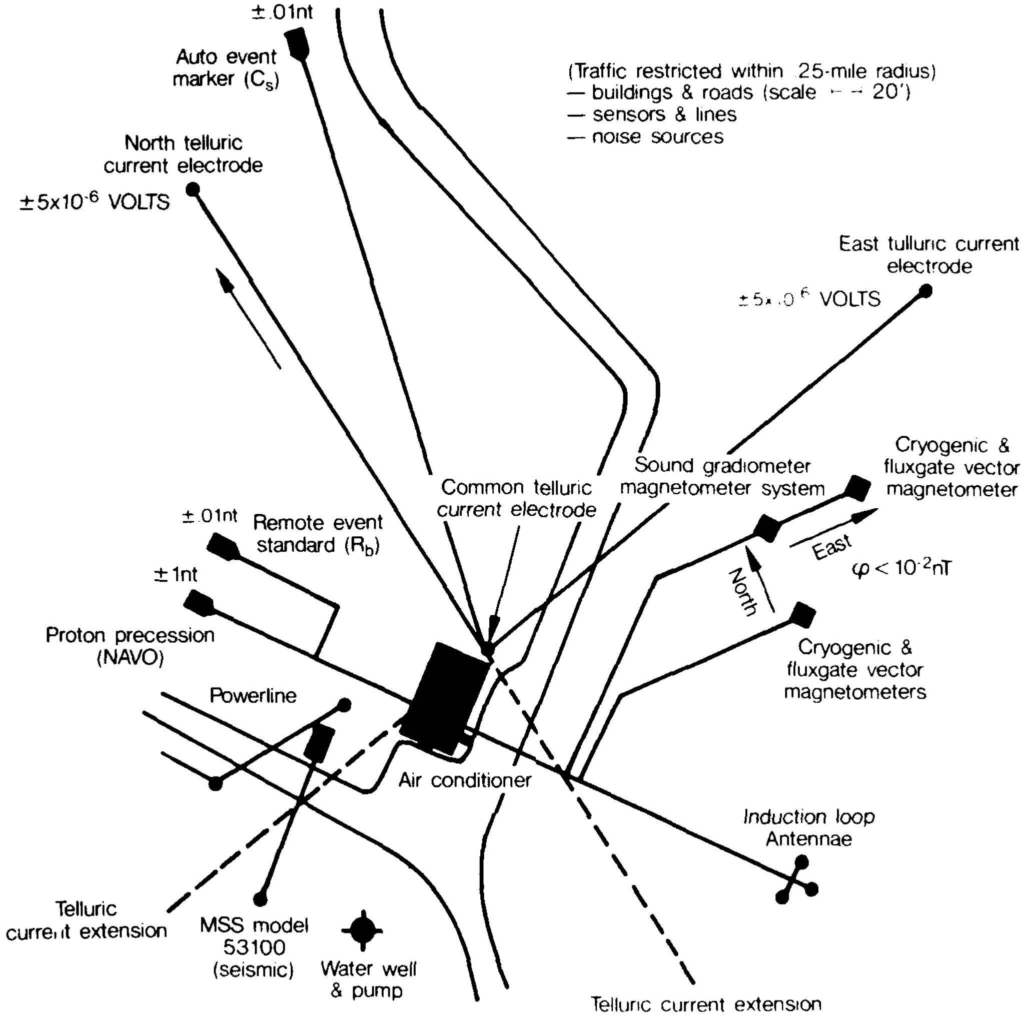

Figure 1. Operational configuration of observatory instruments suite

The observatory instrument suite will be controlled by a single processor system. The remote station suite will consist of a cesium vapor scalar magnetometer, a flux gate vector magnetometer, a telluric current system, and an SGMS. The remote instrument will use variations of this basic scheme, depending upon the location. This suite will also be controlled by a single processor system.

Initial test for local coherence has been performed using the remote processor at the observatory. The test used both scalar and vector magnetometers and a telluric current system. The sensor separation for both the scalar pair and the vector pair of magnetometers was approximately 800 ft. Coherence of the magnetic signal between the two sensors was established to 5×10^{-3} nT below 1 Hz. The 1-Hz limit was imposed by a sampling frequency of 2 Hz. The confinement of the micropulsation signals to the horizontal plane is indicative of a uniform horizontal sheet current flow in the geology. The coherence transform function consisted of a simple identity matrix over the area tested. Again, this is indicative of a deep sedimentary geology and confirms the appropriateness of the site for magnetic observation.

The appropriateness of the site, coupled with the capability of making precise magnetic measurements and storing the data in a digital format, makes the observatory an ideal complement to the USGS observatory network. Data supplied to the National Oceanographic Data Center and used for modeling secular variation will be a subset of the data collected for the geoelectric geomagnetic variability program. These data will aid in constructing both the U.S. variation charts published by the USGS and the world variation charts published by the Naval Oceanographic Office.

Satellite Data Receiving and Processing System

B. Edward Arthur, Jr.
Ocean Sensing and Prediction Division

A basic tool required in using satellite data for ocean research is access to near real-time digital satellite data and the capability to computer manipulate these data. This capability was realized when a Satellite Data Receiving and Processing System (SDRPS) was developed and installed. This system, now in routine operation, can provide oceanographic research programs with real-time digital satellite imagery in the form listed in Table 1. Ninety-day archival of satellite/oceanographic data is being maintained.

Main data sources are the TIROS/National Oceanic and Atmospheric Administration (NOAA) polar-orbiting series of satellites (currently NOAA-6, -8 and -9) and the Defense Meteorological Satellite Program (DMSP) satellites (currently F-6 and -7). These satellites provide high-resolution visible and infrared digital scanner data. Data from the Geostationary Operational Environmental Satellites (GOES-E [East]) and GOES-W [West]) are also collected. These data provide research oceanographers with synoptic views of large Atlantic and Pacific Ocean regions every 30 minutes with their visible and infrared sensors.

Four elements comprise the radio-frequency (RF) portion of SDRPS. The elements are used to acquire GOES-stretched visible infrared spin scan radiometer (VISSR) transmissions, direct readout TIROS high resolution picture transmission (HRPT) real-time data transmissions, recorded global TIROS transmissions, and Station WWV (Colorado) timing information.

Two independent GOES antenna systems are used in SDRPS. One is specifically dedicated to receive GOES-E Mode A stretched VISSR transmissions, and the other is similarly dedicated for GOES-W Mode A stretched VISSR transmissions. At present, only one GOES is operational and data is received from GOES-W (GOES-6) via the GOES-E relay transmission. Each GOES antenna is configured with a 5-m reflector, a limited motion azimuth over elevation mount, prime focus feed (linear dipole and preamplifier), and downconverter. Since only one GOES-stretched VISSR downlink is supported at any one time, a load transfer switch is used to select and provide a down-converted signal from only one of the two antennas. Signals output from the RF switch are amplified by a wide-band amplifier by approximately 30 dB and applied to the input of the PSK (Phase Shift Keying) demodulator. The GOES PSK-encoded signal is then demodulated to produce an NRZ PCM (Nonreturn to zero, Pulse Code Modulation) stream compatible with the front-end signal processing electronics subsystem.

Direct readout TIROS HRPT and Defense Meteorological Satellite Program (DMSP) RTD transmissions are acquired via a Datron Metrak-8 tracking antenna. The antenna was modified with a dual feed to handle both the L- and S-band transmissions. In addition to the tracking mount, an antenna control unit (ACU) facilitates automatic tracking of the polar-orbiting spacecraft from their AOS (acquisition of signal) to LOS (loss of signal) points at or near the horizons. The ACU operates in either an auto-track mode or a programmed track mode. The latter is accomplished via an RS-232C link to the computer system to enable azimuth and elevation commands to be sent to the ACU and, hence, control the antenna tracking in the event of a failure of the auto-track mode. A receiver that contains four crystals is used to select one of the four frequencies broadcast by the two TIROS/ NOAA and two DMSP spacecraft in operation. NRZ PCM signals are then applied to the digital signal processing hardware for signal conditioning and bit/frame synchronization. Since all DMSP RTD transmissions are encrypted, a decryption device is used to decrypt these signals after bit synchronization and before frame synchronization.

Global TIROS AVHRR coverage is provided by means of a receive-only, nonredundant earth station. This earth station is capable of receiving LAC/GAC/HRPT retransmissions played back by either the NESDIS Wallops Island, Virginia, or Gilmore Creek, Alaska, Command and Data Acquisition Stations. The earth station uses a 10-m reflector with a Cassegrain feed assembly to receive nominal 4-GHz C-band downlink transmissions from RCA's SATCOM IIR. Down-conversion to a nominal 52–88 MHz IF is handled by a nonredundant downconverter. The down-converted signals are demodulated and descrambled,

Table 1. NORDA Satellite Data Receiving and Processing System (SDRPS).

Satellite	Sensor	Type Data	Spectral Bands	Spatial Resolution	Repetition Rate	Areal Coverage	Comments
NOAA-6 and NOAA-9	AVHRR (HRPT)	Digital Imagery	0.58 – 0.68 μm 0.725– 1.10 μm 3.55 – 3.93 μm 10.3 –11.3 μm 11.5 –12.5 μm*	1.1 km (Subpoint) 4 km (Edge)	12 hr each satellite	≈ 2900 x 6200 km	Orbiting (806 + 863 km) Direct readout and NOAA CDA Station data relayed via DOMSAT
	(LAC)	Digital Imagery	0.58 – 0.68 μm 0.725– 1.10 μm 3.55 – 3.93 μm 10.3 –11.3 μm 11.5 –12.5 μm*	1.1 km (Subpoint) 4 km (Edge)	12 hr each satellite	≈ 2900 x 5000 km (Selected Global)	Recorded data relayed via DOMSAT
	(GAC)	Digital Imagery	0.58 – 0.68 μm 0.725– 1.10 μm 3.55 – 3.93 μm 10.3 –11.3 μm 11.5 –12.5 μm*	4 km (Subpoint) 16 km (Edge)	12 hr each satellite	≈ 2900 km x Complete orbit (Selected Global)	Recorded data relayed via DOMSAT
	TOVS (HIRS/2) (SSU) (MSU)	Digital Data Digital Data Digital Data	Vis thru CO_2 in IR 15 μm 5.5 μm O_2 Band	17.4–58.5 km 147 km 124 km	12 hr each sat 12 hr each sat 12 hr each sat	2240-km swath width 2240-km swath width 2240-km swath width (Global via DOMSAT)	Direct readout and data relayed via DOMSAT
	DCS	Platform Information	Environmental Measurement (e.g., temperature, pressure, altitude)	NA Location accuracy of platform is 3–5 km	6 hr	Global	ARGOS DCLS by CNES of France Direct readout and data relayed via DOMSAT
DMSP F-6 and F-7	OLS	Digital Imagery	0.5 – 1.1 μm (Day) 0.45– 0.9 μm (night) 10.2 –12.8 μm	"Fine"–0.6 "Smooth"–2.8 km	12 hr each satellite	3050-km swath	Orbiting (835 km) Direct readout (RTD)
	SSM/I	Digital Imagery	19.35 GHz 22.235 GHz 37.0 GHz 85.5 GHz	69 x 41 km 60 x 36 km 35 x 22 km 16 x 10 km	12 hr each satellite	≥1300-km swath width	Future sensor (1986)
GOES EAST and WEST	VAS (Stretched VISSR)	Digital Imagery	0.55– 0.75 μm 10.5 –12.6 μm	0.8 km (Vis) 8.0 km (IR)	30 min	4000 x 4000 km (Vis) Full disc (IR)	GOES-E failed 30 June 84 GOES-W at 108° W

*NOAA-9 only.

the convolutional encoding is removed, and a bit-synchronized TTL level signal is provided to the front-end signal processing hardware. Since only one frame synchronizer exists to handle both the TIROS direct readout HRPT and earth station signals, only one of these two inputs should be active at a time. In addition, the two NESDIS CDA's broadcast the recorded TIROS and AVHRR data on different IF frequency assignments. Although the wideband modem is capable of demodulating/decoding either of the CDA transmissions, by means of two oscillator cards, only one card may be used in the modem at any one time. Hence, in the current system configuration, manual switching is required to receive a particular CDA transmission.

The last RF component is the WWV antenna system. It is used to capture WWV timing signals to accurately time-stamp DMSP RTD data frames and to provide an accurate clock for all SDRPS time-critical computer processing (e.g., scheduled acquisition setup, antenna tracking). A 26-ft fiberglass whip antenna is used to receive the WWV signals. A receiver inputs the selected 5, 10, or 15 MHz WWV signals and provides ticks out at a 1-sec rate to a time code generator/translator, where the time is displayed and subsequently provided as input to the front-end signal processing hardware and computer interface.

The front-end digital signal processing electronics in SDRSPS are comprised of bit and frame synchronizers unique to each satellite input stream. Bit synchronizers are provided with demodulated NRZ PCM data and output serial clock and data signals to the appropriate frame synchronizer. Satellite frame sync pattern identification and serial-to-parallel conversion of the data streams are performed by the frame synchronizer. The parallel data words from each frame are then presented to the SDRPS computer via EMR 732 interface cards.

The GOES-stretched VISSR stream output by the PSK demodulator is presented to two bit synchronizers—one for the infrared data rate (524 Kbps) and the other for the visible data rate (1.747 Mbps). Since the infrared and visible data are interleaved in the stretched VISSR transmission, the two bit synchronizers are never active at the same time. The serial NRZ-L clock and data signals are then applied to the GOES frame synchronizer, which includes a hardware sectorizing unit. The frame synchronizer first performs a correlation of and subsequently removes the pseudo noise (PN) sequence, which precedes the VISSR data and then outputs 16-bit parallel words to the computer interface via direct memory access (DMA) transfers. Automatic identification and extraction of a subset or sector of the incoming data are performed by a single sectorizing unit contained in the frame synchronizer. Sectorizing initialization is under direct software control and specifies the geographic area of interest, data type, and resolution to the unit before acquisition begins. During the real-time acquisition, the sectorizing unit automatically preprocesses the VISSR data. A total of five such sectorizing units may be accommodated by the GOES frame synchronizer.

Demodulated signals from the TIROS HRPT and the DMSP RTD receiver are sent to a bit synchronizer unique to each data stream. Each bit synchronizer operates at a fixed bit rate: 1.024 Mbps for DMSP RTD and 665.4 Kbps for TIROS HRPT. The serial NRZ-L or Bi0-L data and TTL clock signals are then applied to a time frame synchronizer unique to each satellite. The TIROS frame synchronizer is specifically designed for operation only on the HRPT, LAC, and GAC data. Frame sync correlation logic searches and locks on to the 60-bit (six 10-bit words) frame sync pattern and, once lock is achieved, 16-bit parallel data words are output by the frame synchronizer to the computer interface electronics via DMA transfers.

The DMSP frame synchronizer is a generic PCM decommutator that is set up under software control to recognize and decommutate the 150-bit-long frames of RTD data. The serial NRZ-L data and clock signals output by the bit synchronizer are input to the PCM decommutator. A search mode is then entered for pattern correlation of the 13-bit frame sync code. Once found, the unit enters a verify and then lock mode and outputs 16-bit parallel data words to the computer interface via DMA transfers.

As noted previously, bit synchronization for the GAC, LAC, and HRPT transmissions received by the 10-m earth station is handled by the wide-band modem. Serial clock and data streams output from the modem are input to a second port of the TIROS frame synchronizer (i.e., the same frame synchronizer is used for HRPT transmissions received via the 2.4-m tracking antenna, as well as GAC/LAC/HRPT transmissions via the 10-m earth station. This configuration puts a constraint on the use of the frame synchronizer to receive and process data from either the 2.4-m antenna or the 10-m earth station, but never both concurrently.

The computer system supporting SDRPS is a Gould SEL 32/27 that has 2 Mbytes of internal memory, two 675-Mbyte disc drives, a 300-Mbyte disc drive, and a floating point accelerator. As data reception occurs, it is displayed on an I^2S image processing system monitor in real-time, scan line by scan line. Along with the soft copy, a Muirhead K560 hard copy unit, which is a wet process

that gives a good photographic copy, generates within 30 minutes of the receipt of the data, a paper print that is gridded, gamma-corrected and linearized or earth curvature corrected. This formatted data set will then replace the original data image and can be used to determine the quality of the gridding.

Other SDRPS peripherals include a system console, operator terminals, tridensity tape drive, line printer, and a Decwriter terminal, which has a paper printout that is used as a status monitor. During unattended SDRPS operation, the printout provides a history of events that occurred during the course of a night or a weekend. A Hewlett-Packard 8-pen color plotter globally displays the orbiting satellites' paths.

Examples of SDRPS software are unattended operation, antenna positioning and control, formatting setup, data acquisition and extraction, real-time product generation, data management, registration, hard-copy plotter, orbit prediction, calibrations, device control, and archiving. An extensive software array is required to operate a receiving station of this complexity.

This capability enables NORDA to obtain world-wide satellite data coverage to support field experiments, Fleet exercises, and validation of Navy ocean products (sea ice maps, sea surface temperature, etc.). This global capability is critical in resolving many of the Navy's operational and environmental problems that occur in a variety of oceanographic conditions.

The workhorse for this effort is the Interactive Digital Satellite Image Processing System (IDSIPS). This system, established in 1978, consists of an HP-3000 minicomputer interfaced with three I^2S Model 70 image processing terminals. Aside from normal image enhancement software, IDSIPS has additional custom-designed software modules that have been developed for a variety of oceanographic applications, some of which are now available to the Naval Eastern Oceanography Command. These software modules were largely supported by ongoing Navy-funded programs and include routines to produce geometric registration of satellite data to various map projections, multichannel (spectral) sea surface temperatures, atmospheric correction for visible (Coastal Zone Color Scanner—CZCS) satellite data, overlays of geographical and bottom topography contours, warmest pixel compositing for cloud removal, and execution of many image enhancement and interpretation functions. The latter includes contrast enhancement, noise reduction and image sharpening (i.e., edge enhancement), the capability to view consecutive observations of the same area in rapid sequence to study the evolution of oceanographic features, and many other features.

An additional capability that has proven extremely useful has been the transmission of computer-processed imagery to ships at sea. The rapidly changing ocean dynamics of many frontal areas often necessitates daily changes in the oceanographic sampling strategy designed to survey oceanographic features of interest. The utility of having satellite imagery available in the field for real-time planning of oceanographic research readily increases the success and efficiency of an ocean experiment. This was readily apparent during NORDA's Chemical Fronts cruise in the Gulf Stream region in April 1985. Near-real-time processed infrared imagery enabled shipboard scientists to select optimum cruise tracks tailored to their needs to cross well-defined ocean fronts.

NORDA Scientists in the Field

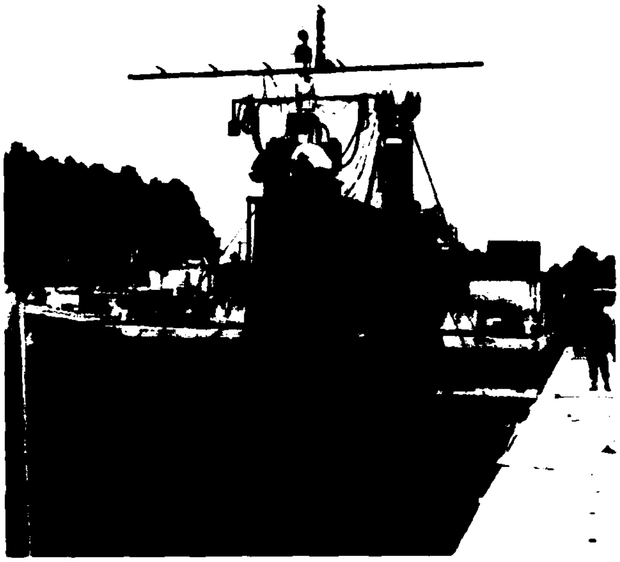

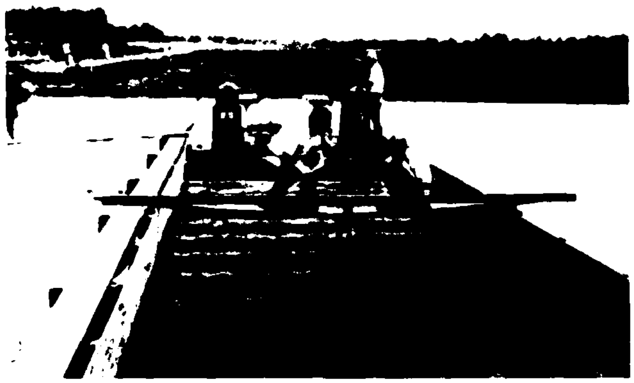

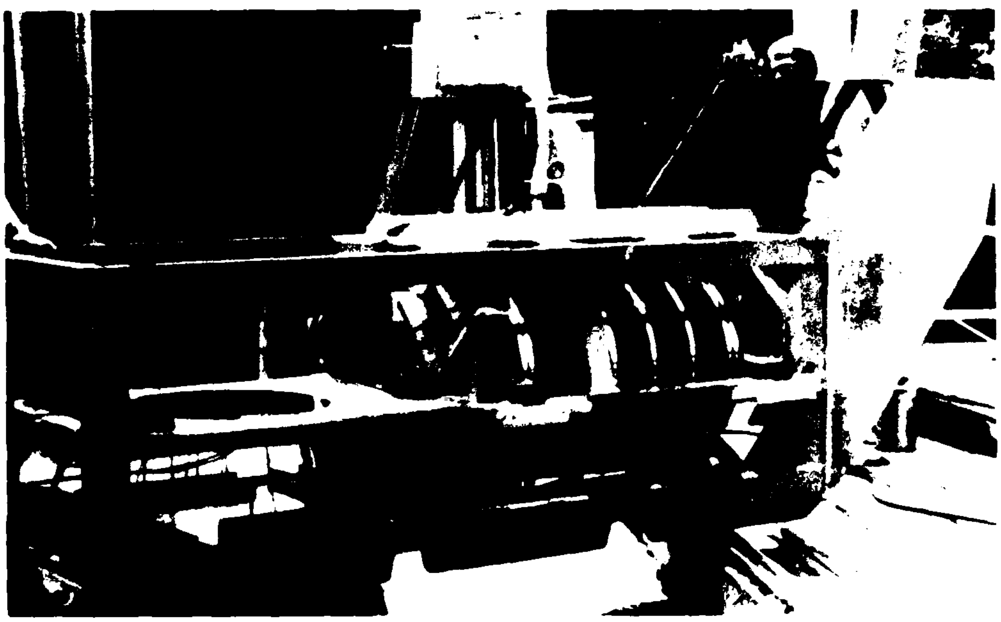

Low-Frequency Noise Fields

William M. Carey and Ronald A. Wagstaff
Office of the Technical Director

Abstract

Very-low-frequency (2 to 20 Hz) and low-frequency (20 to 200 Hz) physical noise models and measurements show long-term, persistent directional characteristics associated with distant shipping lanes and density patterns. Short-term averages show a temporally dynamic field composed of resolved distant shipping and uncorrelated background noise. These results emphasize the importance of the coherent contribution from coastal shipping to the mid-ocean noise field. Vertical directionality measurements by Anderson et al. (1972) show a broad, angular distribution of noise intensity near the horizontal at low frequencies and a peaked distribution about the horizontal at high frequencies. This broad, angular distribution near the horizontal is consistent with sound propagating downslope by means of a bottom reflectivity that favors lower frequencies. The frequency variation near the horizontal was found to be smooth and indicates that, in addition to surface ships, environmental noise influences the vertical directionality.

Introduction

Since the classic paper of Wenz (1962), ambient noise has been an extensively studied phenomenon. Morris (1975) emphasized the importance of enhanced signals as ships cross over seamounts or proceed over the continental slopes. Wagstaff (1981) showed, by comparing measurements and calculations, that coastal shipping (ships over the continental slope and on the shelf near the slope) must be considered so that the horizontal directionality is described correctly. He showed that these coastal sources would also affect the vertical directionality. This paper reinforces these findings with new results from downslope transmission loss (TL) and noise directionality experiments.

Discussion

Signal sound transmission characteristics

Officer (1958) showed that downslope propagation resulted from the conversion of high angle rays (with respect to the horizontal) to lower angle rays by twice the slope angle. The effect was observed by Northrop et al. (1968) with peak pressure amplitudes from shallow explosions over the continental slope. The estimated downslope enhancements averaged 6 dB and ranged as high as 12 dB, and were coined the "megaphone effect" by Smith (1971). Morris (1975) found that the narrowband pressure levels on a vertical array in the upper part of the Pacific sound channel showed a downslope enhancement from the radiated signal of a supertanker to be between 7 and 12 dB from a seamount and 4 and 6 dB from the continental slope. In the Northwest Atlantic, Laplante (1981) and Koenigs et al. (1981), using charges, demonstrated that seamounts and other topographic features that rise into the sound channel significantly affect sofar propagation. The downslope enhancement (DSE) was observed to be most pronounced for near-surface sources (18 m) at frequencies between 25 and 100 Hz, ranging up to 20 dB and averaging 7.5 dB. These results agree with observations in the northeast Pacific (R. L. Martin, NORDA personal communication). The results in this article are comparable and are attributed to the conversion of high-angle energy to low-angle energy by twice the slope angle, with the added frequency-dependent influence of bottom reflectivity.

A downslope to deep ocean sound channel experiment (with an 18-m, 135-Hz source) was conducted in the Northwest Atlantic Ocean (Carey, 1983). The transmission path was from the continental slope off the Sable Island

Bank, through the Gulf Stream, to the edge of the Sargasso Sea. The results agreed with the treatment of downslope propagation converting high-angle energy to low-angle energy, coupled with the effect of the frequency-dependent bottom loss versus grazing angle. Lindrop (1977) defined a slope enhancement by the limiting source angle ($\theta_0 \sim 8^0$) for deep water and the limiting source angle over the slope (θ). The limiting source angle (θ) may be determined by the limiting grazing angle at the bottom and by Snell's law. For a water depth of 1 km, slope angle of 6^0, grazing angles of $11-20^0$, and source angles of $15-25^0$, the DSE = 10 log ($\sin\theta/\sin\theta_0$) = 2.7 to 4.8 dB, which is close to the 4 dB observed. Since the bottom loss increases and the limiting grazing angle decreases with frequency, DSE would not be expected at frequencies greater than 400 Hz.

A similar downslope to bottom-limited region experiment was performed with a towed source driven at 67 Hz and 173 Hz from the Florida Plain toward the West Florida Escarpment (Carey et al., 1985). The DSE at 67 Hz was as high as 6 dB, and most points were between 2 and 4 dB. The 173-Hz data showed a peak DSE of 6 dB with a dramatic increase in transmission loss as the source proceeded up the slope.These low-frequency experimental results show the signal retains a degree of coherence in the downslope propagation.

Beam noise surfaces

Beam noise measurements were obtained using seismic streamers with high density digital recorders (HDDR) and were processed with fast Fourier transform (FFT) techniques on standard minicomputers and array processors. Figure 1 shows results of one such study in a deep basin with shipping lanes. The array was towed near one side of the basin to reduce ambiguity effects. Three coincident beam noise surfaces (beam noise intensity (dB) versus time (Δt = 8 sec) and azimuth ($\Delta\theta \sim 2.5^0$)) are shown for center frequencies of 53, 165, and 320 Hz with equivalent apertures in 0.125-Hz, Hann-shaded frequency bands. Tow-ship noise is observed between 0 and 30^0 while distant ships are shown (light tracks) superimposed on a lower noise level background (environmental noise, unresolved ships, and system noise).

The beam noise surfaces for 165 and 320 Hz show a comparable number of ship tracks. However, the 53-Hz noise surface shows fewer tracks and several with weak intensity levels despite the better transmission loss characteristics at this frequency. Beam-to-beam correlation functions indicate that the individual tracks on 165 and 320 Hz are surface ships within the main beam coverage areas rather than from side-lobe response. A strong signal, which appears on the beam main lobe and also appears on another beam due to the side-lobe response, will produce a cross-correlation function with multiple peaks. The correlation functions did not exhibit this characteristic, which indicates a side-lobe level response better than − 28 dB. Since the system responses are comparable and the transmission loss characteristic shows less loss at 53 Hz, then the fewer tracks observed on this beam noise surface may be due to a characteristic of the surface-

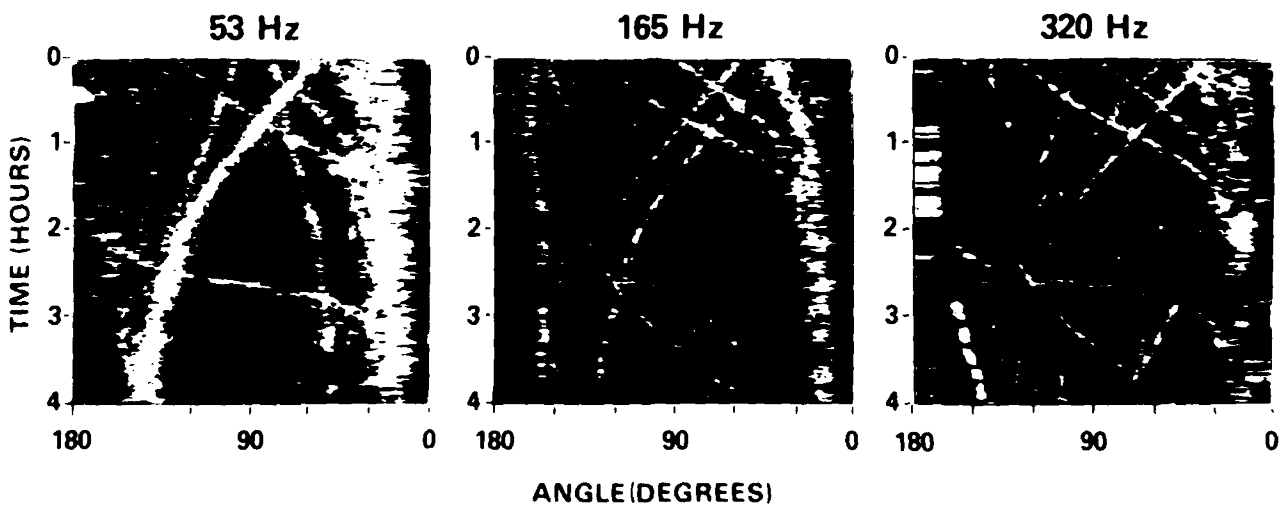

Figure 1. Beam noise intensity versus time and azimuthal angle.

ship-radiated noise spectrum. The lower frequency portion of the spectrum is tonal, whereas the higher frequency portion of the spectrum is a continuum. Consequently, we only observe ships that have energy in the narrow measurement band.

Ambient noise horizontal directionality

Beam noise measurements were performed in the downslope to deep ocean basin and downslope to bottom-limited basin experiments. These noise measurements were used to estimate the noise horizontal directionality with the iterative technique of Wagstaff (1978).

The estimate of the noise horizontal directionality for the Gulf of Mexico (Fig. 2) shows high levels in the northern quadrant and low levels in the southern half-space. The differences between high and low levels range from 10 dB at 150 Hz to 25 dB at 50 Hz with pooled standard deviations of 1.6 and 2.5 dB, respectively. The reasons for the high degree of spatial anisotropy are evident when the acoustic propagation characteristics of the basin surrounding the measurement location and the spectral distribution of noise sources are considered.

Similar results of ambient noise directionality measurements for the Northwest Atlantic Basin are shown as Figure 3. The directional effect (minimum to maximum level deviation) is shown to be about 15 dB at 50 Hz and 7.6 dB at 150 Hz. The directional characteristics of the noise field appear to be similar for the two frequencies. The measurements took place at a location such that the 90° to 180° quadrant was toward the Corner Seamounts in the Mid-Atlantic Ridge, while the northerly sector encompassed the region off Newfoundland. The high noise directions are from approximately 270° clockwise to 90°; a sector including the Grand Banks, the Scotian Shelf, and a major trans-Atlantic shipping lane. Thus, the observed noise directionality is attributable to the combined effect of mid-basin shipping in trans-Atlantic lanes, as well as to ships traversing the continental rise, banks, and shelf.

The directionality plots shown here are consistent with the time-averaged beam response of the bearing time surfaces. Hamson and Wagstaff (1983) have shown that these noise horizontal directionality patterns can be calculated, provided the shipping distribution is known, the transmission loss is calculable, and the ships on the basin margins are included.

Ambient noise vertical directionality

Since high-angle energy from deep ocean noise sources is rapidly attenuated due to multiple bottom interactions, one would expect the energy propagated from these sources

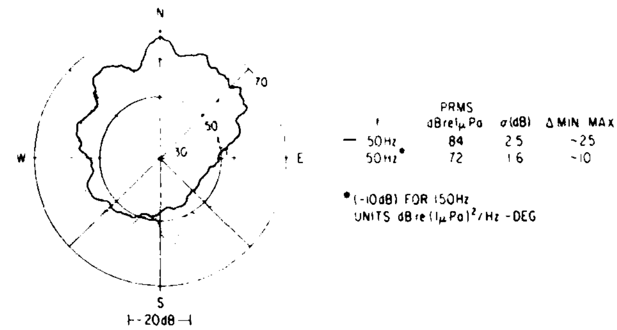

Figure 2. Horizontal noise directionality, Gulf of Mexico.

to be peaked at the sofar channel ray limiting angles (10° to 15° off the horizontal). However, measurements of the vertical distribution of noise intensity in the low-frequency band show a broad angular distribution centered about the horizontal direction. Consequently, the broad distribution of energy about the horizontal requires a mechanism as the downslope conversion process. Figure 4 represents a remarkable set of data collected by Anderson et al. (1972), which illustrates these effects. Here the maximum likelihood method (Edelblute et al., 1966) was used to produce the vertical noise level distribution as a function of vertical angle (90° is the horizontal direction) and frequency. These data were obtained south of Bermuda with a vertical array of 26 elements spanning a distance of 110 m and centered at a depth of 236 m in the deep sound channel with an axis depth of 1 km. Figure 4 shows the vertical arrival structure of the noise as a function of frequency with a resolution of 1.4 Hz. At 150 Hz the noise intensity has maxima at 90° ± 9.5° compared to 90° ± 14° if the array center had been located at the sound channel axis. The Mimi sound source is observed near 400 Hz

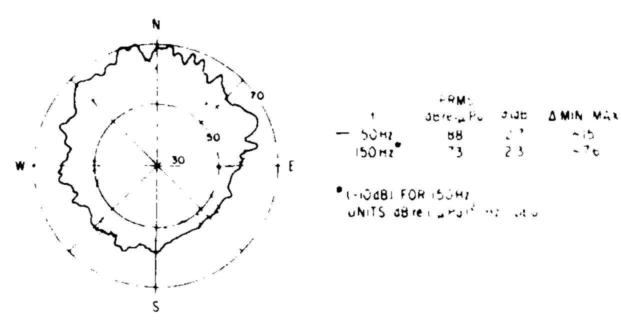

Figure 3. Horizontal noise directionality, NW Atlantic.

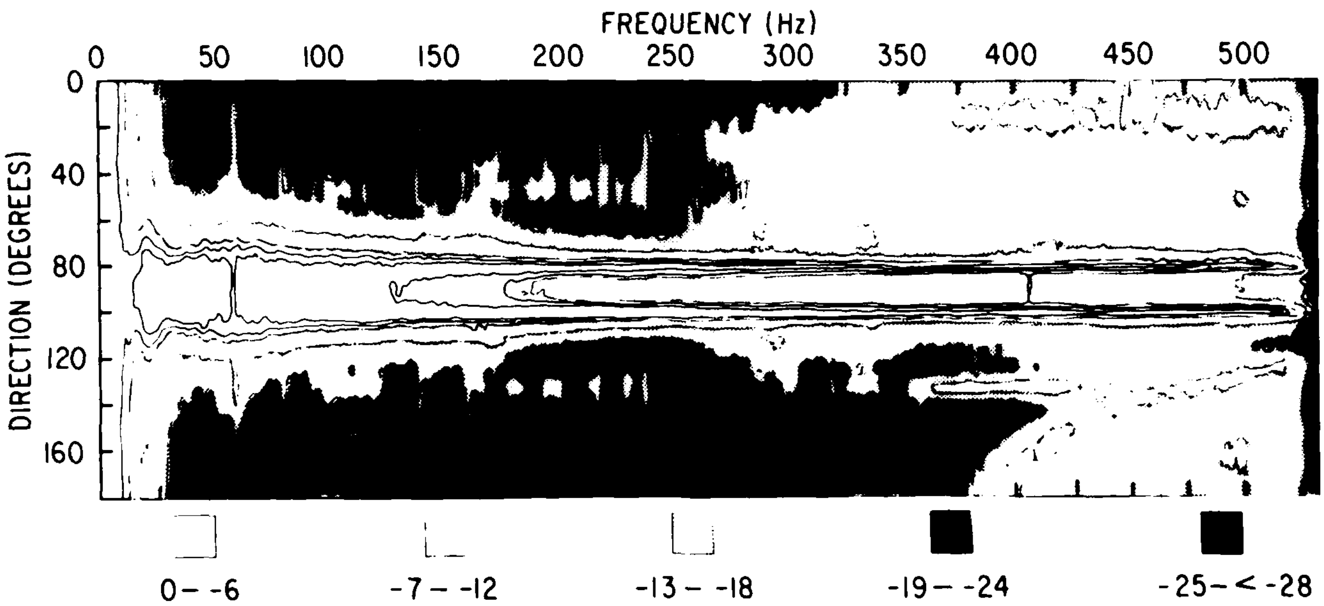

Figure 4. Noise intensity versus vertical arrival direction and frequency

At frequencies greater than 400 Hz, the data show aliasing (180° to 130°) and the peaked distribution of noise intensity at 90° ± 9.5° with a noise minima at 90° of − 10 dB. In comparison, the distribution at 100 Hz shows a broad maximum centered on the horizontal. Anderson (1979) simulated the pattern at the higher frequencies, but was not able to do so at the lower frequencies. He showed that the broad maximum was not due to deficiencies in the measurement technique and analysis. These characteristics persisted for several days, that is, the vertical distribution of energy was broad at the lower frequencies and sharply dual peaked at the higher frequencies, indicating that the horizontal component of noise originates at a distance from the receiver. The smooth noise level variation between 20 and 150 Hz is a significant characteristic of the noise. If the horizontal noise is from distant slope-interacted, ship radiated signatures, why the smooth variation?

These results are consistent with previous and subsequent investigations. Fox (1964) obtained data from a 40-element array near Bermuda in 4.4 km of water. He found that at low sea states, the vertical distribution of noise intensity was broadly peaked near the horizontal over the band of 200 to 1500 Hz. At high sea states he observed an isotropic distribution at higher frequencies (> 200 Hz) but a persistent horizontal component (~ 200 Hz). Measurements by Axelrod et al. (1965) showed a strong low frequency horizontal component and observed that the frequency at which the vertical directionality became isotropic depended on the local wind speed. Anderson (1979) reported noise vertical directionality in a region of the Northeast Pacific Ocean over the 23- to 104-Hz band. He also observed a broad angular distribution of noise near the horizontal. A horizontally stratified, range independent ocean model does not predict a broad angular distribution of noise intensity about the horizontal but, rather, a dual peaked noise intensity distribution (± 10° to ± 15°) and no noise at the horizontal.

Noise generated from surface sources cannot arrive within the limiting angles bracketing this minimum, which is referred to as a horizontal noise notch. Wagstaff (1981) showed, by agreement between calculations and data, that distant shipping over the continental shelf, slope, or a seamount contributes to the broad vertical distribution of low-frequency noise near the horizontal. Data obtained between Cape Hatteras and Bermuda were analyzed in the 45- to 100-Hz band by Wales and Diachok (1981). These data were found to have a broad vertical distribution near the horizontal. Their corresponding noise level versus frequency and arrival angle plot shows a smooth variation in frequency similar to that of the Anderson data. The fact that these data do not show a tonal characteristic is important, as ship radiated noise spectra have been shown to be primarily tonal in this band. Browning et al. (1981) show data obtained in the South Fiji Basin, a region of sparse shipping. Below 200 Hz, he observed a level 4 dB less than Wagstaff, with a broad maximum in the vertical distribution of noise intensity centered at the horizontal

Browning found these results consistent with both surface ship noise and storm noise originating near the basin boundaries coupling to the sound channel. If these results were solely due to ships interacting with slopes and seamounts, one might expect a reflection of the tonal quality of the low-frequency ship signature in the measured noise spectra when the number of ships are small. Since this is not the case, one can draw the inference that another contribution to the noise field at the horizontal is important, such as the noise due to wind and surface waves over continental slopes and seamounts. Furthermore, Burgess and Kewley (1983) found similar results in Australasian waters.

Conclusions

This article has presented measurements showing that surface ship noise coupled into the sound channel produces marked effects on the directional noise field at the lower frequencies. The data presented show that this interaction is similar to a low-frequency pass filter. The expected level of DSE, based on the downslope conversion process for representative bottom loss, yields in 1 km of water DSE = 4.8 at 50 Hz, 2.1 at 200 Hz, and 0.5 at 400 Hz. The lower frequency sound transmission was observed to be more persistent with a fair degree of coherence. Coherent signals from surface ships, readily observed in the beam noise surface plots, were shown to be a dominant characteristic of the ambient noise. The frequency dependence of the beam-noise surfaces is consistent with expectations based on narrowband ship signatures. Calculations and inference suggest that surface ships dominate the low-frequency ambient noise horizontal directionality. The nature of the received signal from distant ships in space and in time provides for a coherent gain over the incoherent environmental noise background. The fact that downslope propagation of sound retains a fair degree of coherence reinforces the idea that the coastal shipping dominates the mid-basin ambient noise horizontal directionality.

Ambient noise vertical directionality data exhibit a low pass filtered effect due to downslope conversion at the basin boundaries, i.e., a broad angular distribution centered about the horizontal at low frequencies and a dual peaked distribution in energy at the higher frequencies. A mechanism for introducing energy into the sound channel is the downslope conversion process. Dashen and Munk (1984) have shown that scattering by internal waves cannot account for this phenomenon; however, Mellen (1985) contends that diffusion is a candidate. Measurements and calculations by Wagstaff demonstrate that coastal shipping could easily account for this effect.

A characteristic of the vertical directionality data was the smooth variation in frequency from 20 Hz to 200 Hz. Since surface ship spectra are tonal in the low-frequency region, expectations are that a spikey nature would be observed, provided the measurement system has the resolution. Furthermore, measurements obtained in remote, sparsely shipped areas, although at lower levels, yield similar findings as the vertical directionality from densely populated basins. Since any sound source such as wind driven noise (capillary to capillary wave interaction, wave turbulence, splashes, impacts and aggregate bubble oscillations) near the surface over the slope, shelf, or seamounts will introduce sound into the sound channel, then environmental noise, in addition to shipping, may be required to explain the broad angular and frequency characteristics.

Acknowledgments

The authors acknowledge D. Edelblute for his permission to use the vertical directionality data.

References

Anderson, C. G., D. A. Anderson, D. J. Edelblute, et al. (1972). *VLAM Data Analysis Site #1*, Bermuda. Naval Ocean Systems Center, San Diego, California, TN 800.

Anderson, V. C. (1979). Variation of the Vertical Directionality of Noise with Depth in the North Pacific. *Journal of the Acoustical Society of America* 66(5), 1446-1452.

Axelrod, E. H., B. A. Schoomer, and W. A. Von Winkle (1965). Vertical Directionality of Ambient Noise in the Deep Ocean at a Site Near Bermuda. *Journal of the Acoustical Society of America* 37(1), 77-83.

Browning, D. G., N. Yen, R. W. Bannister, R. N. Denham, and K. M. Guthrie (1981). Vertical Directionality of Low Frequency Ambient Noise in the South Figi Basin. *Journal of the Acoustical Society of America* 70(1), S66(A).

Burgess, A. S. and D. J. Kewley (1983). Wind-Generated Surface Noise Source Levels in Deep Water East of Australia. *Journal of the Acoustical Society of America* 73(1), 201-210.

Carey, W. M. (1983). Sound Propagation from a Coastal Source to a Deep Ocean Receiver. *Journal of the Acoustical Society of America* 73(S1), S55(AA6).

Carey, W. M., I. Gereben, B. A. Brunson, and M. R. Bradley (1985). Measurement of Sound Propagation, Down

Slope to a Bottom-limited Sound Channel. *Journal of the Acoustical Society of America* 77(1), S14(F7).

Dashen, R. and W. Munk (1984). Three Models of Global Ocean Noise. *Journal of the Acoustical Society of America* 76(2), 540-554.

Edelblute, D. J., J. M. Fisk, and G. L. Kinnison (1966). Criteria for Optimum-Signal-Detection Theory for Arrays. *Journal of the Acoustical Society of America* 41(1), 199-205.

Fox, G. R. (1964). Ambient Noise Directivity Measurements. *Journal of the Acoustical Society of America* 36(8), 1537-1540.

Hamson, M. R. and R. A. Wagstaff (1983). *An Ambient-Noise Model That Includes Coherent Hydrophone Summation for Sonar System Performance in Shallow Water.* SACLANTCEN ASW Research Centre, La Spezia, Italy, Rept. SR-70.

Koenigs, P. D., R. F. LaPlante, D. G. Browning, and R. L. Martin (1981). Long Range Sound Propagation Across the Mid-Atlantic Ridge. *Journal of the Acoustical Society of America* 69(S1), 559(A).

LaPlante, R. F. et al. (1981). *Journal of the Acoustical Society of America* 69 (S1), 559(A).

Lindrop, P. H. (1977). Comments at the *International Workshop on Low Frequency Propagation and Noise.* Woods Hole Oceanographic Institution, Woods Hole, Massachusetts.

Mellen, R. H., 1985. Attenuation at Infrasonic Frequencies in the Deep Sound Channel.

Morris, G. B. (1975). *Preliminary Results on Seamount and Continental Slope Reflection and Enhancement of Shipping Noise.* Scripps Institution of Oceanography, La Jolla, California, SIO Ref. 75-34.

Northrop, J., N. Loughridge, and E. W. Werner (1968). Effect of Near-Source Bottom Conditions on Long Range Sound Propagation in the Ocean. *Journal of Geophysical Research* 73(12), 3905-3908.

Officer, C. B. (1958). *Introduction to the Theory of Sound Transmission.* McGraw-Hill, New York, p. 159.

Smith, P. W. (1971). Sound Transmission in Isogradient Water Over a Plane Sloping Bottom. *Journal of the Acoustical Society of America* 49, 96.

Wagstaff, R. A. (1978). Interactive Techniques for Ambient Noise Horizontal-Directionality Estimation from Towed Line-Array Data. *Journal of the Acoustical Society of America* 63(3), 863-869.

Wagstaff, R. A. (1981). Low Frequency Ambient Noise in the Deep Sound Channel—The Missing Component. *Journal of the Acoustical Society of America* 69(4), 1009-1014.

Wales, S. C. and O. I. Diachok (1981). Ambient Noise Vertical Directionality in the Northwest Atlantic. *Journal of the Acoustical Society of America* 70(2), 577-582.

Wenz, G. M. (1962). Acoustic Ambient Noise in the Ocean: Spectra Sources. *Journal of the Acoustical Society of America* 34, 1936-1956.

Implementation of Rough Surface Loss in Sonar Performance Models

Anthony I. Eller
Office of the Technical Director

Abstract

The past few decades have seen notable advances in the development of widely applicable, robust submodels for the mathematically tractable aspects of ocean acoustic propagation. In contrast, many of the empirically oriented, less tractable aspects of propagation have received less than their due attention, and their inclusion in sonar performance models compromises the accuracy that might have been achieved by the more advanced propagation algorithms. One leading problem area that has not been adequately developed, which in some cases is the weak link in sonar modeling, is the scattering of acoustic energy at the rough sea surface. This article reviews the prevailing inconsistencies associated with how surface scattering has been implemented in current sonar performance models. Some of the measures in progress to achieve consistency within the ocean engineering community are described.

Introduction

Sonar performance models are used to relate how system performance, as measured by received signal-to-noise ratio, is determined jointly by system hardware and processing parameters (such as equipment location, size, and integration time) and by environmental acoustic parameters (such as propagation loss, noise, and reverberation on a path-by-path basis). Extensive R&D effort has been devoted to constructing propagation loss models, and the past two decades have seen notable advances in the development and implementation of widely applicable, robust models for the mathematically tractable aspects of acoustic propagation. At the same time, however, less tractable, and usually empirical, aspects of propagation modeling have received little attention. Their inclusion in sonar models, along with the highly developed aspects of propagation, tends to compromise the overall accuracy of the model and introduces substantial uncertainty into the predictions.

One particular problem area that has not been adequately developed, which in some cases is the weak link in sonar performance modeling, is the scattering of acoustic energy at the rough sea surface. Models currently used for surface reflection loss, as implemented in sonar performance models, often give vastly conflicting predictions, which in turn lead to correspondingly severe discrepancies in predicted propagation loss. The occurrence of such discrepancies is sometimes a more disrupting problem than the actual surface loss. Furthermore, side effects of large modeling discrepancies are that the entire modeling effort loses credibility and, more importantly, users of model predictions are left with unresolved, contradictory guidance.

Discussion

Review of scattering loss inconsistencies

A review of currently used surface loss models has revealed several inconsistencies.

Beckmann-Spizzichino Model—The so-called Beckmann-Spizzichino (B-S) model is a hybrid consisting of

- an angle independent term based jointly on the Marsh (1961) and Marsh et al. (1961) theory of surface duct losses for the limiting ray and on corresponding surface duct data (Marsh, 1963),
- a purely analytic term based on the theory by Beckmann and Spizzichino (1963).

Naming the entire hybrid model "Beckmann-Spizzichino" is considered by many to be a misnomer.

Two versions of the B-S surface loss model presently exist: version I is given in the NUSC Generic Sonar Model (Weinburg, 1981), and version II exists in current versions of the NISSM II model. (Current versions of NISSM II differ from the original NISSM II documentation (Weinburg, 1973) in various ways; one difference is surface loss. The two versions differ by an algebraic sign and by the presence of a term (sin θ)/θ. Reasons for the differences are not known and could be simply an unedited clerical error. The two versions also differ in the selection of which wind speed/wave height relation is built in. The point to note, however, is that the effect of the differences is by no means trivial, and their presence indicates the general confusion and disarray connected with surface loss.

Figure 1 displays predicted surface loss per bounce according to the two B-S model versions. Differences between the predictions are as large as the loss itself.

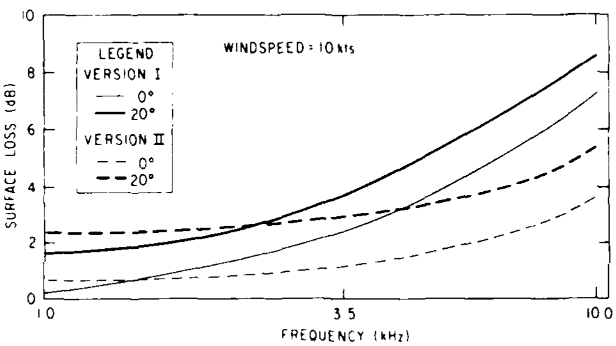

Figure 1. Comparison of surface loss predictions by two versions of the Beckmann-Spizzichino model at grazing angles of 0° and 20°.

Intermodel Comparisons—Comparisons of losses according to four different surface loss models show similar inconsistencies. Figures 2–4 compare predictions of surface loss as a function of significant wave height, grazing angle, and frequency.

The Eckart model (1953) gives surface loss as

$$surface\ loss\ =\ 20\ log\ exp(2g) \tag{1}$$

where

$$g\ =\ (2\pi\, f\, \sigma\, sin\ \theta/c)^2\ . \tag{2}$$

f is frequency, c is sound speed, θ is grazing angle at surface, and σ is rms displacement of surface about the mean. This model is based upon the Kirchhoff approximation, a small surface slope assumption, and a Gaussian distribution of surface vertical displacements. The modified Eckart model represents a mathematical improvement that allows the original Eckart result to be extended. The modified Eckart model is given by

$$surface\ loss\ =\ -20\ log\ [I_o(2g)\ exp(-2g)]\ , \tag{3}$$

where I_o is the zero-order modified Bessel function. The figures show that these two models differ significantly for large values of roughness g.

The Schulkin-Marsh model, called AMOS in Weinburg (1981), is used for example in the LORA performance model Hoffman (1976), where it is given by

$$surface\ loss\ = \begin{cases} 10\ log\ [1\ +\ (fh/4.14)^4],\ fh < 4.2691 \\ 1.59\ (fh)^{1/2},\ fh > 4.2691. \end{cases} \tag{4}$$

where f is frequency in kilohertz and h is average crest-to-trough wave height in feet. The Schulkin-Marsh model is based on measurements of surface duct propagation loss. To convert the measured surface-related losses to a measure of loss per bounce, all losses are assumed to be attributed to propagation of the limiting ray, which is used to define the skip distance between bounces. Consequently, angle dependence does not exist in this model.

The fourth surface loss model used in the comparisons is the B-S model as given in the Generic Sonar Model (Weinberg, 1981).

In Figures 2–4 the two Eckart results group together, as do the Schulkin-Marsh and B-S results, although some differences are indicated.

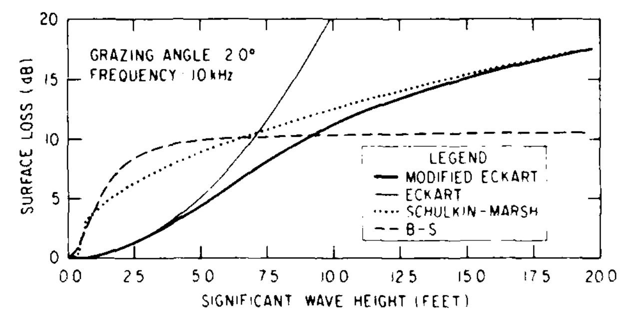

Figure 2. Comparisons of surface loss predictions.

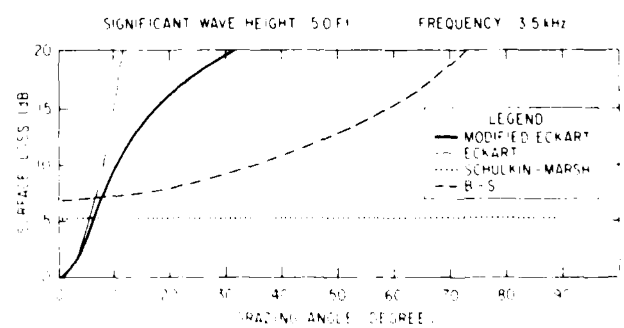

Figure 3. Comparisons of surface loss predictions.

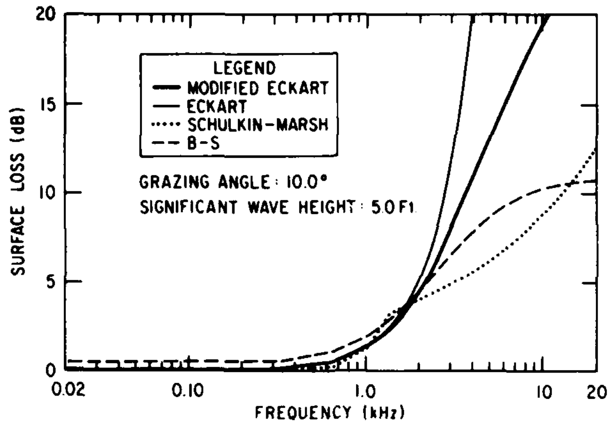

Figure 4. Comparisons of surface loss predictions.

Windspeed-waveheight relations—A further contributor to the confusion surrounding surface loss is an inconsistent use of various wave height measures. For example, when surface loss models are implemented in current sonar performance models, they sometimes are recast to accept wind speed as the environmental input in place of wave height, and several wind speed/wave height relations are available for this purpose. Two examples are

$$H = 2.0 \times 10^{-2} w^2 , \tag{5}$$

attributed to Vine and Volkmann with H in feet and wind speed w in knots, and the corresponding Pierson-Moskowitz (1964) relation

$$H = 1.86 \times 10^{-2} w^2 . \tag{6}$$

Here, H designates the significant wave height, which is generally related to average wave height by (Longuet-Higgins, 1952; Pierson et al., 1955)

$$H = 1.60\ h \tag{7}$$

and to rms wave displacement by

$$H = 4.02\ \sigma . \tag{8}$$

Some performance models (for example, NISSM II) have used the Neumann-Pierson relation

$$h = 0.0026\ w^{2.5} , \tag{9}$$

where h here represents the average wave height, rather than significant wave height H.

In some cases, further inconsistency has resulted in some cases from an incorrect confusion of average and significant wave heights, wherein H and h are interchanged without distinguishing between them.

Why such extensive inconsistency regarding surface loss was able to develop and persist is not clear. Extensive research has been conducted in the basic problem of plane wave interaction with a rough surface. It appears that equal effort has not yet been devoted to the applied problem of implementing scattering theories into full propagation and performance models.

Approach to problem resolution

Recognizing the seriousness of the inconsistent predictive models for surface loss, the ASW Environmental Acoustic Support (AEAS) program in environmental acoustics at NORDA sponsored the formation of a working committee, whose function was to identify and evaluate available surface loss models and to select, at least in an interim sense, a standard for use in sonar performance models. The decision was to be made on the basis of present knowledge, in spite of widespread uncertainties and the temptation to wait until work already in progress was completed.

The committee made the following surface loss recommendations.

- Models that use the AMOS equations for transmission loss of the ducted paths should continue to do so.
- Models that need a "surface-loss-per-bounce" algorithm should use the Modified Eckart (M-E) model.
- The value of 11 dB should be established as an upper limit, even if the M-E algorithm predicts a loss greater than this amount.
- Wind speed is the preferred input parameter and is to be converted internally within the model to wave height by using the Pierson-Moskowitz relation.

The working committee also recognized that a serious deficiency of all of the models is the failure to include nonspecular reflections as a part of propagation modeling. Surface loss indicates only the decrease of the specular component. The nonspecular portion of the scattered field is generally a diffuse, incoherent field that customarily is neglected through the argument that it decreases with distance from the surface more rapidly than the specular component.

Following release of the committee report (Eller, 1984), the most serious criticism was connected with surface duct losses. Experienced sonar performance analysts felt that the Modified Eckart model underestimated losses at low grazing angles and gave overly optimistic predictions of surface duct transmission. A benefit of this response is that it has stimulated an intensive reexamination of surface duct losses, primarily by members of the acoustics community at NORDA and the Naval Underwater Systems Center.

To assess the consistency of surface duct predictions, several calculations of propagation loss were made by using various combinations of propagation and surface loss algorithms. The environment was a surface duct in deep water with a layer depth of 375 ft, a constant gradient of 0.0187 sec^{-1}, and a windspeed of 15 knots.

Propagation loss was computed by means of

- the RAYMODE model with the B-S and the M-E surface loss models;
- the FACT model, also with the B-S and M-E surface loss models;
- the multipath expansion model (MPE) with the B-S surface loss model;
- the AMOS surface duct propagation model with the Schulkin-Marsh surface loss, using the AMOS model as presented in NISSM II (Weinburg, 1973).

Each of these six approaches is one that might be selected and used by a knowledgeable sonar design engineer.

The spread of results is shown in Figure 5. Results based on the M-E surface loss are grouped together and show the least loss. The MPE results were run because this model was expected to represent ground truth, including leakage effects. Its predictions lie in the middle. The AMOS predictions, with other results based on the B-S model, lie together and show the greatest loss. The AMOS results are regarded as nearly equivalent to field data. The comparisons support the belief that the M-E surface loss model underestimates loss at the small grazing angles characteristic of ducted propagation. Failure of the Eckart-based approach at small angles is explained by Brekhovskikh and Lysanov (1982), who use the method of small perturbations to derive the Eckart result for large grazing angles and the relation

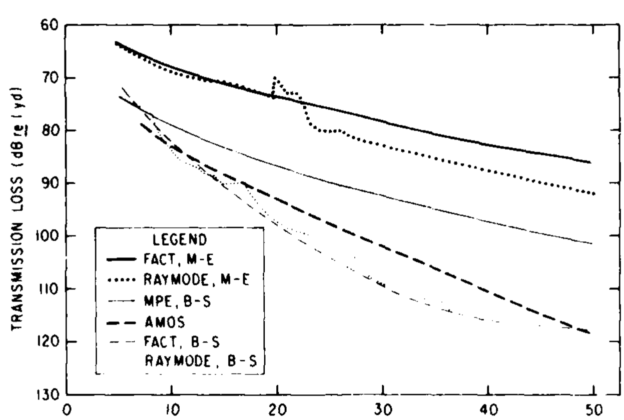

Figure 5. Comparison of propagation loss predictions with various surface loss models.

$$BL\ surface\ loss = -20\ log\ (1 - A f^{3/2} w^4 \sin \theta) \quad (10)$$

at small grazing angle θ, where A represents a constant. Noteworthy here are the dependences on frequency to the $^3/_2$ power and on windspeed to the fourth power. This result is similar to the result

$$MSK\ surface\ loss = -10\ log\ (1 - A\ f^{3/2} h^{8/5} \sin\theta) \quad (11)$$

by Marsh et al. (1961). An unresolved aspect is that Equations 10 and 11 do not agree. These results are compared in Figure 6, which shows also the Eckart predictions. Equations 6, 7 and 8 are used to relate wave height h and rms displacement σ to wind speed.

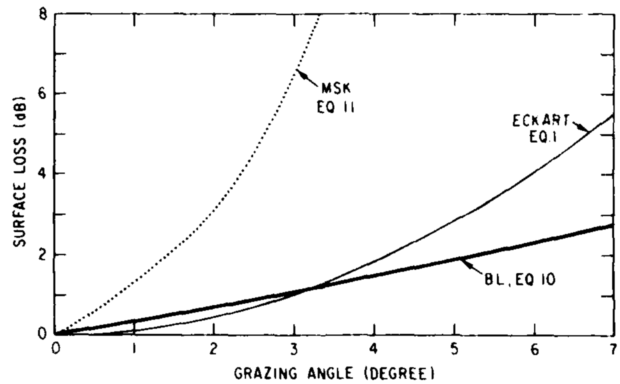

Figure 6. Comparison of surface loss predictions at low grazing angles for a windspeed of 15 knots and a frequency of 3500 Hz.

Summary

In summary, the points addressed here are that

- severe discrepancies exist among presently used surface loss models;
- these discrepancies can lead to equally severe inconsistencies in propagation loss predictions, especially for surface ducts;
- as an interim measure a modified form of the Eckart model was recommended;
- a new look at the theory indicates that the recommended surface loss model underestimates losses at small grazing angles;
- the Marsh et al. (1961) model may resolve the small angle problem, but present inconsistencies with the BL theory need to be resolved first.

References

Beckmann, P. and A. Spizzichino (1963). *The Scattering of Electromagnetic Waves from Rough Surfaces.* Pergamon Press, New York.

Brekhovskikh, L. and Yu. Lysanov (1982). *Fundamentals of Ocean Acoustics.* Springer-Verlag, New York.

Eckart, C. (1953). Scattering of Sound from the Sea Surface. *Journal of the Acoustical Society of America* 25, 566–570.

Eller, A. I. (1984). *Findings and Recommendations of the Surface Loss Model Working Group: Final Report.* Naval Ocean Research and Development Activity, Technical Note 279.

Hoffman, D. W. (1976). *LORA, A Model for Predicting the Performance of Long-Range Active Sonar Systems.* Naval Undersea Center, San Diego, California, TP 541, December.

Longuet-Higgins, M. S. (1952). On the Statistical Distribution of the Heights of Sea Waves. *Journal of Marine Research* 11, 245.

Marsh, H. W. (1961). Exact Solution of Wave Scattering by Irregular Surfaces. *Journal of the Acoustical Society of America* 33, 330–333.

Marsh, H. W. (1963). Sound Reflection and Scattering from the Sea Surface. *Journal of the Acoustical Society of America* 35, 240–244.

Marsh, H. W., M. Schulkin, and S. G. Kneale (1961). Scattering of Underwater Sound by the Sea Surface. *Journal of the Acoustical Society of America* 33, 334–340.

Pierson, Jr., W. J. and L. Moskowitz (1964). A Proposed Spectral Form for Fully Developed Wind Seas Based on the Similarity Theory of S. A. Kitaigorodskii. *Journal of Geophysical Research* 69, 5181.

Pierson, Jr., W. J., G. Neumann, and R. W. James (1955). *Practical Methods for Observing and Forecasting Ocean Waves by Means of Wave Spectra and Statistics.* U.S. Naval Oceanographic Office (Washington, D.C.), NSTL, Mississippi, H.O. Pub. No. 603.

Weinberg, H. (1973). *Navy Interim Surface Ship Model (NISSM II) II.* Naval Underwater Systems Center, Newport, Rhode Island, TR 4527, NUC TP 372, November.

Weinberg, H. (1981). *Generic Sonar Model.* Naval Underwater Systems Center, New London, Connecticut, TD 5971C, December.

Ocean Acoustics and Technology Directorate

W. B. Moseley
Director

The Ocean Acoustics and Technology Directorate was established two years ago to focus a major portion of NORDA's research, development, testing and evaluation resources on improving our understanding of environmental acoustics, on the formulation and use of computerized acoustic models, and on ocean technology and engineering to improve Navy systems and performance.

The articles presented in this portion of the *NORDA Review* trace the development of several major research efforts in these areas. Some of these efforts have already provided specific benefits to the operational Fleet and to the general advancement of ocean science. These include the development of Kevlar technology for acoustic arrays, of an Arctic acoustic capability, and of a sector scan sonar application for mapping, charting, and geodesy; the design and development of a Deep-Towed Array Geophysical System; and the development of coupled mode and nonlinear acoustic models. In a separate portion of the *Review*, you will see a more complete listing of these accomplishments.

Organizationally, our directorate comprises three divisions: Numerical Modeling, Ocean Acoustics, and Ocean Technology. The research work of our people is presently concentrated in the areas of Arctic acoustics, very-low-frequency and high-frequency acoustics, nonlinear acoustic propagation, array technology, acoustic model computer implementation, mine countermeasures, and several allied efforts.

The emphasis of the directorate in the foreseeable future will be to develop the environmental acoustic technology and support necessary to counter the current and future foreign submarine warfare threat, which is becoming dramatically more sophisticated and dangerous. This emphasis, therefore, will be directed toward environmental acoustics support to the Navy's weapons acquisition process, weapons systems effectiveness, and both passive and active tactical and surveillance systems.

Research and Development of Acoustic Models at NORDA

Stanley A. Chin-Bing, Kenneth E. Gilbert, Richard B. Evans,
Michael F. Werby, and Gerard J. Tango
Numerical Modeling Division

Abstract

NORDA has addressed a variety of underwater acoustic studies of Navy interest during its 10 years of existence. These studies fall into three main categories: ocean bottom reflectivity, ocean propagation (both range independent and range dependent), and free-space scattering. Results of these investigations provide the foundation for the study of the more general problem of sound propagation and scattering in an inhomogeneous ocean waveguide. Some of the major thrusts are propagation over rough and sloping ocean bottoms, scattering from rough ocean surfaces, diffractive and resonant scattering from high-aspect-ratio targets, and scattering from targets in a shallow-water waveguide. The research in these areas includes design and support of experiment, as well as fundamental, theoretical studies.

Introduction

The primary purpose of NORDA's efforts is to conduct basic research and exploratory development on underwater acoustic models of interest to the Navy. Theoretical acoustics and modeling support of other researchers within NORDA and of other Navy laboratories is also a major effort.

In the 10 years that NORDA has been in operation, studies in ocean bottom reflectivity, ocean propagation (both range independent and range dependent), free-space scattering and scattering in a waveguide have been conducted. The results of studies performed in each of these categories has helped to build a strong foundation for the present and future research efforts at NORDA.

Discussion

Ocean bottom reflectivity

For many years underwater acoustic propagation was studied only for deep-water scenarios. Recently, many experiments in shallow-water propagation have taken place. In shallow-water propagation, the interaction of sound with the sea floor is a very important mechanism. NORDA scientists have studied acoustic bottom interactions so that a better understanding of the physics could be gained. Mode theory reflection coefficients for the bottom, comparison of mode and ray theory for completely absorbing bottoms and periodically stratified ocean bottoms were some of the early studies performed.

The effect of the lateral wave on bottom-loss measurements was a major study. The Sommerfeld model (isospeed half-space water column over isospeed half-space bottom) was examined to determine the effects of the lateral wave on bottom loss measurements. Results of the study showed the following:

- The "measured" reflection coefficient is geometry dependent. This dependence was found to be true, not only for the Sommerfeld model, but also for a more complex model, viz., an isospeed half-space overlying a geophysical bottom.
- Interference effects occur for incident angles greater than the critical angle where the lateral wave is present and a monotone transition to the Rayleigh reflection coefficient occurs for incident angles less than the critical angle. In addition, this interference region (saddle point greater than the critical angle) shows negative bottom loss—another effect due to the experimental geometry and observed in experiments—which has been associated with bottom-generated caustics. These interference effects are shown in Figure 1, where a comparison is made between

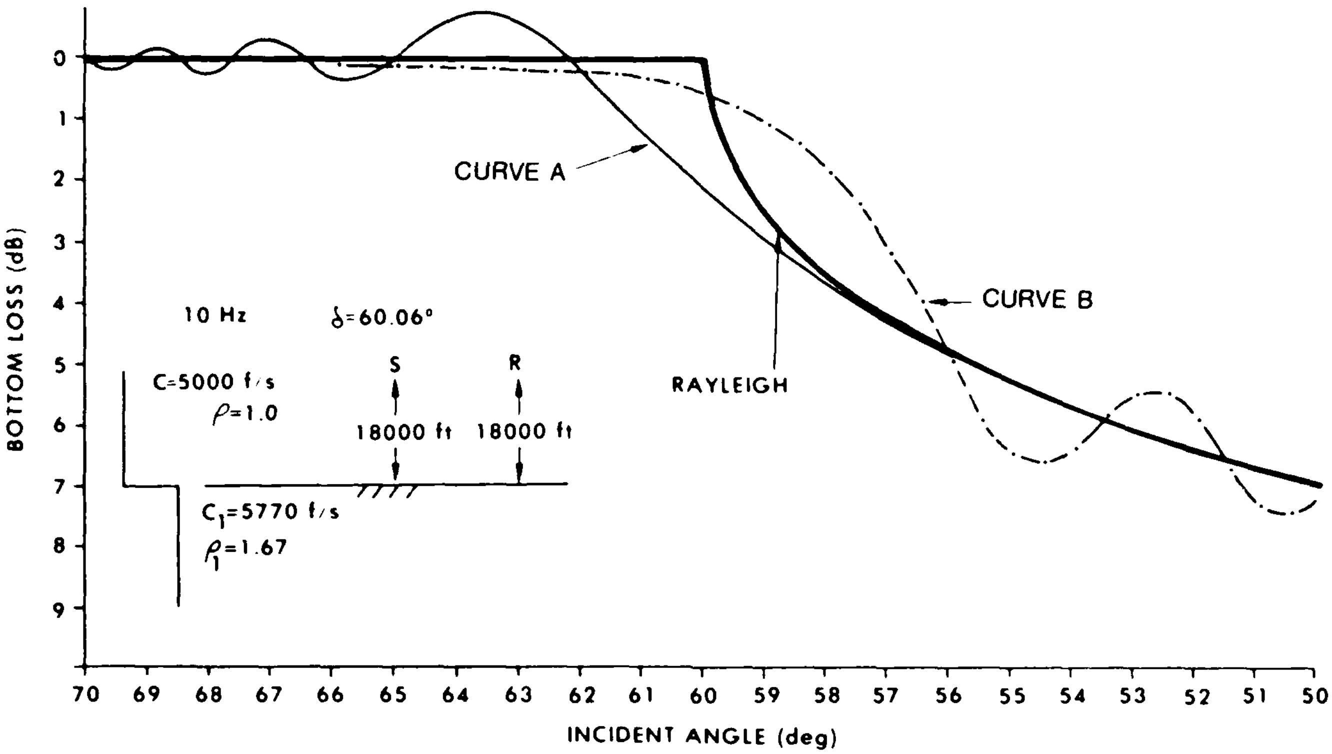

Figure 1. The bottom loss versus the inferred bottom loss, using the seismic technique, for the Sommerfield model.

the Rayleigh reflection coefficient and Curve A, which resulted from this study.

- This study identified the origins of the differences and resolved the discrepancies between results from published studies by Stickler and the well-known text by Brekhovskikh (as shown by Curve B in Fig. 1, which was obtained from Brekhovskikh and Stickler's works).

Ocean propagation

Range independent propagation—The study of range-independent propagation problems is especially valuable to understanding underwater acoustic propagation. Range-independent problems can be solved exactly and thus constitute a standard by which range-dependent solutions can be evaluated when applied to range-independent cases. Normal mode solutions and the Fast Field Program (FFP) are two exact solutions that have been utilized quite extensively by NORDA. A fully complex mode program has been developed and used to study bottom attenuation and target localization. The SAFARI FFP computer algorithm, originally developed at the SACLANT Research Centre (SACLANTCEN) for exact underwater propagation modeling of continuous wave signals, has been extended to a more general applications computer code that now includes broadband pulse and seismogram synthesis. This work was accomplished through a joint NORDA-SACLANT effort.

In deriving a correction to the perturbative treatment of bottom attenuation for shallow-water, low-frequency conditions, comparisons have been made between a perturbative and a total treatment of bottom attenuation in a normal mode expansion for a representative shallow-water, low-frequency problem. The exact treatment introduced bottom attenuation through complex sound speeds and, thus, complex depth functions, whereas the perturbative approach used real sound speed to obtain real depth functions and then introduced mode attenuation only in the range function. Transmission loss calculations resulting from the two approaches could disagree significantly near the cutoff frequency when only a few modes were present. When more than a few modes were present, the other modes dominated the mode nearest cutoff; although this nearest mode was in error, it did not seriously affect the results. For the cases where the perturbative and exact solutions differed significantly, the error in the perturbative approach was mostly due to an incorrect normalizing factor, with mode attenuation differences accounting for a much lesser part of the error. A correction term to the mode normalization factor was derived for the case of an isospeed half-space with attenuation. This correction term

improved the results from the perturbative solution both in phase and in magnitude. The correction term had the added advantage of being composed of terms easily obtainable from the perturbative solution. The results were extendable to any layered bottom with attenuation, which terminated in an isospeed half-space. In Figure 2, line (a) is the exact result, (b) is the perturbative result, and (c) is obtained from applying the correction factor to the perturbative result.

Target depth classification by modal decomposition and correlation has also been studied. Various methods were used to classify and localize submarine targets using real-time information from acoustic sensors. A study was made using another technique, which utilized the environment and its variability to exclude (theoretically) all possible target depths except the correct one. The method involved synthesizing the normal modes using the best available sound speed profile and geoacoustic model as inputs to a complex normal mode model. Both single frequency and broadband fields could be modeled. These synthesized modes were sampled in depth (or range) to form a suite of replicas. The synthesized replicas were then correlated with the modally deconvolved incoming data having the same spatial sampling as the replicas. The ambiguity surface showed relatively high correlation for replicas having the target's true depth.

The SAFARI FFP model mentioned above has been used to study towed array response to ship noise for approximate inverse modeling and to simulate and perform geoacoustic pulse studies of very low frequency bottom interaction.

Range-dependent propagation—Range-dependent acoustic propagation problems are generally not amenable to exact solutions. However, the importance of obtaining very good approximate solutions cannot be understated, since the vast majority of propagation problems in underwater acoustics is range dependent. NORDA has made major contributions to solutions of range-dependent propagation problems. The parabolic equation (PE) model provides a good approximation to the solution of range-dependent problems. The accuracy of the PE model has been significantly improved by the addition of wide-angle capability. Wide-angle PE has been used in cases where other models could not be used. As a result of the NORDA-sponsored PE workshop, it became clear that a need for a benchmark solution was needed to evaluate range-dependent solutions in underwater acoustics.

NORDA has responded to the need for a range-dependent benchmark by developing a fully coupled normal mode model. The coupled mode model contains the effects of both forward and backscatter and all the cross coupling between waterborne and bottom-interacting modes. The coupled mode model has been used to show when the PE approximation is valid and when it fails. The coupled mode model has been extended to be useful on its own. The coupled mode method has been used to study scattering due to bottom roughness and the simultaneous effect of mode coupling and refraction. The latter development has the capability of accurately modeling realistic basin-shelf propagation.

A third new range-dependent model currently under study by NORDA is range-dependent FFP. This model, like the PE model, is a one-way solution to the wave equation. However, unlike the PE model, FFP is an exact solution. Thus, the range-dependent FFP model can serve as a check on the computationally faster PE model.

Free-space scattering

Various numerical techniques and their use in the extension of T-matrix and null-field approaches to scattering have

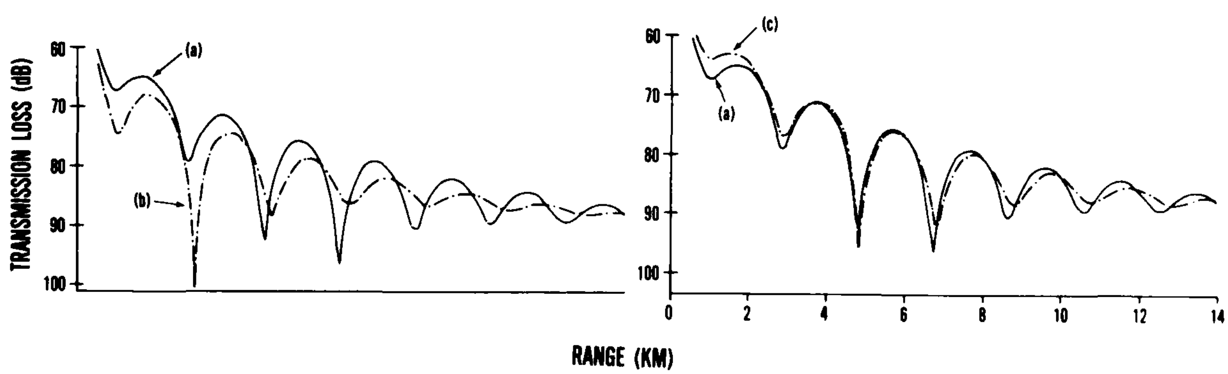

Figure 2. A comparison of transmission loss as a function of range for low-frequency shallow water conditions.

been extensively investigated at NORDA. A number of numerical and theoretical techniques have been developed that extend the range of applicability of these methods beyond the conventional approach.

Scattering from submerged objects consisting of separable boundaries, such as spheres and infinite cylinders, is amenable to closed-formed solution by normal mode theory. Results from extensive investigations of these objects have been extremely fruitful in understanding resonance phenomena, background contributions in the absence of resonances, and geometrical effects that give rise to diffraction phenomena. However, when one wishes to examine arbitrary shapes, it is necessary to resort either to approximate theories (valid under limiting assumptions) or numerical methods that adequately treat the problem in question. It has, in fact, proven very difficult to describe scattering from general objects without resorting to frequency-limiting approximations. In this research effort a numerical procedure was developed—namely, the extended boundary condition (EBC) method, together with its applications for treating a variety of problems. The method was established by Waterman for electromagnetic scattering in 1965, and was extended to acoustical scattering by him in 1969. It is sometimes referred to as the null-field method in electromagnetism, the field equivalent principle, or more generally as the T-matrix method. This last nomenclature is unfortunate, since any of a variety of methods can lead to a transition matrix relating the scattered to the incident field, while the EBC or null-field terminology more properly reflects the fact that one is employing a boundary integral technique.

Some of the salutary features of this approach are that the method yields unique solutions to the exterior problem; the transition matrix is independent of the incident field; the method is not frequency-limited, although it is more efficient for intermediate frequencies; the method can work for a large variety of shapes.

To represent the final results in terms of matrices, one expands all appropriate physical quantities in terms of partial wave basis states and includes expansions for the incident and scattered fields and the surface quantities (i.e., surface displacement, surface tension, etc.). The method then utilizes the Huygen-Poincare integral representation for both the exterior and interior solutions, leading to the required matrix equations. One thus deals with matrix equations, the complexity of which depends on the nature of the problem. We have shown, however, that in general a transition matrix T can be obtained relating the incident field A with the scattered field f having the form $T = PQ$, where $f = TA$. The structure of Q can be quite complicated and can itself be composed of other matrix inversions such as arise from layered objects. We have developed improvements in this method appropriate for a variety of physical problems, and on their implementation. We have conducted research for scattering from very elongated submerged objects and resonance scattering from elastic solids and shells. Significant structural improvements have been made, such as the coupled higher-order method and the unitary method, which lead to more tractable forms of the transition matrix enabling one to avoid matrix inversions and other numerical problems. The final improvement concerns eigenfunction expansions of surface terms, arising from solution of the interior problem, obtained via a preconditioning technique. This effectively reduces the problem to that of obtaining eigenvalues of a Hermitian operator.

This formalism has been developed for scattering from targets that are rigid, sound-soft, acoustic, elastic solids, elastic shells, and elastic layered objects. We present two sets of the more interesting results. The first concerns scattering from elongated objects, the second to thin elastic spheroids.

Figure 3 illustrates scattering from a spheroid with aspect ratio 30 for a $KL/2$ value of 30. Here K is the incident wavenumber and L the object length. We show the case of scattering along the axis of symmetry and 30° and 60° relative to the axis of symmetry and broadside. Elongation effects at 30° and 60° are particularly noticeable where the reflected wave occurs at the same angle as the incident wave relative to the symmetry axis, similar to the plane scattering case. At 0° and 90° the flux is allowed to proceed mainly in the forward direction, with broadside scattering creating the greatest disturbance.

Figure 4a shows resonance phenomena from backscattering from a very thin aluminum spheroid, plotted against $KL/2$. Scattering here occurs along the axis of symmetry for a spheroid of aspect ratio 3. Because of the thin nature the object, its scattering response is like that of a sound-soft object in the absence of resonance. This response is verified by subtracting the sound-soft background from the exact elastic calculation, leaving only the resonance response (Fig. 4b). Figure 4c is a plot of relative phase for the elastic and sound-soft calculations. Note that the phase is almost zero except at a resonance, where it undergoes a rapid phase-change of 180°, typical of this type of resonance.

Another study involving scattering in a free-space environment is the Arctic high-frequency acoustic ice-keel model study. This model stochastically describes the three-dimensional backscattered field (by means of target

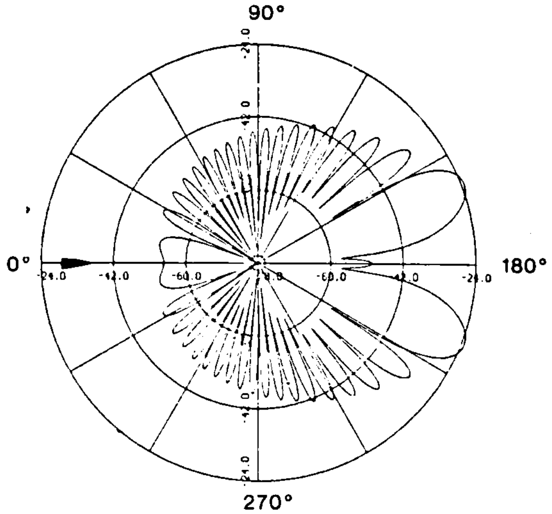

Figure 3a. Scattering along axis of symmetry of spheroid.

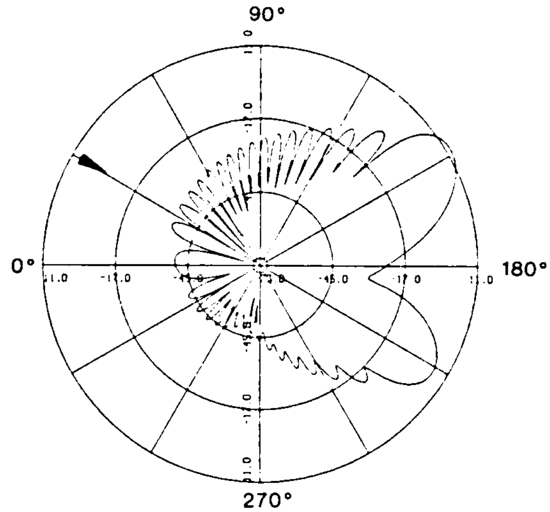

Figure 3b. Scattering at 30° relative to the axis of symmetry of spheroid.

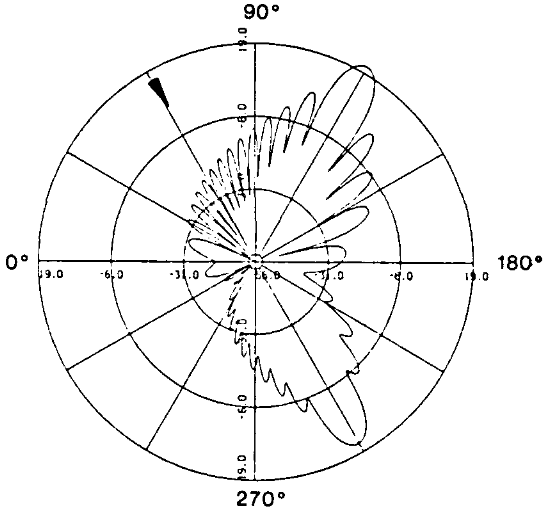

Figure 3c. Scattering at 60° relative to the axis of symmetry of spheroid.

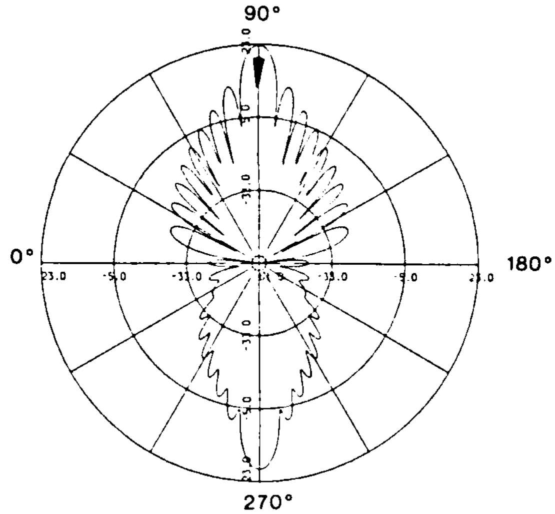

Figure 3d. Broadside scattering from a spheroid.

strength) that results from an ice keel. This model was improved by including different possible facet rotation schemes and by incorporating realistic physical representations of the ice in the model.

Scattering in a waveguide

The field due to a constant sound source together with the inherent noise, can be monitored very precisely for certain underwater regions. If an object intrudes within the region, the field is perturbed; therefore, the intruding object can be detected and located. This "burglar alarm" concept is currently under investigation. Expertise gained in bottom reflectivity, ocean propagation, and free-space scattering is being applied to this problem. Plans are underway for the development of an engineering type model that will assist in experiment design. This project will be followed by an exact calculation of an object in a half-space.

Future directions

NORDA will continue to contribute to the technical base in theoretical acoustics and numerical techniques as applied to modeling underwater sound, to support

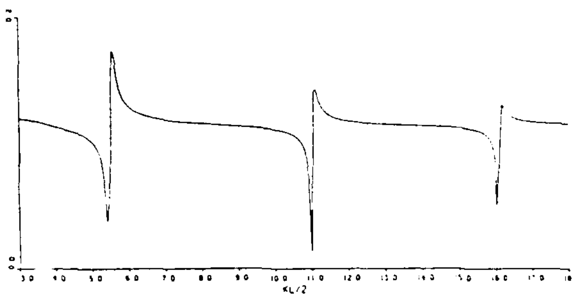

Figure 4a. Form function plot of elastic spheroid end-on incidence.

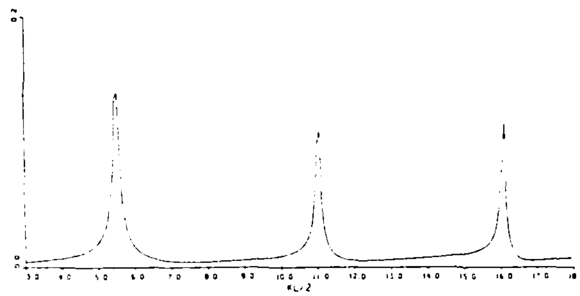

Figure 4b. Resonance reponse of elastic spheroid end-on incidence.

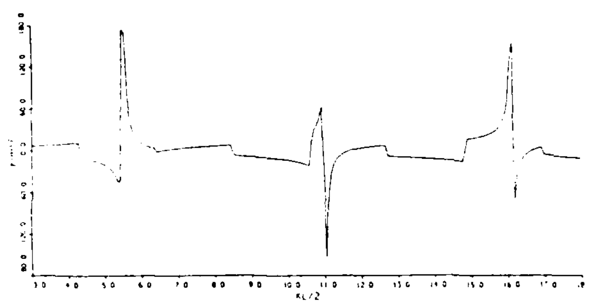

Figure 4c. Relative phase between elastic thin shell and sound-soft object.

experimental design and interpretation, and to evaluate new systems concepts. Specific areas of interest are stochastic modeling, realistic environmental modeling, and volume acoustic field modeling.

The objective in volume acoustic field modeling is to analyze and model the three-dimensional acoustic field on a local to regional basis. In some cases knowledge of pertinent parameters will be limited. Knowledge and understanding of the oceanic processes within the volume will be used to support parameter selection. It is further desirable that the model be portable so that it can be used aboard ships. The difficulty of such an endeavor is obvious, but the benefits are enormous. Such capability would add a new dimension to underwater prediction and surveillance.

Stochastic modeling of the acoustic field and its interactions with boundaries is an area that will be explored. Such boundaries as the underice interface, the marginal ice zones, and rough sea surfaces and ocean bottoms cannot be accurately modeled by deterministic methods.

As acoustic models become more sophisticated and as computationally faster computers with larger memory capability become available, real-world scenarios become feasible. Modeling the interaction of acoustic waves with highly complex boundaries (including such properties as *shear*, *porosity*, *grain size*, *anisotropy*, etc.) are possible. Three-dimensional models that model whole volumes of the world's oceans are needed. Models that include all of the acoustically significant physics will be required. In all of these areas, highly accurate, complete models will be needed as baselines by which to evaluate the accuracy of approximate, but more computationally efficient, models and to undertake detailed sensitivity analyses unavailable by other means. NORDA's task will remain the same, i.e., to research, develop, and assist in the transition of acoustic models that serve the Navy.

Recent Advances in Application of Acoustic Models

Edward A. Estalote, George A. Kerr, and David B. King
Numerical Modeling Division

Abstract

Using acoustic models to simulate the action of the environment on acoustic propagation has been a major activity of NORDA since its beginning. The basis of acoustic application modeling is the use and adaptation of models and principles produced by the research community to "real-world problems." To carry out this program, a large collection of acoustic models and environmental data is required. Over several years the number and quality of the models has increased dramatically. The quality, geographic coverage, and resolution of environmental data bases have also increased to such an extent that application modeling can be done for situations and locations that could not have been considered previously. NORDA has many acoustic models and automated data bases available for use by the research community.

Introduction

Over the last 10 years the application of acoustic models to ocean problems has increased both in scope and in the complexity of the tools available. Since its beginning, NORDA has used acoustic models to address single-issue questions, as well as to perform acoustic model studies of large ocean areas. Due to the variety of problems that have been addressed over the years, NORDA has acquired an extensive collection of acoustic models and automated environmental data bases. The models vary from simple, with limited applicability, to complex. The data bases have evolved from those with limited applicability to those with extensive geographic coverage.

Some tasks require acoustic model surveys of large ocean areas; thus numerous model simulations are carried out. This effort requires numerous user inputs and is subject to human errors. To minimize these errors, the NORDA Acoustic Model Operating System (NAMOS) was established. NAMOS is a menu-driven operating system that enables the user to make many model runs with maximum flexibility in selecting the environmental data and the appropriate model. Also, area-wide surveys tend to collect a large amount of oceanographic data that is not always in the appropriate form for acoustic simulation studies. To help with analyzing and reformatting data, NORDA developed the Naval Oceanographic Raw Data Analysis and Processing System (NORDAPS). NORDAPS helps the oceanographer to select, analyze, and re-form data into a format that is the most compatible with the acoustic models.

The Basic Acoustic Model User Support (BAMUS) Program is used to address short-term or single-issue projects. Through this program, the acoustic models and data bases resident at NORDA are made available to the ASW community. Requests for specific acoustic predictions are provided to naval organizations and those companies under contract with the Navy.

Models and data bases

NORDA has an extensive number of resident acoustic models. An appropriate question at this point would be: Why does the Navy need an extensive number of acoustic models? The answer is that all models use simplifying assumptions and thus are approximations to the real physical ocean environment. It is up to the user to take these assumptions into account and decide which model is most appropriate. Some factors must be considered:

- Can the environment be approximated as range independent, or must the variations be taken into account?
- What is the frequency of interest?

- How accurate does the answer have to be?
- What form does the answer have to be in: e.g., will transmission loss be enough or is complex pressure required?
- How much computer resources are you willing to spend?

The acoustic models fall into three separate categories: propagation (transmission) loss models, ambient noise models, and system performance models. For a full explanation of the different models, see Estalote (1984) where a model synopsis and references to primary sources of information are available.

Propagation loss models

The propagation loss models can be divided into subsections using the type of physics that is being used as a criterion. Generally the models use either physics based on ray theory or wave theory. There are also hybrid models that are combinations of both ray and wave theory. Further separation may also be accomplished by whether or not the model will handle an environment that is a function of range. Table 1 lists the propagation loss models and how they separate into the different categories.

Table 1. Propagation loss models.

Model	Range Dependency*	Model Physics Ray Solution	Wave Solution	Hybrid
FACT	RI			X
RAYMODE	RI			X
NLNM	RI		X	
COMODE	RI		X	
FFP	RI		X	
CRITICAL ANGLE PE	RD		X	
IFDPE	RD		X	
PAREQ	RD		X	
MPP	RD	X		
GRASS	RD	X		
MEDUSA	RD	X		
ASTRAL	RD			X

*Range dependent (RD)
Range independent (RI)

Ambient noise models

Ambient noise, by its very nature, is a difficult process to model properly. Several different mechanisms contribute to the total noise field. For low frequencies (< 200 Hz), shipping contributes the largest share of the noise. Thus, to model the noise properly some accounting of the ships by type and location must be done. NORDA has ship count data bases that are resolved both temporally and spatially, which are instrumental in producing noise predictions. NORDA presently has four noise models: FANM, CNOISE, DANES, and BEAMPL.

The FANM (Fast Ambient Noise Model) is a noise model that uses and internally generates range-independent transmission loss convolved with the noise sources (ships and wind) to produce both vertical and horizontal noise calculations. The model uses user-supplied factors of minimum depth and minimum depth excess to account for topographic interference. Essentially the model stops counting noise sources when the desired values are reached.

The CNOISE model has no internal transmission loss capability. Provisions are made to use an externally generated transmission loss file. The CNOISE model just convolves the noise source (ships only) with the user supplied data. The model will allow for different transmission loss calculation as a function of bearing. CNOISE can provide only horizontal noise calculations.

The DANES (Directional Ambient Noise Estimation System) model is a subset of the Automated Signal Excess Prediction System. This model calculates horizontal ambient noise using ASTRAL as the transmission loss model. It also has its own environmental data bases, including ship counts.

The BEAMPL model can provide beam noise statistics for a beam using random ship traffic on user-supplied ship tracks.

System performance models

Producing performance predictions for systems, both active and passive, requires calculating not only transmission loss, but also other such factors as reverberation or noise. The systems also require the use of beam patterns and other system-specific information. NORDA has five models available for system-specific calculation. Note that some system specific calculations can and have been made by combining the results of other acoustic models, such as PE and CNOISE.

NISSM II (active system) NISSM II (Navy Interim Surface Ship Model) has been designated as the Navy Interim Standard for calculating performance of ship sonars. It is used to predict echo and reverberation levels and is capable of predicting detection probability when environmental, target, and sonar system parameters are defined. The ocean bottom is modeled as a flat, specularly reflecting surface with the bottom loss represented as a range independent function of grazing angle. Volume absorption and surface losses are also incorporated in the model. The sound speed

profile is described by a continuous function, and gradients are to the input sound speed at discrete depths.

SHARPS-III (active system)—SHARPS-III (third generation Ship-Helicopter Acoustic Range Prediction System) is an active system model used for making daily forecasts of detection ranges for a variety of active and passive sonars, including counterdetection. In the prediction of active system detection ranges, SHARPS-III allows the user to specify the prediction mode, e.g., direct path, bottom bounce, or convergence zone. It employs a ray acoustic model that is a modified version of NISSM II, which generates the transmission loss, target echo, and reverberation curves needed for the detection range prediction.

Generic sonar model—The Generic sonar model is a computer program designed to predict and evaluate the performance of various sonar systems. It has significant prediction capabilities for both active and passive systems, and allows the user to choose from an assortment of models to make the necessary calculations. These models include the following:

- ocean sound speed models
- surface/bottom reflection models
- volume attenuation models
- reverberation models
- beam pattern models
- transmission loss models
- passive/active signal excess models
- ray tracing

It should be noted that this model uses a modular approach in that for each basic function (e.g., surface reflection coefficient) a number of choices are available to the user (e.g., table look-up, AMOS, Marsh-Schulkin-Kneale, Beckmann-Spizzichino).

ACTIVE RAYMODE—ACTIVE RAYMODE is used to predict signal excess for active sonar systems. It uses a modified form of the RAYMODE propagation loss model (omits the normal mode portion of the model), together with user input sonar parameters, to compute echo level and reverberation.

Taking these into account, together with the noise (self-noise and ambient noise) and the reverberation recognition differential, the signal excess is calculated as a function of travel time for each transmit/receive beam pair.

ASEPS (passive system) ASEPS (Automated Signal Excess Prediction System) is a system of computer programs and supporting data bases that perform and display passive sonar calculations. Its components are

- DANES: discussed above;
- ASERT: ASTRAL System for the Estimation of Radial Transmission loss;
- TASSRAP: Towed array predictions for short ranges, uses FACT for transmission loss and DANES for ambient noise;
- EXTENDED TASSRAP: Towed array predictions for long ranges, uses ASTRAL for transmission loss and DANES for ambient noise.

This collection of models can predict horizontal/directional ambient noise, transmission loss (radials), signal excess, and probability of detection for both fixed and towed horizontal arrays.

Special software

NORDA Acoustic Model Operating System (NAMOS)—The Navy has many different acoustic models that produce acoustic predictions. By their nature these models require different inputs, and the inputs are required in different formats. Different models are required because each of the models has its own region of applicability as well as its own strengths and weaknesses. A single model (e.g., transmission loss) that is applicable for all situations and cases does not exist. This state of affairs can lead to a lot of wasted effort due to errors and the cumbersome reformatting of inputs for different models. For example, if one is required to carry out an acoustic survey of an ocean area, several different models may be required to produce the results required to give the necessary information. The expense in manpower and time can be prohibitive in running the same problem with different models.

The NAMOS system was designed and developed to minimize the errors and the time required to carry out acoustic model runs. NAMOS is a interactive computer system that sets up a batch runstream to exercise the models. The basic design of NAMOS is to solve the sonar equation by running the selected models for each element's equation, e.g., transmission loss, ambient noise, etc. At its present stage of development NAMOS can extract the required environmental data from the data bases, and run any one of five different transmission loss models and one ambient noise model.

In addition to NAMOS, EAIDS (Environmental Acoustics Interactive Display System) is under development to provide graphic display of both the environmental data bases and the acoustic models. This interactive display system when fully integrated will allow the editing and display of any part of the data bases presently used by the NAMOS models, as well as the display of the acoustic model output. The Color Area Mapper will now display a color representation of shipping density, depth excess, bathymetry, and bottom class for any area of the northern hemisphere. EAIDS will also allow interactive

interpolation of sound speed profiles along a great circle path. Graphic display of acoustic model output is also available in EAIDS. PROFGEN is also resident in EAIDS. This module will permit the merging of bathythermographs to historical deep profiles.

NORDAPS—NORDAPS (Naval Raw Data Analysis Processing System) is an interactive software package that processes and displays Field Exercise Data. This environmental data is typically obtained from oceanographic platforms using conductivity-temperature-depth (CTD) and/or expendable bathythermograph (XBT) sensors. The data is initially recorded on analog tape and is then processed by a shore facility, which in turn, produces the digital data tapes used by NORDAPS. This raw exercise data is read, reformatted, thinned, filtered, and written to direct-access data bases. NORDAPS provides an interactive, menu-driven system for analyzing, editing, extracting, plotting, and displaying this data. The primary functions of NORDAPS are to

- extend CTDs to the bottom,
- attach salinity to XBT data,
- perform absolute difference calculations between bathythermographs (BT's) at standard depths,
- calculate sound speed profiles,
- group data stations into transects,
- plot BT temperature profile against all CTD profiles in range,
- provide interactive editing and displaying of the data,
- perform retrievals of selected data sets for numerical model inputs.

NORDAPS is interfaced to a relational data base system (INGRES) that provides ad hoc query capabilities. Interfaces are provided for updating the RSVP and AUTO-OCEAN data bases along with capabilities to interface with the NAMOS/EAIDS systems. EAIDS is currently under development and will allow the interactive display and modification of environmental parameters.

CHORDS—The advent of new high-resolution digital recorders has led to the requirement to develop an accurate profile thinning algorithm to retain the acoustically significant profile shape while reducing the number of profile points to a manageable size. CHORDS (Kerr, 1984), a new temperature and sound speed profile thinning algorithm, was developed to meet this requirement. The profile is reduced to a series of line segments constructed on the basis of the difference between the actual profile and the existing line segments. The algorithm, already in use in several weapons systems, scans the entire profile in each iteration but retains previous results to increase the algorithm's speed.

Environmental data bases

Acoustic models require environmental inputs to produce simulations. To obtain the required data on a case-by-case basis is both time consuming and error prone. To minimize the problems of obtaining environmental data, NORDA has acquired or built several environmental data bases.

AUTO-OCEAN—AUTO-OCEAN is a low-resolution gridded, 5° by 5° sound speed and wave height data base covering the world's oceans from 60°S to 60°N on a seasonal basis.

STANDARD OCEAN—This data base is used in conjunction with existing models to provide automated retrieval of environmental data along great circle paths in the same manner as AUTO-OCEAN. It contains synthetic data, as opposed to the measured data contained in AUTO-OCEAN, and has a ½° resolution. In addition temperature and salinity profiles can be obtained.

RSVP—The RSVP (Representative Sound Velocity Profile) data base and software allows users to select representative sound speed profiles by region and date. Sound speed profiles are selected on the basis of closeness to the mean sound speed profile calculated from all profiles meeting the query requirements.

SYNBAPS—SYNBAPS (Synthetic Bathymetric Profiling System) is a data base designed to produce rapid generation of bathymetry along any great circle path. It is a finely gridded data base with a resolution of 5 minutes ($\frac{1}{12}$°). The coverage is essentially worldwide.

HITS—December 1983 update of HITS (Historical Temporal Shipping) is a ship-count data base that may be automatically accessed to provide information to be used for ambient noise predictions. The resolution of the data base is 1° squares by ship type. The area of applicability of the data base is essentially worldwide.

AUTO-SHIPS—AUTO-SHIPS (1984 update) is a shipping density data base that can be automatically accessed by the ambient noise models. The coverage is essentially worldwide. The ship count for each square (1°) is the weighted sum (by ship type) of the HITS data base. This data base has the following additional environmental information.

- bottom class
- bathymetry
- depth excess
- wind speed

BAMUS program

The Basic Acoustic Model User Support program (BAMUS) is resident at NORDA, and is jointly funded

on-shore prediction systems. Each arm of the Navy air, surface, subsurface, and shore-based facilities had their own prediction system with different environmental data and different models, which naturally led to different predictions. As a first step toward a goal of consistent results, an environmental data base was created to serve as a master for all environmental data bases to be used in prediction systems. The premise was that the data base should contain the best environmental data at the highest resolution possible. This data base now contains seven parts: Historical Ocean Profiles, Bottom Loss, Ocean Floor Depth, Volume Scattering Strength, Wind Speed, Shipping Noise, and Wind and Residual Noise. After the completion of the data base it was realized that there was not sufficient data of all kinds for all areas. A further analysis of this data base provided a series of maps that defined the areas of data paucity and laid out the survey requirements (King et al., 1984) for each data base, i.e., where and what types of data are required.

Summary

Major strides have been made in acoustic modeling over the last several years. The field has matured from a few models with limited application, environmental data bases of low resolution, and limited geographic coverage to a series of models and automated environmental data bases that make the application of models to real-world situations more credible. Much of the progress can be attributed to increases in computing power that have become available. With a look toward the future one can visualize the ability to do exacting predictions as the environmental data and the knowledge of the processes increase.

References

Estalote, E. (1984). *NORDA Acoustic Models and Data Bases*. Naval Ocean Research and Development Activity, NSTL, Mississippi, Technical Note 293.

Kerr, G. (1984). *CHORDS: A New Temperature or Sound Speed Profile Thinning Algorithm*. Naval Ocean Research and Development Activity, NSTL, Mississippi, Technical Note 272.

King D. B., R. Love, R. A. Fisher, J. Allen, P. Moresdorf, T. Davis, E. Hashimoto, M. Bradley (1984). *Data Survey Requirements Bases on the Acoustic Performance Prediction (APP) Master Data Base*. Naval Ocean Research and Development Activity, NSTL, Mississippi, Technical Note 276.

McGirr R., D. White, and C. Bartberger (1984). *Technical Evaluation of FACT 10A*. Naval Ocean Research and Development Activity, NSTL, Mississippi, NORDA Report 70.

NORDA's High-Frequency, Shallow-Water Bottom Scattering Program

Steve F. Stanic and Richard H. Love
Ocean Acoustics Division

Deep ocean acoustic characteristics of signals, noise, and reverberation are significantly different from shallow or narrow coastal areas. Thus, attempts to extrapolate deep ocean data for use in shallow-water applications have been disappointing. The proximity of the boundaries, the increased substrate and water column inhomogeneity, and the increased density or influence of noise sources contribute to the extreme complexity of the shallow-water acoustic environment. To develop naval systems that can effectively operate in shallow water, a thorough understanding of the interaction of environmental and acoustic parameters is essential.

Because the sea floor is a major factor in shallow-water environments, NORDA has established a program that focuses on the relationships between seafloor properties and acoustic scattering. The program consists of an integrated series of acoustic and environmental measurements designed to identify and isolate various bottom scattering mechanisms, and to resolve their effects on the acoustic back- and forward-scattered fields. Data from these measurements serve as a basis for the ongoing development of shallow-water environmental acoustic models for use in exploratory and advanced development programs.

NORDA has used the expertise available in the offshore oil industry to design and construct two towable, self-deploying, acoustic instrumentation support structures to ensure the success of this program. These towers, designed by Petro Marine in Gretna, Louisiana, are 35 feet long, 20 feet wide, 30 feet high and weigh 17½ tons each.

The acoustic transmitting system uses a pair of nonlinear parametric sources. The low sidelobe capabilities of these sources make them ideal for shallow-water boundary scattering measurements. The receiving systems consist of two 16-hydrophone, two-dimensional spatial arrays with broadband capabilities to 200 kHz. The attitude of each array is controlled by a triaxial positioning system.

The acoustic experiments are supported by a detailed series of oceanographic and seafloor geological characterization measurements. Side-scan sonar surveys are used to locate and identify possible experimental areas. Once an area has been located, high-resolution, close-range, side-scan sensor data are used to characterize large-scale features and the lateral extent of the experimental site. High-frequency precision bathymetric profiles define the large-scale roughness and slope in the selected area. The small-scale roughness properties in the experimental area are obtained from diver-operated stereo camera equipment. A detailed analysis of diver-collected sediment cores and selected in situ probe measurements provides data on the sediment parameters needed to support the acoustic measurement and modeling efforts. Conductivity, temperature, depth, and current measurements are used to continuously monitor water mass properties for acoustic propagation conditions in the water column.

Two experiments have been conducted off the Florida coast. The first experimental site was a homogeneous area characterized by medium-grained sand that contained little shell content and minute small-scale surface roughness. In the second experimental area the small-scale surface roughness was only the result of large shell hash. The other bottom parameters were similar to those measured at the first experimental site. A third experimental site has also been located. In this area the small-scale surface roughness is due to sand waves.

These experimental results will be used to determine the predictability of pertinent bottom parameters; the spatial and temporal variability of these parameters and the extent this variability significantly affects acoustic scattering measurements; the statistics of the acoustic back- and forward-scattered fields as a function of grazing angles (3-30°), frequency (20-180 kHz), pulse length (200 μsec-10 ms), and relevant bottom parameters; the predictability of acoustic bottom scattering given the relevant parameters; and modifications that must be made to available bottom scattering and geoacoustic models or new models that need to be developed.

The program results will provide the exploratory and advanced development programs with high-quality data bases and models needed for successful shallow-water system developments and operations. The acoustic data and models cover a broad range of tactical weapons frequencies and are supported by high-quality environmental measurements.

Arctic Environmental Acoustics

Dan J. Ramsdale and Joe W. Posey
Ocean Acoustics Division

Introduction

Environmental acoustics measurements and models in the Arctic are driven entirely by the unique nature of the ice canopy. The most constant feature about the ice is its variability, both spatially and temporally. The nature and extent of the ice varies seasonally with the changing amount of sunlight in the northern latitudes. Even on a small scale, the thickness of ice on a given floe can range from a few inches to tens of feet, depending on the age of the ice. The spatial characteristics of the ice range from the permanent pack ice of the central Arctic to the marginal ice zones where ice and water mix and are driven by the local wind fields.

One of the challenges facing acousticians at NORDA is to sort out those properties of the Arctic environment, particularly those of the ice canopy, which are relevant to acoustic propagation and which serve as acoustic noise sources. These properties will depend on the acoustic frequency or wavelength of interest. In the high-frequency regime (5–100 kHz), the scales are small and reflection with the complex underice surface includes the consideration of microroughness, penetration into the ice, and the conversion of compressional wave energy into shear waves at the ice-water interface. In the sonar frequency range (50 Hz–5 kHz), the scales of interest are larger, and lower attenuation allows propagation to larger ranges. Here important environmental factors include the ice thickness, the sonic structure of the ice layer, the large-scale roughness, and the number and orientation of ice ridges. As in the high-frequency case, the issues of penetration of acoustic energy into the ice layer and conversion at the ice-water boundary are important.

NORDA acousticians are addressing these problems with a balanced approach of measurements guided by the best environmental acoustic models available. These measurements are designed to expand the data base in the Arctic and to allow critical testing of the existing acoustic prediction models. Two companion research programs are being pursued, one in high-frequency acoustics to support advanced weapons development and one in low-frequency acoustics to support advanced sonar system development. The following sections detail the modeling and measurements research being pursued in each of these efforts.

Discussion

Arctic acoustic models

Sound propagation in Arctic waters is governed by the same physical laws as underwater sound propagation anywhere in the world's ocean basins. Therefore, special Arctic models need not be developed for propagation in the water column or for interaction with the sea floor. However, the presence of sea ice is significant only in the polar regions, so Arctic acoustic modeling at NORDA has been concerned with the interaction of water-borne sound with sea ice.

The acoustical significance of the water-to-ice transition region on the bottom of nominally flat sea ice has been studied using a model that allows the elastic properties of sea ice to vary in the vertical but not in the horizontal directions. One would expect that the thin transition layer, about 6 inches thick, would be important at high frequencies, and this expectation was confirmed. Surprisingly, however, the transition region was found to be important for frequencies as low as 1 kHz, especially at low grazing angles. As a result of these findings, an existing model for acoustic backscatter from ice keels was modified to include gradual rather than abrupt transitions at the ice block faces, and significant changes in backscatter predictions resulted. Also, long-range propagation calculations were made for sound below a flat ice cover, and the inclusion of the water-to-ice transition was found to greatly increase the frequency dependence of the predicted transmission loss. These findings highlight the need for better measurements of the acoustic properties of sea ice at and near the ice-water interface.

The ice keel model referred to above represents a keel as being composed of many randomly oriented blocks which act as independent scatterers. In addition to the

inclusions of the transition region discussed above, this model has been upgraded by allowing for arbitrary stratification within the blocks and by providing alternate block rotation schemes.

Arctic acoustic measurements

Acoustic measurements can be conducted in the Arctic from ice camps, ice breakers, aircraft (using sonobuoys), and submarines. Ice camps and icebreakers severely limit both the geographic and seasonal range of measurements. The sunless Arctic winter is too hazardous, and the summer ice conditions are too precarious to support ice camps and breaker activity. Aircraft afford somewhat better coverage but must depend on finding polynyas (open water) to launch sonobuoys. The submarine platform provides the best capability for year-round acquisition of acoustic data in all locations in the Arctic.

Conducting scientific measurements from an ice camp poses unique logistics problems. In addition to equipment for scientific experimentation, all habitability equipment and supplies must be taken to the ice camp location. This transport is usually done by means of aircraft for small camps (6–12 people) or by using an icebreaker with helicopter support to deploy larger camps (approximately 80 people). Special training is required for all ice camp personnel, including firearms training (in the unlikely event of a polar bear incident), Arctic survival training, and emergency medical training.

Over the last two years NORDA acousticians have participated in two ice camp expeditions in the Arctic. The first camp was approximately 25 nm northeast of Barrow, Alaska. The purpose of this camp was to provide an engineering testbed for the equipment and techniques used in deploying acoustic instrumentation through the ice. A four-hydrophone vertical line array was deployed and used to make ambient noise measurements and also to record signals from lightbulb implosions. The very low ambient noise levels in the Arctic require an extremely quiet preamplifier and signal conditioning unit. The faired Kevlar hydrophone array cable proved to be very flexible, even in extreme cold. When wet cable is removed from the water, however, it must be dried in a warm environment, otherwise icing would occur and render the cable quite inflexible and difficult to handle.

The second NORDA acoustic ice camp, shown in Figures 1 and 2, was part of ICEX 1-85, a multilaboratory experiment conducted in the Beaufort Sea during October 1984. During this second exercise, a multidisciplinary team of NORDA acousticians, oceanographers and engineers deployed four vertical line arrays of hydrophones shown schematically in Figure 3. Three of the arrays contained 4 hydrophones (a) and one contained 16 (b). The 4-element arrays were subsets of the 16-element array so that coherence of the acoustic field in the horizontal direction could be measured. The 16-element array was configured to be a minimal redundancy array so that coherence in the vertical could be measured and beamforming performed to examine the characteristics of individual arrival paths.

A basic acoustic experiment conducted by NORDA scientists during ICEX 1-85 was to measure the reflection loss versus grazing angle for frequencies ranging from 460 to 2200 Hz and for grazing angles from 6° to 60°. This measurement was done (shown in Fig. 4) by using a digitally coded source provided by the University of Miami. The unique feature of this particular digital code is its capability in the decoding process to isolate individual arrival paths for a single hydrophone. Ice cores were taken along the transmission path from source to receiver and used to provide ground truth measurement of ice thickness, as well as the vertical profile of temperature, density, and salinity in the ice core. Even over the short distance of 1000 yds, the cores revealed a great deal of variability (e.g., unfrozen melt ponds were mixed with the ice in some locations). The acoustic reflectivity results, along with the ice cores and measurements of the underice topography, will provide measured values that are vital to testing under ice acoustic propagation models.

Additional experiments in the sonar frequency range during ICEX 1-85 included propagation loss using both narrow- and broad-band sources and broad-band spatial coherence. No high-frequency measurements were conducted at ICEX 1-85.

Future plans

NORDA will be a major participant in ICEX 1-86, another large, multilaboratory series of experiments in the Arctic conducted during the spring of 1986. NORDA will conduct experiments in three environmentally acoustic distinct locations, shallow ice-covered water, deep ice-covered water, and in the marginal ice zone where ice and water are mixed. The measurements will encompass both sonar and high-frequency acoustics, along with ice properties and ocean-bottom sampling.

Figure 1. NORDA ice camp.

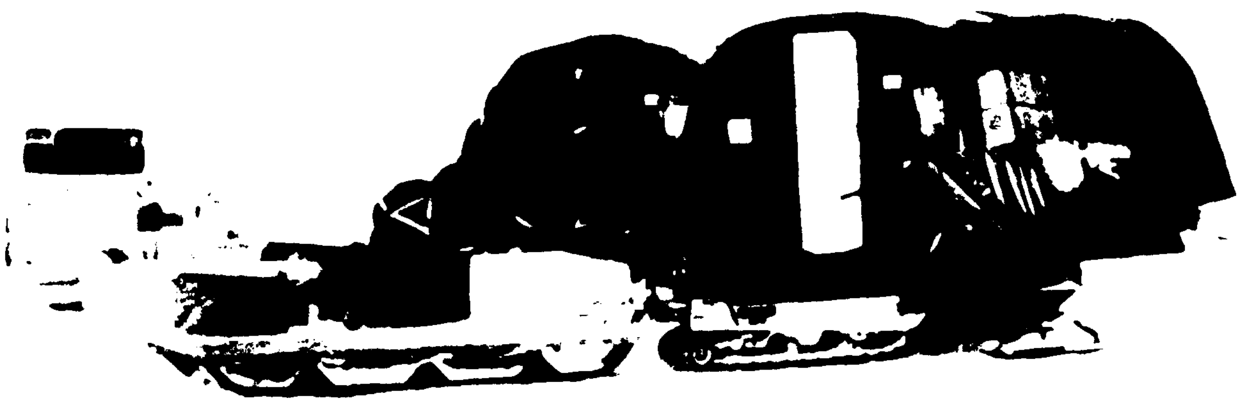

Figure 2. NORDA ice camp.

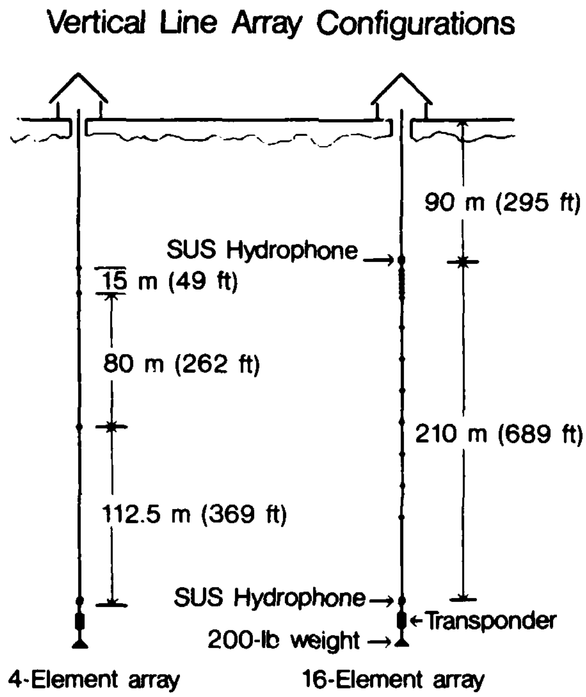

Figure 3. Schematic of vertical line arrays of hydrophones.

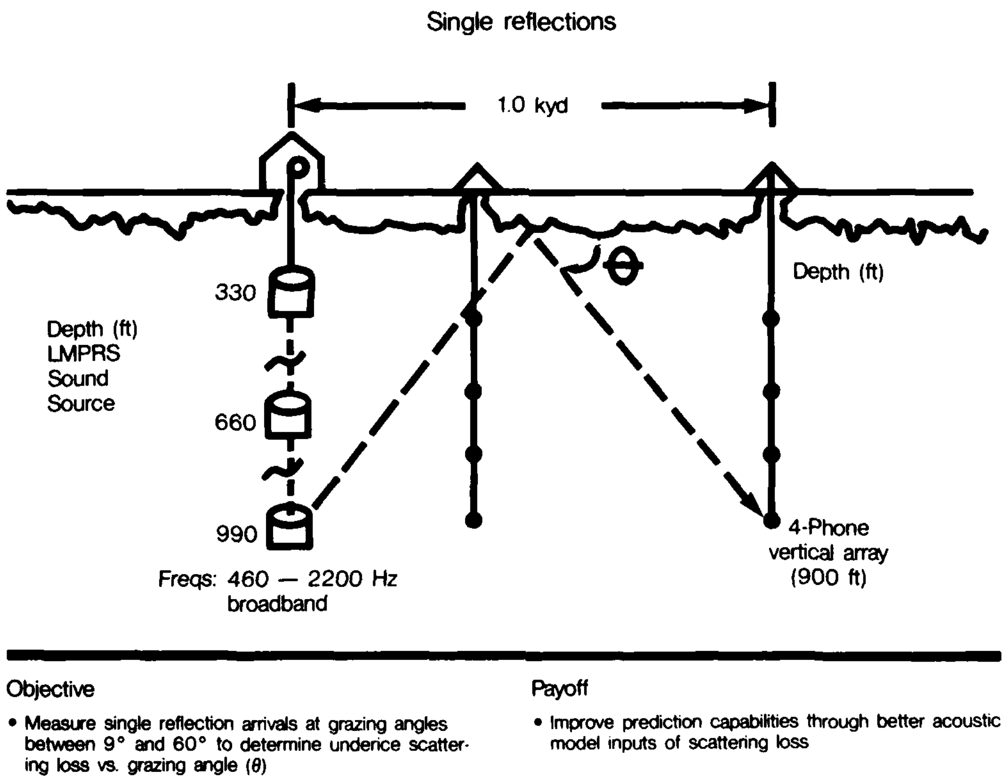

Figure 4. Reflection loss versus grazing angle for frequencies of 460–2200 Hz.

The Development of Directional Ambient Noise Data Bases and Their Application to U. S. Navy Weapons Systems

Ronald A. Wagstaff
Ocean Acoustics Division

Abstract

Knowledge of the ocean acoustic environment in which the Navy must operate is required to predict the performance of a sonar system or to optimize its use. This knowledge is obtained either through a real-time measurement or from historical data bases. Because the operational Navy cannot obtain measured data in real time, historical data bases have become critical. However, the degree to which data is useful often depends on how well the information it contains can be understood and utilized.

This paper presents the rationale for the selection of the particular statistic upon which a data base is built and for the selection of the presentation format. Some of these formats and statistics have been recently developed by NORDA researchers to meet the needs of specific data base users. Several examples are given which illustrate that the particular performance statistic and the presentation format can greatly increase the potential application of a data base. An example is also included to show that the wrong statistic for a given situation can lead to errors and severely limit the usefulness of the data base.

Introduction

Detecting, classifying, localizing, and tracking enemy submarines is a critical mission of the U. S. Navy. One method by which this mission is accomplished is the use of antisubmarine warfare (ASW) sonar systems. Present ASW sonar systems are considerably more sophisticated and complex than their predecessors. They have been intelligently designed to exploit the acoustic and ambient noise environments to enhance their performance. Furthermore, the ASW tacticians and sonar operators are becoming more knowledgeable of how the environment influences the sonar system performance, and more capable of using this knowledge to improve their ASW effectiveness.

NORDA's primary mission is to provide the environmental information that permits ASW sonars to be intelligently designed and effectively utilized. The high level of sophistication of our present sonar systems and the level of knowledge of the sonar tacticians and operators place high demands on the environmental acoustic support that must be provided by the research and development (R&D) community. It is no longer sufficient to provide data bases that simply characterize in general terms the oceanography, acoustic propagation, and ambient noise. Data bases and analysis products must be provided that can be used to adequately characterize or correctly predict a given sonar system's performance for a particular situation in a specific acoustic and ambient noise environment.

This paper presents the rationale for selecting the particular statistic upon which a data base is built and for selecting the presentation format. Some of these formats and statistics have recently been developed by NORDA researchers to meet the needs of specific data base users. Several examples are given, which illustrate that the particular performance statistic and the presentation format can greatly increase the potential application of a data base. An example is also included to show that the wrong statistic for a given situation can lead to errors and severely limit the usefulness of the data base. Discussions of these examples are followed by a summary.

Background

Modeling sonar performance has at least one advantage over measuring performance; modeled results are generally better understood than measured results. This is because the significant parameters and mechanisms that influence the measured results are often not known or are not well understood. In modeling, however, the influence of each parameter and mechanism modeled can be identified and considered separately to provide a much clearer picture of what is happening, even though the model may not be completely representative of the real situation.

This advantage of modeling over measurement also applies to data bases. Hence, some of the discussions presented herein rely on modeled results rather than actual measured data. The simulated data were obtained from modeling the measurement of beam noise by a towed line array, and the resulting data are completely interchangeable with beam noise data that might have been measured in a similar situation. Furthermore, intermediate products in the modeling process can be obtained to give a more complete understanding of the problems involved in selecting the best statistic and the presentation format for the data base. Hence, the generation of simulated beam noise data will be discussed in this section, while the following section will discuss the application of these data in creating different data bases.

The generation of simulated array beam noise data is illustrated by Figure 1. The dots and arrows in Figure 1a correspond to the positions and the courses of merchant ships in a shipping lane. These position data were observed by a maritime patrol aircraft at the beginning of a 9-hour-long ambient noise measurement exercise. In the actual measurement situation, the beam noise data were measured for 15 minutes each hour of the 9-hour period by an acoustic towed line array located at site 5. The array heading was changed after each data acquisition period to permit the unambiguous horizontal directionality of the noise field to be estimated from the beam noise data.

The shipping data in Figure 1a were used to simulate the beam noise data that were measured by the towed array at site 5. The simulation was accomplished by assuming a speed for each ship and dead reckoning it to a new position. Nine such dead-reckoning periods were used, with the simulated array on the same headings used during the actual measurements to permit the modeled results to correspond directly with the measured results. The agreement between the measured and simulated results was excellent. However, this agreement is not critical for the discussions that follow. Therefore, the comparison of those results will not be discussed herein.

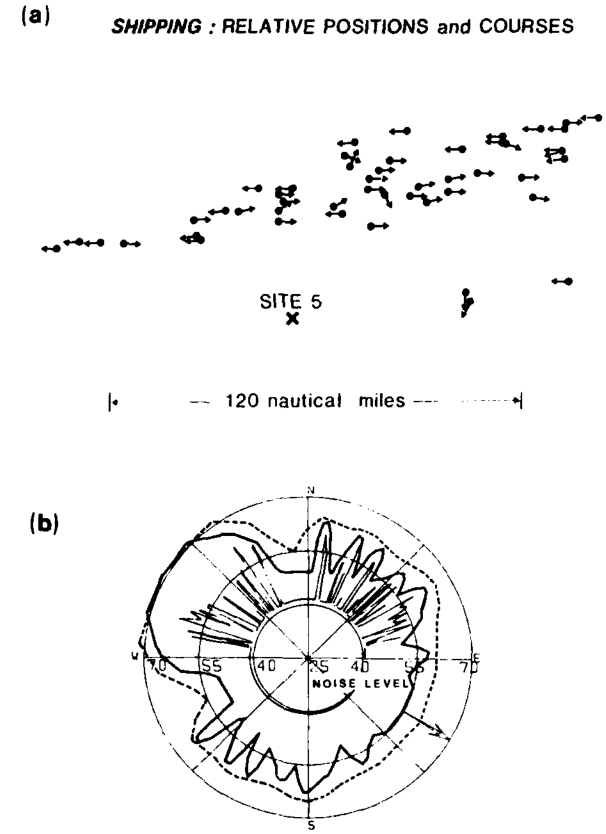

Figure 1. Representation of the ambient noise measurement process including (a) the locations of ships relative to the measurement site 5, and (b) the "true noise field" due to shipping and wind/sea state noise and measured beam noise levels from a small aperture array (dashed curve) and a long aperture array (solid curve).

The curves in Figure 1b are the modeled results for the third dead-reckoned period. These results were obtained from, but do not correspond directly to, the shipping data for the initial time period in Figure 1a. The center-most solid curve, which consists of radial lines superimposed on a uniform (circular) background, represents the ambient noise field horizontal directionality due to the dead-reckoned shipping distribution (the radial lines) and the wind and sea state (the uniform or circular background). Each radial line is along the azimuth of a ship and the length of the line is proportional to the noise level received at the array from that ship. The plot resolution of 1° makes some of the noises appear to be broader than they are, but this is only an artifact of the plotting

format. Since all ships are to the north of site 5, there are no radial noise lines in the southern half-space, only the uniform noise due to wind and sea state.

The two remaining curves in Figure 1b, the solid and the dashed curves, represent the mean beam noise levels that would be measured by two different towed line arrays at site 5 during the same period for which the "spiked" noise field was obtained. Because towed arrays have finite length, the beam noise has a smeared or broad spatial (angular) response. The towed array to which the dashed beam noise curve corresponds is one-third as long as the array to which the solid beam noise curve corresponds. Therefore, the shorter array has three times the spatial smearing effects that the longer array has. The low beam noise levels are no longer evident in the pattern corresponding to the shorter array, even though they exist in the pattern corresponding to the longer array.

The line array has an inherent left-right (or front to back) ambiguity resulting from its conical beam patterns. Angles relative to the axis of the array can be determined, but one side of the axis cannot be distinguished from the other, i.e., clockwise versus counterclockwise. This is evident in the beam response plots in Figure 1b. Both beam response plots are symmetric about the array heading arrow (at 120°) even though the major noise components (the radial lines) are all in the northern half-space (i.e., most are on the left side of the array, or counterclockwise from the array heading arrow).

The amount of spatial smearing in the beam noise data depends on the design parameters of the array and can vary considerably from one sonar system to another, as is illustrated in Figure 1b. Hence, measured array beam noise data are unique to the particular sonar system that made the measurement. To extrapolate the data to another sonar system having different design parameters or to determine characteristics of the ambient noise environment (i.e., the curve consisting of the series of spikes on a uniform background in Fig. 1b), special processing techniques are required to remove the effects in the beam noise that make the data unique to the measurement system. The characteristics of a different system can then be imposed on the result to extrapolate the data to that system.

An engineer might be required to design an advanced towed array sonar system to satisfy a new ASW requirement for high-speed operation, fine spatial resolution and low beam noise levels. Increased resolution is achieved by increasing the array length, which in turn decreases the spatial smearing with a corresponding decrease in the beam noise levels (see Fig. 1b), a desirable effect. However, as the array length and tow speed increase, the array geometry tends to depart from linear, which degrades its signal performance. Furthermore, the handling difficulty of the array and the cost increase with increasing array length. Hence, the engineer must make a trade-off involving beam noise level, signal performance, array length, tow speed, and cost. Thus, an ambient noise data base of beam noise level as a function of array length (or equivalently as a function of beamwidth) is required to make the trade-off. It tells the engineer how wide and deep (low in level) the "holes" in the noise are and permits him to tailor the beamwidth to achieve the required beam noise levels.

An ASW sonar operator, on the other hand, is interested in detecting submarines. He requires a data base that can be used to help him determine the best array heading to maximize the chances of detecting a submarine. In this case, the design parameters of the array are already determined and the historical data base would be used to increase the effectiveness of the sonar system. A data base of beam noise as a function of array length required by the engineer would not provide the information needed by the sonar operator. An entirely different statistic is needed.

There are many different types of ambient noise data bases and a multitude of different users, which range from the scientists who study the physical mechanisms of the ambient noise, to the engineers who design and build sonar systems, to the operators who use the systems. All have urgent needs for data bases, but each addresses the sonar performance problem from a different perspective and with a different technical background.

Discussion and examples

Examples will now be given that illustrate attempts to maximize the usefulness of the data by selecting or devising statistics to answer the user's questions, by appropriately designing the data processing, and by tailoring the presentation format to a user's specific requirement. The examples will all address questions regarding ambient noise. The need, however, is not unique to ambient noise but extends to areas of research that include acoustic propagation, computer modeling, marine geophysics, signal processing, and oceanography.

The first three examples deal with the beam noise measured by a towed line array. The original data consist of time-averaged beam noise levels at a given frequency for many steering angles that range from forward endfire to aft endfire. Since the line array has conical beam patterns, the absolute direction from which signal and noise arrive at the array cannot be determined from

measurements on a single array heading; a left-right ambiguity is inherent in the data as is illustrated in the symmetry of the beam noise curves in Figure 1b. This ambiguity must be resolved to determine the best heading for detection (the operator's question), but it doesn't need to be resolved to determine the beam noise statistics for a longer array (the design engineer's question). A different type of processing is required in each of these two cases.

Now consider the requirement for the engineer to design a high-speed ASW sonar array with fine spatial resolution and low beam noise levels. Estimates of the mean beam noise levels for the new array must be obtained. The measured beam noise data of a much shorter conventional towed array would not have the same mean level statistics as data acquired in the same noise field by a longer array with much narrower beamwidths. This effect is illustrated by the two different plots of mean beam noise levels in Figure 1b. The statistics for a single dominant source would be about the same, but the statistics would be different when there are many sources or if the ambient noise is distributed over azimuth angle as is often the case.

The mean beam noise levels measured by a given towed line array can be used to estimate the corresponding levels for another towed line array by the following procedure. The array response characteristics responsible for the spatial smoothing inherent in the data are deconvolved from the data to get an estimate of the noise field without the smoothing effects of the array. The iterative technique by Wagstaff and Berrou (1984) is an effective way to obtain this estimate. In terms of the curves in Figure 1b, the procedure is to use one of the beam noise curves to generate a spiked field similar to the spiked field in Figure 1b but without the left-right ambiguities being resolved. This ambiguous noise field estimate is then used to generate the other beam noise curve or any other beam noise curve desired. This sampling process can be done for response patterns corresponding to arrays that range in length from very long (solid curve in Fig. 1b) to relatively short (dashed curve in Fig. 1b). The beamwidths of such a collection of arrays might run from 0.5° to 10°. When this process is repeated for several data sets and the beam noise levels accumulated according to beamwidth and beam noise level, the results can be presented in a format called the Azimuthal Anisotropy Cumulative Distribution Function (AACDF) plot. Figure 2a presents a typical AACDF plot. The ordinate is the beamwidth and the abscissa is the percent of azimuth angle the beam noise level would be less than a given amount. The curves are for equal beam noise level. Essentially this plot presents the statistics

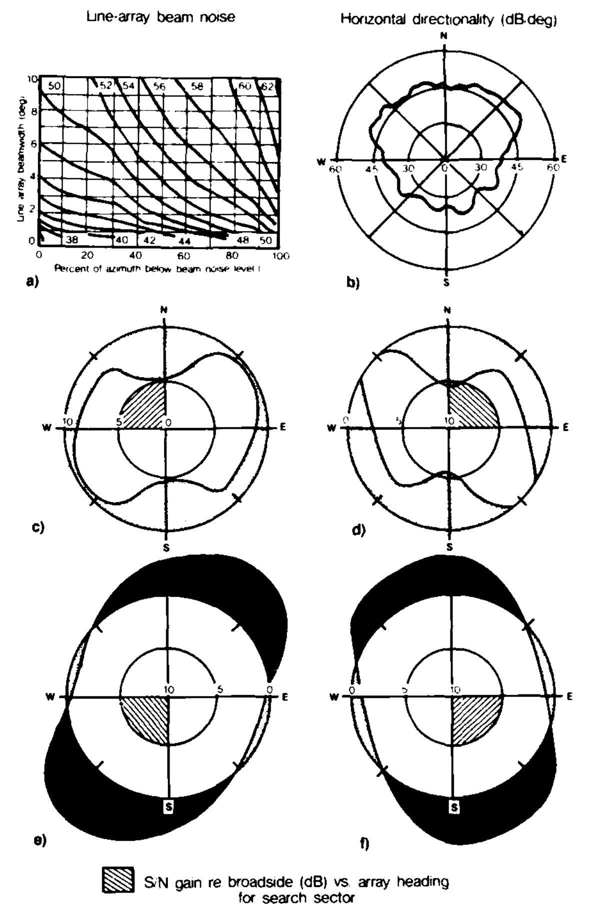

Figure 2. Example of products derived from towed line-array beam noise data. (a) Azimuthal Anisotropy Cumulative Distribution Function (AACDF) plot; (b) ambient noise horizontal directionality plot; (c-f) array heading roses.

of how wide (azimuthal width) and how deep (beam noise level) the "holes" in the noise field are. Since the AACDF is an ordered collection of cumulative distribution functions, it can represent an unlimited amount of data.

The ACCDF plot in Figure 2a was generated from the simulated beam noise data obtained in the modeling referred to previously. The plot is for site 5 of Figure 1a and for a given frequency, but it is not unique to the array that made the simulated measurements. In fact, the mean beam noise levels for any other line array (for that frequency and location) can be obtained from this plot, provided the beamwidths of the array are within the range of the plot, 0.5° to 10°. For example, consider an array that has a beamwidth of 2°. Mean beam noise levels less than about 48 dB will be measured by that array over 45% of azimuth space and less than about 54 dB over

80% of azimuth space. However, the corresponding values for an array with an 8° beamwidth would be about 56 dB and 60 dB respectively. If only a single mean beam noise level were desired, 46 dB for the 2° beamwidth array and 52 dB for the 8° beamwidth array could be used (i.e., the 50 percentile values). However, a distribution function is more realistic and more powerful, and the AACDF plot contains an azimuthal (spatial) cumulative distribution function on each horizontal line (corresponding to a given beamwidth). Hence, by using the AACDF plot, the mean beam noise levels for a particular array can be easily obtained by the engineer, and it is presented in terms he understands.

The mean beam noise data that were used to create the AACDF can also be used to estimate the mean ambient noise level as a function of azimuth provided the data sets were acquired on at least three (preferably more) different array headings (see Wagstaff, 1978). A polar plot of the unambiguous mean ambient noise level as a function of azimuth is commonly called a "noise rose." Although a noise rose has been generated from ambiguous beam noise data acquired by a towed line array, it has no ambiguities. Figure 2b presents an example of a noise rose obtained from the same ambiguous towed line array data that were used to produce the AACDF plot in Figure 2a. Such a noise rose can be used by an operations research analyst to estimate the mean beam noise levels for any array, whether the array is linear, circular, planar, or spherical, provided the beam is along the horizontal and the noise field is concentrated near the horizontal. The latter is generally true at frequencies below about 200 Hz where the noise from distant shipping is usually dominant and arrives at the array at nearly horizontal angles. For example, consider a spherical array with a beam having a 10° beamwidth. Such an array steered to the northeast in the noise field represented by Figure 2b would measure 57 dB (47 + 10 log 10°/1°). This ignores sidelobe contributions that could be easily estimated and included.

Since the noise rose provides an estimate of the mean ambient noise level as a function of azimuth angle, it is also useful for checking the accuracy of ambient noise models. A corresponding plot generated by a noise model can be compared with the measured noise rose to determine whether the noise source levels are correct and the noise source spatial distributions (or geographic positions) are adequately modeled. Agreement between the measured and modeled omnidirectional ambient noise levels can happen by coincidence, but this is not true for the shapes of the noise roses. Disagreement along an azimuth indicates that something is in the acoustic propagation environment or the noise source distribution along that azimuth that the noise model does not include or properly model. The deficiency in the model can often be determined and corrected once the azimuth is known. For example, if a shipping lane was incorrectly modeled to the south instead of to the north, where it actually was, the modeled and measured omnidirectional ambient noise levels could agree, but the error would be clearly evident by the disagreement in the measured and modeled noise roses.

Unlike the engineer who selects the design parameters of the sonar system, the sonar operator can control only the way the sonar is used to improve his chances for detecting submarines. One very important parameter in his control is the heading of the tow ship (and therefore the heading of the towed array). Data bases for improved detection performance as a function of array heading would be very valuable to such an individual. This need was generally ignored until recently, when NORDA researchers devised a statistic and presentation format to address this problem in terms that were meaningful to the sonar operator. Presently, a data base is being generated at NORDA to address this need. A description of the statistic and data base presentation format is given below.

Neither of the plots in Figure 2a or Figure 2b will easily permit the sonar operator to determine the best towed array heading to maximize the chances for detecting a submarine, although the same measured beam noise data are used to generate the AACDF plot and the noise rose that must be used to determine the best array heading for detection. This is done by determining the signal-to-noise ratio (S/N) for all possible array headings and then choosing the heading that will maximize the S/N within the operational constraints imposed on the allowable headings. To make the problem tractable, the sector for detection is specified in advance. The problem can be simplified further by assuming that the signal received by the array is independent of relative bearing (the angle relative to the array axis). In addition, the S/N performance is compared to broadside S/N performance, such that the answer is the gain above broadside performance that can be expected for a given array heading. Furthermore, since the performance is relative to broadside performance and is not in absolute values, a single result applies to all towed line arrays at that location, not just the particular array for which the calculations were performed. The rationale behind normalizing to broadside performance is that the broadside beam is the narrowest of all the beams, and in a cylindrically isotropic noise field, it would give the best performance. This normally will not be the case, since realistic noise fields are usually quite directional in nature.

A plot that gives the S/N gain improvement over broadside performance can be generated from the noise rose, since the array beam noise for any array heading and beam steering angle can be estimated from the noise rose. Beam noise estimates are obtained by convolving the beam patterns of the array with the noise rose. The mean beam noise levels of the beams with steering angles within the detection sector are averaged, and the resultant is subtracted from the average noise level of a broadside beam in that sector. The result is plotted along the azimuth of the array heading and represents the S/N gain improvement over broadside performance for detecting targets in the detection sector for the array heading along that particular azimuth. When this calculation is carried out for all possible array headings and is plotted in polar form, array heading plots (such as Figs. 2c-2f) are obtained. Each of these plots is for a different detection quadrant. The specific quadrant for each is denoted by the cross-hatched area. Sectors with other orientations and widths could have been chosen; however, these sectors (the four principal quadrants) are sufficient to illustrate the value of the array heading roses.

The array heading roses in Figure 2 correspond to the same noise field as do the AACDF plot and the noise rose in Figures 2a and 2b and were derived from the very same beam noise data. The points on the curves outside the large circles of the array heading roses correspond to array headings for which there is a S/N gain improvement over broadside performance for detection of targets in the detection sector (cross-hatched sector), while the associated value indicates how many decibels of improvement to expect. The points on the curves inside the large circles correspond to array headings for which the S/N gain performance is degraded relative to broadside performance, while the associated value gives the expected degradation in decibels. The plots aid in selecting the best array headings for detection. The headings in the black areas (azimuths where the curves are outside the large circles) should be chosen and the headings in the gray areas (azimuths where the curves are inside the large circles) should be avoided if possible.

Given array heading plots similar to those in Figure 2, it is an easy task for the sonar tactician and sonar operator to select the best array heading to maximize detections in a particular sector, within the constraints imposed by their current operations (i.e., compatible with sea state or transiting requirements). For example, if the array heading rose in Figure 2e is considered, the sonar operator has a wide latitude in selecting array headings that will provide better detection performance than would be expected with the broadside beam. Array headings within the 125° wide sectors centered at 022° and 212° should give performance improvements of up to 6 dB. On the other hand, array headings outside these two sectors would give performance about 1 dB worse than broadside beam performance. However, when the detection sector (cross-hatched sector) is to the northwest and northeast (see Figs. 2c and 2d), none of the headings will give better than broadside performance, and the possible degradation is as much as −6 dB for some headings. In addition, the headings that give the best S/N gain performance are localized to small sectors, while the headings corresponding to S/N gain degradation are spread over broad sectors. This is not the case for the detection sector to the southeast (Fig. 2f). The azimuth ranges of favorable headings are about 100° wide centered around 175° and 355°. The extent to which an unfavorable array heading can degrade the S/N gain improvement in this case is limited to about 1.5 dB, several decibels better than the two previous cases.

The three types of plots in Figure 2 illustrate methods of processing and formatting array beam noise data to create data bases for different applications. The AACDF plot presents a parameterized beam noise data base for a technically oriented individual. The array heading rose presents S/N gain improvement as a function of array heading to the sonar tacticians and operators. Finally, the noise rose is useful to the researcher studying the ambient noise and the noise source distributions. Each of these three data formats in Figure 2 conveys a different type of information to a different user but all were derived from a common source—the beam noise data.

The need for data bases to support the design and utilization of ASW sonar systems is not limited to measured sonar performance data. Data bases are also required to support modeling sonar system performance in areas and for situations when measured results do not apply. For example, in a time of war the shipping traffic in an ocean basin is likely to be reduced and the traffic patterns altered to minimize exposing the ships to hostile submarines. Beam noise data previously collected in the basin during peacetime would not be representative of the wartime situation. Such data, however, if documented with the appropriate acoustic, oceanographic, and noise source data bases, would be useful in assessing the validity of a model to extrapolate the sonar performance to the wartime situation.

Historical shipping is one of the ambient noise source data bases often used in the sonar performance extrapolation process. Several statistics and formats have been used

to construct shipping data bases, none of which seems to be ideal. This is probably due to the complex nature of shipping.

The difficulty in devising meaningful shipping data base statistics and presentation formats is illustrated by the two ship position plots in Figures 3a and 3b. These data result from two of ten observations of ship positions conducted on different days in the southern Baltic Sea during February. Comparison of these two plots illustrates the highly variable nature of the ship's positions in time and in space. Even for a smaller time scale, such as a few hours difference, the two corresponding ship positions plots would be significantly different from each other because the ship movement forms tracks, and the positions are simply points on the tracks corresponding to a particular time. As the time increment over which the shipping is considered increases, the tracks become longer and the concept of an average position makes less sense. For this reason the shipping density statistic has been adapted by the Navy for use in sonar performance modeling.

Shipping density focuses attention on standard geographical areas and provides an average occupation statistic. Figure 3c illustrates a shipping density plot corresponding to the 10 observations of ship positions previously mentioned. Two observations from the set of 10 are those plotted in Figures 3a and 3b. The standard geographical area in this case is 0.5° latitude by 1.0° longitude. The number in each standard area corresponds to the average number of ships observed in that area for the 10 observations. Additional examples of historical shipping data bases are given by Ross et al. (1974) and Dyer (1973).

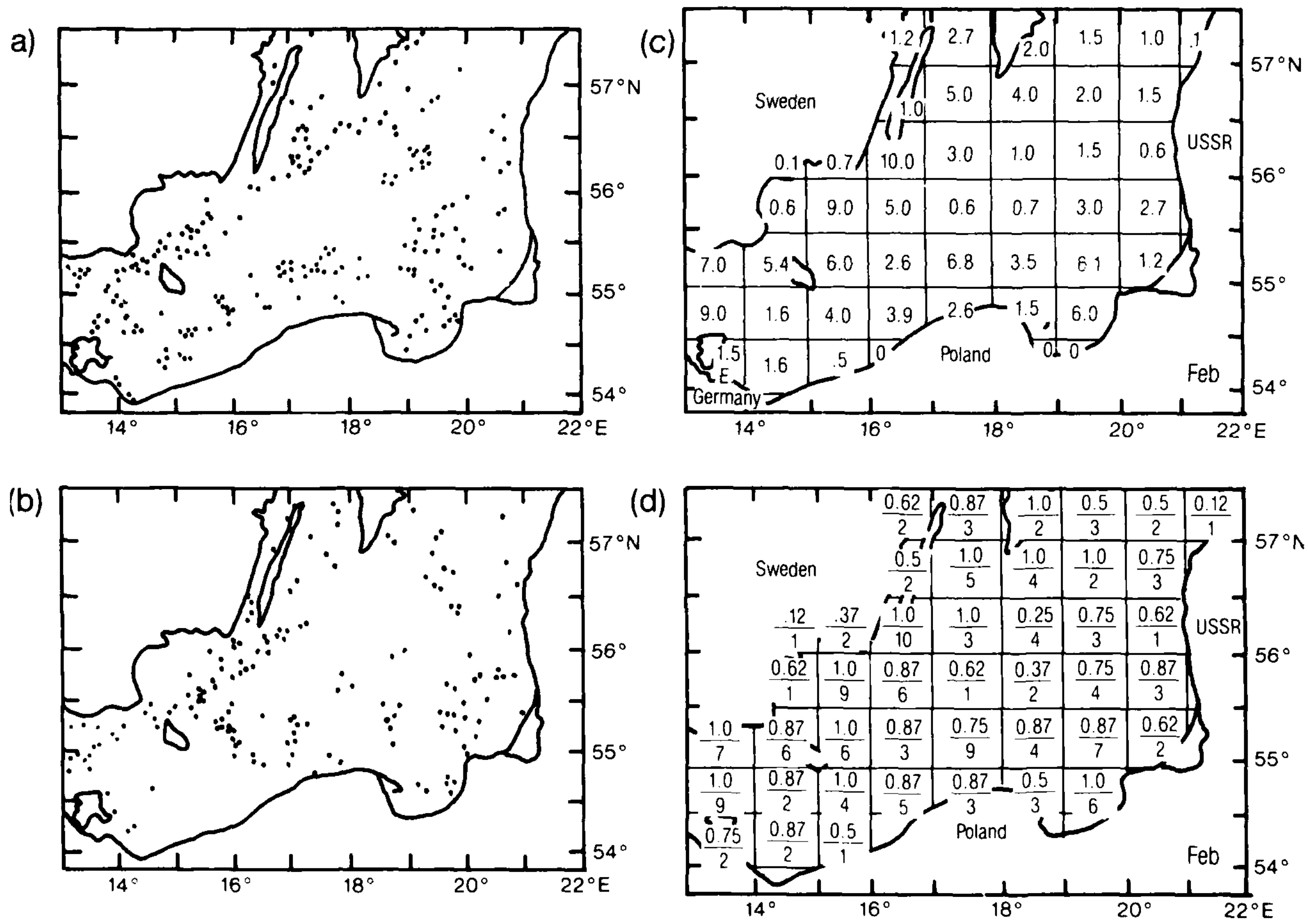

Figure 3. Example of shipping data plots of the southern Baltic Sea. (a,b) "Fly speck" ship position plots for two different times; (c) shipping density plot (average number of ships observed in each area; (d) plot of probability of an area being occupied by ships (above line) and median number of ships, given area is occupied by a ship (below line).

The advantages of shipping density are that it provides a statistic that permits a shipping data base to be developed and a format for that statistic to be presented and utilized. Furthermore, it is readily apparent at a glance where major shipping activity occurs and some indication of where there is not, i.e., 10.0 ships within 56°N–56.5°N by 16°E–17°E and 0.1 ships within 57°N–57.5°N by 21°E–22°E. A disadvantage of shipping density is that it fosters a notion that shipping is a continuum, rather than a distribution of discrete quantities, and this encourages it to be modeled as a continuum. This spatial smearing of the ship's positions to conform to the density continuum is a severe problem that is not fully appreciated by modelers, or the Navy as a whole, and can be responsible for erroneous results. For example, the spatial smearing of the ship's positions has a similar azimuthal smearing affect on the beam noise data as the azimuthal smearing caused by decreasing the array length, illustrated by the two beam noise curves in Figure 1b. Furthermore, there is no physical significance of a fractional ship (i.e., a component of density less than 1), and it is not clear how it would be correctly modeled. This problem can be illustrated by a simple example in which one ship crossing an ocean basin on a seldom-traveled route is observed on four observation days out of ten to be the only ship in each of four standard areas. The corresponding densities for these four areas would each be 0.1 ships/standard area. This situation would be modeled with 0.1 ships in each of the four areas. Not only does 0.1 ships not make physical sense, but one-tenth of the original ship would appear in four different standard areas at the same time, which makes even less sense. Furthermore, one-tenth of the noise from that ship would appear at four different azimuths in the beam noise modeling for sonar performance prediction.

Researchers at NORDA believe that the advantages of shipping density can be maintained, while eliminating some of the disadvantages by using different statistics, instead of density, that will permit and encourage the shipping to be modeled as discrete, whole ships. Such statistics could be obtained by processing the original shipping surveillance data in a slightly different manner. Two statistics could be calculated to replace the single density statistic. The first statistic calculated for each standard area is the probability of the area being occupied by at least one ship. For example, if ships are observed in a standard area during eight of ten observations, the corresponding probability of occupation would be 0.8. The second and accompanying statistic calculated for each standard area is the median (not average) number of ships observed in the area, given the area is occupied. These two statistics, then, replace the single shipping density statistic, and the standard geographical area format is retained. An example of these new historical shipping statistics is given in Figure 3d for the data set previously discussed. The probability of occupation is above the horizontal line, and the median value is below the line in each standard area.

Now consider the results in Figure 3d, which contains the probability of occupation statistics and the median number of ships given area occupation, and compare them with the shipping density results in Figure 3c. The areas that are infrequently populated by ships are obvious from the low probabilities of occupation, i.e., less than 0.5, while this is not necessarily true in the case of shipping density. For example, the standard area bounded by 18°–19°E and 56.0°–56.5° has a density of 1.0, but the probability of occupation was only 0.25. Such a low probability suggests that the chances are slim that the area would be found occupied at some random time in the future. As a result, this area would probably be considered free of shipping for sonar performance modeling purposes. Based on shipping density, however, the modeling would be done with one ship in the area. The former approach would be more representative of what is likely to occur.

The median number of ships in a standard area will always be an integer. This number emphasizes the discrete nature of shipping and encourages modeling individual ships at discrete locations. This entity is more realistic than density data and should give results in better agreement with data. However, if density information is absolutely necessary, an approximation can be obtained by multiplying the probability statistic by the median statistic. In the previous example, both the density and the approximation to the density (0.25 times 4 ships) gives 1.0. Hence, the cost due to doubling the data base to provide two statistics instead of one (density) is more than offset by the usefulness of the data base. Future NORDA shipping data bases will be provided in these new statistics, as well as in the density statistic, to permit the user to select the one that makes the most sense for the particular application.

Summary

The task of satisfying the Navy's requirements for data to support sonar design, utilization, and performance prediction is monumental, considering the temporal and spatial variability of all parameters involved and considering the limited budget and resources with which this must be done. Therefore, it is mandatory that the R&D community be innovative and clever in processing and

reporting relevant data to maximize its utility to the various users. This requirement is facilitated when the researcher understands and is motivated by the following.

- The statistic presently provided in the data base should be changed if it is not the best one to describe the characteristic of the data that is the most important to the user.
- The data base format should be changed if it is not the best one to facilitate the user's understanding and correct utilization of the data base.
- Statistics should be devised and data base formats should be chosen to answer particular user's specific questions.
- Data base formats should be chosen that extend the application of the data base to as many different situations, systems, and users as possible without being unnecessarily complicated.

The researcher must provide the user with a data base that the user needs and can apply for the data base to be fully utilized.

As a primary supplier of environmental/acoustic data bases for the Navy, NORDA has taken the lead in understanding the needs of the individual data base user and devising statistics and data base formats that facilitate the user understanding and correctly using the data bases, and NORDA will continue to do so in the future.

References

Ross, D., J. Mahler, and L. Solomon (1974). *Navy Interim Shipping Distribution Model*, Enclosure to Planning Systems, Inc., memo of 17 Dec 1974.

Dyer, I. (1973). Statistics of Distant Shipping Noise. *Journal of the Acoustical Society of America* 53(2), 564–570.

Wagstaff, R. A. (1978). Iterative Technique for Ambient-noise Horizontal-Directionality Estimation from Towed Line-Array Data. *Journal of the Acoustical Society of America* 63(3), 863–869.

Wagstaff, R. A. and J. L. Berrou (1984). A Fast and Simple Nonlinear Technique for High-Resolution Beamforming and Spectral Analysis. *Journal of the Acoustical Society of America* 75(4), 1133–1141.

Ocean Technology

James H. Elkins
Ocean Technology Division

Ocean technologists at NORDA are performing engineering research and development based upon a wide spectrum of new, emerging, state-of-the-art technologies and capabilities directed toward the support of existing or projected Navy operational requirements and in-house projects for solving measurement problems. Some recent successes are listed.

- The Airborne Data Acquisition and Processing System, which has been completed and transitioned to the user. Similar systems have been requested from other activities.
- The Deep Towed Array Geophysical System was successfully completed with engineering test at a tow depth of 5100 m.
- Several deployments of the Versatile Experimental Data Acquisition Buoy system were successful (Fig. 1).
- Development and multiple deployments of the Cavitation Ocean Profiling System were completed.
- A Vertical Line Array for the follow-on mine program was tested.
- Two studies were completed (submarine counterdetectability and magnetic capability and safety study resulted in development effort) and several new projects initiated (Ice Buster, ice thickness measurement, and inverted echosounder).

NORDA's ocean technologists plan to attract more programs from external sponsors, build credibility in basic research, and maintain support of the Navy community. Emphasis will be on innovative thinking in the exploratory development area and generating new concepts to solve old, current, new, or projected problems in response to Navy operational requirements.

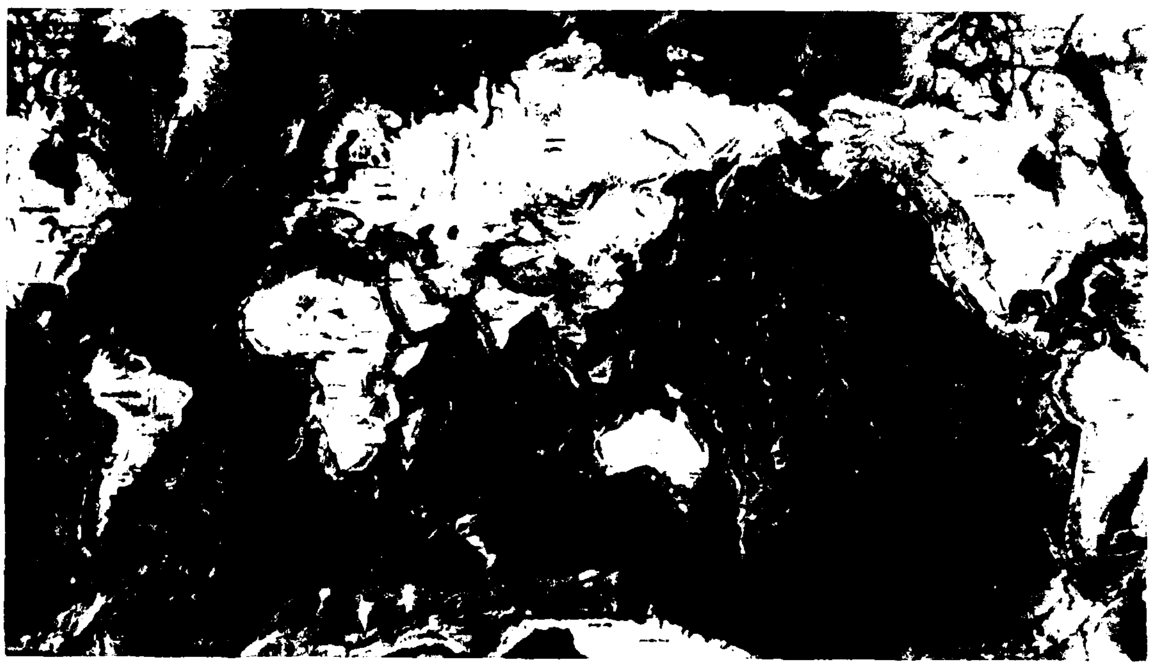

Figure 1. Versatile Experimental Data Acquisition Buoy system deployment locations (indicated by circles).

Development of a Deep-Towed Seismic System: A New Capability for Deep-Ocean Acoustic Measurements

Martin G. Fagot and Stephen E. Spychalski
Ocean Technology Division

Abstract

The development of a deep-towed seismic profiling system has been completed after four years of design, fabrication, and testing. This system provides the capability to determine the detailed acoustic character of the sea floor and upper 500–1000 m of subbottom structure. The system is designed for tow depths of 6000 m while operating at an altitude of 100 m above the sea floor. The major components of the system include a sound source located in the deep-towed vehicle, which operates over a frequency range from 260 Hz to 650 Hz at a peak source level of 201 dB re 1 micropascal at 1 m; a 24 channel, 1000 m long array attached as a tail to the deep-towed vehicle; a duplex digital telemetry link to communicate with the deep-towed system over a coaxial tow cable; a digital data record system; a real time engineering data display system; a short baseline navigation system; handling hardware to deploy and retrieve the system; and two instrumentation vans to support system operations. This paper discusses the unique hardware developed for the deep-towed seismic system and focuses on the acoustic subsystems. Also reviewed is a performance prediction analysis initially performed to define geoacoustic parameter measurement improvements achievable with a deep-towed configuration. Field measurement engineering results acquired during the system's final performance evaluation are presented. Data was acquired at tow depths of 4500 m during the September 1984 evaluation.

Introduction

The Naval Ocean Research and Development Activity (NORDA) carries out broadly based research and development in ocean science and technology to understand the effects of the ocean environment on Navy systems and operations. Specifically, one area of responsibility is developing definitive models of the ocean floor and subbottom as a transmission medium that refracts, diffracts and dissipates, as well as reflects, acoustic energy. These models are used to predict, and thus improve, the performance of naval systems that acoustically interact with the bottom. Critical for developing these models is high-resolution data to describe the geological, geophysical, and geoacoustical character of the deep-ocean sea floor and upper subbottom structure. These high-resolution data can be obtained using a low-frequency sound source and multichannel array system capable of operating at an altitude of 100–500 m in ocean depths of 6000 m. This configuration is depicted in Figure 1. A development program entitled "Deep-Towed Array Geophysical System" (DTAGS) was initiated in 1981 to provide a hardware suite to meet this high-resolution data requirement.

System performance prediction studies[1,2,3,4,5] showed substantial improvement in measuring geoacoustic parameters with the DTAGS configuration. A comparison between the deep-towed configuration and a surface-towed configuration for measuring a critical geoacoustic parameter, interval velocity, as a function of layer thickness is given.

The initial hardware development focused on a Helmholtz resonator sound source system. This unit was successfully tested to a depth of 2000 m in December 1981.

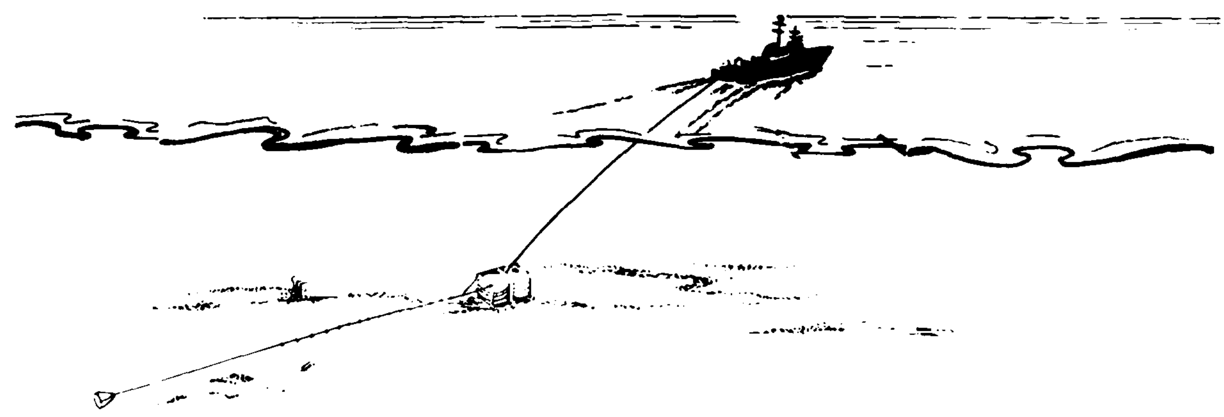

Figure 1. Deep-towed system configuration.

Subsequent effort concentrated on developing the multichannel hydrophone array (672 m long) and high data rate telemetry system. These systems were integrated with the sound source system and sea tested to a depth of 4500 m during the summer of 1983. The hardware development concluded with extending the array to a total length of 1000 m, fabricating a digital data record system, and incorporating into the system a short baseline navigation system. The total hardware suite was tested to a depth of 4500 m in September 1984.

Discussion

Performance prediction analysis

The basic objective of the deep-towed system is to provide measurements for extracting the geoacoustic parameters of the near subbottom. Such parameters include sound speed as a function of depth and vertical thickness between acoustic reflectors. The geoacoustic parameter addressed here is termed interval velocity, where interval velocity is defined as the RMS sound speed in the layer (interval) of interest. For a layer of constant sound speed, the interval velocity reduces to simply the sound speed in the layer. Analysis by Gibson et al.[6] and Gholson and Fagot,[4] more advanced than that presented here, addresses the problems associated with estimating sound speed gradients.

Estimating the interval velocity of a layer bounded above and below by acoustic reflectors can be accomplished by exercising the Dix[7] equation shown below:

$$Vi = \left[\frac{V_{A2}^{\,2}\, T_2 - V_{A1}^{\,2}\, T_1}{T_2 - T_1}\right]^{1/2}$$

Errors in measuring normal incidence travel time (T_1, T_2) were modeled as zero mean independent errors uniformly distributed with bounds ± Tpick where Tpick is the precision of measuring (picking) reflected energy arrival times. Errors in the measured array velocities V_{A1}, V_{A2} are much more difficult to model. The approach was to assume that the fitted T^2 (X^2) curve never departs from the true T^2 (X^2) by more than that associated with the picking error Tpick. Further, it is assumed that the just-mentioned is reliably true over a horizontal span, X, equal to one-half the physical array length. The last assumption is equivalent to assuming the array is one-half its actual length and a moveout curve is successfully fitted (± Tpick) through returns from every hydrophone group. Stoffa[8] and simulations using realistic signal-to-noise ratios indicate the one-half array length assumption to be reasonable for an array with 24 equally spaced groups. This error analysis allowed for system optimization, as well as general system performance prediction.

This type of error analysis was used in comparing a surface-towed system with a deep-towed system. A geoacoustic model, along with a surface versus deep-towed system comparison, is shown in Figure 2. The surface-towed system differs from the deep-towed system both in array length and altitude above the layer of interest. The increasing error for small Z is due to the water column sound speed dominating the measured array velocity. This effect is much worse for the surface-towed system, since the water column is much thicker.

Hardware description

A block diagram of DTAGS hardware configuration is given in Figure 3. The sound source transducer and power amplifier system, telemetry system, and associated electronics are located within a deep-towed vehicle (fish)

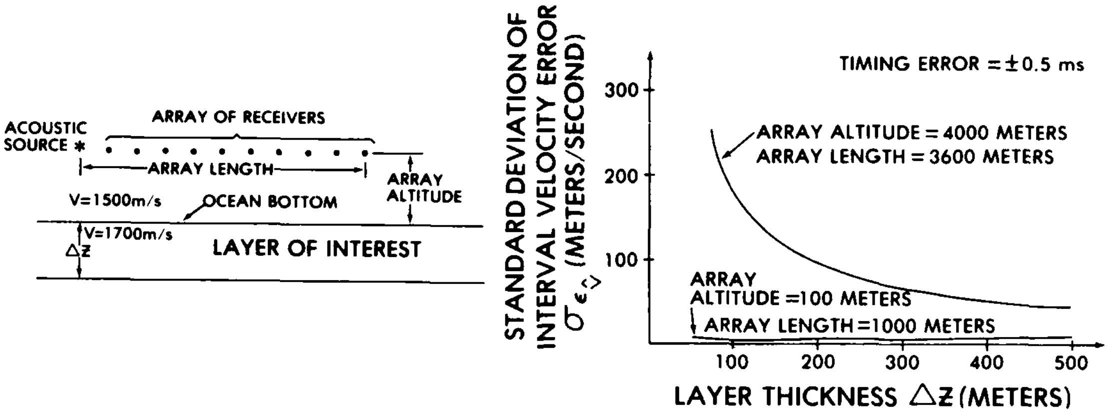

Figure 2. Geoacoustic model and performance comparison between a surface-towed and deep-towed system.

towed at the head of a multichannel array. The deep-towed system is tethered to the tow ship with a 9150-m long coaxial steel tow cable. A duplex telemetry system communicates via the tow cable with the deep-towed system. Data from the fish system is then digitally recorded at the tow ship. Monitoring of system performance is through a real-time display system. The position of the fish relative to the tow ship is provided by a short baseline navigation system. Global position is obtained through satellite and Loran-C navigation. A tow cable heave accumulator and an array handler winch constitute the system handling hardware. The operation systems are located in a portable van with a maintenance facility and spares storage located in a second van. The component designs of these major subsystems are optimized to meet the basic geophysical data requirement while still maintaining a hardware suite that can be easily deployed, operated, and maintained. A detailed description of the total hardware suite is described by Fagot.[9]

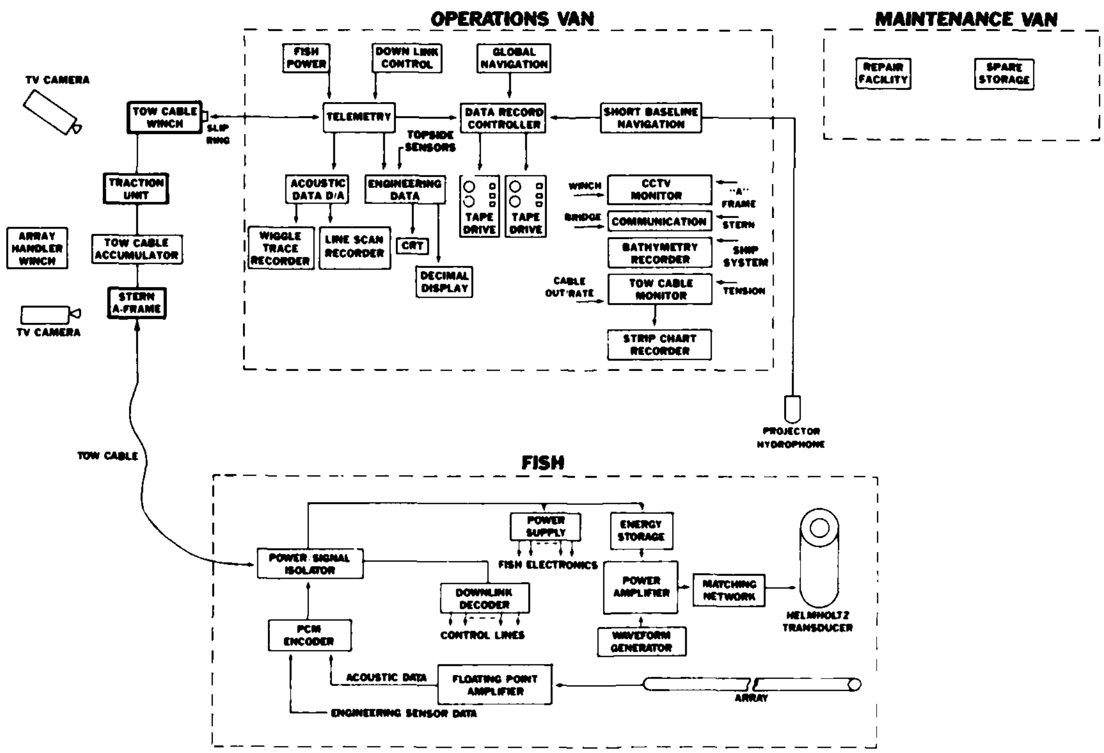

Figure 3. Block diagram of deep-towed system hardware configuration.

Sound Source System—The sound source system hardware consists of a piezoelectric Helmholtz resonator transducer and a power amplifier. The amplifier was designed and packaged for operation at full depth. The transducer and power amplifier are mounted together in the deep-towed vehicle (fish) as shown in Figure 4. Also identified are other major subsystems located on the fish.

The sound source system is capable of full performance from near surface to full ocean depth. The system is capable of a nominal peak source level of 201 dB//1 μPa @ 1 m. This level can be achieved over a frequency range from 260 Hz to 650 Hz. Directivity over this range of frequencies is omnidirectional. Output pulse length is programmable from 5-ms minimum to a maximum of 250 ms in duration. The system is capable of a full power 250-ms output pulse once every 12 seconds.

The transducer consists of a Helmholtz cavity and orifice driven by five piezoelectric-segmented ceramic ring drivers. As built, the transducer is approximately 0.7 m in outside diameter, is 1.1 m long, and weighs 800 kg. The design, development, and fabrication of this transducer was performed by the Naval Research Laboratory, Underwater Sound Reference Detachment and is described by Young.[10]

A Class S switching amplifier was chosen as the driver for the Helmholtz resonator transducer due to its small relative size compared to a linear amplifier, such as a Class B. The Class S power amplifier system weighs approximately 232 kg (including pressure vessel) and is housed in a 0.6 m diameter spherical pressure vessel. Due to the inefficiency of a deep water broadband sound source, the power amplifier is required to deliver 16 kVA of reactive power. Other requirements of the system called for control of output waveshape and frequency. Also due to inaccessibility and remote location of electronics during an at-sea operation, reliability of the power amplifier was of prime concern. The design, development, and fabrication of the power amplifier was performed by NORDA.

The power amplifier system located at the tow vehicle consists of a waveform generator, power amplifier modules, energy storage bank, and a load matching network. Four drive waveforms are stored in an erasable, programmable, read only memory (EPROM) that is programmed prior to deployment. Selection of the source drive waveform, along with the source firing key signal, is accomplished via the downlink telemetry system. Energy for the highpower output pulse is stored in a 0.132 farad capacitor bank. This bank is trickle charged between pulses at an average rate of 300 watts via the tow cable. The power

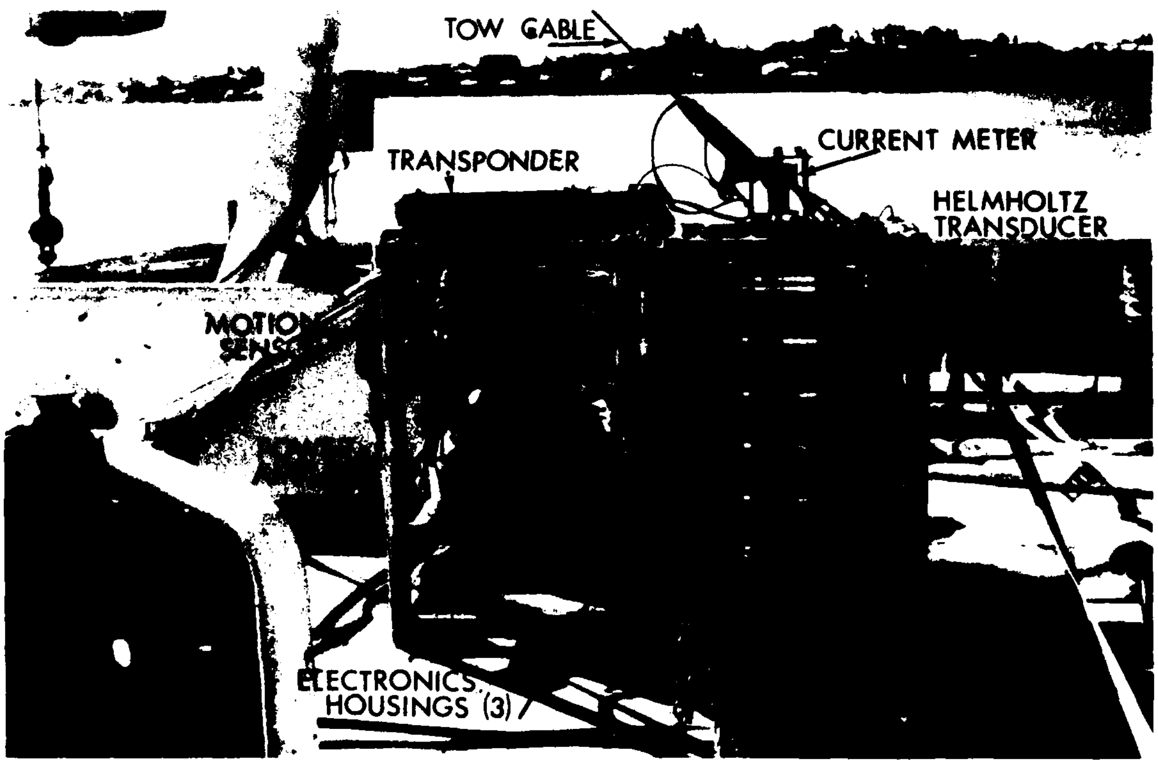

Figure 4. Deep-towed vehicle (fish) with major subsystems identified.

amplifier module controls the power drive level and waveshape supplied to the Helmholtz resonator transducer. Power transfer to the source is optimized through the load matching network, which consists of a power factor correction network and an impedance matching transformer. The matching network is housed in a separate pressure vessel.

Array System—The array design selected for the deep-towed geophysical system is a multichannel hydrophone array similar to the type used by the marine exploration community. The standard oil-filled design, hose, spacers, and oil-immersed electromechanical coupling presently used are compatible with high operating pressures. The array is 1000 m long and consists of 12 active sections that contain a total of 48 hydrophone groups. Only 24 groups will be used for a specific configuration to reduce the telemetry data rate requirement. A 2-m interconnect section is located at the head of each 82-m active section. Each 82-m active section has an outside diameter of 4.61 cm; the 2-m interconnects are either 7.62 cm or 10.16 cm, depending on the sensor suite, and a 50-m stretch section at the head of the array has a diameter of 6.6 cm. The entire array is designed to have a tensile strength greater than 1200 kg and for a maximum tow speed of 1.5 m/sec (3 knots). A drogue parachute is attached to the array tail for tow stability. The interconnect sections contain heading sensors, depth sensors, and hydrophone preamplifiers. Each active section contains four hydrophone groups. Figure 5 shows the array on the handler winch.

The array acoustic design is tailored to the deep-tow geophysical system operational performance requirements. Forty-eight hydrophone groups are spaced uniformly along the array with a 21-m separation between adjacent groups. Each hydrophone group consists of six elements with a total length of less than 60 cm. The individual hydrophones are a piezoelectric cylinder type that are tolerant to high operating pressures. Outputs of the hydrophones are connected to the preamplifiers located in the 2-m interconnect section at the head of the associated active section via a twisted pair shielded cable. Because of the large separation between the hydrophone group and preamplifier (approximately 74 m for the last group of each active section) and the low group capacitance, a balanced input charge amplifier is used for the preamplifier to accommodate these conditions. The combined sensitivity of an acoustic channel (hydrophone group plus preamplifier) is a nominal -150 dB//1 V/μPa with a frequency response from 150 to 1000 Hz. The bandwidth is limited by filters in the preamplifier and can be opened to a band ranging from 10 to 2000 Hz by appropriate component changes in the preamplifier. The self-noise of each acoustic channel is less than 35 dB (// 1 μPa/$\sqrt{\text{Hz}}$) over the operating frequency band, which is less than deep-ocean Sea State 0 ambient noise. Each channel preamplifier has a built-in calibration oscillator with a unique frequency that provides easy channel identification and an in situ functional check of the entire acoustic channel, including the hydrophone group. Gain of the preamplifiers can also be lowered 20 dB by an external control signal.

The array is equipped with a suite of engineering sensors to measure array tow dynamics, such as array shape, tension, and tow attitude. Each interconnect section contains a depth sensor and four heading sensors are spaced uniformly over the array length. A load cell at the head of the array is used to monitor in-line array tension in real time.

Ancillary systems—A number of other subsystems are required to support the deep-towed operations. An overview of these subsystems is presented.

Telemetry System. The telemetry system for the deep-towed geophysical system provides full duplex communication between the tow ship and the tow vehicle via a 9150-m coaxial tow cable. System requirements call for a data transfer rate of 1.5 M bit/sec. The telemetry system is capable of handling tow fish power (300 W) down the cable, as well as the 1.5 M bit/sec pulse code modulation (PCM) uplink data and low data rate FSK downlink control signals.

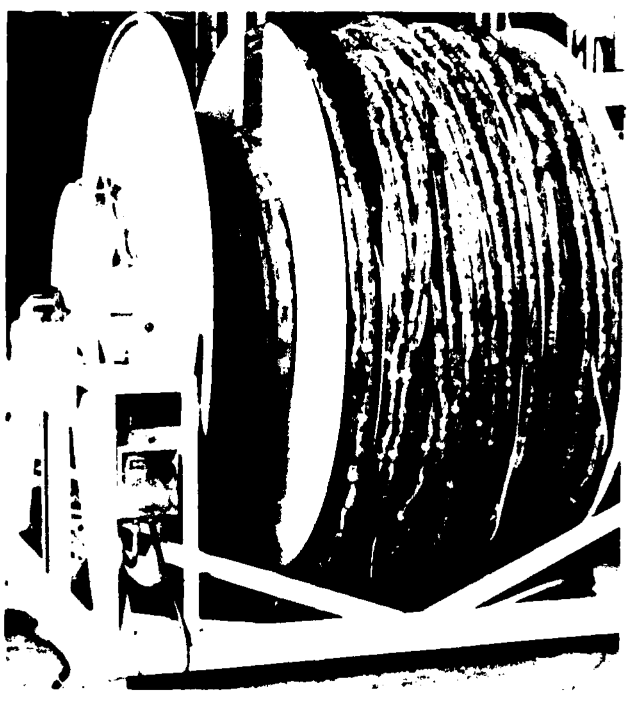

Figure 5. Deep-towed array on the array handler winch.

The acoustic signals from the towed array are digitized by a 12-bit A/D with a 4-bit gain exponent floating point amplifier at a 3125-Hz sample rate. The FSK downlink control system operates at a 10 bit/sec rate. The telemetry equipment contained in the tow vehicle includes the PCM encoder and FSK decoder electronics. Cable equalization circuits are located on the tow ship.

The PCM uplink system provides 30 multiplexed channels for data transmission from the deep-towed vehicle to the tow ship. Twenty-seven of these channels are utilized for transmitting acoustic channel data that has been digitized by a common floating point amplifier (FPA). The FPA low pass filters the data at 800 Hz. The digital outputs of the floating point amplifier are time division multiplexed with two 16-bit frame synchronization words and a submultiplexed engineering sensor channel to form a frame containing thirty 16-bit words. This data stream is Manchester encoded and transmitted to the surface via the tow cable.

The submultiplexed engineering sensor channel is capable of handling 256 sensor channels. Data such as the array depth sensors, array heading, and other engineering sensors are transmitted via these subchannels. The subchannels are also used to transmit subsystem operational status for real-time monitoring by the system operator.

Data Record System. The data record system provides the capability to record the high data rate and large volume of data generated by the deep-towed system. The data is tape formatted in the Society of Exploration Geophysicist's SEG-D (Demultiplexed 2½-byte binary exponent word) as defined by the Society of Exploration Geophysicists.[11] The format provides the flexibility through header blocks to record both the global and short baseline navigation parameters simultaneously with the geophysical reflection data. Thus, each data tape will contain all the information required for geophysical processing.

The ability to play back prerecorded data is also incorporated into the system. The engineering sensor data for the deep-towed system is extracted from the recorded data tape in a format directly compatible with the engineering real-time display system. Also, up to 8 channels of acoustic array data can be input directly into the real-time D/A converter for display.

Real-time display system. The capability to monitor the performance of the deep-towed system is provided by a real-time display system. This system, located in the operations van, includes monitoring, displaying, and recording engineering sensor data from the array and fish located sensors; displaying acoustic array data; monitoring and recording tow ship located subsystem sensor data; and closed circuit television monitoring of the deployment/retrieval handling systems.

Navigation system. The navigation suite consists of two subsystems: a short baseline system to position the fish relative to the tow ship and a global system, Satnav and Loran C, to geographically position the tow ship. The output of both systems is fed to the data record system.

Deep-towed vehicle (fish). The fish is an aluminum open-framed structure (Fig. 4). Since the fish drag is small at low tow speeds (0.5–1.5 knots) in comparison to the tow cable, an unstreamlined structure is employed. The fish envelope size is 1.83 mL x 0.86 mW x 1.35 mH. The fish consists of two substructures of approximately equal size, with a total weight of 1360 kg in air and 1090 kg in water. One substructure houses the Helmholtz transducer, which is shock-mounted to provide vibration isolation. The other substructure houses the sound source power amplifier spherical pressure vessel, two oil-filled junction boxes, motion sensors, a current meter, an array tensiometer, and an acoustic transponder. Three cylindrical pressure vessels containing system electronics are located vertically between the two substructures.

Vehicle heave accumulator system. The ship surge motion effects on the towed system are minimized with a tow cable tension accumulator system. The unit is primarily effective when the fish system is near the sea surface. Incorporated into the system is a cable tension-monitoring sensor. The lead sheave, separate from the accumulator system and located at the tow point, is instrumented with a cable-out sensor.

Array handler winch. The array handler, a large motorized drum (Fig. 5), is used for deployment and retrieval, as well as storage of the array. The winch is mounted near the fish deployment area to facilitate array launch and retrieval.

Tow cable. The tow cable is a coaxial-type construction with two contrahelically wound layers of galvanized, high-strength steel wires wrapped around a coaxial cable core. The core has electrical characteristics similar to RG-8U. The steel wire geometry provides a very low cable torsional characteristic, which eliminates the need for an electrical-mechanical swivel within the tow cable system.

Portable vans. The flexibility to meet a ship-of-opportunity operation scenario is provided by self-contained vans. An operations van and maintenance van are part of the deep-towed hardware suite. The vans are sized to allow air shipment if necessary.

Host ship support. The host ship provides the deep-sea winch, cable traction unit, and the tow point stern

"A" or "U" frame. This set of hardware is generally available for ships engaged in deep-sea geophysical research. The deep-sea winch/traction unit must be capable of smooth and precise control of tow cable movement. Slow, creep, cable in/out speeds are required when lifting the fish off or placing the fish on the deck, and then speeds up to 45 m/min are required for deep deployment and retrieval. The ancillary units are highlighted in Figure 3 by heavy, broader outlines. The slip ring assembly incorporated into the deep-sea winch for termination of the coaxial tow cable is a part of the deep-towed system hardware suite. The ship must be capable of making 0.5 knots (relative the water) on any course in a fully developed Sea State 6, with the ship heading within 45° of the course.

Engineering field test

The final engineering evaluation test was performed in September 1984 while on a transit from Miami, Florida, to St. George, Bermuda. This test concluded the hardware development with extending the array to a total length of 1000 m, fabricating the digital record system, and incorporating a short baseline navigation system.

The sound source system again performed reliably during the test. An excess of 20,000 shot-receive sequences were initiated. The predominant source waveform used was a 260 Hz to 650 Hz linear FM slide with 10% leading and trailing amplitude shading on a 125-ms pulse. Some data was acquired with a 400 Hz, 5-ms pulse. A 20-second pulse repetition rate was typical.

The array also performed well during the test. The array shape typically experienced throughout the test is pictured in Figure 6. The real time display system generates this type figure for tow performance monitoring. Depth data is annotated as D1 through D9 on the figure. Fish depth is annotated as DF with the actual depth value given (4343 m in this case). Also, at the top of the figure are critical tow parameters. They include; tow speed (1.22 knots); array tilt (6°); delta depth between DF and D9 (127 m); depth rate of change (0 m/min); and array tension (245 pounds). The dip at D6 was caused by array low fill oil. For the conditions typified by Figure 6 the tow noise was a nominal 65 dB (//1 μPa/$\sqrt{\text{Hz}}$) over the operating frequency band.

Figure 7 is an unprocessed reflection field trace for a single array group offset 297 m from the source. This type trace is monitored in the field for quality control. The FM slide source waveform was used for this data section. The apparent bottom slope results from a slight change in system tow depth during the two and one-half hours required for the 5.7 km long profile. Static corrections are necessary to correct for this type change.

The seismic data acquired during this engineering evaluation test is being used to complete the geophysical processing software. A short data section has been processed using DISCO, a standard processing package used principally by the oil exploration community.

A processed data section using this package is presented in Figure 8. This is a short section from the same location as the field trace (Fig. 7). An 11-fold CDP stacked section was generated. A match filter routine was used to collapse the FM slide source signature. No static corrections were made for this section. Although this processed section is only preliminary, it does show the potential of the deep-towed system. In particular, the discontinuity

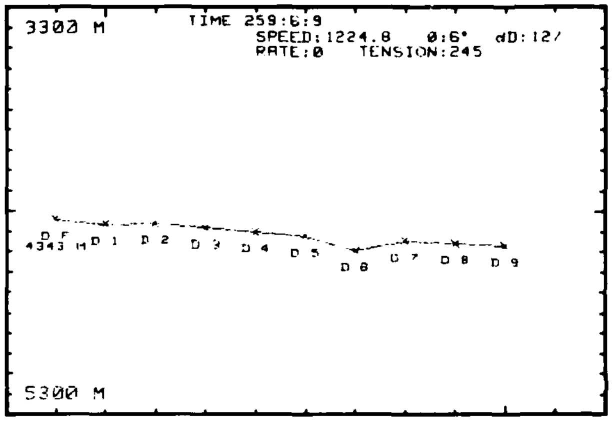

Figure 6. Array shape pictorial generated during field test by real-time display system.

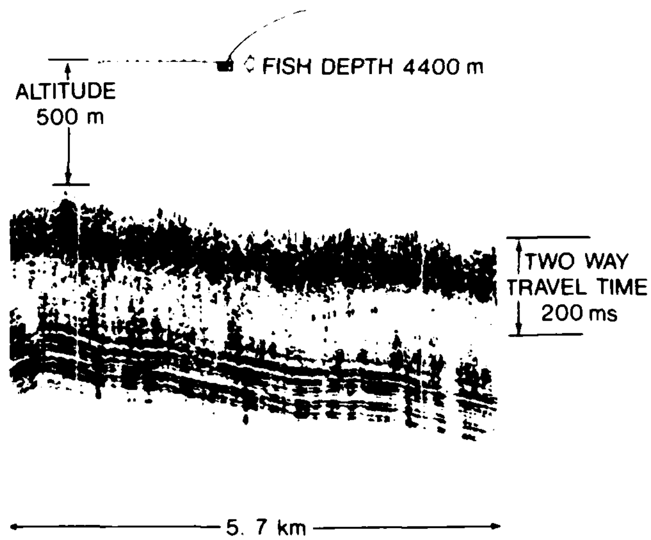

Figure 7. Single channel reflection field trace obtained at a 4400-m system tow depth.

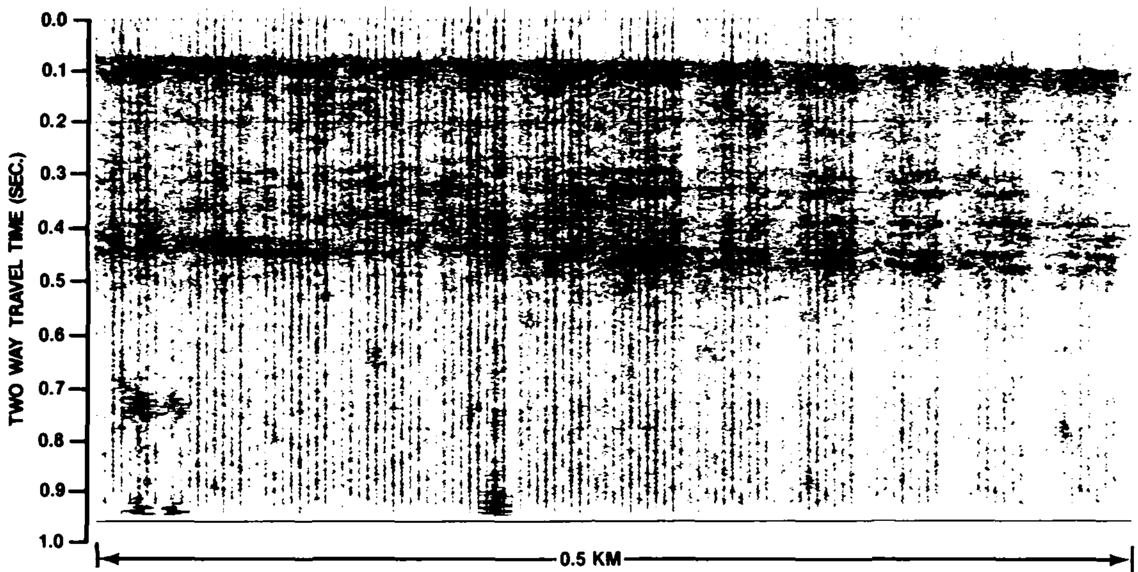

Figure 8. An 11-fold CDP stacked section of deep-tow data acquired at a tow depth of 4200 m.

of beds at 0.3 seconds would be difficult to detect with a conventional surface-towed system.

The present effort focuses on optimizing this standard processing software for the deep-tow data set. Areas of concentration include: static corrections using array depth sensors and moveouts measured for the source to sea-surface to array reflection path; deconvolution techniques to optimize source signature collapse; and interval velocity measurement routines for the high-resolution data set.

Summary

A new capability for deep-ocean acoustic measurements is available with the Deep-Towed Array Geophysical System. The unique hardware suite provides the ability to extract high-resolution geoacoustic parameters. The deep-towed sound source and array and the ancillary support systems have been developed and tested over the past four years. The final field engineering evaluation test successfully operated the total system to a tow depth of 4500 m. The geophysical data acquired during the test is being used to optimize processing software for the deep-towed application.

References

1. Milburn, D. A. and Fagot, M. G., 1979, *The Steady-State Analysis of Candidate Towing Cables for the Deep-Towed Geophysical Array System*, NORDA Technical Note 40, Naval Ocean Research and Development Activity, NSTL, Mississippi.

2. Fagot, M. G., Gholson, N. H., Moss, G. J., and Milburn, D. A., 1980, *Deep-Towed Geophysical Array System-Development Program Review*, NORDA Technical Note 75, Naval Ocean Research and Development Activity, NSTL, Mississippi.

3. Fagot, M. G., Moss, G. J., Milburn, D. A., and Gholson, N. H., 1981, Deep-Towed Seismic System Design for Operation at Depths up to 6000 Meters, presented at the *Offshore Technology Conference*, Paper OTC 4082, Houston, Texas.

4. Gholson, N. H. and Fagot, M. G., 1980, *A Moments Approach for Analyzing Geophysical Reflection Data*, NORDA Report 30, Naval Ocean Research and Development Activity, NSTL, Mississippi.

5. Gholson, N. H. and Fagot, M. G., 1983, A Deep-Towed Sound Source and Hydrophone Array System—Performance Analysis and Design, in: *Handbook of Geophysical Exploration at Sea*, Richard A. Geyer, ed., CRC Press, Inc., Boca Raton, Florida, pp. 267-292.

6. Gibson, B., Odegard, M., and Sutton, G., 1979, Non-linear Least-Squares Inversion of Traveltime Data for a Linear Velocity Depth Relationship, *Geophysics*, 44-2:185-194.

7. Dix, C. H., 1955, Seismic Velocities from Surface Measurements, *Geophysics*, 44-2:185-194.

8. Stoffa, P., 1979, *Design Criteria for a Deep Towed Source and Multichannel Array*, Chute Stoffa, Inc., Nyack, New York.

9. Fagot, M. G., and Spychalski, S. E., 1984, *Deep-Towed Array Geophysical System (DTAGS): A*

Hardware Description, NORDA Report 71, Naval Ocean Research and Development Activity, NSTL, Mississippi.

10. Young, A. M., Tims, A. C., and Henriquez, T. A., 1982, *The Development of a High Power, Low Frequency Underwater Acoustic Source for Use in a Deep-Towed Geophysical Array System*, NRL Report 8633, Naval Research Laboratory-Underwater Sound Reference Detachment, Orlando, Florida.

11. Society of Exploration Geophysicists, 1980, *Digital Tape Standards*, Published by Society of Exploration Geophysicists, Tulsa, Oklahoma.

Ocean Sciences Directorate

Herbert C. Eppert, Jr.
Director

NORDA's Ocean Sciences Directorate comprises four divisions: Ocean Sensing and Prediction; Oceanography; Mapping, Charting and Geodesy, and Seafloor Geosciences. Our aim is to gain a better understanding of the ocean, to devise ways of measuring and predicting the state of the ocean and its boundaries in terms of both time and space, and to learn more about the effects of the ocean environment on Navy systems, plans and operations.

In our portion of this *NORDA Review*, we present more than a score of technical articles prepared by the researchers in our divisions covering a variety of disciplines and technologies. These areas range from remote sensing of the ocean surface, and measurement and prediction of ocean variability at various temporal and spatial scales, to investigations of the shape, structure, and evolution of the sea floor. In some of these studies, we trace the entire history of a program at NORDA; in others, we highlight current efforts and provide a glimpse of where we feel we are heading in the near future.

Among our highest priority programs are the development of numerical models that assimilate remote sensing and in situ data to provide forecasts of the ocean. Our goal is to merge these models with atmospheric and acoustic models to give the Navy a virtually real-time, total environmental forecast system.

Another major thrust is our nonacoustics program, which is directed toward defining the natural background conditions in the ocean. This includes hydrodynamics, chemical, biological and potential fields to support nonacoustic antisubmarine warfare and submarine vulnerability programs. Our work in nonacoustics has already resulted in the development of state-of-the-art instruments, experimental techniques, and prediction models.

In the long term, the efforts of the directorate will continue to focus on remote sensing, oceanography, ocean forecasting, acoustic boundary interaction and nonacoustics. However, increased emphasis will be placed on mapping, charting and geodesy, the development of a total environmental forecast system, especially on tactical scales, and environmental support for the Navy's weapons acquisition process.

Remote Sensing at NORDA

Jeffrey Hawkins
Ocean Sensing and Prediction Division

Abstract

NORDA is actively involved in a variety of basic, exploratory, and advanced development research aimed at satisfying naval needs by using remotely sensed data. These tasks are addressed by incorporating appropriate space-borne instruments as required. These efforts are complex and varied. GEOSAT altimeter sea surface topography data is combined with infrared imagery to locate fronts and eddies and to study the ocean's energetics. Passive microwave measurements are applied to map out polar sea ice and to investigate the effects of wind-induced ambient noise. Field programs test the capabilities of synthetic aperture radars, passive microwave, and altimetry to define such parameters as sea ice and surface wave fields. Application development for using remotely sensed data aboard naval vessels and at regional centers for present satellites (GEOSAT and NOAA-9) and future satellites (NROSS) is actively pursued. Artificial intelligence and expert systems to upgrade image processing techniques are investigated. Investigation of the western Mediterranean Sea circulation by means of an international NORDA-led experiment is ongoing. The rapidly growing field of satellite oceanography has enabled the Navy to begin incorporating new global synoptic data sources to address its ever-increasing needs for environmental data.

Introduction

The U.S. Navy has a major interest in the application of remote sensing data, especially satellite data, to provide accurate synoptic views of oceanic parameters for real-time analyses. There is also a growing naval need to use these data to initialize, force, and verify ocean variabilities expressed in the form of numerical model forecasts. The basic, exploratory, and advanced development research on the Navy's oceanographic applications of remotely sensed environmental data is a vital activity at NORDA.

One of NORDA's major efforts is toward obtaining quantitative oceanographic parameters (i.e., sea surface temperature, phytoplankton concentration, sea surface topography, sea ice concentration, etc.). Thus, a prime concern is the refinement of geophysical algorithms to provide increased absolute accuracy. The goal of these efforts is to apply the corrected data toward fulfilling Navy requirements.

To improve our understanding of remotely sensed data and its correlation with other geophysical parameters, we use image enhancement techniques and the accurate navigation or registration of the data. The latter is most important, since it allows the data to be coregistered with other oceanographic data and to be quantitatively compared with remotely sensed data from other periods. Combining high-precision geometric coregistration of remote sensing data sets with other data bases (i.e., bathymetry, coastline, digitized fields, etc.) can provide maximum understanding and precision of many oceanographic problems.

This report focuses on present research within NORDA and on some of the future roles that remote sensing has for Navy oceanographic applications.

Discussion

Present research

Thermal infrared—Early work centered primarily around the use of infrared sensors and their capability to detect surface thermal signatures of various ocean features. A major program focused on using GOES data (8 km) to eliminate the masking effects of clouds. The "warmest pixel" compositing technique was routinely used to save

the cloud-free or warmest portions of multiple images, so that the composite represented the least cloud-contaminated data set. Five months of data have been processed this way to qualitatively compare the Gulf of Mexico's circulation with the numerical model results of Hurlburt and Thompson (1980) (Hawkins and Thompson, 1982).

Present research programs utilize the NOAA thermal infrared sensors (Advanced Very High Resolution Radiometer—AVHRR) because of their high spatial and thermal resolution and multi-infrared channel capability. Algorithms have been developed similar to those of Strong and McClain (1984), where multiple thermal infrared channels correct for atmospheric contamination and obtain absolute sea surface temperatures with an accuracy of 0.5°C (Holyer et al., 1983). These results have come from numerous comparisons of satellite data with research ship expendable bathythermograph and bucket temperatures, while real-time imagery was used to guide the vessel to the mesoscale features of interest. Partly as a result of these findings, the "weighting" of multichannel sea surface temperatures used to produce sea surface temperature analyses with ship and bathythermograph reports at the Fleet Numerical Oceanography Center (FNOC) has been increased. NORDA has also developed a two-satellite technique that produces very accurate, absolute sea surface temperatures by geometric pathlength corrections instead of the multispectral approach previously outlined (Holyer, 1984).

Oceanographic circulation studies have also been conducted by rapidly displaying time sequences of NOAA infrared imagery in the Gulf of Mexico, the Grand Banks (La Violette, 1983), the western Mediterranean Sea, and the Gulf Stream. In these studies, numerous NOAA satellite images are geographically registered to within 1 km accuracy and atmospherically corrected to obtain absolute sea surface temperatures. Movements of major fronts and eddies can readily be detected by forming a movie loop of these images. Such studies have provided information on both the temporal and spatial variability needed to correlate with ship hydrographic data and to enhance the understanding of the ocean's dynamic circulation.

Figure 1 is a false color image of NOAA-7 channel 4 (10.3-11.3 μm) on 28 April 1983. This striking cloud-free calibrated image of the Gulf Stream shows the development of meanders and the presence of cold and warm core rings. The warm core ring at 67°W is easily noted as being warmer than the older one northeast of Norfolk, Virginia. This westernmost ring has entrained cooler slope water during its journey to this position and now has a cool center at the surface with warmer water on the edges. Other features, such as warm filaments and large diurnal heating north of Bermuda and the diffuse nature of the Gulf Stream near 63°W, are also clearly evident. This information is important to Navy acoustic propagation prediction and represents a prime NORDA study area.

A higher resolution (1 km) subsection of Figure 1 has been processed with a modified Frei-Chen edge enhancement filter (Fig. 2). Filter weights were chosen so that the intensity at each point was replaced by a 3x3 finite difference approximation to the original image. A linear contrast enhancement was applied to the image prior to the filtering. The results provide the impression of relief based upon the sea surface temperature. The relief shown is the reverse of that in nature, in that the white (cold core) rings should represent a depression in the ocean surface and not a rise (courtesy of M. Lybanon, NORDA).

Visible—The applications of visible satellite sensors were directed toward both coastal hydrographic problems and mesoscale oceanographic variability (Arnone and Holyer, 1984; and Arnone and La Violette, 1985). As a result of the frequent repeat time (3 consecutive days of coverage followed by a 2-day absence), the CZCS imagery aboard Nimbus-7 is presently being used for studies of dynamic bio-optics and physical oceanography. Subtle changes in ocean color detected by CZCS result from biological and chemical changes within the upper ocean surface. Since the ocean color represents about 10% of the total signal sensed by CZCS, effective methods of eliminating the atmospheric contamination are critical. Algorithms are presently being developed and validated in which atmospheric correction and quantitative images of the phytoplankton concentration and diffuse attenuation coefficients of the upper ocean surface are being derived. The probable causes of the ocean color signals are under investigation, as is the influence resulting from the biochemical optical properties.

The CZCS data provides temporal and spatial variability of the bio-optical properties and updates our understanding on how ocean productivity is linked to ocean dynamics. Our understanding of the upper ocean dynamics is improved by examining the correlation between the ocean color (CZCS) and the sea surface temperature (AVHRR).

Hydrographic applications have been established in coastal areas by using Landsat multispectral data. Programs have addressed the potential of using remote sensing for charting water depth and coastal water clarity. The digitization and subsequent overlay of bathymetric charts clearly reveal areas of concern where currents and waves have modified the bottom topography to the extent that navigation hazards might exist.

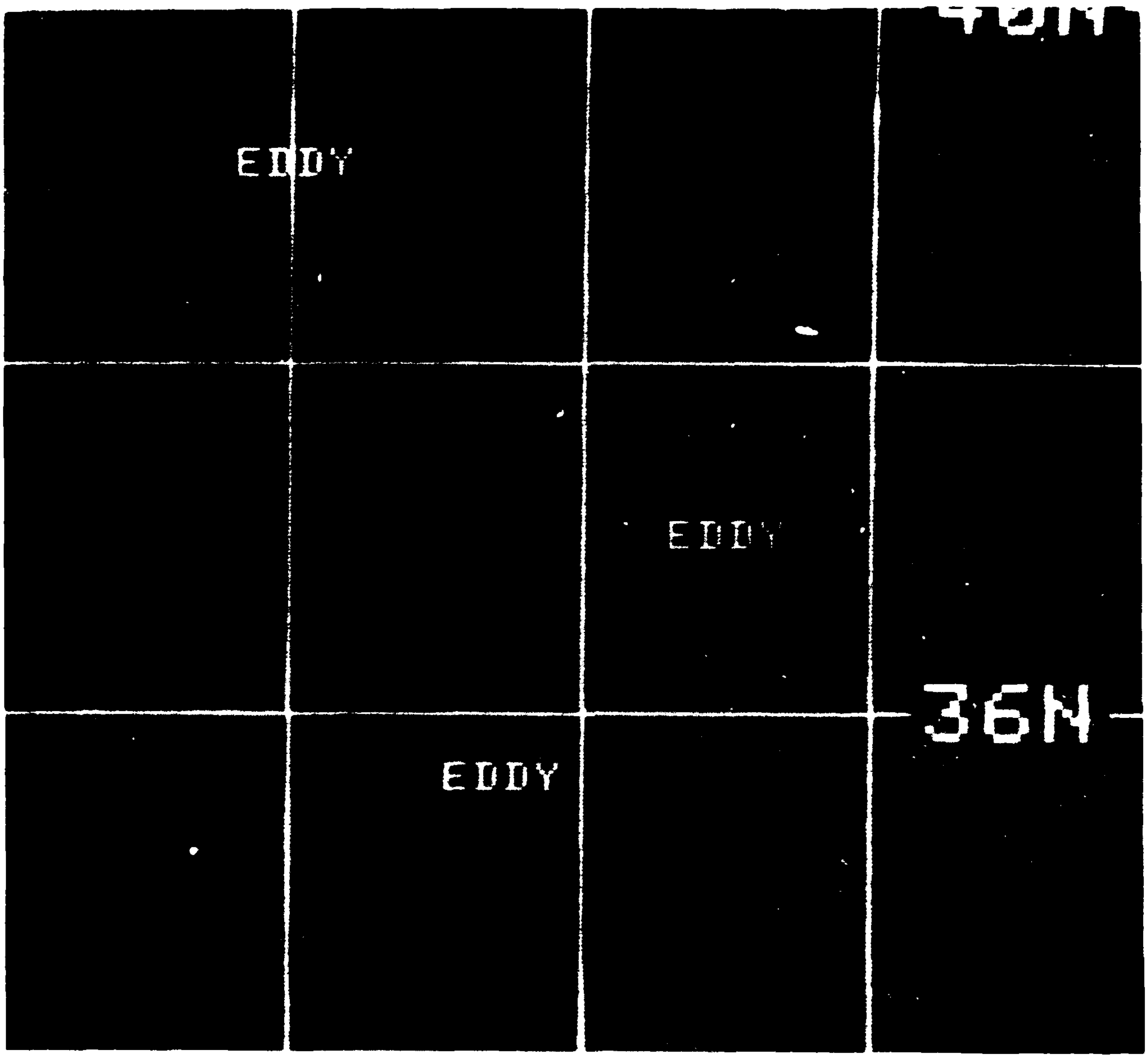

Figure 1. NOAA-7 infrared channel 4 (10.3–11.3 μm) false color image illustrates mesoscale features of the Gulf Stream system.

Microwave—In recent years, active microwave instruments have taken on a larger role in oceanographic remote sensing. The use of altimeters for deriving sea surface topography, significant wave height (H ⅓), sea ice edge, and surface wind speed is now being actively pursued in NORDA's GEOSAT Oceanographic Applications Program and the Northwest Atlantic Regional Energetics Experiment (REX). The combination of the altimeter (launched 12 March 1985) sea surface topography, airborne expendable bathythermographs, in situ inverted echo sounders with bottom pressure gauges, conductivity-temperature-depth probes, and coincident high-resolution infrared data will provide the basis for developing methods to map the quasi-synoptic ocean mesoscale activity.

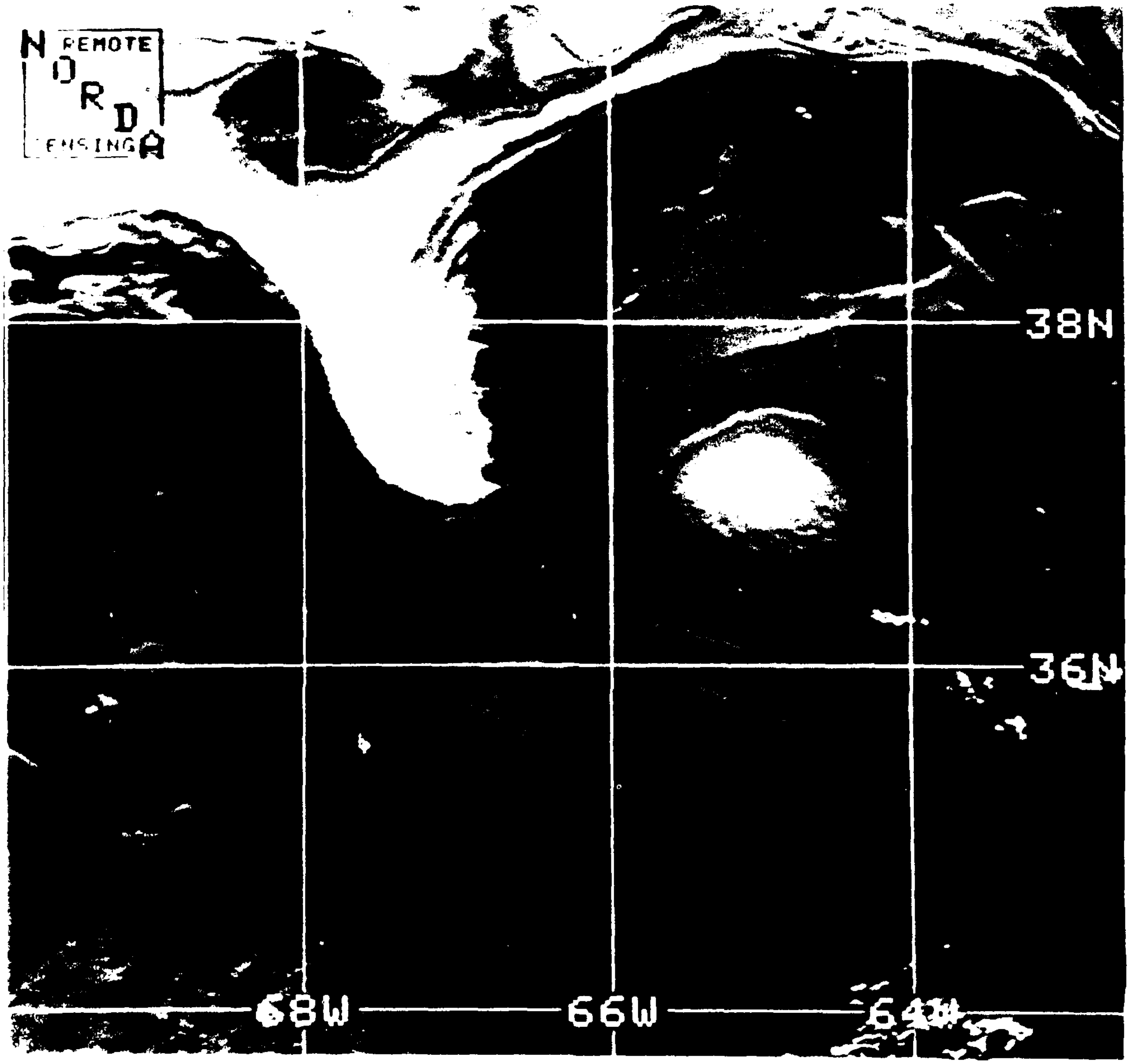

Figure 2. Full resolution (1.1 km) subsection of NOAA 7 infrared photo processed with a modified Frei Chen edge enhancement filter. Filter weights were chosen so that the intensity at each point was replaced by a 3 x 3 finite difference approximation to the original image. A linear contrast enhancement was applied to the image prior to the filtering. The results provide the impression of relief based upon the sea surface temperature. The relief shown is the opposite of reality in that the white (cold core) rings should represent a depression in the ocean surface and not a rise. Photo courtesy of Matt Lybanon.

The basic objectives of the REX project are to examine

- the effects of the New England Seamount chain on the spatial temporal scales of Gulf Stream fluctuations;
- the relationship between dynamic topography, barotropic topography and the available potential energy distributions in the NW Atlantic;

• data assimilation methods for ingestion of altimetric data into regional numerical circulation models.

A major objective of the associated GOAP to demonstrate a real-time capability to process satellite altimetry for use in standard Navy environmental products, such as maps of fronts and eddies, wave models, marine wind analyses and, eventually, mesoscale resolving circulation models and resulting products (Lybanon, 1984). Oceanography from GEOSAT will be greatly enhanced if present plans for an extended repeat mission come to fruition after the initial 18-month geodetic study (Mitchell, 1983). Properly spaced colinear tracks would open up many new areas of research and operational demonstration potential.

The synthetic aperture radar (SAR) is another active sensor taking on increased importance in NORDA's research. The SAR's high resolution, all-weather capability for sea ice and ocean surveillance presents substantial potential for Navy applications (La Violette, 1983). However, a major concern is the high signal processing requirements. NORDA plans active participation in ground truth efforts for the Shuttle Imaging Radar, SIR-C instrument. This effort will serve as a precursor to Navy applications of a SAR satellite to be launched in the late 1980s or early 1990s.

The active microwave scatterometer planned for the Navy Remote Ocean Sensing System promises to provide global synoptic surface wind stress values that will apply to a wide range of Navy needs. The successful assimilation of scatterometer retrievals with conventional data sources will provide the potential to significantly improve wind forcing forecasts required by the Navy's three-dimensional thermal prognostic models, as well as the spectral ocean wave, ambient noise, ocean current, and ice drift models. The surface wind vector information will also have great potential for providing nowcasts for large swaths of the ocean in and around naval operational areas. This wealth of data will significantly upgrade carrier flight operations, sea state forecasts, and several aspects of antisubmarine warfare, as well as search and rescue.

Research is continuing this year with regard to applications of passive microwave satellite data. NORDA is in the process of preparing the Special Sensor Microwave/Imager (SSM/I), scheduled for launch in 1986, for Navy use. Adding this sensor to the DMSP platforms will provide global coverage of sea ice conditions, surface wind speed, water vapor, rain rate, and several other parameters. This sensor is similar in many respects to the SEASAT and Nimbus-7 Scanning Multichannel Microwave Radiometer, but differs in that it will retrieve a different suite of frequencies (19, 22, 37 and 85 GHz) optimized for sea ice and atmospheric water vapor, but lacking sea surface temperature measurement capabilities.

The 12-km resolution sea ice edge and 25-km sea ice concentration and age data from the SSM/I will be of prime concern to the Naval Polar Oceanography Command in Suitland, Maryland (Eppler, 1983). NORDA is working with FNOC, the Naval Research Laboratory, and the Atmospheric Environment Service of Canada to ensure that the SSM/I sea ice algorithms are accurately validated (Eppler and Hawkins, 1985). The SSM/I continuing series, now set for DMSP launch through the early 1990s, guarantees the accessibility of this critical data for Navy polar operations.

Coordinated studies

The method of solving a specific oceanographic problem that has shown the best return for the effort required is the combination of several sensors covering different spectral bands. Such studies emphasize the cross comparison of several remotely sensed data sets with themselves and with in situ data. This cross comparison results in a synergism not possible if the studies were done individually. Such studies were carried out in 1982 in the Alboran Sea where satellite visible and infrared data were combined with aircraft remote sensing instruments, onshore specialized radars, ship data, and deep-sea moorings. The results from these data sets are currently being analyzed and combined with numerical ocean models to solve one oceanographic process: the circulation of the Alboran Sea (Donde Va?, 1984). In this regard, NORDA is working with other U.S. and European institutions.

A larger program with a similar purpose is an experiment planned for October 1985 through October 1986. Called the Western Mediterranean Circulation Experiment, this NORDA-led effort will combine the continuous monitoring by satellites of the entire Western Mediterranean with in situ measurements taken by strategically placed ships and current meter moorings. Aircraft data will also be collected to further provide detailed synoptic remote sensing data along with those provided by expendable aircraft instruments. The effort will combine the advantages of the broad, synoptic data sweeps provided by satellite (and aircraft) remote sensing instruments with the detailed finescale measurements provided by ships and moorings. The results of these data sets will be interactively combined with models to provide an understanding of the regions' surface and subsurface circulation.

Conclusions

During its first 10 years in operation, NORDA's remote sensing capabilities and expertise have developed considerably, as has satellite oceanography in general. One of the purposes of this article is to familiarize the oceanographic and remote sensing communities with NORDA's expanding role in satellite oceanography for basic and applied ocean research. The newly acquired realtime Satellite Data Receiving and Processing System represents an asset that will be used extensively in research programs that cover a wide range of current and future NORDA programs.

As noted earlier, a major goal within NORDA has been to assimilate in situ oceanographic data with processed satellite environmental data to answer specific oceanographic questions. This difficult and costly undertaking requires extensive preparation and resources, especially in Arctic programs. The oceanographic research community is urged to take advantage of NORDA's remote sensing capabilities through cooperative programs. Questions, comments, and inquiries from researchers conducting similar or complementary work are welcome.

References

Arnone, R. A. and R. J. Holyer (1984). *Ocean Optical Remote Sensing Capability Statement*. Naval Ocean Research and Development Activity, NSTL, Mississippi, Technical Note 264.

Arnone, R. A. and P. E. La Violette (1985). Satellite Definition of the Bio-Optical and Thermal Variation of Coastal Eddies Associated with the African Current. *Journal of Geophysical Research*, in press.

Donde Va? Group (1984). Donde Va? An Oceanographic Experiment in the Alboran Sea. *EOS, Transactions of the American Geophysical Union.*

Eppler, D. T. (1983). *Assessment of Potential SSM/I Ice Products in Light of ESMR and SMMR Ice Classification Algorithms*. Naval Ocean Research and Development Activity, NSTL, Mississippi, Technical Note 220.

Eppler, D. T. and J. D. Hawkins (1985). *NORDA Participation in the SSM/I Sea Ice Validation Experiment.* Naval Ocean Research and Development Activity, NSTL Mississippi, Technical Report 129, in press.

Hawkins, J. D. and J. D. Thompson (1982). Analysis of the Loop Current in the Gulf of Mexico Using Satellite IR Imagery. *EOS, Transactions of the American Geophysical Union* 63(18), 356.

Holyer, R. J., J. D. Hawkins and P. E. La Violette (1983). A NOAA-7 Split Window Sea Surface Temperature Algorithm Based on Lowtran-5a Simulation of Atmospheric Radiative Transfer. *EOS, Transactions of the American Geophysical Union* 64(18), 232.

Holyer, R. J. (1984). A Two-Satellite Method for Measurement of Sea Surface Temperature. *International Journal of Remote Sensing* 5(1), 115-131.

Hurlburt, H. E. and J. D. Thompson (1980). A Numerical Study of Loop Current Intrusions and Eddy Shedding. *Journal of Physical Oceanography* 10, 1611-1651.

La Violette, P. E. (1983). *The Grand Banks Experiment: A Satellite/Aircraft/Ship Experiment to Explore the Ability of Specialized Radars to Define Ocean Fronts.* Naval Ocean Research and Development Activity, NSTL, Mississippi, NORDA Report 49.

Lybanon, M. (1984). *GEOSAT Ocean Applications Program (GOAP) Initial Data Processing and Analysis System Test and Evaluation Plan*. Naval Ocean Research nd Development Activity, NSTL, Mississippi, Technical Note 270.

Mitchell, J. L. (1983). *A Position Paper: Mesoscale Oceanography from GEOSAT*. Naval Ocean Research and Development Activity, NSTL, Mississippi, Technical Note 226.

Strong, A. E. and E. P. McClain (1984). Improved Ocean Surface Temperature from Space-Comparisons with Drifting Buoys. *Bulletin of the American Meteorological Society* 65, 138-142.

Western Mediterranean Circulation Experiment

Paul E. La Violette
Ocean Sensing and Prediction Division

Abstract

The Western Mediterranean Circulation Experiment is planned for November 1985–September 1986. The preliminary objective of this NORDA-led, interdisciplinary, multiplatform experiment is to gather the knowledge and data base for an area-wide ocean laboratory useful in evaluating satellites in the 1990s. The experiment design will center on determining the circulation of the western Mediterranean Sea on scales ranging from basin-sized to 1 km. The result will be a dynamically and statistically correct representation of the circulation in terms adequate for understanding chemical and biological transport and for climatic studies.

Introduction

In the 1990s, satellites will be orbited with suites of diverse sensors unparalleled by previous orbited systems. Practical methodology suggests that for these new sensors to be developed to full oceanographic potential, they should be "field-tested" over an ocean area whose physical parameters are well known. Such an oceanic laboratory is provided by the Mediterranean Sea. The compact size of this sea, its physical properties, and comparative moderate climate, as well as the accessibility and quality of its shore facilities and research institutions, combine to make it a unique, ideal area for satellite sensor development.

Although the basic events that determine the Mediterranean Sea's physical characteristics are understood, a great deal is unknown. Recent technological advances, the availability of cooperative laboratories, and the coincident timing of several complementary oceanic experiments provide a rare opportunity to overcome these knowledge deficits.

An international NORDA-led experiment will take place during November 1985–September 1986. The experiment will take advantage of the coinciding events mentioned to endow the western Mediterranean Sea as an oceanic laboratory suitable for fully developing satellites for the future.

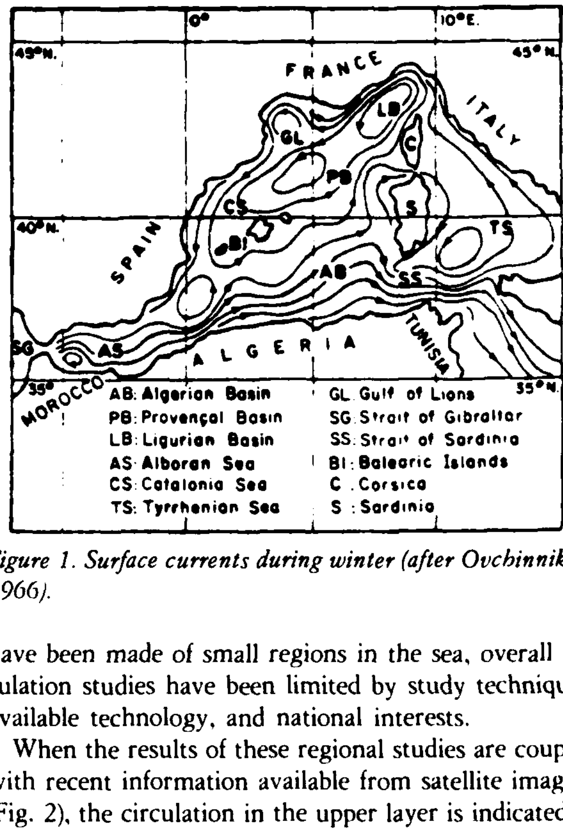

Figure 1. Surface currents during winter (after Ovchinnikov, 1966).

Discussion

The scientific problem

The western Mediterranean Sea circulation is described in simplified patterns (Fig. 1). Although intensive studies have been made of small regions in the sea, overall circulation studies have been limited by study techniques, available technology, and national interests.

When the results of these regional studies are coupled with recent information available from satellite imagery (Fig. 2), the circulation in the upper layer is indicated to be more complex than the generalized studies show. The combined data indicate that this circulation is composed of a series of interconnected mesoscale patterns or gyres modified by bathymetry, seasonal changes, meteorology,

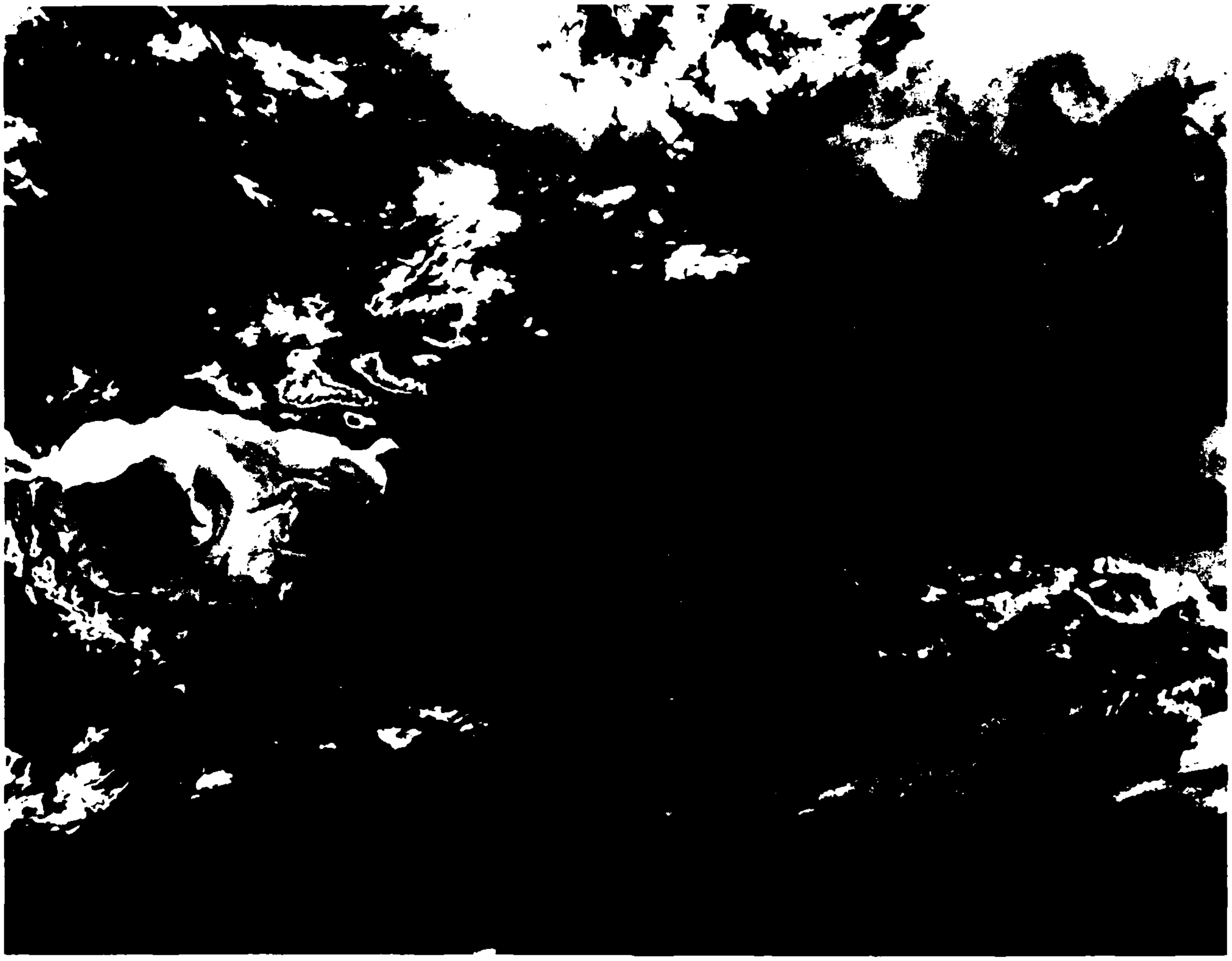

Figure 2. NOAA 6 infrared image taken of a portion of the western Mediterranean Sea on 6 June 1960. (Image received by Centre de Meteorologie Spatiale, Lannion, France.)

and tides (Philippe and Harang, 1982; Millot, 1984; and Arnone and La Violette, 1986).

Until the recent availability of computer-registered and atmospherically corrected satellite imagery (Figs. 3 and 4), no attempt could be made to study the physical interrelationships of these phenomena. Now that such technology is available, a study using a multidisciplinary approach is possible. This is the rationale for the Western Mediterranean Circulation Experiment (WMCE). WMCE could provide answers for several oceanic questions.

- What are the prime features of the western Mediterranean Sea circulation, and how do these features spatially and temporally vary?
- What are the basic forcing mechanisms that control the circulation?
- How does the circulation affect the chemical, biological, and optical properties of the western Mediterranean Sea?
- How can this knowledge be implemented into numerical models?

The WMCE approach

State-of-the-art numerical methods are capable of realistically modeling a basin the size of the western Mediterranean Sea (i.e., from the Strait of Gibraltar to the Strait of Sicily) and to resolve the mesoscale circulation. Such modeling, in conjunction with the synoptic measurements of boundary conditions (i.e., the flow through both straits and the meteorology) and field

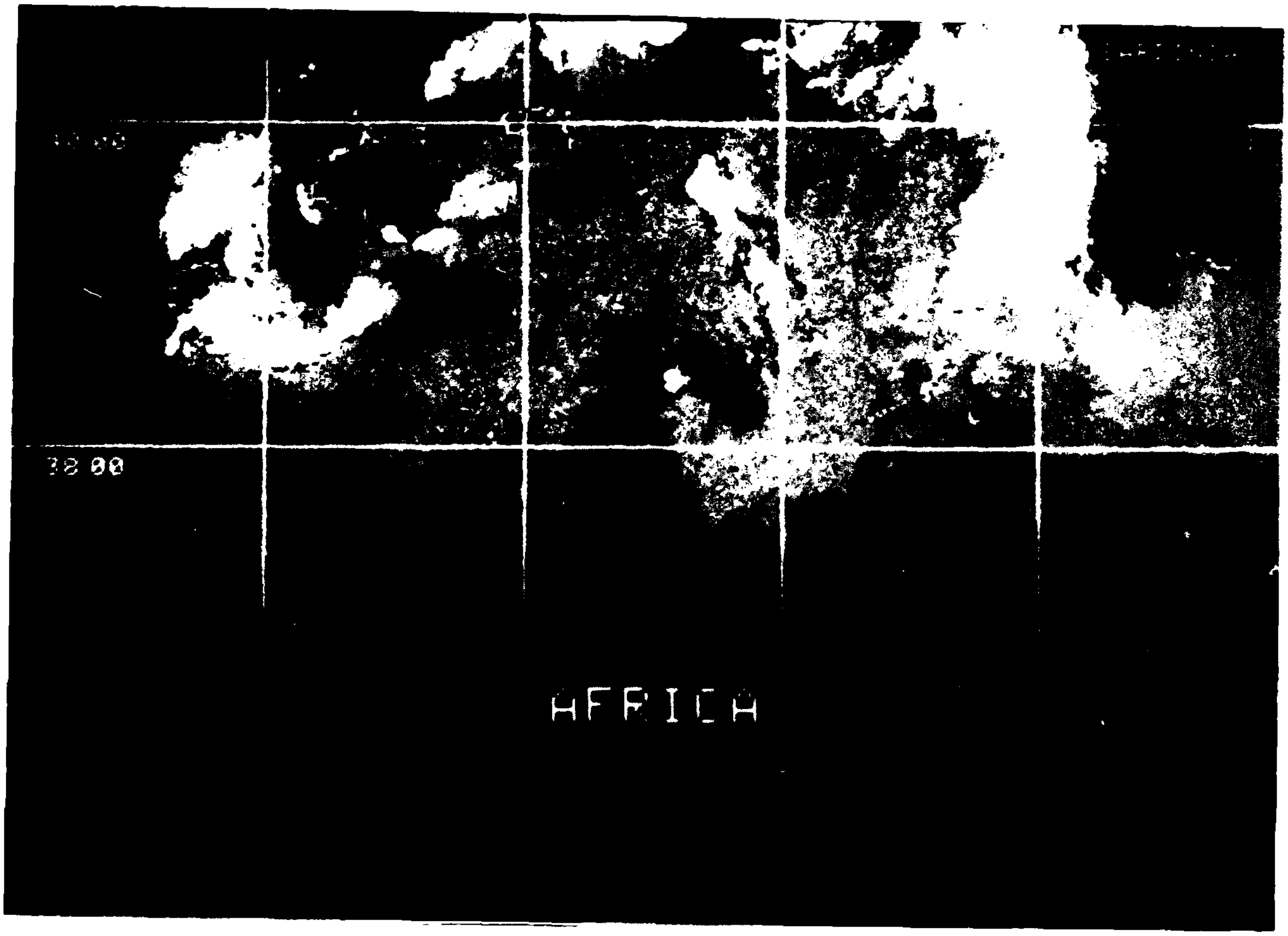

Figure 3. A Nimbus-7 Coastal Zone Color Scanner image taken November 29, 1979. This visible-range image has been atmospherically corrected and represents the ratio of upwelling radiance at 443:550 nanometers. The patterns presented are directly related to the phytoplankton concentration and diffuse attenuation coefficient. The ellipsoid-shaped eddies in the figure extend approximately 120 km offshore (Arnone and La Violette, 1986).

measurements to conform or suggest modification to models, provides the natural framework for WMCE.

Logically included in WMCE are studies of the Intermediate and Deep Waters. Knowledge of the details of their formation and subsequent flow paths is critical toward understanding the circulation of the sea (equally important, such knowledge can provide an understanding of similar processes occurring in other less accessible areas of the world's oceans).

The WMCE approach includes intensive studies in several critical regions within the sea. The most important of these are studies of the inflows and outflows through the boundary straits at Gibraltar and Sicily. Knowledge of these flows is required to understand the local dynamics of flow near these straits and the fluxes of water, heat, salt, nutrients, and pollutants in both the Mediterranean and the North Atlantic (estimates of these fluxes through these straits are presently based on a limited number of short-term measurements and assumptions).

During WMCE, a continuous set of moorings will be maintained for one year in the Strait of Gibraltar (these will be part of an ongoing cooperative experiment — the ONR-sponsored Gibraltar Experiment) and for a slightly shorter period, in the Strait of Sicily. In addition to the moorings in the straits, several shorter-term moorings will be installed in selected areas during the seasonal intensive phases of the experiment. The spot information provided by these measurements will be expanded by spatial measurements made from satellites, ships, aircraft, and drifter buoys. The analyses of these various data sets will

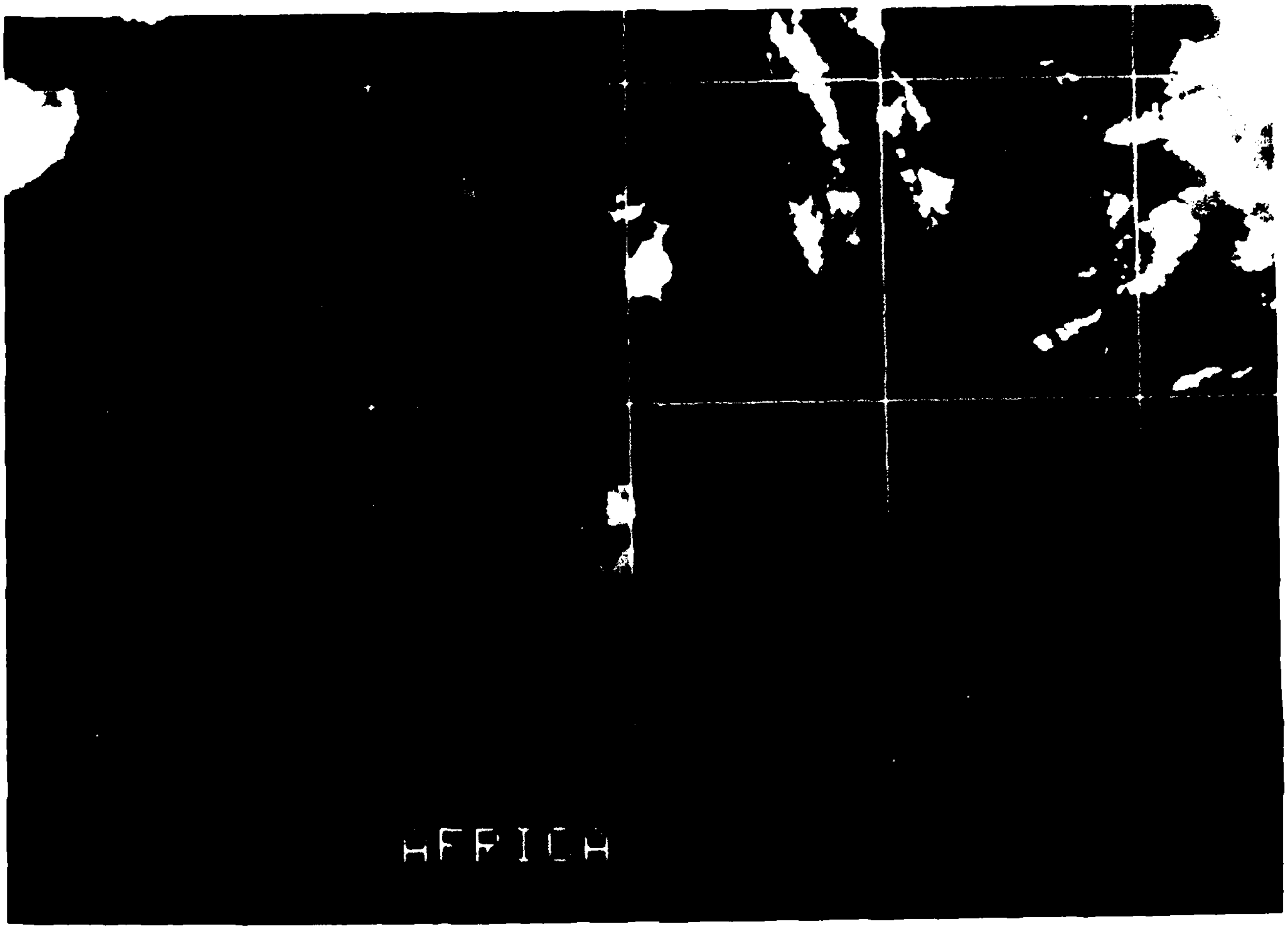

Figure 4. The full resolution of the image in Figure 3. The higher resolution shows details of the high color signatures that dominate the western periphery of the anticyclonic eddies.

be integrated to derive the spatial and temporal variability of the western Mediteranean circulation.

WMCE methodology and operation plan

It is important to emphasize that an interdisciplinary methodology is the mainstay of WMCE. Because of this, the international team of investigators formed to conduct the experiment is composed of biological, chemical, modeling, physical and remote-sensing oceanographers, as well as meteorologists.

An operation plan describing the field events proposed by the individual investigators is presented in Table 1. The 12-month field experiment will allow physical, biological, and chemical data to be collected during a complete seasonal cycle.

Summary

In essence, the WMCE is an interdisciplinary, multiplatform experiment whose preliminary objective is to determine the circulation of the western Mediterranean Sea on scales ranging from basin-sized to 1 km. The result will be a dynamically and statistically correct representation of the circulation in terms adequate for understanding chemical and biological transport and for climatic studies. Its results will form the basis for future interdisciplinary experiments and provide a solid data base to evaluate the satellites that will be orbited in the 1990s.

Table 1. WMCE field operation schedule.

October 1985 Moorings positioned in Strait of Gibraltar by Experiment team investigators. POEM investigators commence experiments in eastern Mediterranean November 1985 1–15 November: Italian ship positions moorings in Strait of Sicily; conducts ocean survey of the Straits of Sicily and Sardinia. Intensive NOAA satellite data collection of Straits area (image received every 6 hours). Begin GEOSAT coverage of WMCE area. Begin sea level and meteorological data collection of WMCE area. 1–7 November: Space Shuttle conducts intensive photographic coverage of southern portion of WMCE area with special emphasis on coast of Algeria and the Straits of Sicily and Sardinia. U.S. helicopter/aircraft conduct study of same regions. Italian ship conducts ocean studies in coordination with airframes and Space Shuttle. 15 November: NOAA satellite data collection shifts to one image per week. NOAA data collection will continue at this rate through September 1986, except during intensive survey periods. At these times collection rate will increase to the rate stated in this schedule. December 1985 and January 1986 At this time, no field campaigns are scheduled for this period. February 1986–Winter Campaigns 4 February: Winter Campaigns preoperation meeting (place to be determined). 5–27 February: Italian ship and U.S. aircraft conduct winter ocean survey of southern portion of WMCE area. Spanish ship conducts studies in eastern portion of WMCE area. Satellite drifters released in eastern Alboran sea. British Royal Navy radar at Windmill Hill, Gibraltar, commences monitoring eastern end of the Strait of Gibraltar for 30 days. NOAA satellite data collection shifts to daily coverage of WMCE area for all of February, first half of March. 27, 28 February: Italian ship and U.S. aircraft conduct ocean survey of Straits of Sardinia and Sicily. Coordinate field studies with NILDEX experiment units. 23 February–15 March: NILDEX scatterometer experiment in the Strait of Sicily involving DSVLR aircraft and tower. (DSVLR aircraft may also work with U.S. aircraft and Italian ship in the early February study of southern portion of WMCE area). March 1986 1–15 March: NILDEX experiment continues in Strait of Sicily.	April 1986 Field campaigns scheduled at end of month (see May). May 1986–Spring/Summer Campaigns 28 April–20 May: U.S. ship and aircraft conduct field studies of the southern portion WMCE area. NOAA satellite weekly coverage shifts to daily coverage. This coverage will stay in daily mode throughout period 27 April–30 June. Satellite drifters at this time should be well along Algerian coast. When possible, U.S. ship and aircraft (and French ship—see below) will adjust their cruise tracks to augment the drifter data. Real-time NOAA satellite imagery and drifter buoy data will be sent to both the U.S. and French ships to aid their operational decisions in the field. 24 May: Spring/Summer Campaign mid-operation meeting Toulon, France. 27 May–27 June: French ship will replace U.S. ship in field study of southern portion WMCE area. Basic operations of both ships will be similar. Real-time data reception of satellite and drifter buoy data will continue. Possibility of Spanish ship conducting ocean studies in northwest portion of WMCE area. June 1986–Spring/Summer Campaigns 1–27 June: French ship continues field study of southern portion WMCE area. NOAA satellite coverage continues as described above. The eastward movement of the satellite drifters along the Algerian coast will be slow, and the drifters should stay in the operation area until August/September. July 1986 At this time, no field campaigns scheduled for this month. August 1986 1–15 August: Italian ship conducts ocean survey of Straits of Sicily and Sardinia then recovers moorings. Possible Space Shuttle (mission STS 61-K) coverage of entire WMCE area during this or following month (tentative plans include the possibility of hand-held spectrometer, special lens on multiple-band cameras and television cameras included in this mission). If this does occur helicopter/aircraft studies similar to November 1985 will be made. September 1986 Moorings recovered in Strait of Gibraltar. Satellite coverage of WMCE area halted. Sea level and meteorological data collection for WMCE area halts. All of the planned WMCE field data collection ceases.

References

Arnone, R. A. and P. E. La Violette (1986). Satellite Definition of the Bio-Optical and Thermal Variation of Coastal Eddies Associated with the African Current. *Journal of Physical Oceanography*, in press (to be published in JGR 91 (C1)).

Millot, C. (1984). Some Features of the Algerian Current. *Journal of Physical Oceanography* 90(C4), 7169-7176.

Ovchinnikov, I. M. (1966). Circulation in the Surface and Intermediate Layers of the Mediterranean. *Oceanology* 6, 48-59.

Philippe, M. and L. Harang (1982). Surface Temperature Fronts in the Mediterranean Sea from Infrared Satellite Imagery. In *Hydrodynamics of Semi-Enclosed Seas*, J. C. J. Nihoul (ed.), Elsevier, 70-90.

Ocean Surface Wave Studies at NORDA

Ming Y. Su and Robert E. L. Pickett
Oceanography Division

The study of nonlinear dynamics of surface gravity waves started at NORDA in 1978. A 52-foot-long mechanical wavemaker was constructed at that time in the outdoor Flood Plain Basin at the National Space Technology Laboratories (NSTL) site. A 12-foot section of the wavemaker was occasionally installed on an indoor tow tank at NSTL.

Among the most significant results of this continuing study of the fundamental characteristics of finite amplitude waves were that the three-dimensional instabilities have a greater growth rate than the essentially two-dimensional Benjamin-Feir instability for wave steepness. These instabilities show a propagation speed that is equal to the phase speed of the unperturbed waves.

We also found that the Benjamin-Fier instabilities lead to a frequency downshift from the fundamental frequency of the wave train, or packet. They also generate stable two-dimensional envelope solitons.

A symmetric bifurcation of two-dimensional Stokes waves into a three-dimensional array of crescent-shaped wavelets has also been observed. These wavelets show a 180° phase shift between successive rows with slopes greater than 0.25. These waves resemble the three-dimensional breaking waves often observed at sea. For slopes between 0.16 and 0.18, the two-dimensional Stokes waves again transitioned into three-dimensional wave groups that are then further subject to the Benjamin-Feir instability.

In addition, an extensive statistical analysis of ocean storm waves collected in the Gulf of Mexico and the North Sea led to the discovery of several new features in the characteristics of wave groupings, and in the joint probability density of wave heights and periods. Also, a new concept of extreme wave groups is under investigation.

Most recently, an air-sea interaction measurement system was installed on a portable research tower located in Lake Pontchartrain, near New Orleans, Louisiana. The data analysis of the first set of measurements of three-dimensional waves is underway.

Another area of wave study is being conducted to develop techniques to verify and upgrade the global surface wave model at the Fleet Numerical Oceanography Center (FNOC). The approach being taken includes reviewing all operational wave prediction models to identify candidates for comparison with the FNOC wave prediction model; developing test procedures for running the intercomparisons; and creating techniques for verifying wave models that may include GEOSAT and instrumented drifters.

Thermal Analysis and Prediction at NORDA: An Overview

Paul W. May, Paul J. Martin, Alex C. Warn-Varnas, and John M. Harding
Ocean Sensing and Prediction Division

Abstract

Extensive research into the analysis and prediction of the temperature field of the upper 500 m of the ocean is being conducted at NORDA. Because the upper ocean thermal structure is an important element in predicting ocean sound propagation. This research led to the operational implementation of upper ocean thermal analysis and prediction systems, designated OTIS and TOPS, respectively. This overview briefly describes the need for an upper ocean analysis and forecast capability, outlines the physical basis for analyzing and predicting the upper ocean thermal field, describes some formal aspects of the OTIS and TOPS software systems, and presents representative results from both.

Introduction

Numerical ocean modeling covers a broad range of activities of interest to naval operations. In general, its aim is to quantitatively determine a set of ocean fields in both space and time by solving the governing equations of motion or conservation. Most commonly these fields consist of temperature and the horizontal components of velocity, but might also include salinity, density, nutrient concentrations, surface height, sound speed, or any other ocean properties.

Analyzing and forecasting the upper ocean temperature field is of particular interest because of its significance for climate, biological resources, and acoustic propagation. The "upper ocean" refers to that part of the ocean from the free surface to the depth where atmospheric effects are negligible over the course of a year. Typically this region generally extends from the ocean/atmosphere interface to a depth of about 500 m. Research into atmosphere-ocean interactions has shown that the heat stored and transported in the surface layers of the ocean is a significant factor in determining gross climate and seasonal fluctuations over the continents. Commercially important marine organisms generally found in the upper few hundred meters of the ocean are also affected.

Thermal effects on acoustic propagation interest the Navy, since antisubmarine warfare (ASW) depends on sound waves to "see" into the ocean depths. By listening for acoustic energy radiated (passive mode sonar) or reflected (active mode sonar) by a target, Navy ASW operators can perform their assigned surveillance, detection, and localization functions. The operational measure of successfully detecting underwater objects is the so-called sonar equation (Urick, 1983), within which dispersion and absorption of acoustic energy are parameterized by the transmission loss term. Through this term the thermal structure of the upper ocean directly impacts naval ASW operations. Because sound speed is primarily a function of temperature and depth, the upper layer temperature changes are the chief cause of refraction (and, hence, energy dispersion) of sound waves generated at or near the surface. By knowing the upper ocean temperature structure, Navy ASW operators gain an advantage in acoustic prediction modeling.

Forecasting conditions in the upper ocean is not a simple task because of the direct forcing by a highly variable atmosphere. The ocean temperature field is also dynamically connected to other oceanic fields, such as velocity. This variability is customarily described in terms of the length and time intervals over which significant changes occur, that is, in frequency-wavenumber space. In such a description the thermal variability covers broad ranges in both space and time. While it is generally true that long time

and length scales contain the most energetic motions, it is also true that shorter scales of motion are energetic enough to significantly affect tactical operations. Thus, the prediction problem is not confined to a certain narrow set of phenomena but encompasses a wide range of physical effects.

Navy scientists have seriously considered upper ocean analyses and forecasts over the past two decades (James, 1966, and Mooers et al., 1982). While ASW became an important concern as long ago as World War I, only recently has knowledge of the ocean environment advanced enough to make a real-time analysis and forecast possible (see Krauss, 1977, for a good overview of this subject). This capability stems from both an increased understanding of ocean physics and a substantial observational effort. With the advent of large-scale computers and satellite observation platforms, the moment seems propitious for great advances in this area.

NORDA scientists have approached the upper ocean analysis/forecast problem by attacking three different areas: thermal analysis, dynamic forecasting, and statistical forecasting. This effort roughly parallels comparable research into atmospheric predictability. In the following discussion, which reviews NORDA's progress in the first two areas, "analysis" refers to an inferred spatial "snapshot" of an ocean field as it is at a particular moment, based on a limited amount of present and past observations. "Dynamic forecast" refers to the prediction of what an ocean field will look like at some time in the future based on its present state and on some knowledge of the operative physical laws. Some combination of these ideas will likely result in a truly "optimum" forecast.

Discussion

Thermal analysis

The primary function of an automated thermal analysis scheme is to supply estimates of the temperature field in regions where the data are either sparse or nonexistent. Analyses commonly convert randomly spaced observations into estimates on some well-defined, uniform grid. The gridded estimates of the fields are typically contoured for visual examination, incorporated as initial conditions or updates into numerical forecast models, or both.

In the past, the primary sources of data for such analyses were expendable bathythermographs (XBTs), for subsurface temperature profiles, and surface ship observations for the sea surface temperature field. Presently about 200 XBT reports and about 3000 ship reports, mostly from the northern hemisphere, are received at the Fleet Numerical Oceanography Center (FNOC) every day. By contrast, almost 5000 surface land observations are available every 3 hours for surface meteorological analyses. Planned and operational satellite observational platforms promise to deliver many orders of magnitude more data with visual, infrared, and microwave sensors; unfortunately, this data is mainly surface information, which leaves the bulk of the upper ocean inaccessible to daily or even weekly analysis.

In addition to interpolating data to a uniform grid, a useful analysis scheme should have certain other features. It should supply some estimate of the error in the fields that it produces. By doing so the operator has a measure of how much he can trust a particular analysis and an indication of where additional data should be gathered. A useful analysis should be capable of detecting erroneous data and eliminating it from further consideration. Furthermore, the analysis should be based on some sound physical principles. By insisting that this condition is met, the analysis is constrained to be truly objective and free from arbitrary assumptions. Finally, it should be capable of using observations of different ocean fields from diverse instruments to produce the best possible analysis of the specified field.

Several options for automated analysis techniques have been investigated at NORDA for application to the upper ocean thermal field (May, 1985): polynomial interpolation, successive approximation, variational analysis, spectral interpolation, and optimal interpolation. Most of these techniques have been tested and used for meteorological purposes. The shortcomings of these schemes vary but can be separated into a few categories. The primary criticism of most of the techniques is the arbitrary nature of the interpolation criterion. This complaint results in large numbers of changeable constants or unrealistic interpolated fields, which tend to belie the "objective" nature of a good analysis. In addition, error fields are often difficult to define, leaving one uncertain of the validity of a particular analysis. Finally, some schemes show poor characteristics when extrapolation (estimation outside of some data "cloud") is being performed. Since an oceanographic analysis scheme must often operate with sparse quantities of data, this consideration is quite important.

The analysis technique most suitable for the ocean thermal field is based on optimal estimation theory. This analysis method, pioneered by Russian meteorologist L. S. Gandin, has its mathematical foundation in statistical work by Gauss and Markov. It has been successfully adapted and used by oceanographers for mapping synoptic

eddy fields as well as entire ocean basins (Bretherton et al., 1976).

Instead of basing an estimate on physical laws, the optimal interpolation technique produces a statistically optimal estimate based on known or inferred statistical characteristics of the field. Optimal estimation theory assumes that an estimate of some scalar quantity can be expressed as the weighted sum of any number of observed values of that quantity or of some related quantity. The best linear estimate of $T(\vec{x},t)$ at the point $(\vec{x}_0,t_0)$ using N data values at points $(\vec{x}_i,t_i)$ is

$$T(\vec{x}_0,t_0) = \sum_i a_i\, D(\vec{x}_i,t_i) \qquad i = 1,N ,$$

where the parameter of interest is $T(\vec{x},t)$, the estimate of the parameter is $T(\vec{x},t)$, and the datum at point i is $D(\vec{x}_i,t_i)$. The unknown weighting coefficients, a_i, are chosen to minimize the squared error, defined by

$$E(\vec{x}_0,t_0)^2 = <[T(\vec{x}_0,t_0) - T(\vec{x}_o,t_0)]^2>$$

$$= <T_0^2> - 2\sum_i a_i <T_0D_i>$$

$$+ \sum_i \sum_j a_i a_j <D_iD_j> ,$$

where $< >$ represents an ensemble average. Minimizing the error in the usual way gives a set of linear equations which can be solved for the unknown weighting coefficients. That is,

$$\frac{\partial E^2}{\partial a_i} = 0 ,$$

gives the linear set of equations

$$\sum_i a_i <D_iD_j> = >D_jT_0> .$$

Solving for the unknown coefficients gives

$$a_i = \sum_j <D_iD_j>^{-1} <D_jT_0> .$$

Noise or errors in the measurements can be explicitly accounted for by including them in the expression for observed quantities:

$$D_i = D(\vec{x}_i,t_i) = T(\vec{x}_i,t_i) + \epsilon(\vec{x}_i,t_i),$$

which, when substituted in the bracketed terms above, gives

$$<D_iD_j> = <T_iT_j> + <\epsilon_i\epsilon_j> .$$

Other than data, the most essential information needed in the optimal interpolation scheme is knowledge of the spatial and temporal covariance functions,

$$R(\vec{x}_i, \vec{x}_j,t_i,t_j) = <T(\vec{x}_i,t_i)\; T(\vec{x}_j,t_j)> = R_{ij} .$$

Simply stated, the covariance function is related to the statistical correlation of the field at point i to the field at point j; i.e., it is a measure of how relevant observations of a field at one point are to making an estimate of the field at another point. Observations that are highly correlated with the field at the point where the estimate is to be made will produce a good estimate. On the other hand, observations that are highly correlated with each other are not independent and are considered redundant when forming the estimate. Calculating these functions requirε large numbers of observations or a good physical model and is a significant step in creating an optimal interpolation analysis system.

NORDA has developed an optimal interpolation thermal analysis system for the Navy's operational upper ocean analysis needs (Innis, 1985). This system, the Optimum Thermal Interpolation System (OTIS), has been delivered to FNOC and will soon replace the existing operational thermal analysis software, the Expanded Ocean Thermal Structure (EOTS). OTIS will produce upper ocean thermal analyses for the northern hemisphere (with approximately 320-km resolution), as well as high-resolution (20–40 km) regional analyses for such important areas as the Gulf Stream, the Kuroshio region, the Mediterranean Sea, etc. By putting the analysis procedure on a firm rational base, dramatic improvements in the Navy's ocean thermal analysis capabilities are anticipated. Preliminary examples of open ocean vertical temperature profiles and a contoured northern hemisphere 300-m temperature field obtained from an OTIS analysis can be seen in Figures 1 and 2.

For tactical applications, where resolution, timeliness, and data communication constraints are more stringent, NORDA is also developing optimal analysis software for carrier battle groups. Recent advances in microcomputer technology have made such ship-board systems feasible.

Dynamic forecasting

Dynamic forecast models seek to predict the state of the ocean thermal structure in the future or to modify observed fields to a dynamically consistent state by applying

AD-A170 212 THE NORDA (NAVAL OCEAN RESEARCH AND DEVELOPMENT ACTIVITY) REVIEW(U) NAVAL OCEAN RESEARCH AND DEVELOPMENT ACTIVITY NSTL STATION MS MAR 86 2/3

UNCLASSIFIED F/G 8/10 NL

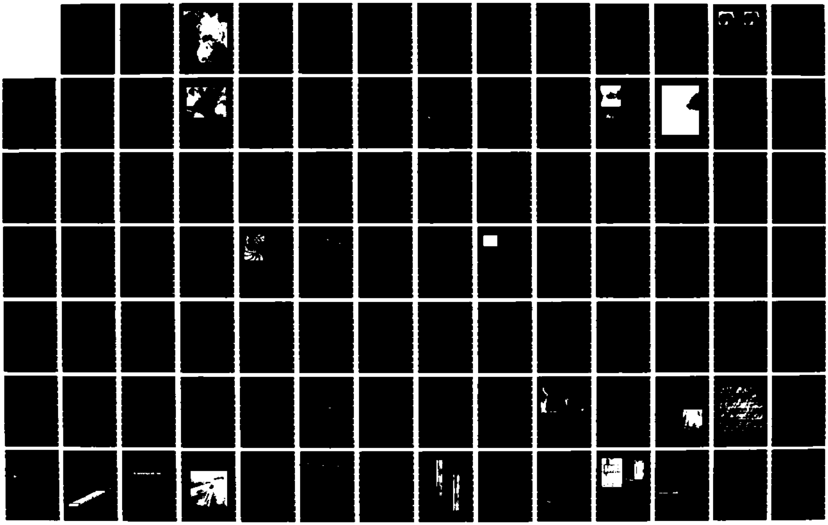

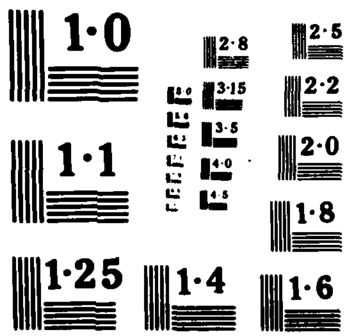
1·0
2·8
2·5
3·15
2·2
3·5
1·1
2·0
4·0
4·5
1·8
1·25
1·4
1·6

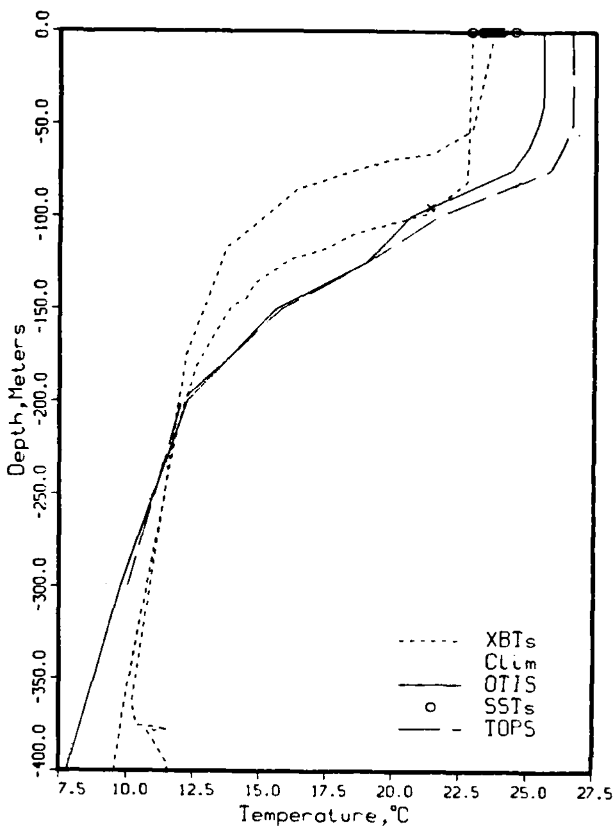

Figure 1. Vertical profiles of temperature at 6.5°S and 110.9°E obtained from XBTs, satellite sea-surface temperature (SST), climatology, TOPS, and OTIS.

the laws of physics to the ocean. These laws are the well-known conservation principles that govern momentum, internal energy, and chemical constituents of sea water.

Because the physical processes of the ocean cover such a broad range of space and time scales, it is impossible to solve the complete set of equations (the Navier-Stokes equations) for the upper ocean thermal structure. The equations must be simplified before any progress can be made. This simplification is achieved in two different ways: first, by ignoring terms in the equations that are small compared to the terms whose magnitudes are first order, and second, by rewriting large, unmanageable terms in simpler form. With these simplifications one hopes to eliminate the terms that make the problem hopelessly complex and yet retain the physics that produce a particular phenomenon. Even so, the equations must usually be solved numerically.

The most fundamental simplification is to decouple the shallow surface layer of the ocean from the deep interior. This involves treating the processes of the deep ocean as a boundary condition on the domain of interest—the upper ocean. Because the upper ocean is forced by the atmosphere, which exhibits significant changes over one- or two-day time scales, it is reasonable to expect that the slower motions of the deep ocean can be approximated by a steady-state background to the vigorously forced upper ocean circulation.

An additional, related simplification is to ignore horizontal pressure gradients in the momentum balance. This approximation is valid where large spatial scales prevail (in the interior of the ocean, far from lateral boundaries). A special advantage is that ignoring pressure gradients eliminates the problems associated with "initialization shock," a phenomenon that occurs when a numerical model is initialized with data that are not balanced with pressure gradient terms. Geostrophic currents, which are lost in this approximation, are generally unimportant in the mixed layer (except in western boundary currents such as the Gulf Stream or Kuroshio) but can be reinstated as advective forcing if desired.

Perhaps the most difficult simplification concerns the way the model handles the turbulence effects. The turbulent Reynold's stresses, which are expressions for important transfers of momentum on length and time scales that are too small for the model to resolve, must be accounted for in such a way that the relevant physics are preserved without rendering the equations unsolvable. Mixed-layer models generally fall into one of two categories with regard to how the turbulent energy affects the model. The first type of model, the turbulent closure model, seeks to parameterize the Reynold's stress terms as functions of known quantities, such as the shear or buoyancy. The second type of model, the bulk model, assumes that the mixed layer is homogeneous and introduces expressions that describe the vertically integrated properties (often the turbulent kinetic energy) of the mixed layer.

Since mixing in the upper ocean is not well understood, parameterizations proposed by different modelers vary considerably. Several mixed-layer-model studies have been carried out at NORDA to understand the important physical processes governing mixing in the upper ocean, to determine which of the alternate ways of handling the turbulence is most suitable for operational modeling, and to develop mixed-layer models that give consistently good predictions in different regions and conditions. Data used for model testing and evaluation includes specific mixed-layer experiments, such as MILE (Warn-Varnas et al., 1981), ocean buoys (Martin, 1982), and ocean weathership stations (Martin, 1985).

Figure 3 shows a comparison of several mixed-layer models at Weathership Station PAPA in the northeastern

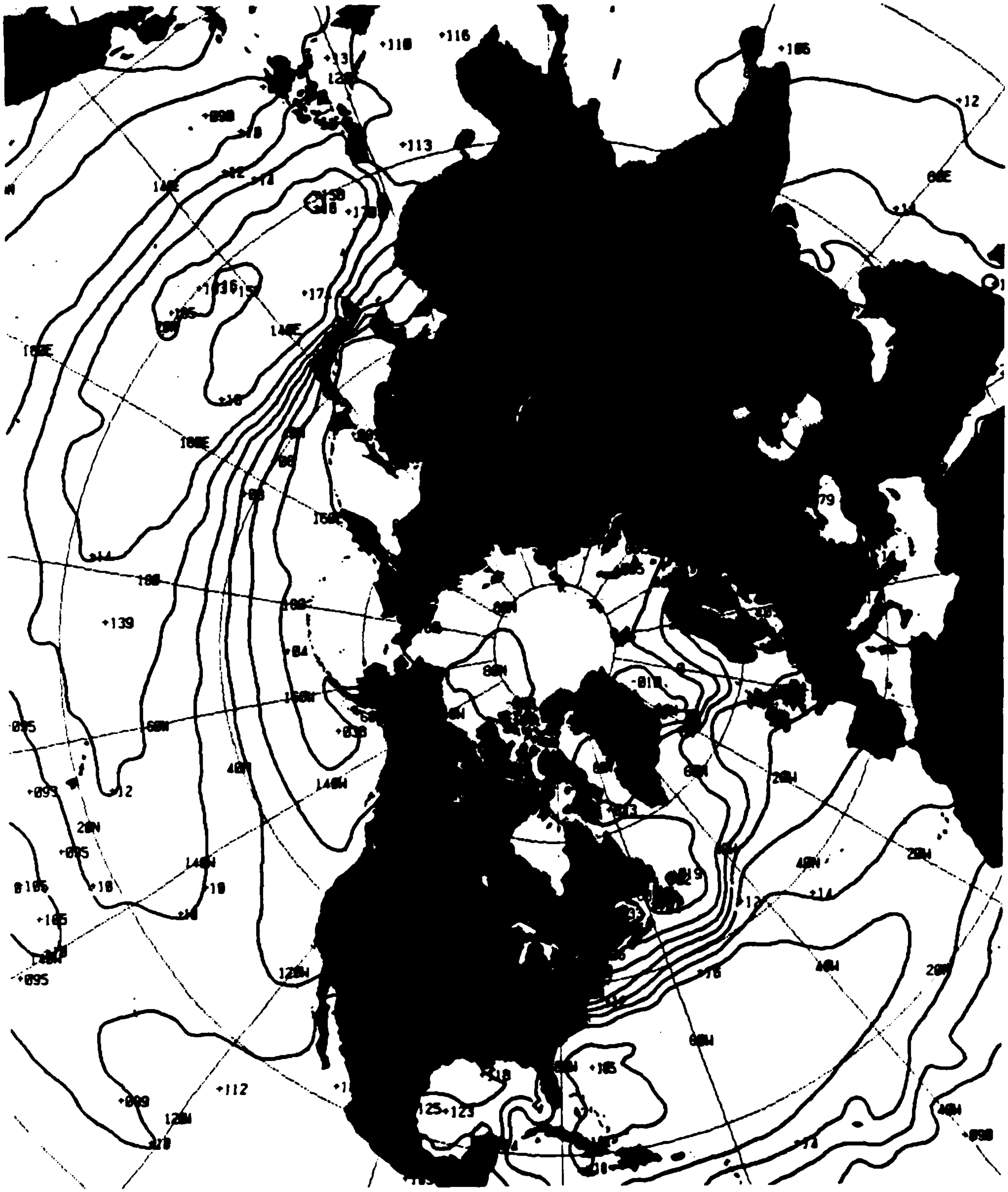

Figure 2. OTIS analysis of northern hemisphere 300 m temperature on FNOC 63 x 63 polar stereographic grid for 14 May 1982.

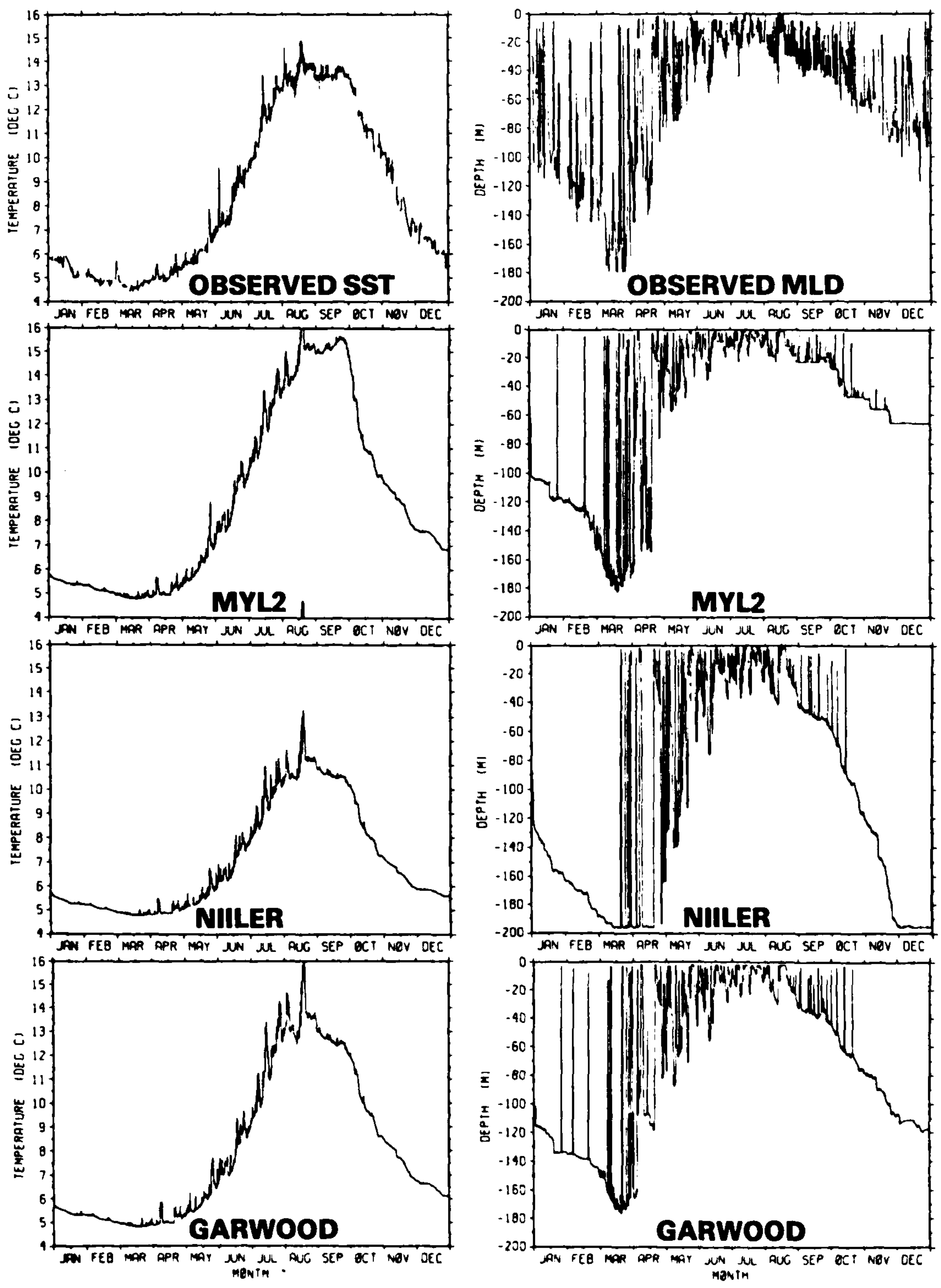

Figure 3. Year long simulations of sea surface temperature (SST) and mixed layer depth (MLD) at ocean station PAPA for the year 1961. Comparisons show the Mellor Yamada Level 2 turbulence scheme (MYL2), the Niiler bulk model, and the Garwood bulk model.

Pacific. Because changes in the upper ocean are usually caused by the surface momentum, heat, and moisture fluxes, all the models show a strong correlation with the observations on diurnal, synoptic, and seasonal timescales—the major timescales of weather variability. Discrepancies are mainly due to biases in determining the model mixed-layer depth, errors in calculating the surface forcing (from the meteorological observations), and advection. Advective effects are usually less significant in more quiescent regions (such as the central ocean gyres) but can be important in areas with strong gradients and currents. The neglect of advection in the PAPA simulations of Figure 3 does not noticeably bias the results until the fall, when all the models slightly underpredict the sea surface temperature.

The Thermal Ocean Prediction System (TOPS) is the current operational implementation of an upper ocean mixed layer model at FNOC. This model, developed at NORDA in the early 1980s, provides from one- to five-day forecasts (based on available forcing fields from atmospheric models) of the upper ocean temperature structure for the northern hemisphere and for various other regional areas.

Complete details of the model can be found in Clancy and Pollack (1983) or in Clancy and Martin (1979). An example of a prediction from the TOPS model is shown in Figure 4. The equations governing the TOPS model express conservation of temperature, salinity, and momentum in the upper ocean in the form

$$\frac{\partial T}{\partial t} = \frac{\partial}{\partial z} < -w'T' > - \nabla \cdot (\vec{V} T) + A \nabla_h^2 T + \frac{1}{\varrho c} \frac{\partial F}{\partial z}$$

$$\frac{\partial S}{\partial t} = \frac{\partial}{\partial z} < -w'S' > - \nabla \cdot (\vec{V} S) + A \nabla_h^2 S$$

$$\frac{\partial u}{\partial t} = fv + \frac{\partial}{\partial z} < -w'u' > - Du$$

$$\frac{\partial v}{\partial t} = -fu + \frac{\partial}{\partial z} < -w'v' > - Dv ,$$

where T is the temperature, S is the salinity, $\vec{v} = (u,v,w)$ is the (x,y,z)-components of current velocity, c is the specific heat of seawater, ϱ is the density of seawater, F is the solar radiation flux, D is a damping coefficient, f is the Coriolis parameter, A is the horizontal eddy diffusion,

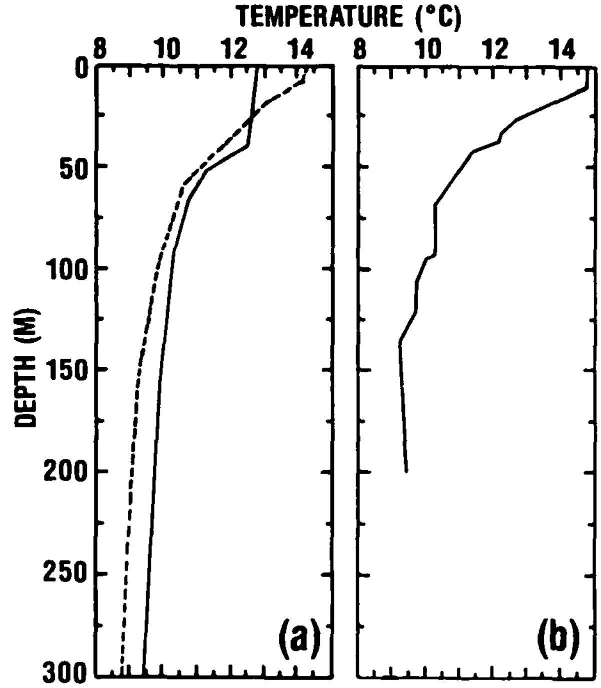

Figure 4. Temperature profiles from climatology (solid line) and TOPS 24-hour prediction (dashed line) from ocean weather station LIMA for 00Z 25 July 1984 (a). Verifying XBT, taken at 09Z is shown in (b).

and $\vec{V} = (U,V,W)$ is the advective velocity. The horizontal components of the gradient operator terms, defined by

$$\nabla_h^2 = \frac{\partial^2}{\partial x^2} + \frac{\partial^2}{\partial y^2}, \quad \text{and}$$

$$\nabla = i \frac{\partial}{\partial x} + j \frac{\partial}{\partial y} + k \frac{\partial}{\partial z},$$

are retained to properly account for advective tendencies due to Ekman drift and geostrophic currents.

The turbulence is parameterized in the TOPS model using the Mellor-Yamada Level-2 (MYL2) turbulent closure scheme, which expresses the Reynolds flux terms as

$$< u'w' > = -(lqQ_m + \nu) \frac{\partial u}{\partial z}$$

$$< v'w' > = -(lqQ_m + \nu) \frac{\partial v}{\partial z}$$

$$< w'T' > = -(lqQ_n + \nu) \frac{\partial T}{\partial z}$$

$$< w'S' > = -(lqQ_n + \nu) \frac{\partial S}{\partial z}$$

where q is twice the square root of the turbulent kinetic energy, l is the turbulent length scale, ν is a background diffusion, and Q_h and Q_m are functions that depend on the local current shear and gravitational stability (i.e., the gradient Richardson number). This treatment of the turbulent Reynolds stresses was chosen for its physical foundations and because it accurately models the continuous stratification at the base of the mixed layer, which bulk models show as a discontinuous jump.

Operational numerical integration of these equations is carried out for the 63 x 63 northern hemisphere grid on the FNOC Cyber-205 computer using forcing fields from the Navy Operational Global Prediction System (NOGAPS) and the Global Surface Contact Layer Interface (GSCLI) models. In addition, temperature fields over two high-resolution (40 km) regional grids, the eastern and western Mediterranean, are forecast on an operational basis, although in nonadvective mode. In its present configuration the TOPS forecast is cycled with the FNOC operational upper ocean analysis (EOTS) using the TOPS forecast fields as a "first guess" for the analysis and the analyzed fields as initial conditions for the forecast model. This procedure, known as TOPS-EOTS or TEOTS, is comparable to that used for atmospheric forecast and analysis operations.

Verification studies of TOPS predictions (Clancy and Pollack, 1983) show that the TEOTS system does exhibit forecast skill. These studies compared forecast sea-surface temperature and mixed-layer depth changes to changes in the analyzed fields for the same period. Good correlations between the forecast and analyzed fields were obtained for forecasts out to 72 hours.

Conclusions

The future holds many advances in the Navy's upper-ocean analysis and forecasting capabilities. Some advances will come from improved computer resources and increased use of satellite observations but many will result from basic research efforts into physical and statistical modeling. Additional improvements will come through developmental efforts in model verification, algorithm development, and software support. NORDA will continue to actively support the Fleet's upper ocean analysis and prediction needs through research in these areas and through continued development and improvement of such operational products as OTIS and TOPS.

References

Bretherton, F. P., R. E. Davis, and C. B. Fandry (1976). A Technique for Objective Analysis and Design of Oceanographic Experiments Applied to MODE-73. *Deep-Sea Research* 23, 559–582.

Clancy, R. M. and P. J. Martin (1979). *The NORDA/FLENUMOCEANCEN Thermodynamical Ocean Prediction System (TOPS): A Technical Description.* Naval Ocean Research and Development Activity, NSTL, Mississippi, Technical Note 54.

Clancy, R. M. and K. D. Pollak (1983). A Real-Time Synoptic Ocean Thermal Analysis/Forecast System. *Progress in Oceanography* 12, 383–424.

Innis, G. E. (1985). *Further Development and Implementation of the Optimum Thermal Interpolation System (OTIS) at FNOC.* Science Applications International Corporation, La Jolla, California.

James, R. W. (1966). *Ocean Thermal Structure Forecasting.* ASWEPS Manual Series Vol.5 (SP-105). U.S. Naval Oceanographic Office (Washington, D. C.), NSTL, Mississippi, 217 p.

Krauss, E. (ed.) (1977). *Modelling and Prediction of the Upper Layers of the Ocean.* Pergamon Press, Oxford, 325 p.

Martin, P. J. (1982). Mixed-Layer Simulation of Buoy Observations Taken During Hurricane Eloise. *Journal of Geophysical Research* 87, 409–427.

Martin, P. J. (1985). Simulation of the Mixed Layer at OWS November and Papa With Several Models. *Journal of Geophysical Research* 90, 903–916.

May, P. W. (1985). *Evaluation of Objective Thermal Analysis Techniques for Battle Group Support.* (NORDA Technical Publication in preparation).

Mooers, C. N. K., S. A. Piacsek, and A. R. Robinson (1982). Ocean Prediction: The Scientific Basis and the Navy's Needs. *Proceedings of the Ocean Prediction Workshop*, Monterey, California.

Urick, R. J. (1983). *Principles of Underwater Sound.* McGraw-Hill Book Co., New York. 423 p.

Warn-Varnas, A. C., G. M. Dawson, and P. J. Martin (1981). Forecast and Studies of Oceanic Mixed Layer During the MILE Experiment. *Geophysical and Astrophysical Fluid Dynamics* 17, 63–85.

Numerical Modeling and Assimilation of Altimeter Data in the Gulf Stream System

J. Dana Thompson, Harley E. Hurlburt and John C. Kindle
Numerical Modeling Division

Abstract

The dynamics of portions of the Gulf Stream System have been studied by using numerical simulations, comparisons with in situ and remotely sensed data, and simplified dynamical models. We have developed a simple potential vorticity-conserving model that can account for the size of shed eddies, the eddy-shedding period, and the westward eddy drift.

Recent work concentrated on the Gulf Stream dynamics downstream from Cape Hatteras. We found that the generation of deep flow by Gulf Stream instabilities can provide a mechanism that causes the New England Seamount Chain to influence the mean path of the stream, the amplitude of its meanders, and the eddy distribution in the seamount vicinity. We have also found that a single vertical-mode, reduce gravity model and a two-layer model with small-amplitude topography consistent with the quasi-geostrophic assumption gives results quite different from those given by the two-layer primitive equation model with full topography.

We believe results from these studies can be applied to the assimilation of GEOSAT data in the upcoming NORDA Regional Energetics Experiment in the northwest Atlantic.

Introduction

In the next decade, oceanographers will organize and participate in several exciting and ambitious programs, inspired in part by the rapidly emerging technologies of satellite remote sensing, new in situ instrumentation, a new generation of numerical ocean models, and a new class of supercomputers. These programs will be part of a larger effort to monitor, understand, and predict the ocean and atmosphere on many time and space scales. Obvious practical applications of this work will encompass climate studies, naval operations, and commercial activities. At least one of these programs will include a concerted attempt to predict the evolution of some part of the Gulf Stream System (GSS). Before addressing that task, we examine the prediction problem in light of our basic understanding of Gulf Stream dynamics and the potential of present and future observing systems. We can now make very accurate predictions of some ocean parameters (tides, for example) with little or no basic understanding of ocean dynamics or physics, but for most elements of ocean prediction, where we lack adequate observing systems and historical data, our knowledge of ocean dynamics is critical for efficient use of very limited resources.

Predictions are desirable for several classes of ocean phenomena. As noted by Hurlburt (1984) and shown in Table 1, one means of distinguishing these classes of ocean processes is by their response to atmospheric forcing. Each class has its own particular requirements for accuracy of the initial state, time scales for skillful forecasts, modeling strategy, data types, and data acquisition and sampling strategies. For the most part, predictions related to the GSS, at least those related to Gulf Stream meandering and eddy shedding, are identified with Class 2. This class is most sensitive to initial conditions not directly related to atmospheric forcing and is subject to contamination by errors in boundary conditions over time scales comparable to that needed to propagate information across the forecast domain.

Table 1. Classes of oceanic response to atmospheric forcing where predictive skill is feasible.

Class	Implications	Examples
1. Strong, rapid (<1 wk) and direct	A. short-range forecasts limited by the time scale for atmospheric predictive skill B. less sensitive to errors in the initial state; more sensitive to errors in the forcing functions	surface mixed layers, surface and some internal waves, Ekman drift currents, some coastal and equatorial processes such as upwelling (in some cases), coastal storm surges, and the onset of some equatorial and coastal waves.
2. Slow (weeks to months) and direct	A. long-range forecasts (potentially a month or more) B. more sensitive to errors in the initial state, less sensitive to errors in the forcing functions C. statistical properties of features and ensembles may be predicted by skillful simulation D. prediction of individual features requires oceanographic data. Altimeter data are the most promising operational source now on the horizon	mesoscale eddies, meandering currents, some frontal positions, features caused by mesoscale flow instabilities.
3. Slow (weeks to years) but direct (i.e., integrated response)	A. long-range forecasts B. sensitive to errors in atmospheric forcing functions on long time scales (e.g., monthly means); but less sensitive to errors on short time scales (e.g., daily fluctuations) C. nowcasting and forecasting are potentially feasible without good oceanic data by means of simulations that use appropriate ocean circulation models	El Niño, much of the tropical ocean circulation (in the Atlantic, Pacific, and Indian Oceans), equatorial waves, part of the large-scale ocean circulation, features such as gyres directly driven by persistent or repeated patterns in the wind, often in conjunction with geometric constraints, e.g., most of the circulation features in the Mediterranean Sea with scales >100 km.

We have been involved in the Class 2 problem for the GSS through work on the Gulf of Mexico and, more recently, on the Gulf Stream downstream from Cape Hatteras. The strategy for both regions has consisted of the following basic steps:

- Develop the simplest model of the system that has some hope of simulating the consistently observed features.
- Using the best forcing functions and boundary conditions available, drive the model to statistical equilibrium; perturb the forcing functions and boundary conditions to explore the full range of possible model response.
- Compare model results with observations, noting what processes exhibit close agreement and substantial disagreement.
- Explain the model results in terms of basic dynamics. Can a simple analytical model account for the observations?
- Once the numerical model has been validated, use it to make predictions of features yet to be observed and for developing techniques to improve the utilization and collection of observational data.

This article briefly describes how we have used this strategy in studying the dynamics and predictability of the GSS.

Discussion

GSS modeling—south

In the southern portion of the GSS the Loop Current enters through the Yucatan Strait and traces an anticyclonic path that may extend almost to the Mississippi Delta before turning southward and exiting through the Florida Straits. The Loop Current volume transport is approximately 30×10^6 m^3/sec and eventually becomes a principal component of the Gulf Stream. Maximum geostrophic surface currents in the Loop can exceed 150 cm/sec and the dynamic height change across the stream can be greater than 75 cm, easily detectable by a satellite altimeter. Large anticyclones (also termed rings) which have diameters larger than 300 km, have been observed to break off from the Loop Current and are believed to move into the western Gulf. Elliott (1979) has estimated the mean westward drift speed after break-off to be about 2.4 cm/sec, although recent observations suggest the speed of eddy drift can be quite variable. Figure 1b, from near-synoptic hydrographic data by Leipper (1970), shows the Loop Current and a large anticyclonic ring about to be shed from it. Much earlier, Ichiye (1962) suggested that detached Loop Current eddies could drift across the Gulf and maintain an anticyclonic circulation in the western basin. Sturges and Blaha (1976) proposed that wind stress curl might drive a mean anticyclonic gyre in the western Gulf.

The Loop Current was once thought to penetrate into the Gulf during the spring and summer, shed an anticyclone during late summer and fall, and exhibit minimum penetration in the winter. This cycle was believed to be due to seasonal variations in the flow through the Yucatan

Strait (Cochrane, 1965). New oceanographic and satellite data have shown that the eddy shedding period ranges from eight to 15 months (Molinari, 1980) and that the earlier interpretation of a dominant seasonal cycle was due to a bias in the data set (Molinari et al., 1977). Results from low-order vertical mode primitive equation numerical models of Hurlburt and Thompson (1980), henceforth referred to as HT, show that approximately an annual period of eddy shedding can occur with no variations in the inflow transport and that for realistic constant values of inflow transport, the mean period between major eddy breakoff is about 10 months. The model Loop Current spontaneously and regularly sheds eddies with realistic diameter, amplitude, and speed of propagation. Agreement between model and observations and the theoretical basis for Loop Current penetration, the ring sizes, the shedding rate, and the westward translation speed are discussed in terms of momentum and potential vorticity conservation

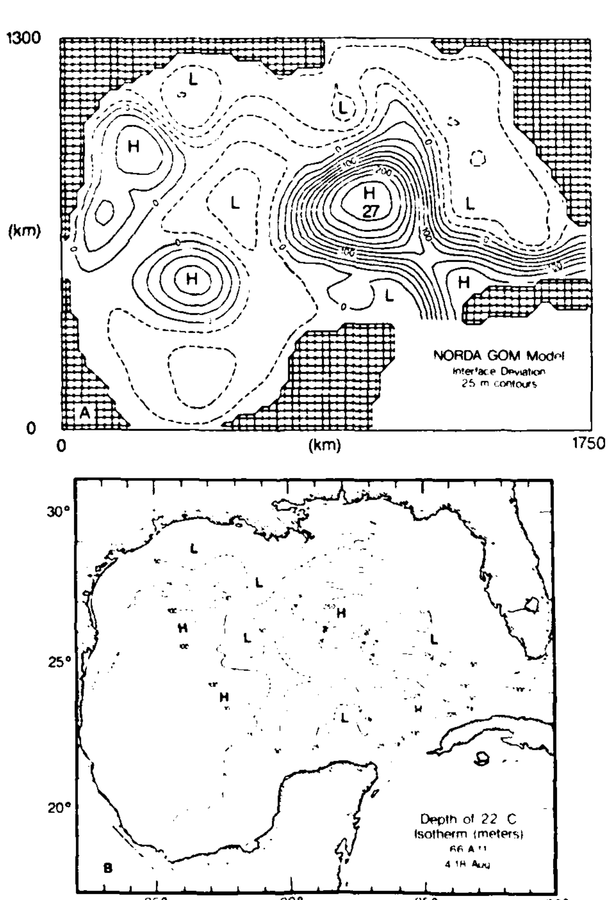

Figure 1. (a) Model experiment by Hurlburt (1984) and (b) near synoptic hydrographic data by Leipper (1970).

and Rossby wave dynamics in HT. An energetics analysis of model experiments exhibiting baroclinic and/or barotropic instability is provided in Hurlburt and Thompson (1982).

The first semi-implicit eddy-resolving primitive equation model retaining realistic geometry and bottom topography for any deep ocean basin was developed for the Gulf of Mexico by Wallcraft and Thompson (1984), who extended the rectangular-basin model of HT to include an irregular coastline. A two-layer, hydrodynamic version of the model on a beta-plane was driven from rest to statistical equilibrium by steady inflow through the Yucatan Strait and exactly compensated by outflow through the Florida Straits. Figure 1a is a snapshot from a model experiment (Hurlburt, 1984) near the same phase of eddy shedding as found by Leipper (1970). A benchmark experiment using a similar model is discussed below. Model parameters for the present benchmark experiment are given in Table 2. The principal difference between this experiment and the one described by Hurlburt (1984) is the vertical distribution of volume transport through the Yucatan Strait. By allowing a larger fraction of the total transport to be carried by the deep flow, we have found more consistent agreement between model and observations, both in terms of the size of the anticyclones and the amplitude of the fluctuating component of the dynamic sea surface height. Existing data on the long-term vertical distribution of transport through the Yucatan Strait is inadequate to validate any particular choice of transport forcing within a rather wide range in each layer although the total transport value of 30×10^6 cm^3/sec is a well-accepted mean.

Figure 2 shows a sequence of dynamic sea surface height anomaly maps (height above an initial uniform level) for the benchmark experiment following spin-up to statistical equilibrium. The first five panels are snapshots every 30 days from Day 1450 to Day 1570; the last panel is Day 1890, during the subsequent shedding cycle. Once the Loop penetrated sufficiently far into the Gulf, it became barotropically unstable and rapidly shed an anticyclone

Table 2. Model parameters for Benchmark experiment.

A	$300\ m^2\ sec^{-1}$	β	$2 \times 10^{-11}\ m^{-1}\ s^{-1}$
C_B	2×10^{-3}	ϱ	$10^{-3}\ kg\ m^{-3}$
f_o	$5 \times 10^{-5}\ s^{-1}$	$\vec{\tau}$	0
g	$9.8\ m\ sec^{-2}$	$\Delta x, \Delta y$	0.2°
g'	$\frac{0.03\ (H_1 + H_2)}{H_2}\ m^2\ s^{-2}$	H_1, H_2	200 m, 3400 m

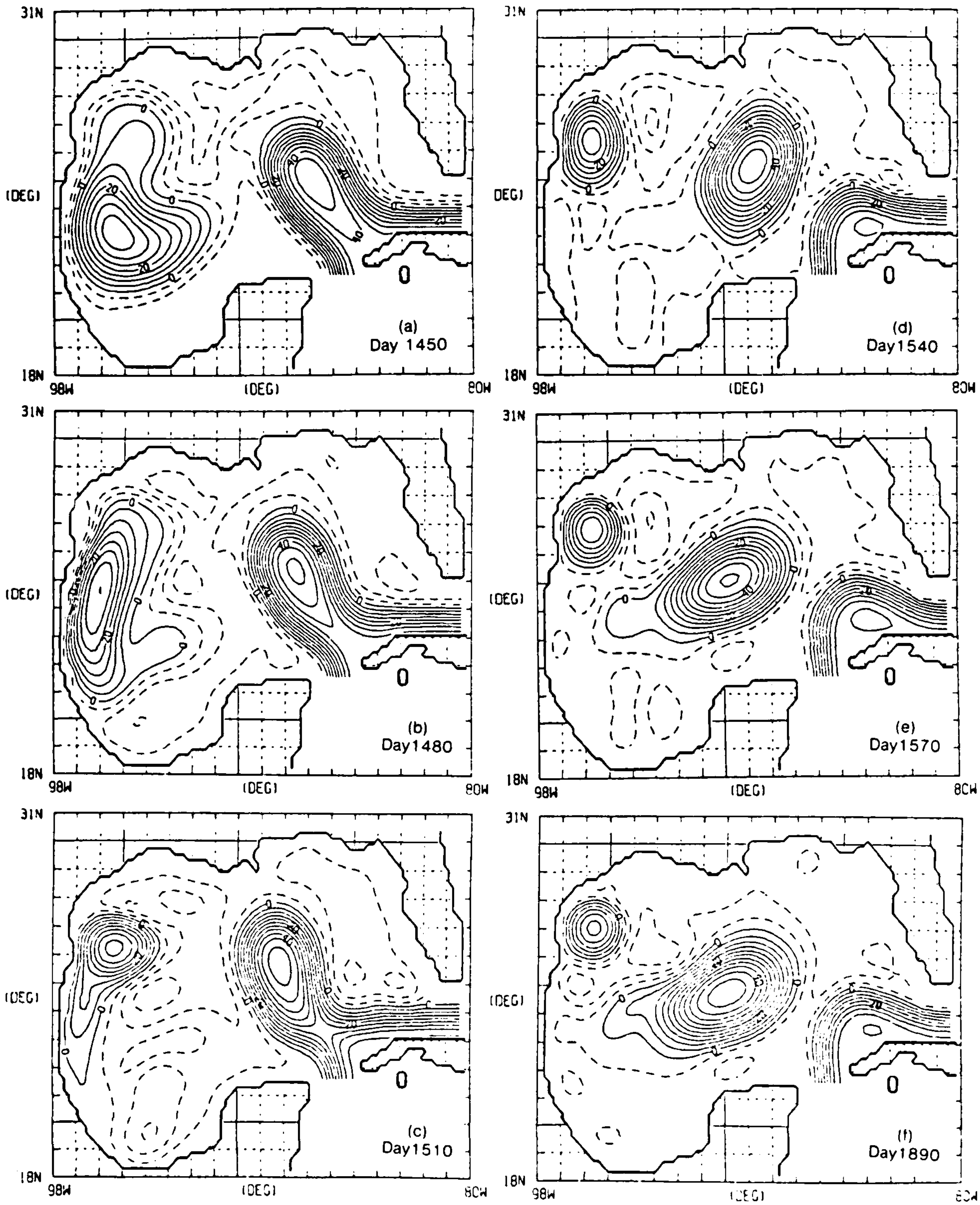

Figure 2. Sequence of dynamic sea surface height anomaly maps

(Day 1450—Day 1540). During this period an anticyclone shed in the previous cycle impinged on the western Gulf, rapidly distorted its shape as it decayed, and evolved to a small, residual anticyclone in the northwestern Gulf by Day 1540. In the eastern Gulf the development of a cold intrusion and a closed cyclonic circulation on the east side of the Loop is evident between Days 1510 and 1540. This feature was often seen in satellite imagery and has been directly observed from shipboard hydrographic data. The shedding rate of large anticyclones from the Loop Current in this experiment was 316 days. The shed anticyclone drifted toward the southwest at about 4 cm/sec. As the main ring drifted into the central and western Gulf, a weak cyclonic circulation developed to its west and northwest. This event is a precursor of the cyclone/anticyclone pair found in the observations and in other numerical experiments.

The model, driven by realistic forcing to statistical equilibrium, is capable of producing dynamic sea surfaces that can be compared with both altimeter and in situ data. Moreover, one can combine the model results, in situ data, and the altimeter data for an optimal estimation of both the dynamic heights and the geoid (Wunsch and Gaposchkin, 1980; Marshall, 1985). Thompson (1985) has compared in detail the mean dynamic height and variability of the sea surface in the Gulf as determined by Maul and Herman (1985) from hydrographic data and the correlation of temperature and salinity in the deep waters of the Gulf; the mean sea surface and its variability as determined from GEOS-3 and SEASAT altimeter crossover data presented by Marsh et al. (1984), henceforth termed MC; and the mean sea surface height and variability as determined from the numerical model after reaching statistical equilibrium.

The variability of the sea surface from altimeter crossover differences as determined by MC and from the numerical model are shown in Figures 3a and 3b respectively. In the eastern Gulf the sea surface height variability amplitude and approximate position were very similar for model, altimeter, and in situ data (not shown). However, in the central Gulf, while the model variability map and the altimeter map agree very well and indicate a ridge of high variabilty extending from the Loop Current toward the southwestern Gulf, they both differed substantially from the map that was determined from the in situ data. The existence of the ridge of high variability toward the southwest in the model and in the altimeter data supports the hypothesis that eddies shed from the Loop Current do drift southwestward. This result has important implications for the fate of materials transported by the Gulf circulation and the role of anticyclones in the circulation of the western Gulf. However, the fact that this ridge does not appear in the in situ data is very disconcerting. This is not merely a minor discrepancy in interpretation or analysis procedure and has considerable dynamical significance. The reasons for these discrepancies are presently being investigated.

Because of the close agreement between model sea surface variability and that observed from altimeters, the dynamical consistency of the results with such auxiliary data as drifter trajectories in shed eddies (Kirwan et al., 1984, and personal communication), and the evaluation of the model through comparison with synoptic observations, we conclude that the model is sufficiently realistic so that we can begin to use it as a tool for studying how to use altimeter data for ocean monitoring and prediction in the GSS.

Altimeter data and the GSS

Once the validity of the model was established by comparisons with in situ and altimeter data, we were able to use it in the study of Gulf circulation predictability by using altimetrically derived sea surface heights. As part of the Office of Naval Research Accelerated Research Initiative in Ocean Dynamics from Altimetry at NORDA, three studies have been conducted using various versions of the Gulf of Mexico model: geoid error and initialization, conversion of surface to subsurface information, and sampling strategies using a single nadir-beam altimeter. The latter two experiments used the rectangular-domain, idealized Gulf of Mexico geometry.

In the first study the experiment described previously was used as a benchmark and was compared with results from four experiments in which the model was initialized with fields modified from archived benchmark data. The experiments differed only in the initialization fields. Each experiment was integrated for 100 days and inflow transport remained constant throughout the integration. The experiments were initialized geostrophically (1) with the exact sea surface and pycnocline height fields, (2) with only the exact sea surface heights and the pycnocline assumed to exactly compensate such that the deep flow vanished, (3) just as in (2) but with a geoid error component added, and (4) just as in (3) except that the geoid error model included an additional contribution in strong geoid gradient regions. The experiments are outlined in more detail and reported in Thompson (1985).

The results of the experiments are summarized in Figure 4, where the normalized root mean square (NRMS) error of the free surface anomaly (FSA), the pycnocline height anomaly (PHA), and the lower layer pressure is plotted

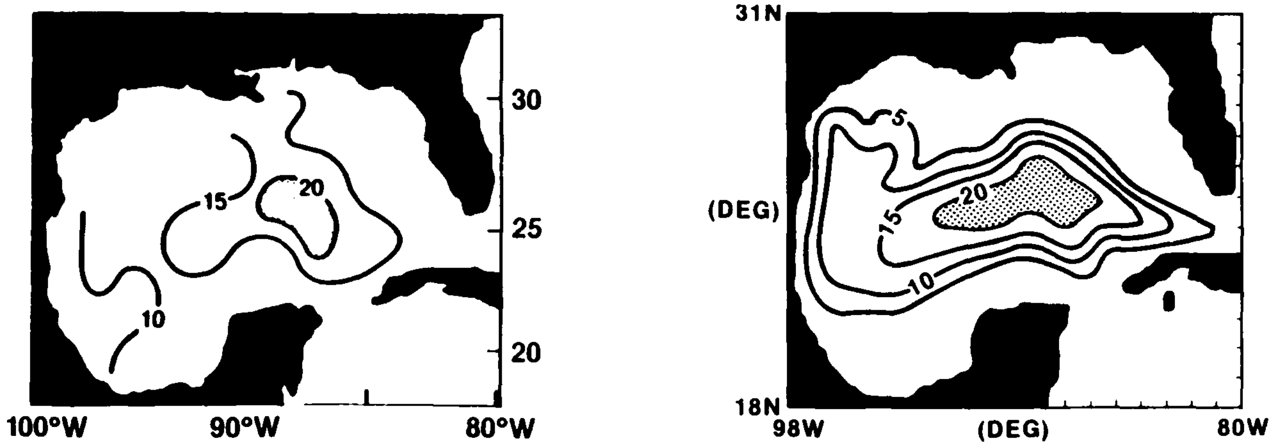

Figure 3. Sea surface variability from GEOS 3 and SEASAT cross-overs (cm) (from Marsh, et al., 1984) and sea surface variability (cm) from NORDA model (b).

The normalization factor is the RMS variability of each field from the benchmark case. The lower layer pressure field is the most difficult field to predict from initial knowledge of the free surface only. At the initial time the NRMS error of lower layer pressure (P2) for Experiment 2 is 100% and increases to over 120% before gradually decreasing to less than 40% by the end of the period.

Experiments 1 and 2 dealt with perfectly known sea surface height information. Experiments 3 and 4 focused on errors likely to be introduced by uncertainties in the geoid on small spatial scales, comparable to the length scale of seamounts or, more generally, the scale of very rapid changes in geoid height associated with strong bottom slopes. These errors may prove difficult to remove from the sea surface height signal, particularly because they may be correlated with dynamic ocean processes over the same scales. In Experiment 3 the error field is represented as random noise with a normal probability distribution function, a zero mean, and a standard deviation of + 5 cm. The range of variation over the domain is > 34 cm. The error field is uncorrelated over the 0.2° model grid. Experiment 4 contains an error field that reflects the fact that geoid errors are likely to be larger on the small scale in the vicinity of strong geoid gradients such as the Campeche escarpment, where the geoid gradient approaches a meter in 10 km. The range of variation in this case is > 47 cm, and the impact of the strong gradient areas on the error field is especially large in the southwestern Gulf.

From the sequence of four numerical experiments we found that even when only the sea surface height information was provided to the numerical model at the initial time, the forecasts of FSA, PHA and even deep pressure were superior to persistence or climatology over the 100-day forecast period. We also found that noise in the initial field, at least on the amplitude and scales of that used in the experiments, did not seriously degrade the forecasts. This result occurred despite the obvious excitation of growing waves on the Loop Current and in the western Gulf.

While the preceding experiments were instructive, they did not provide a comprehensive view of how well altimeter

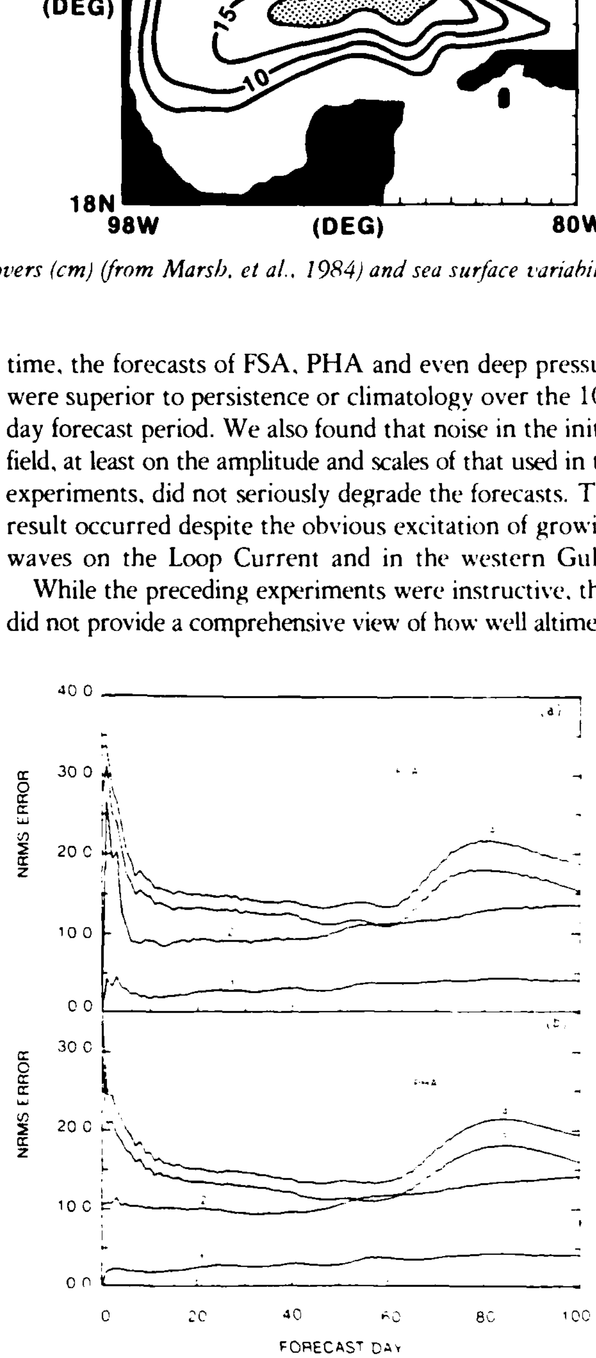

Figure 4. Experiment results.

data might be utilized in different dynamical regimes. Hurlburt (1985) has examined this problem in the context of converting well-observed surface altimeter data into subsurface information. This conversion was done for a variety of dynamical regimes with barotropic, baroclinic, mixed, and episodic instabilities; flat bottoms or large amplitude topogaphy; relatively vigorous or gentle exchanges of energy between the layers; major time scales that are short (~ 60 days), long (~ 1 year) or both; and unstable currents and isolated eddies. In all cases the pattern of the deep pressure field is much different from that of the current-related variations in the sea surface elevations and is sometimes not obviously related to it. Given only the free surface elevation (simulated altimeter data) from the true model solution, the model was able to reconstruct the deep pressure field, even in situations with energetic shallow and deep circulations, baroclinic instability, and a vigorous vertical exchange of energy. However, in such experiments the frequency of updating for the free surface was critical. In this study the maximum update interval that allowed successful dynamic surface-to-subsurface transfer was about half the shortest major time scale (SMTS), which is from 50 to 60 days in the experiments with baroclinic instability (Fig. 5).

Without knowledge of the deep pressure field, numerical predictions of the surface pressure field and the depth of the pycnocline were typically better than climatology for $^1/_4$ to $^1/_2$ the SMTS, but with successful dynamic surface to subsurface transfer, forecasts without updating were better than cimatology for the SMTS or more. The time scale for predictive skill is substantially longer than the maximum update interval permitted because the update interval must be short enough to allow decreasing error in the deep pressure field from one free surface update to the next until the error asymptotes at some acceptable level, approximately 30% to 50% in these results. Forecasts of isolated eddies demonstrated predictive skill for three months or more even when the subsurface initial state was unknown.

In the third study, Kindle (1985) utilized the one-layer, reduced-gravity model of the Gulf of Mexico to study the spatial and temporal sampling problem associated with a single nadir-beam altimeter. The two previous studies assumed data was available over the entire domain at a given time rather than along narrow swaths staggered in time. The simulated data were obtained by flying an imaginary altimeter over the model ocean and sampling the sea surface in a manner similar to a real altimeter (see Fig. 6). The numerical model was geostrophically initialized using the asynoptic data, which are assumed to be valid at the mid-point of the observing period. Figure 7a shows the RMS errors of the forecasts generated using only the data from the ascending tracks for each of the three periods (72, 36, and 24 days) of the exactly repeating satellite tracks. Figure 7b demonstrates that if the descending track data are used, the RMS error can be significantly different. Surprisingly, in the descending track forecast the error decays more rapidly, even though the initial value of the RMS error is substantially greater than the representation based on the ascending track observations. Figure 7c shows the results of applying an intermittent updating scheme during the nowcast period to reduce the effects of asynopticity. The numerical nowcast is initialized with the asynoptic data (Figs. 6a, b, c) at the beginning of the

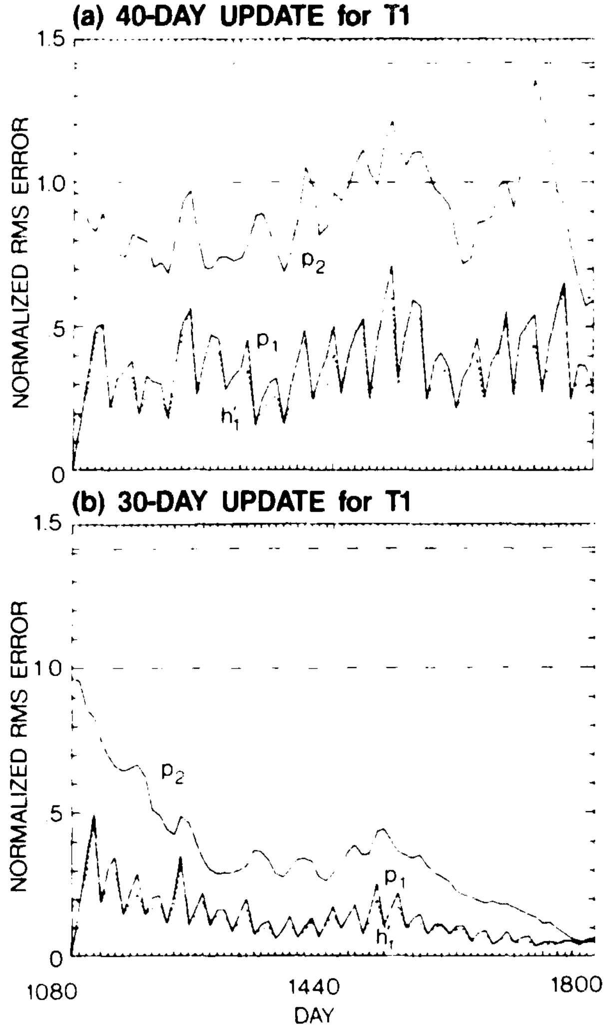

Figure 5. Baroclinic instability experiments

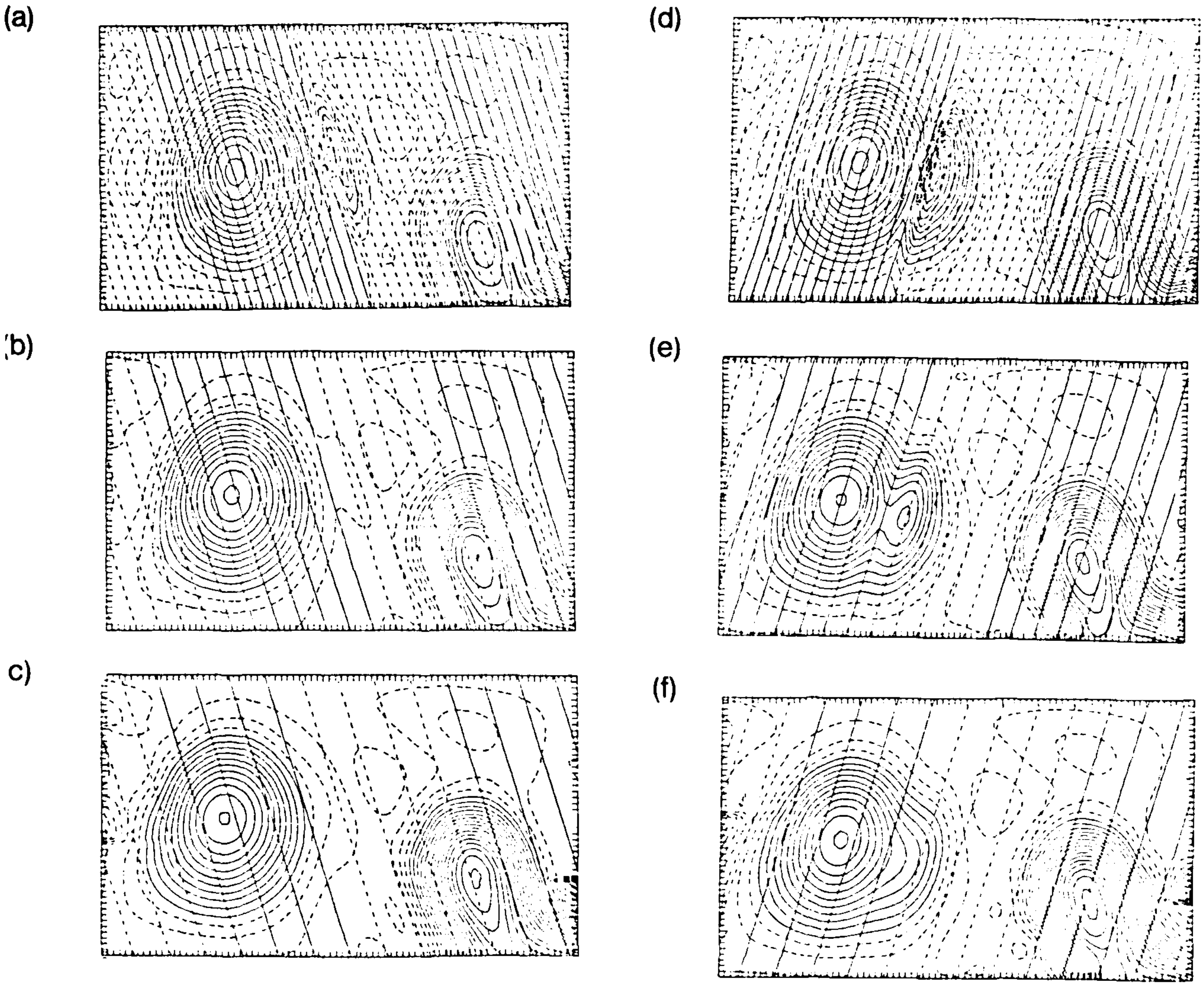

Figure 6. Simulated data.

observing period and the data are reinserted into the numerical solution 4 tracks at a time (i.e., every 12 days) until Day 0 of the forecast. No data are inserted into the model during the forecast. The results demonstrate that the asynopticity of the 72-day repeat track observations were reduced so effectively that the forecast was just as accurate as the one using the 24-day repeat track data. A similar experiment using the descending track data (not shown) exhibited virtually identical results.

The essence of Kindle's study is that the sampling trade-off between track spacing and repeat period may not be as difficult as once thought. The interaction between synoptic altimeter data and a hydrodynamic numerical model indicates that in many regions both adequate spatial and temporal resolution may be possible with a single nadir-beam altimeter. The observations form the basis of the model initialization and, in turn, the model "corrects" the asynopticity of the data. The result is an accurate nowcast which, for highly asynoptic data, would not have been possible without the model. A sampling strategy should favor spatial resolution and resolve the important dynamic features; the inherent asynopticity of the measurements can be reduced by applying an initialization/updating scheme to the numerical nowcast.

GSS modeling—north

We have begun to employ the strategy used for modeling the southern portion of the GSS to the northern portion

downstream of Cape Hatteras. Recently, Thompson and Hurlburt (1982) and Hurlburt and Thompson (1984), both henceforth referred to as HTG, have developed a primitive equation (PE) model of the Gulf Stream, including bottom topography. In the HTG study, the model domain extended from Cape Hatteras to the Grand Banks. The domain was rotated 28° counterclockwise from zonal. To avoid unknown specification of open-boundary segments, the model domain was closed except for an inflow port at Cape Hatteras and an outflow port roughly at the mean position of the Gulf Stream as it passes south of the Grand Banks. In all the experiments reported, the flow of the Gulf Stream was confined to the upper layer of the model. Thus, this work departs significantly from other studies of flow over topography in that the flow is not directly forced to impinge on the topography. Here, any flow in the lower layer must be driven from above due to pressure fluctuations associated with the active upper ocean. Any influence of the seamount chain on the path of the Gulf Stream must be a back interaction driven by the upper ocean.

Five numerical experiments were conducted. All but one used two active layers, the minimum allowing baroclinic instability, and both a thermocline and bottom topography. One experiment used a reduced gravity model with an active upper layer and a lower layer infinitely deep and at rest. The other experiments were identical except for the bottom topography used. In experiment 3, a Gaussian ridge with a maximum height of 2500 m was added across the channel with an e-folding half-width of 50 km. For the seamount experiments a set of four Gaussian seamounts with an amplitude of 2500 m for Experiment 4 and 500 m for Experiment 5 were aligned across the channel with the same e-folding halfwidth as for the ridge. The seamounts were spaced 200 km apart. The separation and the diameter of the seamounts are substantially greater than for the real seamounts, a compromise dictated by the affordable grid resolution and the desired domain size. The diameter (radius) of the real (model) seamounts is comparable to the baroclinic radius of deformation.

The five numerical experiments were integrated from rest for seven years. Approximately four years were required to reach statistical equilibrium, and another three years were added for a stable, long time series. Results of the modeling study can be briefly summarized.

- The model New England Seamount Chain (NESC) was found to have a substantial influence on the Gulf Stream even when the Stream did not directly impinge on the topography.

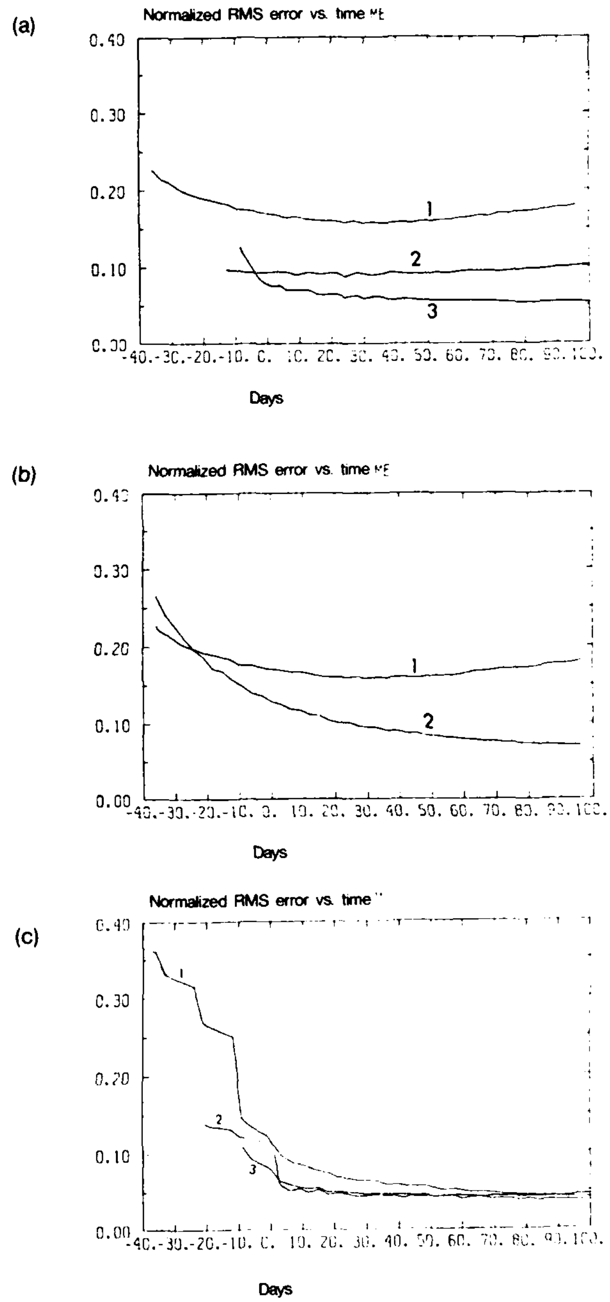

Figure 7. Forecast errors.

- Results from the reduced-gravity model were quite unrealistic, which suggests that addition of the barotropic mode, which yielded a more realistic GS, is critical to modeling the GS in this region.
- Warm core ring generation was enhanced by the NESC. Prolific generation of warm core rings occurs

immediately upstream of the NESC with a frequency of about two a year.

- When compared to the flat bottom experiment, the NESC increased both baroclinic and barotropic instabilities as measured by the rate of transfer of mean potential to eddy potential energy and mean kinetic to eddy kinetic energy (EKE).
- Maximum EKE in the large seamount experiment exceeds 2000 cm/sec in the upper layer and 130 cm/sec in the lower layer. These values are comparable to observations, but are located too near Cape Hatteras in the model
- Maximum sea height variability, >35 cm, was found in the large amplitude seamount experiment, comparable to that observed by Douglas et al. (1983) and MC from altimeter data from GEOS-3 and SEASAT. Location of the maximum was upstream of the seamounts, however, unlike the observations.

Thus, by using a limited-domain model with open boundary conditions we have shown that the NESC can have a significant influence on the GS mean path and its eddy statistics. We clearly showed that baroclinic instability of the Gulf Stream could generate deep mean flows, which interacted with the bottom topography and, in turn, influenced the upper ocean circulation. However, to answer a broader range of questions—for example, how might the large-scale topography influence the mean path and the eddy statistics—a much larger domain is required. This step is certainly required before we can continue our strategy of developing the models to the point where the same model/data and altimeter studies we have done for the Gulf of Mexico can be done for the REX and SYNOP region. At the same time, the eddy-resolving capability of the model must not be sacrificed. Thus, a realistic numerical model of the GSS is expensive, both in manpower for model development and in actual computer time. In some respects this expense must be considered in the same category as ship time or mooring costs. Great care and forethought must be taken to ensure that the model is as efficient as possible, while choosing research problems that have some chance of success with limited computer resources. Therefore, in proposing experiments in modeling the GSS, it is important to determine what problems are "do-able" on present and near-future computers.

The domains for our proposed experiments are shown in Figure 8. Domain A includes the Gulf Stream and its principal recirculation region, but does not encompass the Gulf of Mexico, the Caribbean, and part of the North Atlantic. However, this domain closely parallels Holland's (1982) quasi-geostrophic (QG) domain, and should provide a good benchmark for assessing the differences between the PE and QG models and the influence of large-scale topography. Domain B, while bigger, will be more costly and is of more limited use in terms of possible experiments. It will, however, allow us to evaluate the limitations of Domain A for studying the GSS and should provide some useful information on the role of the Caribbean and the Gulf of Mexico in modulating the transport in the Gulf Stream under time-varying wind forcing. The southern latitude of Domain B was chosen, based on some numerical experiments by NORDA's G. Heburn, by using a coarse grid ($1\frac{1}{2}^{0}$ x $1\frac{1}{4}^{0}$) one-active-layer, reduced-gravity world ocean model driven by climatological monthly mean winds. In Figure 9a the solution for the interface deviation after nearly five years of integration is shown, while in Figure 9b a no-slip barrier has been placed at 9^{0}N. While the details do have differences, the basic circulation of the Gulf Stream at mid-latitudes remains unchanged. We have developed an eddy-resolving (0.2^{0}) spherical geometry, arbitrary n-layer primitive equation, semi-implicit model for the North Atlantic. The first version of the model (with a flat bottom and two layers and driven by a simple zonal wind) is now being run on the newly installed Cray-XMP 12 at the Naval Research Laboratory. More realistic wind forcing and bottom topography are now being added.

A wide range of scientific issues form the basis for research on the GSS. Some of those issues are directly amenable to observational study, while others will require more theoretical effort. It seems clear, however, that for the foreseeable future, observational efforts in the GSS should be coupled with a serious, stably funded modeling program. The models will provide valuable guidance in determining sampling strategies, in interpreting field data from sparse observational networks, and in generating new hypotheses for field testing. In some instances, for example, in using altimeter data for ocean forecasting, the models will be critical for data assimilation in space and time.

At least three areas of GSS research are timely and are of critical concern: First, while numerical models have become more realistic, some serious discrepancies still exist between model simulations and the sparse observations. This problem is due to inadequacies in the models and in the data density. The models have failed to simultaneously account for both the mean path of the Gulf Stream and its penetration far into the interior of the North Atlantic, and for the high energy levels in the deep water downstream of the NESC at 55°W, where long time series from moored current meters are available. This discrepancy

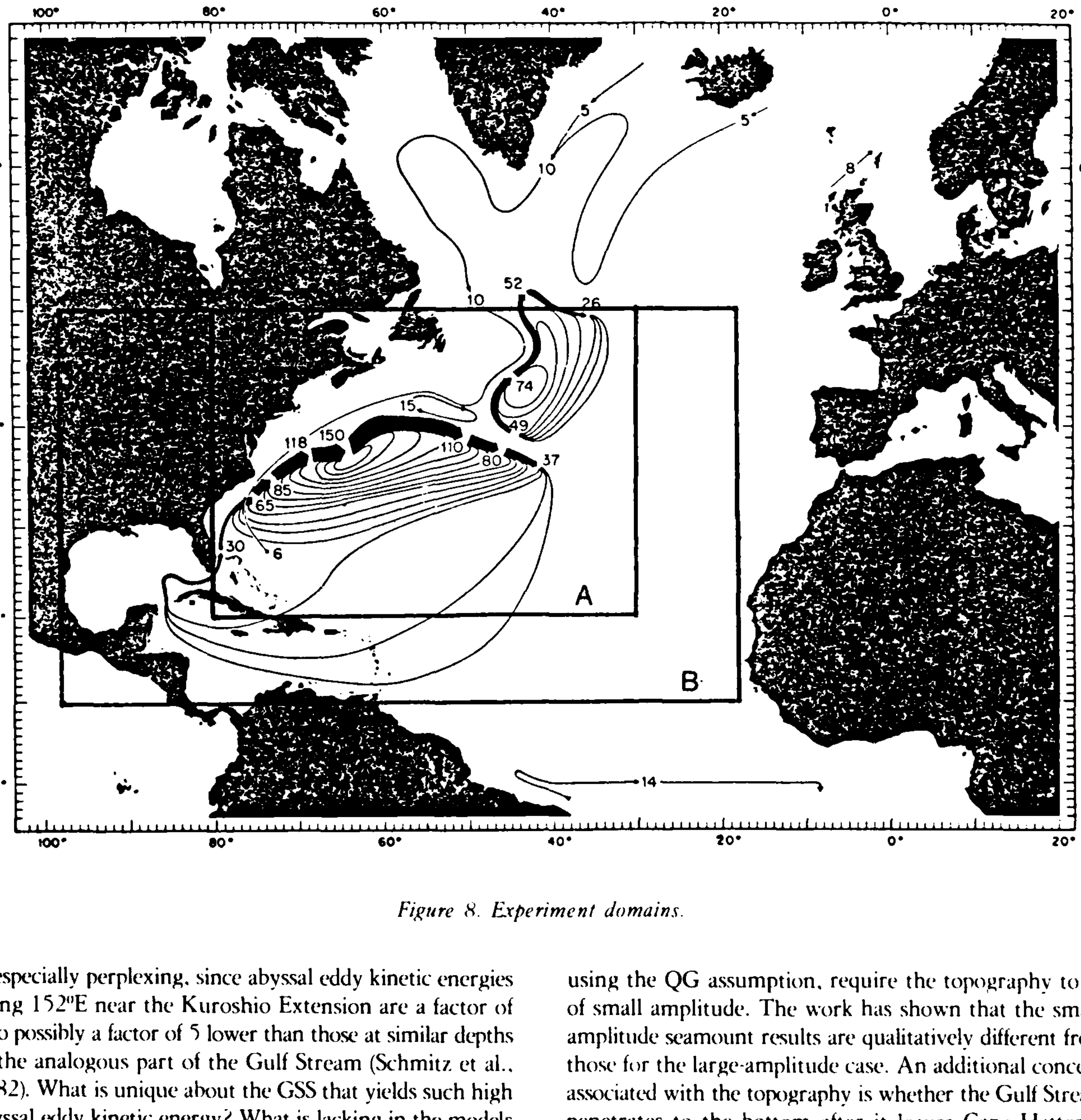

Figure 8. Experiment domains.

is especially perplexing, since abyssal eddy kinetic energies along 152°E near the Kuroshio Extension are a factor of 2 to possibly a factor of 5 lower than those at similar depths in the analogous part of the Gulf Stream (Schmitz et al., 1982). What is unique about the GSS that yields such high abyssal eddy kinetic energy? What is lacking in the models that prevents them from generating such energies so far away from the western boundary?

A second question involves the importance of topographic control on the dynamics and statistics of the Gulf Stream downstream from Cape Hatteras. Increasing observational evidence and the modeling work suggest an important role for the continental shelf and slope, as well as such obvious topographic anomalies as the NESC in influencing the Gulf Stream. However, most of the existing models of the GSS either use a flat-bottom model or, by using the QG assumption, require the topography to be of small amplitude. The work has shown that the small-amplitude seamount results are qualitatively different from those for the large-amplitude case. An additional concern associated with the topography is whether the Gulf Stream penetrates to the bottom after it leaves Cape Hatteras. Direct current meter observations along the continental slope are often contaminated by low-frequency topographic Rossby waves, which makes it difficult to determine the relationship between deep fluctuations and meanders of the Gulf Stream (Bryden, 1982). How are these waves generated and can a model account for them? Hogg (1981) traced the origin of the TRWs observed near 70°W back to a generation region near 38°N and 68°W at the northern end of the NESC. Is it possible that meanders of the GS, interacting with the seamounts might be the trigger

for these waves? Another aspect of the topographic influence is related to ring generation, movement, and decay. Work clearly indicates that warm core ring generation efficiency is increased by the seamounts and that eddy activity in the deep water in the vicinity of the seamounts was increased compared to the flat bottom experiment. It is also quite evident in the observations that the continental shelf and slope influence the movement and decay of the rings.

The third scientific issue is related to the measurement of various statistical quantities, both from the models and in the observations. We have evaluated the complete energetics budget for our model experiments and can map each term in the kinetic and potential energy equations, both for the means and for the fluctuations, which is much easier to do in the models than in the observations. The best that can be done observationally is to monitor some of the terms in the energy equations, estimate the magnitude of the energy reservoirs, and make educated guesses at the total picture. By subsampling the model with "imaginary" current meters, inverted echo sounders, altimeters, etc. and recomputing certain energetic quantities that one might observe in the ocean, then comparing them to the "true" solutions from the full model output, we can begin to make statements about how sensitive eddy-mean calculations are to record length, measurement resolution, and error contamination. This should aid the design of new observational programs as well as improve our efforts to compare models and observations. Other quantities, such as mass transport, relative and potential vorticity, vertical velocity, sea surface height, and Lagrangian drifter statistics are readily obtained from the model. Much work still needs to be done on the optimum means for intercomparing models and oceanic data and on standardizing the rules for determining when a model realistically compares with the observations.

Acknowledgments

This work was funded by the Office of Naval Research at NORDA under the basic research Accelerated Research Initiative, "Ocean Dynamics from Altimetry." We wish to thank Jim Mitchell of NORDA, Tom Davis of the Naval Oceanographic Office, George Born of the University of Texas, Bob Cheney of NOAA/NGS, and Pierre DeMey, CNES, Toulouse, France, for their helpful ideas, comments and technical suggestions during this research. Jim Marsh of NASA/GSFC kindly provided the altimetric data, George Maul of NOAA/AOML generously permitted the use of his hydrographic data, and Norman Huang and his colleagues at NASA/Wallops provided material concerning the DMA geoid for the Gulf. Monte Peffley, Cindy Duarte, and Darren Grant performed many of the diagnostic calculations and produced many of the graphics. Graphics software was provided by the National Center for Atmospheric Research (sponsored by the National Science Foundation). Alan Wallcraft of JAYCOR provided the fast vectorized Helmholtz solver and the irregular coastline version of the model originally designed by Harley Hurlburt. Calculations were performed on the two-pipeline Texas Instruments Advanced Scientific Computer at the Naval Research Laboratory in Washington, D.C., and on the NORDA VAX 11/780.

References

Bryden, H. S. (1982). Review of Gulf Stream Measurements in the Region South of New England. *Proceedings: Workshop on Gulf Stream Structure and Variability*, Office of Naval Research, J.M. Bane, Jr. (ed.), University of North Carolina, Chapel Hill, 48-59.

Cochrane, J. D. (1965). *The Yucatan Current and Equatorial Currents of the Western Atlantic*. Unpublished report, Department of Oceanography, Texas A&M University, College Station, Ref. (65-17T), 20-27.

Douglas, B. C., R. E. Cheney, and R. W. Agreen (1983). Eddy Energy of the Northwest Atlantic and Gulf of Mexico Determined from GEOS-3 Altimetry. *Journal of Geophysical Research* 88, 9595-9604.

Elliott, B. A. (1979). *Anticyclonic Rings and the Energetics of the Circulation of the Gulf of Mexico*. Ph.D. Thesis, Department of Oceanography, Texas A&M University, College Station, 188 pp.

Hogg, N. G. (1981). Topographic Waves along 70W on the Continental Rise. *Journal of Marine Research* 39, 627-649.

Holland, W. R. (1982). Simulation of North Atlantic Variability. *Proceedings: Workshop on Gulf Stream Structure and Variability*, Office of Naval Research, J. M. Bane, Jr. (ed.), University of North Carolina, Chapel Hill, pp. 114-126.

Hurlburt, H. E. (1984). The Potential for Ocean Prediction and the Role of Altimeter Data. *Marine Geodesy* 8, 17-66.

Hurlburt, H. E. (1985). Dynamic Transfer of Simulated Altimeter Data into Subsurface Information by a Numerical Ocean Model. *Journal of Geophysical Research*, Oceans, Special Issue on Remote Sensing of the Ocean and Troposphere (to appear).

Hurlburt, H. E. and J. D. Thompson (1980). A Numerical Study of Loop Current Intrusions and Eddy Shedding. *Journal of Physical Oceanography* 10, 1611-1651.

Hurlburt, H. E. and J. D. Thompson (1982). The Dynamics of the Loop Current and Shed Eddies in a Numerical Model of the Gulf of Mexico. In: *Hydrodynamics of Semi-Enclosed Seas*, J. C. J. Nihoul (ed.), Elsevier, Amsterdam, 243-298.

Hurlburt, H. E. and J. D. Thompson (1984). Preliminary Results from a Numerical Study of the New England Seamount Chain Influence on the Gulf Stream. In: *Predictability of Fluid Motions*, G. Holloway and B. J. West (eds.), American Institute of Physics, New York, New York, 489-503.

Ichiye, T. (1962). Circulation and Water Mass Distribution in the Gulf of Mexico. *Geofisica Internacional* (Mexico City) 2, 47-76.

Kindle, J. C. (1985). Sampling Strategies and Model Assimilation of Altimetric Data for Ocean Monitoring and Prediction. *Journal of Geophysical Research*, Oceans, Special Issue on Remote Sensing of the Ocean and Troposphere (to appear).

Kirwan, A. D., Jr., W. J. Merrell, Jr., J. K. Lewis, and R. E. Whitaker (1984). Lagrangian Observations of an Anticyclonic Ring in the Western Gulf of Mexico. *Journal of Geophysical Research* 89, 3417-3424.

Leipper, D. F. (1970). A Sequence of Current Patterns in the Gulf of Mexico. *Journal of Geophysical Research* 75, 637-657.

Marsh, J. G., R. E. Cheney, J. J. McCarthy, and T. V. Martin (1984). Regional Mean Sea Surfaces Based Upon GEOS-3 and SEASAT Altimeter Data. *Marine Geodesy* 8, 385-402.

Marshall, J. C. (1985). Sea-surface Topography Determination and Geoid Improvement from Satellite Altimetry. *Journal of Physical Oceanography* (to appear).

Maul, G. A. and A. Herman (1985). Mean Dynamic Topography of the Gulf of Mexico with Application to Satellite Altimetry. *Marine Geodesy* (to appear).

Molinari, R. L. (1980). Current Variability and Its Relation to Sea-Surface Topography in the Caribbean Sea and the Gulf of Mexico. *Marine Geodesy* 3, 409-436.

Molinari, R. L., S. R. Baig, D. W. Behringer, G. A. Maul, and R. Legeckis (1977). Winter Intrusions of the Loop Current. *Science* 198, 505-507.

Schmitz, W. J., Jr., P. P. Niiler, R. L. Bernstein, and W. R. Holland (1982). Recent Long-Term Moored Instrument Observations in the Western North Pacific. *Journal of Geophysical Research* 87, 9425-9440.

Sturges, W. A. and J. P. Blaha (1976). A Western Boundary Current in the Gulf of Mexico. *Science* 192, 367-369.

Thompson, J. D. (1985). Altimeter Data and Geoid Error in Mesoscale Ocean Prediction: Some Results from a Primitive Equation Model. *Journal of Geophysical Research*, Special Issue on Remote Sensing of the Ocean and Troposphere (to appear).

Thompson, J. D. and H. E. Hurlburt (1982). A Numerical Study of the Influence of the New England Seamount Chain on the Gulf Stream: Preliminary Results. *Proceedings: Workshop on Gulf Stream Structure and Variability*, Office of Naval Research, J. M. Bane, Jr. (ed.), University of North Carolina, Chapel Hill, 346-362.

Wallcraft, A. J. and J. D. Thompson (1984). Ocean Modeling and Drifters. *Proceedings: 1984 Drifting Buoy Workshop*, Marine Technology Society, Gulf Coast Section, 81-98.

Wunsch, C. and E. M. Gaposchkin (1980). On Using Satellite Altimetry to Determine the General Circulation of the Oceans with Application to Geoid Improvement. *Review of Geophysics and Space Physics* 18, 725-745.

NORDA Studies of Medium Scale Flow Dynamics in Marginal Seas and Straits

Thomas H. Kinder
Oceanography Division

Abstract

The techniques of experimental physical oceanography, numerical circulation modeling, and remote sensing measurements have been applied to the Southeastern Caribbean and Western Mediterranean Seas. Flows channeled by narrow passages enter these semi-enclosed seas as jets which become unstable and form medium scale eddies and gyres. Improved descriptions and dynamical understanding of the medium scale features have emerged from NORDA studies.

Introduction

Marginal or semi-enclosed seas, such as the Caribbean and the Mediterranean, exhibit hydrodynamical phenomena similar to the oceans. Their smaller size and partial isolation, however, make them more tractable for both experimental and modeling investigations than the great oceans they typically border. A natural laboratory for studying oceanic fluid dynamics exists in marginal seas, particularly where strong flows enter or exit through narrow straits or passages. Flows through these straits are often concentrated into well-defined jets, but unstable, jets.

These features of marginal seas can make posing experimental and modeling questions clearer. For instance, mesoscale eddies located near the downstream side of straits are most likely recently formed locally, and their formation is probably associated with the strong flows that form in the vicinity of the strait. Boundaries for both observational grids and numerical models are also defined well, whereas in open-ocean experiments and models there is often a nagging uncertainty about the upstream and downstream conditions; indeed, it is often not known which is upstream and which is downstream.

Sea straits are oceanographically important because they influence adjacent water bodies and contain highly energetic hydrodynamic phenomena. They impose a geographic constriction on the water flow (and, frequently, on the flow of air above them). Bathymetric gradients are also large, and continental slopes and submarine canyons are often located near straits. These features cause water flow to intensify, water masses to juxtapose, and atmospheric forcing to modify. Strait geometries make various boundary effects important, such as lateral and bottom friction, coastal upwelling, sidewall eddies, setup, and sharp curvature of streamlines. The energetic flows cause nonlinear effects, mixing, and turbulence to become important. For large straits, the earth's rotation remains significant.

To address basic scientific questions about the complex flows in marginal seas and near straits, investigators from three NORDA groups were combined, so the techniques of experimental physical oceanography, numerical circulation modeling, and satellite and aircraft remote sensing could be applied to the problem. The goal was to learn how to use these techniques synergistically while working on meaningful and clearly defined scientific problems.

Two NORDA projects have combined in situ measurements with other techniques to elucidate medium-scale (about 10–100 km) variability downstream of straits. In the Caribbean project, hydrographic and current measurements were combined with numerical modeling to investigate eddy formation as the westward-flowing Caribbean Current exits the passages of the southern Lesser Antilles. In the Mediterranean project, in situ measurements and numerical modeling were combined with remote sensing techniques from aircraft and satellite to study the gyre that forms from the Atlantic Water that debouches the Strait of Gibraltar.

These two projects emphasize NORDA's contributions. Obviously, many non-NORDA investigators have contributed to mesoscale and strait flows in the Caribbean

and the Mediterranean, but the discussion focuses on NORDA work. For more balanced overviews, see Kinder et al. (1985) and Parrilla and Kinder (1985).

Discussion

Mesoscale eddies in the southeastern Caribbean Sea

In the late 1970s, the southeastern Caribbean Sea was determined to have a high level of mesoscale variability (Fig. 1). Details of this variability were not known because closely spaced hydrographic surveys had not been done and current measurements were few. Satellite infrared images are not very useful in this area because of atmospheric interference and uniform sea surface temperatures (visible and radar sensors hold some promise). A numerical circulation model that seemed useful became available (Hurlburt and Thompson, 1980), and we decided to combine in situ and modeling techniques to study eddy formation there.

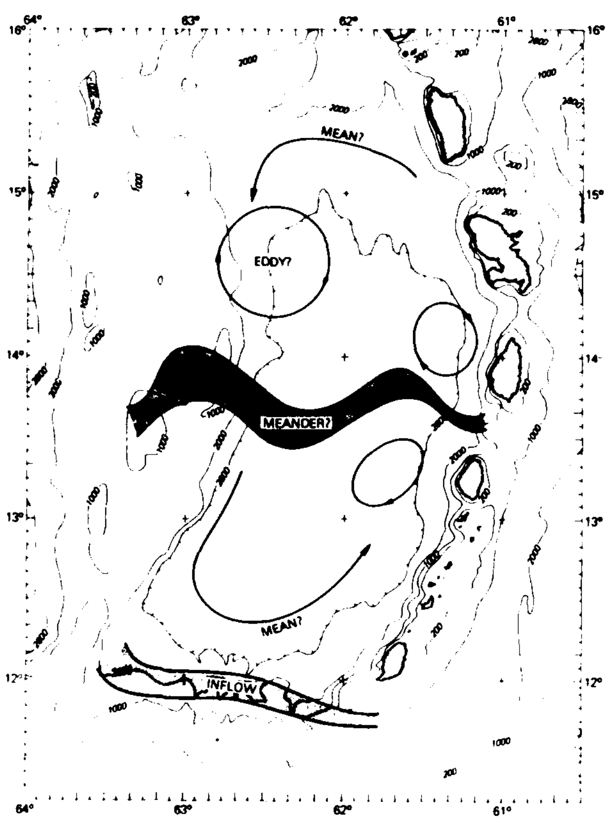

Figure 1. A conceptual schematic of mesoscale variability in the southeastern Caribbean Sea. The two inflows (stippled) through Grenada Passage (south) and St. Vincent Passage (north) carry about 40% of the total transport that enters the Caribbean.

The working hypothesis for the study was that strong inflows through the narrow passages of the southern Lesser Antilles are the direct cause of the mesoscale variability immediately downstream. Thus, the model used inflow as forcing. The measurement program was aimed at assessing the inflow to provide realistic values for these critical boundary conditions, and also at observing the nature of the variability to validate model results. The role of the model was not merely to simulate the flow, but to provide dynamical understanding.

Hydrographic measurements taken east of the Antilles, as well as a careful literature review, suggested that the southern passages were major entrances for Caribbean inflow, but with only about one-half the previously accepted transports (Mazeika et al., 1980). Current meter moorings in the two major passages, Grenada and St. Vincent, showed that St. Vincent Passage had the most energetic inflow (Mazeika et al., 1983). Inflow through both St. Vincent and Grenada showed fluctuations at 30-day periods (Fig. 2).

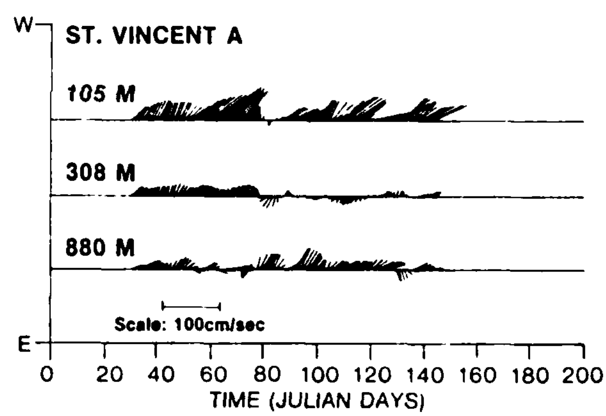

Figure 2. A vector plot of low passed filtered current meter records obtained in 1977 from St. Vincent Passage. The record shows important fluctuations on scales longer than 10 days.

The numerical model used two versions, either two-layer or reduced gravity (one active layer overlying a quiescent layer). Both used a primitive equation formulation with high horizontal resolution (7.5 X 7.5 km). Model results using constant inflow boundary conditions (open western boundary) showed that the St. Vincent inflow alternately shed cyclonic and anticyclonic eddies (Fig. 3) with a period of about 35 days (Heburn et al., 1982). The mechanism was a horizontal shear instability. Further

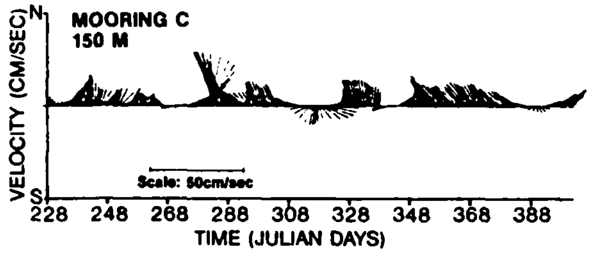

Figure 3. A vector plot of low-passed filtered currents obtained in 1978–1979 from Grenada Basin (near 13°N, 62°W; cf. Fig. 1). Note that there are energetic fluctuations near periods of 30 days.

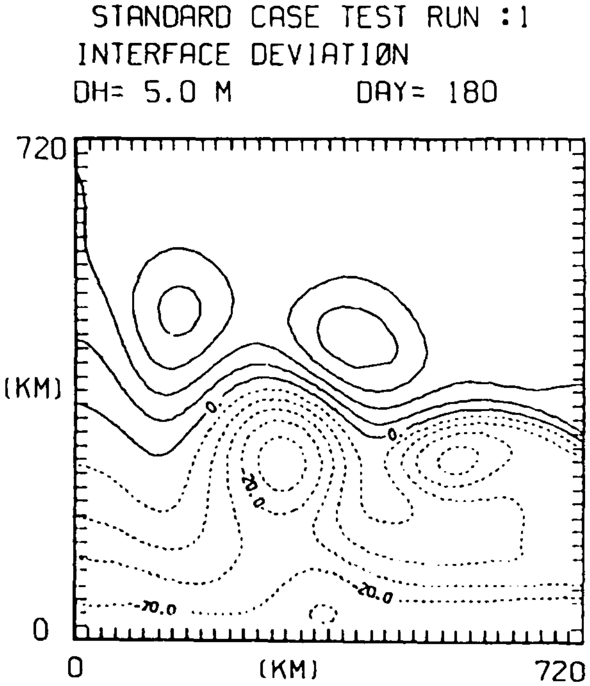

Figure 4. Pycnocline fluctuations from a two-layer numerical model experiment forced by inflow on the eastern (right) boundary and with the western boundary open. Even with steady inflow, eddies form with properties that are consistent with the observations.

modeling (Heburn and Hurlburt, 1985) has shown the effects of variable inflow and interaction between the inflow jets.

Satelite-tracked drifter measurements showed eddies of the same size, polarity, and location as predicted by the model (Heburn et al., 1982; Kinder, 1984). A hydrographic survey (Burns et al., 1981) and current meter moorings (Boyd and Kinder, 1980; Fig. 4) confirmed the scales and energy levels of the eddies.

Mesoscale and strait flows in the western Mediterranean Sea

The Mediterranean project differed from the Caribbean project in two important respects. First, the major mesoscale feature, the Alboran Sea gyre, and the inflow forcing were reasonably well known (Lanoix, 1974; Lacombe and Richez, 1982). We were thus able to formulate more specific scientific questions early in the project and to judge preliminary experimental and modeling results against existing knowledge. Second, the Mediterranean Sea is an excellent region for applying satellite infrared techniques. We included remote sensing as the third important technique.

An international team of investigators was formed, and the principal objective was to understand the dynamics of the Alboran Sea gyre. The experimental plan was coordinated by NORDA and the Instituto Espanol de Oceanografia. Overviews of the project, entitled Donde Va?, and preliminary results have been published (Donde Va Group, 1984; Parrilla, 1984), but many important results are still being prepared for publication.

The numerical model was, again, an adaptation from Hurlburt and Thompson (1980) with high horizontal resolution (5 X 10 km). We hypothesized that the gyre was directly forced by the narrow eastward jet of Atlantic Water, and that the major gyre fluctuations were caused by variations in this inflow jet. The model experiments suggested that the gyre size is strongly dependent on the velocity (both speed and direction) and vorticity of the incoming current (Preller and Hurlburt, 1982; Preller, 1985). The gyre develops as an instability of the inflow (Figs. 5 and 6) and, once formed, it can be interpreted as a standing Rossby (planetary) wave.

Although some caution is required in inferring the gyre and jet structure from infrared images (Bucca and Kinder, 1984), during June–October 1982 the infrared images accurately reflected the general gyre and jet shape, as well as location (Champagne-Phillipe and La Violette, 1984; La Violette, 1984; Kinder, 1984). The images showed a fully developed gyre throughout the period, except for one 10-day interval in September. June and October hydrographic data and current meter data throughout the period confirmed a close correlation between the sea surface temperature pattern and the shallow (to 200-m depth) hydrographic and velocity distributions. Visible satellite and aircraft images showed a strong negative correlation between sea surface temperature and calculated chlorophyll concentrations (Arnone and La Violette, 1985; Fig. 7). Rapid fluctuations present in apparent chlorophyll

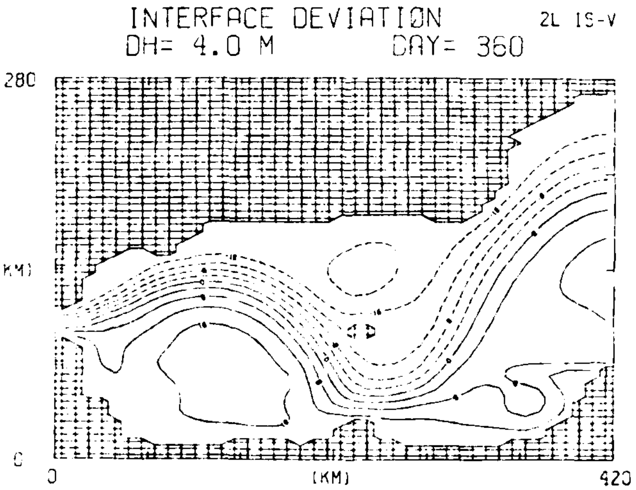

Figure 5. Pycnocline fluctuations from a two-layer numerical model experiment forced by upper layer inflow through the Strait of Gibraltar (left). The western boundary is open to the upper layer. Note the strong meandering in flow jet and the anticyclonic gyre (cf. Fig. 6).

concentrations are not yet understood. La Violette (1984) found small (10-km), cool, surface temperature anomalies that appeared to extend through the Atlantic Water and that were advected around the gyre. Each anomaly seemed to be generated twice daily near the strait exit.

Velocity measurements included moored current meters during June–October and various short-term measurements during October: surface drifters (La Violette, 1985), shore-based radar (Janopaul and Frisch, 1984), and detailed profiler sections (Perkins and Saunders, 1984). The low-passed current data were highly correlated across the array, which spanned both the jet and the gyre. The most startling event was the absence of any strong eastward flow in the northern Alboran during the 10 day period that corresponded to the absence of the gyre in satellite infrared images (Kinder, 1984; Fig. 8). The short-term (4- to 5-hour) drifter tracks showed that the surface speed maximum (< 120 cm/sec) was found near cool sea surface temperatures (La Violette, 1985). Velocity cross sections showed a close correspondence to hydrography and regions of high shear (Perkins and Saunders, 1984; Fig. 9).

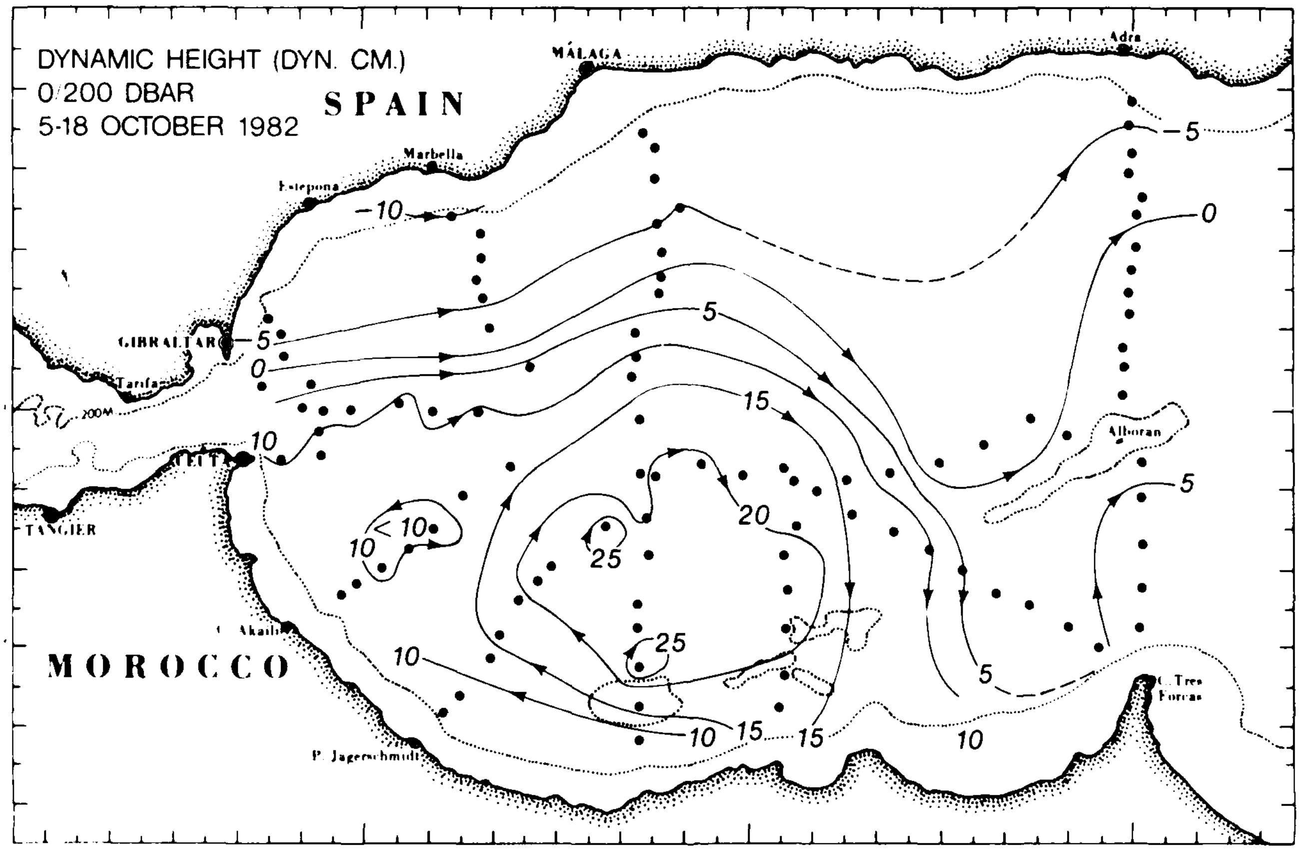

Figure 6. Surface dynamic height using a 200 dbar reference level (which is both a traditional and reasonable choice). The data were gathered by U.S. and Spanish ships during two weeks in October 1982. Both the inflow jet and the gyre are evident (cf. Fig. 5).

Figure 7. A Coastal Zone Color Scanner image from 7 October 1982. The high chlorophyll concentrations (darker shades) corresponded to cool sea surface temperatures in satellite infrared images (cf. Figs. 5 and 6).

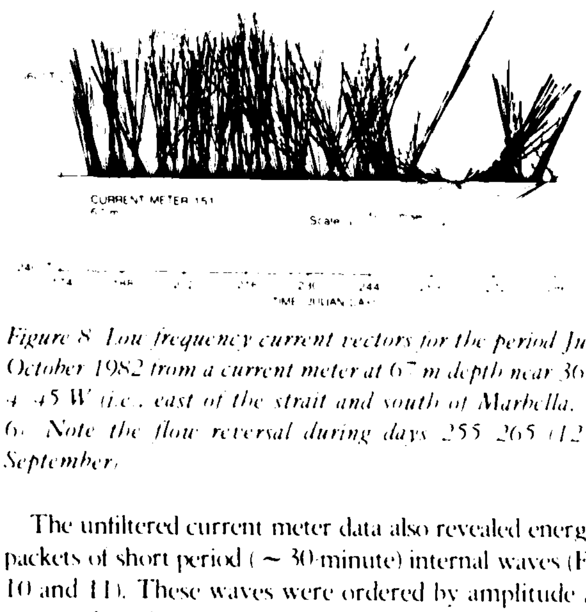

Figure 8. Low frequency current vectors for the period June–October 1982 from a current meter at 67 m depth near 36° N, 4° 45' W (i.e., east of the strait and south of Marbella, Fig. 6). Note the flow reversal during days 255–265 (12–22 September).

The unfiltered current meter data also revealed energetic packets of short period (~30-minute) internal waves (Figs. 10 and 11). These waves were ordered by amplitude and appeared to be internal solitons (Kinder, 1984). They originate in the extremely energetic hydraulic regime of the strait (Lacombe and Richez, 1984). A similar wave packet was correlated to an arcuate (concave westward) pattern observed in a visible satellite image by La Violette (1984). The geometric evolution of this surface manifestation of the internal waves has been further traced by using radar in the strait (La Violette, Kinder and Green,

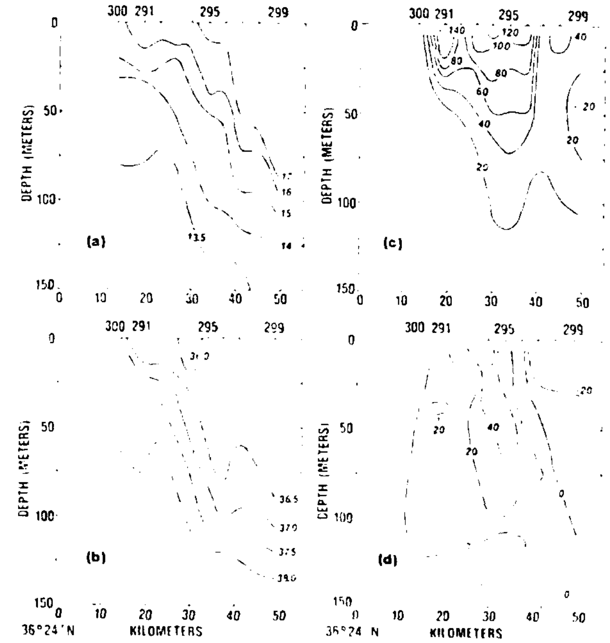

Figure 9. Hydrographic and velocity cross section obtained south of Estepona (see Fig. 6) in October 1982 using the NORDA finescale profiler: (a) temperature, (b) salinity, (c) eastward velocity, and (d) northward velocity. The velocities are measured, and not calculated from the hydrographic data.

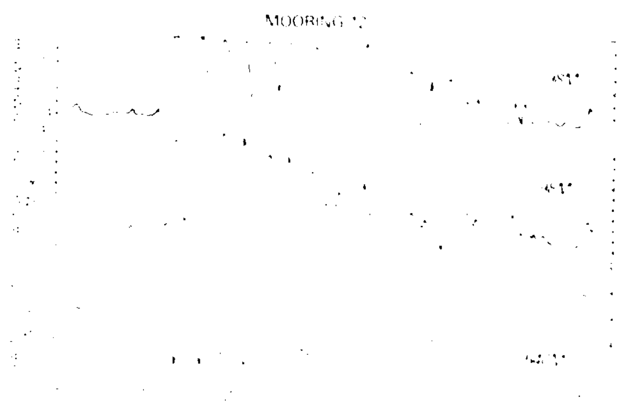

Figure 10. High frequency internal wave packet at mooring 12 (near 36° 15' N, 4° 50' W). Note that the largest amplitude waves arrived first, and that the shallow (98 m) velocity and temperature were 180° out of phase with the deep (540 m) velocities.

Figure 11. A space shuttle photograph obtained from an altitude of 200 km on 12 October 1984. The arcuate lineations east of the Strait are surface manifestations of an internal wave packet similar to that measured two years earlier (cf. Fig. 10). (Photograph courtesy of P. E. La Violette.)

unpublished manuscript) and by using both aircraft and Space Shuttle photographs in the strait and the Alboran Sea (La Violette and Arnone, personal communication).

The pattern and the dynamics of the Mediterranean water beneath the gyre have also been elucidated (Parrilla et al., 1985). They showed that the concentration of intermediate water as a broad current in the northern Alboran and the deep water as a narrow current in the southern Alboran is understandable as an effect of the earth's rotation. In the first case the absence of bottom topography is crucial; in the second case the bottom topography imitates variations in the rotation rate ("topographic beta effect") and causes a boundary current to form.

Summary

The Caribbean and the Mediterranean projects have already been fruitful, although important results are still in preparation for publication. The first basic description of the energetic mesoscale variability in the southeastern Caribbean has been obtained, and the nature of its genesis is now understood. The origin of the Alboran gyre and the cause of the Mediterranean water currents are now understood. Internal solitons and submesoscale thermal anomalies were discovered.

The attempt to combine different techniques was also successful. The nature of this success is probably best demonstrated by the papers by Heburn et al. (1982) and Parrilla et al. (1985), in which fundamental points in the papers depended critically on both of the represented techniques. Publications that are now in preparation will provide further examples, either within single papers or within closely coupled pairs of papers. NORDA has strong expertise in the areas of experimental physical oceanography, numerical circulation modeling, and satellite remote sensing. Future collaborations should be equally fruitful.

Acknowledgments

NORDA coworkers who do not appear in the references include Louis Banchero, Steve Sova, and Richard Myrick. Funding for the Mediterranean work was primarily from the Office of Naval Research Coastal Studies Program (Code 422 CS).

References

Arnone, R. A. and P. E. La Violette (1985). The Ability of Nimbus-7 Coastal Zone Color Scannner (CZCS) to Detect Bio-Optical Changes in the Alboran Sea. Submitted to *Journal of Physical Oceanography*.

Boyd, J. D. and T. H. Kinder (1980). *Current Meter Data from the Southeastern Caribbean Sea, August 1978–February 1979*. Naval Ocean Research and Development Activity, NSTL, Mississippi, Technical Note 76.

Burns, D. A., M. E. Gove, N. V. Lombard, J. D. Boyd, S. E. Raffa and T. H. Kinder (1981). *Hydrographic Measurements in Grenada Basin, Southeastern Caribbean Sea*. Naval Ocean Research and Development Activity, NSTL, Mississippi, Technical Note 202.

Bucca, P. J. and T. H. Kinder (1984). An Example of Meteorological Effects on the Alboran Sea Gyre. *Journal of Geophysical Research* 89, 751–757.

Champagne-Phillippe, M. and P. E. La Violette (1984). *NOAA-7 AVHRR Images Obtained During the Donde Va? Experiment in the Alboran Sea, 1–20 October 1982*. Naval Ocean Research and Development Activity, NSTL, Mississippi, NORDA Report 65.

Donde Va Group (1984). Donde Va? An Oceanographic Experiment in the Alboran Sea. *EOS* 65, 682–683.

Heburn, G. W., T. H. Kinder, J. H. Allender, and H. E. Hurlburt (1982). A Numerical Model of Eddy Generation in the Southeastern Caribbean Sea. In: *Hydrodynamics of Semi-Enclosed Seas*, J. C. J. Nihoul, (ed.), Elsevier, pp. 299–328.

Heburn, G. W. and H. E. Hurlburt (1985). A Numerical Study of Mesoscale Variability in the Eastern Caribbean Sea. Submitted to *Journal of Physical Oceanography*.

Hurlburt, H. E. and J. D. Thompson (1980). A Numerical Study of Loop Current Intrusions and Eddy Shedding. *Journal of Physical Oceanography* 10, 1611–1651.

Janopaul, M. M. and A. S. Frisch (1984). CODAR Measurements of Surface Current in the Northwestern Alboran Sea During the Donde Va? Experiment. *Annales Geophysicae* 2, 443–448.

Kinder, T. H. (1983). Shallow Currents in the Caribbean Sea and Gulf of Mexico as Observed with Satellite-tracked Drifters. *Bulletin of Marine Science* 33, 239–246.

Kinder, T. H. (1984). Net Mass Transport by Internal Waves Near the Strait of Gibraltar. *Geophysical Research Letters* 11, 987–990.

Kinder, T. H., G. W. Heburn, and A. W. Green (1985). Some Aspects of the Caribbean Circulation. *Marine Geology*, in press.

Lacombe, H. and C. Richez (1982). The Regime of the Strait of Gibraltar. In: *Hydrodynamics of Semi-Enclosed Seas*, J. C. J. Nihoul (ed.), Elsevier, pp. 13–73.

Lacombe, H. and C. Richez (1984). *Hydrography and Currents in the Strait of Gibraltar*. Office of Naval Research, Sea Straits Report 3. Available from Naval

Ocean Research and Development Activity, NSTL, Mississippi.

Lanoix, F. (1974). *Project Alboran*. Etude Hydrologique et Dynamique de la Mer d'Alboran. NATO Technical Report 66, Brussels. 39 pp.

La Violette, P. E. (1984). The Advection of Submesoscale Thermal Features in the Alboran Sea Gyre. *Journal of Physical Oceanography* 14, 550–565.

La Violette, P. E. (1985). Short-term Measurements of Surface Currents Associated with the Alboran Sea Gyre During Donde Va?. Submitted to *Journal of Physical Oceanography*.

Mazeika, P. A., D. A. Burns, and T. H. Kinder (1980). Mesoscale Circulation East of the Southern Lesser Antilles. *Journal of Geophysical Research* 85, 2743–2758.

Mazeika, P. A., T. H. Kinder and D. A. Burns (1983). Measurements of Subtidal Flow in the Lesser Antilles Passages. *Journal of Geophysical Research* 88, 4483–4488.

Parrilla, G. (ed.) (1984). *Donde Va? Preliminary Results*. Informe Tecnico 24, Instituto Espanol de Oceanografia, Madrid, 264 pp.

Parrilla, G. and T. H. Kinder (1985). The Physical Oceanography of the Alboran Sea. *Proceedings of the NATO Advanced Research Workshop on Mediterranean Oceanography*, H. Charnock (ed.), in press.

Parrilla, G., T. H. Kinder, and R. E. Preller (1985). Deep and Intermediate Mediterranean Water in the Alboran Sea. Submitted to *Deep Sea Research*.

Perkins, H. T. and K. D. Saunders (1984). Sections of Current, Salinity, and Temperature in the Northwestern Alboran Sea, October 1982, pp. 143–149, in Parrilla (1984).

Preller, R. H. (1985). A Numerical Model of the Alboran Sea Gyre. Submitted to *Progress in Oceanography*.

Preller, R. and H. E. Hurlburt (1982). A Reduced Gravity Model of Circulation in the Alboran Sea. In: *Hydrodynamics of Semi-Enclosed Seas*, J. C. J. Nihoul (ed.), Elsevier, pp. 75–90.

Bioturbation of Ocean Sediments

Dave K. Young and Kevin B. Briggs
Oceanography Division

Bioturbation is defined as all biological activity that physically alters sediments. Research at NORDA has shown that bioturbation also alters sediment geoacoustic and roughness properties important to modeling and predicting high-frequency acoustic bottom scattering. Bioturbation by benthic animals can alter sediment impedance properties by either compacting or "fluffing" the sediment; bioturbation can also alter bottom roughness properties by smoothing the sediment surface or by building sediment mounds (Fig. 1). Benthic animals can also alter sediment acoustic volume scattering properties because the animals create feeding voids that become filled with sediments that have densities different from the surrounding sediments, of the animals create or destroy layered sediments. Large benthic animals, especially those with shells, are important bottom and volume point scatterers of acoustic energy.

High-frequency acoustic bottom scattering is known to limit the effectiveness of mine-hunting sonar systems, torpedo guidance and control systems, and ASW systems in general. NORDA research has shown that biological alteration of sediment is predictable, and NORDA researchers have demonstrated the magnitude of this alteration on acoustic bottom scattering using theoretical and empirical bottom scattering models.

For example, changes in bottom roughness due to smoothing of the sediment surface in sandy sediments can result in a decrease in bottom backscatter strength by one to two orders of magnitude for a 20-kHz signal at low grazing angles. Acoustic volume scattering by sediment inhomogeneities created by bioturbation may be the most important factor determining bottom scattering in soft sediments.

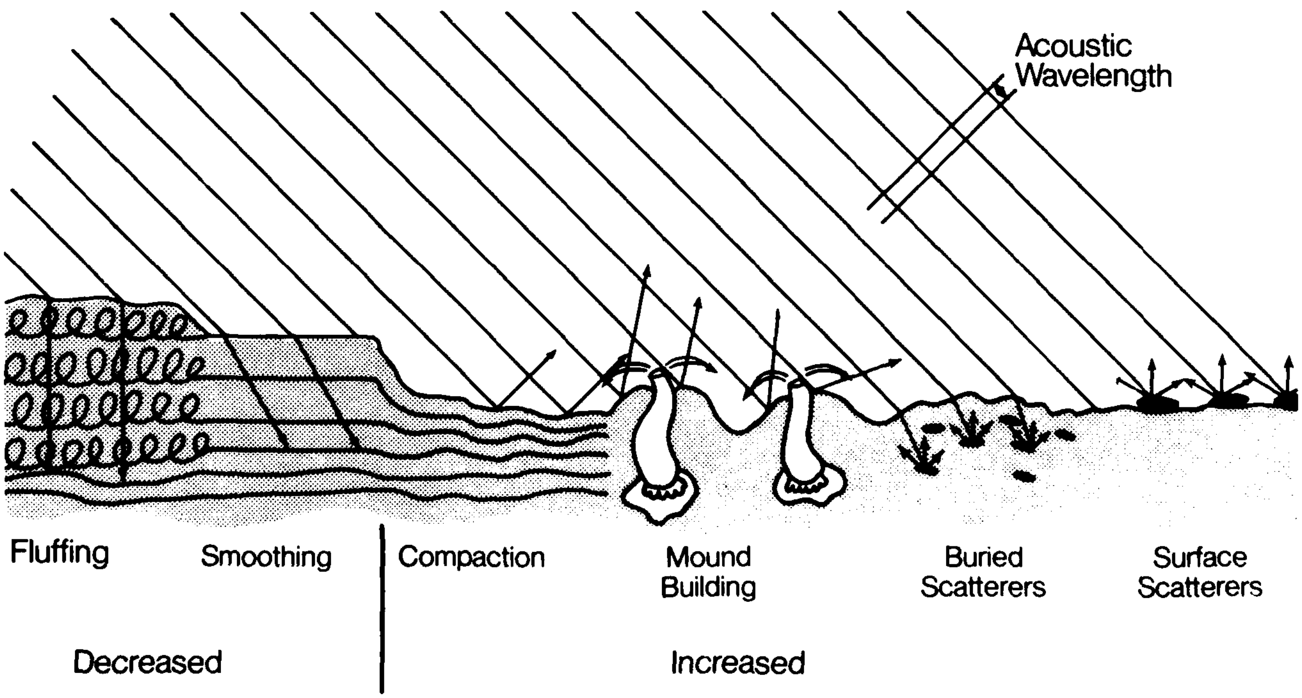

Figure 1. Examples of how benthic animals can alter bottom roughness properties.

NORDA Polar Oceanography

James P. Welsh, Duane T. Eppler, and Alan W. Lohanick
Oceanography Division

Introduction

The polar regions are characterized by unique environments and are potential theaters of naval operations. The environments are characterized by consistently low temperatures, long periods of darkness, erratic and unreliable communications, large areas of ice-covered shallow seas (Arctic), remote to centers of population, the shortest (great circle route) distance airline routes between northern hemisphere centers, etc. These and other features peculiar to polar regions, especially the Arctic, often translate into constraints on the U.S. Navy's capability to carry out missions. Until recently, the U.S. made only a minimal effort to study Arctic phenomena, especially how it affects military operations. Increased activity and improved capabilities by Soviet forces in the Arctic, particularly surface and subsurface operations, has focused U.S. Navy interest on the Arctic as a potential theater of operations. NORDA has been involved in research on ice, snow, sea ice, ice dynamics, airborne and satellite remote sensing, and ice camp logistics in the Arctic and the Antarctic since the early 1960s. Specific areas of studies have developed through the years that are principally centered on understanding the environmental physics and advanced remote sensor technology.

The majority of the study programs have developed specific capabilities required for research in polar environments. Establishment of camps on floating sea ice for supporting 10–15 scientists for durations ranging from weeks to months is one example of the unique capabilities NORDA has developed. The variety of disciplines required to solve many problems must be merged and coordinated within the pervading hostility of the polar environments. The threats to man and machines posed by the environment underlies the challenge of scientific investigations in the polar regions. Highlights of a few areas of polar regions research in progress at NORDA follows.

Discussion

Analysis of single-band passive microwave imagery

The K_a-band Radiometric Mapping System (KRMS) is a passive airborne microwave imager that operates at a center frequency of 33.6 GHz. The instrument produces images of surfaces during heavy cloud cover or darkness. As such, KRMS-like instruments are well suited to all-weather Arctic reconnaissance applications.

Digital images produced by KRMS represent maps of the areal variation in radiometric brightness temperatures across a scene. Brightness temperature is a function of physical surface characteristics. Differences in salinity, liquid water content, porosity, and the character of overlying snow determine, in large part, the radiometric characteristics of sea ice. Insofar as such physical characteristics differ between different types of ice, passive microwave imaging systems provide a means of mapping the abundance and distribution of different ice types encountered along a flight track.

Work to date shows that four Arctic surfaces can be mapped unambiguously in winter conditions if only static (point measurement) K_a-band brightness temperatures are considered. Open water, frazil (agglomerated into clumps, stringers, and tadpoles), old ice (multiyear and second-year), and first-year ice (including young ice) are characterized by ranges of brightness temperatures that do not overlap. New ice and nilas, however, display a wide range of brightness temperatures that overlap brightness temperatures characteristic of old ice and first-year ice. Although new ice and nilas confound classification schemes based solely on static brightness temperature measurements, areal variation in temperatures across different types of ice produces characteristic patterns and textures. Descriptors that characterize these patterns can be used in conjunction with static temperature measurements to distinguish between different types of ice that display similar brightness temperatures.

Textural descriptors are being developed to classify ice in scenes of passive K_a-band imagery. Our ultimate objective is to provide basic research in digital image processing that will permit automated ice reconnaissance sensor systems to be constructed. We envision a semiautomated system that will record the abundance of different ice types overflown at regular intervals along track. Advantages of implementing such a system versus using present ice reconnaissance methods are several fold. The all-light, all-weather capability of passive microwave imagers removes limitations imposed on conventional visual ice reconnaissance methods. Passive microwave imagers can be used at higher altitudes and will cover broader regions than human ice observers can. Finally, data gathered by an automated system can be near-real-time telemetered or recorded and archived for later analysis and interpretation. Such synoptic records of regional, seasonal, and annual ice variability are valuable as input to models for Arctic acoustics, ice drift, and heat exchange between ocean and atmosphere.

Analysis of archived aerial photographs

Since 1962 a substantial archive of remotely sensed (airborne) data in Arctic regions has been accumulated. These data show ice conditions in the central Arctic and in regions adjoining the United States, Canada, Greenland, Iceland, and Norway. Most data are aerial photographs and laser profiles, although limited sequences of infrared, passive microwave, and multifrequency radar images also are available.

Individual records in the archive have been used for specific projects, but the data set has never been analyzed, as a whole, for the synoptic information it contains. Because these data depict ice conditions over a wide range of geographic regions in most seasons for more than 20 years, a comprehensive picture of regional, seasonal, and annual variation in ice conditions is present in the archive. More than 10,000 high-resolution aerial photographs are being reduced to a form in which they can be used to study regional and seasonal variation in ice type, thickness, and concentration. Image processor programs were developed to measure the relative abundance of different surface types in a photograph. This information is preserved in tabular form. Each line of the table corresponds to a different frame of photography and gives the percentage of the scene covered by open water, shuga, dark nilas, light nilas, gray ice, gray-white ice, first-year ice, old ice, and icebergs. Meltpond and ridge coverage is given where it can be determined. The end product is an environmental data base that provides the distribution of surface types present at specific times and places in the Arctic.

Ice/snow physics and ground-truth validation

The Arctic ice pack constitutes a complex physical system not easily described by mathematical models in any but a gross statistical sense. Dynamical models are derived from physical principles and typically contain a small number of parameters that must be merged with airborne or ground-based measurements. But, if the properties of the medium vary significantly over relatively small distances (as they do in the Arctic ice pack), the model appropriate for a small volume of the medium may not apply (if it contains typical limiting approximations) to the adjoining volume.

Physical properties relevant to remote sensing in the Arctic include physical temperature (usually, if not always, varying with distance from the top surface), ice and snow salinities, porosity (the amount of air trapped in the ice), ice and snow densities, dielectric constant (which could, in principle, be derived from the other properties if they were uniform), brine volume (the percentage of salt water trapped in the ice), free water content (extremely important to the dielectric constant of snow cover), snow and ice grain size (still suffering from a lack of universally accepted definition), crystal orientation, and ice thickness. None of these properties can be measured remotely *a priori* (except the surface temperature part of the physical temperature profile) with remote sensors, but they can be inferred once the model parameters have been established, if the surface is uniform over some distance.

Therefore, surface-based (ground truth) measurements must be made to establish the measurable physical properties and their typical spatial variability (to determine the statistical portion of the models). Validation consists of matching remotely inferred physical property and parameter values (e.g., ice thickness), with a second set of ground-based measurements taken at the time of the remote-sensor "flyover."

Spatial variability of the physical properties contributes uncertainties in the parameters that must be inferred from measurements. The scientific process—hypothesis, experiment or test, and improved hypothesis—is very difficult to maintain in the Arctic due to the limitations of experimental control. However, recent work at NORDA has shown progress in sorting out the sources of the variability in electromagnetic properties of sea ice. This basic work will help in developing a mathematical physical model that links the near surface and remote measurements of sea ice electromagnetic radiation.

Finescale Variability Studies at NORDA

Janice D. Boyd, Kim D. Saunders, Henry T. Perkins
Oceanography Division

Abstract

NORDA is investigating finescale oceanographic processes and the means by which they can be studied. "Finescale processes" loosely include those with vertical scales of tens of meters or less and horizontal scales of hundreds of meters or less. From a basic science perspective, a better understanding of these processes sheds light on the nature of the oceanic internal wave field and on the mechanisms and rates of horizontal and vertical mixing. From a Navy perspective, the work yields insights into wake turbulence and second-order effects on acoustic propagation. Initial efforts concentrated on developing a unique profiling instrument, the VCTD, that allows simultaneous measurement of temperature, conductivity, pressure (depth), and three components of velocity. Now that the instrument has been perfected, present and future work deals with the use of the VCTD and supplemental instrumentation in better understanding the nature of the finescale processes.

Introduction

Many upper ocean processes are intimately related to turbulent mixing. For example, to study the transport of heat by the ocean from the equator to the pole, we must first understand how the downward mixing of heat is balanced by the upward transport of deep, cold water that sank in the polar regions. The wind-driven currents are generated by a stress acting directly at the surface and by waves generated by pressure fluctuations acting on that surface. The currents are formed when the wind's momentum is mixed downward and is transferred to the deeper water. The upper layers of the ocean become stratified as heat is input from the sun and is mixed to deeper levels. One of the great unresolved problems of modern oceanography is understanding the mechanisms underlying the mixing processes and the distribution and intensity of those processes.

The simplest assumption about ocean mixing is that it is distributed uniformly, or at least smoothly, in both space and time—an assumption that is supported by the most elementary formulations of diffusion theory: that is, although the level of mixing might vary from place to place and from time to time, the transition would always be smooth. However, recent studies have shown this is not the case; in fact, mixing appears to occur as isolated events localized in both space and time. These events appear to be rare in the sense that most of the mixing is the result of widely separated regions of intense mixing. If the concept of smoothly varying mixing can be applied at all, it can only be in a statistical sense, in which the net effect of the mixing can be given regional or seasonal characterizations.

These regions of strong mixing appear as anomalies in the smooth background of temperature, salinity (and often, but not necessarily, density) and velocity. Anomalous patches with vertical scales on the order of 1-100 m and horizontal scales on the order of 10-1000 m are grouped under the general term "oceanic finestructure," while smaller scales are termed "microstructure." These terms are not well defined, the distinction being based mainly on the differences in instrumentation required to observe the smaller scales, so they are sometimes grouped under the general category of "fine- and microstructure."

Interest in the occurrence of fine- and microscales in the ocean thus arises from their close relation to the natural mixing processes. The fact that they are small in scale and infrequent makes their study challenging. We need to know how the natural processes occur, whether their occurrence can be predicted (at least on a statistical basis), and what the statistics of intensity and occurrence of the

mixing events are. Only then will we be able to make reasonable estimates of the probability of encountering natural patches of turbulence.

Because the mixing processes associated with fine- and microstructure are so widely distributed, but occur in small localized patches, it is necessary to develop techniques by which the frequency and distribution of these mixing events can be determined by routine surveys. One of the original and primary goals of the finescale processes program at NORDA was (and remains) to develop and test methods for obtaining this information.

Fine- and microscale variations in oceanic properties occur almost everywhere in the ocean. In certain areas, however, specific types of finescale structure occur more often and with greater intensity than in other areas.

For example, a region of intense finestructure activity is southeast of Barbados. The finestructure is characterized by a step-like appearance in the trace of temperature, salinity and density plotted against depth. The steps are really layers of water on the order of 10–40 m thick, separated by high gradient layers (usually called sheets) on the order of a meter or less in thickness.

Other types of finestructure are associated with oceanic fronts. Very clear finestructure signatures can be seen in the temperature, salinity, and velocity fields in the North Atlantic Subtropical Convergence Front (1984 study area, see later). Other fronts, such as the New England Shelf-Break Front and the Iceland-Faeroe Front, exhibit similar instances of clear finestructure activity.

Even as the turbulent events responsible for oceanic mixing occur as isolated patches in space, so is their occurrence in time a localized phenomenon. This statement needs to be qualified, as different mechanisms are responsible for the existence of different finescale structures, which necessarily possess different time scales. In some models of fine- and microscale processes, the frequency distribution in both space and time is thought to be log-normal. If that assumption is correct, the form of the distribution implies that the rarer events are responsible for most of the mixing activity. If we are to determine the fluxes over an oceanic area due to mixing from field measurements, we must have good statistics of the finescale structures and a good knowledge of the processes involved.

Mechanisms

A number of different processes lead to fine- and microstructure in the ocean. Among these are double diffusion, shear instability, external mixing, and internal wave straining.

Double diffusion

The possible existence of double diffusion was suggested by three oceanographers in 1956 (Stommel et al., 1956). For nearly 15 years double diffusion was termed an "oceanographical curiosity" and felt to have no major significance in the ocean. However, over the past 10 years or so it has become more and more apparent that under the right conditions double diffusion is not only a very important process in oceanography, but also in such diverse fields as astrophysics, metallurgy, chemical engineering, solid earth geophysics, and solar pond technology (Huppert and Turner, 1981; Chen and Johnson, 1984).

Double diffusion arises when two components in a fluid diffuse at different rates on a molecular scale and when these components contribute, in opposing senses, to the vertical density gradient. In the ocean these components are heat and salt: heat diffuses nearly 100 times faster than salt, and the more heat the water has, the lighter it is; when water has more salt, it is heavier.

If more than two components are involved—in stars this might include angular momentum, heat, magnetic field, and helium—the process is called multicomponent diffusion.

When well developed, both forms are characterized by extremely well-mixed convective layers separated by relatively thin interfaces. Figure 1 is a schematic drawing of the two forms. The so-called diffusive form, arising when temperature and salinity both increase with depth, is

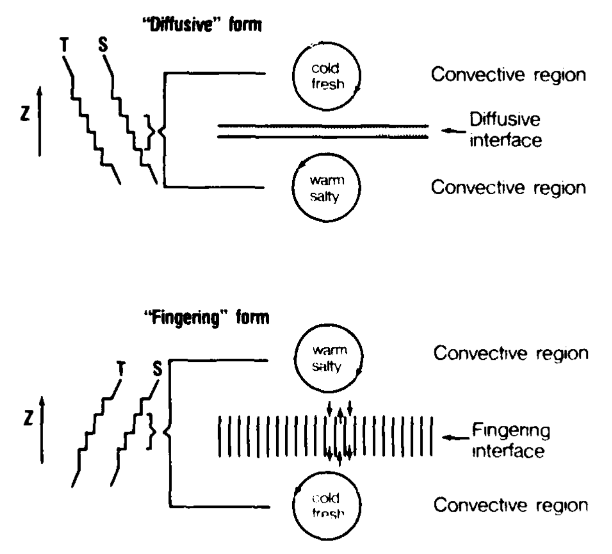

Figure 1. The two forms of double diffusion. T is temp. or the faster diffusing substance; S is salt, the slower diffusing substance.

characterized by a sharp interface, across which large temperature and salinity gradients exist. Heat and salt are transported upward, primarily by molecular diffusion across the interface (hence the name "diffusive" form), but because heat diffuses faster than salt, the heat flux is larger than the salt flux. The convective regions on either side keep the interface sharp and the gradients maximized.

The second form, the fingering form, occurs when both temperature and salinity decrease with depth. The fingering interface consists of a field of upward- and downward-moving columns of water—the fingers—which transport fluid from one side of the interface to the other. Because heat diffuses through the side walls of the fingers much faster than salt does, some heat lost through the sidewalls by the downward-moving fingers is returned upward by the upward-moving fingers. As a consequence, the downward flux of salt is greater than the downward flux of heat. As with the diffusive form, the convective regions on either side of the interface keep the gradients through the interface maximized. Turner (1985) gives a recent review of the field.

Under some oceanic conditions, both forms are important. It is impossible to explain frontal processes without invoking double diffusion, particularly the dynamics and evolution of intrusions and vertical and horizontal mixing in such regions (e.g., Gregg and McKenzie, 1979; Toole and Georgi, 1981). On a smaller scale, double diffusion may be important in the mixed layer for mixing small-scale thermohaline anomalies into the surrounding fluid (Delnore, 1980).

Under other circumstances, one form or the other predominates. The diffusive form is possible where temperature and salinity increase with depth, a situation that occurs most commonly in polar regions (e.g., Neshyba et al., 1971; Foster and Carmack, 1976) and near seafloor geothermal sources (e.g., Voorhis and Dorson, 1975; Wiesenburg, 1980). Schmitt (1981) has suggested that intermittent salt fingering may be the controlling mechanism in the shape of the potential temperature-salinity curve in the Central Waters of the world's oceans. The existence of a widespread subsurface salinity maximum in many parts of the tropical and subtropical ocean (Pickard and Emery, 1982) suggests that salt fingering may be common in these regions. Miller and Browning (1974) observed the large-scale isothermal steps, which are considered a hallmark of intense salt-fingering activity, in a 53-km transect across the equator along 84°25' W in the eastern Pacific. Similar staircases have been observed off the northeast coast of South America (1985 study area, see later) in the Tyrrhenian Sea (e.g., Johannessen and Lee, 1974), the Gulf of Cadiz (e.g., Elliott et al., 1974), and the northeast Caribbean (Lambert and Sturges, 1977).

Conditions allowing the formation of large-scale, well-developed and long-lived thermohaline staircases are not as common as conditions that permit less vigorous salt fingering. However, the occurrence of staircases may well indicate regions of significant vertical mixing and water mass modification (Lambert and Sturges, 1977). In addition, less dramatic steps appear to be fairly common wherever two water masses with the proper temperature and salinity relationships are in contact (e.g., Evans, 1981; Schmitt and Georgi, 1982; Larson and Gregg, 1983; Armi and Zenk, 1984). If laboratory results may be extrapolated to oceanic conditions, then salt fingering is causing substantial downward transport of heat and salt wherever staircases are found and may be a very important vertical mixing mechanism. In addition, preliminary work has indicated the staircases have a significant impact on acoustic propagation (S. Chin-Bing and D. King, NORDA, personal communication; R. Schmitt, Woods Hole Oceanographic Institution, personal communication).

Shear instabilities

Fine- and microstructure variations of oceanic properties can also result from turbulence generated by shear instabilities. Two closely related classes of instabilities may be defined: Kelvin-Helmholtz instabilities and internal wave breaking.

The simplest model of the Kelvin-Helmholtz instability is that of a flag waving in the breeze. Suppose you start with a thin, flexible membrane (a flag, for instance) with a constant breeze blowing by it. Now, impose a small wavy disturbance on the membrane. Where the membrane is convex, the streamlines of the wind will be forced together and will increase its speed; conversely, on the concave portion of the membrane, the wind will be slowed. From Bernoulli's law, we can see that the pressure acting on the membrane in the convex regions will be lowered and the pressure on the concave regions increased. This pressure distribution will tend to move the membrane in a manner such that the concave regions become more concave and similarly for the convex regions.

The same physics applies to a horizontal membrane separating two regions of flow moving at different speeds, if you allow the membrane to move at the average speed of the flow in both regions. As long as the density is the same in both regions of flow, the instability will occur. If the upper region has less dense fluid than the lower region, work will have to be done against gravity to raise fluid from the lower region into the upper region and vice

versa. If the density difference is great enough, the disturbance will not grow and no instability will occur.

The ocean does not have thin, flexible membranes or infinite gradients, such as in the simple model described. Nevertheless, the same physics applies to regions of flow where the density and velocity gradients vary with depth. As long as the ratio of the density gradient to the square of the velocity gradient remains above a certain threshold, Kelvin-Helmholtz instabilities cannot occur. The density gradient is usually multiplied by the gravitational acceleration and divided by the mean density to get a number that is the square of the Brunt-Vaisala frequency, the frequency at which a parcel of water would oscillate if displaced vertically from its resting position. When this number is divided by the square of the vertical velocity gradient, a nondimensional number, the Richardson number, Ri, is formed. The critical value for Kelvin-Helmholtz instabilities is Ri = ¼.

Internal wave breaking can arise when internal waves occur in a region where the fluid velocity varies with depth, i.e., in a shear regime. Suppose you have a weak shear field with velocity increasing upward. If an internal wave is generated moving in the same direction as the shear, the upper part of the wave will be advected forward faster than the lower portion of the wave. Eventually the upper part of the wave will move far enough ahead of the rest of the wave that denser fluid will overlay less dense fluid and result in a Rayleigh-Taylor instability that collapses into a turbulent patch. (This instability is responsible for the ultimate development and turbulent collapse of the Kelvin-Helmholtz instability.)

In the ocean, the shear field may be due to a large-scale feature such as an eddy or front or to other larger scale internal waves. Frontal regions may possess both the large-scale shears associated with the actual front and large-scale internal-inertial waves. Strictly speaking, the instability associated with the breaking of internal waves should be called an "advective instability." This can take place without any ambient shear—just the shear present in the background internal wave field.

External mixing

Another source of fine- and microscale structure related to turbulence arises from the passage of various types of objects through the ocean. When a vessel or large animal moves through a fluid, it leaves a wake of turbulent fluid behind. For most bodies the wake is large enough to generate turbulent patches. The initial transverse diameter of the wake is on the order of the diameter of the generating body. In a stratified fluid the wake will tend to collapse and flatten out under the influence of the surrounding fluid. The initial collapse is quite rapid, typically on the order of a few minutes in the ocean, but the time for flattening is on the order of the reciprocal of the Brunt-Väisälä frequency of the ambient fluid. As the wake collapses it will lose energy by turbulent dissipation and radiation of internal waves. After a time, the turbulent velocity fluctuations will be damped by the viscosity of the fluid, and the variations in temperature and salinity will be smoothed out by diffusive processes. The time needed to smooth out the fluctuations to the original background state is known as the *lifetime* of the disturbance. Wu (1966) gives a good discussion of the hydrodynamic phenomena associated with the collapse of a turbulent wake in a stratified fluid.

Internal wave straining

The above mechanisms of generating finestructure are called "irreversible" mechanisms because the mixing they cause irreversibly changes the temperature, salinity, and density fields. Another mechanism, internal wave straining, is termed "reversible" because it only temporarily leads to changes in these fields. Perturbations in the fields occur as the wave passes, but once it has gone by, the temperature, salinity, and density fields return to their prewave condition.

This has been a quick survey of some of the mechanisms generating finestructure and turbulence in a fluid. The action of some of these mechanisms (action) is commonly observed in the atmosphere when cloud and moisture conditions are favorable. On days when a strong vertical shear is near or just above a stratus cloud, Kelvin-Helmholtz instabilities and subsequent billow/roll formation and, finally, turbulent mixing and smoothing can be seen. External mixing is evident when a high-flying aircraft creates the classic contrail formation. These formations result from the wing-tip vortices of the aircraft and eventually interact with one another to twist and form "smoke-ring" patterns far back in the wake.

Instrument development

In a few special instances it is possible to directly observe the formation and evolution of fine- and microstructure in the ocean. Woods (1968) observed the formation of billows and rolls on a thermocline sheet by introducing dye into the stratification and photographing its evolution. Some of the first direct measurements of shear in the main thermocline were made by dropping dye pellets from the submersible ALVIN and making a series of stereoscopic photographs of the dyed pellet wakes.

Microstructure in the thermal (or more accurately, the refractive index) field is often observed by divers as they pass through the seasonal thermocline in large lakes. In general, however, fine- and microstructure must be studied indirectly through a suite of instruments, including sensors that measure temperature, conductivity, velocity, optical properties, and high-frequency acoustic backscatter.

In the mid 1950s, an instrument was developed to obtain very rapid measurements of temperature, pressure, and conductivity. The temperature and conductivity were combined in the instrument to get salinity, and the values of temperature, salinity, and conductivity were transmitted up a conducting cable to a readout unit and plotter on the ship. This instrument evolved into the the Bissett-Berman STD (salinity-temperature-depth measuring device). At the time the STD was developed, the need for matching the time response of the temperature and conductivity sensors was not recognized, nor were digital computers inexpensive, reliable or small enough to use in routine data processing at sea. The mismatch between the sensor time responses resulted in erroneous salinity "spikes" whenever the instrument passed through very strong temperature gradients. The conductivity, temperature, and depth profiler (CTD) developed by Neil Brown to overcome many of the problems inherent in the STD design has been manufactured by Neil Brown Instrument Systems Corporation (NBIS) since the 1970s, and has become one of the standard instruments for oceanographic research.

The acoustic current meter (ACM) was also developed by NBIS. This instrument uses the principle that the time required for an acoustic pulse to travel from one set of transducers to another is equal to the speed of sound plus a factor proportional to the speed of the water. If pulses are sent at the same time and in opposite directions, then the time difference of the pulse travel is directly proportional to projection of the water velocity on the sound path. This type of current meter is very rugged and has no moving parts or negligible zero drift. The pathlength is short, on the order of 20 cm, making it a good sensor for the larger microscale to the larger finescale velocity fluctuations.

A major undertaking at NORDA has been the development of a hybrid instrument combining the features of the NBIS CTD and ACM. This finescale profiler measures velocity, conductivity, temperature, and pressure (depth) and is termed the VCTD. The primary sensors for temperature and conductivity are the same as for the NBIS CTD. As in the CTD, there is a temperature sensor with a very rapid response but low accuracy, and another temperature sensor has a slow response but very high accuracy. The temperature signals from both sensors are sent to the deck unit separately for subsequent data processing on the ship or in the laboratory. The velocity sensors are similar to those used in the ACM, but while the ACM has two acoustic paths, the VCTD has three independent paths and can therefore resolve the full three-dimensional velocity vector.

In addition to the basic oceanic sensors, two sets of auxiliary sensors determine the orientation and motion of the instrument. The first sensor is an orthogonal triad of accelerometers that measures instrument acceleration along three axes. A triaxial magnetometer is also installed to measure the components of the earth's magnetic field vector in the instrument coordinate system.

When the instrument was initially ordered, the suite of sensors was thought to be sufficient for determining both the instrument orientation and the motion of its center of mass. It was also thought that these quantities could be resolved and that the effect of the instrument's motion could be removed by appropriate numerical treatment of the data, but this assumption has proved incorrect. Over the past several years NORDA has investigated a number of methods for mechanically decoupling ship-induced motion from the VCTD, subject to the constraint of keeping the instrument tethered to the ship. Tethering would permit control of the sampling depths of the instrument, provide power, obtain real-time data, and avoid the time and expense of VCTD redesign and construction.

Both passive and active systems were considered for providing the decoupling before finally settling on an actively controlled winch with external feedback. The winch was constructed by the SeaMac division of Harvey Lynch, Inc., of Houston, Texas, and the control and feedback system was designed and constructed at NORDA. The first tests of the motion isolation system were performed with reasonable success on the Finescale Variability Experiment cruise in July 1984, and the VCTD is becoming an indispensable tool in NORDA's finestructure investigations.

A number of expendable instruments have been or will be used in finescale studies. They include the expendable dissipation profiler (XDP), developed by Lueck and Osborne of the Naval Postgraduate School; the expendable current profiler (XCP), developed by Sanford of the University of Washington Applied Physics Laboratory; and the ubiquitous expendable bathythermograph (XBT) and its air-launched version, the AXBT. The XDP is the newest of these instruments and is presently the only expendable instrument capable of making microscale turbulence

estimates. These expendables are invaluable in supplementing CTD and VCTD measurements.

Field studies

1980

The first sea tests of the VCTD were performed on a cruise to the Bay of Campeche in autumn 1980. The primary goal of the cruise was to check out the instrument at sea, correct design faults, if any, and test different methods for deploying the instrument to facilitate reduction of ship-induced motion.

Several easily corrected errors were found in the electrical design of the instrument. The instrument was tested by deploying it in the same manner as the CTD (from the starboard davit arm). Also tried were several variations of a catenary deployment, which proved very successful in reducing the vertical motion of the instrument at the expense of increasing its horizontal motion.

While at sea, also tested were several methods for determining the vertical velocity component of the instrument to be used in correcting the observed vertical velocity. These methods worked sucessfully, and were later improved on shore, prior to the next cruise (Saunders et al., 1981).

1981

The VCTD was used next on a joint cruise aboard the RV GYRE in November and December 1981. The working track of the cruise began near the equator at 25°W and ran west-northwest to Barbados. Most of the VCTD stations were taken between the equator and 4°N along that track.

Good observations of the equatorial undercurrent were obtained, although data had to be filtered about 10-m resolution to remove ship-induced motion effects. Some extremely homogeneous layers in the undercurrent were observed, which may have been indicative of strong mixing. Results from this cruise have been published in Perkins and Saunders (1982).

1982

The following year, NORDA scientists participated in a cruise to the Alboran Sea and the Gulf of Cadiz, spanning both sides of the Strait of Gibraltar. A second VCTD was purchased that had a pressure sensor capable of depths to 3200 m. The initial plan was to use this profiler in examining the Mediterranean outflow in the Gulf of Cadiz and to use the older, shallow profiler in the Alboran Sea. Unfortunately, the new profiler developed conductivity problems, but measurements taken with the CTD yielded good information on the larger finescale structures (Perkins and Saunders, 1984a).

The second part of the cruise was part of the Donde Va? international experiment to study the Alboran Sea Gyre. The seas were extremely calm, and all the data from the older profiler were of very high quality. Two good velocity and CTD sections were made across the Atlantic inflow, and a moderately long time series station was made just off Gibraltar. Findings have been presented in Perkins and Saunders (1984b).

1983

In July 1983 NORDA oceanographers once again returned to the tropical Atlantic as participants in the international SEQUAL/FOCAL program. Two equatorial sections were made: the first extended from 10°N to 10°S along 24°W, and the second extended from 3°S to 10°N along 26°W. The older profiler functioned well, yielding good data down to 320 m, but unfortunately, conductivity problems recurred with the new profiler. CTD measurements were made to obtain conductivity and temperature down to 800 m, and the sections were filled in by XBT drops. Results were published in Perkins and Saunders (1984c).

On the westward transit from the equator into Barbados the ship passed through a well-known region of large-scale, salt-fingering-generated thermohaline steps. As a pilot study for the 1985 C-SALT work (see later) XBTs were dropped and a number of VCTD and CTD casts were made. Results have been reported in a number of presentations and publications, including Boyd et al. (1983), Boyd and Perkins (1984), Boyd et al. (1985), Boyd and Perkins (1985a), and Boyd and Perkins (1985b).

1984

By 1984, the original project had evolved into a Special Focus Program project with more emphasis on the nature of the finescale processes themselves, rather than the methods by which they can be observed. This overall project involved NORDA, the Naval Research Laboratory (NRL) and the Contract Research Program Office of ONR. The first phase of the program began in 1984 with the Finescale Variability Experiment (FVX-84), which was planned as a two-ship operation to investigate the finestructure in the North Atlantic Subtropical Convergence Front.

The scientific objectives of the study were to determine the spatial distribution of finescale patches in relation to the front and to the distribution of internal wave activity; to measure the morphology of the patches and determine

the processes operating in the patches; to study the internal wave variability; to determine, if possible, the cause of sheet and layer structures; and to determine the large-scale structure of the front. To accomplish these objectives, a two-ship operation was planned. The NRL ship would be responsible for obtaining the large-sca' · thermal background and locating potentially interesting patches using their high-resolution thermistor chain, while the NORDA team would make detailed profiles of conductivity, temperature, and velocity in the patches. Airborne AXBT flights would be used to locate the front, and the ships would use this information for detailed sections. The experiment was to be divided into three phases: the front would be located; NORDA would take repeated profiles at a point in the front while NRL would run a star pattern around the NORDA ship in the front; the second phase would be repeated in a "quiet" region away from the front.

This plan was generally followed, with the addition of a cross-frontal VCTD and CTD section during a maintenance period for the NRL chain, and a study of an active patch. The patch study began with its location by NRL and the tagging of the patch with a NORDA drogue. The drogue was then followed by the NORDA ship, and nearly continuous profiles were taken while following the patch center. During this period the NRL ship ran nearly continuous tracks across the patch.

Very strong shears were observed in the patch study. The current speed did not vary greatly with depth, but the direction of the current changed radically, giving rise to strong shears. During most of the study a great deal of internal wave activity was witnessed, and the thermistor chain profiles showed numerous indications of Kelvin-Helmholtz like structures. Analysis of the data is approaching completion.

1985

Double diffusion is the focus of the 1985 work. A number of institutions, including NORDA, NRL, the Naval Postgraduate School, the Woods Hole Oceanographic Institution, and the University of Washington will conduct an intensive study of the thermohaline staircase field off the northeast coast of South America.

The 1985 study area is shown in Figure 2. Thermohaline staircases have been reported here for at least the past 15 years (Delnore and McHugh, 1972; Mazeika, 1974; Perkins and Saunders, 1982; Bruce et al., 1984; Boyd et al., 1985). A survey of the historical reports suggests the steps are found over approximately the region outlined, covering roughly 1.2 x 10 km^2. An example of what is meant by "large-scale thermohaline staircase" is shown in Figure 3 from the small pilot study NORDA carried out in the area in 1983.

The upper 1000 m of this area is a region of high variability where waters formed in the North and South Atlantic come together and serve as a source for both the westward-flowing Caribbean Current and the eastward-flowing North Equatorial Counter Current, and the eastward-flowing Equatorial Undercurrent (Richardson and McKee, 1984; Pickard and Emery, 1982). Centered at about 100 m is the warm, salty North Atlantic Subtropical Underwater (SUW) (Defant, 1961; terminology from Wuest, 1964). Somewhat deeper, at about 800 m, is found the relatively cool and fresh Antarctic Intermediate Water (AAIW) (Wuest, 1978; terminology from Pickard and Emery, 1982), which can be traced well into the Caribbean.

The salt fingering and the staircases they generate occur in the water column between the SUW and the AAIW. The high gradient interfaces between the well-mixed convective layers are typically several meters thick, but the layers can range from several meters thick to up to 200 m thick in some parts of the world. The salt fingers are located within the interfaces, probably across several smaller scale interfaces imbedded within the larger interfaces. The small interfaces are too small to be resolved by ordinary oceanographic instrumentation. The collective effect of the fingers is to drive a vigorous flux of salt and a somewhat lesser flux of heat downward from the SUW into the AAIW.

The region is excellent for the first oceanographic investigation of double diffusive processes. The salt fingering is much more vigorous than in many other parts of the world ocean where the signatures of the process would be contaminated to a much greater extent by other mechanisms that generate finescale variability. We hope the understanding gained in this area will improve our understanding of what is happening in much more complex areas.

The field work in 1985 will occur in two phases. A spring phase includes an AXBT survey and a ship survey that will also implant a current meter mooring. The fall phase will begin with an AXBT survey and the two 2-ship investigations using a vast array of oceanic finescale instrumentation, including VCTD profilers. The investigation has five scientific goals.

- To define the extent of the staircase field in this region and to assess its variability in both time and space.
- To determine the local temperature, salinity, and shear environment.
- To examine the evolution of the staircases over several inertial periods.

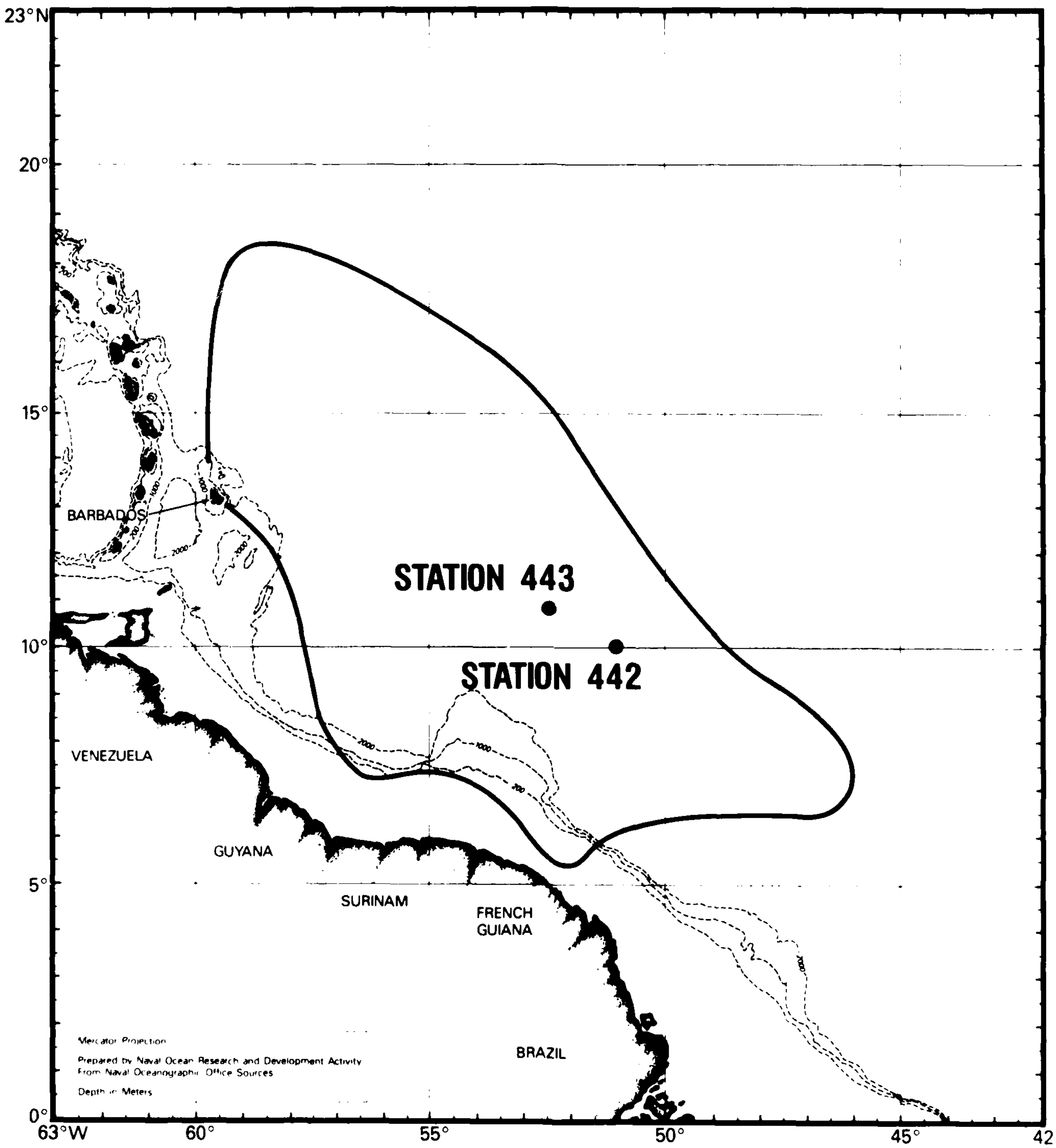

Figure 2. The study area in 1985. Earlier reports of large scale staircases fall within the area outlined. Stations 442 and 443 are two multicast hydrographic stations taken in July 1983, which formed a pilot study for the 1985 work

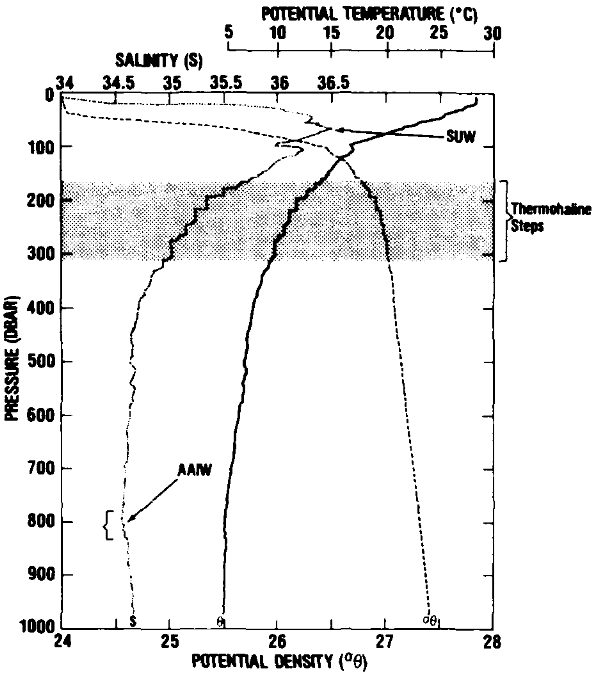

Figure 3. Typical hydrographic cast from Stations 442 and 443 (July 1983). The warm salinity maximum of the SUW, the large scale thermohaline steps, and the salinity minimum of the AAIW are indicated.

- To compare microstructure measurements in the staircases with theoretical flux models and with laboratory flux laws.
- To evaluate the role of the steps in the maintenance of regional hydrographic and tracer fields.

The spring phase of C-SALT proved very successful and as this article goes into publication the fall phase has had a successful beginning.

1986

In the spring of 1986, the Finescale Variability Project plans a cruise in the Alboran Sea to observe the generation of finescale structure near the Strait of Gibraltar, to follow the structures as they are advected into the Alboran Sea Gyre, and to observe their decay.

References

Armi, L. and W. Zenk (1984). Large Lenses of Highly Saline Mediterranean Water. *Journal of Physical Oceanography* 14, 1560-1576.

Boyd, J. D. and H. Perkins (1984). Estimates of Vertical Heat and Salt Fluxes in a Thermohaline Staircase. *EOS, Transactions of the American Geophysical Union* 65, 954.

Boyd, J. D. and H. Perkins (1985a). Estimates of Double Diffusion Heat and Salt Fluxes off the Northeast Coast of South America. Submitted to *Oceanologica Acta*.

Boyd, J. D. and H. Perkins (1985b). Characteristics of Thermohaline Steps off the Northeast Coast of South America, July 1983. Submitted to *Deep Sea Research*.

Boyd, J. D., H. T. Perkins, and K. D. Saunders (1983). Characteristics of Thermohaline Step Structures off the Northeast Coast of South America. *EOS, Transactions of the American Geophysical Union* 64, 1058.

Boyd, J. D., H. Perkins, and K. D. Saunders (1985). *Hydrographic Measurements off the Northeast Coast of South America, July 1983*. Naval Ocean Research and Development Activity, NSTL, Mississippi, NORDA Technical Note 305, 181 pp.

Bruce, J. G., J. L. Kerling, and W. H. Beatty III (1984). Temperature Steps off Northern Brazil. *Tropical Ocean-Atmosphere Newsletter*, January, 10-11.

Chen, C. F. and D. H. Johnson (1984). Double-Diffusive Convection: A Report on an Engineering Foundation Conference. *Journal of Fluid Mechanics* 138, 405-416.

Defant, A. (1961). *Physical Oceanography, Volume 1*. Pergamon Press, 729 pp.

Delnore, V. E. (1980). Numerical Simulation of Thermohaline Convection in the Upper Ocean. *Journal of Fluid Mechanics* 93, 803-826.

Delnore, V. E. and J. McHugh (1972). *BOMEX Period III Upper Ocean Soundings*. National Oceanic and Atmospheric Administration, Rockville, Maryland, 352 pp.

Elliott, A. J., M. R. Howe, and R. I. Tait (1974). The Lateral Coherence of a System of Thermohaline Layers in the Deep Ocean. *Deep-Sea Research* 21, 95-107.

Evans, D. L. (1981). Velocity Shear in a Thermohaline Staircase. *Deep-Sea Research* 28, 1409-1415.

Foster, T. D. and E. C. Carmack (1976). Temperature and Salinity Structure in the Weddell Sea. *Journal of Physical Oceanography* 6, 36-44.

Gregg, M. C. and J. H. McKenzie (1979). Thermohaline Intrusions Lie across Isopycnals. *Nature* 280, 310-311.

Huppert, H. E. and J. S. Turner (1981). Double Diffusive Convection. *Journal of Fluid Mechanics* 106, 299-329.

Johannessen, O. M. and O. S. Lee (1974). A Deep Stepped Thermohaline Structure in the Mediterranean. *Deep-Sea Research* 21, 629-639.

Lambert, R. B. and W. Sturges (1977). A Thermohaline Staircase and Vertical Mixing in the Thermocline. *Deep-Sea Research* 24, 211-222.

Larson, N. G. and M. C. Gregg (1983). Turbulent Dissipation and Shear in Thermohaline Intrusions. *Nature* 306, 26–32.

Mazeika, P. A. (1974). Subsurface Mixed Layers in the Northwest Tropical Atlantic. *Journal of Physical Oceanography* 4, 446–453.

Miller, R. R. and D. G. Browning (1974). Thermal Layering between the Galapagos Islands and South America. *Deep-Sea Research* 21, 669–673.

Neshyba, S., V. T. Neal, and W. Denner (1971). Temperature and Conductivity Measurements under Ice Island T3. *Journal of Geophysical Research* 76, 8107–8120.

Perkins, H. T. and K. D. Saunders (1982). Physical Oceanographic Observations in the Northwest Tropical Atlantic. *Tropical Ocean-Atmosphere Newsletter*, September, 7–9.

Perkins, H. T. and K. D. Saunders (1984a). Measurements of the Mediterranean Outflow South of Cape St. Vincent, September, 1982. In *Preliminary Results of the Donde Va Meeting in Fuengirola*, G. Parrilla (ed.), Instituto Espanol de Oceanografia, *Informes Technios*, 24 1982, 25–32.

Perkins, H. T. and K. D. Saunders (1984b). Sections of Current, Salinity, and Temperature in the Northwestern Alboran Sea, October, 1982. In *Preliminary Results of the Donde Va Meeting in Fuengirola*, G. Parrilla (ed.), Instituto Espanol de Oceanografia, *Informes Technios*, 24 1982, 141–149.

Perkins, H. T. and K. D. Saunders (1984c). Atlantic Equatorial Sections During July, 1983. *Geophysical Research Letters* 11, 769–772.

Pickard, G. L. and W. J. Emery (1982). *Descriptive Physical Oceanography*. Pergamon Press, New York, 249 pp.

Richardson, P. L. and T. K. McKee (1984). Average Seasonal Variation of the Atlantic Equatorial Currents from Historical Ship Drifts. *Journal of Physical Oceanography* 14, 1226–1238.

Saunders, K. D., H. Perkins, L. Banchero, S. Sova, and J. Vega (1981). Sea Trials of a Lowered Three-Axis Current Meter. *Proceedings, Oceans '81*, 245–249.

Schmitt, R. W. (1981). Form of the Temperature-Salinity Relationship in the Central Water: Evidence for Double-Diffusive Mixing. *Journal of Physical Oceanography* 11, 1015–1026.

Schmitt, R. W. and D. T. Georgi (1982). Finestructure and Microstructure in the North Atlantic Current. *Journal of Marine Research* 40 (suppl.), 659–705.

Stommel, H., A. B. Aarons, and D. Blanchard (1956). An Oceanographical Curiosity: The Perpetual Salt Fountain. *Deep-Sea Research* 3, 152–153.

Toole, J. M. and D. T. Georgi (1981). On the Dynamics and Effects of Double-Diffusively Driven Intrusions. *Progress in Oceanography* 10, 123–145.

Turner, J. S. (1985). Multicomponent Convection. *Annual Reviews of Fluid Mechanics* 17, 11–44.

Voorhis, A. D. and D. L. Dorson (1975). Thermal Convection in the ATLANTIS II Hot Brine Pool. *Deep-Sea Research* 22, 167–175.

Wiesenburg, D. A. (1980). *Geochemistry of Dissolved Gases in the Hypersaline Orca Basin*. Ph.D. dissertation, Texas A&M University, College Station, Texas, 265 pp.

Woods, J. D. (1968). Wave-Induced Shear Instability in the Summer Thermocline. *Journal of Fluid Mechanics* 32, 372–378.

Wu, J. (1966). *Flow Phenomena Caused by the Collapse of a Mixed Region in a Density-Stratified Medium*. Hydronautics Technical Report 231-11.

Wuest, G. (1964). *Stratification and Circulation in the Antillean-Caribbean Basin*. University Press, 130 pp.

Wuest, G. (1978). *The Stratosphere of the Atlantic Ocean*. W. J. Emery, ed., Amerind Publishing Company, New Delhi, 112 pp.

An Analytical Evaluation of Microbiologically Induced Corrosion

Brenda J. Little and Patricia A. Wagner
Oceanography Division

Abstract

The corrosion resulting from the colonization of bacterial isolates on nickel, copper, and carbon steel surfaces has been quantified using a newly developed technique. In all cases the presence of the microorganisms created anodic currents. Further, it has been shown that the observed currents can be due to respiration, which creates differential aeration cells, and secretion of acidic metabolites.

Introduction

Microfouling and corrosion commence immediately after a metal is exposed to an aquatic environment. Microfouling is the accumulation of microbial forms, such as bacteria, fungi, and microalgae, and their secretions. Corrosion, as applied to metals, consists of oxidation and reduction reactions that take place in areas known as anodes and cathodes, respectively.

Most metals are found in nature in thermodynamically stable forms. An investment of energy is required for refining these metallic ores. Immediately after refinement, oxidations and reductions that involve energy changes via electron transport convert these metals to their original low-energy state. Microorganisms have evolved elaborate, efficient systems for electron transport, using a variety of metals to serve energy manipulation requirements (Alexander, 1967; Zajic, 1969).

Despite the obvious interrelationship between corrosion and microfouling, these two processes have traditionally been evaluated individually. However, the economic ramifications of microbial corrosion have created a need for measurement tools to quantify the process. The traditional weight-loss method for measuring corrosion does not distinguish between biological and abiological contributions. In addition, the method is destructive—only one measurement can be made per specimen. Electrochemical methods, such as potentiodynamic polarization scans and Tafel extrapolations, permit many observations on one specimen over time, but, again, there is no distinction between the biotic and abiotic components of corrosion. Furthermore, the patchy nature of microbial colonization of surfaces invalidates the data derived from electrochemical techniques that are based on the assumption that the measured corrosion is taking place uniformly on the surface.

NORDA scientists developed an analytical approach that can be used to quantify the corrosion current resulting from microbial colonization of metal surfaces and to determine the nature of the microbial mediation. The effects of a marine pseudomonad, an obligate thermophilic filamentous bacterium and an iron-oxidizing stalked bacterium, isolated from corroding copper, nickel, and carbon steel surfaces, respectively, were examined using this approach. Possible mechanisms for the observed corrosion have also been evaluated.

Methods and materials

Corrosion experiments

A schematic diagram of the corrosion-measuring device is presented in Figure 1. Ground glass bases from 47 mm Millipore filter supports were joined to the sides of two 500-ml flasks. A 0.1-μm pore Millipore cellulose acetate/cellulose nitrate filter disc was placed between the two supports, and the flasks were clamped together and filled with 500 ml of the basal salts medium supplemented with 0.025% each tryptone and yeast extract. Duplicates of either nickel, copper, or carbon steel 1-cm^2 electrodes were placed into the flasks. The entire assemblage was autoclaved for 15 min at 120°C and 15 psi. Water-saturated air was bubbled into one of the flasks. Previous experiments have shown that oxygen diffused across the membrane

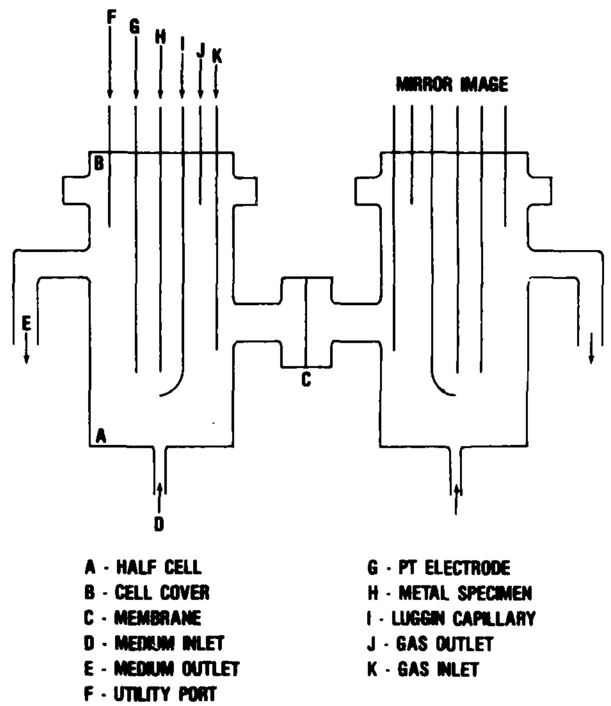

Figure 1. Corrosion measurement cell.

and that the water in the two flasks was saturated with oxygen after 2 hours of aeration. The membrane ensured electrolytic conductivity between the discs, while maintaining microorganisms on one side of the membrane and an abiotic system on the other side. One flask was inoculated with a metal disc previously colonized by microorganisms, while a sterile disc was dropped into the flask to be kept in an abiotic condition. The electrodes were then galvanically coupled and the resulting currents measured with an EG&G PARC corrosion measuring device (Model 350).

In such a system the measuring device functions as a zero resistance ammeter; i.e., the potential of the galvanic cell is not perturbed by the current measurements. If the identical metal specimens are galvanically coupled and are isolated in identical electrolyte solutions, the current flow between them is zero, even in the presence of active corrosion. They corrode at the same rate and neither functions as an anode or cathode in reference to the other. If this balance is disturbed by the presence of colonizing microorganisms, a current flows between the two specimens. If the reaction that is taking place at the surface of the inoculated electrode is an oxidation, an anodic current will be recorded; if it is a reduction, a cathodic current results.

Experiments were designed to abiotically test the individual effects of bacterial respiration and acid metabolite production on the corrosion of the metal substrata. Platinum electrodes were used as chemically unreactive surfaces with which to compare the electrochemical responses of the other metals. The 0.1 μm Millipore filter was replaced with a Teflon disc to ensure chemical separation of the compartments. A KCl/agar bridge maintained electrolytic conductivity.

Bacteria

The bacterium designated as B-3 (Pseudomonas sp.) was isolated from a surface that was painted with cuprous oxide and tributyl tin and exposed in seawater. Thermus aquaticus, an obligate thermophile, was isolated from a failed nickel heat exchanger that had been maintained with distilled water. The iron-oxidizing bacterium was isolated from a corroding carbon steel water box that had been filled with (naturally occurring) lake water. Standard microbiological techniques were used to isolate and maintain pure cultures. Organisms that had a greater ability to attach to surfaces were selected by providing metal discs in the culture. These discs were used for subsequent transfers and for the inoculation of the electrode in the corrosion-measuring experiments.

Results and discussion

In all cases, the specimen in the cell inoculated with bacteria became the anode of the galvanic couple with currents ranging from 1.0 μA cm^{-2} to 10.4 μA cm^{-2} (Fig. 2). The range of observed currents is indicative of the varying susceptibilities of the metal substrata and the varying impacts of the three isolates on those substrata.

The optimum growth temperature for the obligate thermophile is 60–70°C, and the organism is completely

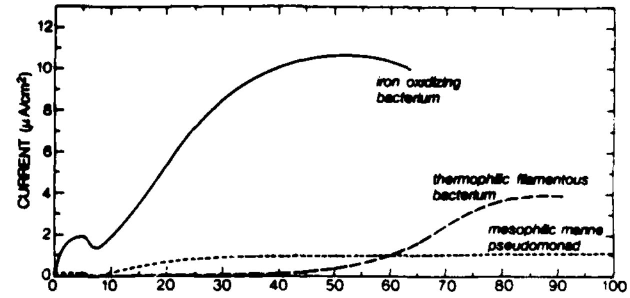

Figure 2. Corrosion current versus time for three bacterial species.

inactive below 50°C. The dual compartment cell, which held nickel specimens, was submerged in a water bath maintained at 60°C, and one compartment was inoculated with the organism. After about 20 hours, the current at the inoculated electrode began to increase anodically, and finally stabilized at 3.8 μA cm^{-2}. At ambient temperature, where the organism is inactive, no current between the compartments was observed. Similarly, no current was observed when the organisms colonizing the nickel electrode were heat-killed. These results suggest that these organisms must be metabolically active to affect corrosion.

Bacterium B-3 was inoculated into one side of the dual compartment cell that held copper specimens. After a 10-hour incubation time at ambient temperature, the current at the inoculated electrode began to increase anodically to about 1.0 μA cm^{-2}. Similar results were obtained when the stalked iron-bacterium was inoculated into the system containing carbon steel electrodes. An anodic current of 10.4 μA cm^{-2} was measured after approximately 40 hours. However, the iron-oxidizing bacteria on the carbon steel surface produced tubercles of ferric hydroxide, which prevented diffusion to and from the surface and created differential aeration cells that were independent of the biochemical activity of the bacteria. When these microorganisms were heat-killed, the anodic current remained stable at 8.6 μA cm^{-2}.

Several possible mechanisms have been proposed for microbial effects on corrosion under aerobic and microaerobic conditions. Among these are the formation of differential concentration (aeration) cells between areas covered by bacteria and the bare areas and the production of acids by microorganisms. With the aid of the dual-compartment cell described in this paper, it is possible to abiotically simulate conditions to individually evaluate proposed mechanisms.

Under sterile conditions, oxygen was bubbled through both compartments of the cell containing nickel, copper, carbon steel, or platinum electrodes. The current between the compartments was, in all cases, zero. Differential aeration was created by replacing the oxygen in one of the compartments with nitrogen. The carbon steel and copper electrodes in the compartment containing nitrogen became the anode of the galvanic couple with stable currents of 5.3 μA cm^{-2} and 4.8 μA cm^{-2}, respectively. No current was observed with the platinum and nickel electrodes in the presence of differential aeration at room temperature.

Evans (1925) stated that any geometrical factor that results in a higher concentration of oxygen at one part of a metal surface and a lower or zero concentration at another will result in the former becoming the cathode and the latter the anode of the corrosion cell. The experiments described here demonstrate the differential aeration principle defined by Evans, but they also demonstrate that the impact of differential aeration on corrosion current varies among metal substrata from virtually no current in the case of platinum to stable corrosion currents for copper, carbon steel, and nickel.

Most heterotrophic bacteria secrete organic acids during the fermentation of organic substrates. Organic acids from bacteria have been shown to enhance corrosion of a number of different types of metals. The types and amounts of acids produced in nature depend on the kinds of organisms present and the substrate molecules available. However, in natural microaerobic habitats, acetic acid is the major organic acid produced during fermentation.

The impact of acetic acid on the corrosion of nickel, carbon steel, and copper was experimentally evaluated in the two-compartment cell, with platinum serving as a control. The experiments were conducted in 3 parts per thousand synthetic salt solution in which the electrodes were incubated overnight. Once the electrical connections were made, each cell was allowed to reach its own characteristic baseline value. One of the compartments in each of the cells was made 10 millimolar (mM) with respect to acetic acid. In all cases the electrodes in the compartment containing acetic acid became the anodes of the two-compartment apparatus with currents which stabilized at 0.11, 1.87, 7.54 μA cm^{-2}, respectively, for nickel, copper, and carbon steel. The current between the platinum electrodes remained stable at 0 μA cm^{-2} (Fig. 3). The acetic acid apparently caused anodic depolarization with the corroding metals.

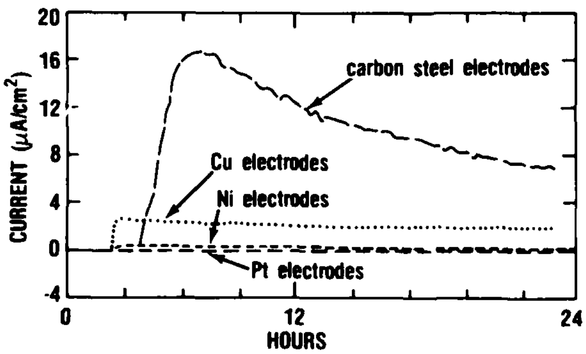

Figure 3. Impact of 10 mM acetic acid on corrosin current versus time for nickel, copper, carbon steel, platinum electrodes.

The impact of specific metabolites varies among substrata as shown in Figure 3. Burnes et al. (1967) demonstrated that organic acids formed metallic salts of copper in the presence of oxygen. Ashton et al. (1973) suggested that the acidic secretions of *Escherichia coli* were reponsible for the enhanced corrosion of carbon steel due to the dissolution of iron-oxide formed on the metal surface. Similarly, nickel forms a passivating film in slightly alkaline solutions. Acidic metabolites secreted by microorganisms can prevent passivation or destroy an existing passivation film.

Conclusions

The corrosion measurements presented in this paper confirm that three bacterial isolates are responsible for anodic corrosion currents. Further, we demonstrated that respiration and acid metabolites contribute to these anodic processes. The corrosion of carbon steel colonized by microorganisms can continue after the microorganisms have been killed because persistent ferric hydroxide tubercles are present. Their presence creates differential aeration cells that are independent of the biochemical activity of the microorganisms.

References

Alexander, M. (1967). *Introduction to Soil Microbiology*. John Wiley, New York, 467 pp.

Ashton, S. A., J. D. A. Miller, and R. A. King (1973). Corrosion of Pourous Metals in Batch Cultures of Nitrate Reducing Bacteria. *British Corrosion Journal* 8, 185-189.

Burnes, J. M., E. E. Staffeld, and O. H. Calderon (1967). Corrosion Caused by Organic Acids Reacting with Three Metals, with Special Emphasis on Kreb Cycle Acids. *Developments in Industrial Microbiology* 8, 327-334.

Evans, U. R. (1925). Oxygen Distribution as a Factor in the Corrosion of Metals. *Industrial and Engineering Chemistry* 17, 363-370.

Zajic, J. E. (1969). *Microbial Biogeochemistry*. Academic Press, New York, 345 pp.

An Overview of Basic Bioluminescence Research at NORDA

Richard V. Lynch III and Arthur V. Stiffey
Oceanography Division

Abstract

Bioluminescence occurs throughout the world's oceans at all times of the year and at every depth. In some regions it creates spectacular displays. It can be stimulated in a number of ways—notably mechanically, chemically, photically, barometrically and, possibly, acoustically. Most naval research has concentrated on mechanical stimulation to facilitate remote detection of ships at night moving through waters containing luminous organisms. Such movement will stimulate the organism to flash or glow, creating a signal that can be detected by airborne low-light-level, image-intensifying television camera systems. NORDA research has also concentrated on vertical distribution of bioluminescence in the water column, on correlations with physical and chemical parameters in seawater, and on stimulation and quenching mechanisms. A correlation between bioluminescence and temperature gradients has been established. Lasers and small pressure pulses have been used successfully to stimulate bioluminescence in dinoflagellates. Studies of chemical effects on bioluminescence have led to the development of assay techniques with many potential applications. Instrumentation development is being promoted to enhance naval capabilities in this field.

Introduction

"The ship dropped depth charges and in 30 minutes sank the last German U-boat. The phosphorescence of the sea was so intense that the movements of the shining U-34 under surface were clearly visible."

> Luminescence of the Sea,
> N. I. Tarasov (1956), from
> Newbolt's *Operations of the British Fleet in World War I.*

Marine bioluminescence has been observed since ancient times. Aristotle refers to light in the sea that can only be bioluminescence. Later observers believed that it was produced by phosphorus and called it phosphorescence of the sea, a term still frequently used by mariners. However, the proper term is bioluminescence because it is light produced by living organisms.

Bioluminescence occurs throughout the world's oceans at all times of year and at every depth. Luminous organisms have been observed at the bottom of the Marianas Trench and have been thawed from Arctic ice. Below the photic zone of the ocean, it has been estimated that perhaps 90% of the individuals and 70% of the species are luminous (Lynch, 1978). Even within the photic region, large numbers of luminous organisms occur. Luminescence appears in most marine phyla from one-celled dinoflagellates and radiolarians up through fish and squid. Bioluminescence is also common on land; fireflies are the best-known examples. In fresh water, however, only a single luminous organism lives—a limpet from New Zealand.

Luminous marine organisms are known to create spectacular displays. Primarily in the Arabian Sea, Bay of Bengal and South China Sea, displays called "milky seas" and "phosphorescent wheels" occur. A milky sea is a large, lighted area in the ocean, which frequently extends from horizon to horizon and sometimes lasts all night or longer. A phosphorescent wheel is a display in which alternating arms of light and dark appear to rotate around a center similar to a fireworks pinwheel (see Figure 1 for

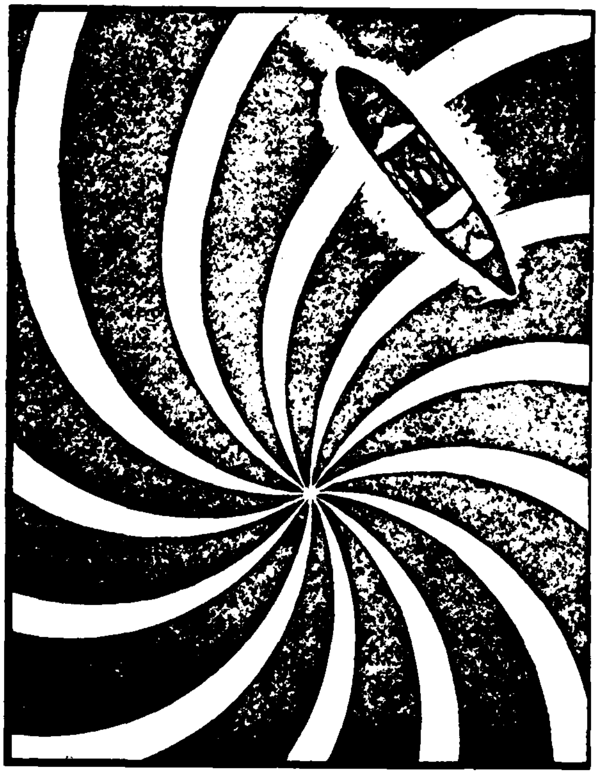

Figure 1. Artist's conception of a phosphorescent wheel (from Hilder, 1962).

an artist's conception of a wheel). These pinwheels range in size from one meter to several kilometers in diameter. Indeed, it is speculated that another display consisting of moving, parallel stripes of light is only the arms of a wheel the center of which is over the horizon. The causes of these displays are unknown.

Bioluminescence can be stimulated in many ways. In nature, the most common means is probably mechanical—touching or shaking a luminous organism will cause it to flash or glow. Thus, an object moving through water containing luminous organisms will stimulate them to emit light. Another natural means is photic—some organisms respond to flashes from their own species or others with an answering flash. In the laboratory electrical and chemical stimuli are the means most often used. Stimulation by acoustic pulses may also occur.

Naval interest in bioluminescence stems from incidents such as the one quoted from Tarasov. If such happenings would occur often, an obvious need would exist to understand the probability of that occurrence. However, marine bioluminescence is not usually sufficiently intense to be seen by the human eye. Therefore, serious study was believed to be unnecessary until the 1970s. At that time the National Marine Fisheries Service, using "starlight scope" technology developed for use in Vietnam, developed an airborne low-light-level, image-intensifying TV camera system (LLLII) for spotting fish schools moving at night (Roithmayr, 1970). The motion of the fish through water containing luminous organisms would stimulate them to emit light, which could then be detected by the LLLII and used to locate and entrap the school. This system was capable of intensifying light too dim to be seen by eye until it could easily be seen on a TV screen. Suddenly, a means of detecting remote objects moving in the water at night was available, and the Navy became interested in bioluminescence. However, many questions remained to be answered.

Discussion

Distribution

NORDA's present bioluminescence research program began in 1973 at the Naval Research Laboratory (NRL). The program was transferred to NORDA in 1983 upon the closing of NRL's Environmental Sciences Division. NORDA's initial program goal was to study the seasonal and geographic distribution of bioluminescence and attempt to correlate that distribution with physical and chemical parameters in the ocean. To do this, a literature survey and a series of research cruises were instituted. The Seventh Fleet also assisted by observing bioluminescence in its operating areas, primarily the Arabian Sea, for several years.

The major result of this work has been the publication of a series of articles, reports, and atlases establishing the ubiquitous occurrence of bioluminescence, suggesting the predominant luminous organisms, and estimating the probability of encountering surface bioluminescence of given intensity levels (Figs. 2 and 3). Individual encounters with bioluminescence occurrences in the Indian Ocean are shown for the different quarters of the year, each of which roughly corresponds to a season (Fig. 2). Estimates of the probability of encountering bioluminescence in the Indian Ocean in July-September are shown in Figure 3. Similar maps have been prepared for all the oceans of the world and all yearly quarters. This work continues and updates the pioneering work of R. F. Staples (1966) of the U.S. Naval Oceanographic Office (NAVOCEANO) and R. J. Turner (1965) of the National Institute of Oceanography. The conclusion to be drawn from these works is that on a large scale, some level of bioluminescence activity will be encountered anywhere in the ocean anytime at night.

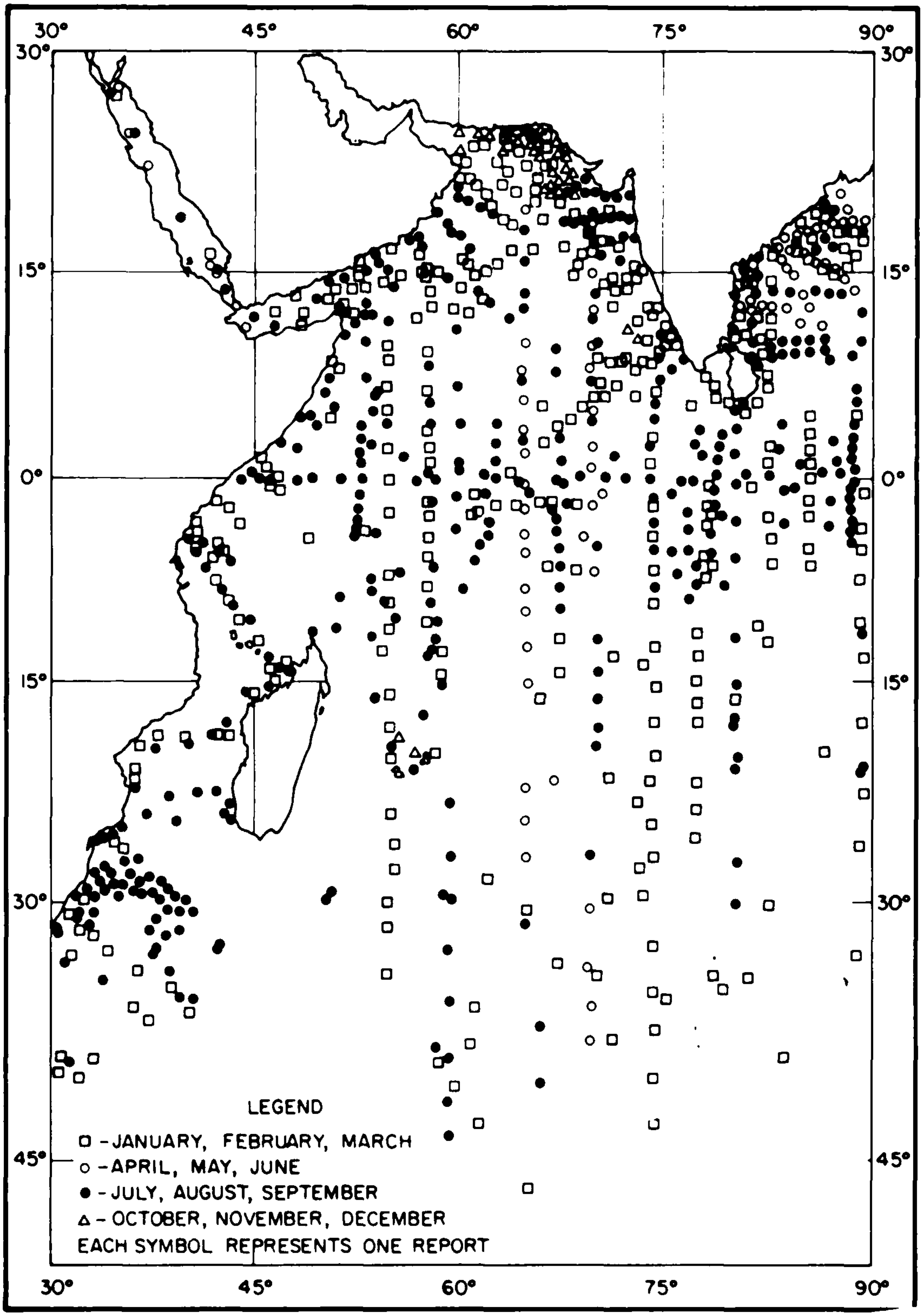

Figure 2. Seasonal distribution of bioluminescence in the central and western Indian Ocean and adjacent seas (from Lynch, 1978).

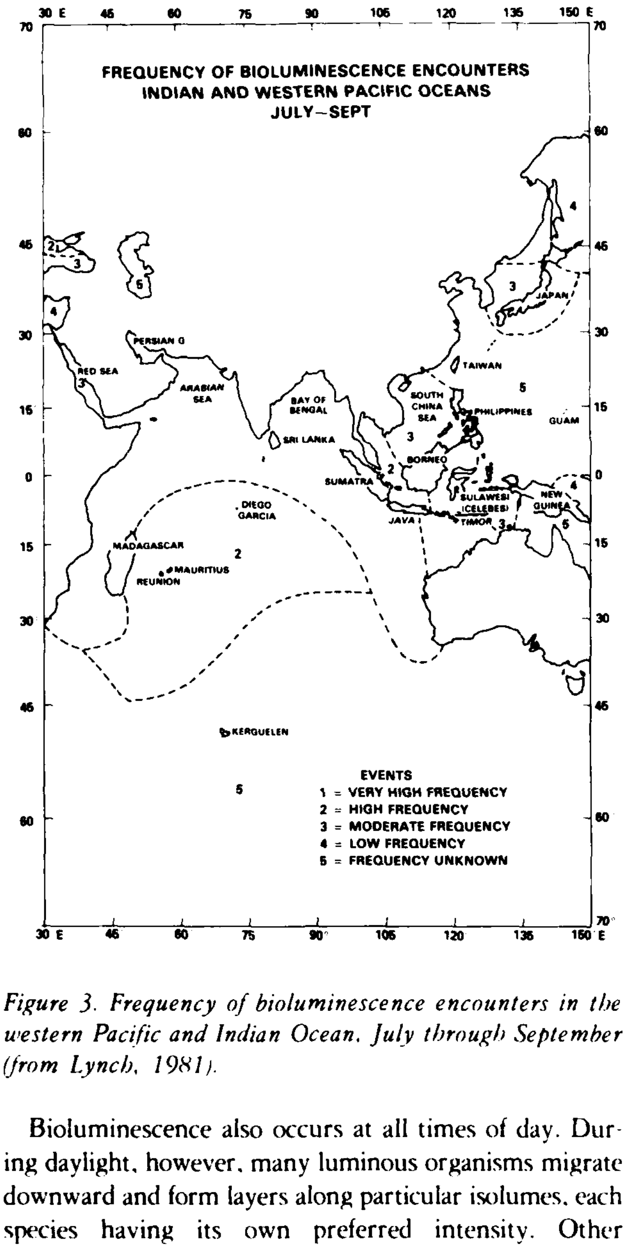

Figure 3. Frequency of bioluminescence encounters in the western Pacific and Indian Ocean, July through September (from Lynch, 1981).

Bioluminescence also occurs at all times of day. During daylight, however, many luminous organisms migrate downward and form layers along particular isolumes, each species having its own preferred intensity. Other organisms—notably photosynthetic dinoflagellates—are photically inhibited; that is, the light suppresses activity of luciferose, the enzyme that catalyzes the luminescence reaction, so that light emission will occur only very weakly and under extremely high levels of stimulation. Still other organisms neither migrate nor become inhibited, but exhibit the same luminous behavior both day and night. Therefore, luminous activity continues through the day, but with a very different vertical distribution from that of night. Even if the activity near the surface were the same in day and night, sunlight (even through heavy clouds) is so much more intense than bioluminescence that the bioluminescence signal is completely masked. The human eye, adapted to (relatively) strong sunlight, cannot detect the (relatively) weak bioluminescence signal, and instruments designed to measure bioluminescence saturate unless they are heavily shielded or lowered to depths where the sunlight is dim (around 70 m). Until recently, daytime bioluminescence was not thought to be of naval interest. Thus, all of the observations cited in the reports were made at night and the statistics developed assume night conditions. (In fact, of the thousands of observations examined, fewer than a dozen were made during the day, more than half of those since the last report was published.)

In addition to supporting the above conclusion, the observations of the Seventh Fleet in the Arabian Sea have been particularly useful in scrutinizing theories on the origins of luminous displays. Several theories on the causes of these displays have been advanced without supporting experimental evidence. Although inability to perform specialized scientific measurements has prevented testing some of the theories, the normal meteorological and oceanographic observations made by the Fleet have been sufficient to discredit others, thereby reducing the confusion and controversy over these phenomena.

The fact that bioluminescence is ubiquitous still does not mean that it is useful to the Navy. Successful remote sensing of bioluminescence depends upon both the strength of the initial signal and its penetration distance through the water and atmosphere. Signal penetration distance is dependent on scattering and absorption. In the atmosphere this is not considered a problem except when clouds are present. Thus, airborne remote sensing must be accomplished below cloud cover.

In the water, however, scattering and absorption are critical concerns. These concerns are related to particulate matter in the ocean; the presence of many particulates causes decreased penetration. Conversely, high particulate concentrations are frequently associated with high signal levels, since luminous organisms form some proportion of the particulate mass. Horizontally, particulate concentrations can change quite abruptly on a small scale, a phenomenon known as patchiness. Vertically, particulate concentrations also can change radically within a few meters. Organisms are known to form layers in daytime. These layers are known as deep scattering layers because they can be detected with an acoustic signal.

Different acoustic frequencies can be used to detect different size classes of organisms. During the day the layers

are well defined, their positions determined by the physical and chemical parameters of the water. For many luminous organisms, the forcing function is the intensity of penetrating sunlight; particular species like to remain close to particular isolumes. At night, however, the deep scattering layers rise toward the surface and diffuse. Layering nevertheless continues to occur, driven by as-yet undetermined parameters, and can be detected by nonacoustic means. For example, Soviet scientists (Gitel'zon et al., 1967) first suggested layering of bioluminescence in connection with the thermocline. This layering has been confirmed in joint research by NORDA, the Naval Ocean Systems Center (NOSC), and NAVOCEANO. Furthermore, NORDA, NOSC, and NAVOCEANO have established that small-scale bioluminescence maxima occur in conjunction with thermal fronts or boundary layers, the horizontal equivalents of the thermocline. In one instance a front has been detected with an airborne LLLII. However, the correlation between bioluminescence and temperature gradients is not perfect. The research effort at NORDA is currently being redirected from large-scale geographic and seasonal studies of bioluminescence distribution to studies of patchiness and vertical distribution. The approach taken is to conduct joint ship-air exercises to correlate remotely sensed data with in situ measurements, and to use manned submersible platforms to correlate direct eye observations with instrumental measurements, both approaches pioneered by NORDA and NOSC. If the Navy is to make full use of bioluminescence, these small-scale, short-term variations must be understood.

In addition to the established correlation between bioluminescence and temperature gradients, correlations with many other chemical and physical parameters have been suggested. On a small scale, no other correlations appear to hold true consistently. On a large scale, a correlation with chlorophyll fluorescence (which indicates the presence of phytoplankton) appears promising. Further research is required to establish this correlation definitively, to determine the scale at which it breaks down, and to understand why.

Stimulation

Some problems with bioluminescence distribution studies are the time and expense involved in shipborne surveys. Aerial coverage could be increased and short-term variations monitored rapidly if remote sensing techniques could be used. Airborne LLLII's for this purpose exist, but with a major drawback, namely, that if an overflown area exhibits no bioluminescence, it is not possible to distinguish whether this is due to a lack of luminous organisms or a lack of sources of stimulation such as fish schools or breaking waves, since most light is emitted only by stimulation. Furthermore, if light is detected, its appearance reflects a combination of the distribution of stimuli and the distribution of luminous organisms rather than the latter alone. To overcome this statistical problem, a source of remote stimulation must be developed.

A laser is an attractive potential stimulus source. Not only can it be used from long distances, but also it involves no expendables and is, therefore, relatively inexpensive to operate. Furthermore, some luminous planktonic organisms are known to respond to flashes of light. Finally, one naval program is attempting to develop a laser system for communications purposes. Therefore, investigations into stimulating bioluminescence by using lasers could affect other strategic naval research.

The laser chosen for experimental use was a pulsed blue-green dye laser with a pulse energy of up to 2 Joules, pulse width of 1 microsec, repetition rate of 1 pulse/sec, beam diameter of 12 mm, and beam divergence of 1 mrad. The dye was Rhodamine 6G, with an optimum lasing wavelength of 586 nm. A gated photomultiplier tube was used to detect the light emission and the dinoflagellate *Pyrocystis lunula*, an organism not known to be stimulated by light, was chosen as the test subject. The laser was pulsed and the photomultiplier tube gated to avoid saturation of the tube by the pulse (Hickman and Lynch, 1981). The experimental arrangement is shown in Figure 4 and the result in Figure 5. As can be seen, a well-defined pulse follows the stimulus. Remaining work involves establishing the threshold and action spectrum, testing other organisms for their response, and testing the effectiveness of other lasers with greater potential for flight than the

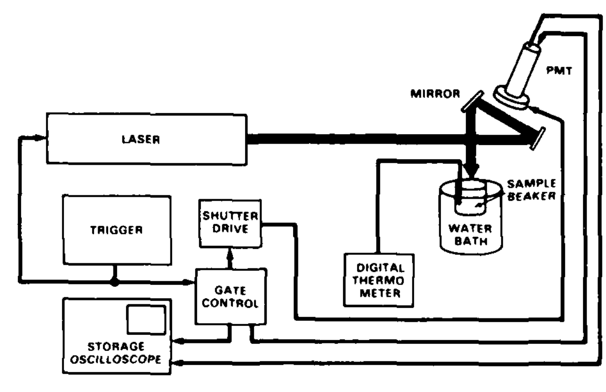

Figure 4. Schematic diagram of laser induced bioluminescence experimental set-up (from Hickman et al., 1983).

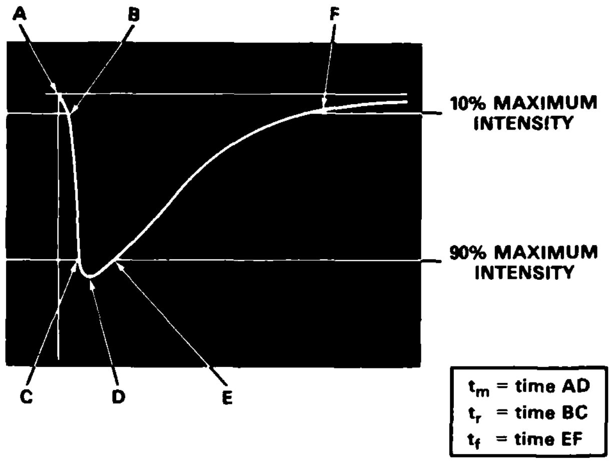

Figure 5. Typical laser-induced bioluminescence response (from Hickman et al., 1983).

dye laser. The laser also has potential as a probe into the microstructure of the dinoflagellate cell because it can be focused to an extremely small diameter. Because the time between the stimulus and the emission maximum is dependent upon the ambient temperature, this stimulation technique may be used to determine water temperature to ±0.5°C (Hickman et al., 1983). Finally, time-gating the response may provide some data on the depth distribution of bioluminescence.

Because dinoflagellates are not known to emit light in response to weak light pulses, it has been suggested that the response to a laser pulse is due, not to the light itself, but to some side effect of the light—most likely a photoacoustic effect. If an intense beam of light strikes water, an acoustic signal is generated. Field reports of bioluminescence stimulated by acoustic signals have been received, but the effect has so far not been duplicated in the laboratory. Visual observation of the bioluminescent response of *P. lunula* to a laser pulse shows that only those organisms directly in the light path are stimulated (Hickman et al., 1984). From measurements of the propagation distance of the stimulus normal to the light beam, it can be calculated that, if a photoacoustic effect is the cause of stimulation, it must have a frequency on the order of 15 to 20 MHz. This corresponds to a wavelength of approximately the same size as the diameter of the dinoflagellates and suggests a resonance effect as the immediate stimulus. This further suggests that other luminous organisms would have their own characteristic resonance frequencies and that the failure of the laboratory experiments to date is due to improperly selecting a test organism for the frequencies used (up to 100 kHz).

An acoustic signal in water is no more than a series of pressure pulses. The results of an experiment to stimulate bioluminescence in *P. lunula* using a small pressure pulse are shown in Figure 6. This work was done with students at the Naval Postgraduate School. Pressure decreases were found to be much more effective than pressure increases. Further work with students at the Naval Academy established that the rate of decrease rather than the magnitude was the stimulus, and a threshold of about 0.25 atm sec^{-1} was established (Holderied, 1984). The same experiments were performed with *Gonyaulax polyedra*, another dinoflagellate with a greatly different morphology. Pressure changes were much less effective on *G. polyedra*, with rates >0.95 atm sec^{-1} required for stimulation, and pressure increases and decreases were almost equally effective (Donaldson et al., 1983). These differences may be used to understand the approximate cause of mechanical stimulation (shear, turbulence, acceleration, velocity, or some other factor), which is presently difficult to determine because of difficulty in designing an experiment that adequately isolates the possible factors.

Chemical quenching

In the laboratory, chemicals are frequently used to stimulate bioluminescence. Conversely, chemicals can be used to quench, wholly or partially, the bioluminescence reaction. It has been hypothesized that bioluminescence generated by moving ships could be masked in this way. To test this hypothesis a methodology to evaluate chemicals for their ability to suppress bioluminescence in a marine environment in a minimal contact time was developed.

The test organism chosen was again *P. lunula*, which is widely distributed in the oceans, produces a large amount

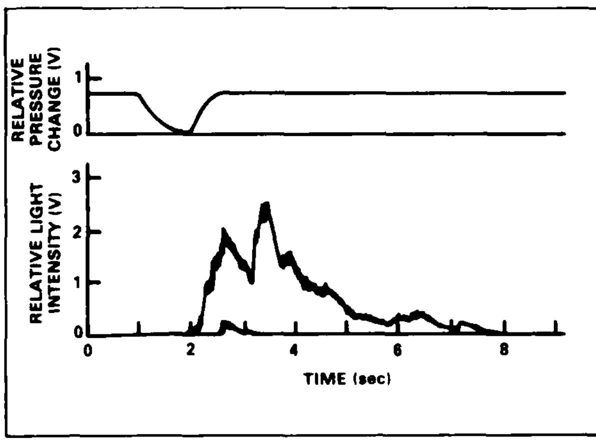

Figure 6. Responses of P. lunula to pressure changes (from Donaldson et al., 1983)

of light upon stimulation in laboratory conditions, is easily handled and maintained, and reacts quickly to a wide variety of chemicals. The assay procedure consists of adding an aliquot of samples to a vial containing a fixed, predetermined number of *P. lunula* cells, stirring vigorously for a short time in a small photometer apparatus, and recording the photomultiplier output with a strip chart recorder set in exponential mode. Quenching of bioluminescence is calculated as light output of the treated vial at a given time divided by light output of one identical control vial (to which an aliquot of sample was not added at the same time) and expressed as percent inhibition.

Using this assay, a number of compounds have been found effective in quenching bioluminescence. Among these is the class of compounds known as mycotoxins or tricothecenes. Produced by molds of the genera *Fusarium* and *Stachybotrys*, common contaminants of stored grains, these compounds are widely believed to be the active components in "yellow rain," the term given to the unknown mixture reputedly used by the Soviets in Southeast Asia in chemical warfare against dissident villages. Some 40 or 50 tricothecenes, differing from one another in structure and toxicity, have been isolated. They act by inhibiting protein synthesis and are difficult to assay by conventional immunological techniques. However, all the tricothecenes tested (obtained through the University of Maryland) exhibited unique quenching kinetics (Fig. 7). Using the bioluminescence assay, the presence of very small quantities of toxin could be established in minutes. Furthermore, the uniqueness of each curve could potentially be used as a diagnostic for each toxin; T-2 toxin, the most toxic of all, could be detected in quantitative as low as 250 nanograms per ml, approximately one order of magnitude lower than the minimum detectable by the immunological assays, which require hours rather than minutes to perform.

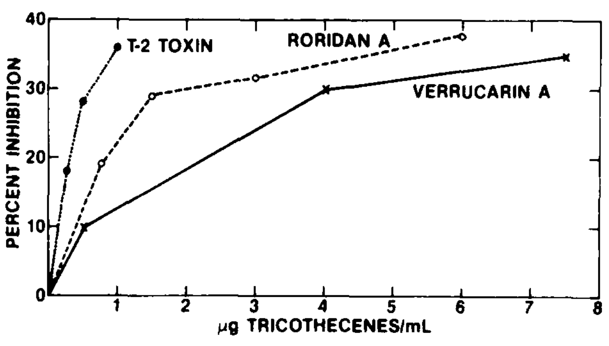

Figure 7. Dose response of selected tricothecenes as measured by bioluminescence assay.

The bioluminescence assay has been used to test the stability of tricothecenes in contact with biological material. Stored in solutions in glass containers, or dry, tricothecenes exhibit great stability and show little or no degradation over periods of weeks. However, when exposed to biologically active material (such as leaves), all traces of activity disappear within a few days, as measured by this assay. These results have been confirmed using gas chromatography. Thus, one cannot expect to find any traces of tricothecenes on vegetation samples removed from Southeast Asia, since weeks will have elapsed between the reported contact with "yellow rain" and the analysis, and the controversy of Soviet use of chemical warfare cannot be resolved by this means.

Another class of compounds active in quenching bioluminescence activity is a group of neoplastic agents. These anticarcinogenic compounds are effective against various forms of cancer, especially leukemia. Preliminary testing has shown that compounds effective against cancer quench bioluminescence, while related ineffective compounds do not. The test compounds have been supplied by the Charles Pfizer Pharmaceutical Company. These results suggest a possible rapid screening technique for anticarcinogenic compounds that will reduce the need for animal testing.

One drawback to the use of the bioluminescence assay for identifying various chemicals is its lack of specificity. While this would not be a problem in screening anticarcinogenic agents, it would be a problem in identifying components of a chemical mixture that might be used in chemical warfare or found in contaminated grain. However, various techniques for separating the components of mixtures exist. One that may be particularly well suited for use with a bioluminescence assay is two-dimensional, thin-layer chromotography (TLC), coupled with bioautography. By the proper choice of eluting solvents, TLC can effectively resolve complex mixtures of closely related compounds by "mapping" their spot positions after treatment. Such mapping is normally a slow procedure because each spot must be analyzed separately. However, the entire map can be analyzed at once using bioluminescence and bioautography. A layer of luminous dinoflagellates can be placed between the TLC map and a plate of film, in direct contact with both, then stimulated. After development, dark spots on the film can be identified by density analysis. These dark spots will correspond to those points where bioluminescence was quenched, and the degree of darkness will correspond to the amount of quenching. Thus, mixtures of compounds can be quickly separated and resolved.

The success of such a technique requires immobilization of the dinoflagellates. NORDA has developed a technique for immobilizing dinoflagellates for up to five weeks on solid medium. This technique, coupled with laser stimulation, has additional applications in basic research on cell structure and response characteristics, because it allows manipulation of individual cells without complex and expensive handling apparatus. It is also potentially possible to substitute luminous bacteria for luminous dinoflagellates. Bacteria can be stored and transported more easily than dinoflagellates because they can be freeze-dried without harm, but the different reactions of different genetic strains to identical stimuli lead to problems with specificity and sensitivity unless several strains are used simultaneously. Although preliminary experiments with bacteria have been successful, much work remains to be done.

Now let us return for a moment to the original impetus for these investigations, namely, suppression of bioluminescence ship signatures through quenching. Although a number of chemicals are effective in various degrees in quenching bioluminescence in dinoflagellates, a literature survey shows that chemicals effective against some organisms will actually stimulate others to increased light production. Since sea water contains a mixture of organisms, it seems unlikely that chemicals will be effective in practical quantities against all organisms present. Thus it seems unlikely that the original goals will be achieved. However, the possibilities of chemical bioluminescence assays, which spun off from the initial work, appear extremely promising and worthwhile.

Instrumentation

One final area of research concerns instrumentation improvements. The present LLLIIs use technology that is more than ten years old. Developments during that time in low-light-level technology have greatly surpassed their capability. Furthermore, the LLLII is degraded by certain environmental conditions, such as bright light sources that saturate the tube in a manner similar to that of the laser already described. Research efforts are underway to overcome these limitations and to determine and utilize the most effective of modern technology for remotely sensing bioluminescence. Efforts are also being made in the area of image processing to enhance the effectiveness of the LLLII in the field. Finally, research is underway to determine the possibility of detecting bioluminescence from space. Two space detection experiments have been mounted by other laboratories, one of which produced an image showing light in the sea for which all explanations other than bioluminescence can be eliminated. However, a lack of sea truth prevents unequivocable identification of the light. A ship/aircraft/shuttle experiment is in the planning stages to resolve the question conclusively.

This research leads directly into NORDA's bioluminescence applications programs.

References

Donaldson, Thomas Q., Stevens P. Tucker, and Richard V. Lynch (1983). *Stimulation of Bioluminescence in Dinoflagellates by Controlled Pressure Changes*. Naval Research Laboratory, Washington, D.C., Report 8772.

Gitel'zon, I. I., R. I. Chumakova, V. S. Filimonov, A. S. Artemkin, and V. F. Schatokhin (1967). Instrumental Bioluminescence Measurements in the Tropical Part of the Pacific. Scientific Report, *Yokosuka City Mus* 13, 6–11.

Hickman, G. Daniel and Richard V. Lynch (1981). Laser-induced Bioluminescence. *Proceedings, SPIE* 288, 263-268.

Hickman, G. Daniel, John A. Edmonds, and Richard V. Lynch (1984). Laser-induced Marine Bioluminescence Measurements and the Potential for Airborne Remote Sensing. *Remote Sensing of the Environment* 15, 77-89.

Hickman, G. Daniel, John A. Edmonds, Robert D. Pike, Nicholas Antonoff, and Richard V. Lynch (1983). Temperature Dependence of Laser-induced Bioluminescence in *Pyrocystis lunula*. *Proceedings, SPIE* 380, 411-414.

Holderied, Kristine (1984). *The Effect of Controlled Pressure Changes on the Stimulation of Bioluminescence in Pyrocystis lunula*. U.S. Naval Academy, Report TSPR-129.

Lynch, Richard V. (1978). *The Occurrence and Distribution of Surface Bioluminescence in the Oceans during 1966 through 1977*. Naval Research Laboratory, Washington, D.C., Report 8210.

Roithmayr, Charles W. (1970). Airborne Low-Light Sensor Detects Luminescing Fish Schools at Night. *Commercial Fisheries Review* 32, 42-51.

Staples, Robert F. (1966). *The Distribution and Characteristics of Surface Bioluminescence in the Oceans*. Naval Oceanographic Office, NSTL, Mississippi, Report TR 184.

Tarasov, N. I. (1956). *Luminescence of the Sea*. Academy of Sciences USSR, Moscow.

Turner, R. J. (1965). *Notes on the Nature and Occurrence of Marine Bioluminescent Phenomena*. National Institute of Oceanography, Internal Report B-4.

Environmental Influences on Cavitation

Dennis M. Lavoie
Oceanography Division

As the technology of acoustic detection and signature identification becomes more sensitive, the cavitation characteristics of submarine propellers increase in importance. Unfortunately for the design engineer, the cavitation characteristics as determined from calculations and from scale model tests do not always seem to hold when the full-scale propeller is put into service.

One clue to the problem is that for any given submarine, propeller cavitation is not a constant but, instead, seems to vary with the water mass in which the submarine is operating. From the data available before this study, it appears that the cavitation of submarine propellers in oligotrophic waters has less variation than in more productive waters. Evidently, some factor or factors in the seawater environment are affecting the way cavitation occurs on the propeller. This phenomenon is not surprising, given the results of previous theoretical and experimental studies of cavitation, but these studies have not definitively identified the cause of cavitation in natural bodies of water. Thus, the question remains, "What factors in the real environment, as opposed to the test tank, are responsible?"

To study the problem in a systematic way (and to eliminate the need for a submarine in the study), a probe has been developed by NORDA that can cause cavitation in seawater reproducibly and under controlled conditions without the complications of wall effects. For the first time, we can measure the cavitation potential of various water masses in situ to determine cavitation variability with depth and with region. With this ability, we can now gather concurrent measurements on environmental parameters that are likely to be influencing the cavitation in some way, i.e., the concentration of microbubbles; the concentration and size distribution of suspended particulates; the concentration of organic material, both dissolved and particulate; the concentration of surfactant compounds; the concentration of dissolved gases, such as oxygen; the amount of biological activity in the water column, which is estimated by the concentration of chlorophyll a; and the temperature and salinity of the water.

Working jointly with the David Taylor Naval Ship Research and Development Center, NORDA is in the process of conducting several cruises to make these measurements in several different oceanic regions, including the Gulf of Mexico; the subtropical, the western, and the northern regions of the North Atlantic; and the Greenland Sea. We are also building a unique data base from which we hope to deduce those environmental factors influencing cavitation in the ocean. With a better understanding of how the environment affects the acoustic character of his craft, the submarine commander may improve his tactical advantage, and the engineer may be able to design quieter, more efficient propellers.

Electronic Environmental Filter

Kuno Smits
Mapping, Charting, and Geodesy Division

Discussion

Geological background noise is the largest environmental noise source affecting Magnetic Anomaly Detection (MAD) operations. The term, "geological noise," is applied to noise that has as its source naturally occurring magnetic anomalies, which are caused by magnetic material present in the earth's crust.

When this noise appears on the MAD trace, the identification of target MAD signals is extremely difficult, if not impossible, in certain antisubmarine warfare operating areas. Therefore, MAD performance is seriously impaired in areas of moderate-to-high geological noise.

The approach taken for reducing the effects of geological noise was to alter the standard MAD bandpass filter so that moderate to high geological noise could be selectively filtered. Our initial efforts were directed toward theoretical studies and computer-generated modeling. Electronic filter specifications were prepared from the mathematical filter models, and 14 electronic units were constructed for installation aboard P-3 aircraft. These units were independently tested against the standard filter by the fleet P-3 community.

At the test conclusion, all the participants involved in the test and evaluation program concluded that the electronic environmental filter (EEF) tests demonstrated that an improved signal-to-noise ratio can be achieved in ASW operating areas where moderate to high geological noise is present. Typical data showed that the standard filter trace was continuously saturated, because the geological background noise was high and no target signals could be identified. In contrast, the EEF trace clearly identified each target signal, since most of the geological noise was suppressed on this trace.

Commander, Patrol Wings Pacific, summarized all the participating squadron reports to the Commander, Naval Air Pacific, and recommended incorporating the EEF in P-3 configuration, and also stated that the EEF would be a valuable asset to ASW capabilities. This recommendation was endorsed by Commander, Naval Air Pacific, and forwarded to the Commander, Naval Air Systems Command for action.

Optical Character Recognition

Charles L. Walker
Mapping, Charting, and Geodesy Division

Abstract

The Optical Character Recognition task developed procedures for the computer recognition of handprinted numerical and alphabetical characters. The effort concentrated on digitizing numeric handprinted soundings on hydrographic smooth sheets. Based on a limited set of individual recognizable numerals scanned from smooth sheets, the algorithms achieved an accuracy of 99.7% and an efficiency of 96%. Preliminary results were obtained for handprinted capital letters.

Introduction

The Optical Character Recognition (OCR) task sponsored by the Defense Mapping Agency investigated and developed techniques to provide for the automatic computer recognition of handprinted mapping and charting symbols, particularly numerals and alphabetic characters. A software system was developed for recognizing numerals at a high degree of accuracy and with high efficiency for individual numerals. Algorithms were incorporated into the Raster Scan Character Recognition (RSCR) System with the objective of digitizing archival hydrographic smooth sheets. Further work was done on recognizing free-form, unconstrained, handprinted alphabetic characters.

Digitizing handprinted bathymetric soundings on hydrographic smooth sheets received the greatest attention and serves as a typical example. A smooth sheet is the basic result of a hydrographic bathymetry survey and consists of numerous corrected soundings written on a particular map projection base with each sounding in its proper geographic (latitude-longitude) position. The digitization of this manuscript must capture the value (depth) of the handprinted soundings, as well as their precise locations. The sounding orientation is arbitrary, and style and authorship can vary.

Smooth sheets have historically contained the source bathymetric data used for producing nautical charts. Typically, these smooth sheets have been produced by the Navy (Naval Oceanographic Office surveys) and given to DMA for chart production in response to Navy requirements for mapping, charting, and geodesy products. Work is underway to completely digitize the data collection process so that bathymetric soundings are produced in a digital form with the smooth sheet being a machine-generated proof sheet. The motivation for digitizing existing archived smooth sheets is to make past nondigital survey data available in a digital hydrographic bathymetry data base.

Analyzing the problem of digitizing handwritten, free form material for DMA led to partitioning the effort into a few distinct tasks: document handling, preprocessing (thinning), recognition, and composition.

Discussion

The document-handling tasks involve optically scanning the original source to produce a digitally coded tape of the black and white areas. This tape is input to the software system, which decodes the tape and isolates connected black areas which are potential characters. Very large and very small areas corresponding to contours on shorelines or to dirt spots are eliminated in this section of the code. The isolated candidate characters are then passed to a preprocessor, which thins the image into a set of connected vector-like points.

The preprocessor or thinning algorithms were found to be crucial for high accuracy and efficiency. The basic model used in recognition was based on the concept that a character is composed of strokes; each stroke is the "centerline" of the pen being used, and that all of the information on the identity of the symbol is contained in the form and relationships of the strokes. Thus, we are led to the concept of a pen model that gives a finite width to the strokes. In common with many other recognition systems, the Medial Axis Transformation (MAT) was

used for thinning to generate stroke information. However, it was discovered that many problems were encountered using the MAT such that a new concept called "unthinnable regions" was developed to extract stroke information. Using the unthinnable regions concept allowed the generation of "stick figures" with few artifacts and even allowed filled in regions of 8s, 6s, 4s, and 9s to be properly thinned.

The features extracted for character recognition were primarily the topological properties of the smoothed stick figures. Basic features are the numbers of segments, numbers of enclosed regions, and numbers and types of branch points. Further measures were made on individual segments by joining the end points with an axis. Various axis crossings, as well as a maxima and minima relative to the axis, were categorized. To analyze the feature measures and to partition the feature space, a binary decision tree was used. Because misidentification is costly (e.g. calling a 9 a 4), it was insufficient merely to partition the feature space and make a hard decision for most characters. Normally, after a character has been classified into only one possible class, further quality control checks are made. If these checks are not passed, the character is rejected and assigned to the unrecognizable class. Efficiency is the measure of the proportion of recognizable characters not rejected. Accuracy is the proportion of the characters not rejected and correctly classified. Based on a limited set of individual recognizable characters scanned from smooth sheets, the algorithms achieved an accuracy of 99.7% and an efficiency of 96%.

A major problem area that arose in correctly identifying soundings on smooth sheets was the occurrence of connected and broken characters. Connected characters occur when two or more adjacent numerals touch. Broken characters occur when one or more strokes do not touch the rest of the characters. A typical example is the numeral 5 in which the top stroke does not join the bottom one. Connected and broken characters are rejected as unrecognizable by the algorithms. Algorithms have been developed to handle broken 5s and a large subset of connected character pairs. To handle the rejected characters, an editor was developed to allow operator interaction to correctly identify rejected characters.

After the majority of characters are classified, the next step in digitizing smooth sheets is to compose the individual characters into words or soundings. This task has been achieved through the simple procedure of making proximity measures on adjacent characters.

Summary

The OCR task has provided a system which can recognize handprinted characters on hydrographic smooth sheets to a high degree of accuracy. After scanning and digitizing the smooth sheet characters are passed through a thinning process. The topological structure of the stick figures resulting from the thinning process are inspected to identify the numeral. An accuracy of 99.7% was achieved.

Further research has been done on incorporating alphabetic handprinted characters into the software system developed for numerals. The initial phases of this effort concentrated on upper-case letters. Most of the preprocessing and feature extraction modules developed for numerals was used. By making changes only to the decision logic we have obtained a high degree of performance.

Future areas of research pointed to by experience using the OCR algorithms include incorporating a control structure that would allow feedback communication among the various modules involved. This improvement would permit the use of context information to enhance performance.

Future research and development work needs to be done in the area of recognizing handprinted alphabetic characters, both capital and lower case, as well as punctuation marks. This would allow handprinted source material from a variety of sources to be digitized. Another area for further research is in the recognition of variable or multifont machine-printed material using techniques developed for handprint recognition.

Map and Chart Formats for a Digital Production Environment

Gail L. Langran
Mapping, Charting, and Geodesy Division

Abstract

Digital technology has introduced new design possibilities for standard topographic, hydrographic, and aeronautical maps and charts. To exploit the benefits offered by computers, current cartographic practices must be reevaluated and, if necessary, tailored to the strengths and weaknesses of digital equipment. Early planning saves time and money when implementing new charting techniques.

Introduction

Mapping is entering a new age. Digitized geographical data, collected and stored in data bases, is a tool for future chart compilation. Computer graphics equipment will free cartographers from drafting tables, and software will perform many mapping tasks without human intervention. Although such technological innovations are used on a largely provisional basis today, the future mapping environment will be entirely digital. Digital terrain elevations, shoreline vectors, bathmetry, and chart feature locations and attributes will be data based for large areas of the world. To make a map or chart, an area's digital data will be compiled, content selected according to scale, symbols assigned interactively and automatically, and a graphic will be generated.

Both hardcopy (paper) and softcopy (digital or video) charts will be utilized, and the media selected according to the user's needs. With communications links, full-color chart facsimiles can be transmitted to distributed sites for timely updates to standard charts or for customized graphics drawn from a central data base. Digital data sets maintained on naval platforms will generate charts in real time, provide responses to interactive queries on chart data, and allow chart and sensor data to be interfaced.

Computer technology will allow the Defense Mapping Agency to support new command, control, communication, and intelligence products and produce today's standard maps and charts more quickly. Users benefit from improved data coverage and currency, as well as from lowered response time. However, digital technology's impact on chart production and use must be fully evaluated. New media, methods, and formats could adversely affect perception of symbol sizes, shapes, and colors, or introduce other ergonomic problems that can lead to mistakes or confusion by chart users. Some design methods used on today's products are difficult to replicate with digital equipment, which delays introducing new technology and adds to its expense.

NORDA, the Navy's lead laboratory in mapping, charting, and geodesy, works with the DMA to exploit computer technology in map and chart generation, thus improving DMA's ability to support military intelligence needs. Because all aspects of chart production and use will be affected by digital equipment, the DMA tasked NORDA in FY84 to study the production and human factors impacts of digital technology. The NORDA study was intended to recommend ways to improve production efficiency and exploit the technological benefits inherent in computer-assisted mapping.

Discussion

Paper chart production

Today's paper charts are compiled and constructed using a mixture of manual and photomechanical methods. Charts are reproduced by passing their production negatives through a five-color printing press. Centralized mass production should continue in the digital age. However, charts will be compiled from digital data bases and their linework, symbols, and areal fills will be generated and applied to film by digital equipment.

Design adaptations are essential for efficient digital mass production. Three problem areas exist.

- Techniques that are relatively simple to render manually may be intractable to perform digitally.
- Digital production equipment has physical limitations that should be accommodated by chart designs to minimize implementation costs.
- Inefficiencies that exist for historical or traditional reasons need to be exorcised.

It is not surprising that many tasks that are easily performed manually are difficult to render using digital equipment, since computer capabilities differ decidedly from those of humans (Table 1). Because the techniques used to compile and symbolize today's maps and charts have evolved to suit human capabilities, in many cases they are difficult or expensive to simulate by computer. Map layout requires a number of subjective or artistic judgments, which can be emulated by using topological data structures and setting spatial parameters according to psychophysical test findings. Geographic knowledge allows cartographers to select the most important features to map for a particular area, but simulating the human process would require extensive data bases, which are difficult to collect and maintain. An alternative is to use mathematical models for feature selection: models of geographic location for topographic maps, models of visual prominence for aeronautical charts, and line-of-sight computations for hydrographic charts.

Table 1. Strengths and weaknesses of computers.

Strengths	Weaknesses
computation	subjective decisions
data processing	knowledge-based decision
consistency	nondiscrete graphic tasks
speed	
precision	

Unless map and chart designs are altered slightly, some digital production equipment must be specially built. This adds considerably to procurement time and expense. The dimensions of the largest aeronautical and navigational charts exceed common scanner and filmwriter format sizes. Reducing chart sizes by as little as half an inch allows procurement of off-the-shelf equipment. The dot densities of the standard line screens and area fills used to produce tints and patterns on maps do not coincide with the fixed scanning densities of filmwriting equipment (Dunn, 1985). New dot patterns can be designed that produce the required number of repeatable intensity levels and are also efficient to generate digitally.

Some traditional cartographic practices are innately inefficient, whether production is digital or manual. Unnecessary detail—features not needed by the users, ornate symbols, or excessive symbol subdivisions—adds to production time and impedes graphic communication (French, 1954; Bowen et al., 1960; Promisel, 1964; Andrews and Ringle, 1964; Mackworth, 1965; Yoeli and Loon, 1972; Dobson, 1980). All content and symbolization should be continuously reviewed to stay abreast of changing needs. One practice that could be eliminated immediately without harm to map readers is the traditional use of type styles to impart qualitative information. Few map readers are capable of decoding information thus encoded, and research has shown that numerous type styles slow the map-reading process (Bartz, 1970; Foster and Kirkland, 1971; Amachree et al., 1977; Phillips et al., 1978).

In the future, paper maps will be printed at distributed sites from transmitted data sets using laser or ink-jet plotters that employ raster treatments to apply color to paper in combinations dictated by software, rather than by hardcopy negatives. Because local graphics may be of lower quality or repeatability, maps must be readable with reduced color constraint or resolution. Simple symbols are crucial for design robustness, since ornate symbols could become unrecognizable if pixels are lost during scanning or transmission.

Softcopy products

Softcopy and hardcopy graphics are perceived differently by humans. Several factors unimportant to hardcopy graphic design influence symbol size perception on softcopy displays. Irradiation (the tendency of a light image on a dark background to appear larger than a dark image on a light background) is stronger when an image transmits, rather than reflects or refracts, light (Greenberg, 1971). Irradiation may cause users to see line widths, symbol sizes, and lettering differently on a CRT than on a paper map. Symbol sizes should be adjusted accordingly, especially when using a black map format (light figure on a dark background). Color, too, affects softcopy symbol size perception, although it affects hardcopy symbol size perception only nominally (Shurtleff, 1980; Dobson, 1983). The accuracy of estimating areas of colored symbols and filled regions on softcopy media varies with the colors of both the target and the background, but the exact nature of the variation is not and may never be known.

True, consistent color reproduction is a particular problem for maps stored on and accessed from optical disks, since video devices and photographic films generally have individual spectral weaknesses that make uniformity

difficult to maintain. Cartographers can do little to prevent these problems, but they can design defensively by using redundant color codes and choosing colors that contrast well with one another.

Resolution for softcopy devices is problematic in two ways. Graphic resolution affects discriminability of symbols. Taylor (1976) found that the high levels of information shown on current paper maps and charts cannot be shown on softcopy displays, in part because of decreased graphic resolution. Data resolution can also be a problem. The scale of a paper chart is controlled by its designer. The scales of softcopy charts can be controlled by their users. Softcopy chart designers must guard against users assuming improved accuracy when they zoom to scales that exceed the source data's resolution. One way to prevent such assumptions is to prevent excessive zooming.

Softcopy charts can be either static or dynamic. Static displays are generated by projecting photographed charts or, more recently, by using optical disks. Film and disk are compact storage media, but they do not provide the benefits of charts generated dynamically from stored data, commonly termed "interactive" or "electronic" charts. The electronic chart will be an important navigation and tactical device for the Navy in the future. The few digital displays planned for naval platforms today are forerunners of powerful information systems that will be possible when digital data and the software to drive it are available.

The simplest electronic charts automate position plotting by displaying a ship's progress in a real time on a softcopy chart display. Ship's position is established by Loran C, GPS, Doppler sonar logs, or automated dead reckoning using signals from the ship's gyrocompasses. Correlating such a display with radar adds considerably to its usefulness, since uncharted features are displayed simultaneously with charted obstacles. Connecting the electronic chart to a collision prevention or automatic steering system, or interfacing the display with real-time sensor data results in a sophisticated electronic navigational system. Commercial vendors are actively pursuing these possibilities in the United States, Canada, and Japan for use on fishing boats, ferries, yachts, cruise ships, and patrol vessels.

Electronic navigation charts are being used in the U.S. by civilians and by the Coast Guard. Although not yet integrated into ship controls, such charts are a boon to navigators. Data for charted features is stored digitally so systems can support such queries as "what color is this buoy?" or "display only lighted buoys." Overlaying the chart onto radar displays allows the movement of other ships to be tracked (Gilman, 1983; Eaton et al., 1983; and Hammer, 1984).

While the electronic chart is generating excitement among seagoers, it is also fostering a number of questions among those who will be called on to support its requirements. Commercial developers are concerned with data sources, data updates, and legal liability, since alterations to the digital data that drives electronic charts are invisible without an established audit trail. Standards for data currency, organization, accuracy, and resolution are sought, as are human factors standards regarding graphic format and user interface. Naval concerns echo those of civilians. The Submarine Advanced Combat System (SubACS) is one of the first Navy systems to approach electronic chart implementation. The SubACS designers have expressed a need for Navy-wide electronic chart standards, particularly for the operator's interface, for feature content and density, and for algorithms to perform the various charting functions (IBM, 1984).

Current progress and future plans

During the first year of this study (FY84), a report (Langran, 1984) was prepared that surveyed the literature of cartographic communication, design, and digital production, and recommended ways for DMA to tailor the designs of its standard maps and charts to the strengths and weaknesses of digital equipment without impacting chart readability. In FY85, an experimental 1:100,000 ground/air product was designed to demonstrate mapping techniques that are efficient to render digitally. A report describing the design rationale will be published in early FY86.

Plans for NORDA to assist DMA in supporting the Navy's electronic chart began in FY85. A survey of the Navy's plans for electronic chart development was incorporated in a Navy-sponsored survey of the digital mapping, charting, and geodesy data needs of planned naval systems. The results of the survey will be published this fiscal year. After gauging the status of naval electronic charting plans, a program to coordinate development, to standardize products, and to supply data can be designed and NORDA's supporting role can be defined.

Conclusions

Computer technology will change the way we use and perceive maps and charts. To exploit technology's potential, current practices must be evaluated for their suitability to a digital environment. Comprehensive digital data bases and improved efficiency will move cartography's focus

away from standardized mass-production, and allow maps and charts to be customized to user needs. More attention will focus on maintaining the chart data and on employing special-purpose formats that optimize the transfer of geographic information from map to map reader.

As applications of digital chart data become more sophisticated, all available data that are tied to geographic locations will be displayable and correctable on demand. Chart use will be incorporated with other planning functions into integrated information processing systems. These innovations are expected, but implementation dates are not yet known. Careful planning today will minimize future problems.

References

Amachree, Tomlinson K. P., Hubertus L. Bloemer, and Bob J. Walter (1977). Typographic Legibility on Maps: A Comparative Study. *Society of University Cartographers Bulletin* 11, 27–39.

Andrews, R. S. and S. Ringle (1964). *Certitude Judgments and Accuracy of Information Assimilation from Visual Displays.* USA PRO Technical Research Note 145.

Bartz, Barbara S. (1970). Experimental Use of the Search Task in an Analysis of Type Legibility in Cartography. *Journal of Typographic Research* 4, Spring, 147–167.

Bowen, H.M., J. Andreas, S. Truax, and J. Orlansky (1960). Optimum Symbols for Radar Displays. *Human Factors* 2, 28–33.

Dobson, Michael W. (1980). The Influence of the Amount of Graphic Information on Visual Matching. *The Cartographic Journal* 17, 26–32.

Dobson, Michael W. (1983). A High Resolution Microcomputer-based Color System Examining the Human Factors Aspect of Cartography in a Real-Time User Environment. *Auto-Carto VI, Proceedings of the International Symposium on Computer-Assisted Cartography*, October, 352–360.

Dunn, S. Thomas (1985). *Filmwriter Interim Report.* Prepared for U.S. Army Corps of Engineers, Engineering Topographic Laboratories. Dunn Technology, Inc., Vista, California. Contract No. DACA 76-84-C-0009, January.

Eaton, R.M., N.M. Anderson, and T.V. Evangelatos (1983). The Electronic Chart. Paper presented at the *Canadian Hydrographic Service Centennial Conference*, Ottawa, April.

Foster, J.J. and W. Kirkland (1971). Experimental Studies in Map Typography. *Bulletin of the Society of University Cartographers* 6, 40–45.

French, Robert J. (1954). Pattern Recognition in the Presence of Visual Noise. *Journal of Experimental Psychology* 47, January, 27–31.

Gilman, David (1983). The Silicon Ship. *Oceanvoice*, July, 9–12.

Greenberg, G.L. (1971). Irradiation Effect on the Perception of Map Symbology. *International Yearbook of Cartography* 11, 120–126.

Hammer, J.L. (1984). The Electronic Chart It's on Our Doorstep. *Sea Technology*, March, 10 15.

IBM, Federal Systems Division (1984). *SubACS Management/Technical Support Documentation Digital Navig.. ion Charts for use in the Submarine Advanced Combat System*. Report 84-E75-003, Manassas, Virginia, February.

Langran, Gail (1984). *Map Design for Computer Processing: Literature Review and DMA Product Critique*. Naval Ocean Research and Development Activity, NSTL, Mississippi, NORDA Report 72.

Mackworth, N.H. (1965). Visual Noise Causes Tunnel Vision. *Psychonomic Science* 3, 67 68.

Phillips, Richard J., Elizabeth Noyes, and R.J. Audley (1978). Searching for Names on Maps. *The Cartographic Journal* 15, December, 72 77.

Promisel, D.M. (1964). Visual Target Location as a Function of Number and Kind of Competing Signals. *Journal of Applied Psychology* 45.

Shurtleff, D.A. (1980). *How to Make Displays Legible*. Human Interface Design, La Mirada, California.

Taylor, Robert M. (1976). *Projected Map Display Legibility: An Evaluation of an Experimental 1:250,000 Topographical Map*. RAF Institute of Aviation Medicine, Farnborough, Hampshire, Report 545, March.

Yoeli, Pinhas and J. Loon (1972). *An Examination of Map Symbols*. Final Technical Report for the European Research Office, U.S. Army, London, England, June.

Airborne Electromagnetic Bathymetry

I. J. Won and K. Smits
Mapping, Charting, and Geodesy Division

Abstract

An experimental airborne electromagnetic (AEM) survey was carried out in the Cape Cod Bay area to investigate the potential of extracting bathymetric information for a shallow ocean. A commercially available Dighem III AEM system was used for the survey without any significant modification. The helicopter-borne system operated at 385 Hz and 7200 Hz, both in a horizontal coplanar configuration. A concurrent ground truth survey included extensive acoustic soundings, as well as spot water conductivity measurements.

Because of a lack of knowledge about the absolute system calibration figures, an acoustic-sounding calibration was made for each flight line using a small portion of AEM data to derive the zero-level signal, amplitude, and phase calibration factors for each coil pair. The interpreted bathymetric profiles show excellent agreement with corresponding acoustic depth profiles up to one (possibly more) skin depth of the source frequency. It is envisioned that with further improvements in hardware and software, the bathymetric resolution may extend beyond the skin depth. AEM data can also produce (as by-products) conductivity profiles of both seawater and bottom sediments that may find potential applications in mine warfare and offshore geotechnical engineering.

Introduction

NORDA has been investigating a possible application of the airborne electromagnetic (AEM) method to bathymetric charting in a shallow ocean. The Navy has a requirement for a cost-effective rapid, airborne, shallow-ocean bathymetric method capable of supplementing or even replacing the traditional shipborne acoustic sounding methods, which are time-consuming and often not suited to shallow coastal areas. Periodical and repetitive bathymetric mapping of heavily trafficked shallow-ocean regions is necessary for monitoring bottom sediment movements, ship lane maintenance, and a variety of geotechnical operations, as well as for routine charting.

Discussion

Test Survey in the Cape Cod Bay

All flights and ground truth surveys were performed during a 3-day period in the test survey area in June 1984 (Fig. 1). The AEM system used was a commercially available Dighem III, described in detail by Fraser (1978, 1979, and 1981). The system was equipped with two horizontal coplanar coil pairs operating at 385 Hz and 7200 Hz. Both pairs had an 8-m coil separation (an additional coaxial coil pair operating at 900 Hz was deactivated due to an electronic malfunction).

The sensor platform, or "bird," towed by a Sikorsky S58T twin-engine helicopter using a 30-m cable, maintained an average altitude range between 40 and 50 m above the sea surface. The aircraft altitude was measured by a radar altimeter (Sperry Model 220 mounted on the aircraft) that had a manufacturer-specified accuracy of 5%. A total of about 200 line-km AEM data consisting of 13 segment profiles was obtained in three separate flights in less than 7 hours. The sampling rate was 1 sec and corresponded to about 50 m along the ground track (about a 3 km/min ground speed). The maximum water depth in the survey area is about 40 m, according to the bathymetric chart (NOAA Chart: 13,246).

The flight plan included data collection before and after each profile at an altitude of about 270 m to calibrate the zero-level signal of the receiver coils. In addition, three

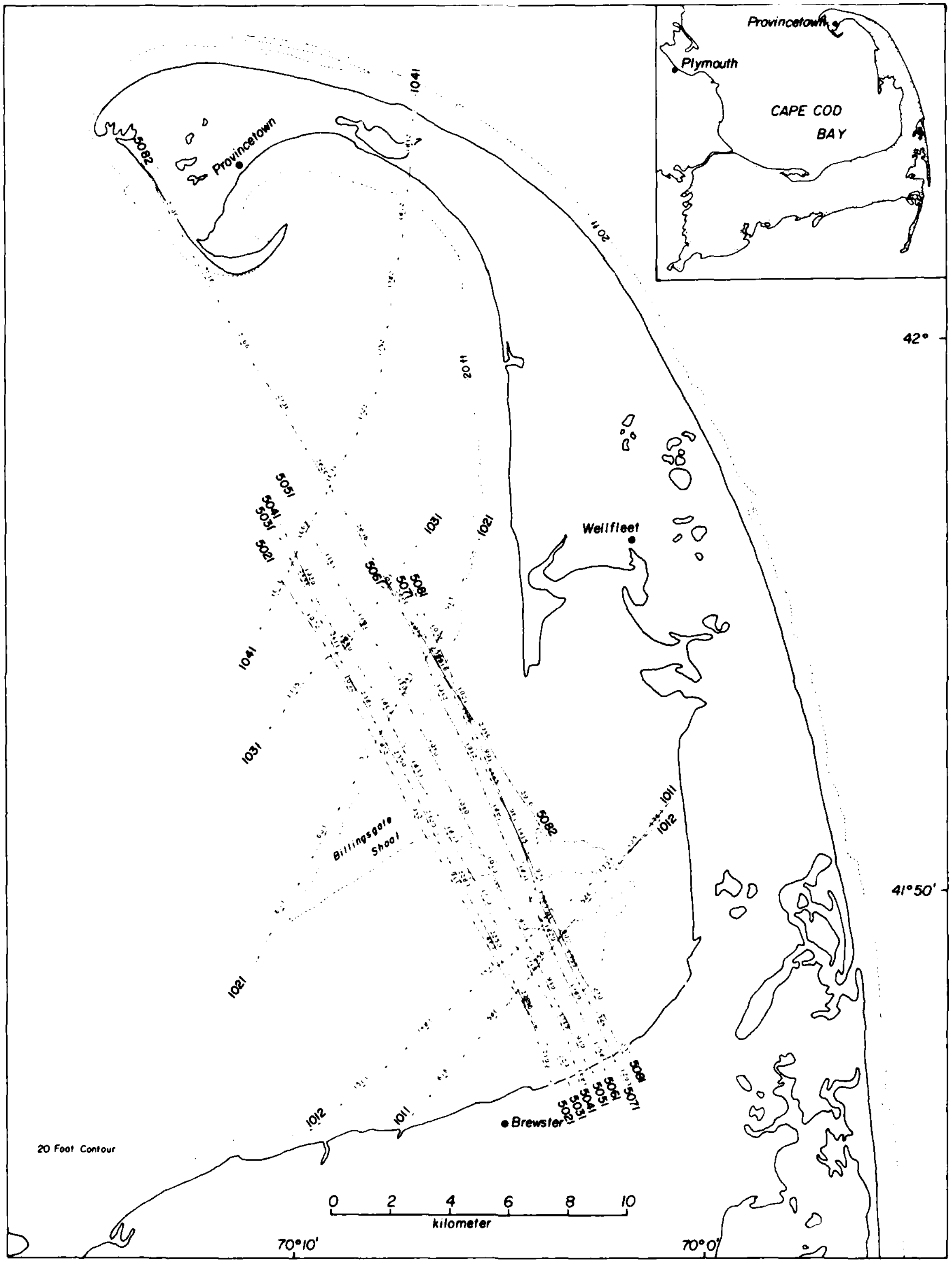

Figure 1. The Cape Cod Bay test area and AEM flight lines. The line numbers are shown on ends of each line.

short calibration flights were made in a location about 15 km east of the Cape, where the bathymetric chart indicated water depth in excess of 60 m. These data were intended to be used for determining the absolute calibration constants for amplitude and phase of each coil pair by assuming that the water body below could be considered a uniform conductive half-space. It turned out, however, that this calibration method is not accurate enough for bathymetric processing. As discussed in Data Calibration, zero-level signal and amplitude/phase calibration constants are derived from a small portion of each actual flight line data.

Figure 2 shows a raw AEM data profile accompanied by a corresponding radar altimeter profile along Line 5021 (see Fig. 1 for location). Clearly, the AEM data are overwhelmingly correlatable with variations in altitude. A very crude indication of water depth may be observed from the ratio of the quadrature component to the inphase component of the 385 Hz data: the ratio increases with a decreasing water depth. Unfortunately, this relationship is highly nonlinear. Even though the aircraft altitude is maintained mostly within a 10-m range (between 40 and 50 m), the corresponding variations of the AEM responses amount to more than 500 parts per million (ppm). Owing to the high water conductivity, errors induced by inaccurate altimetry pose a critical problem. At a 45-m bird altitude, a 1% altitude change at a given water depth of 10 m generates amplitude differences of 22 ppm at 385 Hz and 33 ppm at 7200 Hz. It can also be shown that for a 1-m depth change at the same water depth of 10 m, the predicted amplitude differences amount to only 10 ppm at 385 Hz and 0 ppm at 7200 Hz.

Since the employed radar altimeter has a specified accuracy of 5%, it soon became evident that the radar altitude could not be trusted for the bathymetric processing. Instead, a new algorithm was developed to use the 7200-Hz response to derive the electromagnetic altitude during the inversion process. The new altitudes thus derived show fairly random zero-biased differences (with respect to the radar altitudes) whose RMS amounts to about 2–3%.

Navigation was originally planned to employ a Del Norte navigation system supported by three ground transponders. Excessive distances caused poor reception; therefore, a Loran-C system was installed on site with a makeshift arrangement of a printer that produced coordinates at 5-sec intervals. These coordinates were later interpolated to produce 1-sec interval coordinate data corresponding to the AEM data rate.

A ground truth bathymetric survey concurrent with the AEM flights was carried out using an acoustic depth sounder. A total of about 120 line-km depth profiles was obtained, which covered about 60% of the AEM flight area. Unfortunately, due to many practical reasons, the

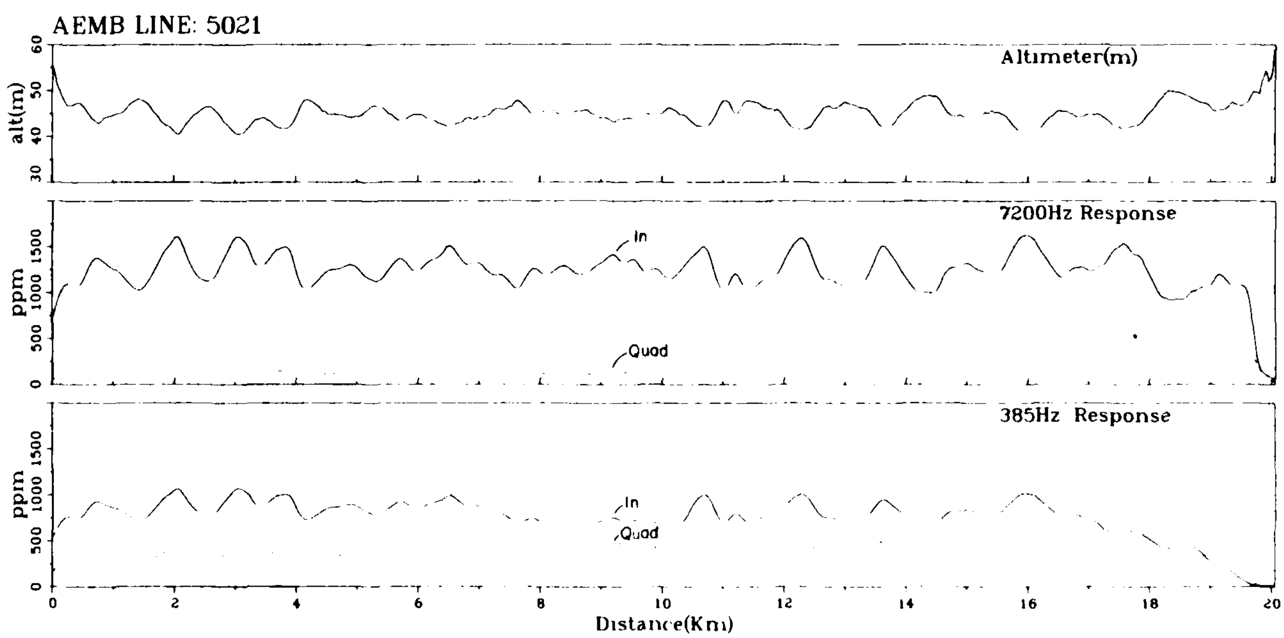

Figure 2. Raw AEM and radar altitude data along Flight Line 5021

flight lines and the ship track did not coincide and were often more than 500 m apart. Therefore, the best available ground truth still reflects another interpolated approximation (unless the bottom topography fluctuates rapidly, the ground truth is considered to be accurate within 1-2 m).

Spot measurements of water conductivity were made at eight different locations along the ship track at a 3-m depth. They ranged between 4.0 mho/m and 4.12 mho/m. While these values may be fairly representative for deep water, there are considerable uncertainties over very shallow water (~ 3 m) where water temperature may rise significantly during the day (particularly during sunny days in June, as in this case). A mere 4°C difference in the water temperature at a given salinity can result in as much as a 10% change in water conductivity. Unfortunately, no ground truth measurements were made during the survey to confirm this possibility.

Interpretation

The high conductivity of seawater (between 3 and 5 mho/m, depending on salinity and temperature with no fresh-water inlets) severely restricts the ability of electromagnetic waves to penetrate the water. Bathymetric range and resolution, therefore, are primarily governed by the source frequency. Figure 3 shows the skin depths in a frequency range between 40 Hz and 40 kHz for assumed water conductivities of 2, 3, 4, and 5 mho/m (skin depth is the ability of electromagnetic waves to penetrate seawater to depths determined by frequency and seawater conductivity).

For the employed frequencies of 385 Hz and 7200 Hz for seawater with a conductivity of 4 mho/m, we may, therefore, expect skin depth of 12.8 and 3.0 m, respectively. From Figure 3 the source frequency obviously should be less than 100 Hz to achieve a depth range of 50 m or more.

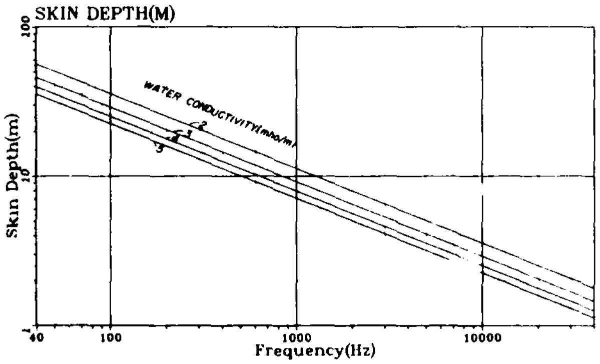

Figure 3. Skin depths as a function of frequency for seawater having a conductivity ranging from 2 mho/m to 5 mho/m.

The Cape Cod test data were initially interpreted and reported by Fraser (1985) using a least-squares algorithm by Anderson (1979). Subsequently, the data were reprocessed at NORDA using a different Marquardt least-squares algorithm, notably Subroutine ZXSSQ, in the IMSL package. The inverted bathymetry in both cases agreed approximately in trends with known bathymetry but showed a considerable static bias that often exceeded 5-10 m. Further careful inspection of the least-squares inversion results leads us to the following conclusions:

- Computer inversion time is unacceptably long: one-point inversion of the two-frequency data consumes from 5 sec to 1 min on a VAX 11/780 computer, even when the water depth is the only sought parameter, while all other parameters are prescribed and fixed.
- AEM response is too sensitive to the bird altitude to accept the specified 5% accuracy of the radar altimeter used for the survey.
- Both the water and the sediment conductivities must be allowed to float, albeit in constrained ranges.

The AEM bathymetric profiles reported here are derived from yet another method: analytic solutions of simultaneous nonlinear equations. At each data location, we have four measured quantities; i.e., inphase and quadrature components at two frequencies. From this data set we derive exact solutions of four parameters: water conductivity, water depth, sediment conductivity, and electromagnetic altitude. When unconstrained, the solutions are exact (since the number of knowns and unknowns is the same), which results in zero residuals regardless of data error. However, severe data error may produce physically unacceptable solutions (e.g., negative depth or conductivities). While least-squares methods (in which the number of knowns is usually much more than that of unknowns) may produce a stable solution set (even though its root-mean-square (rms) error may be high) from a noisy data set, the present analytic approach is understandably sensitive to data error. Under this circumstance, a low-pass filtering of the inverted profile is justifiable to countermeasure the random data errors.

An inversion algorithm using a modified Newton-Raphson method is then applied to the data. Initially, we derive the sensor altitude and water conductivity from the 7200-Hz data and, subsequently, water depth and bottom conductivity from the 385-Hz data. Inversion time for deriving all four parameters amounts to 0.5-2.0 sec on a VAX 11/780 computer. The analytic method, as in the least-squares method, also requires initial guesses

and, to ensure physically acceptable solutions, reasonable solution constraints. The constraints used for the final processing of the Cape Cod data follow.

Water conductivity (σ_1): 3–5 mho/m
Sediment conductivity (σ_2): 0.01–2 mho/m
Water depth (d): 0–50 m
Altitude (b): positive

Spot measurements of water conductivity at a 3-m depth at eight locations ranged from 4.0 to 4.12 mho/m. No bottom sediment conductivity data are available. However, an extensive in situ study of carbonate sediments (Hulbert et al., 1982) off the Florida coast shows a common range of 0.4 mho/m to 1.4 mho/m within the first 5-m depth, decreasing only slightly with increasing depth of burial.

The inversion process is initiated as follows: For the very first point, we prescribed starting values of σ_1 = 4 mho/m, σ_2 = 1 mho/m, d as read from the hydrographic chart, and b as indicated by the radar altimeter. Once the process starts, the solution set at the present location is prescribed as the initial parameters for the next location. Thus, after the first data point of a profile, the interpretation becomes completely autonomous.

We present only the bathymetric results in this article. Note, however, that (1) the derived electromagnetic altitude is well within ± 1 m of the radar altitude (less than the manufacturer-specified 5% error), (2) water conductivity is mainly 4 ± 0.2 mho/m except for very shallow-water regions, and (3) bottom sediment conductivity ranges between 0.5 mho/m and 1.5 mho/m in most profiles.

Results

The interpreted AEM bathymetry for Line 5021 is depicted in Figure 4 (see Fig. 1 for location). The solid line represents the water depth inferred from the AEM data. Solid circles denote the depths determined from acoustic profiles. Depths are computed at approximately 50-m intervals. Small numerals at the bottom are the flight line fiducials that represent every 20th data point. The profile length is about 20 km.

The agreements are excellent up to a water depth corresponding to about one skin depth (12.8 m) of the 385-Hz signal. In fact, the agreements up to this depth are well within the interpolation accuracy of ground truth data. Below the skin depth we notice progressively degrading resolution that results in oscillatory bathymetric profiles.

In essence, the oscillatory behavior is a direct result of the decreasing signal-to-noise ratio with respect to the altitude uncertainty. At a 20-m depth, for instance, the maximum theoretical 385 Hz response (against an infinitely deep water) is expected to be about 10 ppm, while a mere 0.2 m error in altitude will result in the same amount of difference in response. Since the bathymetric errors appear to be random, yet strongly correlated with the aircraft altitude, we tentatively conclude that the error sources are likely related to the altimeter resolution and to such bird attitude uncertainties as pitching and yawing associated with the aircraft altitude variations. The bird attitude can be monitored in the future using inclinometers whose output can be incorporated into the interpretation.

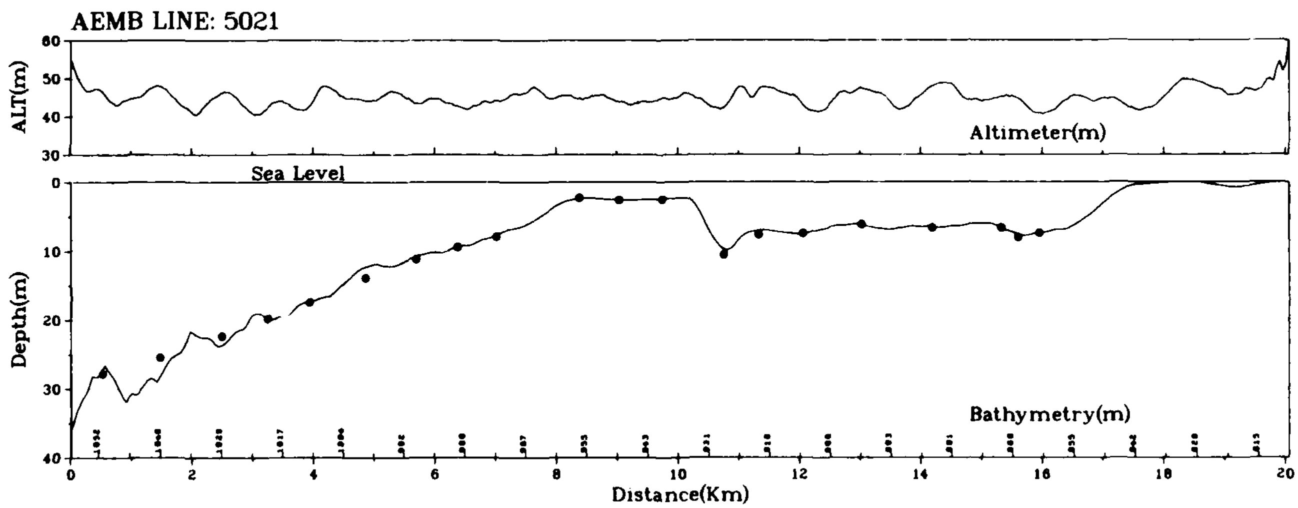

Figure 4. AEM bathymetric profile for Line 5021 after applying an 11-point running average filter. Solid circles represent acoustic depths.

Such an oscillatory behavior can sometimes be suppressed if we use a least-squares inversion method when a sufficient number of redundant measurements is available. The resultant solutions in this case will carry large rms errors, yet may give a deceptively smooth solution profile. The present analytic inversion method produces zero-residual solutions that fit the observed data regardless of the measurement errors. Although the two approaches are equivalent in the sense of error budgeting, the analytic inversion method appears to be superior in field logistics and in computational speed. Figures 5–8 show additional AEM bathymetric profiles produced by the above described procedure.

A composite of seven AEM profiles is shown in Figure 9. We notice striking details of the sea bottom morphology, which show subtle trends and developments of slopes, trenches, and shoals. The fact that each profile is independently derived and yet shows remarkable correlations with neighboring profiles renders further credence to the AEM results.

Conclusions

From our experience through the Cape Cod AEM bathymetry experiment, we summarize some of the error sources that degrade the bathymetric resolution:

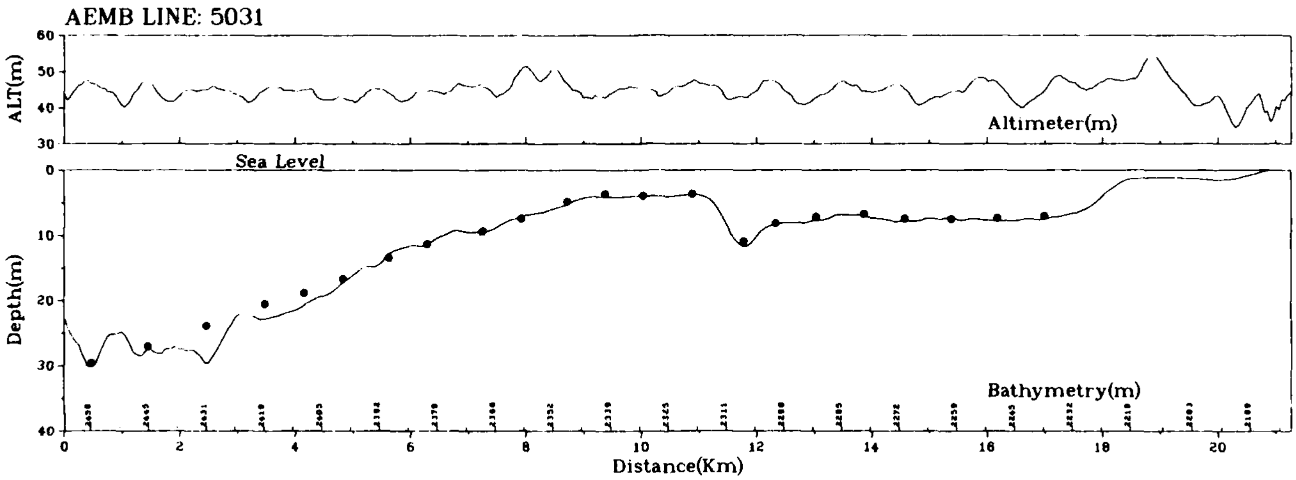

Figure 5. AEM bathymetry profile for Line 5031. Solid circles represent acoustic depths.

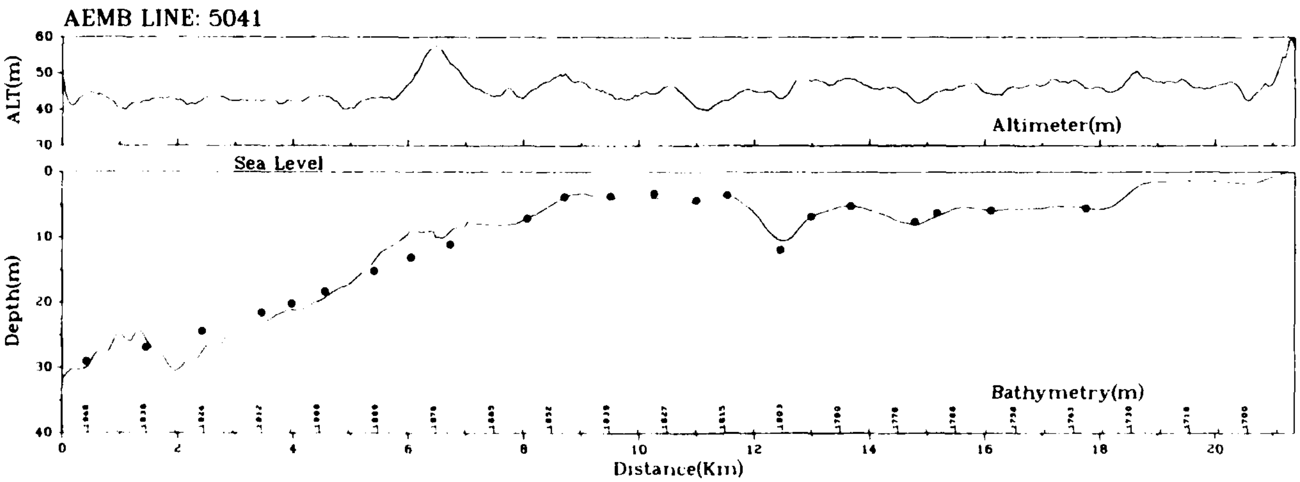

Figure 6. AEM bathymetry profile for Line 5041. Solid circles represent acoustic depths.

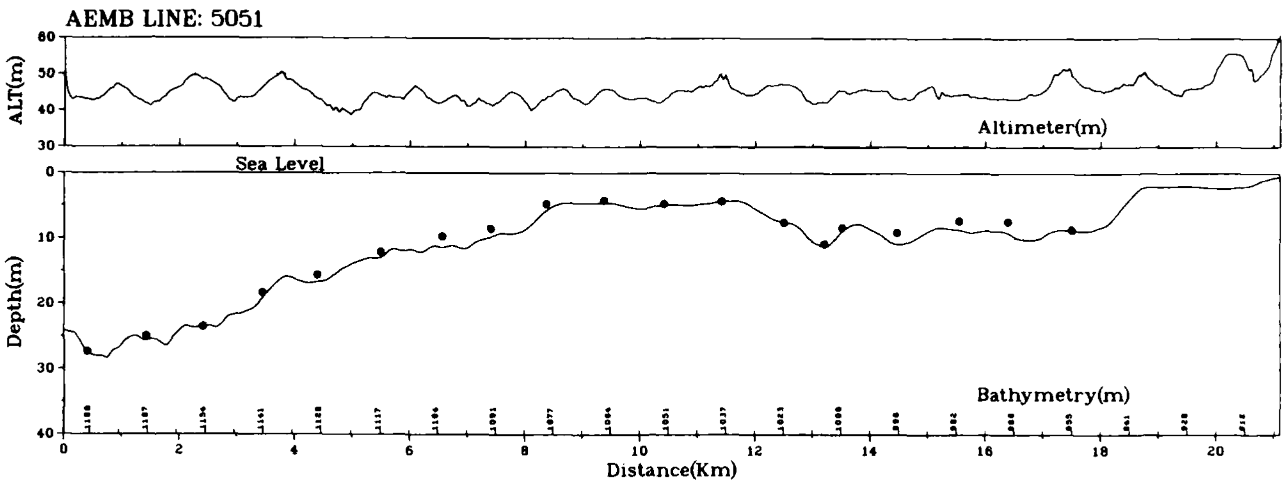

Figure 7. AEM bathymetry profile for Line 5051. Solid circles represent acoustic depths.

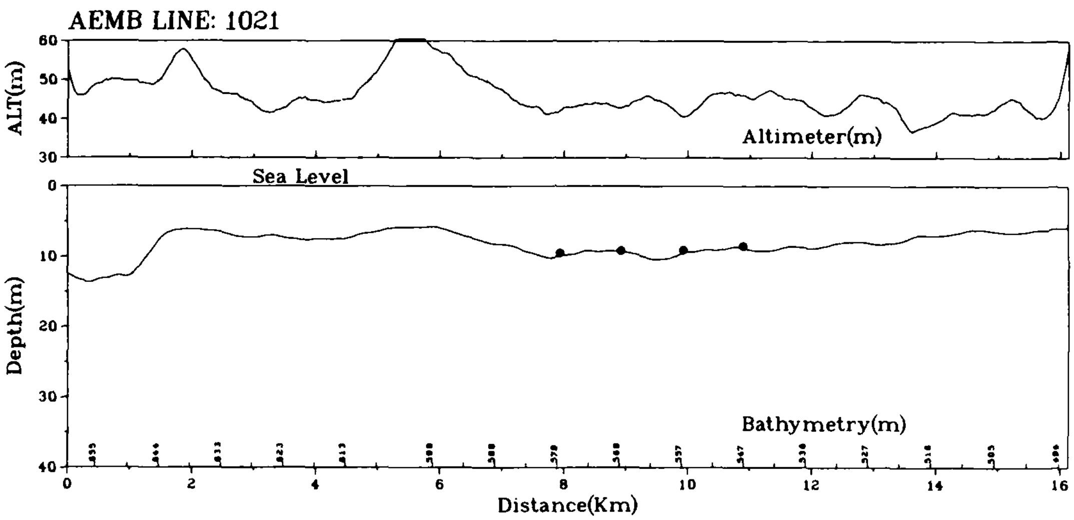

Figure 8. AEM bathymetry profile for Line 2021. Solid circles represent acoustic depths.

- calibration errors—amplitude, phase and zero-level;
- error in the interpretative ocean model, particularly assuming the vertically homogeneous bottom sediment layer;
- altimeter error;
- measurement error due to pitching and yawing of the bird—negligible up to 10° if the bird altitude is 50 m or higher;
- ground truth interpolation error due to noncoincidence of tracks by boats and aircraft;
- electronic measurement noise.

Most of these error sources can be significantly reduced by improving equipment and software interpretation.

We envision that with additional research and development efforts, the AEM method will produce accurate bathymetric charts over a shallow ocean (perhaps up to 100 m in depth). Compared with the traditional acoustic sounding techniques, the AEM method can provide an order-of-magnitude faster survey speed at a reduced cost and thus yield a synoptic knowledge of ocean-bottom topography. With improved interpretation schemes, even a real time data processing appears to be a realizable goal.

In addition, the method has potential applications to remotely measure electrical conductivities of ocean water and bottom sediments. The bottom sediment conductivity, in particular, is closely related to certain mechanical

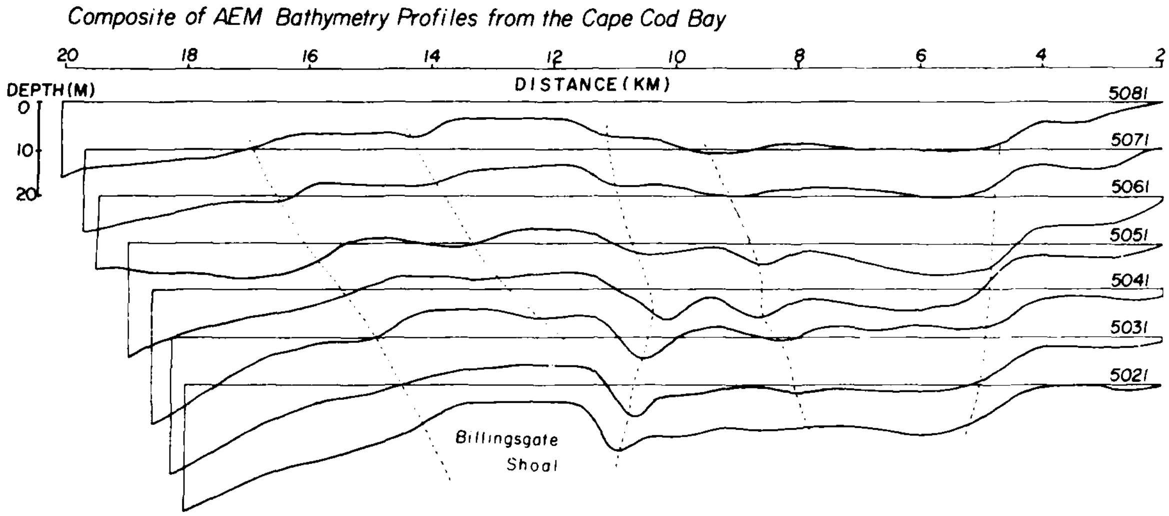

Figure 9. A composite of seven AEM bathymetry profiles from the Cape Cod Bay.

characteristics, such as compaction, porosity, density, and (indirectly perhaps) sediment types, all of which carry broad geotechnical implications for many offshore activities.

References

Anderson, W. L. (1979). *Program MARQLOOPS: Marquardt Inversion of Loop-loop Frequency Soundings*. USGS Open File Report 790240, p. 75.

Fraser, D. C. (1978). Resistivity Mapping with an Airborne Multicoil Electromagnetic System. *Geophysics* 43, 144-172.

Fraser, D. C. (1979). The Multicoil II Airborne Electromagnetic System. *Geophysics* 44, 1367-1394.

Fraser, D. C. (1981). Magnetic Mapping with a Multicoil Airborne Electromagnetic System. *Geophysics* 46, 1579-1593.

Fraser, D. C. (1985). *Airborne Electromagnetic (AEM) Bathymetric Survey and Data Analysis, Cape Cod, Massachusetts Area*. Final Report to NORDA, Contract No: N62306-84-C-0013, Submitted by Carson Geoscience Co. Inc., Perkasie, Pennsylvania, p. 67.

Hulbert, M. H., D. N. Lambert, R. H. Bennett, G. L. Freeland, J. T. Burns, W. B. Sawyer, and P. Field (1982). In Situ Electrical Resistivity Measurements of Calcareous Sediments. *American Society for Testing and Materials*, Special Publication STP 777, 414-428.

Hydrographic Information Handling

Herman J. Byrnes
Mapping, Charting, and Geodesy Division

NORDA conducts research, development, test, and evaluation of systems, equipment, or techniques in the general areas of charting, surveying, photogrammetry, remote sensing, reconnaissance, bathymetry, geophysics, precise positioning, and ocean surveillance in support of the Defense Mapping Agency and the U.S. Navy. NORDA is the primary activity within the Navy conducting research and development in direct support of naval mapping, charting, and geodesy requirements.

Under the above charter, a hydrographic information handling (HIHAN) system is being developed for the Hydrographic Division of the U. S. Naval Oceanographic Office. That office plans and conducts hydrographic surveys in response to charting deficiencies identified by the Defense Mapping Agency. Until recently, surveys have been conducted and the results processed via labor-intensive manual techniques.

The project HIHAN develops the application software that will operate on both shipboard and in-house computers and that will perform automated tasks to assist hydrographers in selecting, merging, and editing hydrographic data; overlaying features and annotations; and calculating, file manipulating, and other processing to produce digital field sheets, smooth sheets, and management accession files. The project is sponsored by the Defense Mapping Agency, since digital smooth sheet products are high on their list of priorities.

The capability resulting from this development is to be used by NAVOCEANO in a production environment. Products generated by the system must have been generated via observable, acceptable hydrographic standards and must be acceptable to DMA and legal entente, consistent with International Hydrographic Organization (IHO) standards. Critical aspects of this software design are that the software must emulate procedure already employed manually and that the hydrographer's decisions must dominate any edit and sounding selection process, even when the user has little computer training.

Since the program was initiated in 1983, interactive data editing and verification system modules to process hydrographic data have been designed and implemented as a system for use onboard NAVOCEANO survey ships; the system acronym is "HPTS," which stands for Hydrographic Post Time System. The HPTS is a basic shipboard capability that is to be expanded both on ship and for base plant processing. The HPTS emerged from implementing modules emulating manual methods. The task level modules are Extract, Thin, Select, Plot Status, Edit, Merge, Plot Track, Plot Soundings, and Contour.

To ensure detection of minimum depth, survey procedure requires NAVOCEANO to collect more soundings than can be plotted on a sheet. The desire of the data processor is to reduce the volume of data requiring full treatment as rapidly as possible. The Extract and Thin modules reduce data volume while satisfying IHO standards. The standards require that shoalest soundings appear at 5.0-mm intervals on the sounding sheet and that the soundings be positioned on the sheet to 1.0-mm accuracy. To ensure that the 1.0 mm accuracy requirement is not violated, the Extract and Thin modules generate a file of maximum and minimum soundings for each time interval not exceeding 1.0 mm of ship "sheet travel," depending on the scale of development. For a scale of development of 1/10,000, a reduction in data volume by 10:1 can be realized; for a 1/50,000 scale, the reduction can be 50:1.

The Select module applies a few rudimentary selection rules that emulate the hydrographer in the selection process and set a status bit that indicates which soundings the computer thinks should be plotted at 5.0-mm intervals on the sheet.

The Status Plot module generates a plotter profile of the 1.0-mm max/min thin depth file so that a hydrographer can evaluate the data in general and, in particular, evaluate the designated sounding selections. The proximity and status of navigation lines of position are also plotted relative to the profile. When the status plot is completed, the hard copy is removed and studied by the hydrographer in preparation for editing. The profile and designated select depths are compared with a hard copy echogram by visual inspection.

The Edit module provides both a video display of the data files and a user-friendly means to change the files by means of a keyboard. The Edit module can select or deselect soundings, insert, change, provide a tabular snapshot of a sequence of observations, or provide a profile of a sequence.

When the editing and sounding selection is complete, the next operation is to merge soundings, positions, and tide information. For each selected sounding a position is computed from interpolated lines of position for the exact time of the sounding. Soundings with computed positions outside the designated survey area are removed from the file. The appropriate tide table versus sounding position and time is consulted and a relevant tide corrector is acquired.

The data files resulting from the merge process are ready for plotting. The Plot Track module provides a sheet showing the actual track of selected segments of track for the ship or launch data actually used. The track is annotated with time date and platform tags. The Plot Sounding module provides a field sheet where soundings values are plotted in their sheet locations.

The contour module provides a quick, first-look set of contours that can be overlaid on the tracksheet or the sounding sheet for evaluation. The contours are generated via a subdivided triangle technique, Delaunay tessellation (Watson, 1982), because the computer capacity is too small to deal with larger data sets, i.e., 20,000 soundings per sheet, and the desire to infer no additional or interpolated soundings as in the result of grid contouring techniques.

Continuing software applications in the HIHAN program will focus on using the computer interactive graphics capability. The primary goal will be to improve the hydrographer's ability to evaluate data and his/her ability to interact with the DMA hydrographic data base. Further efforts will include utilization of Global Positioning System and capabilities to extract hydrographic information from airborne laser systems and multispectral image systems.

References

Watson, D. F. (1982). ACORD: Automatic Contouring of Raw Data. *Computers and Geosciences* 8(1),97-101.

Seafloor Geosciences

Richard H. Bennett and Donald J. Walter
Seafloor Geosciences Division

Abstract

Effective utilization of the sea floor is realized by the Navy as a result of basic and applied geological, geophysical, and geotechnical investigations conducted at NORDA. Major thrusts are directed toward the characterization and quantification of geological materials, structure, morphology, and seafloor processes that provide critical environmental data for naval applications. NORDA's geosciences research supports specific naval requirements in mine and Arctic warfare, acoustic bottom interaction, coastal engineering, mapping, geoacoustic/geophysical modeling, and antisubmarine warfare.

Introduction

Seafloor geosciences research at NORDA provides the Navy with advanced capabilities to describe and model, qualitatively and quantitatively, marine geological environments, sediments, and rocks in terms that relate to Navy systems design, construction, and operations. Effective utilization of the sea floor by the Navy is realized as a result of basic and applied geological, geophysical, and geotechnical investigations that contribute to the fundamental knowledge and understanding of the oceanic crust and overlying sediments. Interdisciplinary research programs are an integral aspect of these activities and are designed to maximize the return on ocean science investment, to optimize the scientific contributions to Navy needs and applications, and to maintain a leading edge in advancing the state of the art in geosciences.

Major thrusts in geosciences are directed toward the characterization and quantification of geological materials, structure, morphology, and seafloor processes in both site-specific and regional areas of Navy interest. Investigations provide critical environmental data, geoacoustic properties, and other seafloor engineering properties (geotechnical data) for naval applications (construction, mines, geoacoustic modeling and prediction). Specific studies involve not only site investigations at sea but also extensive laboratory studies coupled with theory and modeling. From an interdisciplinary studies perspective, the geological inputs provide the descriptive analysis and background of an investigation. Geophysical measurements and remote sensing techniques provide qualitative and quantitative assessment of the seafloor and subseafloor structure and materials, both laterally and vertically. Geotechnical studies provide the quantitative measure, or "ground truth," of the physical, mechanical, and geoacoustic properties of the seafloor and subseafloor geological materials (Fig. 1).

NORDA's geosciences assets and support facilities include such state-of-the-art geophysical instrumentation as multichannel seismic profilers, e.g., Deep Towed Array Geophysical System, Ocean Bottom Seismographs, magnetometers, computer facilites and specialized software; geotechnical in situ (e.g., electrical conductivity, piezometers, geomechanical, and geoacoustical) laboratory instrumentation. Geological facilities include coring and sampling tools and underwater photographic equipment. A high-pressure (69 MPa, 10,000 psi) test and calibration facility is operated routinely by NORDA. Currently, this facility is being used to test and calibrate differential sediment pore water pressure sensors for deep-sea measurements at high pressure (69 MPa).

Discussion

Investigations in geosciences

Geological investigations focus on seafloor processes and sedimentary materials in time and space. Transport and deposition of sediments reflect the geological processes active in submarine environments; these processes are critical to naval activities in such areas as mine burial, high frequency acoustic scattering, and geoacoustic modeling. Bathymetric and geological mapping, as well as

morphological investigations are integral aspects of geological activities in both shallow water and deep ocean environments.

Basic research in geomagnetics is directed toward the study of the geologic history and evolution of the ocean basin. Seismology studies address vital questions regarding acoustic energy propagation and related fine-scale stratigraphy of sediments and crusts. These investigations provide the Navy with fundamental seafloor environmental data for geoacoustic modeling, predictive modeling for remote areas, estimates of bottom and subbottom roughness, scattering, attenuation, estimates of acoustic impedance, reflection coefficients, energy partitioning and other derived geoacoustic parameters. Investigations of fine-scale geoacoustic properties and boundary layer acoustics are critical in assessing the subsurface variability and sediment acoustic velocities in shallow water and in deep ocean environments.

Thrusts in marine geotechnique include the development of in situ probes for measuring the physical and mechanical properties of seafloor sediments. Field and laboratory testing of marine sediments and samples provide the Navy with critical data for engineering applications, geoacoustic modeling, and a variety of seafloor environmental requirements. Testing and evaluation of remote sensing techniques (acoustic and electromagnetic) for determining seafloor sediment properties and identifying marine soil types are ongoing activities because of the pressing requirements for rapid survey systems to meet Navy requirements. Quantitative geotechnical studies provide "ground truth" for the remote sensing systems and are a fundamental basis for evaluating problems in seafloor stability, bearing capacity predictions, mine burial estimates, and the response and behavior of sonar systems.

Mine warfare—Applicable areas of interest to mine burial problems are seafloor mapping of bathymetry and morphology, mapping of seafloor geotechnical properties, seafloor sediment/bottom typing and characterization, bottom roughness measurements, and bottom and subbottom structure determination. These research areas provide information vital to the Mine Counter Measures Program. Specific capabilities include a side-scan sonar laboratory (seafloor mapping, bottom roughness), a geotechnical sediment (soil) properties laboratory (geotechnical properties of the sea floor, bottom typing and characterization), a core laboratory (sediment/bottom typing and characterization, bottom and subbottom structure), and a geophysics laboratory (subbottom structure). An acoustic bottom characterization system (complete with a new instrumentation laboratory) has been recently added.

Arctic warfare research—Subsurface ice characterization in the future will become an important topic of consideration in undersea Arctic warfare. NORDA has the research tools and the expertise to develop a program for investigating the environmental characteristics of Arctic sediments and ice. Ice roughness and structure, as well as stability, are critical factors to be considered by subsurface craft before transiting ice-covered areas. In addition to other subsurface interests, seafloor geotechnical properties and acoustic techniques should be considered with respect to mine burial and bottom-mounted structures.

Acoustic bottom interaction—Acoustics has developed to the point where it is one of the most important considerations in undersea warfare. Methods have been

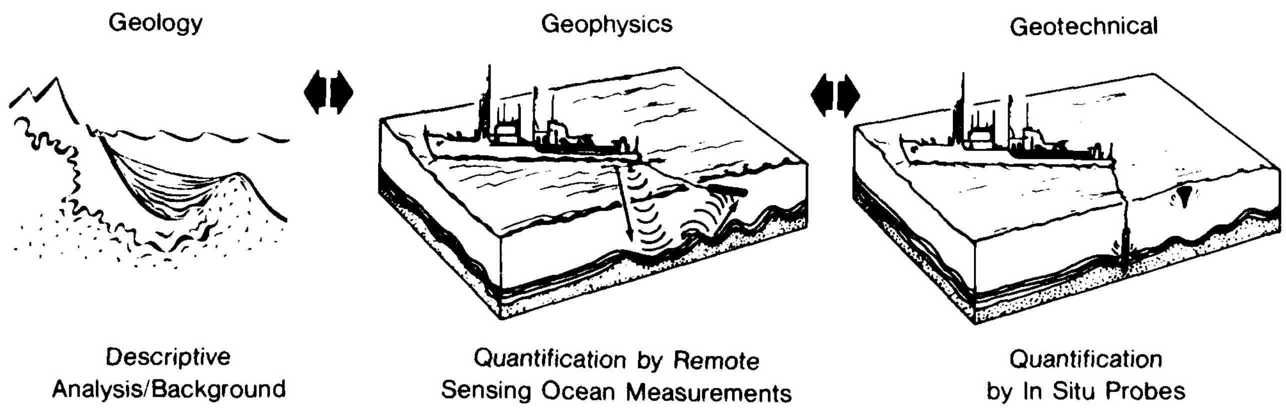

Figure 1. A general view of individual research efforts that contribute to interdisciplinary studies.

developed to adequately detect and track enemy sea craft (surface and subsurface) almost anywhere in the world's oceans. However, with the development of new technology for acoustically quiet craft (especially subsurface) it becomes inherently more imperative to develop techniques to detect or predict acoustic transmissions from quieter sources. Theoretical studies have been completed and models developed that predict acoustic wave behavior in the ocean and on the sea floor; however, these techniques take into account only a "theoretical" or "simple" environment. Future models must begin to account for the real-earth environment; that is, measurements must be made of seafloor and subseafloor properties and their variability on the transmission of sound through the geological materials.

NORDA has devoted a considerable effort during the last few years, and will devote an increasing effort in the coming years, to applying seafloor and subseafloor research to acoustical problems. Beginning with sediment and bottom characterization (e.g., roughness and morphological features) and advancing through the geotechnical realm into the geophysical structure of the subbottom, NORDA has conducted significant studies in terms of geological, geotechnical, and geophysical enhancement of present acoustic models of sound propagation through the bottom. The development of state-of-the-art instrumentation related to acoustic behavior of geological materials is an integral aspect of this research.

Coastal engineering—The Navy has always been interested in coastal processes. In conventional areas, successful amphibious landings require a significant amount of personnel and materials. To accomplish these missions, the shallow (beach front) bottom structure must be capable of supporting first the equipment, then the required personnel. Methods are needed to rapidly characterize and analyze near-shore bottom environments. Geological and geotechnical methods developed by NORDA are used to investigate and characterize the bottom from both a mapping and a surficial structure point of view. Geotechnical probes have been developed and tested to determine in situ physical and mechanical properties of the sea floor.

A joint program with Sandia National Laboratories has been underway for a number of years. This program has investigated seafloor stability requirements for deep-sea nuclear waste burial. Technology developed during this research is now being applied to naval coastal engineering and geoacoustic requirements.

Seafloor mapping—On-scene Commanders, especially while operating in coastal areas (on the continental shelf), must have an accurate "picture" of the sea floor. Seafloor mapping and characterization have been accomplished by NORDA using acoustical methods. Researchers utilize advanced seafloor imaging technologies that contribute to the development of new systems currently evolving. One such system is the Sea MARC IV acoustic mapping system being developed in cooperation with Texas A&M University. These capabilities provide the Navy and the scientific community with new dimensions in seafloor mapping and acoustic signal processing.

Summary

Seafloor geosciences researchers are now able to answer many questions pertinent to naval environmental problems of the sea floor and subseafloor regions. Such areas as mine warfare, Arctic warfare, acoustic bottom interaction, coastal engineering, seafloor mapping, geoacoustic/geophysical modeling, and submarine detection require seafloor environmental data for concise predictions of conditions on and under the sea floor.

Marine Geological Studies, Data Resources, and Archives

Julius Egloff
Seafloor Geosciences Division

Abstract

Specialized marine geological data, listed by oceanic regions and principal investigators are available within NORDA. Geological data holdings and related sources are represented by the geographic and technologic subjects of the numerous papers produced by NORDA. Deep-sea sediment cores and dredged oceanic rock samples, together with seismic reflection, 3.5 kHz bathymetry, and computerized data bases, combine to form a unique research archive within NORDA. This archive serves Navy needs and is open to scientists of every discipline.

Introduction

NORDA inherited a wealth of significant data and experience from the divisions of previous parent organizations. Regional studies carried out by NORDA geologists in its formative years have been enhanced by information gained from recently completed multipurpose, multisponsor Navy projects. Additional excellent marine geological data have been gathered from NORDA-sponsored research cruises during the last decade.

Discussion

The majority of the shipborne seismic reflection and 3.5 kHz bathymetric profiling, magnetic surveys, photography, and sediment core and rock sampling of the sea floor have been collected in the following regions (see Fig. 1):

- Northern North Atlantic, southeastern North Atlantic, Bermuda Rise, U. S. continental margin, Caribbean Sea and Gulf of Mexico, and central South Atlantic.
- North Pacific in the vicinity of Panama, the Galapagos, East Pacific Rise, northeastern Pacific, west-northwestern Pacific, and east-west transits from Hawaii.
- Indian Ocean between the Ninety-East Ridge and Wharton Basin, from Australia to Java and Singapore, including the Banda and Timor Seas.
- U. S. coastal waters, bays and harbors of Navy interest.

In addition to original data that have direct applications to future projects at NORDA, regional studies with related base maps, reports, computerized data files, and bibliographical materials are held in-house. A listing of NORDA geology publications by author may be requested, or a listing of papers and holdings by regional interest is available on request. Several less well-known previous efforts, which may not have been fully published, may be of interest. Examples of regional significant basic analysis (with geological/geophysical study parameters emphasized) are listed.

- North Pacific Ocean/Evaluation of Seamount Occurrence: by study of water depth, topographic relief, age of crust, proximity to known relief, spread of shiptrack control, and theoretical considerations.
- North Atlantic Ocean/Evaluation of Seamount Occurrence: by study of water depth, topographic relief, age of crust, proximity to known relief, spread of shiptrack control, and theoretical considerations.
- Northeast Pacific/Sediment Thickness Compilation: involves digitization of seismic sections and isopach maps, standard Navy ocean area NP-9.
- Equatorial Eastern Pacific/Earthquake, volcano, and bathymetric geologic data correlations, emphasizes regional plate tectonics.
- Eastern South Pacific/Geophysical studies of the eastern margin of the plate.
- Central North Atlantic/Geophysical Studies of the Mid-Atlantic Ridge crest, including morphology, composition (petrochemistry), crustal thickness, etc.
- South Atlantic Ocean/Basin evaluation, preliminary data compilation, bibliography, seismic and 3.5 kHz

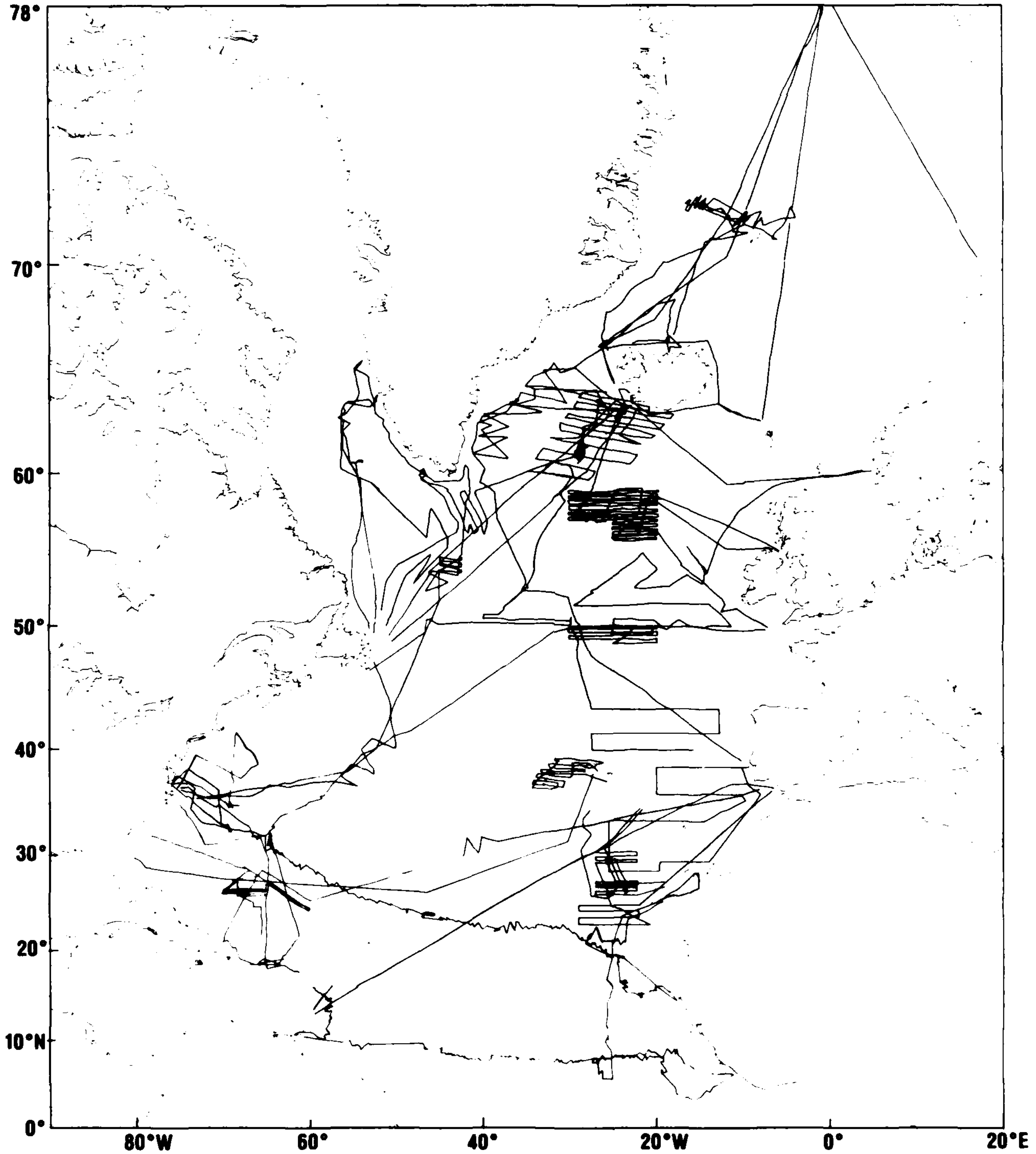

Figure 1. Seafloor survey regions.

profiling, magnetic surveys, bottom photography, geological sampling.

- Caribbean Sea/geological and geophysical data synthesis of data to produce a set of maps, and study of many specific features of seabed, sediments, and crust; includes geological/geophysical/geotechnical data off northern and western margin of St. Croix.
- U. S. Coastal Waters/Side-scan sonar and related sedimentology studies.
- Western Atlantic and Eastern Pacific/Evaluation of selected seamounts.
- Eastern coast of U.S./Mid-Atlantic States offshore/Wilmington Canyon and vicinity.

Several studies are available as larger scale sets of graphics and maps, and computer listed data. Seismic reflection profiles over most of the regions listed above have been analyzed and described, at least preliminarily, and most are available on microfilm from the National Geophysical Data Center, Boulder, Colorado 80303. Most original records are retained by NORDA for future analysis and as a reference library.

Graphics showing the distribution of shiptrack control for most surveys are available from the National Geophysical Data Center or from NORDA. Data are identified by ship, year, and region.

Quality of survey data

In the early 1970s, single-channel seismic reflection data were recorded on Raytheon Precision Seismic Recorders. These data are still some of the cleanest, sharpest seismic records available for the northern North Atlantic—several are with airgun sources and most are with 33,000 or 66,000 joule sparker sources. Later data are clear in less stormy conditions in mid-latitudes and equatorial waters and were recorded on Raytheon UGR. Navigational control was usually by satellite, except for selected offshore areas where radio control was used (Raydist, Decca, and radar). In higher latitudes the satellite navigation was extremely accurate and allowed detailed surveys of smaller geologic features. Magnetic data utilizing Varian or similar proton precession sensors were taken as a standard practice on most cruises. Gravity data were acquired occasionally but were limited in extent because of acceleration problems on the small ships.

Possibly the most extensive high-quality 3.5 kHz shallow seismic profiles within the Navy, next to those generated as a standard practice by the Naval Oceanographic Office, are archived at NORDA. These data represent most of the regions previously listed in which NORDA researchers worked.

Sediment samples and dredged rock collection

Sediment cores from all oceans investigated are kept as a reference sample collection in NORDA's Core Repository, along with an extensive dredged rock collection. The cores were taken mainly in deep ocean basins and the dredged rock samples were taken principally from the mid-ocean near hot-spot-related island groups and from isolated seamounts. This set of seamount rock collections is unique in the U. S.

Core and dredged rock samples date from the late 1960s to the present. Mineral and sediment properties studies have been run on selected cores and rocks; these cores are available for more detailed studies. Partial lists and subsamples have been extracted for detailed studies by academia and institutions. These samples were formerly used to support thesis research and scientific investigations, as well as Navy requirements for seafloor engineering and acoustic applications. Manganese samples and other data from these rock samples are held by the U. S. Geological Survey. Smithsonian Institution scientists have subsampled the volcanic glass and fresh basalt. A few magnetic properties studies were done with selected samples of basalts from around Iceland and the East Pacific Rise.

Questions by interested scientists regarding NORDA-held data bases and samples are invited.

Marine Geology: Research and Support in Naval Ocean Science

Frederick A. Bowles and Peter Fleischer
Seafloor Geosciences Division

Abstract

The behavior of naval systems is significantly influenced by seafloor characteristics; thus, the Navy must continually improve its understanding of these aspects of the ocean environment. At NORDA, marine geologic investigations address both shallow- and deep-water environmental problems as they relate to Navy needs. Regional investigations are often multidisciplinary and are designed to enhance the Navy's fundamental knowledge of the geology of the deep ocean basins. Site-specific and shallow-water investigations are generally more directed because they usually support applied Navy programs relating to acoustics or engineering. NORDA is developing a strong survey capability using undersea remote sensing systems that provide acoustic imaging of the sea floor for detailed geological investigations.

Introduction

Geology studies are concerned with such matters as the earth's origin, composition, history, morphology, and processes that shape it or have shaped it. Past interest focused primarily on the continents and ignored the major part of the earth, which lies beneath the oceans. Marine geology is the study of this submerged area and, until recently, it was the least-developed branch of the geological sciences. Interest in marine geology has grown enormously since World War II. The great breakthrough in knowledge of the deep sea floor has come primarily from research conducted by academic oceanographic institutions and subsidized by grants from the U. S. Navy and the National Science Foundation.

The continuing evolution and development of naval equipment and systems require a continual advance in understanding the vast ocean environment in which the Navy operates. It is becoming increasingly more apparent that seafloor characteristics significantly influence the behavior of Navy systems. Bottom geometry and sediment type/structure, for example, affect acoustic reflectivity; sediment dynamics and seafloor properties affect the choice of seafloor installation sites of cable routes. Topography can be used in subsurface navigation or may represent a navigational hazard. Improvement of the Navy's operational and defense capabilities is dependent on developing a thorough understanding of the physical characteristics of ocean basins, as well as the processes that form and continue to shape them.

Within the naval laboratory structure, NORDA addresses the marine geological environment as it relates to Navy needs. Marine geologic investigations of coastal and deep-ocean environments are directed toward the fundamental understanding of sedimentology, morphology, acoustic stratigraphy, seafloor processes, and environmental parameters. Field and laboratory techniques are used to improve the resolution of geological parameters. Regional and site-specific studies are designed to provide descriptions of geological environments for high-frequency acoustics, mine countermeasures, bottom installations, and to develop state-of-the-art predictive modeling.

Discussion

Sediment patterns and deep ocean circulation

This research represents a composite approach to studying seafloor environments and abyssal water mass circulations by understanding sediment distribution, biostratigraphy, paleoclimatology, bedforms, sediment composition, sediment acoustics, and acoustic stratigraphy. Knowing

how water circulation affects sediment patterns and seafloor geometry, and also how the sedimentary environment and processes affect water circulation, give data we can use to predict microtopography and acoustic responses of the bottom as a function of geographic area. Research has primarily concentrated on analyzing geological and geophysical data collected in the North Atlantic Ocean, Indian Ocean, Caribbean Sea, and the Gulf of Mexico. Seismic reflection and bathymetric data have been used to define the stratigraphic and sedimentation history in the western North Atlantic (Bermuda Rise) and the eastern Indian Ocean (Nicobar Fan), and to delineate the bottom current flow pattern on the south flank of the Iceland-Faeroe Ridge and Northeast Atlantic Basin. These and similar studies provide valuable environmental data bases (sediment thickness and bathymetric maps) that can be applied to bottom-related Navy activities. Sediment thickness (Fig. 1), for example, is important in environmental acoustic modeling for the Fleet (Bottom Loss Upgrade Program and research support for geoacoustic models). Geoacoustic models simulate the real sea floor in terms of sediment thickness, layering, physical properties, and velocities, and are used by the Navy in acoustic-related activities. These models are basic to underwater acoustics and are useful in guiding theoretical studies, reconciling field experiments with theory, or predicting the effects of the sea floor for experimental design. Sediment core data, echo-sounder profiles, seismic reflection profiles, etc., permit geological province boundaries to be defined within which geoacoustic models can be applied. Such data is also significant in acoustic scattering experiments, blockage of sound propagation (obstructions), and deployment of bottom-mounted equipment.

In addition tc supporting Navy needs, marine geological investigations have also resulted in scientific contributions. Investigations in the Caribbean Sea/Gulf of Mexico region, for example, have led to positively identifying the Orinoco River as a source area and to developing sediment transport models that explain the spatial and temporal input of Orinoco/Amazon River sediments to the eastern Caribbean. Models for the post-Miocene evolution of the northwest Caribbean have been postulated and refined. Stratigraphy and paleoenvironment investigations of carbonate sediments on the Florida escarpment have revealed a history of Late Cretaceous and Cenozoic erosion and subsidence.

South Atlantic Geocorridor

The Navy faces increasing responsibilities in distant geographic areas that are potentially strategic and where current knowledge of the environment is limited. The South Atlantic Geocorridor Project (Fig. 2) is designed to provide a systematic approach toward gaining increased understanding in such an area. Recent interest in the South Atlantic is based on a concern for protecting and monitoring shipping routes for strategic supplies. One of the first steps in determining the best, most effective approach for conducting surveillance is to define the acoustically relevant environmental characteristics of an ocean basin. Ultimately, the optimum performance of surveillance systems will depend, in part, on a quality environmental data base. From a scientific point of view, our current understanding of the South Atlantic is extremely deficient. Knowledge of the tectonic history, structural framework, sedimentation, stratigraphy, sediment dispersal and related process, etc., is inadequate. Suitable environmental data bases do not exist. A major field program is presently underway to collect baseline geophysical and sedimentological data from the South Atlantic to develop a better understanding of tectonic and sedimentation patterns and their influence on the geoacoustic environment in that region.

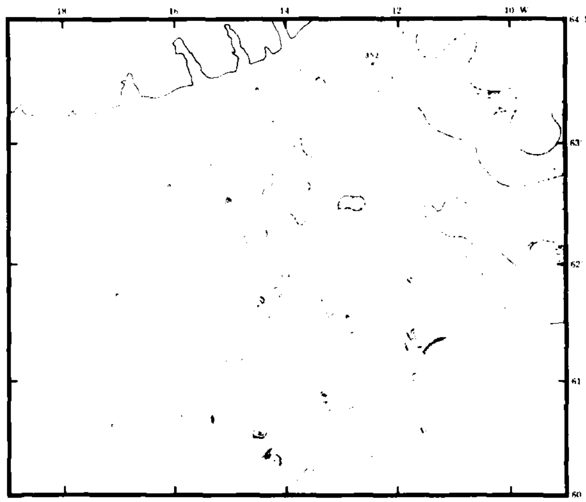

Figure 1. Sediment isopach map of south flank and crestal area of Iceland-Faeroe Ridge and adjacent Hatton Drift area. Contour interval is 0.1 sec. Sediment thickness was read every 15 min, or about every 2 km. Stippling indicates areas of little or no sediment. Dashed contours indicate uncertainty in the position of the contours due to lack of data. Question marks indicate area of uncertain sediment thickness because acoustic basement reflector is not visible in seismic reflection profiles.

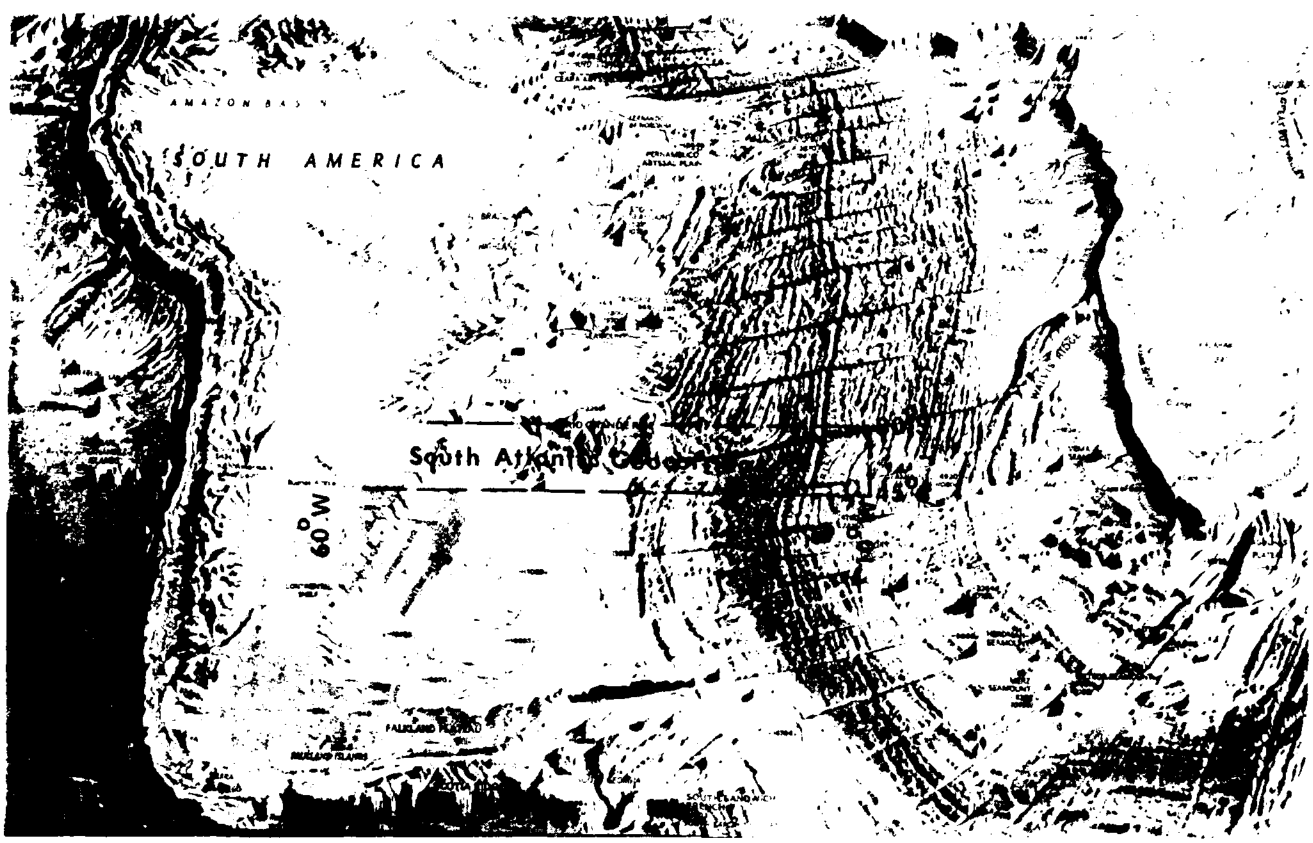

Figure 2. Physiographic map showing location of corridor (30°S-45°S, 10°W-60°W).

Site surveys and regional assessments

Geologic/geoacoustic assessments of specific areas and site-specific surveys are among the principal means by which marine geology directly benefits the Navy.

A major environmental assessment of the northwest Pacific was completed by NORDA in support of the Marine Seismic System (MSS) Project funded by the Defense Advanced Research Projects Agency. The thrust of this program was the use of marine borehole instruments to monitor nuclear testing. The report presents comprehensive data compilations to aid in planning and site selection for the MSS. Data were compiled for two geographic regions—the northwest Pacific (40°-56°N, 145°-170°E) and the Kurile-Kamchatka earthquake region. Included for the northwest Pacific were cultural, meteorological, oceanographic, geological, geophysical, and seismological data to define the environment in which the MSS would operate. Two MSS site areas were proposed, primarily for their advantageous local geology.

Often, detailed geophysical and geological data collection are needed to assess an area properly. NORDA geologists, for example, have conducted four surveys in the St. Croix area. During these investigations, precision bathymetric profiling, seismic reflection profiling, dredging, coring, geotechnical testing, and photographic operations were conducted. In addition to practical application for the Navy, the St. Croix surveys gave NORDA geologists the opportunity to address more fundamental scientific questions, such as the age of the opening of the Virgin Island Trough and the characteristics of the carbonate sediments and their physical properties.

A better knowledge of the seafloor characteristics that form the north and west margins of St. Croix, and in the Virgin Island Trough, is essential to long-range planning of Navy activities for the area. Such information is necessary to locate optimal sites for seafloor installations, determine cable routes, and specify requirements for protecting and stabilizing cables and other equipment. Two

surveys were directly related to planned expansions of the St. Croix tracking range located at the western end of St. Croix Island.

The Jordan Basin (Gulf of Maine) represents a similar situation, where geological/geophysical/geotechnical techniques were directed toward more applied Navy needs—specifically, to provide seafloor environmental support for shallow-water ASW acoustic experiments. Relevant geological information was collected in conjunction with the shallow-water acoustic experiment. The analysis and interpretation of geologic samples and data were intended to address two basic factors affecting acoustic bottom interaction in the experiment: the significant characteristics of the bottom in terms of such parameters as sediment type, sound velocity, and porosity; and the areal and vertical variation of these parameters within the experiment sites.

Geologic mapping

The conventional surface ship echo-sounder has been the standard approach to distinguishing and mapping the topographic features of the sea floor. Even in the most precise and detailed bathymetric surveys, however, contours must be extrapolated between ship survey lines, which leads to questions concerning the actual sea floor. Moreover, the shapes of contours have been used to infer the nature of the processes that create seafloor relief. These inferences have not always been accurate.

The technique and philosophy of seafloor mapping has changed considerably in recent years with the development and improvement of new undersea remote sensing systems that provide acoustic imaging of the sea floor. Side-scan sonar imaging systems are readily available to marine geologists for studying the details of the sea floor and shallow subsurface. These instruments, coupled to modern electronic navigation equipment, have opened a new era of geological understanding of shallow- and deep-water environments. Standard methods of direct seafloor sampling (gravity piston coring, grab sampling, and dredging) now provide better data because we are now able to understand the seafloor features from which they are selected. These methods of both remote and direct data collection are employed to develop an understanding of seafloor environments not previously possible.

NORDA's ability to obtain detail and "big-picture geology" of the sea floor will improve significantly with the development of Sea MARC IV (Fig. 3). This is the latest member in a family of instrumentation called the Sea Mapping and Remote Characterization system. These side-scan systems allow geologic mapping in water depths of 50–5000 m with a single system and a minimum of ship time in the survey area. The various Sea MARC systems differ primarily in the operational frequency of their mapping sonars and their relative modes of operation (e.g., slow, deep towing versus more rapid, shallow towing). Sea MARC IV is being developed by NORDA, Texas A&M University, and Lamont-Doherty Geological Observatory as a portable, state-of-the-art system. It will be an integrated towed system that will simultaneously provide quantified acoustic backscatter images, swath bathymetry, and echosounding over a wide range of towing altitudes, swath widths, and water depths.

Remote characterization is a cost-effective way to map the sea floor and to increase our understanding of geologic processes and bottom morphology. With this technology, a large volume of information can be gathered during cruises. The nature of Sea MARC IV data is such that bottom backscatter can be quantified and correlated with geologic features on a detailed scale. Thus, geologic/acoustic models can be enhanced on the basis of a single, routine survey. These models, in turn, will lead to a vital predictive capability for critical Navy areas.

Shallow-water geology

In general, the acoustic characteristics of signals, noise, and reverberation in shallow continental shelf or narrow

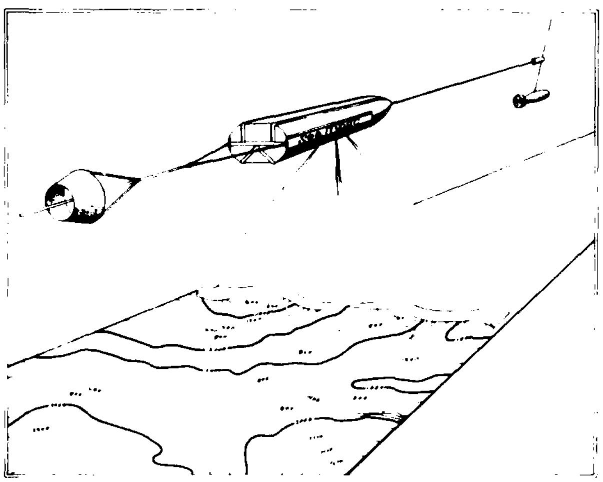

Figure 3. Sea MARC IV mapping geometry. The Sea MARC IV neutrally buoyant towfish and umbilical cable stream behind a dead weight depressor. This arrangement yields a very quiet and stable sonar platform for acoustic imaging and bathymetric mapping (from International Submarine Technology, Ltd.).

coastal areas are significantly different from deep ocean areas. Attempts to extrapolate deep ocean acoustic data to shallow-water applications have been disappointing. In recent years, concern about the way Navy systems perform in shallow-water environments has led to increased emphasis on understanding and exploiting those features that characterize these environments. The proximity of boundaries (surface, bottom, shoreline), inhomogeneity of the water column, sea floor, and substrate; short-term temporal variability, and influences of noise sources contribute to the extreme complexity of the acoustic environment in shallow water.

Clearly, environmental acoustics are so complex that an interdisciplinary approach to investigations is required. NORDA geologists, together with acousticians and oceanographers, have developed an integrated, long-range environmental acoustics program that addresses basic and applied issues in the bottom interaction of high-frequency sound in shallow-water environments. Phases of this program are currently supported by the Office of Naval Research and the Naval Sea Systems Command. The objective of this program is to develop a fundamental understanding of the physics of high-frequency, shallow-water bottom scattering.

Because acoustic wavelengths are very short at high frequencies (10–100 kHz), small seafloor features (such as ripple marks) will cause acoustic scatter. Thus, high-frequency bottom interaction depends mainly upon small-scale seafloor rou;hness. The seafloor features most important to high-frequency acoustic scattering are discernible on side-scan sonar records.

In support of the high-frequency program, NORDA has developed a strong shallow-water survey capability built around the ability to conduct precisely navigated sonar imaging (Figs. 4 and 5) and shallow subbottom profiling measurements.

Extensive geological site investigations for high-frequency bottom scattering experiments have been conducted off Panama City, Florida (Figs. 4 and 5), and in the Arafura Sea, off the northern coast of Australia. In these experiments, sonar imaging, integrated with in situ physical properties measurements and stereophotography, is used to map the finescale spatial variability of sediment type and bottom roughness.

Within NORDA's high-frequency acoustics program, side-scan imagery, subbottom profiles, and precision positioning were provided for the SQQ14 minehunting sonar evaluation study conducted off Charleston, South Carolina. The pre-experiment environmental assessments demonstrated the considerable variability in bottom character encountered at this location.

Future shallow-water efforts will include geological investigation of areas where high-frequency scattering experiments will be conducted. Improved survey techniques will also be developed.

Summary

Many of the most important direct applications of marine geology support within the Navy research structure are in fields of underwater acoustics and engineering. As new or improved systems are developed, the Navy will continue to require a better understanding of the extensive seafloor environment and the ocean in which it operates. Marine geology programs within NORDA advance the Navy's fundamental and applied knowledge of geology to meet current and future Navy requirements.

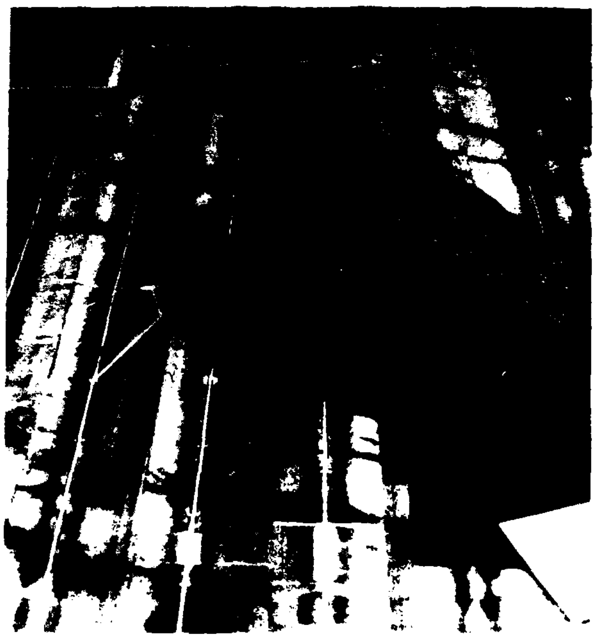

Figure 4. NORDA scientist preparing side scan sonar mosaic of sea floor.

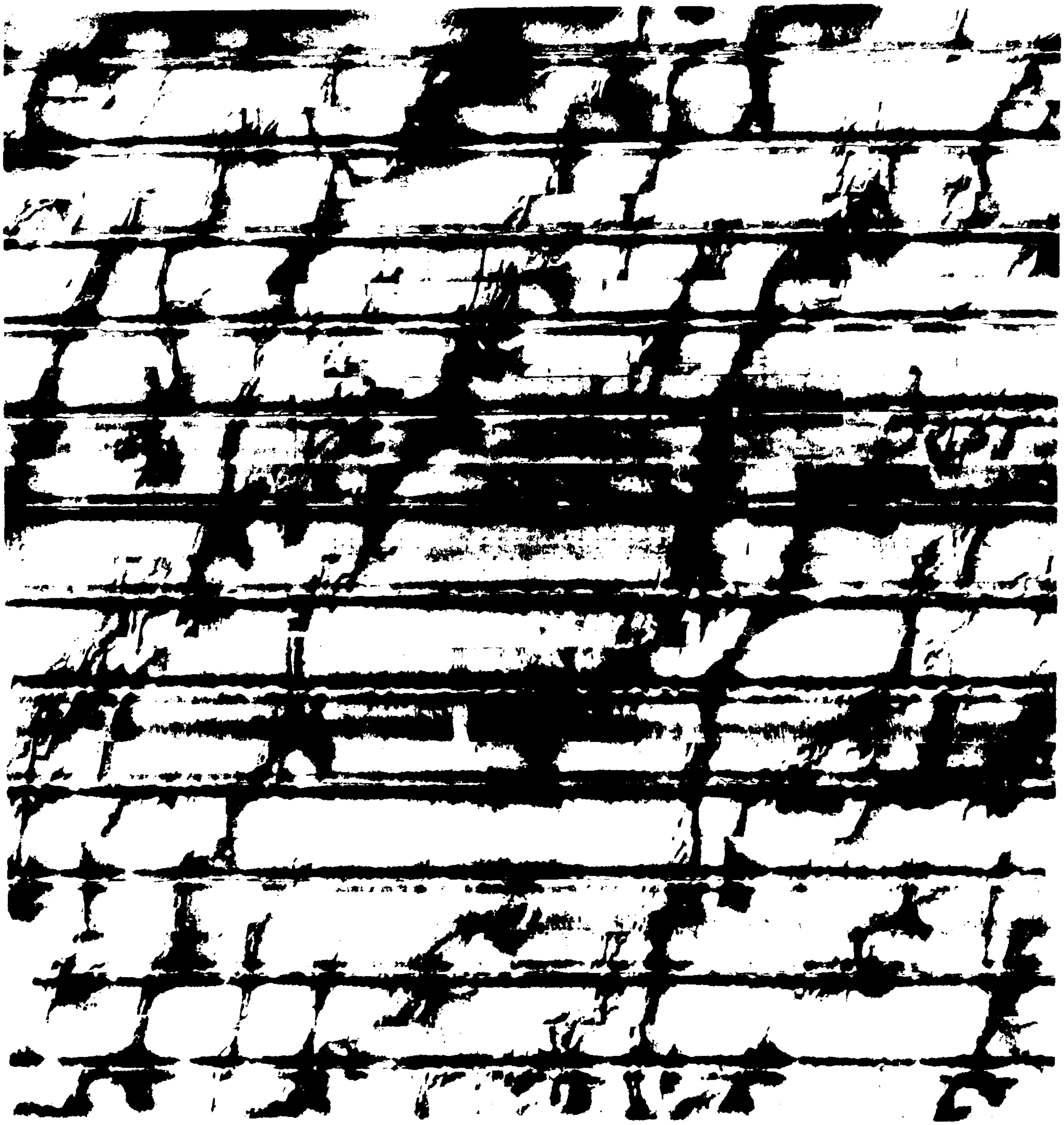

Figure 5. Side scan sonar mosaic (2 x 2 nautical miles) of sea floor off Panama City, Florida (water depth 30 m). Dark areas represent linear sand ridges with a coarse grained rippled crest. Light areas represent medium grained unrippled sand.

Geophysics Probes the Seafloor/Subseafloor Environment

Joseph F. Gettrust and David W. Handschumacher
Seafloor Geosciences Division

Abstract

The marine geophysics program at NORDA focuses on geomagnetic/plate tectonics and seismic research. These research efforts span the spectrum from developing a basic understanding of earth processes to supporting advanced system development. Broadly stated, the research projects are directed toward providing the Navy with a better understanding of how the sea floor and subbottom affect sound propagation, as well as defining the source and spatial and temporal variability of potential fields and the effects of these features on Navy systems and operations.

Introduction

NORDA's charter is to address the marine environment and its impact on the Fleet. To address problems of immediate concern (e.g., detection of seamounts) and environmental issues that impact longer range needs (e.g., very low frequency antisubmarine warfare surveillance), the marine geophysics activities focus on geomagnetism/plate tectonics and seismic research.

The development of methods by which to predict the topography and geoacoustic properties of the bottom in areas where direct measurements cannot be easily made critically depends upon the fundamental understanding of past and present dynamic processes within the solid earth. Following World War II, the Office of Naval Research supported marine geophysical research at a level that led to significant breakthroughs in our knowledge of the earth. This work led to the syllogism of plate tectonics, a model for tectonic processes that explains the gross structure of the ocean basins and continental margins. One of the aspects most critical to the development of this model is the concept of seafloor spreading in which marine magnetic anomaly lineations could be related to the age of the oceanic crust. Ultimately, this model makes it possible to predict in a systematic manner the bottom topography, sediment type and structure and, thus, the gross distribution of geoacoustic properties of the sea floor.

Discussion

Geomagnetism/plate tectonics program

In 1979 NORDA established a basic research program to further investigate the geology and geomagnetism of ocean basins within the framework of plate tectonic theory. The program's objectives are broad-based and address fundamental questions concerning the origin and nature of seafloor structure, magnetism and tectonism (Fig. 1). The research approach is empirical and predicated on field investigations that involve airborne and shipborne deep-tow/surface-tow magnetic surveys.

One of the first areas identified for an extensive aeromagnetic survey effort was the western Pacific. The seafloor structure in this region is anomalously complex. Numerous deep basins are seen to be transected or bounded by oceanic rises, plateaus, troughs, and ridges. In addition, the area contains an unusually large number of seamounts, which occur in linear chains, amorphous groups, and isolated settings. Prior attempts to develop a coherent tectonic model for the evolution of these structures had been hampered by the presence of a regional magnetic "quiet zone" (Fig. 1).

According to a widely accepted hypothesis, sea floor underlying this quiet zone and other quiet zones marginally located over coeval crust of the North Atlantic and Indian Ocean basins was formed during the mid- to late Jurassic (approximately 150 to 180 million years age)

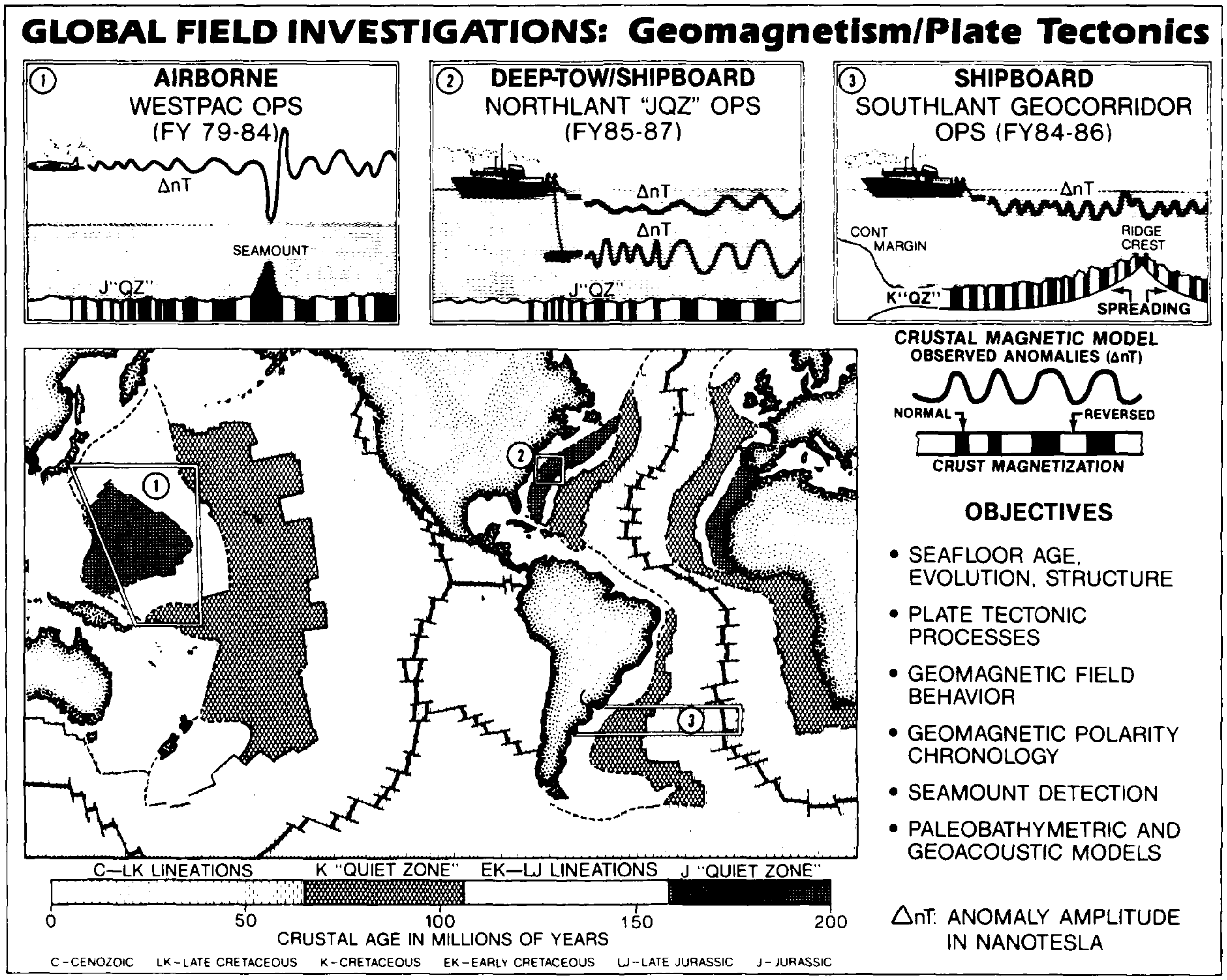

Figure 1. This figure schematically illustrates the empirical approach taken by NORDA's geomagnetism and plate tectonics program in addressing fundamental questions concerning seafloor structure, magnetism, and tectonism. Examples of research operations discussed in the text are presented and experiment sites located with respect to seafloor age.

period of constant, i.e., nonreversing, geomagnetic field behavior. Interpreted as such, the Jurassic quiet zones (JQZs) represent blank sections in the marine magnetic record within which detailed study of the earliest spreading history of these oceans is precluded by the absence of crustal isochron control provided by magnetic reversal anomalies.

Shipboard and deep-tow magnetometer records, however, had provided tenuous evidence that at least the youngest portions of the JQZs contain short wavelength (< 50 km), reversal-type anomalies, which could be related to seafloor spreading during a period of frequency reversals rather than a period of constant polarity. This conclusion, if valid for older portions of the JQZs, would significantly impact not only tectonic studies of the JQZ regions, but also studies seeking to define the chronology and mechanism of the earth's magnetic field reversals. A primary goal of NORDA's western Pacific (WESTPAC) aeromagnetic operations was to regionally test the frequent reversal model for the origin of the JQZs by determining whether or not seafloor spreading lineations can be resolved in these regions.

During WESTPAC operations, NORDA collected over 100,000 nm of low-altitude (1000–2000 feet) aeromagnetic

measurements in sparsely surveyed areas of the western Pacific aboard P-3 Orion aircraft. Much of this data was collected during flight operations specifically targeted to search for linear anomalies in the JQZ.

The search was an unqualified success. A well-defined sequence of low amplitude (10–50 nT), short wavelength (10–40 km) anomalies was identified in the JQZ east of the Mariana Trench. Interpreted to be of the seafloor spreading variety, these magnetic anomalies have been used as the criteria for extending the geomagnetic reversal time scale backward in time to the earliest stages in the evolution of the Pacific, Atlantic, and Indian Oceans (Fig. 2).

The success of the WESTPAC operations provides incentive and precise criteria for re-examining the magnetic morphology of JQZs elsewhere. While the Pacific data are significant, a global correlation of the Pacific anomaly sequence would make the frequent reversal hypothesis for the origin of the JQZs more conclusive. In addition, if these anomalies are to be used for detailed tectonic studies, mapping programs must be initiated. It should be noted that the Pacific anomalies were mapped in a region where the crust is inferred to have formed at a relatively high spreading rate (~10 cm/yr). Crust formed at slower spreading rates will produce a less resolvable magnetic signature because individual polarity bands within the crust will be narrower. In the North Atlantic, for instance, model studies based on the predicted spreading rate of less than 3 cm/yr indicate that it will not be possible to resolve the predicted anomaly record in the JQZ with airborne or shipborne surface-tow magnetic surveys (Fig. 3). However, the predicted anomaly pattern would be easily resolvable with a magnetometer towed at mid-depths (3000 m). For this reason, we plan to conduct a specialized deep-tow magnetometer operation off the east coast of the United States to test the frequent reversal model for the JQZ. If successful, this operation will show that detailed isochron information, which is critical to deciphering the initial rifting processes that produced the Atlantic ocean basin, exists and is resolvable in the JQZs.

The WESTPAC operations also provided scientists with an opportunity to field test the application of aeromagnetic surveys to locate such uncharted bathymetric structures as seamounts (which produce a characteristic geomagnetic signal that can be resolved during low-altitude airborne magnetic surveys). This effort addressed the Navy's continuing requirement to detect and chart seamounts within its operational areas. In extreme cases, these seamounts can be hazardous to surface or submarine navigation. More often, they represent significant environmental features that can adversely affect sensor/weapons systems. The introduction of deeper running submarines with increased operational ranges has expanded this requirement to large

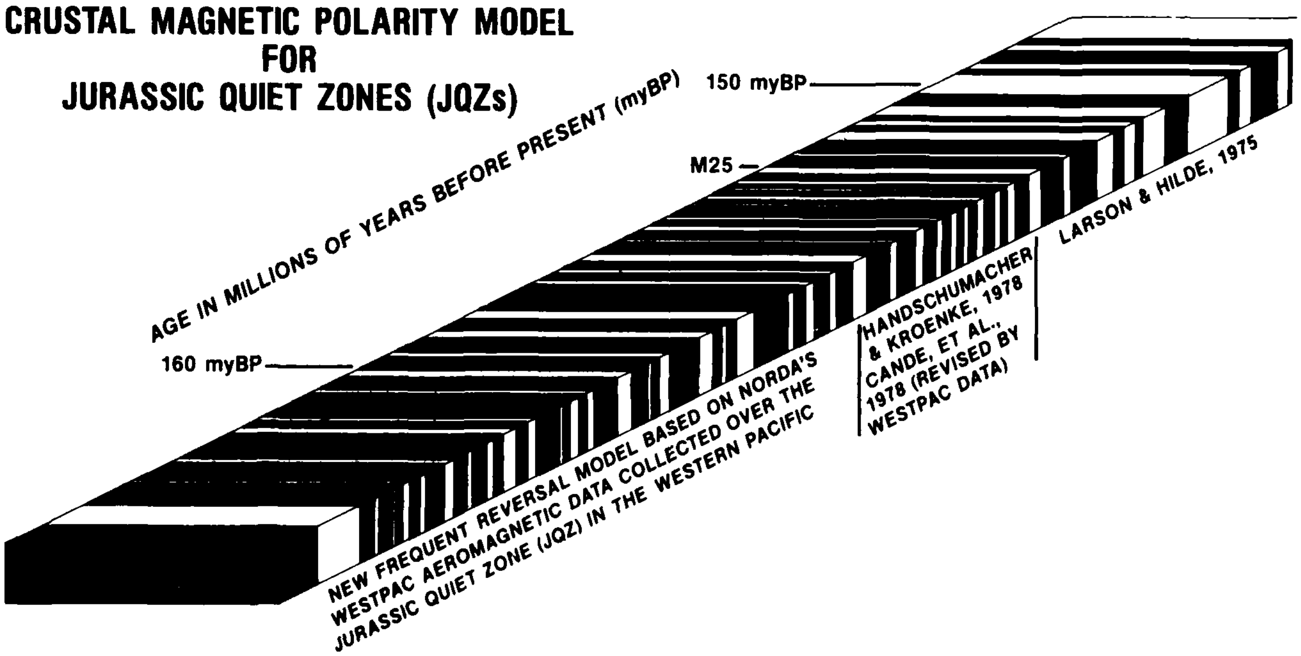

Figure 2. New crustal magnetic polarity model for the Jurassic quiet zones developed from magnetic lineations resolved in data during WESTPAC aeromagnetic survey operations. The model shows narrow banding of alternating polarity, which is attributed to seafloor spreading during a period of frequent reversals prior to anomaly M25 time. Age extrapolations were made using a constant spreading rate assumption and the time scale for post M25 anomalies of Larson and Hilde (1975).

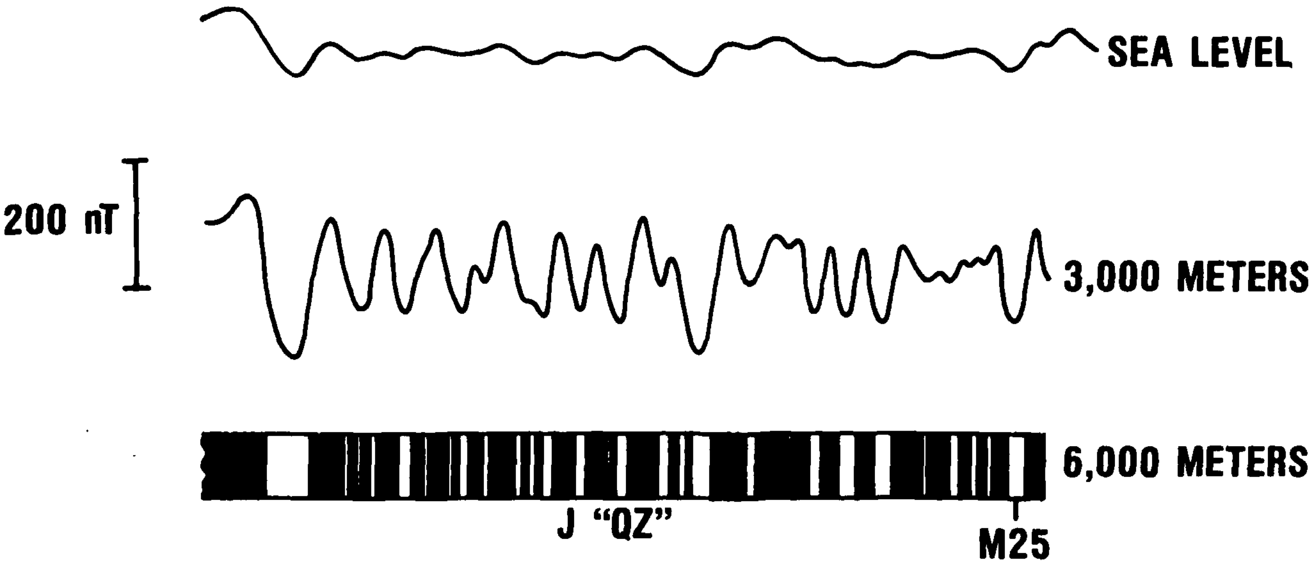

Figure 3. Predicted North Atlantic JQZ crustal magnetic polarity model based on Pacific data with synthetic anomaly profiles generated at sea level and at a depth of 3000 m. These profiles demonstrate the requirement for deep-tow magnetometer operations to resolve the predicted JQZ anomalies in the North Atlantic JQZs.

ocean areas where only reconnaissance grade bathymetry is available. One area of particular concern is the western Pacific. This region contains an anomalously high number of randomly distributed seamounts. Outside localized areas that have been bathymetrically surveyed in detail, the probability is high of encountering uncharted seamounts or seamounts that shoal at depths less than those reported.

During WESTPAC OPS79, aeromagnetic survey data was used to predict the existence of three large, uncharted seamounts near Wake Island. Subsequent bathymetric surveys conducted by the Hawaii Institute of Geophysics (HIG) under NORDA/ONR sponsorship confirmed the aeromagnetic results. One seamount was found to rise over 4000 m above the surrounding sea floor and shoal at a depth of less than 1200 m (Fig. 4). Subsequent flight operations were used to field test the potential application of aeromagnetic surveys to validate predicted sites of uncharted seamounts derived from SEASAT radar altimetry data. Although numerous sites were overflown, only one yielded an apparent magnetic confirmation for the SEASAT prediction (Fig. 5).

The western Pacific represents an area where the understanding of the gross structure, age, and evolution is still a significant issue. By contrast, these aspects of plate reconstruction are no longer a first priority issue in the South Atlantic. NORDA scientists are using geomagnetic data from the South Atlantic (SOUTHLANT GEOCORRIDOR OPS) to address more detailed questions. Because the gross tectonic history of the South Atlantic basins is well understood, it will be possible to take the detailed information from the geocorridor and extrapolate parameters of interest to the Navy to the whole of the South Atlantic basin.

Seismology program

NORDA's seismology program complements the geomagnetic/plate tectonics effort by measuring geoacoustic properties in regions of Navy interest (Fig. 6). The design and location of seismic experiments is often predicated on earth models derived from geomagnetic observations.

NORDA's seismic program is relatively young; the first major seismic refraction/reflection field program was conducted in 1979 when NORDA scientists participated in the Rivera Ocean Seismic Experiment (ROSE). This experiment was unique in that essentially every major marine geophysics group in the United States participated. The goal of this project was to investigate the structure of young oceanic crust near the East Pacific Rise using the seismic refraction technique. More than 80 ocean bottom seismographs (OBSs) recorded both explosive "shots" fired from ships and earthquakes generated by the spreading of the oceanic crust. The indirect sampling of the evolving oceanic crust is of interest to the Navy because very low frequency acoustic waves (roughly 5 to 30 Hz) might become important to ASW surveillance, and acoustic signals at these low frequencies interact with the oceanic crust.

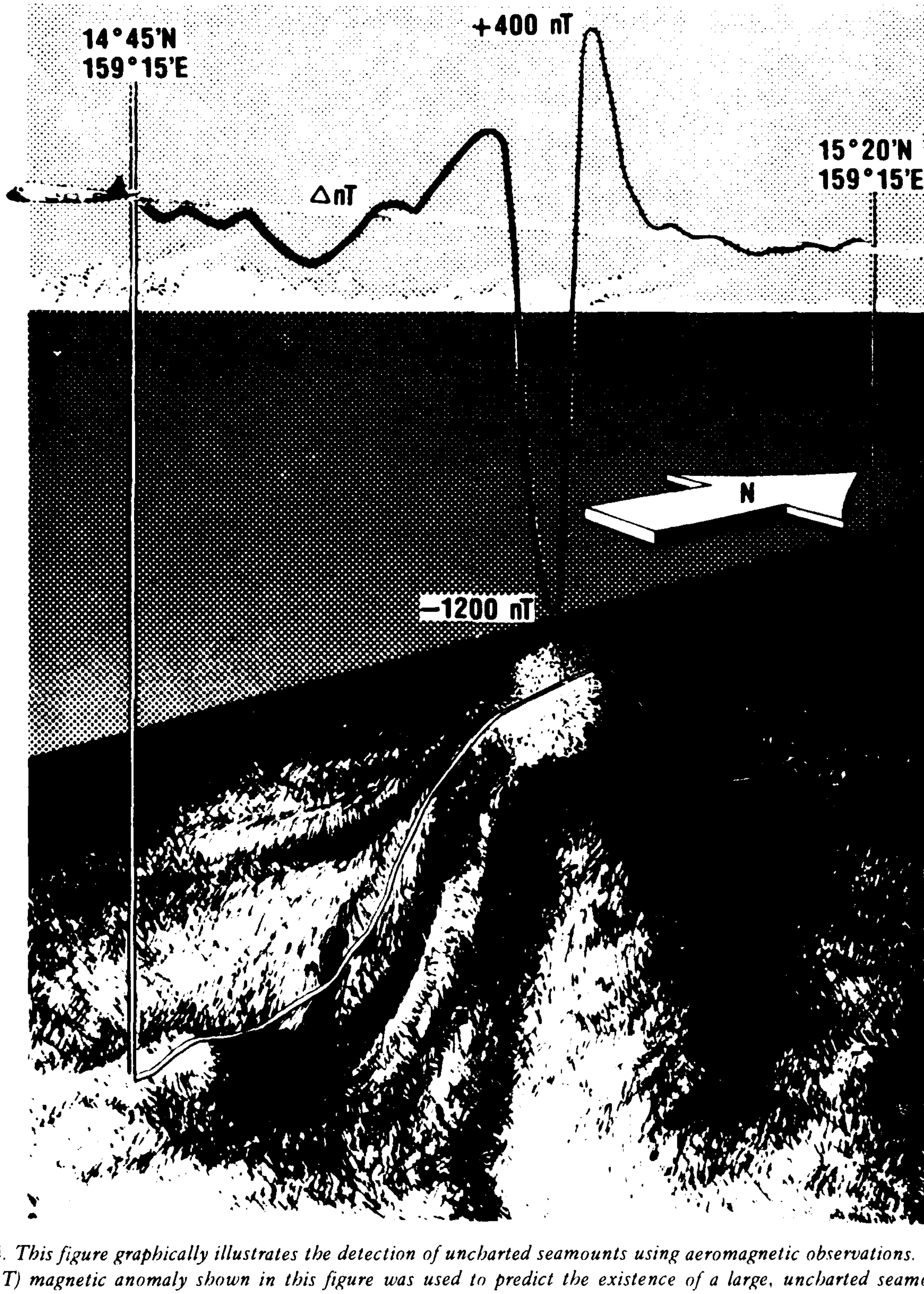

Figure 4. This figure graphically illustrates the detection of uncharted seamounts using aeromagnetic observations. The large (1600 nT) magnetic anomaly shown in this figure was used to predict the existence of a large, uncharted seamount near Wake Island. This prediction was confirmed by the Hawaii Institute of Geophysics, which ran bathymetric profiles over what is now known as SEASCAN seamount. An artist's conception of the seamount's bathymetry derived from the Institute's data is shown.

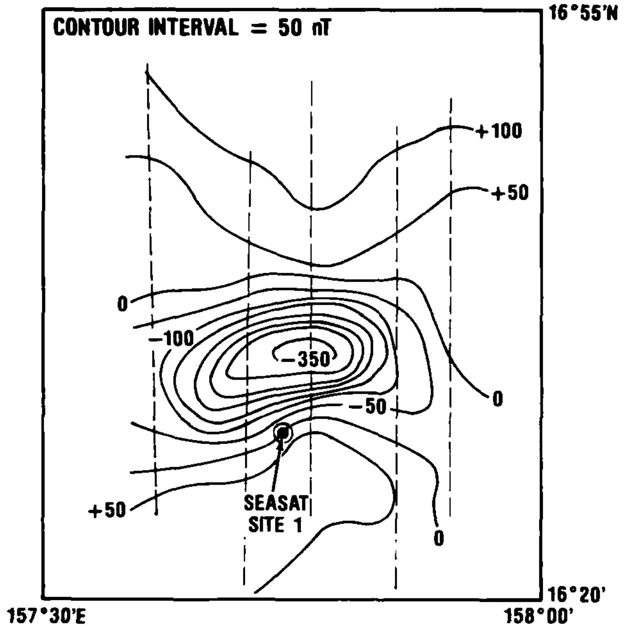

Figure 5. WESTPAC aeromagnetic contour map (flight tracks dashed lines), which provides independent confirmation of a SEASAT radar altimetry predicted site for an uncharted seamount.

Interpretations made of the crustal structure and seismicity in the ROSE area show that the oceanic crust structure is heterogeneous, that seismic (acoustic) velocity anisotropy in the upper mantle (which underlies the crust) is nil, and that measurable changes in the seismic velocities exist within the crust over the age range from 0.5 to 4.5 million years.

NORDA seismologists also played a role in evaluating subbottom borehole seismic systems. The thrust of this program was to evaluate marine borehole instruments as sensors to verify compliance with future test ban treaties and for ASW surveillance. Preliminary results from a 1982 borehole instrument experiment off the Kamchatka Peninsula suggest that the signal-to-noise ratio of the borehole instruments might be significantly better (20 dB in certain frequency bands) than those found for conventional OBSs and bottom-mounted hydrophones. This improved signal-to-noise ratio could impact the design of future ASW systems.

In a similar experiment carried out in the South Pacific, the Marine Seismic System borehole instrument produced similar results. Further research efforts will be directed toward Navy applications.

Although the structure of the oceanic crust beneath the deep oceans might be of long-range interest to the Navy, bottom and subbottom acoustic wave interaction is presently of considerably greater importance in shallow water (the continental shelf). NORDA is currently carrying out a very low frequency acoustic/seismic special focus project in which the energy partitioning between the water column and solid earth is being studied. During the first very low frequency field program (June 1985 on the continental shelf off Cape Fear, North Carolina), acousticians and seismologists from NORDA measured the acoustic signal and noise distribution within the water column, compared the signal-to-noise ratio of solid earth path and pure water path signals, and related these observations to the geologic structure of the subbottom (Fig. 7). By combining the expertise of acousticians and seismologists in a single experiment, the propagation characteristics of very low frequency acoustic signals can be related to earth structure of a passive continental margin: this relationship makes it possible to better predict geoacoustic properties in similar geologic environments.

Another focus of NORDA's seismology program is the Deep Towed Array Geophysical System (DTAGS), which was developed by NORDA engineers (Fig. 8). DTAGS is a multichannel seismic system similar to those used with great success in petroleum exploration. The array can be towed at full ocean depths, which allows NORDA scientists to investigate the structure of deep-water marine sediments in significantly greater detail than with conventional systems previously used. Estimates of the acoustic impedance and attenuation of the sea floor and subbottom at midrange (300–600 Hz) frequencies, and the spatial variability of these properties will significantly improve the accuracy and predictive power of the Navy's geoacoustic models.

Engineering field tests of DTAGS were completed in September 1984. During this field exercise, seismic profiles were taken south of Bermuda (Fig. 9); these profiles are the first "geophysics" data collected with DTAGS. Data from this cruise has been used to make a preliminary seismic section of the sediment structure in 4900 m of water south of Bermuda. We now know that with a complete 24-channel seismic data set taken at 16-m intervals along the profile, it will be possible (for the first time) to obtain excellent in situ compressional velocity estimates in the upper several hundred meters of sediments at full ocean depths. The dense sampling made possible with DTAGS will make it possible to develop a viable statistical model for the spatial variability of sediment properties in that environment.

Modeling of seismic propagation within complex sediment structure is being carried out in cooperation with

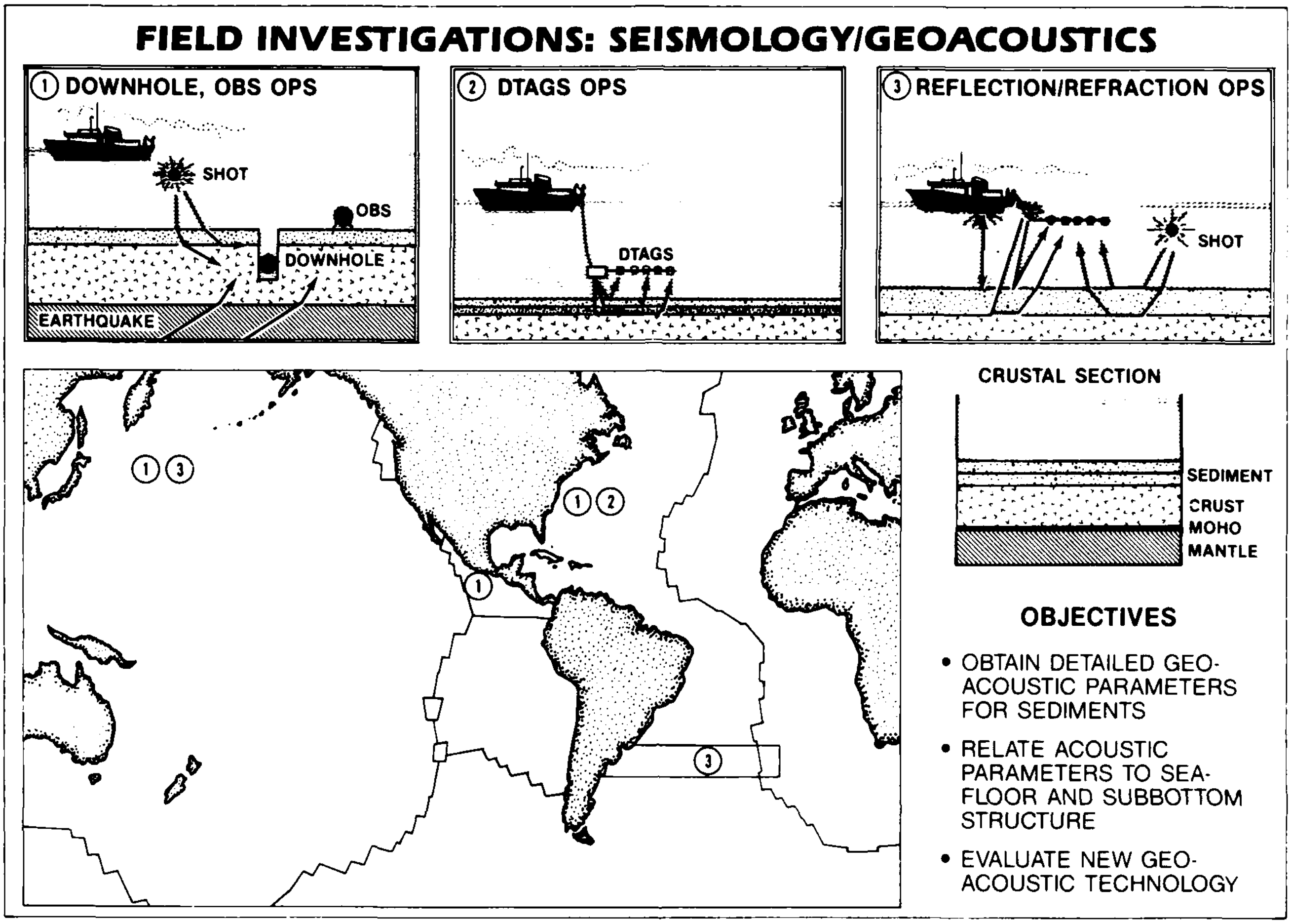

Figure 6. This figure schematically illustrates the research efforts and regions in which NORDA's seismologists have conducted field projects. The ocean bottom seismograph, borehole seismic, and deep-towed multichannel seismic systems are emphasized in the text.

the University of Houston. There, Seismic Acoustic Laboratory scientists have developed facilities where small-scale analogs of the marine sediment column can be constructed and used to test seismic propagation through known, complex earth models.

Marine geophysics scientists are also engaged in the application of existing fleet sonars to mapping the seafloor morphology and geoacoustic properties in areas of Navy interest. This program (SWATHMAP) complements our cooperative effort with Texas A&M University to develop and implement the next generation of quantitative side-scan sonar systems.

Summary

Geomagnetism/plate tectonics and seismology/geoacoustics research at NORDA emphasizes the measurement of environmental properties of interest to the Navy. The programs complement other ongoing research efforts of NORDA, academia, and other governmental laboratories. The emphasis of cooperative research efforts is in recognition of the fact that a multidisciplinary approach to marine studies will enhance our ability to study the complex marine environment, and to refine earth models to the degree required to meet current and potential Navy needs.

References

Larsen, R. L. and T. W. C. Hilde (1975). A Revised Time Scale of Magnetic Reversals for the Early Cretaceous and Late Jurassic. *Journal of Geophysical Research* 80, 2586–2594.

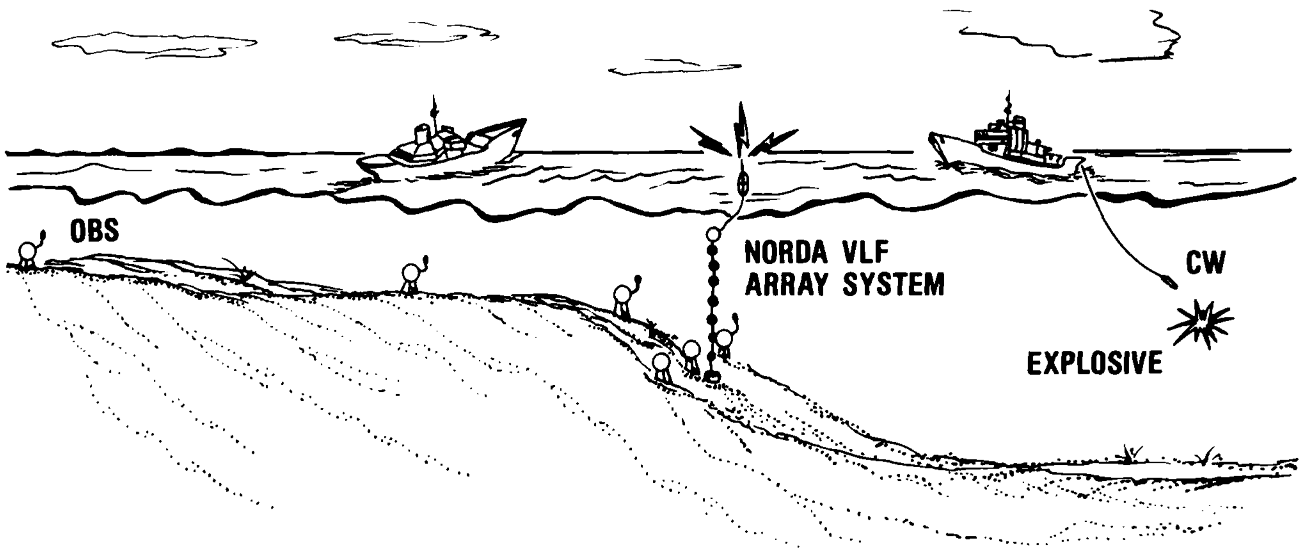

Figure 7. A schematic presentation of the Cape Fear experiment, which was carried out in June 1985. NORDA acousticians deployed the vertical hydrophone array shown in this figure. NORDA seismologists deployed the ocean bottom seismometers in various configurations. Both impulsive and continuous wave acoustic sources will be used to study the geoacoustic properties of the region.

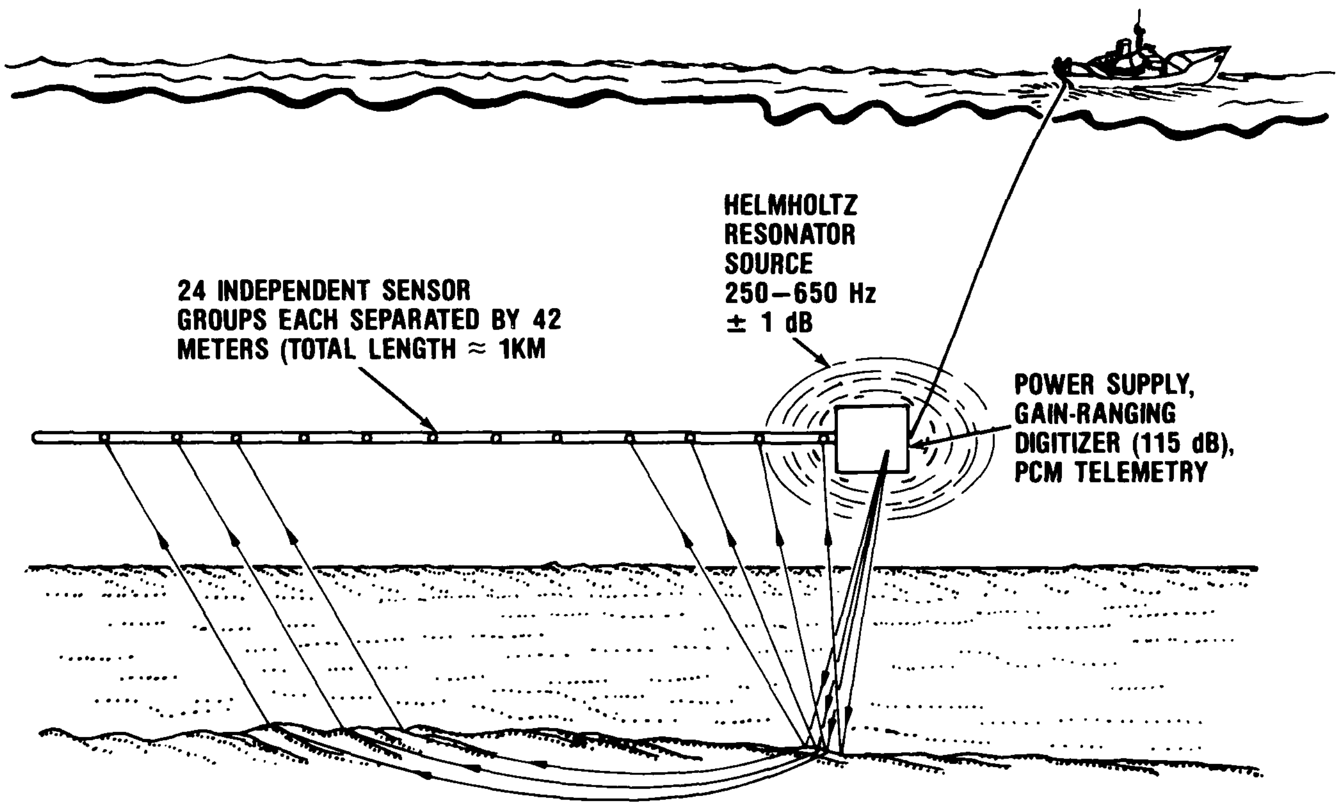

Figure 8. This figure presents the general configuration of DTAGS. Note that the acoustic source and multichannel hydrostreamer are towed close (500 m) to the bottom at full ocean depths. The deep-tow configuration limits towing speeds to approximately 1.5 knots; however, the increased resolution that results from this geometry improves our sampling of the deep sea sediments by an order of magnitude.

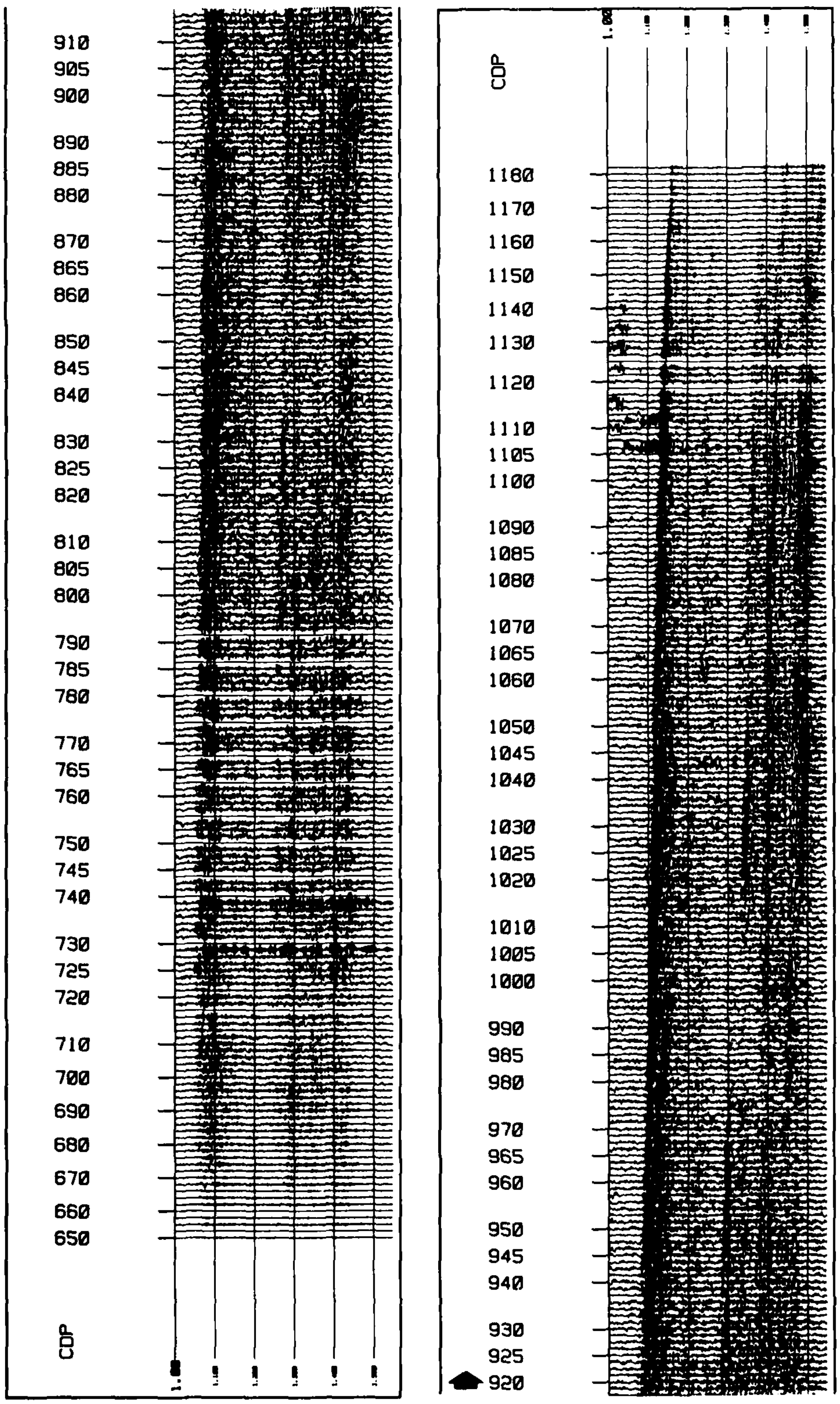

Figure 9. A common depth point stack of DTAGS data taken south of Bermuda during September 1984. This seismic section was produced by Digicon Corporation for NORDA as a benchmark evaluating their DISCO multichannel seismic analysis system.

The Prediction of Geoacoustic/Geotechnical Properties

Philip Valent, Douglas Lambert, Dawn Lavoie, and Huon Li
Seafloor Geosciences Division

Abstract

Geotechnical activities within NORDA include fundamental studies of marine sediment behavior under various loading conditions, including acoustic overpressures. Development efforts leading to specialized probes and remote techniques for measuring geoacoustic/geotechnical properties are integral aspects of the research. Support services in preparing geoacoustic/geotechnical environmental models and site assessments for Navy users are important projects by NORDA researchers. Studies addressing the fundamental nature of submarine sediments are essential basic research efforts.

Introduction

NORDA scientists conduct basic and applied research to improve understanding of the acoustic and geotechnical properties of marine sediments and shallow rock, and the variation of these properties with change in source material and environment. Geotechnologists also provide environmental support to other research, development, and test and evaluation efforts, in the form of predictions and in situ measurements of seabed sediment acoustic and geotechnical properties, profiles, and lateral variability. These research and support functions are accomplished in the field and in the laboratory by using a suite of NORDA-designed and -built advanced sensors and probes. This article describes research efforts directed toward understanding marine sediment properties and some of the tools developed for this effort.

Discussion

Basic and applied research

Marine geotechnologists are relative newcomers to the NORDA community and as such are first developing a basic research program. A special interest is in developing an improved understanding of the geoacoustic and geotechnical behavior of marine gravels and carbonate sediments with near-term emphasis on continental shelf carbonates. Also under study are the sediment changes and deformation caused by the insertion of probe-type devices for measuring in situ sediment properties and to extend, in detail, earlier models. NORDA is attempting to theoretically describe the impact of probe insertion on the sediment and on the measured sediment properties. These predictions are being verified/calibrated against measurements made from the prototype probe shape/configuration in the laboratory and in the field. Measurements of excess pore water pressures generated by probe insertion have been and are being obtained in the laboratory and in the field and compared to theoretical predictions (Bennett et al., 1985b, and Riggins et al., 1985; Fig. 1),

Figure 1. Piezometer pore pressure response during probe insertion (1 psi = 6.895 kPa).

with good success to date in one reconstituted ocean sediment and three in situ "undisturbed" sediment tests. This work is being extended to include identification and development of techniques to determine the impact of probe insertion on measured sediment electrical conductivities and compression and shear wave velocities.

Geoacoustic/geotechnical sensor development

Improved and new laboratory and field sensor technology that can be applied to help the Navy accomplish its mission are being identified and evaluated. Currently, research centers around developing acoustic subbottom survey systems, probe-type in situ measurement systems, and improved laboratory test equipment and techniques.

NORDA has contracted for the development of a software subsystem to be integrated with a Honeywell-ELAC acoustic sediment classifier. The system integrates the reflected acoustic energy per unit time from the subseabed after insonification at either 15 kHz or 30 kHz and uses this measure of reflected energy to broadly classify the sediment type (Fig. 2). First tests of this acoustic sediment classifier indicate that while the system can readily identify the transition between two sediment types, it cannot classify sediments without ground-truth from cores or in situ probe measurements from the subseabed. Field evaluation of the acoustic sediment classifier continues while complementary technologies are being explored to determine the feasibility of augmenting the acoustic reflectivity data with other remotely measured data to produce a more reliable remote sediment classification.

NORDA has a number of probe types in various stages of development for measuring in situ the properties of seafloor sediments. The geoacoustic/geotechnical probe development, laboratory testing, and fielding (at sea) activities are strong in-house capabilities. Efforts include not only the electronics and mechanical design functions to engineer durable, yet precise systems, but also the technical evaluations to properly relate the data measured to the mechanisms of soil behavior. Perhaps the most developed of these probes is the differential pore pressure system developed for the Department of Energy's (DOE) Seabed Disposal Program (SDP). The instrument measures sediment differential pore pressures to a precision of ±0.3 kPa (±0.05 psi) at ambient pressures to 70 MPa (10,000 psi) (Bennett et al., 1985a; Fig. 3). The Department of Energy has supported the development of this piezometer probe to measure the pore water pressure gradients, which will result from an experimental, recoverable, long-term heat source to be placed in the sediments. The test will model the influence of the thermal and pore water pressure fields generated by a buried canister containing high-level radioactive waste, and will provide high-quality field data to be used in validating predictive computer codes being used in the SDP. Calibration of the differential pressure transducers used in the SDP work has required in-house development of a calibrator unit (Fig. 4) to be used in conjunction with NORDA's high-pressure test facility.

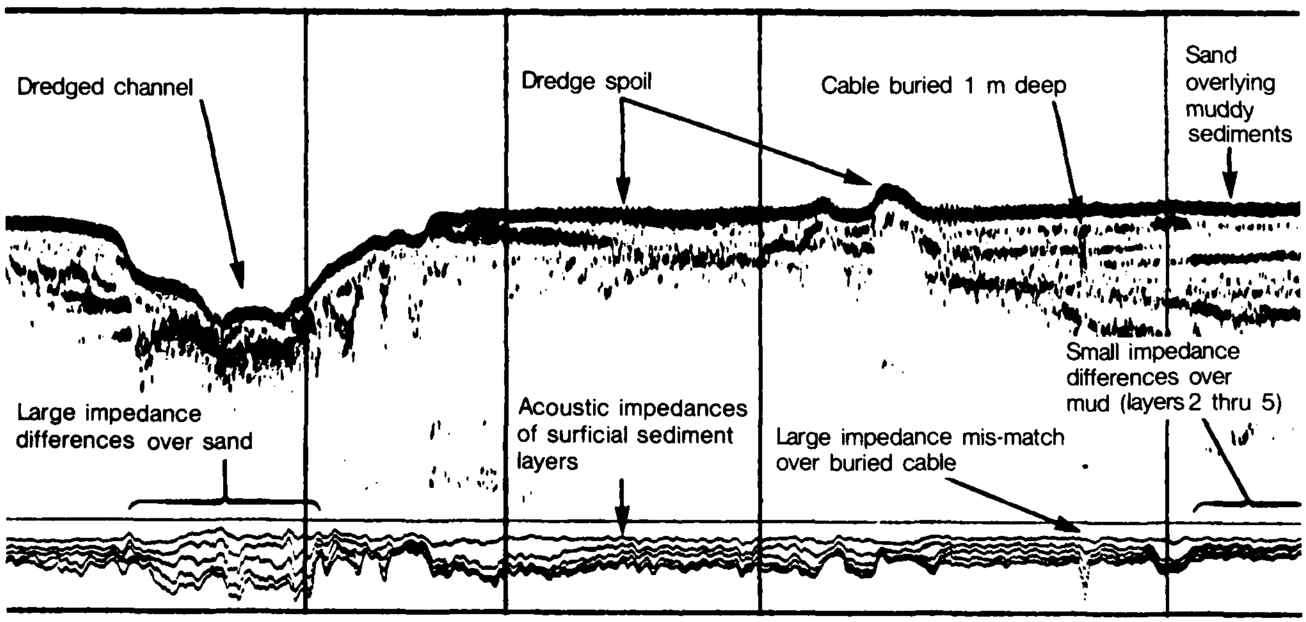

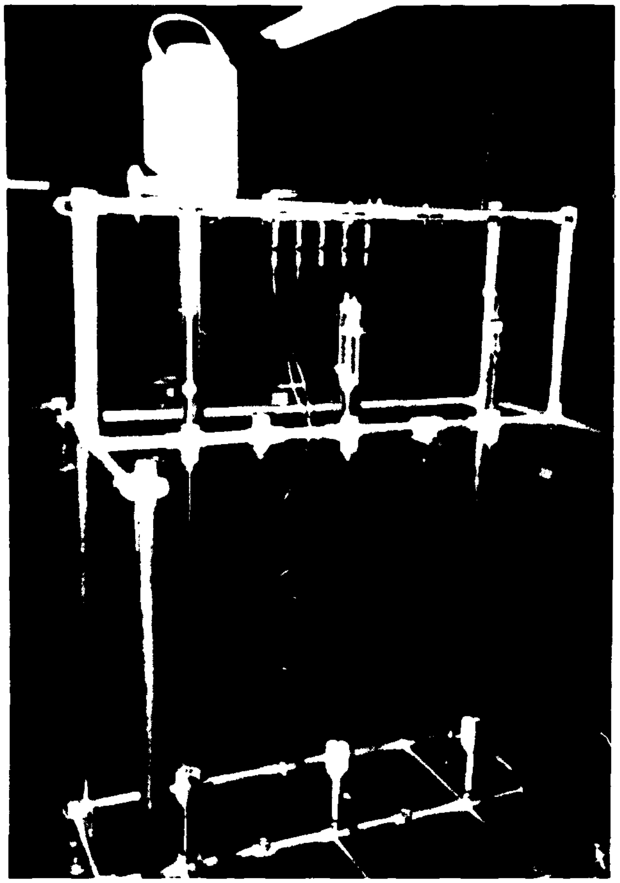

Figure 3. Deep water differential pore pressure probes in various stages of assembly.

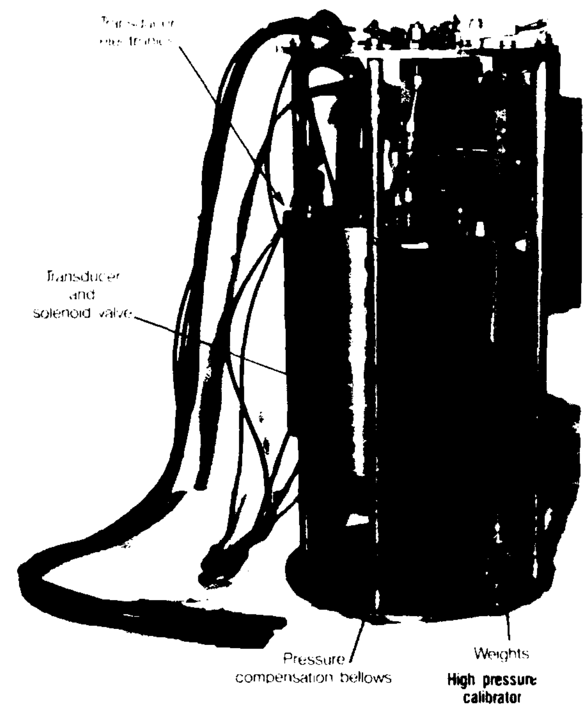

Figure 4. NORDA high pressure calibrator for deep ocean pressure transducers.

The sediment conductivity probe is also a well-developed system that is used to provide direct measurements of sediment electrical conductivity for mine countermeasures assessment. The probe provides an indirect measure of sediment porosity and classification and, to some extent sediment consistency (shear strength). The sensing element of the conductivity probe is wedge-shaped to minimize driving resistance with four needle-like electrodes protruding in advance of the wedge (Fig. 5). The electrode design is based on the Wenner spread electrode configuration (Griffiths and King, 1965) commonly used in geophysical exploration. This probe design has been applied to a 130 mm (5 inch) diameter probe driven to 12 m penetrations by a vibrocorer (Hulbert et al., 1981), and to a diver-embedded, self-contained probe carrying the electrodes in a small wedge mounted on a 10-mm (⅜-inch) diameter, 0.5-m-long shaft. This in situ conductivity/porosity measuring technique provides the best means for determining in situ porosities and densities of cohesionless

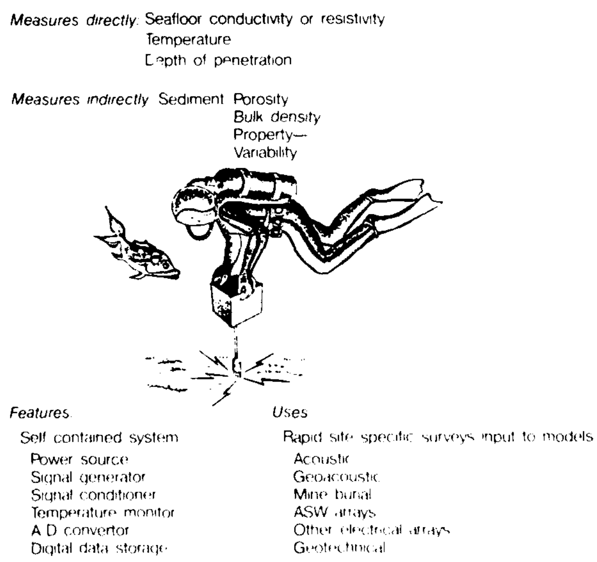

Figure 5. Diver operated conductivity probe.

sediments, i.e., gravels, sands and many silts, when performing research or test and evaluation studies. A few cores are normally taken in conjunction with the in situ conductivity measurements to identify infrequent, but possible, misclassifications from the conductivity data—e.g., stiff, overconsolidated clays may be classified as silts or sands when operating without benefit of ground-truth data. Development of the conductivity probe has permitted bridging a gap in in situ measurement technology—that of obtaining reliable measurements of in situ density/porosity in cohesionless sediments. Such measurements were formerly made on gravity or diver push cores of the sediments; density measurements on cores of cohesionless sediment have been shown to yield unreliable density and porosity measurements (Bailard, 1982).

NORDA geotechnologists have developed diver-operated probes for measuring compressional and shear wave velocities. These probes are used in sets of three (Fig. 6) with one end probe used to produce the source signal and the other two used to measure the difference in acoustic wave arrival time at each probe. The shear wave probes use a bimorph-type transducer element to enhance sediment-sensor coupling in the soft and loose surficial seafloor sediments. These probes are being used to examine the near-surface variability of sediment sound velocities to better understand high-frequency scattering phenomena.

The bimorph transducer element has also been incorporated in the specimen end caps of the Hamilton frame (Brunson, 1983) and used to measure shear wave velocities on soft sediments in the laboratory. Studies are now underway to improve our understanding of shear wave velocity and velocity anisotropy variations in carbonate sediments using specimens collected on Leg 101 of the Ocean Drilling Project. Additional development work with the bimorph shear wave transducers is proposed to improve their ease of operation and to systemize their operation to enhance the repeatability of the measured data. Further work with the shear wave transducers has shown that a number of wave arrivals exist: study of the full set of generated and received waves is proposed to clearly delineate the transducer performance and to help identify possible improvements, to identify possible improvements in the test frame, and to identify the optimum test specimen geometry for shear wave velocity determinations.

The remote, in situ probe, and laboratory geoacoustic/geotechnical sensors developed by geotechnical personnel are all targeted toward improving our understanding of the fundamental properties and variability of seafloor sediments and toward improving our ability to rapidly delineate that variability laterally and vertically.

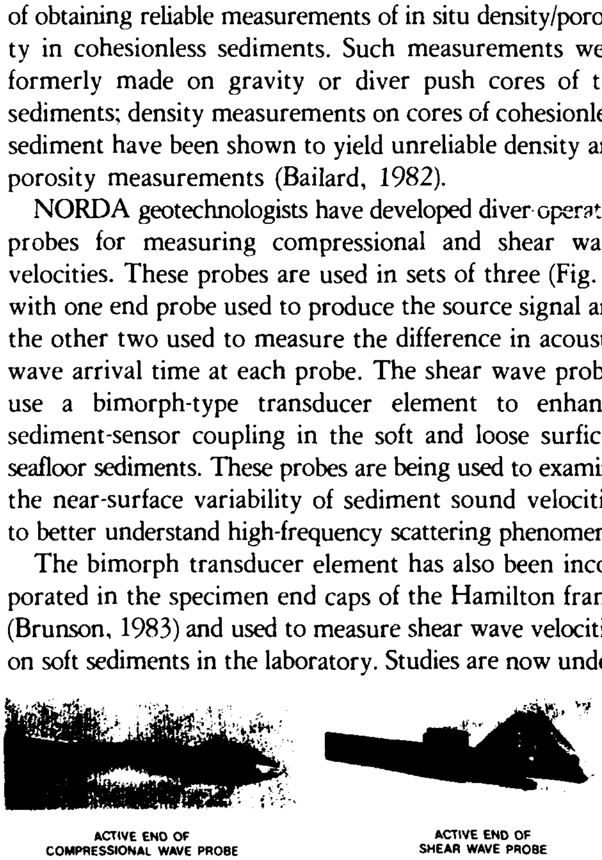

MEASURES DIRECTLY: COMPRESSIONAL WAVE VELOCITY
COMPRESSIONAL WAVE ATTENUATION
SHEAR WAVE VELOCITY

MEASURES INDIRECTLY: SEDIMENT: BULK MODULUS
SHEAR MODULUS
YOUNG'S MODULUS
POISSON'S RATIO

FEATURES: 1. FREQUENCY: COMPRESSIONAL~70 kHz, SHEAR~2 kHz
2. GOOD COUPLING IN SOFT SEDIMENTS
3. CAN BE EMBEDDED IN SANDS WITH MINIMAL DISTURBANCE

USES: GEOACOUSTIC MODEL INPUTS
EMPIRICAL DATA ON Vp/Vs RATIOS

Figure 6. Compressional and shear wave probes.

Environmental support

Another important role of the geotechnical scientists is to provide geoacoustic/geotechnical environmental support to other NORDA researchers and to other Navy laboratories and contractors. This seafloor environmental work normally requires gathering a complete description of the geologic environment from the literature (particularly from Deep Sea Drilling Project reports), reviewing the open data bases and those held by the Naval Oceanographic Office and, when possible, reviewing offshore well-drilling logs sometimes available from the petroleum companies or from the U.S. Geological Survey. This information is assembled and used to prepare a geologic map and stratigraphic profiles of the area of interest—a test site a few miles on a side or an entire ocean basin (Fig. 7). Densities and sound velocities are then obtained, if available, from nearby drillhole logs or geophysical records or, in lieu of data, the densities and sound velocities are estimated using available relationships (Hamilton, 1980). Development work continues to improve understanding of the sediment contribution to acoustic bottom interaction and the performance of analytical models developed to describe acoustic bottom interaction.

Summary

NORDA marine geotechnical scientists perform basic and applied research in the geoacoustic and geotechnical areas. They design, fabricate, test, and use in the laboratory

Washington Coast Province 1

	Depth (m)	Vp (m/sec)	Vs (m/sec)	Kp (dB/m/kHz)	Ks (dB/m/kHz)	Density (g/cc)
Sea Surface Bottom Water	50-200	1483				
	0	1654	55	0.37	13.2	1.9
	5	1772	201	0.30	10.7	1.9
	10	1791	244	0.27	9.8	1.9
	15	1802	273	0.26	9.3	1.9
very	20	1810	296	0.25	8.9	1.9
fine	25	1816	315	0.25	8.9	1.9
sands	50	1835	383	0.22	7.8	1.9
	75	1846	429	0.21	7.5	1.9
	100	1854	465	0.21	7.5	1.9
	125	1860	495	0.20	7.1	1.9
	150	1865	521	0.19	6.8	1.9
Acoustic Basement (Siltstone)		3000	1500	0.03	3.0	2.54

Figure 7. Representative geoacoustic model.

and field a number of special-purpose sensors and probes. These sensors allow the measurement of soil behavior from the infinitesimal strains of acoustic stress levels to the large strains of engineering stress levels associated with mine impact burial and sediment mass movement. This effort in the development and understanding of sensor performance is supported by a moderate basic research effort directed toward better understanding of the interaction between sensors (probe) and the sediments, while use of the sensors in the field provides data for evaluating performance/adequacy of a number of Navy and Marine Corps systems interacting with the sea floor.

In addition to this general support of Navy requirements, major focus has been directed toward improvement of understanding and predictive capability of the properties/behavior of carbonate sediments, shallow- and deep-water, and of gravels; and the range of property anisotropy in seafloor sediments, the fundamental reasons for the anisotropy, and its impact on sediment behavior. These thrusts are directed toward providing understanding of in situ sediment data and behavior to improve the Navy's capability to model the ocean environment.

References

Bailard, J. A. (1982). *Geotechnical Diver Tool Development*. Naval Civil Engineering Laboratory, Port Hueneme, California, Technical Report R892, 7-23.

Bennett, R. H., J. T. Burns, F. L. Nastav, J. Lipkin and C. M. Percival (1985a). Deep-Ocean Piezometer Probe Technology for Geotechnical Investigations. *Journal of Oceanic Engineering* OE-10(1), 17-22.

Bennett, R. H., H. Li, P. J. Valent, J. Lipkin and M. I. Esrig (1985b). In Situ Undrained Shear Strengths and Permeabilities Derived from Piezometer Measurements. In *Strength Testing of Marine Sediments: Laboratory and In Situ Measurements*.

Brunson, B. A. (1983). *Shear Wave Attenuation in Unconsolidated Laboratory Sediments*. Naval Ocean Research and Development Activity, NSTL, Mississippi, Technical Note 159.

Chaney, R. C. and K. R. Demars (eds.), American Society for Testing and Materials STP 883, 83-100.

Griffiths, D. H. and R. F. King (1965). *Applied Geophysics for Engineers and Geologists*. Pergamon Press, New York, p. 27.

Hamilton, E. L. (1980). Geoacoustic Modeling of the Sea Floor. *Journal of the Acoustical Society of America* 68(5), 1313–1340.

Hulbert, M. H., D. N. Lambert, R. H. Bennett, G. L. Freeland, J. T. Burns, and W. B. Sawyer (1981). *Electrical Resistivity/Conductivity of Submarine Sediments Measured by In Situ Techniques*. Atlantic Oceanographic and Meteorological Laboratories, Miami, Florida, NOAA Technical Report ERL 416-AOML 31, 46 p.

Riggins, M., P. J. Valent, H. Li, C. E. Hickox and J. T. Burns (1985). *Pore Pressure Response to Probe Insertion and Thermal Gradient: ISIMU-II*. Naval Ocean Research and Development Activity, NSTL, Mississippi, NORDA Technical Note 259, 80 p.

AD-A170 212 THE NORDA (NAVAL OCEAN RESEARCH AND DEVELOPMENT ACTIVITY) REVIEW(U) NAVAL OCEAN RESEARCH AND DEVELOPMENT ACTIVITY NSTL STATION MS MAR 86 3/3

UNCLASSIFIED F/G 8/10 NL

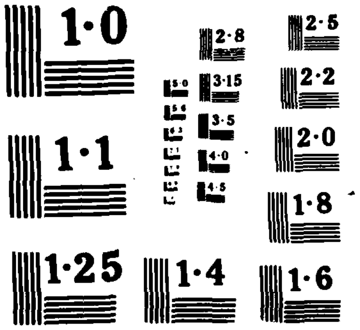
1·0
2·8
2·5
3·15
2·2
3·5
2·0
1·1
4·0
4·5
1·8
1·25
1·4
1·6

Refereed Journal Contributions, 1976–1984

(from Jenkins, Linda H. (1984). *NORDA Journal Index 1976–1984*. Naval Ocean Research and Development Activity, NSTL, Mississippi.)

Adaptations Within Antarctic Ecosystems

Richardson, Michael D. and Joel W. Hedgpeth (1977). Antarctic Soft-bottom, Macrobenthic Community Adaptations to a Cold, Stable, Highly Productive, Glacially Affected Environment; p. 181-186.

American Association of Petroleum Geologists

Egloff, J. and G.L. Johnson (1978). Erosional and Depositional Structures of the Southwest Iceland Insular Margin: Thirteen Geophysical Profiles; Memoir 29.

Egloff, J. and G.L. Johnson (1979). Sedimentary Structures of the SW Iceland Outer Shelf and Slope; Memoir 29.

Holcombe, Troy L. (1978). Geomorphology and Subsurface Geology West of St. Croix, U.S. Virgin Islands; Memoir 29.

American Geophysical Union Transactions

Lowrie, A., T. Aitken, and P. Grim (1978). Extinct Spreading Zone Within the Panama Fracture Zone; v. 59, p. 378.

Williams, G.O., G.E. Innis, and R.M. Clancy (1982). Improvements to Ocean Thermal Field Mapping at FNOC; v. 63, p. 1006.

American Journal of Physics

Lybanon, Matthew (1984). Comment on Least Squares When Both Variables Have Uncertainties; v. 52, n. 3, p. 276-278.

American Meteorological Society Bulletin

Blake, D., T.N. Krishnamurti, S.V. Los-Nam, and J.S. Fein (1983). Heat Low Over the Saudi Arabian Desert During May 1979 (Summer MONEX); v. III, p. 1759-1775.

Clancy, R. Michael and Paul J. Martin (1981). Synoptic Forecasting of the Oceanic Mixed Layer Using the Navy's Operational Environmental Data Base: Present Capabilities and Future Applications; v. 62, n. 6, p. 770-784.

American Physical Society, EM²

Su, M.Y. and C.L. Chen (1982). Schwartz-Christoffel Theory of Flow Past and Opening; v. 108, p. 399-418.

American Scientist

Heirtzler, J.P., P.T. Taylor, R. Ballard, and J. Houghton (1977). A Visit to the New England Seamounts; v. 65, n. 4, p. 466-472.

American Society of Testing and Materials

Hulbert, M.H., D.N. Lambert, R.H. Bennett, G.L. Freeland, J.T. Burns, W.B. Sawyer, and P. Field (1982). In Situ Electrical Resistivity Measurements of Calcareous Sediments; Spec. Pub. 777, p. 156-179.

Arctic Institute Journal

Tooma, Samuel G. (1978). Summer Circulation Patterns, Northern Smith Sound; v. 31, pt. 2, p. 85-96.

Botanica Marina

Itturriaga, R. and A. Zsolnay (1981). Differentiation Between Auto- and Heterotrophic Activity: Problems in the Use of Size Fractionation and Antibiotics; v. XXIV, p. 399-404.

Itturriaga, R. and A. Zsolnay (1983). Heterotrophic Uptake and Transformation of Phytoplankton Extracellular Products; v. XXXVI, p. 375-381.

Boundary-Layer Meteorology

La Violette, P., S. Peteherych, and J.F.R. Gower (1980). Oceanographic Implications of Features in NOAA Satellite Visible Imagery; v. 18, p. 159-175.

Canadian Journal of Fisheries and Aquatic Sciences

Wiesenburg, D.A. and J.M. Brooks (1983). Eddy-enhanced Dispersion of Ocean-dumped Organic Waste at Deep Water Dumpsite 106; v. 40, suppl. 2, p. 248-261.

Climatic Change

Thompson, J. Dana (1978). Ocean Deserts and Ocean Oases; v. 1, p. 205-230.

Copeia

Fisher, Robert A. (1983). Protandric Sex Reversal in Gonostoma Elongatum (Pisces: Gonostomatidae) from the Eastern Gulf of Mexico; n. 2, p. 554-557.

Deep-Sea Research

Clancy, R. Michael (1983). The Effect of Observational Error Correlations on Objective Analysis of Ocean Thermal Structure; v. 30, n. 9A, p. 985-1002.

Green, A. W. (1984). The Bulk Dynamics of the XBT (T-7); v. 31, n. 4A, p. 415-426.

Lavoie, D.M., C.M. Burney, and J.M. Sieburth (1979). Dissolved Carbohydrate and Microbial ATP in the North Atlantic: Concentrations and Interactions; v. 26, p. 1267-1290.

Love, R.H. (1981). A Model for Estimating Distributions of Fish School Target Strengths; v. 28A, n. 7, p. 705-725.

Perkins, H.T. (1981). Low-frequency Forcing of the Tropical Atlantic Ocean Under the ITCZ During GATE; GATE Suppl. I, v. 26, p. 225-236.

Richardson, M.D., H.R. Harvey, and J.S. Patton (1984). Lipid Composition and Vertical Distribution of Bacteria in Aerobic Sediments of the Deep Venezuela Basin; v. 31, p. 403-414.

Earth and Planetary Science Letters

Boyle, E.A., D.F. Reid, S.S. Huested, and J. Hering (1984). Trace Metals and Radium in the Gulf of Mexico: An Evaluation of River and Continental Shelf Sources; v. 69, p. 69-87.

MacDonald, Ken C. and Troy L. Holcombe (1978). Inversion of Magnetic Anomalies and Sea-floor Spreading in the Cayman Trough; v. 40, p. 407-414.

Reid, David F., Robert M. Key, and David R. Shink (1979). Radium, Thorium, and Actinium Extraction from Seawater Using an Improved Manganese-Oxide-Coated Fiber; v. 23, p. 223-226.

Reid, David F., Willard S. Moore, and William M. Sackett (1979). Temporal Variation of 228-Ra in the Near Surface Gulf of Mexico; v. 43, p. 227-236.

Reid, David F. and William M. Sackett (1982). Radium in the Near-Surface Caribbean Sea; v. 60, p. 17-26.

Electro-Optical Systems Design

Guagliardo, J. (1979). CRT Displays Monochromators A-O Modulators; v. 11, n. 2.

Guagliardo, J. (1979). Program for Subsurface Lidar Scattering; v. 11, n. 2, p. 42-43.

Engineering and Mining Journal

Case, J. and Holcombe, T.L. (1977). Simplified Geologic/Tectonic Map of the Caribbean Region; v. 178, n. 11j, p. 49-51.

Environmental Contamination and Toxicology Bulletin

Wiesenburg, D.A., J.M. Brooks, and G. Bodennec (1981). Volatile Liquid Hydrocarbons Around a Production Platform in the Northwest Gulf of Mexico; v. 27, p. 167-174.

Environmental Geology

Reid, D.F. and E.R. Landa (1983). Sorption of Radium-226 from Oil-production Brine by Sediments and Soils; v. 5, n. 1, p. 1-8.

Environmental Science and Technology

Brooks, J.M., D.A. Wiesenburg, R.A. Burke, and M.C. Kennicutt (1981). Gaseous and Volatile Hydrocarbon Inputs from a Surface Oil Spill in the Gulf of Mexico; v. 15, p. 951-959.

Sester, P.J., N.L. Guinasso, N.L. Condra, D.A. Wiesenburg, and D.R. Shink (1983). A Deep-towed Pumping System for Continuous Underway Sampling; v. 17, p. 47-49.

Wiesenburg, D.A., J.M. Brooks, and R.A. Burke (1982). Gaseous Hydrocarbons Around an Active Offshore Gas and Oil Field; v. 16, p. 278-282.

Estuarine, Coastal and Shelf Science

Kinder, T.H., G.L. Hunt, D. Schneider, and J.D. Schumacher (1983). Correlations Between Seabirds and Oceanic Fronts Around the Pribilof Islands, Alaska; v. 16, p. 309-319.

Estuarine Coastal Marine Sciences

Richardson, M.D., S.L. Richardson, and J.L. Laroche (1980). Larval Fish Assemblages and Associations in the Northeast Pacific Ocean Along the Oregon Coast, Winter-Spring, 1971-1975; v. 11, p. 671-699.

Geojournal

Holcombe, Troy L. (1977). Ocean Bottom Features—Terminology and Nomenclature; v. 1, n. 6, p. 25-48.

Geological Society of America Bulletin

Eppler, Duane T., R. Ehrlich, D. Nummedal, and P.H. Schultz (1983). Sources of Shape Variation in Lunar Impact Craters: Fourier Shape Analysis; v. 94, p. 274-291.

Greenewalt, D. and P.T. Taylor (1977). Near-bottom Magnetic Measurements Between the FAMOUS Area and DSDP Sites 332 and 333; v. 89, p. 571-576.

Handschumacher, D.W., R.H. Pilger, J.A. Foreman, and J.F. Campbell (1981). Structure and Evolution of the Easter Plate; Memoir 154, p. 63-76.

Pilger, R.H. and D.W. Handschumacher (1981). The Fixed Hotspot Hypothesis and Origin of the Easter-Salay Gomez-Nazca Trace; p. I, v. 92, p. 437-446.

Geological Society of France Bulletin

Richardson, M.L. (1983). The Effects of Bioturbation on Sediment Elastic Properties; v. 25, p. 505-513.

Geology

Holcombe, T.L. and G.F. Sharman (1983). Post-miocene Cayman Trough Evolution: A Speculative Model; v. 11, p. 714-717.

Lowrie, Allen (1978). Buried Trench South of Panama; v. 6, p. 434-436.

Geo-Marine Letters

Almagor, Gideon, Richard H. Bennett, B.A. McGregor, and L.E. Shephard (1982). Stability Studies of Surficial Sediments in the Wilmington-Lindenkohl Canyons Area, Eastern U.S. Margin; v. 2, p. 129-134.

Bennett, Richard H., James R. Hooper, and Robert Bea (1982). Geological and Geotechnical Research on Seafloor Stability of Continental Margins; v. 2, p. 115-116.

Egloff, J. and G.L. Johnson (1982). Growth Fault on Insular Slope/Rise of Western Iceland: Comparison with SE Greenland Canyons and Slumps; v. 2, p. 143-148.

Hulbert, M.H., R.H. Bennett, and D.N. Lambert (1982). Seabed Geotechnical Parameters from Electrical Conductivity Measurements; v. 2, p. 219-222.

Lambert, D.N. (1982). Submersible Mounted In Situ Geotechnical Instrumentation; v. 2, p. 209-214.

Matthews, James E. (1982). Shear Wave Velocity Measurements in Marine Sediments; v. 2, p. 215-217.

Geophysical and Astrophysical Fluid Dynamics

Warn-Varnas, A., G.M. Dawson, and P.J. Martin (1981). Forecasts and Studies of the Oceanic Mixed Layer During the MILE Experiment; v. 16, p. 1-12.

Warn-Varnas, Alex C. and Steve A. Piacsek (1979). An Investigation of the Importance of Third-order Correlations and Choice of Length Scale in Mixed Layer Modeling; v. 13, p. 225-243.

Geophysical Journal of the Royal Astronomical Society

Frazer, L.N. and J.F. Gettrust (1984). On a Generalization of Filon's Method and the Computation of the Oscillatory Integrals of Seismology; v. 76, n. 2, p. 461-481.

Geophysical Research Letters

Clark, J.R. and P.E. La Violette (1981). Detecting the Movement of Oceanic Fronts Using Registered TIROS-N Imagery; v. 8, n. 3, p. 229-332.

Kinder, T.H. (1984). Net Mass Transport by Internal Waves Near the Strait of Gibraltar; v. 11, n. 10, p. 987-990.

Perkins, H.T. and K.D. Saunders (1984). Atlantic Equatorial Sections During July 1983; v. 11, n. 8, p. 769-772.

Reid, David F. (1976). On the Half-life of 228-Ra and the Errors in Oceanographic Data Due to the Use of the 6.7 Year (Wrong) Value; v. 3, n. 5, p. 253-256.

Geophysics

Ballard, J. Alan (1982). Shear Wave Symposium; v. 47, p. 1741-1746.

Health Physics Press

Reid, David F., William M. Sackett, and Roy F. Spalding (1977). Uranium and Radium in Livestock Feed Supplements; v. 32, p. 535-540.

Initial Reports of the Deep Sea Drilling Project

Ballard, J. Alan, Carl C. Mulcahy, R.L. Wallerstedt, and E.L. Kiser (1984). The Borehole Seismic Experiment in Hole 395A: Engineering and Installation; v. LXXVIII, p. 743-757.

Bowles, F.A., B.E. Tucholke, and P.R. Vogt (1979). Site Survey, DSDP Site 386; v. XLIII, p. 1013-1017.

Vogt, Peter R. and Anna M. Einwich (1979). Magnetic Anomalies and Sea-floor Spreading in the Western North Atlantic, and a Revised Calibration of the Keathley (M) Geomagnetic Reversal Chronology; v. XLIII, p. 857-876.

International Journal of Remote Sensing

Ketchum, R.D., Jr. (1984). SEASAT SAR Sea-Ice Imagery: Summer Melt to Autumn Freeze-up; v. 5, n. 3, p. 533-544.

Isotope Geoscience

Reid, David F. (1984). The Occurrence and Behavior of Radium in Saline Formation Water of the U.S. Gulf Coast Region; v. 2, p. 153-174.

Journal of Analytical and Applied Pyrolysis

Zsolnay, A. (1982). A New Pyrolysis-Mass Spectrometry Approach to Organic Marine Chemistry Using Chemical Ionization; v. 4, p. 47-58.

Zsolnay, A. and Brenda Little (1983). Characterization of Fouling Films by Pyrolysis and Chemical Ionization Mass Spectrometry; v. 4, p. 335-341.

Journal of Atmospheric Sciences

Cheng, Andrew F. and Steve A. Piacsek (1978). A Study of Stratospheric Turbulence and Mean Flow by Constant-level Tracer Balloons in the Northern Hemisphere; v. 35, n. 5, p. 890-898.

Journal of Computational Physics

Madala, Rangarao V. and Steve A. Piacsek (1977). A Semi-implicit Numerical Model for Baroclinic Oceans; v. 23, n. 2, p. 167-178.

Journal of Energy Resources Technology

Bennett, R.H., F.A. Bowles, D.N. Lambert, F.L. Nastav, G.F. Merrill, G. Almagor, and W.J. Burton (1984). Geotechnical and Geological Factors Affecting Offshore Engineering and Seabed Utilization on a Carbonate Margin: St. Croix, V.I.; v. 106, p. 120-129.

Journal of Experimental Marine Biology and Ecology

Briggs, Kevin B., Kenneth R. Tenore, and Robert B. Hanson (1979). The Role of Microfauna in Detrital Utilization by the Polychaete, Neresis Succinea (Frey and Leuckart); v. 36, p. 225-234.

Journal of Fisheries Research Board, Canada

Levenson, Coleman and William T. Leapley (1978). Distribution of Humpback Whales (Megaptera novaeangliae) in the Caribbean Determined by a Rapid Acoustic Method; v. 35, p. 1150-1152.

Journal of Fluid Mechanics

Beardsley, R.C., K.D. Saunders, Alex C. Warn-Varnas, and John M. Harding (1979). An Experimental and Numerical Study of the Secular Spin-up of a Thermally Stratified Rotating Fluid; v. 93, pt. 1, p. 161-184.

Su, M.Y. (1982). Three-dimensional Deep-water Waves, Part 1: Experimental Measurement of Skew and Symmetric Wave Patterns; v. 124, p. 73-108.

Su, M.Y., M.T. Bergin, P. Marler, and R.K. Myrick (1982). Experiments on Nonlinear Instabilities and Evolution of Steep Gravity-Wave Trains; v. 124, p. 45-72.

Warn-Varnas, Alex, William W. Fowlis, Steve A. Piacsek, and Sang Myung Lee (1978). Numerical Solutions and Laser-Doppler Measurements of Spin-up; v. 85, pt. 4, p. 609-639.

Journal of Geophysical Research

Bucca, Paul J. and Thomas H. Kinder (1984). An Example of Meteorological Effects on the Alboran Sea Gyre; v. 89, p. 751-757.

Brooks, James M., David F. Reid, and Bernie B. Bernard (1981). Methane in the Upper Water Column of the Northwestern Gulf of Mexico; v. 86, n. C11, p. 11,029-11,040.

Fenner, Don F. (1978). Sound Speed Structure Across and Anticyclonic Eddy and the Gulf Stream North Wall; v. 83, n. C9, p. 4599-4605.

Hawkins, Jeffrey D. and Peter G. Black (1983). SEASAT Scatterometer Detection of Gale Force Winds Near Tropical Cyclones; v. 88, n. C3, p. 1674-1682.

Hsu, V., J.F. Gettrust, C.E. Helsley, and E. Bert (1983). Local Seismicity Preceding the March 14, 1983, Petatlan, Mexico, Earthquake (Ms = 7.6); v. 88, p. 4247-4262.

Kempner, W.C. and J.F. Gettrust (1982). Ophiolites, Synthetic Seismograms, and Oceanic Crustal Structure: 1. Comparison of Ocean Bottom Seismometer Data and Synthetic Seismograms for the Bay of Islands Ophiolite; v. 87, n. B10, p. 8447-8462.

Kempner, W.C. and J.F. Gettrust (1982). Ophiolites, Synthetic Seismograms, and Oceanic Crustal Structure: 2. A Comparison of Synthetic Seismograms of the Samail Ophiolite, Oman, and the ROSE Refraction Data from the East Pacific Rise; v. 87, n. B10, p. 8463-8476.

Kinder, Thomas A., Paul A. Mazeika, and Donald A. Burns (1983). Measurements of Subtidal Flow in the Lesser Antilles Passages; v. 88, n. C7, p. 4483-4488.

Martin, Paul J. (1984). Mixed Layer Simulation of Buoy Observations Taken During Hurricane Eloise; v. 87, p. 409-427.

Mazeika, P.A., D.A. Burns, and T.H. Kinder (1980). Mesoscale Circulation East of the Southern Lesser Antilles; v. 85, n. C5, p. 2743-2758.

Regan, R.D., D.W. Handschumacher, and M. Suguira (1981). A Closer Examination of Satellite Magnetometer Data for Geological Studies; v. 86, n. B10, p. 9567-9573.

Saunders, Kim D. and F.C. Hamrick (1982). A Note on Cross-Spectrum and Coherence Calculations; v. 87, p. 9699-9703.

Thompson, J. Dana, George H. Born, and George A. Maul (1983). Collinear-track Altimetry in the Gulf of Mexico from SEASAT: Measurements, Models, and Surface Truth; v. 88. n. C3, p. 1625-1636.

Vogt, P.R., P.T. Taylor, L.C. Kovacs, and G.L. Johnson (1978). Detailed Aeromagnetic Investigation of the Arctic Basin; v. 84, p. 1071-1090.

Von Zweck, Ortwin H. and Kim D. Saunders (1981). Contamination of Current Records by Mooring Motion; v. 86, n. C3, p. 2071-2072.

Journal of Glaciology

Ketchum, R.D., Jr. (1983). Dual Frequency Radar Ice and Snow Signatures; v. 29, n. 102, p. 286-295.

Radl, C.J. and J.P. Welsh (1983). Inventory of Arctic Laser Terrain Profiles (1983); v. 29, n. 101, p. 127-132.

Journal of Great Lakes Research

Boyd, Janice D. (1980). Metalimnetic Oxygen Minima in Lake Ontario, 1972; v. 6, n. 2, p. 95-100.

Pickett, R.L., J.E. Campbell, and A.H. Clites (1983). Satellite-tracked Current Drifters in Lake Michigan; v. 9, n. 1, p. 106-108.

Schwab, David J., Paul C. Liu, H.K. Soo, Roland D. Kistler, Howard L. Booker, and Janice D. Boyd (1980). Wind and Wave Measurements Taken from a Tower in Lake Michigan; v. 6, n. 1, p. 76-82.

Journal of Marine Research

Smith, Walker O., George W. Heburn, Richard T. Barber, and James J. O'Brien (1983). Regulation of Phytoplankton Communities by Physical Processes in Upwelling Ecosystems; v. 41, p. 539-556.

Young, D. and M. Young (1977). Regulation of Species Densities of Seagrass-associated Macrobenthos: Evidence from Field Experiments in the Indian River Estuary, Florida; v. 36, p. 569-593.

Journal of Mathematical and Physical Sciences

Li, Huon, S.E. Pai, and M.M. Das (1980). Compactness Effects on Drift of Arctic Pack Ice; v. 14, n. 2.

Journal of Mathematical Physics

Wenzel, Alan R. (1980). Spectral Broadening of Waves Propagating in a Random Medium; v. 21, n. 8, p. 2131-2139.

Journal of Physical Oceanography

Allender, J., J. Albrecht, and G. Hamilton (1983). Observations of Directional Relaxation of Wind Sea Spectra; v. 13, n. 8, p. 1519-1525.

Allender, James H. and James H. Saylor (1979). Model and Observed Circulation Throughout the Annual Temperature Cycle of Lake Michigan; v. 9, n. 3, p. 573-579.

Hallock, Z.R., W.J. Teague, and R.D. Broome (1982). A Deep, Thick Isopycnal Layer Within an Anticyclonic Eddy; v. 11, p. 1674-1677.

Hurlburt, H.E. and J.D. Thompson (1980). A Numerical Study of Loop Current Intrusions and Eddy Shedding; v. 10, p. 1611-1651.

Kinder, Thomas H., James D. Schumacher, and Donald V. Hansen (1980). Observation of a Baroclinic Eddy: An Example of Mesoscale Variability in the Bering Sea; v. 10, n. 8, p. 1228-1245.

La Violette, Paul E. (1984). The Advection of Submesoscale Thermal Features in the Alboran Sea Gyre; v. 14, n. 3, p. 550-565.

McClain, C.R., N.E. Huang, and P.E. La Violette (1982). Measurements of Sea-State Variations Across Oceanic Fronts Using Laser Profilometry; v. 12, n. 11, p. 1228-1244.

Perkins, H.T. and E.A. D'Asaro (1984). The Near-inertial Internal Wave Spectrum in the Late Summer Sargasso Sea; v. 14, p. 489-505.

Schumacher, J.D. and T.H. Kinder (1983). Low Frequency Current Regimes Over the Bering Sea Shelf; v. 13, n. 4, p. 607-623.

Schumacher, J.D., T.H. Kinder, D.J. Pashinski, and R.L. Charnell (1979). A Structural Front Over the Continental Shelf of the Eastern Bering Sea; v. 9, n. 1, p. 79-87.

Teague, W.J. and R.J. Wahl (1983). Estimation of Brunt-Vaisala Frequency from Temperature Profiles; v. 13, p. 2236-2240.

Journal of Sedimentary Petrology

Feuillet, Jean-Pierre and Peter Fleischer (1980). Estuarine Circulation: Controlling Factor of Clay Mineral Distribution in James River Estuary, Virginia; v. 50, n. 1, p. 0267-0279.

Journal of the Acoustical Society of America

Berkson, Jonathan M. (1980). Measurements of Coherence of Sound Reflected from Ocean Sediments; v. 68, n. 5, p. 1436-1441.

Chin-Bing, S., J.A. Davis, and R.B. Evans (1982). Nature of the Lateral Wave Effect on Bottom Loss Measurements; v. 71, p. 1433-1437.

Dicus, R.L. (1981). Impulse Response Estimation with Underwater Explosive Charge Acoustic Signals; v. 70, n. 1, p. 122-?.

Evans, R.B. (1983). A Coupled Mode Solution for Acoustic Propagation in a Waveguide with Stepwise Depth Variations of a Penetrable Bottom; v. 74, n. 1, p. 188-195.

Gilbert, Kenneth E. (1980). Reflection of Sound from a Randomly Layered Ocean Bottom; v. 68, p. 1454-1458.

Gilbert, Kenneth E. (1983). A Propagator Matrix Method for Periodically Stratified Media; v. 73, n. 1, p. 137-142.

Gold, Barry A. and Wayne E. Renshaw (1978). Joint Volume Reverberation and Biological Measurements in the Tropical Western Atlantic; v. 63, n. 6, p. 1809-1819.

Hackman, Roger H. and Michael F. Werby (1984). Nearfield Effects in Acoustic Scattering; v. 75, n. 3, p. 1001-1003.

Kinney, Wayne A. (1983). Scattering from a Corrugated Surface: Comparison Between Experiment, Helmholtz-Kirchoff Theory and the Facet-Ensemble Method; v. 73, n. 1, p. 183-194.

Kinney, Wayne A. and C.S. Clay (1984). The Spatial Coherence of Sound Scattered from a Wind-driven Surface: Comparison Between Experiment, Eckart Theory, and the Facet-Ensemble Method; v. 75, p. 145-148.

Kinney, Wayne A. and Allan D. Perce (1980). Caustics and the Spreading of Adjacent Acoustic Rays; v. 67, n. 4, p. 1145-1148.

Levenson, Coleman and Randy Doblar (1976). Long-range Acoustic Propagation Through the Gulf Stream; v. 59, n. 5, p. 1134-1141.

Love, R.H. (1977). Target Strength of an Individual Fish at Any Aspect; v. 62, p. 1397-1403.

Love, R.H. (1978). Resonant Acoustic Scattering by Swimbladder-bearing Fish; v. 64, p. 571-580.

Mackenzie, Kenneth V. (1981). Discussion of Sea Water Sound-speed Determinations; v. 70, n. 3, p. 801-806.

Matthews, James E. (1980). Heuristic Physical Property Model for Marine Sediments; v. 68, n. 5, p. 1361-1375.

Ramsdale, Dan J. and Roger A. Howerton (1980). Effect of Element Failure and Random Errors in Amplitude and Phase on the Sidelobe Level Attainable with a Linear Array; v. 68, n. 3, p. 901-906.

Richardson, Michael D. (1984). Environmental Bottom Characterization Required for Modeling and Prediction of High Frequency Acoustic Bottom Scattering; Suppl. 75, p. 550-551.

Welsh, J.P. (1983). Characterization of Sea Ice; v, 74, suppl. 1.

Wenzel, Alan R. (1982). Radiation and Attenuation of Waves in a Random Medium; v. 71, p. 26-35.

Wenzel, Alan R. (1982). A Method for Analyzing Wave Propagation in Random Media; v. 71, p. 249-254.

Wenzel, Alan R. (1983). Supersaturation of Complex-Amplitude Fluctuations of Waves Propagating in a Random Medium; v. 74, p. 1021-1024.

Werby, Michael F. and L.H. Green (1984). A Comparison of Acoustical Scattering from Fluid-loaded Elastic Shells and Soft Objects; v. 76, n. 4, p. 1227-1230.

Journal of the Water Pollution Control Federation

Harrison, W., D.L. McCown, K.D. Saunders, and J.D. Ditmars (1979). Wintertime Raw-water Contamination at Chicago's South Water Filtration Plant; v. 51, n. 10, p. 2432-2446.

Journal of Underwater Acoustics

Marshall, Samuel W. (1983). Topographic Noise Stripping: Introduction; v. 33, n. 1.

Marshall, Samuel W. (1984). High Resolution Beamforming; v. 34, n. 2, p. 75-76.

Ramsdale, Dan J. and M.Z. Lawrence (1984). Horizontal Line Array Performance Using Maximum Entropy Beamforming; v. 34, n. 2, p. 93-114.

Limnology and Oceanography

Burke, Roger A., David F. Reid, James M. Brooks, and Dennis M. Lavoie (1983). Upper Water Column Methane Geochemistry in the Eastern Tropical North Pacific; v. 28, n. 1, p. 19-32.

Tucker, W.A. and A.W. Green (1977). A Time-dependent Model of the Lake-averaged, Vertical Temperature Distribution of Lakes; v. 22, n. 4, p. 687-699.

London Geological Society

Gorsline, D.S., H.A. Karl, D.E. Drake, R.L. Kolpack, S.E. Thornton, and P. Fleischer (1984). California Borderland Suspended Sediment Studies; Spec. Pub. 15.

Marine Biology

Zsolnay, A. and R. Iturriaga (1981). Transformation of Some Dissolved Organic Compounds by a Natural Heterotrophic Population; v. 62, p. 125-129.

Marine Geodesy

Born, George H., David B. Lame, and Jim L. Mitchell (1984). A Survey of Oceanographic Satellite Altimetric Missions; v. 8, n. 1-4, p. 3-16.

Hurlburt, Harley E. (1984). The Potential for Ocean Prediction and the Role of Altimeter Data; v. 8, n. 1-4, p. 17-66.

Marine Geology

Andrews, J., G. Friedrich, G. Pautot, W. Pluger, V. Renard, M. Melguen, D. Cronan, J. Craig, M. Hoffert, P. Stoffers, S. Shearme, T. Thijssen, G. Glasby, N. LeNotre, and P. Saget (1983/1984). The Hawaii-Tahiti Transect: The Oceanographic Environment of Manganese Nodule Deposits in the Central Pacific; v. 54, p. 109-130.

Bowles, F.A. (1980). Stratigraphy and Sedimentation of the Archipelagic Apron and Adjoining Area Southeast of Bermuda (1980); v. 37, p. 267-294.

Bowles, Frederick A. and Walter H. Jahn (1983). Geological/Geophysical Observations and Inferred Bottom-current Flow: South Flank Iceland-Faeroe Ridge; v. 52, p. 159-185.

Bowles, F.A, W. Ruddiman, and W.H. Jahn (1978). Acoustic Stratigraphy, Structure, and Depositional History of the Nicobar Fan, E. Indian Ocean; v. 26, p. 269-288.

Firek, F., G.L. Shidler, and P. Fleischer (1977). Heavy-Mineral Variability in Bottom Sediments of the Lower Chesapeake Bay, Virginia; v. 23, p. 217-235.

Holcombe, Troy L. and Willard S. Moore (1977). Paleocurrents in the Eastern Caribbean: Geologic Evidence and Implications; v. 23, p. 35-66.

Lowrie, Allen, Julius Egloff, Jr., and Walter H. Jahn (1978). Kane Seamount in the Cape Verde Basin, Eastern Atlantic; v. 26, M29-35.

Lowrie, A., J. Stewart, R.H. Stewart, Tj. Van Andel, and L. McRaney (1982). Location of the Eastern Boundary of the Cocos Plate During the Miocene; v. 45, p. 261-279.

Richardson, M.D. and D.K. Young (1980). Geoacoustic Models and Bioturbation; v. 38, p. 205-218.

Richardson, Michael D., David K. Young, and Kevin B. Briggs (1983). Effects of Hydrodynamic and Biological Processes on Sediment Geoacoustic Properties in Long Island Sound, U.S.A.; v. 52, p. 201-226.

Ruddiman, W.F. and F.A. Bowles (1976). Early Interglacial Bottom-current Sedimentation on the Eastern Reykjanes Ridge; v. 21, p. 191-210.

Stanley, M. and P.T. Taylor (1977). Sediment Transport Down a Seamount Flank by a Combined Current and Gravity Process; v. 23, n. 1, p. 77-88.

Marine Geophysical Researches

Lowrie, Allen, Thomas Aitken, Paul Grim, and Linda McRaney (1979). Fossil Spreading Center and Faults Within the Panama Fracture Zone; v. 4, p. 153-166.

Marine Science Bulletin

Kinder, T.H. (1983). Shallow Currents in the Caribbean Sea and Gulf of Mexico as Observed with Satellite-tracked Drifters; v. 33, n. 2, p. 239-246.

Marine Technology Society Journal

Jahn, W.H., T. Simkin, D.J. Stanley, and P.T. Taylor (1982). Deep-ocean Photography: A Study of the Gilliss Seamount; v. 16, p. 11-22.

Materials Performance

Little, Brenda J., John Morse, George Loeb, and Frank Spiehler (1981). Gulf of Mexico Study of Biofouling on OTEC Heat Exchanger Candidate Alloys; v. 20, n. 8.

Monthly Weather Review

Clancy, R.M. (1981). A Note on Finite Differencing of the Advection-Diffusion Equation; v. 109, n. 9, p. 1807-1809.

Clancy, R.M., J.D. Thompson, H.E. Hurlburt and J.D. Lee (1979). A Model of Mesoscale Air-sea Interaction in a Sea Breeze-Coastal Upwelling Regime; v. 107, n. 11, p. 1476-1505.

Sweet, W., R. Fett, J. Kerling, and P.E. La Violette (1981). Air-Sea Interaction Effects in the Lower Troposphere Across the North Wall of the Gulf Stream; v. 109, n. 5, p. 1042-1052.

Nature

Harding, John M. (1977). Long-term Variations in Western Tropical Pacific Cyclogenesis Associated with the Southern Oscillation; v. 262, p. 41-42.

Ocean Engineering

Welsh, J.P., I.M. Lissauer, G.L. Hufford, T.S. Ellis, B.D. Thompson, L.D. Farmer, and R.R. Hiltabrand (1977). Some Dynamics of Spilled Oil in a Fractured Ice Field in Buzzards Bay, Massachusetts; v. 4, p. 197-203.

Ocean Optics

Arnone, Robert A. (1984). Secchi Depth Atlas of the World Coastlines; Society of Photo-optical Instrumentation Engineers, VII, v. 489, p. 195-201.

Bright, Duane, Jerald W. Caruthers, and George Kattawar (1984). The Effect of Detector Field-of-View on Laser Backscatter and Bottom Reflection Measurements; VII, v. 489, p. 281-286.

Photogrammetric Engineering and Remote Sensing

Farmer, L.D. and R.Q. Robe (1977). Photogrammetric Determination of Iceberg Volumes, v. XLII, p. 183-189.

Lissauer, Ivan M. and L. Dennis Farmer (1980). Determining Synoptic Surface Current Patterns Using Aerial Photography; v. 46, n. 3, p. 333-336.

Physics of Fluids

Su, M.Y. (1982). Evolution of Groups of Gravity Waves with Moderate to High Steepness; v. 25, n. 12, p. 2167-2174.

Su, M.Y. and A.W. Green (1984). Coupled Two- and Three-dimensional Instabilities of Surface Gravity Waves; v. 27, p. 2595-2597.

Progress in Oceanography

Clancy, R. Michael and Kenneth D. Pollak (1983). A Real-time Synoptic Ocean Thermal Analysis/Forecast System; v. 12, p. 383-424.

Remote Sensing of the Environment

Hickman, G.D., J.A. Edmonds, and R.V. Lynch (1984). Laser-induced Marine Bioluminescence Measurements and the Potential for Airborne Remote Sensing; v. 15, p. 77-89.

Holyer, Ronald J. (1978). Toward Universal Multispectral Suspended Sediment Algorithms; v. 7, p. 323-338.

Ketchum, R.D., Jr. and A.W. Lohanick (1980). Passive Microwave Imagery of Sea Ice at 33 GHz; n. 9, p. 211-223.

Review of Geophysical Space Physics

Allen, J.S., R.C. Beardsley, J.O. Blanton, W.C. Boicourt, B. Butman, L.K. Coachman, A. Huyer, T. Kinder, T.C. Royer, J.D. Schumacher, R.L. Smith, W. Sturges, and C.D. Winant (1983). Physical Oceanography of Continental Shelves; v. 21, n. 5, p. 1149-1181.

Review of Scientific Instrumentation

Guagliardo, J.L. and H.L. Dufilho (1980). Range-resolved Brillouin Scattering Using a Pulsed Laser; v. 51, n. 1, p. 79-81.

Science

Shokes, Robert F., Peter K. Trabant, Bob J. Presley, and David F. Reid (1977). Anoxic, Hypersaline Basin in the Northern Gulf of Mexico; v. 196, p. 1443-1466.

Sea Technology

Pickett, R.L., R.A. Arnone, R.M. Partridge, and J.A. Galt (1984). The Persian Gulf, Oil and Natural Circulation; v. 25, p. 23-25.

Seismological Society of America

Casanova, D., V. Hsu, Eduard Berg, Charles E. Helsley, and Joseph F. Gettrust (1984). Aftershock Activity of the Petatlan Earthquake: The First 54 Hours; v. 74, p. 2451-2461.

Society of Economic Paleontologists and Mineralogists

Bennett, R.H. and T.A. Nelson (1983). Seafloor Characteristics and Dynamics Affecting Geotechnical Properties at Shelfbreaks; Spec. Pub. 33, p. 333-355.

Wave Motion

Wenzel, Alan R. (1983). Radiation and Attenuation of Low- and High-frequency Waves in a Random Medium; v. 5, p. 215-223.

Journal Addendum

Arnone, R. A. and **P. E. La Violette** (1984). A Method of Selecting Optimal Angstrom Coefficients to Obtain Quantitative Ocean Color Data from Nimbus-7 CZCS. *Ocean Optics VII, SPIE* 489, 187.

Arnone, R. A., S. P. Tucker, and F. A. Hilder (1984). Secchi Depth Atlas of the World Coastlines. *Ocean Optics VII, SPIE* 489, 195.

Barker, F. S. and D. R. Barraclough (1985). The Effects of the Non-uniform Distribution of Magnetic Observatory Data on Secular Variation Models. *Physics of the Earth and Planetary Interiors* 37, 65–73.

Bennett, R. H., J. T. Burns, F. L. Nastav, J. Lipkin, and C. M. Percival (1985). Deep-ocean Piezometer Probe Technology for Geotechnical Investigations. *Journal of Oceanic Engineering* IE-10(1), 17–22.

Bennett, R. H., L. Lehman, M. H. Hulbert, G. R. Harvey, S. A. Bush, E. B. Forde, P. Crews, and **W. B. Sawyer** (1985). Interrelationships of Organic Carbon and Submarine Sediment Geotechnical Properties. *Marine Geotechnology* 6(1), 61–98.

Born, G. H., D. B. Lame, and **J. L. Mitchell** (1984). A Survey of Oceanographic Satellite Altimetric Missions. *Marine Geodesy* 8(1-4), 3–16.

Briggs, K. B. (1985). Deposit Feeding by Some Deep-sea Megabenthos from the Venezuela Basin: Selective or Non-selective. *Marine Ecology—Progress Series* 21, 127–134.

Evans, R. B. and **K. E. Gilbert** (1985). The Periodic Extension of Stepwise Coupled Modes. *Journal of the Acoustical Society of America* 77, 983-988.

Evans, R. B. and **K. E. Gilbert** (1985). Acoustic Propagation in a Refracting Ocean Waveguide with an Irregular Interface. *Computers and Mathematics with Applications* 11(7/8), 795–805.

Hall, M., D. F. Gordon, and **White, D.** (1983). Improved Methods for Determining Eigenfunctions in Multilayered Normal Mode Problems. *Journal of the Acoustical Society of America* 73, 153–162.

Heburn, G. W. (1985). Effects of Wind Versus Hydraulic Forcing on the Dynamics of the Western Mediterranean Sea. *Rapp. Comm. int. Mer Medit.* 29(3), 65–67.

Kinder, T. H. (1984). Net Mass Transport by Internal Waves Near the Strait of Gibraltar. *Geophysical Research Letters* 11(10), 987–990.

Kinney, W. A. and J. G. Zornig (1985). Azimuthal Dependence of Bistatic Surface Scattering: Comparison Between Theory and Experiment. *Journal of the Acoustical Society of America* 77(4), 1403.

La Violette, P. E. (1985). A Report on the CIESM Session on the Western Mediterranean Circulation Experiment, 17 October 1984. *Rapp. Comm. int. Mer Medit.* 29(3), 27–30.

La Violette, P. E. and **R. A. Arnone** (1985). A Preliminary Study of a Standing Internal Wave in the Western Approaches to the Strait of Gibraltar. *Rapp. Comm. int. Mer Medit.* 29(3), 131–132.

Little, B. J. and J. Jacobus (1985). A Comparison of Two Techniques for the Isolation of Adsorbed Dissolved Organic Material from Seawater. *Organic Geochemistry* 8(1), 27–33.

Little, B. J. and **A. Zsolnay** (1985). Chemical Fingerprinting of Adsorbed Organic Materials on Metal Surfaces. *Journal of Colloid and Interface Science* 104(1).

Lybanon, M. (1985). A Simple Generalized Least-Squares Algorithm. *Computers and Geosciences* 11(4), 501–508.

Martin, P. J. (1985). Simulation of the Mixed Layer at OWS November and Papa with Several Models. *Journal of Geophysical Research* 90(C1), 903–916.

McDonald, B. E., S. A. Piacsek, and **G. Dawson-Martin** (1985). Computational Methods for Two Problems in Air-Sea Interaction. *Rapp. Comm. int. Mer Medit.* 29(3), 53–54.

Perkins, H. T. and **T. H. Kinder** (1985). The Flow of Atlantic Water Into the Alboran Sea During Donde Va. *Rapp. Comm. int. Mer Medit.* 29(3), 139–140.

Perkins, H. T. and **K. D. Saunders** (1984). Atlantic Equatorial Sections During July 1983. *Geophysical Research Letters* 11(8), 769–772.

Pickett, R. E., R. M. Partridge, **R. A. Arnone**, and J. A. Galt (1984). The Persian Gulf, Oil and Natural Circulation. *Sea Technology*, September.

Pickett, R. E., R. M. Partridge, J. A. Galt, and **R. A. Arnone** (1984). The Persian Gulf Via Satellites. *Oceanographic Monthly Summary* IV(9), OceaNotes.

Reid, D. F. (1984). Radium Variability Produced by Shelf-water Transport and Mixing in the Western Gulf of Mexico. *Deep Sea Research* 31(12), 1501–1510.

Richardson, M. D. (1983). The Effects of Bioturbation on Sediment Elastic Properties. *Bulletin of the Geological Society of France* 25, 505-513.

Richardson, M. D. (1984). Environmental Bottom Characterization Required for Modeling and Prediction of High Frequency Acoustic Bottom Scattering. *Journal of the Acoustical Society of America* S75, 550-551.

Wenzel, A. R. (1985). Comment on "Second-order Rytov Approximation." *Journal of the Optical Society of America A* 2, 774.

Werby, M. F. and **S. A. Chin-Bing** (1985). Some Numerical Techniques and Their Use in the Extension of T-Matrix and Null-field Approaches to Scattering. *Comput.* 11(7/8), 717-731.

Werby, M. F., K. Davey, and J. P. Miller (1985). The Use of Integral Equations and the Conjugate Gradient Method in Field Theory Problems. *Journal of Mathematics Computer in Simulation*, Special Issue, Z. Candes (ed.).

Werby, M. F., C. Feuillade, and G. Gaunaurd (1984). Scattering from Fluid Loaded Layered Elastic Objects. *Journal of the Acoustical Society of America* 76(S1).

Werby, M. F. and G. Gaunaurd (1984). Criteria for Suitable Background Choice in Resonance Acoustic Scattering by Shells. *Journal of the Acoustical Society of America* 76(S1).

Werby, M. F. and G. Gaunaurd (1985). Resonance Response of Submerged, Acoustically Excited Thick and Thin Shells. *Journal of the Acoustical Society of America* 77.

Werby, M. F. and G. Gaunaurd (1985). Scattering from Spheroidal Elastic Shells at Various Incident Angles. *Journal of the Acoustical Society of Ameri a* 77(S1).

Werby, M. F. and **K. E. Gilbert** (1985). Target Characteristic from High Aspect Ratio Objects. *Journal of the Acoustical Society of America* 77(S1), 1038.

Werby, M. F. and L. H. Green (1983). An Extended Unitary Approach—Acoustical Scattering from Elastic Shells Immersed in a Fluid. *Journal of the Acoustical Society of America* 74, 625.

Werby, M. F. and L. H. Green (1985). Calculation of Monostatic Angular Distributions for Elongated Elastic Shells. *Journal of the Acoustical Society of America* 76(S1).

Publications*

Allender, J. H. and **M. Lybanon** (1982). *A Discrete Nonlinear Spectral Model for Ocean Wave Prediction, Description of Computer Program*. Naval Ocean Research and Development Activity, NSTL, Mississippi, Technical Note 147.

Allender, J. H. and M. Lybanon (1982). *Application of a Discrete Nonlinear Spectral Model to Ideal Cases of Wind Wave Generation*. Naval Ocean Research and Development Activity, NSTL, Mississippi, Technical Note 148.

Almagor, G., **R. H. Bennett, D. N. Lambert,** E. B. Forde, and L. S. Shephard (1983). Analysis of Slope Stability, Wilmington to Lindenkohl Canyons, U.S. Mid-Atlantic Margin. *Seabed Mechanics, Proceedings of IUTAM/IUGG Symposium*, University of Newcastle Upon Tyne, U.K., 5-9 September, 77-86.

Anderson, R. S. (1979). *Cruise Report for USNS DESTEIGUER Operations in OUTPOST GUMBO*. Naval Ocean Research and Development Activity, NSTL, Mississippi, Technical Note 48.

Anderson, R. S. and R. Dicus (1982). *Effective Low-frequency Geoacoustic Sediment Properties*. Naval Ocean Research and Development Activity, NSTL, Mississippi, NORDA Report 21.

Arnone, R. A. (1981). Interpretation of Satellite Imagery Related to Bathymetric Features. *Proceedings of the Ocean Survey 8th Hydrographic Survey Conference*, Norfolk, Virginia, 12-16 January.

Arnone, R. A. (1981). Bathymetric and Hydrographic Coastal Feature Recognition Using Landsat and CZCS Imagery. *Applications of Aerospace Remote Sensing in Marine Research at the International Council for the Exploration of the Sea, 69th Statutory Meeting*, Woods Hole, Massachusetts, 5-15 October.

Arnone, R. A. (1982). *Annotated Bibliography of Water Optical Properties of Ocean Waters*. Naval Ocean Research and Development Activity, NSTL, Mississippi, Technical Note 115.

Arnone, R. A. (1983). *Water Optics of the Mississippi Sound*. Naval Ocean Research and Development Activity, NSTL, Mississippi, NORDA Report 63.

Arnone, R. A. (1983). Optical Variability in the Alboran Front Monitored by CZCS. *Proceedings of the Fourth Annual Gulf of Mexico Information Transfer Meeting*, Minerals Management Service, Gulf of Mexico Regional Office, 87-91.

Arnone, R. A. (1985). *Coastal Secchi Depth Atlas*. Naval Ocean Research and Development Activity, NSTL, Mississippi, NORDA Report 83.

Arnone, R. A. (1983). Evaluation of CZCS and Landsat for Coastal Optics and Water Properties. *Seventeenth Symposium on Remote Sensing of the Environment*. Ann Arbor, Michigan, 9-13 May.

Arnone, R. A. and **E. Arthur** (1980). *Interpretation of Hydrographic Features Using Landsat Images*. Naval Ocean Research and Development Activity, NSTL, Mississippi, NORDA Report 39.

Arnone, R. A., **R. Brown**, F. Townsend, and A. Zied (1983). *Water Penetration Photogrammetry: Volume I, Feasibility and Evaluation Study*. Naval Ocean Research and Development Activity, NSTL, Mississippi, Technical Note 186.

Arnone, R. A., G. M. Dawson, G. W. Heburn, T. H. Kinder, P. E. La Violette, B. E. McDonald, H. T. Perkins, S. A. Piacsek, et al. from other agencies (1985). *Contributions to the Oceanography of the Western Alboran Sea*. Naval Ocean Research and Development Activity, NSTL, Mississippi, Technical Note 315.

Arnone, R. A. and **R. J. Holyer** (1984). *Ocean Optical Remote Sensing Capability Statement*. Naval Ocean Research and Development Activity, NSTL, Mississippi, Technical Note 264.

Arnone, R. A. and **P. E. La Violette** (1984). *Bio-optical Variability in the Alboran Sea as Assessed by NIMBUS-7 CZCS*. Naval Ocean Research and Development Activity, NSTL, Mississippi, Technical Note 283.

Arnone, R. A. and **P. E. La Violette** (1984). *Satellite Definition of the Geo- and Bio-optical Variation of Coastal Eddies Associated with the African Current*. Naval Ocean Research and Development Activity, NSTL, Mississippi, Technical Note 291.

*This listing contains all unclassified NORDA publications other than refereed journals.

Arnone, R. A. and **P. E. La Violette** (1984). A Method of Selecting Optimal Angstrom Coefficients to Obtain Quantitative Ocean Color Data from NIMBUS-7 CZCS. *Proceedings, Ocean Optics VII*, v. 489, 187.

Arnone, R. A., S. P. Tucker, and F. A. Hilder (1984). Secchi Depth Atlas of the World Coastlines. *Proceedings of Ocean Optics VII*, v. 489.

Ballard, J. A. (1977). *Interpretation of Single Channel Seismic Reflection Records*. Naval Ocean Research and Development Activity, NSTL, Mississippi, NORDA Report 1.

Ballard, J. A. (1982). *Geology of a Stable Intraplate Region: The Cape Verde/Canary Basin*. Naval Ocean Research and Development Activity, NSTL, Mississippi, NORDA Report 45.

Ballard, J. A. and R. C. Mitchell-Thome (1978). Cape Verde Islands. *Encyclopedia of World Regional Geology, Part II*, R. W. Fairbridge (ed.), Dowden, Hutchinson, and Ross, Inc.

Becker, A., H. Morrison, and **K. Smits** (1983). *Analysis of Airborne Electromagnetic Systems for Mapping Thickness of Sea Ice*. Naval Ocean Research and Development Activity, NSTL, Mississippi, Technical Note 261.

Bennett, R. H. (1983). *Seafloor Geosciences Division: Mission, Technical Specialties, Accomplishments, and Activities, 1982 to 1983*. Naval Ocean Research and Development Activity, NSTL, Mississippi, Technical Note 214.

Bennett, R. H., F. A. Bowles, D. N. Lambert, F. L. Nastav, G. F. Merrill, G. Almagor, and W. J. Burton (1983). Geotechnical and Geological Factors Affecting Offshore Engineering and Seabed Utilization on a Carbonate Margin: St. Croix, V.I. *Proceedings, Second International Offshore Mechanics and Arctic Engineering Symposium*, American Society of Mechanical Engineers, 311–321.

Bennett, R. H., J. T. Burns, T. L. Clarke, J. R. Faris, E. B. Forde, and A. F. Richards (1982). Piezometer Probes for Assessing Effective Stress and Stability in Submarine Sediments. *Marine Slides and Other Mass Movements*, S. Saxov and J. K. Nieuwenhuis (eds.), Plenum Publishing Corp., 129–161.

Bennett, R. H., J. T. Burns, J. Lipkin, and C. M. Percival (1983). Piezometer Probe Technology for Geotechnical Investigations in Coastal and Deep-ocean Environments. Secretariat, Range Commanders Council, White Sands Missile Range, New Mexico. *Proceedings, Twelfth Transducer Workshop*, L. Bates and K. D. Cox (eds.), Melbourne, Florida, 7–9 June, 377–404.

Bennett, R. H., D. N. Lambert, M. H. Hulbert, **J. T. Burns, W. B. Sawyer**, and G. L. Freeland (1983). Electrical Resistivity/Conductivity in Seabed Sediments. *CRC Handbook of Geophysical Exploration at Sea*, R. A. Geyer (ed.), CRC Press, Inc., Boca Raton, Florida, 333–374.

Bennett, R. H., F. L. Nastav, and W. R. Bryand (1984). Strength Measurements. *Sedimentology, Physical Properties, and Geochemistry in the Initial Reports of the Deep Sea Drilling Project, Volumes 1–44: An Overview*, G. R. Heath (ed.), World Data Center A, National Academy of Sciences, Washington, D.C., World Data Center A for Marine Geology and Geophysics Report MGG-1, 129–146.

Bennett, R. H. and T. A. Nelsen (1983). Seafloor Characteristics and Dynamics Affecting Geotechnical Properties at Shelfbreaks. *The Shelfbreak: Critical Interface on Continental Margins*, D. T. Stanley and G. T. Moore (eds.), SEPM Special Pub. No. 33, 333–355.

Bergin, M. and **T. H. Kinder** (1983). *Expendable Bathythermograph (XBT) Measurements in the Western Alboran Sea, October 1982*. Naval Ocean Research and Development Activity, NSTL, Mississippi, Technical Note 224.

Berkson, J. M. and **J. E. Matthews** (1983). Statistical Properties of Seafloor Roughness. *Acoustics and the Sea Bed*, N. G. Pace (ed.), Bath University Press, Bath, England, 215–223.

Blake, D. W. (1982). *The Structure and Energy Budget of the Heat Low Over the Empty Quarter in Saudi Arabia During May 1979*. Naval Ocean Research and Development Activity, NSTL, Mississippi, Technical Note 170.

Botseas, G., D. Lee, and **K. E. Gilbert** (1983). *IFD: Wide Angle Capability*. Naval Underwater Systems Center, Technical Report 6905.

Bowles, F. A. and **P. Fleischer** (1983). Orinoco/Amazon River Sediment Input to the Eastern Caribbean Basin. *EOS, Transactions of the American Geophysical Union* 64(52), 1076.

Boyd, J. D. (1982). *Ocean Current Effects on Marine Seismic Systems and Deployments*. Naval Ocean Research and Development Activity, NSTL, Mississippi, Technical Note 132.

Boyd, J. D. (1984). Currents Near DSDP Hole 395A and Effects on Components of the Marine Seismic System Project. *Initial Reports of the Deep Sea Drilling Project*, v. 78B, B. Biju-Duval et al. (eds.), Washington, D.C., U.S. Government Printing Office.

Boyd, J. D. and **T. H. Kinder** (1979). *Current Meter Data from the Southeastern Caribbean Sea, August 1978-February 1979.* Naval Ocean Research and Development Activity, NSTL, Mississippi, Technical Note 76.

Boyd, J. D. and **T. H. Kinder** (1982). Vertical Wavenumber Spectra of Temperature, Salinity, and Sigma-t Profiles in the Southeastern Caribbean. *EOS, Transactions of the American Geophysical Union* 63, 344.

Boyd, J. D. and **H. T. Perkins** (1984). Estimates of Vertical Heat and Salt Fluxes in a Thermohaline Staircase. *EOS, Transactions of the American Geophysical Union* 65, 954.

Boyd, J. D., H. T. Perkins, and **K. D. Saunders** (1983). Characteristics of Thermohaline Step Structures Off the Northeast Coast of South America. *EOS, Transactions of the American Geophysical Union* 64, 1058.

Boyd, J. D., H. T. Perkins, and **K. D. Saunders** (1985). *Hydrographic Measurements Off the Northeast Coast of South America, July 1983.* Naval Ocean Research and Development Activity, NSTL, Mississippi, Technical Note 305.

Briggs, K. B. (1984). *Physical and Acoustical Properties of Surface Sediment from the Venezuela Basin: A Data Report.* Naval Ocean Research and Development Activity, NSTL, Mississippi, Technical Note 238.

Briggs, K. B. and **M D. Richardson** (1983). Physical and Acoustic Properties of Surface Sediments from the Venezuela Basin, Caribbean Sea. *EOS, Transactions of the American Geophysical Union* 64(52), 1076.

Briggs, K. B. and **M. D. Richardson** (1984). *The Abyssal Megabenthic Fauna of the Venezuela Basin, Caribbean Sea* (abs.). Benthic Ecology Meetings, Goucher College, Baltimore, Maryland, 23-25 March.

Bright, D. C. (1983). *A Plan for Optical Oceanography R&D to Support Mapping, Charting and Geodesy.* Naval Ocean Research and Development Activity, NSTL, Mississippi, Technical Note 201.

Brock, H. K. (1978). *The AESD Parabolic Equation Model.* Naval Ocean Research and Development Activity, NSTL, Mississippi, Technical Note 12.

Brooks, J. M., L. A. Barnard, **D. A. Wiesenburg**, M. C. Kennicutt, and K. A. Kvenvolden (1983). Molecular and Isotopic Composition of Hydrocarbons at Site 533, Deep Sea Drilling Project, Leg 76. *Initial Reports of the Deep Sea Drilling Project*, v. 76, R. E. Sheridan, F. M. Gradstein, et al. (eds.), U.S. Government Printing Office, Washington, D.C., 377-389.

Brooks, J. M., **D. A. Wiesenburg**, G. Bodennec, and T. Sauer, Jr. (1983). Dispersion and Background Measurements of Volatile Organic Wastes at the Puerto Rico Deep Water Industrial Waste Dumpsite. *Industrial and Seawater Wastes in the Ocean*, I. W. Duedall et al. (eds.), John Wiley and Sons, Inc., New York, 171-198.

Brooks, J. M., **D. A. Wiesenburg**, and T. Ichiye (1982). Use of Volatile Organics as Tracers of Waste Dispersion at an Ocean Dumpsite. *EOS, Transactions of the American Geophysical Union* 63, 77.

Brooks, J. M., **D. A. Wiesenburg**, C. R. Schwab, E. L. Estes, and R. Shokes (1981). Surficial Sediments and Suspended Particulate Matter. *Environmental Effects of Offshore Oil Production—The Buccaneer Gas and Oil Field Study*, B. S. Middleditch (ed.), Plenum Press, New York, 69-115.

Brown, R. M. (1983). *Pattern Analysis in the Marine Environment: An Ocean Science and Technology Workshop, 24-26 March 1982.* Naval Ocean Research and Development Activity, NSTL, Mississippi, Technical Note 176.

Brown, R. M. (1985). *Preprocessing for Symbol Recognition.* Naval Ocean Research and Development Activity, NSTL, Mississippi, Technical Note 210.

Brown, R. M., R. A. Arnone, A. Zied, F. Townsend, and F. Scarpace (1983). *Water Penetration Photogrammetry, Volume 1: Feasibility and Evaluation Study.* Naval Ocean Research and Development Activity, NSTL, Mississippi, Technical Note 186.

Brown, R. M. and C. F. Cheng (1983). *Optical Character Recognition for Automated Cartography: The Advanced Development Handprinted Symbol Recognition System.* Naval Ocean Research and Development Activity, NSTL, Mississippi, Technical Note 187.

Brown, R. M. and **L. K. Gronmeyer** (1980). Recognition of Handprinted Characters for Automated Cartography. *Technical Papers for the American Congress on Surveying and Mapping, 40th Annual Meeting.*

Brown, R. M., L. K. Gronmeyer, and **M. Lybanon** (1979). Recognition of Handprinted Characters for Automated Cartography: A Progress Report. *Image Understanding Systems II, Proceedings of the Society of Photo-Optical Instrumentation Engineers.*

Brown, R. M., A. Zied, A. E. Barnes, and E. C. Gough (1983). *Advanced Type Placement and Geonames Database: Comprehensive Coordination Plan.* Naval Ocean Research and Development Activity, NSTL, Mississippi, Technical Note 189.

Brunson, B. A. (1980). *Acoustic Model Sensitivity to Input Data Differences: Objective Analysis Scheme*

Outputs, Volume II. Naval Ocean Research and Development Activity, NSTL, Mississippi, Technical Note 73.

Brunson, B. A. (1984). *Shear Wave Attenuation in Unconsolidated Laboratory Sediments*. Naval Ocean Research and Development Activity, NSTL, Mississippi, Technical Note 159.

Bucca, P. J. (1979). *Environmental Variability During the Church Stroke II Cruise 5 Exercise*. Naval Ocean Research and Development Activity, NSTL, Mississippi, Technical Note 44.

Bucca, P. J., C. Sellinger, and **J. E. Matthews** (1985). *A Preassessment of Environmental Conditions on the Continental Shelf Adjacent to Jacksonville, Florida*. Naval Ocean Research and Development Activity, NSTL, Mississippi, NORDA Report 88.

Burns, D. A. (1977). *The Oceanographic/Meteorological Environment West of St. Croix*. Naval Ocean Research and Development Activity, NSTL, Mississippi, Report 13.

Burns, D. A. (1982). *Data Summary, XCP Profiles in the Vicinity of the Faeroe Islands, October 1980*. Naval Ocean Research and Development Activity, NSTL, Mississippi, Technical Note 142.

Burns, D. A. (1982). *Physical Oceanographic Summary for the Gulf of Maine/Georges Bank*. Naval Ocean Research and Development Activity, NSTL, Mississippi, Technical Note 157.

Burns, D. A., M. A. Gove, N. V. Lombard, J. D. Boyd, S. E. Raffa, and **T. H. Kinder** (1981). *Hydrographic Measurements in the Grenada Basin, Southeastern Caribbean Sea, January 1980*. Naval Ocean Research and Development Activity, NSTL, Mississippi, Technical Note 86.

Burton, W. J., **F. A. Bowles, J. Egloff, Jr., R. H. Bennett, D. N. Lambert,** G. F. Merrill, and **F. L. Nastav** (1982). *Seafloor Environments North of St. Croix Margin and Virgin Islands Trough*. Naval Facilities Engineering Command, Chesapeake, Maryland, Technical Report FPO-1-92.

Byrnes, H. J. (1978). *Optimal Filtering and Analysis of Scanning Laser Data*. Naval Ocean Research and Development Activity, NSTL, Mississippi, Technical Note 24.

Byrnes, H. J. (1979). *Operating Scenario for a Hydrographic Airborne Laser Sounder*. Naval Ocean Research and Development Activity, NSTL, Mississippi, Technical Note 34.

Byrnes, H. J. (1982). *HALS Post-processing Software*. Naval Ocean Research and Development Activity, NSTL, Mississippi, Technical Note 161.

Byrnes, H. J., J. Caruthers, H. Mesick, and **G. Vega** (1983). *Hydrographic Information Handling System (HIHAN) Concept Development*. Naval Ocean Research and Development Activity, NSTL, Mississippi, Technical Note 194.

Campbell, J., E. Gough, and **Langran, G. L.** (1984). *Commercial Data Base Management System for Geonames Data Base*. Naval Ocean Research and Development Activity, NSTL, Mississippi, NORDA Report 73.

Caruthers, J. W. (1982). *An Assessment of Soviet Development of Optimum Signal Discrimination Techniques*. Naval Ocean Research and Development Activity, NSTL, Mississippi, Technical Note 168.

Caruthers, J. W., R. A. Arnone, W. Howard, C. Haney, and **D. Durham** (1985). *Water Depth Determination Using Wave Refraction Analysis of Aerial Photography*. Naval Ocean Research and Development Activity, NSTL, Mississippi, NORDA Report 110.

Chin-Bing, S. A. (1984). *Soviet Research in Ocean Acoustics*. Naval Ocean Research and Development Activity, NSTL, Mississippi, Technical Note 242.

Chin-Bing, S. A. (1985). *Arctic High Frequency Acoustic Keel Model Study*. Naval Ocean Research and Development Activity, NSTL, Mississippi, Technical Note 257.

Chin-Bing, S. A. and **D. B. King** (1984). The Effect of Large Thermohaline Steps on Acoustic Propagation Near the Northeast Coast of South America. *Journal of the Acoustical Society of America* 76(S1), S84.

Chen, (B.) Y.-H. and **D. A. Milburn** (1984). The Effect of Nonlinear Wave Interactions on an Offshore Structure. *Proceedings of Marine Technology Society-IEEE Conference and Exposition*, Washington, D.C., 10-12 September.

Chen, (B.) Y.-H. and C. Y. Yang (1984). Random Wave Force Transformation on Sloping Beach. *Proceedings of 5th ASCE-EMD Specialty Conference*, 1-3 August.

Clancy, R. M. (1979). *The NORDA Hemispheric Mixed-Layer Model System (HMLMS): A Functional Description*. Naval Ocean Research and Development Activity, NSTL, Mississippi, Technical Note 45.

Clancy, R. M. and **P. J. Martin** (1979). *The NORDA/FLENUMOCEANCEN Thermodynamical Ocean Prediction System (TOPS): A Technical Description*. Naval Ocean Research and Development Activity, NSTL, Mississippi, Technical Note 54.

Clancy, R. M., P. J. Martin, and **S. A. Piacsek** (1981). *Test and Evaluation of an Operationally Capable Synoptic Upper-ocean Forecast System*. Naval Ocean

Research and Development Activity, NSTL, Mississippi, Technical Note 92.

Coachman, L. K., **T. H. Kinder**, J. D. Schumacher, and R. B. Tripp (1980). Frontal Systems of the Southeastern Bering Sea Shelf. *Proceedings of the Second International Symposium on Stratified Flows*, Volume II, T. Carstens and T. McClimans (eds.), Tapir, Trondheim, 917-933.

Cornyn, J. J. (1982). *Guideline for Coding Fortran Programs*. Naval Ocean Research and Development Activity, NSTL, Mississippi, NORDA Report 41.

Daubin, S. C. and **E. Hashimoto** (1983). Comparison of Observed Data and GDEM/Standard Ocean Data, Part II: Monthly Sea Surface Temperature (SST) Plots and Temperature/Salinity Vertical Cross Sections Along Great Circle Tracks in the Mediterranean Sea. Naval Ocean Research and Development Activity, NSTL, Mississippi, Technical Note 195.

Davis, J. A. and **S. A. Chin-Bing** (1978). Mode Theory Reflection Coefficient. *Journal of the Acoustical Society of America* 64(S1), S24A.

Davis, J. A. and **S. A. Chin-Bing** (1978). Mode and Ray Theory Comparison for a Completely Absorbing Bottom. *Journal of the Acoustical Society of America* 64(S1), p. S24A.

Davis, J. A. and **D. White** (1982). *Parabolic Equation Workshop*. Naval Ocean Research and Development Activity, NSTL, Mississippi, Technical Note 143.

Donde Va? Group (1984). Donde Va? An Oceanographic Experiment in the Alboran Sea. *EOS, Transactions of the American Geophysical Union* 65(36), 682-683.

Eckstein, B. E., C. R. Holland, F. A. Rakoczy, R. R. Rumpf, and **R. L. Williams** (1981). *Operation and Maintenance Manual for the NORDA Vertical Profiler*. Naval Ocean Research and Development Activity, NSTL, Mississippi, Technical Note 96.

Eckstein, B. E., C. R. Holland, and **R. L. Williams** (1982). *Operation and Maintenance Manual for the Atmospheric Profiler System*. Naval Ocean Research and Development Activity, NSTL, Mississippi, Technical Note 164.

Egloff, J. (1980). *A Digital File of Gridded Minimum, Maximum, and Average Depths for the North Pacific Ocean*. Naval Ocean Research and Development Activity, NSTL, Mississippi, Technical Note 50.

Einwich, A. M. and P. R. Vogt (1978). *Magnetic Pattern of the Western Atlantic South of 40°N*. Naval Ocean Research and Development Activity, NSTL, Mississippi, NORDA Report 16.

Einwich, A. M. (1981). Geology Related to Acoustic Transmission: Eastern Caribbean. Naval Ocean Research and Development Activity, NSTL, Mississippi, NORDA Report 28.

Eller, A. I. (1985). *Findings and Recommendations of the Under-Ice Scattering Loss Model Working Group*. Naval Ocean Research and Development Activity, NSTL, Mississippi, Technical Note 255

Emery, W. (1984). Physical Oceanography of the Continental Shelf Region Off Juan De Fuca Strait. Naval Ocean Research and Development Activity, NSTL, Mississippi, Technical Note 231.

Eppler, D. T. (1982). *Possible Application of GEOSAT-A Radar Altimeter Data: Ice Forecast Polar Region*. Naval Ocean Research and Development Activity, NSTL, Mississippi, Technical Note 177.

Eppler, D. T. (1983). Possible Applications of Satellite Altimetry Data Acquired Over Sea Ice. *Oceanography from GEOSAT Workshop*, Naval Ocean Research and Development Activity, NSTL, Mississippi.

Eppler, D. T. (1983). *Assessment of Potential SSM/I Ice Products in Light of ESMR and SMMR Ice Classification Algorithms*. Naval Ocean Research and Development Activity, NSTL, Mississippi, Technical Note 220.

Erlich, R., P. J. Brown, J. M. Yarus, and **D. T. Eppler** (1980). Analysis of Particle Morphology Data. *Advanced Particulate Morphology*, J. D. Beddow and T. P. Meloy (eds.), CRC Press, Inc., Boca Raton, Florida, 101-119.

Estalote, E. (1983). *NORDA Code 323 Acoustic Model and Data Bases*. Naval Ocean Research and Development Activity, NSTL, Mississippi, Technical Note 211.

Estalote, E. (1984). *Acoustic Models and Data Bases*. Naval Ocean Research and Development Activity, NSTL, Mississippi, Technical Note 293.

Estalote, E., J. Davis, D. King, and **G. Kerr** (1982). *Environmental Data Base Development and Acoustic Model Survey of the South Atlantic*. Naval Ocean Research and Development Activity, NSTL, Mississippi, Technical Note 126.

Evans, R. B. (1985). *Acoustic Scattering from a Rigid Object in a Half-space and a Slab Waveguide*. Naval Ocean Research and Development Activity, NSTL, Mississippi, Technical Note 304.

Fagot, M. G. (1978). *Marine Seismic Display, Volume I: Results*. Naval Ocean Research and Development Activity, NSTL, Mississippi, Technical Note 13.

Fagot, M. G. (1978). *Marine Seismic Display, Volume II: Processing Software*. Naval Ocean Research

and Development Activity, NSTL, Mississippi, Technical Note 14.

Fagot, M. G. (1978). *Marine Seismic Display, Volume III: User's Handbook.* Naval Ocean Research and Development Activity, NSTL, Mississippi, Technical Note 15.

Fagot, M. G. (1978). *Reconnaissance Sonar for OSP Survey Ships, Final Report.* Naval Ocean Research and Development Activity, NSTL, Mississippi, Technical Note 17.

Fagot, M. G. (1978). Reconnaissance Sonar for Deep Ocean Seamount Detection. *Proceedings, IEEE International Conference on Acoustics, Speech, and Signal Processing*, Tulsa, Oklahoma.

Fagot, M. G. (1983). A Deep-Towed Sound Source and Hydrophone Array System: Performance Prediction Analysis and Hardware Description. *Acoustics and the Sea-Bed*, N. G. Page (ed.), Bath University Press, Bath, U. K.

Fagot, M. G. and **B. E. Eckstein** (1979). *Deep-Towed Geophysical Array Development Program Progress Report (FY-78).* Naval Ocean Research and Development Activity, NSTL, Mississippi, Technical Note 41.

Fagot, M. G., N. H. Gholson, G. J. Moss, and **D. A. Milburn** (1980). *Deep-Towed Geophysical Array System, Development Program Review.* Naval Ocean Research and Development Activity, NSTL, Mississippi, Technical Note 75.

Fagot, M. G., G. J. Moss, D. A. Milburn, and **N. H. Gholson** (1981). Deep-Towed Seismic System Design for Operation at Depths up to 6000 m. *Proceedings, Offshore Technology Conference 4082*, 141–147.

Fagot, M. F. and **S. E. Spychalski** (1982). Deep Towed Seismic System: A Hardware Description. *Proceedings of the Society of Exploration Geophysicists 52nd Annual International Meeting and Exposition*, Dallas, Texas, Paper S10.3.

Fagot, M. G. and **S. Spychalski** (1984). *Deep-Towed Array Geophysical System (DTAGS): A Hardware Description.* Naval Ocean Research and Development Activity, NSTL, Mississippi, NORDA Report 71.

Fagot, M. G. and **S. E. Spychalski** (1984). Development of a Deep Towed Geophysical Sound Source, Multichannel Array, and Telemetry System. *Proceedings of the Remotely Operated Vehicle Conference and Exposition*, San Diego, California.

Farmer, L. D., D. Eppler, and **A. Lohanick** (1984). *Digital Processing of Passive K-Band Microwave Images for Sea Ice Classification.* Naval Ocean Research and Development Activity, NSTL, Mississippi, NORDA Report 51.

Fay, T. and **C. Walker** (1985). *Handprint Symbol Recognition Alphabetic Character Recognition.* Naval Ocean Research and Development Activity, NSTL, Mississippi, NORDA Report 114.

Fenner, D. F. (1979). *Sound Speed and Oceanic Frontal Variability in the Western Alboran Sea (January–March 1979).* Naval Ocean Research and Development Activity, NSTL, Mississippi, Technical Note 52.

Fenner, D. F. (1982). *Sound Speed Structure of the Western Atlantic Ocean.* Naval Ocean Research and Development Activity, NSTL, Mississippi, Technical Note 107.

Fenner, D. F. and **P. J. Bucca** (1982). *The Sound Velocity Structure of the North Indian Ocean.* Naval Ocean Research and Development Activity, NSTL, Mississippi, Technical Note 65.

Ferer, K. M. (1977). *Effects of Long-term Tension on Kevlar Aramid Fiber.* Naval Ocean Research and Development Activity, NSTL, Mississippi, Technical Note 8.

Ferer, K. M. (1977). *NAVSEA Kevlar Coaxial Cable Development Program FY 1977.* Naval Ocean Research and Development Activity, NSTL, Mississippi, Technical Note 10.

Ferer, K. M. (1978). *NAVSEA Kevlar Coaxial Cable Development Program, FY-78, First Quarterly Report.* Naval Ocean Research and Development Activity, NSTL, Mississippi, Technical Note 16.

Ferer, K. M. (1978). *NAVSEA Kevlar Coaxial Cable Development Program, FY-78, Second Quarterly Report.* Naval Ocean Research and Development Activity, NSTL, Mississippi, Technical Note 22.

Ferer, K. M. (1978). *Kevlar Coaxial Cable Development.* Naval Ocean Research and Development Activity, NSTL, Mississippi, NORDA Report 20.

Ferer, K. M. (1979). *NAVSEA Kevlar Coaxial Cable Development Program, FY-79 Report: First Quarterly Report.* Naval Ocean Research and Development Activity, NSTL, Mississippi, Technical Note 43.

Ferer, K. M. (1979). *NAVSEA Coaxial Cable Development Program, FY-79 Report: Second Quarterly Report.* Naval Ocean Research and Development Activity, NSTL, Mississippi, Technical Note 46.

Ferer, K. M. and **R. Swenson** (1978). *Kevlar Cable Development Program.* Naval Ocean Research and Development Activity, NSTL, Mississippi, NORDA Report 15.

Feuillade, C. and **M. F. Werby**. Scattering from Fluid-loaded, Layered Elastic Objects. *Journal of the Acoustical Society of America* 76(S1), Fall.

Feuillet, J. P. and **P. Fleischer** (1982). Effect of Circulation on Clay Mineral Distribution on the Southeastern U. S. Continental Slope. *EOS, Transactions of the American Geophysical Union* 63, 991.

Flax, L., L. H. Green, and **M. F. Werby** (1983). Scattering from Submerged Infinite Cylindrical Elastic Thin Shells. *Journal of the Acoustical Society of America* 73(S1), Spring.

Fleischer, P. (1980). *Weather and Currents in the Vicinity of 23°N, 46°W, North Atlantic Ocean*. Naval Ocean Research and Development Activity, NSTL, Mississippi, Technical Note 74.

Fleischer, P. (1981). *Evaluation and Selection of Test Sites for BURMMS*. Naval Ocean Research and Development Activity, NSTL, Mississippi, Technical Note 90.

Fleischer, P. (1984). *Guide to Dauphin Island Bridge Rubble Locations*. Alabama Sea Grant Extension Bulletin, Circular CRD-27, 4 p.

Foreman, J. A. and **D. W. Handschumacher** (1977). Interaction Between Primary Basement Structure and Secondary Crustal Extrusion Along the Hawaiian Ridge. *EOS, Transactions of the American Geophysical Union* 58(12), 1231.

Gaunaurd, G. and **M. F. Werby** (1984). Criteria for Suitable Background Choices in Resonance Acoustic Scattering by Shells. *Journal of the Acoustical Society of America* 76(S1), Fall.

Gholson, N. H. (1982). *Electrical Characteristics of Sea Water Return Transmission Loss*. Naval Ocean Research and Development Activity, NSTL, Mississippi, NORDA Report 52.

Gholson, N. H. and **M. G. Fagot** (1980). *A Moments Approach for Analyzing Geophysical Reflection Data*. Naval Ocean Research and Development Activity, NSTL, Mississippi, NORDA Report 30.

Gholson, N. H. and **M. G. Fagot** (1983). A Deep Towed Sound Source and Hydrophone Array System—Performance Analysis and Design. *Handbook of Geophysical Exploration at Sea*, R. A. Geyer (ed.), CRC Press, Inc., Boca Raton, Florida.

Gholson, N. H. and **P. Harris** (1981). *Analog Data Compression for Versatile Experimental Kevlar Array (VEKA) Telemetry*. Naval Ocean Research and Development Activity, NSTL, Mississippi, Technical Note 131.

Gilbert, K. E. and **R. B. Evans** (1985). A Green's Function Method for One-way Wave Propagation in a Range-dependent Ocean Environment. *Proceedings of the Conference on Ocean Seismoacoustics*, La Spezia, Italy.

Gilbert, K. E., **R. B. Evans**, **S. A. Chin-Bing**, **D. White**, and **W. A. Kuperman** (1983). Some New Models for Sound Propagation in Bottom-limited Ocean Environments. *Acoustics and the Sea-Bed*, N. G. Pace (ed.), Bath University Press, Bath, U. K., 243-250.

Gorsline, D. S., R. L. Kolpack, H. A. Karl, D. E. Drake, **P. Fleischer**, S. E. Thornton, J. R. Schwalback, and C. E. Savrda (1984). Studies of Fine-grained Sediment Transport Processes and Products in the California Continental Borderland. *Fine-grained Sediments: Deep-water Processes and Facies*, D. A. V. Stow and D. J. W. Piper (eds.), The Geological Society of London, Blackwell Scientific Publications, London, 395-415.

Gove, M. (1978). *NORDA ADP Workload Analysis and System Requirements*. Naval Ocean Research and Development Activity, NSTL, Mississippi, Technical Note 19.

Green, A. W. (1982). Possible Applications of Pattern Recognition Methods in Physical Oceanography. *Workshop on Pattern Analysis in the Marine Environment*, CNR/NORDA, NSTL, Mississippi, April.

Green, A. W. (1982). Wave Measurement in the 1980's. *Proceedings of a Symposium and Workshop on Wave Measurement Technology*, 22-24 April 1981, Washington, D.C., National Academy Press, Washington, 210-223.

Green, A. W. (1983). Influence of the Eastern Caribbean Circulation on Productivity and Sediment Distribution. *EOS, Transactions of the American Geophysical Union* 64, 1076.

Green, A. W. and **T. H. Kinder** (1981). An Unusually Strong Temperature Perturbation Detected by Two Current Meter Moorings in the Southeastern Caribbean Sea. *EOS, Transactions of the American Geophysical Union* 62(17), 305.

Green, A. W. and **K. D. Saunders** (1981). Dynamical and Empirical Fall Rates of XCP's and XBT's. *Proceedings of OCEANS '81*, 382-386.

Green, A. W. and **M. Y. Su** (1983). Nonlinear Dynamics Applied to Interpretation of Storm Wave Statistics. *Proceedings of XVIII General Assembly*, August, Hamburg, Germany, *Proces Verbaux* 16, 127.

Green, J. A. and **P. Fleischer** (1980). *Environmental Report of the Northwest Pacific for the Marine Seismic System (MSS)*. Naval Ocean Research and Development Activity, NSTL, Mississippi, NORDA Report 31.

Green, J. A. and **J. E. Matthews** (1983). *Global Analysis of the Shallow Geology of Large-scale Ocean Slopes*. Naval Ocean Research and Development Activity, NSTL, Mississippi, Technical Note 197.

Green, J. A. and **S. D. Trowell** (1981). *Data Report for Oceanographic/Geophysical Surveys in the Northwest Pacific (46–47°N, 159–161°E): USNS SILAS BENT, 2–3 August 1980*. Naval Ocean Research and Development Activity, NSTL, Mississippi, Technical Note 81.

Green, L. H. and **M. F. Werby** (1984). Calculation of Monostatic Angular Distributions for Elongated Elastic Shells. *Journal of the Acoustical Society of America* 76(S1), Fall.

Gronmeyer, L. K., B. W. Ruffin, et al. (1978). *An Overview of Optical Character Recognition Technology and Techniques*. Naval Ocean Research and Development Activity, NSTL, Mississippi, Technical Note 218.

Guinasso, N. L., D. R. Schink, J. J. Johnson, L. W. Quan, K. P. Cole, and **M. D. Richardson** (1983). Radionuclide Bioturbation Rates at Three Sites in the Caribbean Sea. *EOS, Transactions of the American Geophysical Union* 64(52), 1086.

Hackman, R. and **M. F. Werby** (1983). Nearfield Effects in Acoustic Scattering. *Journal of the Acoustical Society of America* 73(S1), Spring.

Hackman, R., **M. F. Werby**, and L. H. Green (1983). Scattering from Layered Material Immersed in a Fluid. *Journal of the Acoustical Society of America* 73(S1), Spring.

Hallock, Z. R. (1982). A Technique for Describing Thermohaline Intrusions in the Presence of Dynamic Variability. *Proceedings of the 1982 International STD Conference and Workshop*, Marine Technology Society, San Diego Section, 17 pp.

Hallock, Z. R. (1982). *A Computer Program for Processing Conductivity-Temperature-Depth (CTD) Data*. Naval Ocean Research and Development Activity, NSTL, Mississippi, Technical Note 196.

Hallock, Z. R. (1983). *The Exchange of Heat and Salt Across the Iceland-Faeroe Front*. Naval Ocean Research and Development Activity, NSTL, Mississippi, NORDA Report 78. Also in *Proceedings of the Chemical Variability of Ocean Areas Workshop*, NSTL, Mississippi, 21–23 September.

Hallock, Z. R. (1983). *Regional Variability of Thermohaline Finestructure*. Naval Ocean Research and Development Activity, NSTL, Mississippi, Technical Note 203.

Hallock, Z. R. (1983). Three-dimensional Structure of Frontal Interleaving in the Southern Norwegian Sea. *EOS, Transactions of the American Geophysical Union* 64, 248.

Handschumacher, D. W. and D. R. Bracey (1981). Northwest Pacific Magnetic Anomaly Map. *EOS, Transactions of the American Geophysical Union* 62(45), 847.

Handschumacher, D. W., L. G. Hemler, E. J. Morgenthaler, and R. Clark (1981). Imaging Conventional Marine Geophysical Data: Caribbean Seismic Example. *Proceedings, Marine Geological and Geophysical Workshop*, National Oceanic and Atmospheric Administration, Boulder, Colorado, 100–104.

Handschumacher, D. W. and L. Kroenke (1978). An Extended Time Scale for Mesozoic Geomagnetic Reversals. *EOS, Transactions of the American Geophysical Union* 52(4), 266.

Handschumacher, D. W., R. H. Pilger, J. A. Foreman, and J. F. Campbell (1981). Structure and Evolution of the Easter Plate. *Nazca Plate: Crustal Formation and Andean Convergence*, L. D. Kulm et al. (eds.), Geological Society of America, Memoir 154, 63–76.

Handschumacher, D. W., P. R. Vogt, and D. R. Bracey (1983). Japanese (M) Lineations: Systematic Anomaly Amplitude Increase Away from Fracture Zones. *EOS, Transactions of the American Geophysical Union* 64(45), 688.

Harding, J. M. (1982). *Relative Numerical Dispersion of Shallow-water Gravity Waves Caused by Three Time Differencing Techniques*. Naval Ocean Research and Development Activity, NSTL, Mississippi, Technical Note 134.

Harding, J. M., R. M. Clancy, and J. P. French (1984). Operational Mixed Layer Forecasts Compared with Ocean Station Data. *EOS, Transactions of the American Geophysical Union* 65(45), 942.

Harding, J. M., R. M. Clancy, J. Hawkins, and **G. W. Heburn** (1984). U.S. Navy Operational Ocean Thermal Analysis and Prediction: Present Capabilities, Future Plans. *Proceedings, 4th Biennial Society of Exploration Geophysicists/U.S. Navy Joint Technical Symposium on Three dimensional Marine Data Collection, Processing, Interpretation, and Presentation*, NSTL, Mississippi, 11 p.

Harding, J. M., H. E. Hurlburt, L. B. Lin, D. R. Moore, and A. J. Wallcraft (1982). Intercomparison of Primitive Equation and Quasigeostrophic Simulations of a Mid-latitude Jet. *EOS, Transactions of the American Geophysical Union* 64(45), 997.

Harding, J. M., R. H. Preller, and **S. A. Piacsek** (1983). *Statistics of Vertical Shear from a Hemispheric Model*. Naval Ocean Research and Development Activity, NSTL, Mississippi, Technical Note 206.

Harding, J. M., R. H. Preller, S. A. Piacsek, and **A. C. Warn-Varnas** (1983). Statistics of Vertical Shear and Richardson Number from a Global Model. *Proceedings, IUGG XVII General Assembly,* Hamburg, Germany.

Hashimoto, E. (1982). *FY-79 APP Task II Report: Comparison of the ICAPS and SIMAS Historical Environmental Data Bases.* Naval Ocean Research and Development Activity, NSTL, Mississippi, Technical Note 66.

Hashimoto, E. (1982). *FY-80 APP Task I Report.* Naval Ocean Research and Development Activity, NSTL, Mississippi, Technical Note 69.

Hashimoto, E. (1980). *FY-80 APP Task II Report.* Naval Ocean Research and Development Activity, NSTL, Mississippi, Technical Note 70.

Hashimoto, E. (1982). *Comparison of Observed Data and GDEM/Standard Ocean Results.* Naval Ocean Research and Development Activity, NSTL, Mississippi, Technical Note 154.

Hawkins, J. D. (1985). *Multichannel Sea Surface Temperature Retrievals for Navy Utilization.* Naval Ocean Research and Development Activity, NSTL, Mississippi, Technical Note 312.

Hawkins, J. D., R. A. Arnone, E. Arthur, C. Daniels, R. Holyer, P. La Violette, M. Lybanon, J. McKendrick, J. Mitchell, B. Moody, S. Peckinpaugh, A. Pressman, J. Schmidt, P. Smith, and **G. Stephenson** (1985). Remote Sensing at NORDA. *EOS, Transactions of the American Geophysical Union* 66(23), 482-483.

Hawkins, J. D., J. M. Harding, J. D. Thompson, and **R. M. Clancy** (1985). *USS AMERICA Emergency Breakaway Environmental Conditions.* Naval Ocean Research and Development Activity, NSTL, Mississippi, NORDA Report 105.

Heburn, G. W. (1983). World Ocean Model—A Preliminary Report. *Coupled Ocean-Atmospheric Modeling for 3-15 Day Numerical Prediction, A Workshop Report,* T. E. Rosmond et al. (eds.), Naval Environmental Prediction Research Facility, Technical Report 83-05, 2-11—2-13.

Heburn, G. W. (1984). *Effects of Wind versus Hydraulic Forcing on the Dynamics of the Western Mediterranean Sea.* XXIXth Congress and Plenary Assembly of International Commission of the Scientific Exploration of the Mediterranean Sea, H. Perkins (ed.), *Rapports et Proces-Verbaux,* 2 p.

Heburn, G. W., J. Allender, H. E. Hurlburt, and **T. H. Kinder** (1981). Dynamical Effects of Inflow Angle on Eddy Formation in the Southeastern Caribbean Sea. *EOS, Transactions of the American Geophysical Union* 62(45), 934.

Heburn, G. W., J. A. Allender, H. E. Hurlburt, and **T. H. Kinder** (1982). A Numerical Model of Eddy Generation in the Southeastern Caribbean Sea. *Hydrodynamics of Semi-Enclosed Seas,* J. C. J. Nihoul (ed.), Elsevier Scientific Publishing Company, Amsterdam, 299-328.

Heburn, G. W. and **H. E. Hurlburt** (1983). Influence of Basin Geometry on the Formation of Eddies in the Southeastern Caribbean Sea. *EOS, Transactions of the American Geophysical Union* 64(52), 1076.

Heburn, G. W., H. E. Hurlburt, and **T. H. Kinder** (1983). Eddy Generation Downstream of the Lesser Antilles. *EOS, Transactions of the American Geophysical Union* 64(18), 248.

Heburn, G. W., T. H. Kinder, and **H. E. Hurlburt** (1983). Eddies Generated by Horizontal Shear in the Southeastern Caribbean. *Tropical Ocean-Atmosphere Newsletter* 19, 11.

Heburn, G. W. and **R. H. Preller** (1984). Influence of Climatological Wind Forcing on the Circulation in the Alboran Sea. *EOS, Transactions of the American Geophysical Union* 65(45), 962.

Hironaka, V. F. and **M. D. Richardson** (1981). *An Investigation of the Effects of Deposit Feeding Invertebrates on the Structural Properties of Clay Minerals.* Naval Ocean Research and Development Activity, NSTL, Mississippi, Technical Note 105.

Holcombe, T. L., A. M. Einwich, F. A. Bowles, and **J. Egloff, Jr.** (1977). *The Geological Environment West of St. Croix.* Naval Ocean Research and Development Activity, NSTL, Mississippi, NORDA Report 5.

Holland, C. R. (1978). *Thermistor Array Impedance Considerations.* Naval Ocean Research and Development Activity, NSTL, Mississippi, Technical Note 26.

Holland, C. R. and **H. L. Dufilho** (1979). *Fiber Optics Applications Study.* Naval Ocean Research and Development Activity, NSTL, Mississippi, Technical Note 56.

Holland, C. R., B. E. Eckstein, R. C. Jackson, and D. A. Johnson (1980). *Operation and Maintenance Manual for the XBT Data Acquisition System.* Naval Ocean Research and Development Activity, NSTL, Mississippi, Technical Note 60.

Holland, C. R., R. Miles, and **R. A. Brown** (1982). *Operation and Maintenance Manual for the Expendable Poles Data Acquisition.* Naval Ocean Research and Development Activity, NSTL, Mississippi, Technical Note 127.

Holland, C. R. and **R. L. Williams** (1983). *Performance Tests of 4-5 Year Old Lithium Sulphur Dioxide Batteries*. Naval Ocean Research and Development Activity, NSTL, Mississippi, Technical Note 239.

Holyer, R. J. and **J. Hawkins** (1982). *Comparison of Multi-channel and Two-satellite Methods for Remote Measurement of Sea Surface Temperature*. Naval Ocean Research and Development Activity, NSTL, Mississippi, Technical Note 162.

Holyer, R. J. and **P. E. La Violette** (1984). *NIMBUS-7 CZCS Data*. Naval Ocean Research and Development Activity, NSTL, Mississippi, NORDA Report 60.

Hubbard, D. K., I. P. Gill, H. H. Roberts, and **F. A. Bowles** (1984). Variations in Shelf-edge and Peri-platform Depositional Styles Around St. Croix, U.S. Virgin Islands. SEPM.

Hufford, G. L., **J. P. Welsh**, I. M. Lissauer, and B. D. Thompson (1977). Along-shore Coherence of Winds Along the North Alaskan Coast for Oil and Spill Analysis. *Offshore Technology Conference*, May, Paper OTC 2947.

Hulbert, M. H., **D. N. Lambert, R. H. Bennett**, G. L. Freeland, **J. T. Burns, W. B. Sawyer**, and P. Field (1982). In Situ Electrical Resistivity Measurements of Calcareous Sediments. *Geotechnical Properties Behavior, and Performance of Calcareous Soils*, K. R. Demars and R. C. Chaney (eds.), ASTM Special Tech. Pub. 777, 156-179.

Hurlburt, H. E. (1981). *An Implicit Form of Upstream Differencing and Its Applications to a Radiation Boundary Condition*. Naval Ocean Research and Development Activity, NSTL, Mississippi, Technical Note 97.

Hurlburt, H. E. (1981). *A Summary of [illegible] ers Related to Mesoscale and Large-scale Ocean Modeling Volume 1*. Naval Ocean Research and Development Activity, NSTL, Mississippi, Technical Note 109.

Hurlburt, H. E. (1984). The Importance of Altimeter and Scatterometer Data for Ocean Prediction. *Frontiers of Remote Sensing of the Oceans and Troposphere from Air and Space Platforms*, J. Goldhirsh (ed.), Marshall Space Flight Center, Alabama, NASA Conference Publication 2303, 587-599.

Hurlburt, H. E. and **J. D. Thompson** (1980). *A Numerical Study of Loop Current Intrusions and Eddy Shedding*. Naval Ocean Research and Development Activity, NSTL, Mississippi, Technical Note 64.

Hurlburt, H. E. and **J. D. Thompson** (1981). *The Dynamics of the Loop Current and Shedding Eddies in a Numerical Model of the Gulf of Mexico*. Naval Ocean Research and Development Activity, NSTL, Mississippi, Technical Note 125.

Hurlburt, H. E. and **J. D. Thompson** (1982). The Dynamics of the Loop Current and Shed Eddies in a Numerical Model of the Gulf of Mexico. *Hydrodynamics of Semi-Enclosed Seas*, J. C. J. Nihoul (ed.), Elsevier Scientific Publishing Company, Amsterdam, 243-297.

Hurlburt, H. E. and **J. D. Thompson** (1982). The Behavior of an Individual Current Meander in Different Dynamical Regimes. *Proceedings, Workshop on Gulf Stream Structure and Variability*, J. M. Bane, Jr. (ed.), sponsored by the Office of Naval Research, 127-152.

Hurlburt, H. E. and **J. D. Thompson** (1984). Preliminary Results from a Numerical Study of the New England Seamount Chain Influence on the Gulf Stream. *Predictability of Fluid Motions*, G. Holloway and B. J. West (eds.), American Institute of Physics, New York, 489-504.

Irish, G., **W. Howard, J. W. Caruthers**, and **D. Durham** (1985). *Multispectral Imagery for Amphibious Preassault Planning*. Naval Ocean Research and Development Activity, NSTL, Mississippi, NORDA Report 109.

Jahn, W. H. (1982). A Remote Controlled Camera System. *Navy Technical Disclosure Bulletin* 7(4), 43-46.

Jones, S. K., **S. E. Spychalski**, and **M. G. Fagot** (1984). Deep-Towed Array Geophysical System Telemetry Equipment. *Proceedings, Offshore Technology Conference*, Houston, Texas.

Karweit, M. (1984). *Analyzing Temperature Data from XBT Grid Surveys*. Naval Ocean Research and Development Activity, NSTL, Mississippi, Technical Note 250.

Keen, D. J., H. E. Morris, and **D. L. Durham** (1978). *The Ocean Science Program of the U.S. Navy—An Overview*. Naval Ocean Research and Development Activity, NSTL, Mississippi, Technical Note 39.

Kerr, G. A. (1983). *An Evaluation of Fleet Mission Program Library: Program V10011/B (Bathythermograph-Sound Velocity Profile)*. Naval Ocean Research and Development Activity, NSTL, Mississippi, Technical Note 192.

Kerr, G. A. (1983). *Bathythermograph/Sound Velocity Profile Program for the HP-41 CV Calculator, Including a Northern Hemisphere Salinity Profile Library*. Naval Ocean Research and Development Activity, NSTL, Mississippi, Technical Note 193.

Kerr, G. A. (1984). *CHORDS: A New Temperature on Sound Speed Profile Thinning Algorithm*. Naval Ocean Research and Development Activity, NSTL, Mississippi, Technical Note 272.

Kerr, G. A. (1984). *A New Salinity Prediction Method for Use with XBTs*. Naval Ocean Research and Development Activity, NSTL, Mississippi, Technical Note 284.

Kerr, G. A. (1985). *An Overview of NORDAPS: NORDA's Raw Data Analysis and Processing System*. Naval Ocean Research and Development Activity, NSTL, Mississippi, NORDA Report 97.

Kerr, G. A. (1985). *An Investigation of the ICAPS Data Base for Use with Shallow Temperature Probes*. Naval Ocean Research and Development Activity, NSTL, Mississippi, NORDA Report 116.

Kerr, G. A., E. Hashimoto, and **R. Lauer**. *Homogeneous Environmental Acoustic Regions: A Low Resolution Global Ocean Data Base*. Naval Ocean Research and Development Activity, NSTL, Mississippi, NORDA Report 89.

Kerr, G. A., R. H. Lauer, and **E. Hashimoto** (1985). *Preliminary Determination of Homogeneous Environmental Acoustic Regions for the Naval Nuclear Warfare Simulation Acoustic Data Base*. Naval Ocean Research and Development Activity, NSTL, Mississippi, NORDA Report 79.

Ketchum, R. D. (1977). *An Evaluation of Side-looking Radar Imagery of Sea Ice Features and Conditions in the Lincoln Sea Strait and Baffin Bay*. Naval Ocean Research and Development Activity, NSTL, Mississippi, Technical Note 7.

Ketchum, R. D. (1977). *Passive Microwave Signatures of Arctic Sea Ice Features*. Naval Ocean Research and Development Activity, NSTL, Mississippi, Technical Note 9.

Ketchum, R. D. (1978). *An Evaluation of ERIM X-L Band Airborne Synthetic Aperture Radar Imagery of Sea Ice*. Naval Ocean Research and Development Activity, NSTL, Mississippi, Technical Note 28.

Ketchum, R. D. (1981). *Dual Frequency Radar Ice and Snow Signatures*. Naval Ocean Research and Development Activity, NSTL, Mississippi, Technical Note 135.

Ketchum, R. D. (1982). *SEASAT SAR Sea Ice Imagery from Summer Melt to Fall Freeze-up*. Naval Ocean Research and Development Activity, NSTL, Mississippi, Technical Note 178.

Ketchum, R. D. (1984). *Observations in the Arctic Environment and the Development of Techniques for Ice Penetration and Sensor Deployment*. Naval Ocean Research and Development Activity, NSTL, Mississippi, Technical Note 187.

Ketchum, R. D. and **L. D. Farmer** (1980). *Eastern Arctic SURSAT SAR Ice Experiment: Radar Signatures of Sea Ice Features*. Naval Ocean Research and Development Activity, NSTL, Mississippi, Technical Note 68.

Ketchum, R. D. and **L. D. Farmer** (1980). Eastern Arctic SURSAT SAR Ice Experiment: Radar Signature of Sea Ice Features. *Proceedings, Final SURSAT Ice Workshop*, Atmospheric Environmental Service, Toronto, Ontario, Canada, 23–27 June.

Ketchum, R. D., L. D. Farmer, and **J. P. Welsh** (1983). *K-Band Radiometric Mapping of Sea Ice*. Naval Ocean Research and Development Activity, NSTL, Mississippi, Technical Note 179.

Ketchum, R. D. and **A. W. Lohanick** (1977). Microwave Scanning the Arctic Pack Ice. *A Symposium on Sea Ice Processes and Models*, 6–8 September, v. II, 11–22.

Ketchum, R. D., S. Tooma, and **H. Li** (1976). *Mission Spring, 1976: Arctic Airborne Remote Sensing Program and Preliminary Analysis of High Resolution Microwave Sea Ice Imagery*. Naval Ocean Research and Development Activity, NSTL, Mississippi, Technical Note 1.

Kinder, T. H. (1981). A Perspective of Physical Oceanography in the Bering Sea, 1979. *Eastern Bering Sea Shelf, Oceanography and Resources*, D. W. Hood and J. A. Calder (eds.), NOAA Office of Marine Pollution Assessment, pp. 5–13.

Kinder, T. H. (1984). *Hydrographic Measurements in the Western Alboran Sea, October 1982*. Naval Ocean Research and Development Activity, NSTL, Mississippi, Technical Note 273.

Kinder, T. H. (1984). *Hydrographic Distribution in the Northwestern Alboran Sea, 22–24 June 1982*. Naval Ocean Research and Development Activity, NSTL, Mississippi, Technical Note 277.

Kinder, T. H., J. Allender, G. W. Heburn, and **H. E. Hurlburt** (1981). Mesoscale Eddies in the Southeastern Caribbean Sea. *EOS, Transactions of the American Geophysical Union* 62(17), 305.

Kinder, T. H., D. A. Burns, Z. R. Hallock, and M. Stirgus (1983). *Hydrographic Measurements in the Western Alboran Sea, June 1982*. Naval Ocean Research and Development Activity, NSTL, Mississippi, Technical Note 202.

Kinder, T. H., G. W. Heburn, J. D. Boyd, J. H. Allender, and **H. E. Hurlburt** (1982). Spatial and Temporal Scales of Physical Variability Near the Southern Lesser Antilles. *EOS, Transactions of the American Geophysical Union* 63, 75.

Kinder, T. H. and J. D. Schumacher (1981). Hydrographic Structure Over the Continental Shelf of the

Southeastern Bering Sea. *Eastern Bering Sea Shelf, Oceanography and Resources*, D. W. Hood and J. A. Calder (eds.), NOAA Office of Marine Pollution Assessment, pp. 31-52.

Kinder, T. H. and J. D. Schumacher (1981). Circulation Over the Continental Shelf of the Southeastern Bering Sea. *Eastern Bering Sea Shelf, Oceanography and Resources*, D. W. Hood and J. A. Calder (eds.), NOAA Office of Marine Pollution Assessment, pp. 53-75.

Kindle, J. C. (1981). On Equatorial Rossby Solitons. *Recent Progress in Equatorial Oceanography*, J. P. McCreary (ed.), Nova University, Dania, Florida, p. 353-360.

Kindle, J. C. (1983). On the Generation of Rossby Solitons During El Nino. *Hydrodynamics of the Equatorial Ocean*, J. C. J. Nihoul (ed.), Elsevier Scientific Publishing Company, Amsterdam, p. 353-368.

Kindle, J. C., H. E. Hurlburt, and **J. D. Thompson** (1984). Sampling Strategies and Four-dimensional Data Assimilation of Altimeter Data for Ocean Monitoring and Prediction. *Frontiers of Remote Sensing of the Oceans and Troposphere from Air and Space Platforms*, J. Goldhirsh (ed.), Marshall Space Flight Center, Alabama, NASA Conference Publication 2303, 587-599.

Kindle, J. C., J. D. Thompson, and **H. E. Hurlburt** (1984). Sampling Strategies and Four-dimensional Assimilation of Altimetric Data for Ocean Monitoring and Prediction. *Proceedings of URSI Commission F Symposium, Frontiers of Remote Sensing of the Oceans and Troposphere from Air and Space Platforms*, Israel, 14-23 May.

King, D. B., G. Kerr, and **R. Lauer** (1985). *Convergence Zone Range Accuracy as a Function of Location and Merge Depth*. Naval Ocean Research and Development Activity, NSTL, Mississippi, NORDA Report 77.

King, D. B. and **R. H. Love** (1985). *Data Survey Requirements Based on the Acoustic Performance Prediction Master Data Base*. Naval Ocean Research and Development Activity, NSTL, Mississippi, Technical Note 276.

Kinney, W. A. and C. S. Clay 3). Numerical and Experimental Studies of the Spati oherence of Acoustic Signals Scattered from a Rough urface. *Proceedings of the Institute of Acoustics Underwater Acoustics Group Conference on Acoustics and the Sea-bed*, Bath University, Bath, U.K., 157-165.

Kuperman, W. A., M. F. Werby, and **K. E. Gilbert** (1983). Mathematical Foundations of Propagation Models in Underwater Acoustics. *Underwater Acoustics, AIAA 8th Aeroacoustics Conference*, Atlanta, Georgia, 11-13 April. American Institute of Aeronautics and Astronautics, New York, Reprint AIAA-83-0684.

Kvenvolden, K., L. A. Barnard, **D. A. Wiesenburg**, and J. B. Brooks (1983). Geochemistry of Natural Gas Hydrates in Oceanic Sediment. *Advances in Organic Geochemistry 1981, Proceedings of the Tenth International Conference on Organic Geochemistry*, Oslo, Norway, 14-18 September 1981, 422-430.

Lambert, D. N., P. J. Valent, M. D. Richardson, and G. F. Merrill (1983). Shear Strength Variability in Three Sedimentary Provinces of the Venezuela Basin. *EOS, Transactions of the American Geophysical Union* 64(52), 1076-1077.

Langran, G. L. (1983). Map Design for Digital Production Efficiency. *Technical Papers, ACSM 45th Annual Meeting*, Washington, D.C., 10-15 March, 467-473.

Langran, G. L. (1984). *Map Design for Computer Processing: Literature Review and DMA Product Critique*. Naval Ocean Research and Development Activity, NSTL, Mississippi, NORDA Report 72.

Langran, G. L. (1985). *Map Design for Computer Process: Literature Review and DMA Critique*. Naval Ocean Research and Development Activity, NSTL, Mississippi, NORDA Report 72.

Langran, G. L. (1985). *Commercial Data Base Management Systems for Geonames Data Base*. Naval Ocean Research and Development Activity, NSTL, Mississippi, NORDA Report 73.

Langran, G. L. (1985). *Geonames Processing System Functional Design Specifications, Volume 1*. Naval Ocean Research and Development Activity, NSTL, Mississippi, NORDA Report 101.

Lauer, R. H., E. Hashimoto, G. Shayne, and M. Bolig (1984). *The Acoustic Performance Prediction Bathythermograph Merge Algorithm*. Naval Ocean Research and Development Activity, NSTL, Mississippi, Technical Note 302.

Lauer, R. H. and **T. N. Lawrence** (1984). *The Feasibility of Adding Confidence Bounds through Fluctuation Modeling or Data Base Development*. Naval Ocean Research and Development Activity, NSTL, Mississippi, NORDA Report 81.

La Violette, P. E. (1980). *Variations in the Frontal Structure of the Southern Grand Banks*. Naval Ocean Research and Development Activity, NSTL, Mississippi, Technical Note 87.

La Violette, P. E. (1981). *Remote Sensing Oceanography: A Synoptic Approach*. Naval Ocean

Research and Development Activity, NSTL, Mississippi, Technical Note 100.

La Violette, P. E. (1983). *The Grand Banks Experiment: A Satellite/Aircraft/Ship Experiment to Explore the Ability of Specialized Radars to Define Ocean Fronts.* Naval Ocean Research and Development Activity, NSTL, Mississippi, NORDA Report 49.

La Violette, P. E. (1984). *NOAA-7 AVHRR Images.* Naval Ocean Research and Development Activity, NSTL, Mississippi, NORDA Report 65.

La Violette, P. E. (1983). *The Advection of Submesoscale Thermal Features in the Alboran Sea Gyre.* Naval Ocean Research and Development Activity, NSTL, Mississippi, Technical Note 240.

La Violette, P. E. (1983). *Short-term Measurements of Surface Currents Associated with the Alboran Sea during Donde Va?.* Naval Ocean Research and Development Activity, NSTL, Mississippi, Technical Note 241.

La Violette, P. E. (1984). *NOAA-7 AVHRR Images.* Naval Ocean Research and Development Activity, NSTL, Mississippi, NORDA Report 65.

La Violette, P. E. and J. L. Kerling (1983). *An Analysis of Aircraft Data Collected in the Alboran Sea During Donde Va?, 6-18 October 1982.* Naval Ocean Research and Development Activity, NSTL, Mississippi, Technical Note 222.

La Violette, P. E., T. H. Kinder, and **H. E. Hurlburt** (1984). Donde Va?: Mesoscale Flow Dynamics Experiment in the Straits of Gibraltar and Alboran Sea. *Raffons ed Proces. Verbous de Reunions* iii-iiV(28), Fascicule 2.

Lavoie, D. L. (1985). *Geoacoustic Models: Washington State Continental Margin.* Naval Ocean Research and Development Activity, NSTL, Mississippi, NORDA Report 85.

Lavoie, D. L., I. DePalma, D. Reid, and **J. Hayes** (1982). *Chemical, Biological, and Physical Measurements from the Mediterranean Sea, Summer 1980.* Naval Ocean Research and Development Activity, NSTL, Mississippi, Technical Note 138.

Lavoie, D. L., I. DePalma, D. Reid, and **J. Hayes** (1982). *Chemical, Biological, and Physical Measurements from the Eastern Tropical Pacific, Spring 1979, USNS DESTEIGUER, Cruise 1207-79, Leg 1.* Naval Ocean Research and Development Activity, NSTL, Mississippi, Technical Note 139.

Lavoie, D. L., I. DePalma, D. Reid, and **J. Hayes** (1982). *Chemical, Biological, and Physical Measurements from the Western Caribbean and Gulf of Mexico, 1979, USNS DESTEIGUER, Cruise 1207-79, Leg 2.* Naval Ocean Research and Development Activity, NSTL, Mississippi, Technical Note 140.

Lavoie, D. L. and **J. E. Matthews** (1983). *Sediments on the Southeastern Flank of the Bermuda Pedestal.* Naval Ocean Research and Development Activity, NSTL, Mississippi, Technical Note 198.

Lee, D. and **K. E. Gilbert** (1982). Recent Progress in Modelling Bottom-interacting Sound Propagation with Parabolic Equations. *Oceans '82 Conference Record,* Washington, D.C., September, 172-177.

Levenson, C., R. H. Love, M. A. Wilson, and **R. A. Fisher** (1981). *Volume Reverberation Measurements in the Eastern Caribbean Sea.* Naval Ocean Research and Development Activity, NSTL, Mississippi, Technical Note 128.

Li, H. (1981). *On Wind Induced Underwater Ambient Noise.* Naval Ocean Research and Development Activity, NSTL, Mississippi, Technical Note 89.

Lin, L. B. and **J. M. Harding** (1978). A Numerical Simulation of the Pacific Equatorial Undercurrent. *EOS, Transactions of the American Geophysical Union* 59(12), 113.

Lin, L. B. and **H. E. Hurlburt** (1981). Maximum Simplification of Nonlinear Somali Current Dynamics. *Monsoon Dynamics,* Sir M. J. Lighthill and R. P. Pearce (eds.), Cambridge University Press, England, p. 541-555.

Lissauer, I. M. and **J. P. Welsh** (1978). Can Oil Spill Movement be Predicted? *Proceedings, In the Wake of the Argo Merchant,* Center for Ocean Management, University of Rhode Island, Kingston.

Little, B. J. (1983). Succession in Microfouling. *Marine Biodeterioration: An Interdisciplinary Study,* J. D. Costlow and R. C. Tipper (eds.), U.S. Naval Institute Press, Bethesda, Maryland, pp. 63-67.

Little, B. J. (1984). An Assessment of the Factors Influencing the Adsorption of Macromolecules from Estuarine and Marine Waters. *Proceedings of the 58th Colloid and Surface Science Symposium,* American Chemical Society.

Little, B. J. and J. Jacobus (1985). A Comparison of Two Techniques for the Isolation of Adsorbed Dissolved Organic Material from Seawater. *Organic Geochemistry* 8(1), 27-33.

Little, B. J. and **D. K. Young** (1979). *Ocean Dumping of Dredged Material at the Jacksonville Harbor Disposal Site: An Environmental Trend Assessment, February 1977 to April 1978.* Naval Ocean Research and Development Activity, NSTL, Mississippi, Technical Note 42.

Liu, P. C. and **A. W. Green** (1978). Higher Order Wave Spectra. *Proceedings of the 16th Coastal Engineering Conference*, American Society of Civil Engineers, Hamburg, West Germany, 370–371.

Locker, S. D. and **W. B. Sawyer** (1984). Lithofacies of Pleistocene Rocks. *Gulf of Mexico, Atlas 6, Ocean Margin Drilling Program, Regional Atlas Series*, R. T. Buffler et al. (eds.), Marine Science International, Woods Hole, Massachusetts, Sheet 32.

Lohanick, A. W. (1979). *Airborne Laser Sea Ice Profiles Near a Drifting Camp, April 1977.* Naval Ocean Research and Development Activity, NSTL, Mississippi, Technical Note 49.

Lohanick, A. W. (1981). *Reducing Laser Profiles on a Tabletop Computer.* Naval Ocean Research and Development Activity, NSTL, Mississippi, Technical Note 77.

Lohanick, A. W. (1982). 33 GHz Brightness Temperature of a Freezing Lead (abs.). *A Workshop on the Microwave Remote Sensing of Sea Ice and Icebergs*, NASA Langley Research Center, Hampton, Virginia, 6–9 April.

Lohanick, A. W. (1982). *Snow Thickness and Brightness Temperature on Multi-year Ice.* Naval Ocean Research and Development Activity, NSTL, Mississippi, Technical Note 171.

Lott, D. F., **R. A. Brown**, and **R. T. Miles** (1985). *Concurrent Testing of Expendable XSV 01 Probes Using the Expendable Probe Data Acquisition System.* Naval Ocean Research and Development Activity, NSTL, Mississippi, Technical Note 309.

Love, R. H. (1977). *A New Model of Resonant Acoustic Scattering by Swimbladder-bearing Fish.* Naval Ocean Research and Development Activity, NSTL, Mississippi, NORDA Report 4.

Lybanon, M. (1982). *Ocean Altimetry Algorithms Status: March 1982.* Naval Ocean Research and Development Activity, NSTL, Mississippi, Technical Note 146.

Lybanon, M. (1983). *GEOSAT—An Ocean Applications Program (GOAP): Initial Data Processing and Analysis System Test and Evaluation.* Naval Ocean Research and Development Activity, NSTL, Mississippi, Technical Note 158.

Lybanon, M. (1984). *GEOSAT Ocean Applications Program (GOAP): Initial Data Processing Analysis Test and Evaluation Plan.* Naval Ocean Research and Development Activity, NSTL, Mississippi, Technical Note 270.

Lybanon, M. (1985). *Ocean Wave Slope Statistics from Automated Analysis of Sunglitter Photographs.* Naval Ocean Research and Development Activity, NSTL, Mississippi, NORDA Report 103.

Lybanon, M. and **J. D. McKendrick** (1983). Some Applications of Image Processing in Oceanography. *The 15th Southeastern Symposium on System Theory*, University of Alabama, Huntsville, 28–29 March.

Lynch, R. V. (1985). *Detection of Bioluminescence Stimulated by Aircraft Using Explosive Charges.* Naval Ocean Research and Development Activity, NSTL, Mississippi, Technical Note 311.

Marmarino, G. O., E. E. Rudd, J. P. Dugan, W. L. Brundage, R. P. Mied, W. D. Morris, R. H. Hill, C. L. Trump, C. Y. Shen, D. Greenewalt, J. A. C. Kaiser, **K. D. Saunders**, and **H. T. Perkins** (1984). *Plans for the NRL/NORDA Fine-scale Variability Experiment—1984 (FVX-84).* Naval Research Laboratory, Washington, D.C., Memorandum Report 5450, 23 p.

Martin, R. L. (1985). *Effects of Ocean Boundaries and Bottom Topography on Acoustic Ambient Noise Fields in the Oceans.* Naval Ocean Research and Development Activity, NSTL, Mississippi, Technical Note 323.

Matthews, J. E. (1980). *An Approach to the Quantitative Study of Sea Floor Topography.* Naval Ocean Research and Development Activity, NSTL, Mississippi, Technical Note 47.

Matthews, J. E. (1982). *Geoacoustic Models for the Straits of Sicily and Sardinia-Tunisia.* Naval Ocean Research and Development Activity, NSTL, Mississippi, Technical Note 99.

Matthews, J. E., P. Bucca, and **C. Sellinger** (1985). *Preliminary Environmental Assessment of the Project Gemini Site, Corpus Christi, Texas.* Naval Ocean Research and Development Activity, NSTL, Mississippi, NORDA Report 120.

Matthews, J. E. and C. Stewart (1982). *An Operational Summary of the BERMEX 81-V3 Experiment, 17–19 September 1981.* Naval Ocean Research and Development Activity, NSTL, Mississippi, Technical Note 153.

Matthews, J. E. and **D. C. Young** (1983). *Mechanical Details of a Modified Hamilton Frame Velocimeter.* Naval Ocean Research and Development Activity, NSTL, Mississippi, Technical Note 227.

May, P. W. (1982). *Climatological Flux Estimates in the Mediterranean Sea: Part I.* Naval Ocean Research and Development Activity, NSTL, Mississippi, NORDA Report 54.

Mazeika, P. A., D. A. Burns, and **T. H. Kinder** (1980). *Measured Flow in St. Vincent and Grenada Passages in 1977.* Naval Ocean Research and Development Activity, NSTL, Mississippi, Technical Note 62.

McDonald, B. E. (1982). *On the Stress-Shear Relation Near a Turbulent Air-Sea Interface*. Naval Ocean Research and Development Activity, NSTL, Mississippi, Technical Note 181.

McDonald, B. E. (1983). *A Second Order Upwind Flux Method for Hyperbolic Conservation Laws*. Naval Ocean Research and Development Activity, NSTL, Mississippi, NORDA Report 57.

McDonald, B. E. (1984). *The Nonlinear Progressive Wave Equation for a Refracting Medium Including Caustics: Deviation*. Naval Ocean Research and Development Activity, NSTL, Mississippi, Technical Note 295.

McDonald, B. E. (1985). *A Conservation Law Related to Kelvin's Circulation Theories*. Naval Ocean Research and Development Activity, NSTL, Mississippi, NORDA Report 75.

McDonald, B. E. and **W. A. Kuperman** (1983). Time Domain Solution of Nonlinear Pulse Propagation. *Proceedings, NATO Workshop on Hybrid Formulation of Wave Propagation and Scattering*, Castel Gandolfo, Italy, September.

McDonald, B. E. and **W. A. Kuperman** (1984). Time Domain Solution of the Parabolic Equation Including Nonlinearity. *Proceedings, Workshop on Computational Ocean Acoustics*, Yale University, New Haven, Connecticut.

McDonald, B. E. and J. M. Witting (1982). *A Conservation-of-Velocity Law for Inviscid Fluids*. Naval Ocean Research and Development Activity, NSTL, Mississippi, Technical Note 184.

McGirr, R. (1983). *Comments and Issues Pertinent to SHARPS III Near-surface Propagation Modeling*. Naval Ocean Research and Development Activity, NSTL, Mississippi, NORDA Report 64.

McGirr, R. (1984). *Passive Broadband Sonar Modeling Methodologies*. Naval Ocean Research and Development Activity, NSTL, Mississippi, Technical Note 271.

McGirr, R. and **D. White** (1984). *Technical Evaluation of FACT 10A*. Naval Ocean Research and Development Activity, NSTL, Mississippi, NORDA Report 70.

McRaney, L. H. (1982). *NORDA Style Manual*. Naval Ocean Research and Development Activity, NSTL, Mississippi, NORDA Report 0.

McWilliams, J. C., E. D. Brown, H. L. Bryden, C. C. Ebbsmeyer, B. A. Elliot, R. H. Heinmiller, B. L. Hua, K. D. Leaman, E. J. Lindstrom, J. R. Loyten, S. E. McDowell, W. B. Owens, **H. T. Perkins**, J. F. Price, L. Regier, S. C. Rise, H. T. Rossby, T. B. Sanford, C. Y. Shen, B. A. Taft, and J. C. van Leer (1983). The Local Dynamics of Eddies in the Western North Atlantic. *Eddies in Marine Science*, A. R. Robinson (ed.), Springer-Verlag, New York, 92–113.

Merrill, G. F. and **R. H. Bennett** (1985). Slope Map of a Geotechnical Corridor on the Atlantic Continental Margin Southeast of Cape May. NOAA/NORDA six-plate, six-color transverse mercator projection map. Scale 1:40,000. Naval Ocean Research and Development Activity, NSTL, Mississippi.

Milburn, D. A. (1982). *JHU/APL Heat Flux Spar Buoy*. Naval Ocean Research and Development Activity, NSTL, Mississippi.

Milburn, D. A. (1983). Hydrodynamic Performance Evaluation of a Newly Developed Kevlar Rope Fairing. *Proceedings of the 1983 Symposium on Buoy Technology*, New Orleans, Louisiana, 27–29 April.

Milburn, D. A. and N. Chhabra (1980). Static and Dynamic Analysis of a Deep-water Subsurface Mooring for Near-surface Current Measurements. *Proceedings of Near Surface Ocean Experimental Technology Workshop*, NSTL, Mississippi.

Miles, R. T. (1984). *ADAPS Operation and Maintenance Manual*. Naval Ocean Research and Development Activity, NSTL, Mississippi, Technical Note 265.

Mitchell, J. L. (1983). *A Position Paper: Mesoscale Oceanography from GEOSAT*. Naval Ocean Research and Development Activity, NSTL, Mississippi, Technical Note 226.

Mitchell, J. L. (1984). *OUTPOST ENCORE Environmental Acoustics Measurements*. Naval Ocean Research and Development Activity, NSTL, Mississippi, Technical Note 266.

Mitchell, J. L. (1984). Regional Ocean Dynamics from GEOSAT: Plans for the Gulf of Mexico. *Proceedings of the 4th Minerals Management Service Gulf of Mexico Information Transfer Meeting*, New Orleans, Louisiana, November.

Mitchell, J. L. and **Z. R. Hallock** (1984). Plans for Oceanography from the U.S. Navy GEOSAT. *Proceedings of the Pacific Congress on Marine Technology (PACON '84)*, Honolulu, Hawaii.

Milburn, D. A. and **M. G. Fagot** (1979). *A Steady-state Analysis of Candidate Towing Cables for a Deep Towed Geophysical Array System*. Naval Ocean Research and Development Activity, NSTL, Mississippi, Technical Note 40.

Milburn, D. A. and P. Rispin (1981). *Hydrodynamic Test and Evalution of a Newly Developed Kevlar Rope Fairing*. Naval Ocean Research and Development Activity, NSTL, Mississippi, Technical Note 118.

Milburn, D. A. and **R. C. Swenson** (1979). *Performance of an Experimental Cable Payout Package.* Naval Ocean Research and Development Activity, NSTL, Mississippi, Technical Note 55.

Mohr, D. L., J. P. French, **A. C. Warn Varnas, J. M. Harding,** and **R. M. Clancy** (1983). Statistical Forecasts of Temperature Profiles in the North Atlantic. *EOS, Transactions of the American Geophysical Union* 64(52), 1058.

Montera-Guiterres, C., G. J. Fryer, and **J. Gettrust** (1984). Deep Crustal Structure and Upper Mantle Anisotropy in the ROSE Area. *EOS, Transactions of the American Geophysical Union* 65, 1013.

Morris, G. B., J. M. Berkson, and T. E. Stixrud (1983). *Short-term Measurements of Omnidirectional Ambient Noise.* Naval Ocean Research and Development Activity, NSTL, Mississippi, Technical Note 183.

Moss, G. J. (1982). *Navigation Hazard Survey Sonar, FY-79 Annual Report.* Naval Ocean Research and Development Activity, NSTL, Mississippi, Technical Note 53.

Moss, G. J. (1983). *Coastal Hydrographic Sonar/Advanced Acoustic Techniques.* Naval Ocean Research and Development Activity, NSTL, Mississippi, Technical Note 199.

Moss, G. J., Jr., C. R. Holland, and **R. A. Brown** (1984). *Under the Hull Diver Location System—System Definition Study.* Naval Ocean Research and Development Activity, NSTL, Mississippi, Report 113.

Nastav, F. L. and **R. H. Bennett** (1984). *Seafloor Geosciences Division: Missions, Technical Specialties, Accomplishments, and Activities, Calendar Year 1983.* Naval Ocean Research and Development Activity, NSTL, Mississippi, Technical Note 281.

Pai, S. I., M. M. Das, and **H. Li** (1976). *Compactness Effects on Drift of Arctic Pack Ice.* Naval Ocean Research and Development Activity, NSTL, Mississippi, Technical Note 3.

Pai, S. I. and **H. Li** (1976). *Mathematical Mode for Dynamics of Pack Ice in the Arctic Ocean and Its Surrounding Sea.* Naval Ocean Research and Development Activity, NSTL, Mississippi, Technical Note 4.

Panchal, C., **B. J. Little**, and J. Larsen-Basse (1984). Biofouling Control for Marine Heat Exchangers Using Intermittent Chlorination. *Proceedings of the 22nd National Heat Transfer Conference*, American Society of Mechanical Engineers and the American Institute of Chemical Engineers.

Perkins, H. T. (1980). *Oceanic Environmental Background Observations in the Sargasso Sea During September 1979.* Naval Ocean Research and Development Activity, NSTL, Mississippi, Technical Note 58.

Perkins, H. T. and **K. D. Saunders** (1982). Physical Oceanographic Observations in the Northwest Tropical Atlantic. *Tropical Ocean-Atmosphere Newsletter* 9, 7-9.

Perkins, H. T. and **K. D. Saunders** (1984). Measurements of the Mediterranean Outflow South of Cape St. Vincent, September 1982. *Preliminary Results of the Donde Va? Meeting in Fuengirola*, G. Parrilla (ed.), Instituto Espanol de Oceanografia, Instituto Espanol de Oceanografia, *Informes Technicos* 24-1984, 25-32.

Perkins, H. T. and **K. D. Saunders** (1984). Sections of Current, Salinity, and Temperature in the Northwestern Alboran Sea, October 1982. *Preliminary Results of the Donde Va? Meeting in Fuengirola*, G. Parrilla (ed), Instituto Espanol de Oceanografia, *Informes Technicos* 24-1984, 141-149.

Perkins, H. T., K. D. Saunders, G. Appel, and T. Mero (1980). Design and Initial Testing of a Three-Axis Current Meter. *OCEANS '80 Conference Record,* IEEE Pub. No. 80CH1572-7, 319-322.

Piacsek, S. A. (1977). A Numerical Simulation of the Interannual Seasonal Forcing of the Equatorial Pacific. *EOS, Transactions of the American Geophysical Union* 58(12), 1168.

Pickett, R. E. (1983). Great Lakes Bottom Currents. *Coastal Oceanography and Climatology News* 5(4), 41-43.

Pickett, R. E., R. M. Partridge, A. H. Clites, and J. E. Campbell (1983). Great Lakes Satellite-tracked Drifters. *Proceedings, 1983 Symposium on Buoy Technology*, Marine Technology Society, New Orleans, Louisiana.

Pierce, A. (1984). *Analytical Modeling of Random Thermal Fluctuations in the NORDA High Frequency Sound Scattering Facility.* Naval Ocean Research and Development Activity, NSTL, Mississippi, Technical Note 280.

Pilger, R. H. and **D. W. Handschumacher** (1980). The Easter-Nazca-Tuamotu and Hawaii-Emperor Chains: Volcanic Traces Incompatible with the Fixed Hotspot Hypothesis. *American Geophysical Union, Fall Meeting Abstracts.*

Poffenberger, D. (1982). *SHARPS III Configuration Management Guidelines.* Naval Ocean Research and Development Activity, NSTL, Mississippi, Technical Note 59.

Posey, J. W. and **C. Levenson** (1982). Propagation in a Random Medium: An Experiment Using Heating and Cooling in a Large Water Tank. *Journal of the Acoustical Society of America* 72(S1), S60.

Posey, J. W., C. Levenson, and **G. H. Branch** (1983). A Thermal Microstructure Measurement System (TMMS) to Support High-frequency Acoustic Experiments. *Journal of the Acoustical Society of America* 73(S1), p. S13.

Preller, R. H. (1985). *The NORDA/FNOC Polar Ice Prediction System (PIPS)—Arctic: A Technical Description*. Naval Ocean Research and Development Activity, NSTL, Mississippi, NORDA Report 108.

Preller, R. H. and **S. A. Piacsek** (1985). *Vertical Shear from TOPS*. Naval Ocean Research and Development Activity, NSTL, Mississippi, Technical Note 300.

Pressman, A. E. and **R. J. Holyer** (1978). *Interactive Digital Satellite Image Processing System for Oceanographic Applications*. Naval Ocean Research and Development Activity, NSTL, Mississippi, Technical Note 23.

Radl, C. J. and **J. P. Welsh** (1982). *Inventory of Arctic Laser Terrain Profiles*. Naval Ocean Research and Development Activity, NSTL, Mississippi, Technical Note 136.

Radl, C. J. and **J. P. Welsh** (1983). *Open Water and Thin Ice Detection in the Arctic Marginal Ice Zone Using Reflectometer Signal Analysis*. Naval Ocean Research and Development Activity, NSTL, Mississippi, Technical Note 209.

Radl, C. J. and **J. P. Welsh** (1985). *Ice Properties Survey: Literature Search, Volumes 1 and 2*. Naval Ocean Research and Development Activity, NSTL, Mississippi, Technical Note 317.

Ramsdell, J. V. and **J. D. Thompson** (1981). *Surface Stress Estimation for Study of the Circulation Dynamics of the Gulf of Mexico*. Naval Ocean Research and Development Activity, NSTL, Mississippi, Technical Note 125.

Regan, R. D., **D. W. Handschumacher**, and M. Sugiura (1979). A Closer Examination of the Utility of Satellite Magnetometer Data in Geologic Studies. *EOS, Transactions of the American Geophysical Union* 60(18), 245.

Reid, D. F., J. F. Todd, **D. A. Wiesenburg**, and J. H. Watkins (1983). Radium Across the Orca Basin Interface. *EOS, Transactions of the American Geophysical Union* 64(52), p. 1063–1064.

Rein, C. R. (1983). *Analysis of Enclosed Internal Combustion Engine Operation with Water as the Working Fluid*. Naval Ocean Research and Development Activity, NSTL, Mississippi, Technical Note 237.

Rein, C. R., D. A. Wiesenburg, and **D. M. Lavoie** (1985). *A Towed Instrument Vehicle for Deep Ocean Sampling*. Naval Ocean Research and Development Activity, NSTL, Mississippi, NORDA Report 90.

Richardson, M. D. (1982). *Acoustic, Physical, and Biological Properties of Surface Sediment Cores Collected from Long Island Sound, August 17–28, 1980*. Naval Ocean Research and Development Activity, NSTL, Mississippi, Technical Note 150.

Richardson, M D. (1983). Standing Stock and Vertical Distribution of Benthic Fauna from the Venezuela Basin. *EOS, Transactions of the American Geophysical Union* 64(52), 1086.

Richardson, M. D., J. H. Tietjen, and R. I. Ray (1983). *Environmental Support for Project WEAP East of Montauk Point, New York, 7–28 May 1982*. Naval Ocean Research and Development Activity, NSTL, Mississippi, NORDA Report 40.

Richardson, M. D., D. K. Young, and R. I. Ray (1983). *Environmental Support for High Frequency Acoustic Measurements at Nose Oceanographic Tower, 26 April–7 May 1982, Part 1: Sediment Geoacoustic Properties*. Naval Ocean Research and Development Activity, NSTL, Mississippi, Technical Note 219.

Riggins, M., **P. J. Valent, H. Li, J. T. Burns,** and C. E. Hickox (1985). *Pore Pressure Response to Probe Insertion and Thermal Gradient: ISIMU-II*. Naval Ocean Research and Development Activity, NSTL, Mississippi, Technical Note 259.

Rowe, P. C. (1983). *SHARPS III Winter Update*. Naval Ocean Research and Development Activity, NSTL, Mississippi, Technical Note 215.

Rowe, P. C. and R. M. Holt (1983). *SHARPS III Update Review—Fall 1983*. Naval Ocean Research and Development Activity, NSTL, Mississippi, Technical Note 221.

Saunders, K. D. (1980). Horizontal Response of the NBIS Current Meter. *Proceedings, OCEANS '80*, IEEE Pub. No. 80CH1472, 220–225.

Saunders, K. D. (1982). *Documentation of Software for Estimating XCP Fall Rates*. Naval Ocean Research and Development Activity, NSTL, Mississippi, NORDA Report 50.

Saunders, K. D. (1982). *Documentation of Software for the Neil Brown Instrument Systems/NORDA Velocity/CTD Profiler*. Naval Ocean Research and Development Activity, NSTL, Mississippi, Technical Note 155.

Saunders, K. D. (1985). *An Active Winch Control System for Ship induced Motion Isolation*. Naval Ocean Research and Development Activity, NSTL, Mississippi, NORDA Report 91.

Saunders, K. D. and **D. A. Burns** (1985). *Atlas of the Sognefjord Section, 1900–1970.* Naval Ocean Research and Development Activity, NSTL, Mississippi, NORDA Report 92.

Saunders, K. D. and W. Crawford (1981). Use of Explosives in Underwater Salvage Operations. *Proceedings, 1981 Explosives Conference of the IADC*, Houston, June.

Saunders, K. D. and **A. W. Green** (1981). *Measurement of High Frequency, High Wave Number Processes in the Upper Ocean: The Acoustically Tracked Oceanographic Mooring Experiment (ATOM '79), Final Report, Part I.* Naval Ocean Research and Development Activity, NSTL, Mississippi, Technical Note 129.

Saunders, K. D. and **A. W. Green** (1982). *Mooring Motion Workshop Summary Report.* Naval Ocean Research and Development Activity, NSTL, Mississippi, Technical Note 119.

Saunders, K. D., A. W. Green, and **M. Bergin** (1981). *A Comprehensive Graphical Representation of Data Obtained in the Acoustically Tracked Oceanographic Mooring (ATOM).* Naval Ocean Research and Development Activity, NSTL, Mississippi, Technical Note 85.

Saunders, K. D., A. W. Green, and F. C. Hamrick (1983). The ATOM '79 Mooring Motion Experiment. *Proceedings of the MTS/NDBC Symposium on Buoy Technology, 27–29 April*, Marine Technology Society, Washington, D.C., 200–209.

Saunders, K. D. and F. C. Hamrick (1982). Problems in Computing Coherence. *EOS, Transactions of the American Geophysical Union* 63(18), 344.

Saunders, K. D., H. T. Perkins, J. J. Vega, and **L. A. Banchero** (1981). Sea Trials of a 3-Axis Current/CTD Profiler. *Proceedings, OCEANS '81*, 245–249.

Sawyer, W. B. (1984). Top of Neogene Rocks, Thickness of Neogene Rocks, Thickness of Pleistocene Rocks. *Gulf of Mexico, Atlas 6, Ocean Margin Drilling Program, Regional Atlas Series*, R. T. Buffler et al. (eds.), Marine Science International, Woods Hole, Massachusetts, Sheets 11, 18, and 19.

Schumacher, J. D., R. Wilcox, and **T. H. Kinder** (1979). Observations of Advective and Diffusive Processes in the Southeastern Bering Sea. *EOS, Transactions of the American Geophysical Union* 60(4), 735–736.

Siquig, R., G. Shayne, L. Ballard, and **E. Hashimoto** (1985). *Navy Standard Analyzed Marine Wind Data Base for Latitudes 0° to 70° North.* Naval Ocean Research and Development Activity, NSTL, Mississippi, Technical Note 313.

Smith, P. M. (1981). *Measurements of Whitecap Coverage and Surface Winds Over the Gulf of Mexico Loop Current.* Naval Ocean Research and Development Activity, NSTL, Mississippi, NORDA Report 43.

Smith, P. M. and C. S. Lin (1984). *A Laser Slope Gauge and a Spar Buoy Wave Gauge: Tools for the Validation of Microwave Remote Sensors.* Naval Ocean Research and Development Activity, NSTL, Mississippi, Technical Note 301.

Smits, K. (1977). *Project Linear Chain Array System.* Naval Ocean Research and Development Activity, NSTL, Mississippi, Technical Note 11.

Smits, K. and **C. J. Crandall** (1981). *Development, Test, and Evaluation of Magnetic Environmental Filter (MEF) for Use with ASW-81 Magnetic Anomaly Detection System (MAD) Aboard Fleet P-3 Aircraft.* Naval Ocean Research and Development Activity, NSTL, Mississippi, Technical Note 112.

Snow, E. C. and **J. E. Matthews** (1980). *A Summary of Selected Data: DSDP Legs 1–19, Volume I*, and *A Summary of Selected Data: DSDP Legs 20–44, Volume II.* Naval Ocean Research and Development Activity, NSTL, Mississippi, NORDA Report 25.

Soileau, J. and **P. J. Bucca** (1984). *An Analytical Approach to the Refraction of Sound in the Water Column: New Atlantic.* Naval Ocean Research and Development Activity, NSTL, Mississippi, Technical Note 268.

Soileau, J. and **P. J. Bucca** (1984). *An Analytical Approach to the Refraction of Sound in the Water Column: Strait of Juan de Fuca.* Naval Ocean Research and Development Activity, NSTL, Mississippi, Technical Note 269.

Stanford, G. E. (1984). *Microwave Radiometric Measurement of Sea Surface Salinity.* Naval Ocean Research and Development Activity, NSTL, Mississippi, Technical Note 267.

Stanford, G. E. (1984). *Evolving Science and Technology Systems.* Naval Ocean Research and Development Activity, NSTL, Mississippi, NORDA Report 56.

Stephenson, G. D. (1983). *A Description of the NORDA Satellite Remote Sensing Hardware/Software for Prospective Users.* Naval Ocean Research and Development Activity, NSTL, Mississippi, Technical Note 205.

Stephensen, G. D. (1985). *A Description of NORDA's Software for Satellite Remote Sensing Data Processing/Analysis Applicable to TESS.* Naval Ocean Research and Development Activity, NSTL, Mississippi, Technical Note 292.

Su, M. Y. (1984). Three-dimensional Deep Water Waves. *Encyclopedia of Fluid Mechanics*, Gulf Publishing Company.

Su, M. Y. (1984). Characteristics of Extreme Wave Groups. *Proceedings, OCEANS 84*, Washington, D.C.

Su, M. Y. and **M. Bergin** (1983). Storm Wave Characteristics in the Gulf of Mexico. *Proceedings, Marine Technology Society/NOAA Data Buoy Center Symposium on Buoy Technology*, New Orleans, Louisiana, 17-19 April.

Su, M. Y., M. Bergin, and S. Bales (1982). Characteristics of Wave Groups in Storm Seas. *Proceedings, Ocean Structural Dynamics Symposium '82*, 118-132.

Su, M. Y., M. Bergin, R. J. Myrick, and J. Roberts (1982). Experiments on Shallow Water Wave Grouping and Breaking. *Proceedings, First International Conference on Meteorology and Air-Sea Interaction of the Coastal Zone*, 107-112.

Su, M. Y. and **A. W. Green** (1981). Experimental Studies of Strong Nonlinear Interactions of Deep-water Waves. *Proceedings, IUCRM Symposium on Wave Dynamics and Radio Probing of the Ocean Surface*, Miami, Florida, 13-20 May, Plenum Press, New York.

Su, M. Y. and **A. W. Green** (1983). Bubble Generation by Surface Wave Breaking. *Proceedings of XVIII General Assembly*, Hamburg, FRG, August. In *Proces-Verbaux* 16, 127.

Su, M. Y. and **A. W. Green** (1983). Experimental Studies of Surface Wave Breaking and Air Entrainment. *Proceedings, International Symposium on Gas Transfer at Water Surfaces*, Cornell University, Ithaca, New York.

Su, M. Y. and **A. W. Green** (1984). On the Predictability of Deep-water Waves. *Proceedings, Workshop on Predictability of Fluid Motions*, Scripps Institution of Oceanography, La Jolla, California, 1-4 February 1983. In *Predictability of Fluid Motions*, G. Holloway and B. West (eds.), American Institute of Physics, New York, 507-514.

Su, M. Y. and **A. W. Green** (1984). Strong Nonlinear Characteristics of Steep Surface Gravity Waves. *Proceedings of the 14th Symposium on Naval Hydrodynamics*, August 1982, Plenum Press, New York.

Su, M. Y. and **A. W. Green** (1984). Breaking Waves and Nonlinear Instability Coupling. *Proceedings, Symposium on Wave Breaking, Turbulence Mixing, and Radio Probing of the Ocean Surface*, Sendai, Japan.

Su, M. Y., A. W. Green, and **M. Bergin** (1984). Experimental Studies of Surface Wave Breaking and Air Entrainment. *Gas Transfer at Water Surfaces*, W. Brutsaert and G. Jirka (eds.), D. Reidel Publishing, Dordrecht, Holland, 211-220.

Sutherland, A. (1981). *Brine Measurement System (BRIMS) Section II: Implant Plan*. Naval Ocean Research and Development Activity, NSTL, Mississippi, Technical Note 94.

Sutherland, A., R. Miles, R. A. Brown, and **R. Williams** (1981). *The Brine Measurement System (BRIMS), Section III: Operation and Maintenance Manual*. Naval Ocean Research and Development Activity, NSTL, Mississippi, Technical Note 110.

Taylor, P. T. (1978). *Henderson Seamount Geological Data*. Naval Ocean Research and Development Activity, NSTL, Mississippi, Technical Note 18.

Taylor, P. T., P. R. Vogt, L. C. Kovacs, **J. A. Green,** and **D. W. Handschumacher** (1979). West-Arctic Ocean Basin: Aeromagnetic Results. *EOS, Transactions of the American Geophysical Union* 60(18), 372-373.

Teague, W. J. (1984). *Conversion of FEB Utilities of ASCII FORTRAN*. Naval Ocean Research and Development Activity, NSTL, Mississippi, Technical Note 275.

Thompson, J. D. (1978). The Role of Mixing in the Dynamics of Upwelling Ecosystems. *Upwelling Ecosystems*, Springer-Verlag, 203-218.

Thompson, J. D. (1981). Climate, Upwelling, and Biological Productivity: Some Primary Relationships. *Resource Management and Environmental Uncertainty: Lessons from Coastal Upwelling Fisheries*, M. H. Glantz and J. D. Thompson (eds.), Wiley-Interscience, 13-25.

Thompson, J. D. (1982). *Collinear Track Altimetry in the Gulf of Mexico from SEASAT Measurements, Models, and Surface Truths*. Naval Ocean Research and Development Activity, NSTL, Mississippi, Technical Note 57.

Thompson, J. D. (1984). The Influence of Actual and Apparent Geoid Error on Ocean Analysis and Prediction. *Frontiers of Remote Sensing of the Oceans and Troposphere from Air and Space Platforms*, J. Goldhirsh (ed.), NASA Marshall Space Flight Center, Alabama, Conference Publication 2303, 613-614.

Thompson, J. D. and **H. E. Hurlburt** (1979). *Gulf of Mexico—OTEC Far-field Numerical Studies: Description and Results of a Two-layer Model*. NORDA Final Report to Department of Energy under Interagency Agreement E(49-26)-1005 with Naval Research Laboratory, Washington, D.C.

Thompson, J. D. and **H. E. Hurlburt** (1982). A Numerical Study of the Influence of the New England Seamount Chain on the Gulf Stream: Preliminary Results. *Proceedings of the Workshop on Gulf Stream Structure and Variability*, J. M. Bane, Jr. (ed.), sponsored by the Office of Naval Research, p. 346-362.

Thompson, J. D., H. E. Hurlburt, and **P. J. Martin** (1978). Results from the Gulf of Mexico—OTEC Far-field Numerical Model. *Proceedings, 5th OTEC Conference*, A. Lavi and T. N. Veziroglu (eds.), 1, III141-164.

Thompson, J. D. and A. J. Wallcraft (1984). Ocean Modelling and Drifters. *Proceedings, 1984 Drifting Buoy Workshop*, Marine Technology Society, Gulf Coast Section, 81-98.

Tooma, S. (1978). *Northern Smith Sound Oceanography 1977*. Naval Ocean Research and Development Activity, NSTL, Mississippi, Technical Note 21.

Tucker, W. and **A. W. Green** (1977). Thermocline Formation in Large and Small Lakes. *Proceedings of the Symposium on Modeling of Transport Mechanisms in Oceans and Lakes*. Fisheries and Environment Canada, Manuscript Report Series No. 43, 193-197.

Valent, P. J., T. L. Holcombe, J. F. Gettrust, and **F. A. Bowles** (1983). *Technical Assessment: Rapid Nearshore Geotechnical Surveying*. Naval Ocean Research and Development Activity, NSTL, Mississippi, Report 68.

VanWyckhouse, R. (1982). *Acoustic Parameter Charts*. Naval Ocean Research and Development Activity, NSTL, Mississippi, Technical Note 166.

Walker, C., R. M. Brown, and W. Osterman (1983). *Raster Scan Character Recognition System*. Naval Ocean Research and Development Activity, NSTL, Mississippi, Technical Note 187.

Warn-Varnas, A. C. (1982). *Studies of Large-scale Thermal Variability with a Synoptic Mixed-layer Model*. Naval Ocean Research and Development Activity, NSTL, Mississippi, Technical Note 156.

Warn-Varnas, A. C. and **G. M. Dawson** (1981). *An Analysis of Modelled Shear Distribution During MILE*. Naval Ocean Research and Development Activity, NSTL, Mississippi, Technical Note 84.

Warn-Varnas, A. C. and **J. M. Harding** (1977). An Investigation of the Importance of Third-Order Correlations in Mixed Layer Models. *EOS, Transactions of the American Geophysical Union* 58(12), 1162.

Wasowski, S. (1980). *Oceanographic Management and Information System (OMIS): The Navy Oceanographic Program, DATABASE*. Naval Ocean Research and Development Activity, NSTL, Mississippi, Technical Note 67.

Wasowski, S. (1981). *Oceanographic Management Information System (OMIS): The Navy Oceanographic Requirements Database, Development Phase*. Naval Ocean Research and Development Activity, NSTL, Mississippi, Technical Note 79.

Watrous, B. A., R. J. VanWyckhouse, and **J. V. Soileau** (1983). *Environmental Variability of the Jordan Basin, Gulf of Maine, August 1982, NRL Cruise 712-82*. Naval Ocean Research and Development Activity, NSTL, Mississippi, Technical Note 243.

Welsh, J. P. (1978). *Test and Evaluation of POLAR STAR, Volumes I-IV*. Naval Ocean Research and Development Activity, NSTL, Mississippi, NORDA Report 22.

Wenzel, A. R. (1982). Attenuation of Low- and High-frequency Waves in a Random Medium. *Journal of the Acoustical Society of America* 72(S1), S60.

Wenzel, A. R. (1983). A Comparison of the Quasi-Rytov and Smooth Methods. *Journal of the Acoustical Society of America* 73(S1), S13.

Werby, M. F. (1983). Convergence and the T-Matrix. *Journal of the Acoustical Society of America* 73(S1), Spring.

Werby, M. F. (1983). Resonance Studies of Submerged Elastic Spheroids for Several Materials. *Journal of the Acoustical Society of America* 73(S1), Spring.

Werby, M. F. (1983). Excitation of Anomalous Resonances for Acoustical Scattering from Fluid-loaded Elastic Spheroids. *Journal of the Acoustical Society of America* 74(S1), Fall.

Werby, M. F. (1983). Rigid Scattering from Fluid-loaded Objects for High Aspect Ratio. *Journal of the Acoustical Society of America* 74(S1), Fall.

Werby, M. F. (1984). *Ocean Data Base Survey*. Naval Ocean Research and Development Activity, NSTL, Mississippi, Technical Note 254.

Werby, M. F. (1984). Numerical Treatment of Scattering from Submerged Objects. *Journal of the Acoustical Society of America* 76(S1), Fall.

Werby, M. F and **S. A. Chin-Bing** (1985). Some Numerical Techniques and Their Use in the Extension of T-matrix and Null-field Approaches to Scattering. *Computational Ocean Acoustics*, M. H. Schultz and D. Lee (eds.), Pergamon Press, Oxford.

Werby, M. F. and G. Gaunaurd (1985). Scattering from Spheroidal Shells. *Proceedings of ASME Conference on Dynamics of Plates and Shells*, New Orleans, Louisiana, June.

Werby, M. F. and L. H. Green (1983). Study of Acoustical Scattering from Submerged Spheroidal Elastic Shells. *Journal of the Acoustical Society of America* 83(S1), Spring.

Werby, M. F. and L. H. Green (1984). A Comparison of Acoustical Scattering from Fluidloaded Elastic Shells

and Sound Soft Objects. *Journal of the Acoustical Society of America* 75(S1), Spring.

Werby, M. F. and R. Hackman (1983). Differential Scattering Cross Sections and the Study of Resonances for Immersed Fluid-loaded Objects. *Journal of the Acoustical Society of America* 73(S1), Spring.

Werby, M. F. and R. Hackman (1983). A Study of Acoustical Scattering from Axially Symmetric Fluid Loaded Elastic Objects with Ridges. *Journal of the Acoustical Society of America* 73(S1), Spring.

Werby, M. F. and R. Hackman (1983). The Isolation of Physical Mechanisms Associated with Acoustical Scattering from Submerged Elastic Spheroidal and Spherical Shells. *Journal of the Acoustical Society of America* 74(S1), Fall.

White, D. and **S. A. Chin-Bing** (1982). Comparison Between Perturbative and Exact Treatment of Bottom Attenuation for Shallow-water, Low-frequency Conditions. *Journal of the Acoustical Society of America* 7(S1), S11.

White, D. and **S. A. Chin-Bing** (1983). Source Depth Classification by Modal Decomposition and Correlation. *Journal of the Acoustical Society of America* 74(S1), S118.

Wiesenburg, D. A. (1985). *Bibliography of Research on Ocean Fronts, 1964-84*. Naval Ocean Research and Development Activity, NSTL, Mississippi, Technical Note 303.

Wiesenburg, D. A. (1985). *Operation Guiding Light—Scientific Program and Field Plan: The Pilot Field Experiment for NORDA Project Chemical Dynamics in Ocean Frontal Areas*. Naval Ocean Research and Development Activity, NSTL, Mississippi, Technical Note 308.

Wiesenburg, D. A., J. M. Brooks, and **D. F. Reid** (1982). Suspended Particulate Distributions Across the Orca Basin Interface. *EOS, Transactions of the American Geophysical Union* 63, 991.

Wiesenburg, D. A. and N. L. Guinasso, Jr. (1982). Thermal Structure and Heat Flow in the Orca Basin, Northern Gulf of Mexico. *EOS, Transactions of the American Geophysical Union* 63, 108-109.

Wiesenburg, D. A., D. F. Reid, D. L. Lavoie, and **I. P. DePalma** (1985). *Chemical, Biological, and Physical Measurements from the Subtropical Western North Atlantic Ocean, Summer 1982, USNS LYNCH, Cruise 710-82*. Naval Ocean Research and Development Activity, NSTL, Mississippi, Technical Note 306.

Wilcox, C. C., B. Hold, and R. McQuinn (1982). *SHARPS III Update Review—Autumn 1982*. Naval Ocean Research and Development Activity, NSTL, Mississippi, Technical Note 169.

Won, I. J. (1985). *Magnetic Fields at the Ocean Bottom Generated by a Vertical Magnetic Dipole Placed On or Below the Ocean Surface*. Naval Ocean Research and Development Activity, NSTL, Mississippi, NORDA Report 96.

Won, I. J. and **K. Smits** (1985). *Airborne Electromagnetic Bathymetry*. Naval Ocean Research and Development Activity, NSTL, Mississippi, NORDA Report 94.

Won, I. J. and **K. Smits** (1985). *Airborne Electromagnetic Measurements of Electrical Conductivities of Seawater and Bottom Sediments Over Shallow Water*. Naval Ocean Research and Development Activity, NSTL, Mississippi, NORDA Report 95.

Won, I. J. and **K. Smits** (1985). *High Resolution Electromagnetic Altimetry Over Oceans*. Naval Ocean Research and Development Activity, NSTL, Mississippi, NORDA Report 104.

Won, I. J. and **K. Smits** (1985). *Determination of Electrical Depths and Bottom Characteristics of Shallow Oceans Using the Airborne Electromagnetic Method*. Naval Ocean Research and Development Activity, NSTL, Mississippi, NORDA Report 106.

Young, D. K. (1982). Nondestructive Measuring of Effects of Bioturbation Sediment Structure. *EOS, Transactions of the American Geophysical Union* 63(3), 104.

Young, D. K. (1983). Photographs of Deep-sea Lebensspuren: A Comparison of Sedimentary Provinces. *EOS, Transactions of the Ameican Geophysical Union* 64(52), 1086.

Young, D. W. and panel members (1982). Effects of Nutrients and Carbon Loadings on Communities and Ecosystems. *Ecological Stress and the New York Bight: Science and Management*, G. F. Meyer (ed.), Estuarine Research Federation, University of South Carolina Press, 53-65.

Young, D. W. and M. W. Young (1982). Macroinvertebrate Invertebrates in Bare Sand and Seagrass (Thalassia testudinum). The Atlantic Barrier Reef Ecosystem at Carrie Bow Cay, Belize, I. Structure and Communities, K. Rutzler and I. C. Macintyre (eds.), *Smithsonian Contributions to the Marine Sciences* 12, 115-126.

Young, D. W. and M. W. Young (1982). Marine Macrobenthos as Indicators of Environmental Stress. *Ecological Stress and the New York Bight: Science and Management*, MESA/NOAA Symposium Volume, Wiley Interscience, New York, 527-539.

Zahuranec, B. J. (1976). *Shark Hazards on Navy Marine Corps Operations*. Naval Ocean Research and Development Activity, NSTL, Mississippi, Technical Note 2.

Zahuranec, B. J. (1977). *Taxonomy and Distribution of Lantern Fishes (Family Myctophidae) of the Eastern Pacific Ocean*. Naval Ocean Research and Development Activity, NSTL, Mississippi, NORDA Report 3.

Zalkan, R. L. and L. B. Wetzel (eds.) (1981). *Describing Ocean Phenomena Using Coherent Radars: Proceedings, NORDA Workshop*. Naval Ocean Research and Development Activity, NSTL, Mississippi, Technical Note 104.

Zollinger, R., A. Becker, and F. Morrison (1985). *Data Analysis of Airborne Electromagnetic Bathymetry*. Naval Ocean Research and Development Activity, NSTL, Mississippi, NORDA Report 93.

Zsolnay, A. (1983). The Classification of Venezuela Basin Sediments with Pyrolysis-Mass Spectrometry. *EOS, Transactions of the American Geophysical Union* 64(52), 1085.

Zsolnay, A., D. M. Lavoie, D. A. Wiesenburg, and **D. F. Reid** (1984). *Environmental Parameters in Exuma Sound and the Straits of Florida*. Naval Ocean Research and Development Activity, NSTL, Mississippi, Technical Note 252.

Presentations

Ballard, J. A. (1976). Geometrical and Environmental Constraints on Single Channel Seismic Record Interpretation. *Seismology Symposium of the Acoustical Society of America*, Annual Meeting, San Diego, California.

Ballard, J. A. (1978). Structural Patterns in the Canary Basin. *48th Annual International Meeting of the Society of Exploration Geophysicists*, San Francisco, California.

Ballard, J. A. (1979). Marine Earthquake Monitoring System. *Ocean Crustal Dynamics Committee Workshop*, La Jolla, California.

Ballard, J. A. (1984). The Marine Seismic System. Invited speaker, *54th Annual International Meeting of the Society of Exploration Geophysicists*, Atlanta, Georgia.

Ballard, J. A., F. K. Duennebrer, R. Stephen, and **J. Gettrust** (1982). Borehole Seismic Station in the Northwest Pacific Ocean. *American Geophysical Union, Annual Meeting*, San Francisco, California.

Ballard, J. A., P. R. Vogt, and **J. Egloff** (1976). Seismic Structure of the J-Anomaly in the Eastern Atlantic. *57th American Geophysical Union Annual Meeting*, Washington, D.C.

Bennett, R. H. (1982). Deep-ocean Piezometer System: Pore Pressure Events During High Pressure Simulation Tests. *SEPM/NORDA Research Conference on the Seafloor Stability of Continental Margins*, Diamondhead, Mississippi, 11-15 October.

Bennett, R. H. (1983). NORDA's Activities in the In Situ Heat Transfer Experiment (ISHTE). *14th Annual Meeting of the Subseabed Disposal Program*, Denver, Colorado, October.

Bennett, R. H. (1984). In Situ Undrained Shear Strengths and Permeabilities Derived from Piezometer Measurements. *ASTM Symposium on Laboratory and In Situ Determination of the Strength of Marine Soils*, San Diego, California.

Bowles, F. A. (1984). Orinoco/Amazon River Sediment Input to the Eastern Caribbean Basin. *American Geophysical Union Ocean Sciences Meeting*, New Orleans, Louisiana.

Boyd, J. D. (1982). Deep Ocean Currents Near DSDP Hole 395A (22°45'N, 46°10'W) and Possible Effects on Ocean Bottom Seismometers. *46th Annual Meeting of the Mississippi Academy of Sciences*, Biloxi, 4-5 March.

Boyd, J. D. and **T. H. Kinder** (1982). Vertical Wavenumber Spectra of Temperature, Salinity, and Sigma-t Profiles in the SE Caribbean. *American Geophysical Union Meeting*, Philadelphia, Pennsylvania, 31 May-4 June.

Boyd, J. D. and **H. T. Perkins** (1984). Estimates of Vertical Heat and Salt Fluxes in a Thermohaline Staircase. *American Geophysical Union/Society of Limnology and Oceanography Meeting*, San Francisco, California, 3-7 December.

Boyd, J. D., H. T. Perkins, and **K. D. Saunders** (1984). Characteristics of Thermohaline Step Structures Off the Northeast Coast of South America. *American Geophysical Union/Society of Limnology and Oceanography Meeting*, New Orleans, Louisiana, 23-27 January.

Briggs, K. B. (1983). Deposit-feeding Strategies of Some Deep-sea Megabenthos from the Venezuela Basin. *Benthic Ecology Meetings*, Florida Institute of Technology, Melbourne, 25-27 March.

Brooks, J. M., **D. F. Reid**, and R. A. Lamontagne (1982). Methane Geochemistry in the Equatorial Pacific and Atlantic. *American Geophysical Union Annual Meeting*, San Francisco, California, December.

Brooks, J. M., **D. A. Wiesenburg**, and T. Ichiye (1982). Use of Volatile Organics as Tracers of Waste Dispersion at an Ocean Dumpsite. *Ocean Sciences 1982*, San Antonio, Texas, 16-19 February.

Brunson, B. A. and **J. E. Matthews** (1982). Laboratory Measurements of Shear Wave Attenuation in Natural and Synthetic Sediments. *Society of Exploration Geophysicists/U.S. Navy Shear Waves and Pattern Recognition Symposium*, NSTL, Mississippi, 22-23 March.

Buffler, R. T., S. Locker, C. D. Cagle, **W. B. Sawyer**, J. C. Crowe, and R. L. Phair (1983). Results of Ocean Margin Drilling Program Synthesis of Gulf of Mexico Basin. *American Association of Petroleum Geologists Annual Convention*, Austin, Texas.

Carey, W. M. (1983). Sound Propagation from a Coastal Source to a Deep Ocean Receiver. *105th Meeting of the Acoustical Society of America*, Cincinatti, Ohio, 10-13 May, Paper AA6, 73(S1), S55(AA6).

Carey, W. M. and M. P. Bradley (1985). Low-frequency Ocean Surface Noise Sources. *110th Meeting of the Acoustical Society of America*, Nashville, Tennessee, 4-8 November.

Carey, W. M. and N. Yen (1984). The Formation of a Synthetic Aperture with Towed Hydrophones. *107th Meeting of the Acoustical Society of America*, Norfolk, Virginia, 9 May, Paper GG6.

Chin-Bing, S. A. (1985). The Influence of Water-to-ice Transition Layers on the Reflection Coefficient and High-frequency Acoustic Backscatter from an Ice Keel. *110th Meeting of the Acoustical Society of America*, Nashville, Tennessee, 4-8 November.

Chin-Bing, S. A. and **D. B. King** (1984). The Effect of Large Thermohaline Steps on Acoustic Propagation Near the Northeast Coast of South America. *108th Meeting, Acoustical Society of America, Minneapolis, Minnesota*, 8-12 October.

Davis, J. A. and **S. A. Chin-Bing** (1978). Mode Theory Reflection Coefficient. *96th Meeting, Acoustical Society of America*, Honolulu, Hawaii, 27 November-1 December.

Davis, J. A. and **S. A. Chin-Bing** (1978). Mode and Ray Theory Comparison for a Completely Absorbing Bottom. *96th Meeting, Acoustical Society of America*, Honolulu, Hawaii, 27 November-1 December.

Del Balzo, D., M. Authement, and C. T. Mire (1985). Calculations of Ocean Ambient Noise Over a Continental Slope. *110th Meeting of the Acoustical Society of America*, Nashville, Tennessee, 4-8 November.

Egloff, J. (1977). Sedimentary Structures of the Southwest Iceland Outer Shelf and Slope. *American Association of Petroleum Geologists Research Conference, Geophysical Investigations of Continental Slopes and Rises*, Galveston, Texas, 12-14 January.

Egloff, J., G. Sommerhoff, and G. L. Johnson (1982). Canyons, Submarine Fans, and Older Structures of Southern Greenland Continental Margin from Seismic Surveys. *American Association of Petroleum Geologists Annual Convention*, Calgary, Alberta, Canada, July.

Egloff, J. and G. L. Johnson (1982). The Discovery of a Tensional Release Feature on the Insular Slope/Rise of W. Iceland, and Comparison with SE Greenland Canyons and Slumps. *SEPM/NORDA Conference on Seafloor Stability*, Diamondhead, Mississippi, October.

Eller, A. (1985). Implementation of Rough Surface Loss in Sonar Performance Models. *OCEANS '85*, San Diego, California, 12-14 November.

Evans, R. B. (1985). The Stabilization of Stepwise Coupled Modes. *110th Meeting of the Acoustical Society of America*, Nashville, Tennessee, 4-8 November.

Fagot, M. G. (1978). Deep-Towed Seismic System Design. *1st Biennial Society of Exploration Geophysicists/U.S. Navy Joint Technical Symposium on Acoustic Imaging Technology and On-board Data Recording and Processing*, NSTL, Mississippi.

Fagot, M. G. (1978). Deep-Towed Seismic System Design. *48th Annual International Meeting of the Society of Exploration Geophysicists*, San Francisco, California.

Fagot, M. G. and **B. E. Eckstein** (1979). Deep-Towed Seismic Profiling System. *Electronics and Aerospace Systems Conference, EASCON 79*, Arlington, Virginia.

Fagot, M. G., N. H. Gholson, G. J. Moss, and **D. A. Milburn** (1980). A Deep-Towed Geophysical Array System. *50th Annual International Meeting of the Society of Exploration Geophysicists*, Houston, Texas.

Fagot, M. G., D. A. Milburn, N. H. Gholson, and **B. E. Eckstein** (1980). A Deep-Towed Array Geophysical System. *2nd Biennial Society of Exploration Geophysicists/U.S. Navy Joint Technical Symposium on High Resolution*, NSTL, Mississippi.

Fagot, M. G., G. J. Moss, D. A. Milburn, and **N. H. Gholson** (1981). Deep-Towed Seismic System Design for Operation at Depths Up to 6000 m. *13th Offshore Technology Conference*, Houston, Texas.

Fagot, M. G. and **S. E. Spychalski** (1982). Deep-Towed Seismic System: A Hardware Description. *52nd Annual International Meeting of the Society of Exploration Geophysicists*, Dallas, Texas.

Fagot, M. G. and **S. E. Spychalski** (1984). Development of a Deep-Towed Seismic System – A Potential New 3-D Tool. *4th Biennial Society of Exploration Geophysicists/U.S. Navy Joint Technical Symposium on Three Dimensional Marine Data Collection, Processing, Interpretation, and Presentation*, NSTL, Mississippi.

Fagot, M. G. and **S. E. Spychalski** (1984). Development of a Deep-Towed Geophysical Sound Source, Multi-Channel Array, and Telemetry System. *Remotely Operated Vehicle Conference and Exposition*, San Diego, California.

Fenner, D. F. (1981). Sound Speed Structure of the South Atlantic Ocean. *NAVOCEANO/NORDA South Atlantic Conference*, NSTL, Mississippi, 19 May.

Fenner, D. F. (1984). Temperature Salinity and Sound Speed Structure Related to the Dynamics of the Argentine Basin. *American Geophysical Union Ocean Sciences Meeting*, New Orleans, Louisiana.

Feuillade, C. and **W. Kinney** (1985). Source Localization in a Waveguide Using a Matched-field Technique. *110th Meeting of the Acoustical Society of America*, Nashville, Tennessee, 4-8 November.

Fleischer, P. (1984). Mine Burial: Field Tests to Assess Its Likelihood in U.S. Waters and to Evaluate Burial

25th Mine Development Conference. Naval Surface Weapons Center, White Oak, Maryland, 13 May.

Fleischer, P., R. M. Fitchko, and R. L. Fleisher (1979). Outcrop Patterns and Cenozoic Continental Slope Development Between Blake Plateau and Cape Hatteras. *Geological Society of America, Southeastern Section Meeting*, Blacksburg, Virginia (invited paper).

Gaunaurd, G., C. Feuillade, and **M. F. Werby** (1985). Scattering from Submerged Solid-, Fluid-, and Air-filled Elastic Shells to the High ka Region. *110th Meeting of the Acoustical Society of America*, Nashville, Tennessee, 4-8 November.

Gershfield, D. A. and **A. I. Eller** (1983). Optimum Frequency of Acoustic Propagation in Shallow Water. *106th Meeting of the Acoustical Society of America*, San Diego, California, 7-11 November.

Green, L. H., M. F. Werby, and R. Wooten (1985). The Interaction of Acoustic Waves with Multi-layered Shells. *110th Meeting of the Acoustical Society of America*, Nashville, Tennessee, 4-8 November.

Harding, J. M., R. H. Clancy, and J. P. French (1984). Operational Mixed Layer Forecasts Compared with Ocean Station Data. *American Geophysical Union Fall Meeting*, San Francisco, California.

Harding, J., R. M. Clancy, J. Hawkins, and **G. Heburn** (1984) U.S. Navy Operational Ocean Thermal Analysis and Prediction: Present Capabilities, Future Plans. *4th Biennial Society of Exploration Geophysicists/U.S. Navy Joint Technical Symposium on Three-dimensional Marine Data Collection, Processing, Interpretation, and Presentation*, NSTL, Mississippi.

Harding, J. M., H. E. Hurlburt, L. B. Lin, D. R. Moore, and A. J. Wallcraft (1982). Intercomparison of Primitive Equation and Quasigeostrophic Simulations of a Mid-latitude Jet. *American Geophysical Union Fall Meeting*, San Francisco, California.

Harding, J. M. and T. Laevastu (1976). Evaporation and Transport of Latent Heat in Relation to Surface and Mid-atmospheric Systems Development. *American Meteorological Society Conference on Atmospheric and Oceanic Waves and Stability*, Seattle, Washington.

Harding, J. M., R. H. Preller, and **S. A. Piacsek** (1982). Vertical Shear from TOPS. *NORDA Ocean Measurement Programs Shear Workshop*, NSTL, Mississippi.

Heburn, G. W. (1984). Effects of Wind Versus Hydraulic Forcing of the Dynamics of the Western Mediterranean Sea. *XXIX Congress and Plenary Session of the International Commission of the Scientific Exploration of the Mediterranean Sea*, Lucerne, Switzerland, 11-19 October.

Holcombe, T. L. (1983). Perspective on Marine Geology and Geophysics Research. *Workshop on Southern Oceans*, Palisades, New York, 14-15 March.

Holcombe, T. L. (1983). Quaternary Turbidites of the Muertos Trough—Composition, Source, and Dispersal Patterns. *Tenth Caribbean Geological Conference*, Cartagena, Colombia, 15-19 August.

Holland, C. R. and E. L. Burdette (1983). In Situ Data Selection and Compression as a Tool for Extending the Lifetome of Remote Acquisition Systems. *OCEANS '83*.

Holland, C. R., R. T. Miles, and **L. B. Stogner** (1983). Adaptive Multiprocessor Data Acquisition System. *International Symposium on Ocean Instrumentation*, Woods Hole Oceanographic Institution, Woods Hole, Massachusetts, October.

Jahn, W. H. (1980). *Deep Ocean Photography Exhibit*. New Orleans Museum of Art, New Orleans, Louisiana, 23 February-7 April.

Jahn, W. H. (1980). *Deep Ocean Photography Exhibit*. San Diego Natural History Museum, Balboa Park, San Diego, California, 12 June-10 August.

Jahn, W. H. (1980-1981). *Deep Ocean Photography Exhibit*. Science Museum of Minnesota, St. Paul, 15 October-18 January.

Jahn, W. H. (1981). *Deep Ocean Photography Exhibit*. National Space Technology Laboratories, Visitor's Center, NSTL, Mississippi, 10 April-12 September.

Jahn, W. H. (1982). *Deep Ocean Photography Exhibit*. Smithsonian Institution, Washington, D.C., January.

Jahn, W. H. (1982). *Selected Photographs from the Deep Ocean Photography Exhibit*. International Hydrographic Conference, Monte Carlo, Monaco, 20-30 April.

Jahn, W. H. (1982). *Selected Photographs from the Deep Ocean Photography Exhibit*. OCEANS '82, Washington, D.C., 20-22 September.

Jahn, W. H. (1983). *Deep Ocean Photography Exhibit*. American Museum of Natural History, New York, New York, 22 January-15 May.

Jahn, W. H. (1983). *Deep Ocean Photography Exhibit*. Intrepid Sea-Air-Space Museum, New York, New York, 20 May-2 October.

Jahn, W. H. (1983-1984). *Deep Ocean Photography Exhibit*. Chicago Museum of Science and Industry, Chicago, Illinois, 27 October-3 January.

Kinder, T. H. (1979). A Perspective on Physical Oceanography in the Bering Sea. Invited talk, *Plenary Session, Bering Sea Symposium* (Sponsored by NOAA/Bureau of Land Management), Anchorage, Alaska.

Kinder, T. H., G. W. Heburn, J. D. Boyd, J. H. Allender, and **H. E. Hurlburt** (1982). Spatial and Temporal Scales of Physical Variability Near the Southern Lesser Antilles. *American Geophysical Union/Society of Limnology and Oceanography Meeting*, San Antonio, Texas, 16–18 February.

Kinney, W. A. (1985). Coherence Versus Time Delay for Spatially Separated Receivers in Deep Water Using a Z-transform Method. *110th Meeting of the Acoustical Society of America*, Nashville, Tennessee, 4–8 November.

Kuperman, W. A., M. F. Werby, and **K. E. Gilbert** (1984). Towed Array Response to Ship Noise: A Nearfield Propagation Problem. *NATO Conference on Underwater Acoustics and Signal Processing*, Luneberg, W. Germany, 30 July.

Lambert, D. G. (1982). In Situ Geotechnical Instrumentation from a Submersible. *SEPM/NORDA Research Conference on Seafloor Stability of Continental Margins*, Diamondhead, Mississippi, 11–15 October.

Lambert, D. N., P. J. Valent, M. D. Richardson, and G. F. Merrill (1984). Shear Strength Variability in Three Sedimentary Provinces of the Venezuela Basin. *American Geophysical Union Ocean Science Meeting*, New Orleans, Louisiana, January.

Langran, G. L. (1983). Automated Point Selection and Labeling for Geographic Data Bases. *Fourth Annual Meeting of the National Computer Graphics Association*, Chicago, Illinois, 26–30 June.

Langran, G. L. (1984). Map Design for DMA's Digital Age. *DoD Mapping, Charting, and Geodesy Users Conference*, Washington, D.C., October.

La Violette, P. E. (1983). Short-term Measurements of the Velocity of Currents Associated with the Alboran Sea Gyre During Donde Va?. *American Geophysical Union Spring Meeting*, Baltimore, Maryland, June

La Violette, P. E. (1983). Results of the Synthetic Aperture Radar Experiment Off the Grand Banks. *American Geophysical Union Spring Meeting*, Baltimore, Maryland, June.

La Violette, P. E. and **R. A. Arnone** (1984). A Preliminary Study of a Standing Wave in the Western Approaches to the Strait of Gibraltar. *XXIX Congress and Plenary Session of the International Commission for the Scientific Exploration of the Mediterranean Sea*, Lucerne, Switzerland, 11–19 October.

Lavoie D. (1984). Methane Production from Oceanic Seston. *47th Annual Meeting of ASLO*, Vancouver, B.C., 11–14 June.

Lavoie, D. L. and **J. E. Matthews** (1983). Sediments on the Southeastern Flank of the Bermuda Pedestal. *Geological Society of America Annual Meeting*.

Lavoie, D. L. and **J. E. Matthews** (1984). Sediment Physical Property Measurements. *Research and Related Activities in the Correlation of Acoustic-Geotechnical Properties Workshop*, Calgary, Canada, 16–17 April.

Li, H. (1979). A Time-Dependent Ice Drift Model in the Arctic Ocean. *American Geophysical Union 1979 Fall Meeting*, San Francisco, California, 3–7 December.

Li, H. (1981). A Study of Recent Data Sets Exhibiting Wind-induced Ambient Noise. *101st Meeting of the Acoustical Society of America*, Ottawa, Ontario, Canada, 18–22 May.

Li, H., S. A. Tooma, R. D. Ketchum, and **J. P. Welsh** (1978). Sea Ice Airborne Infrared Radiometry. *World Meteorological Organization Workshop on Remote Sensing of Sea Ice*, Washington, D.C., 16–20 October.

Lin, L. B. and **J. M. Harding** (1978). A Numerical Simulation of the Pacific Equatorial Undercurrent. *American Geophysical Union Fall Meeting*, San Francisco, California.

Lin, L. B. and **J. M. Harding** (1979). Simulation of the Pacific Equatorial Circulation. *INDEX Theoretical Meeting*, Ft. Lauderdale, Florida.

Little, B. J. (1983). An Assessment of the Factors Influencing the Adsorption of Dissolved Organic Material from Naturally Occurring Waters. *Symposium on Initial Events in Biofouling*, sponsored by the Office of Naval Research, La Jolla, California, December.

Little, B. J. and **A. Zsolnay** (1982). Chemical Fingerprinting of Adsorbed Organic Material. *American Chemical Society Meeting*, Las Vegas, Nevada, March.

Lohanick, A. W. and **J. P. Welsh** (1981). Some Effects of Snow Cover on 33 GHz Passive Signatures of Sea Ice. *URSI Commission F Symposium on Signature Problems in Microwave Remote Sensing of the Surface of the Earth*, University of Kansas, Lawrence, 5–8 January.

Matthews, J. E., M. D. Richardson, B. A. Brunson, and **F. S. Carnaggio** (1982). Shear Wave Measurements at OSTL. *Society of Exploration Geophysicists/U.S. Navy Shear Waves and Pattern Recognition Symposium*, NSTL, Mississippi, 22–23 March.

McIntosh, J. A. and **J. P. Welsh** (1981). A Provisional Calculation of the Icebreaking Resistance of the USCGC POLAR STAR. *Ice Tech 81, Star Symposium, The Society of Naval Architects and Marine Engineers*, Ottawa, Ontario, Canada, 16–19 June.

Milburn, D. A. and **T. Burke** (1985). Ocean Acoustic Measuring Systems: VEKA and VEDABS. *OCEANS '85*, San Diego, California, 12–14 November.

Mohr, D. L., J. P. French, **A. C. Warn-Varnas, J. M. Harding,** and **R. M. Clancy** (1983). Statistical Forecasts of Temperature Profiles in the North Atlantic. *American Geophysical Union Ocean Sciences Meeting*, New Orleans, Louisiana.

Muench, R. D., J. D. Schumacher, and **T. H. Kinder** (1979). Flux of Horizontal Kinetic Energy Over the Southeastern Bering Sea. *IUGG Assembly*, Canberra.

Murphy, D., D. Del Balzo, and **R. Wagstaff** (1985). Computer Simulation of the Vertical Structure of Mid-ocean Ambient Noise. *110th Meeting of the Acoustical Society of America*, Nashville, Tennessee, 4-8 November.

Pai, S. I., M. D. Das, and **H. Li** (1977). Compactness and Thickness Effects on Drift of Arctic Pack Ice. *Symposium on Sea Ice Process and Models*, Seattle, Washington, 6-9 September.

Pedersen, M. A. and **R. McGirr** (1983). Experimental and Theoretical Statistical Distributions of Underwater Acoustic Propagation Losses. *Eleventh International Congress of Acoustics*, Paris, France, Paper 28-11.

Peltzer, R. D., W. D. Garrett, and **P. M. Smith** (1985). A Remote Sensing Study of a Surface Ship Wake. *OCEANS '85*, San Diego, California, 12-14 November.

Perkins, H. T. (1983). Current and Hydrographic Sections in the Mediterranean Inflow and Outflow. *Donde Va? Workshop*, Instituto Oceanografico, Fuengirola, Spain, 19 October.

Perkins, H. T. (1984). First Results from the NORDA Sections in the Tropical Atlantic. *Third FOCAL/SEQUAL Reunion*, Paris (UNESCO), France, 18 February.

Perkins, H. T. and **J. D. Boyd** (1984). Characteristics of Thermohaline Step Structures Off the Northeast Coast of South America. *American Geophysical Union Ocean Sciences Meeting*, New Orleans, Louisiana, 25 January.

Perkins, H. T. and **T. H. Kinder** (1984). The Flow of Atlantic Water into the Alboran Sea During Donde Va?. *XXIX Congress and Plenary Session of CIESM*, Lucerne, Switzerland, 12 October.

Piacsek, S. A. and **J. M. Harding** (1977). A Numerical Simulation of the Interannual Seasonal Forcing of the Equatorial Pacific. *American Geophysical Union Fall Meeting*, San Francisco, California.

Reid, D. F., E. A. Boyle, and A. J. Spivack (1982). Covariance of Radium and Copper in Mediterranean Sea Surface Waters. *American Geophysical Union/ASLO Ocean Sciences Meeting*, San Antonio, Texas, 16-19 February.

Richardson, M. D. (1982). Effects of Bioturbation on Sediment Elastic Properties, as Measured Acoustically. *American Geophysical Union/ASLO Ocean Sciences Meeting*, San Antonio, Texas, 16-19 February.

Richardson, M. D. (1983). The Effects of Bioturbation on Sediment Elastic Properties. Invited paper, *Symposium on Relations Entre Organismes et Sediments*, AGSO/SGF/UOF, Perpignan, France, 7-9 October.

Saunders, K. D. (1985). Design and Initial Testing of a Motion Compensating Winch System. *OCEANS '85*, San Diego, California, 12-14 November.

Saunders, K. D. and F. C. Hamrick (1982). Problems in Computing Coherence. *American Geophysical Union Spring Conference, Philadelphia, Pennsylvania, May.*

Stanic, S., B. Eckstein, and D. Sherman (1985). NORDA's Shallow-water Acoustic Measurements System. *OCEANS '85*, San Diego, California, 12-14 November.

Su, M. Y. (1981). On Nonlinear Energy Transfer and Spectral Evolution in Growing Seas. *American Geophysical Union Fall Meeting*, San Francisco, California, December.

Tango, G. J., M. F. Werby, and R. Wooten (1985). Applications of a Synthetic Array Method for Shallow-water Geobottom Reconnaissance. *110th Meeting of the Acoustical Society of America*, Nashville, Tennessee, 4-8 November.

Tunnell, T. and **A. Kramer** (1985). Propagation of Bottom Interacting Very Low-frequency Acoustic Signals Off the Coast Near Cape Fear, N.C. *110th Meeting of the Acoustical Society of America*, Nashville, Tennessee, 4-8 November.

Wagstaff, R. A. (1985). Ambient Noise Directionality at Two Locations in the Gulf of Mexico. *110th Meeting of the Acoustical Society of America*, Nashville, Tennessee, 4-8 November.

Warn-Varnas, A. C. and **J. M. Harding** (1977). An Investigation of the Importance of Third-order Correlations in Mixed Layer Models. *American Geophysical Union Fall Meeting*, San Francisco, California.

Werby, M. F. and **S. A. Chin-Bing** (1984). Some Numerical Techniques and Their Use in the Extension of T-Matrix and Null-field Approaches to Scattering. *Computational Ocean Acoustic Workshop*, Yale University, August.

Werby, M. D., K. Davey, and J. Montgomery (1984). The Use of Integral Equations and the Conjugate Gradient Method in Field Theory Problems. *ECOMP Conference*, Carnegie-Mellon Institute, Pittsburg, Pennsylvania, 11-12 December.

Werby, M. F., L. H. Green, and R. Wooten (1985). A Study of Angular Distributions from Submerged Spheroidal and Finite Cylindrical Shells. *110th Meeting*

of the Acoustical Society of America, Nashville, Tennessee, 4-8 November.

Werby, M. F. and **G. Tango** (1985). Characterization of Average Geoacoustic Bottom Properties from Expected Propagation Behavior at Very Low Frequencies (VLF) Using Towed Array Simulation. *NATO Conference*, La Spezia, Italy, June.

White, D. and **S. A. Chin-Bing** (1982). Comparison Between Perturbative and Exact Treatment of Bottom Attenuation for Shallow-water, Low-frequency Conditions. *103rd Meeting, Acoustical Society of America*, Chicago, Illinois, 26-30 April.

White, D. and **S. A. Chin-Bing** (1983). Source Depth Classification by Modal Decomposition and Correlation. *106th Meeting, Acoustical Society of America*, San Diego, California, 7-11 November.

Wiesenburg, D. A., J. L. Bird, **D. F. Reid**, and **R. A. Arnone** (1983). Observations at the Mississippi River Plume Front During December. Special Session: Fish and Fronts—How Are They Related?, *46th Annual Meeting, American Society of Limnology and Oceanography*, St. John's, Newfoundland, June.

Wiesenburg, D. A., J. M. Brooks, and **D. F. Reid** (1982). Suspended Particulate Distributions Across the Orca Basin Interface. *Fall Meeting, American Geophysical Union*, San Francisco, California, December.

Wiesenburg, D. A. and N. L. Guinasso, Jr. (1982). Thermal Structure and Heat Flow in the Orca Basin, Northern Gulf of Mexico. *Ocean Sciences 1982*, San Antonio, Texas, 16-19 February.

Wiesenburg, D. A. and **C. Rein** (1985). Towed Underwater Pumping System for Deep Ocean Sampling. *OCEANS '85*, San Diego, California, 12-14 November.

Young, D. K. (1982). Nondestructive Measuring of Effects of Bioturbation Sediment Structure. Invited talk, *American Geophysical Union/ASLO Ocean Sciences Meeting*, San Antonio, Texas, 16-19 February.

Young, D. K. and **W. H. Jahn** (1984). Photographs of Deep Sea Lebensspuren: A Comparison of Sedimentary Provinces. *American Geophysical Union Ocean Sciences Meeting*, New Orleans, Louisiana.

Zsolnay, A. (1982). Determining the Source of Particles in Aquatic Environments with Pyrolysis-Chemical Ionization Mass Spectrometry. *American Geophysical Union/ASLO Ocean Sciences Meeting*, San Antonio, Texas, 16-19 February.

Zsolnay, A. (1982). Use of Pyrolysis-Mass Spectrometry in Oceanography, Geochemistry and Fouling Studies. Invited talk, *13th Annual ACS Symposium on Advances in Applied Analytical Chemistry*, New Orleans, Louisiana.

Patents Granted Since 1982

Brunson, B. A. (9/84). *Single Element Cantilever Mounted Shear Wave Transducer*, 4,471,475.

Ferer, K. M. (2/82). *Quatricalically Laid Torque-Balanced Benthic Cable*, 4,317,000.

Gholson, N. H. (1/85). *A Controller for a Locked Carrier Distributed Multiplexed Telemetry System*, 4,494,115.

Marshall, S. W. (10/83). *A Generalized Drifting Oceanographic Sensor*, 4,408,488.

Perkins, H. T. et al. (2/83). *Three-Axis Current Meter*, 4,391,136.

Stiffey, A. V. et al. (4/85). *Method and Apparatus for the Detection of Toxicants*, 4,513,280.

Sutherland, A. L. (4/83). *Trawl Resistant Sensor Mount*, 4,397,584.

Sutherland, A. L. (5/84). *Shallow-water Environmental Oceanographic Measurement System*, 4,448,068.

Swenson, R. C. (11/82). *Self-deploying Buoy System*, 4,358,834.

Swenson, R. C. (8/85). *Safety Mooring Line*, 4,534,262.

Major Participation by NORDA in Workshops, Seminars, and Symposia

Date	Subject	In conjunction with
1977 January 25–27	Buoy Technology Workshop	NOAA/MTS
December 8–9	Ocean Sciences Board	NAS/NRC
1978 April 25–27	15th Oceanographic Subcommittee	CANADA/US MCC
August 17–18	Acoustic Imaging and Data Processing	SEG/USN
1979 September 5–7	Interpretive Modeling of Deep Ocean Sediments	ONR
October 9–11	Satellite Data in Ocean Analysis and Prediction	ONR
November 6–8	Near Surface Ocean Experimental Technology	ONR
November 13–15	Describing Ocean Phenomena using Coherent Radars	ONR
1980 January 22–23	Kevlar Cables and Rope	--
March 17–18	Resolution of Signals Reflected from the Sea Floor	SEG/USN
1982 March 22–23	Shear Waves and Pattern Recognition	SEG/USN
October 12–15	Seafloor Stability of Continental Margins	SEPM
1983 September 20–22	Chemical Variability in Ocean Frontal Areas	U. of R.I.
1984 January 24–26	Ocean Sciences Meeting—New Orleans	AGU
March 13–15	3-D Marine Data	SEG/USN
1985 May 1–3	Ocean Data—New Orleans	MTS
June 11–14	Arctic Oceanography	CNOC

The NORDA Review Editorial Board

This premier issue of the NORDA Journal was a collaborative effort of the contributing authors, under the cognizance of the senior management staff of NORDA. Of particular note were the contributions of the following:

END
DTIC
9-86